IEA-SHAC-TVI-4

IEA
ILAR R&D

INTERNATIONAL ENERGY AGENCY

solar heating and
cooling programme

Experimental Results from Eleven Evacuated Collector Installations

A Report of Task VI:
The Performance of Solar Heating, Cooling, and Hot Water Systems Using Evacuated Collectors

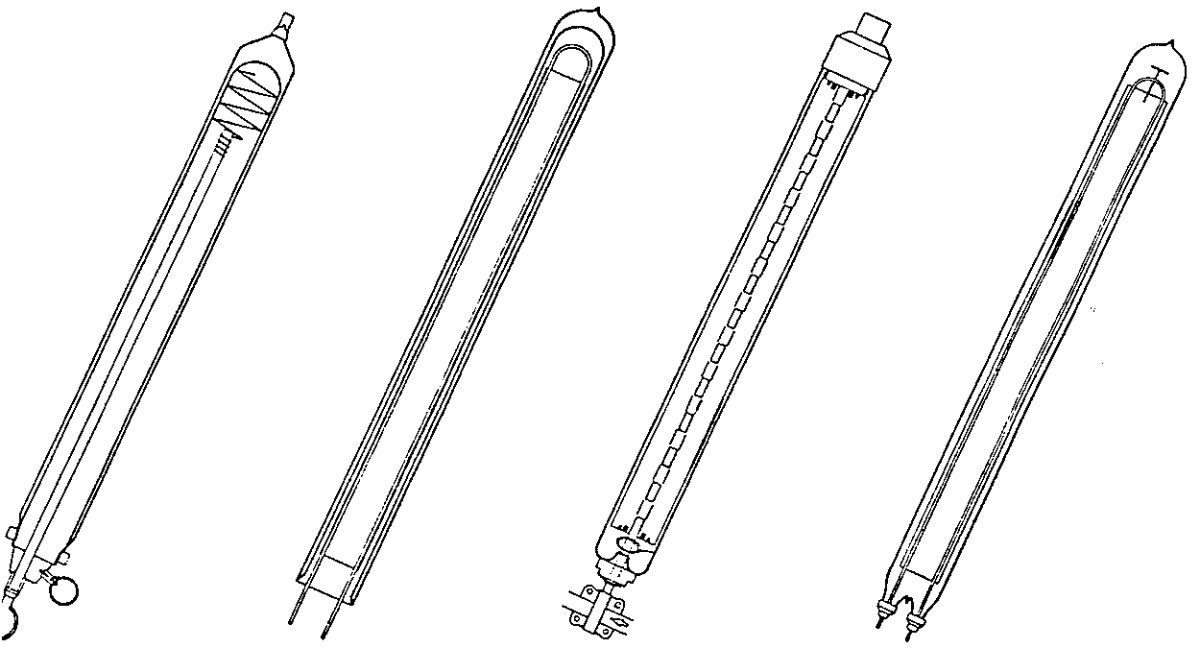

November 1986

Experimental Results from Eleven Evacuated Collector Installations

A Report of Task VI: The Performance of Solar Heating, Cooling, and Hot Water Systems Using Evacuated Collectors

William S. Duff
Colorado State University
United States

PRINCIPAL CONTRIBUTORS:

Roland Schmid
University of Sydney
Australia

William E. Carscallen
National Research Council
Canada

Dolf van Hattem
Joint Research Centre
CEC

H.R. Rauwerdink
Philips Gloeilampenfabrieken
The Netherlands

Elisabeth Kjellsson
Uppsala Kraftvarme
Sweden

Bengt Perers
Studsvik Energiteknik AB
Sweden

Olivier Guisan
University of Geneva
Switzerland

Nigel Potter
BSRIA
United Kingdom

Susumu Karaki
Colorado State University
United States

Klaus Vanoli
IST Energietechnik
Federal Republic of Germany

CONTENTS FINALIZED JANUARY 1988

ABSTRACT

Four years of thermal performance, operation, maintenance, and longevity for eleven evacuated collector installations in the United States, Canada, Europe, and Australia are reported. Also presented are details on each installation's system, controls, loads, climate, components, and experiments. All installations have used a common set of definitions and reporting format so that different installation's results may be easily and unambiguously compared. Thermal performance results are provided on an instantaneous, daily, monthly, and seasonal basis. Comparisons are made to show what effect differences in collector type, evacuated tube type and size, reflectors, tube spacing, preheating, capacitance, snow cover, season, climate, and end use patterns have on thermal performance, operation, maintenance, durability, and longevity. A concise list of conclusions are presented for evacuated collector and system thermal performance, operation, maintenance, and longevity.

TABLE OF CONTENTS

LIST OF TABLES

LIST OF FIGURES

EXECUTIVE SUMMARY

OVERVIEW

This report covers the experimental activity in eleven installations of an International Energy Agency Solar Heating and Cooling Program evacuated collector systems research project. The multi-national effort spans seven years. Installation applications range from single family residential heating and cooling to large scale industrial process heat and district heating. The thermal performance for each installation is reported, as are a great many particulars regarding system components, controls, loads, climate, installation, operation, maintenance, longevity, and snow cover. A previous report addressed the first three years of the project. This report covers the last four years of experimental activity. A list of Task VI reports covering additional subjects investigated during the course of the research is found in the References and Bibliography section.

OBJECTIVE

The project objective was to further the understanding of the performance of evacuated collectors in solar heating, cooling, and hot water systems and to study, document, and compare the performance characteristics of such collectors in various systems and climates.

RESEARCH APPROACH

To accomplish the objective, research teams from the ten participating countries performed experiments, analyzed the results, modeled component and system performance, and reported the findings.

Each of the ten countries provided at least one well instrumented installation with at least two full time scientific staff members and a full time data engineer who was responsible for the instrumentation and data acquisition equipment and the timely correction of system faults.

A mandatory uniform reporting format was adopted which facilitated comparison of performance among different installations and allowed material to be conveniently assembled into Task reports.

EVACUATED COLLECTORS

More than twenty different evacuated collectors were studied during the 1979 to 1986 period of the research project. There were evacuated collectors with round and flat absorbers; glass and metal absorber substrates; soft and hard glass vacuum enclosures; close, moderate, and wide tube spacing; U-tube, heat pipe, thermosyphon, straight through, and direct contact heat extraction; black chrome, cobalt oxide/sulfide, and

Table 1 Philips VTR361 Collector Performance Data
for January 2, 1984, CSU Solar House I.

TIME	TOTAL SOLAR RAD, W/m^2	AVERAGE COLLECTOR FLUID TEMP. ^oC	AMBIENT AIR TEMP. oC	COLLECTOR EFFICIENCY	TIME	TOTAL SOLAR RAD, W/m^2	AVERAGE COLLECTOR FLUID TEMP. ^oC	AMBIENT AIR TEMP. oC	COLLECTOR EFFICIENCY
8:45	468	41.3	-8.5	.545	12:30	1028	69.5	-1.6	.613
50	495	42.0	-8.4	.547	35	1028	70.0	-1.6	.610
55	520	42.7	-7.9	.554	40	1027	70.5	-1.1	.605
9:00	546	43.4	-8.0	.561	45	1024	71.0	-1.3	.603
5	572	44.1	-8.1	.566	50	1015	71.5	-1.0	.597
10	596	44.9	-7.6	.573	55	1006	71.9	-1.0	.592
15	621	45.7	-7.2	.576	13:00	1005	72.3	-1.0	.583
20	644	46.3	-7.2	.578	5	1002	72.8	-0.6	.578
25	668	45.4	-7.2	.555	10	994	73.2	-0.6	.573
30	691	46.8	-6.8	.611	15	986	73.7	-0.8	.570
35	712	47.4	-6.7	.587	20	974	74.2	-1.0	.569
40	731	47.9	-6.8	.590	25	959	74.6	-1.1	.568
45	751	48.3	-6.8	.592	30	944	75.0	-0.6	.568
50	771	48.8	-6.8	.590	35	938	75.5	-0.7	.564
55	790	49.4	-6.4	.592	40	926	76.0	-1.0	.566
10:00	809	50.0	-6.3	.589	45	913	76.4	-0.5	.564
5	827	50.6	-5.9	.590	50	900	76.8	-0.5	.565
10	843	51.3	-5.9	.590	55	888	77.2	-0.2	.565
15	857	52.1	-5.8	.592	14:00	873	77.6	-0.5	.565
20	872	52.9	-5.7	.592	5	856	77.9	-0.3	.563
25	889	53.6	-5.4	.588	10	839	78.4	-0.2	.566
30	904	54.2	-5.1	.588	15	819	78.7	0.2	.565
35	917	54.7	-5.0	.587	20	798	79.0	0.0	.567
40	929	55.4	-4.7	.591	25	778	79.4	0.3	.570
45	942	56.0	-4.7	.592	30	755	79.8	0.4	.575
50	954	56.7	-4.5	.595	35	731	80.1	-0.1	.576
55	966	57.3	-4.2	.594	40	709	80.4	-0.3	.574
11:00	976	58.0	-4.1	.598	45	684	80.6	0.0	.574
5	986	58.7	-4.1	.600	50	657	80.8	-0.2	.571
10	998	59.4	-4.0	.602	55	630	80.9	-0.3	.569
15	1004	60.2	-3.6	.607	15:00	606	81.1	-0.4	.564
20	1007	61.0	-3.4	.601	5	583	81.2	-0.4	.558
25	1012	61.6	-3.5	.611	10	562	81.3	-0.4	.551
30	1017	62.2	-3.4	.612	15	537	81.4	-0.4	.546
35	1020	62.9	-3.1	.616	20	514	81.5	-0.2	.538
40	1025	63.4	-3.0	.614	25	492	81.6	-0.3	.522
45	1029	64.1	-3.0	.618	30	464	81.6	-0.5	.512
50	1029	64.6	-2.5	.618	35	434	81.6	-0.4	.497
55	1028	65.3	-2.5	.624	40	405	81.5	-1.0	.481
12:00	1027	65.9	-2.4	.623	45	376	81.4	-1.1	.460
5	1028	66.6	-2.4	.622	50	344	81.3	-1.1	.434
10	1028	67.2	-2.2	.620	55	315	81.2	-1.3	.407
15	1028	67.8	-2.0	.620	8:45	503	74.5	3.7	.514
20	1023	68.3	-1.8	.619	50	528	75.1	4.1	.509

sintered carbide selective surfaces; and diffuse and mirrored reflectors -- and no reflectors.

NEW EVACUATED COLLECTORS

Though not ready in time for testing as part of this project, some new highly promising evacuated collector tubes are under development. A 125 mm wide tube with an internal mirror is expected to extend the temperature range where evacuated collectors achieve high seasonal collection efficiencies to about 200°C. A 150 mm wide tube with a storage tank internal to the tube is expected to provide the basic building block for a high performance low cost integral tank DHW system.

MAJOR FINDINGS

Efficiency of Energy Collection

For all evacuated collector types efficiency of energy collection reaches a high value when solar radiation levels are high and collector operating temperature differences to ambient are low. As solar radiation levels fall or collector operating temperature differences rise, energy collection efficiencies decline. This decline is significantly slower for evacuated collectors than for most other collector types.

- **Instantaneous collection efficiencies around sixty percent were attained for temperature differences up to almost 80°C during most daylight hours.**

Five minute interval readings for the United States's Colorado State University Solar House I on 2 January 1983 are given in Table 1.

Though high collection efficiencies can be attained over the short term, monthly and seasonal collection efficiencies are invariably lower. For evacuated collectors these longer term efficiencies are still quite high.

- **Monthly collection efficiencies above fifty percent were consistently attained for a DHW and space heating application in a climate with a high level of diffuse radiation.**

As can be seen in Figure 1, monthly collection efficiencies above fifty percent were routinely attained by the Federal Republic of Germany's Solarhaus Freiburg while operating at average temperature differences between 21 and 45°C.

- **Monthly collection efficiencies of close to fifty percent were routinely attained for a space cooling application.**

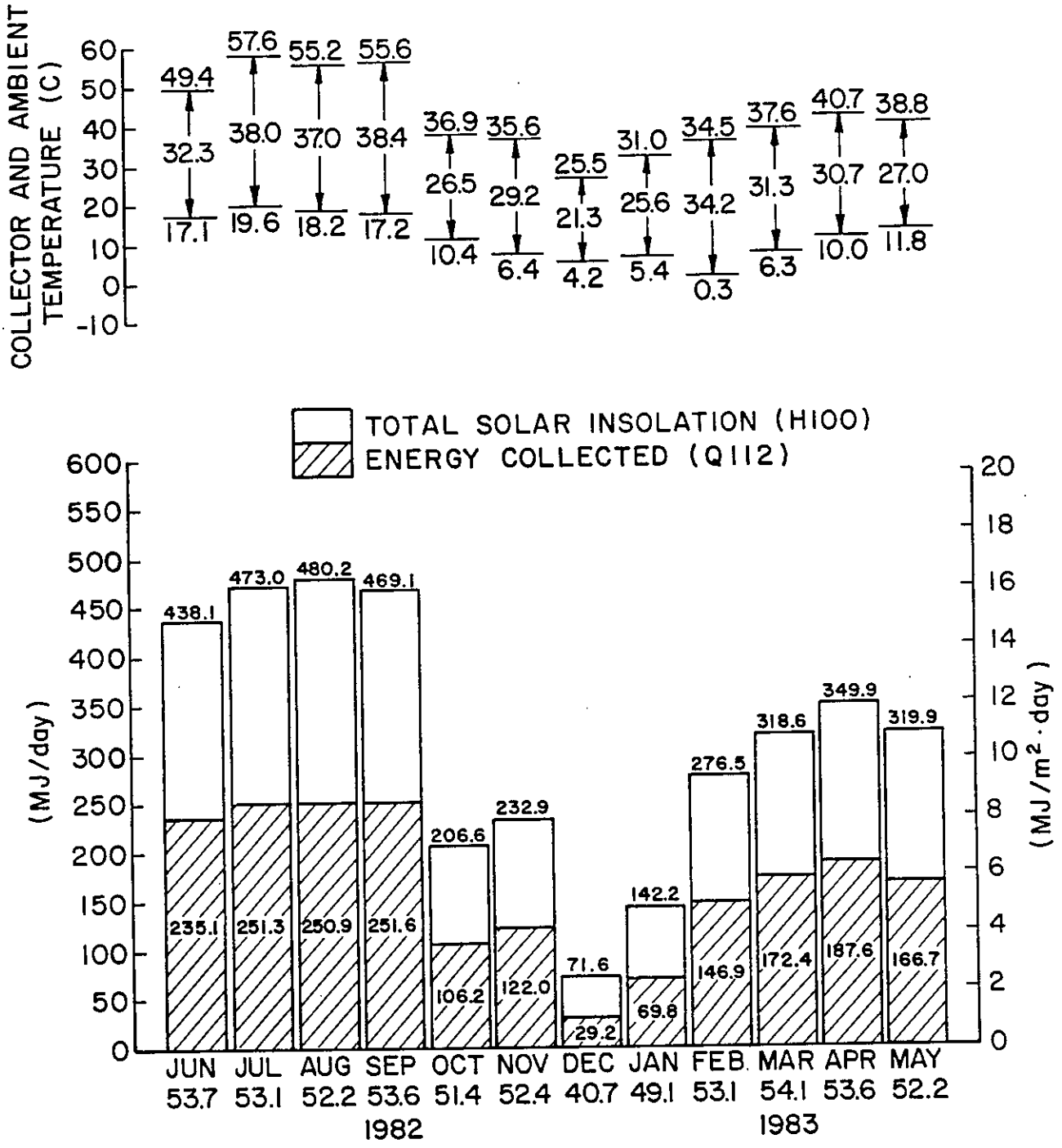

Figure 1 Average Energy Supply Rates for Solarhaus Freiburg, Federal Republic of Germany, for June 1982 to May 1983.

As can be seen in Figures 2 and 3, monthly collection efficiencies of about fifty percent were attained by the Commission of European Communities' Ispra, Italy Solar Laboratory while operating at average temperature differences between 40 and 61°C.

- **Monthly collection efficiencies as high as forty four percent were attained while operating at average monthly temperature differences between 88 and 96°C.**

The Monthly collection performance for the United States's Colorado State University Solar House I for four months in 1984 is shown in Figure 4. During April and May there were several days when the system was not operated for substantial periods and these days were included in the computations of Figure 4. Thus, collection performance for these months is lower than it would have been under normal circumstances.

Performance at Off-Normal Solar Incidence

Collector efficiency is ordinarily stated for solar radiation directly normal to the plane of the collector. For most collectors efficiency falls off only slightly for most other solar radiation angles. This is not the case for evacuated collectors.

- **Evacuated collector efficiencies were greater at nearly every time of day all year long when compared with efficiencies determined when radiation was normal to the collector plane. For some types the difference was substantial, up to greater than twenty percent during the times of the day that most energy is collected.**

Solar collector efficiencies are commonly stated at a solar incidence angle normal to the plane of the collector. When contrasted to flat plate collectors, the efficiencies of most evacuated collectors were greater for incidence angles off normal to the tube in the transverse direction. As can be seen in the experimental data in Figure 5 and the calculated curve for the round absorber in Figure 6, the efficiency response for the round absorber Sydney University collector with wide tube spacing is nearly flat and substantially above that for radiation normal to the collector plane. Exceptions were evacuated collectors with CPC reflectors. Here efficiency at first increases with increasing incidence angles and then declines rapidly once a high incidence angle is exceeded. However, the CPC reflectors are usually designed with an incidence angle cut-off that is sufficiently high to allow collection of most of the available incident energy.

Other Performance Results

- **Two evacuated collectors, the Corning collector and most versions of the long tube Philips collector, outperformed all other evacuated collectors and significantly outperformed the**

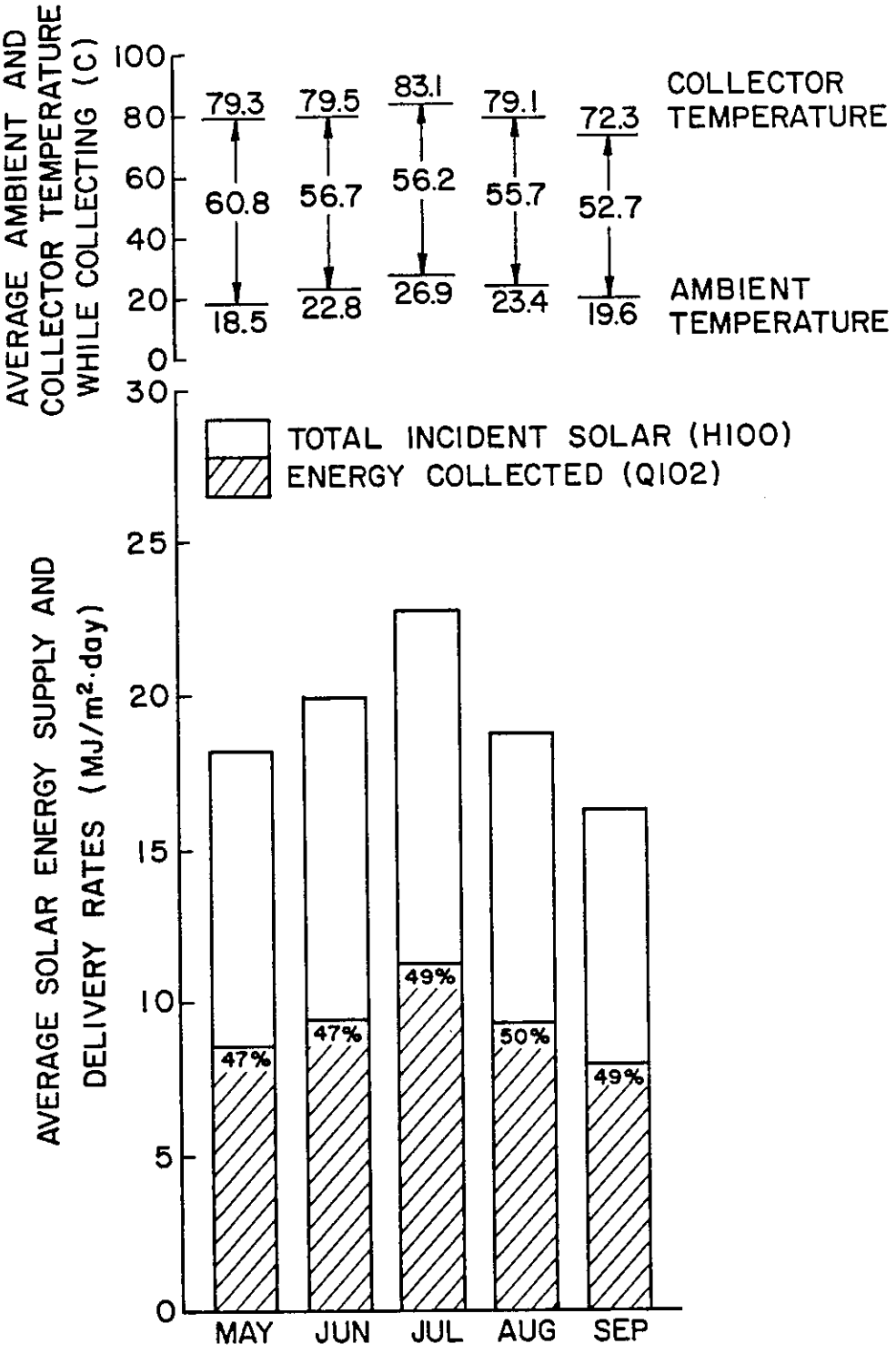

Figure 2 Average Energy Supply Rates for the Philips VTR 261 Collector at the Ispra Solar Laboratory in 1983.

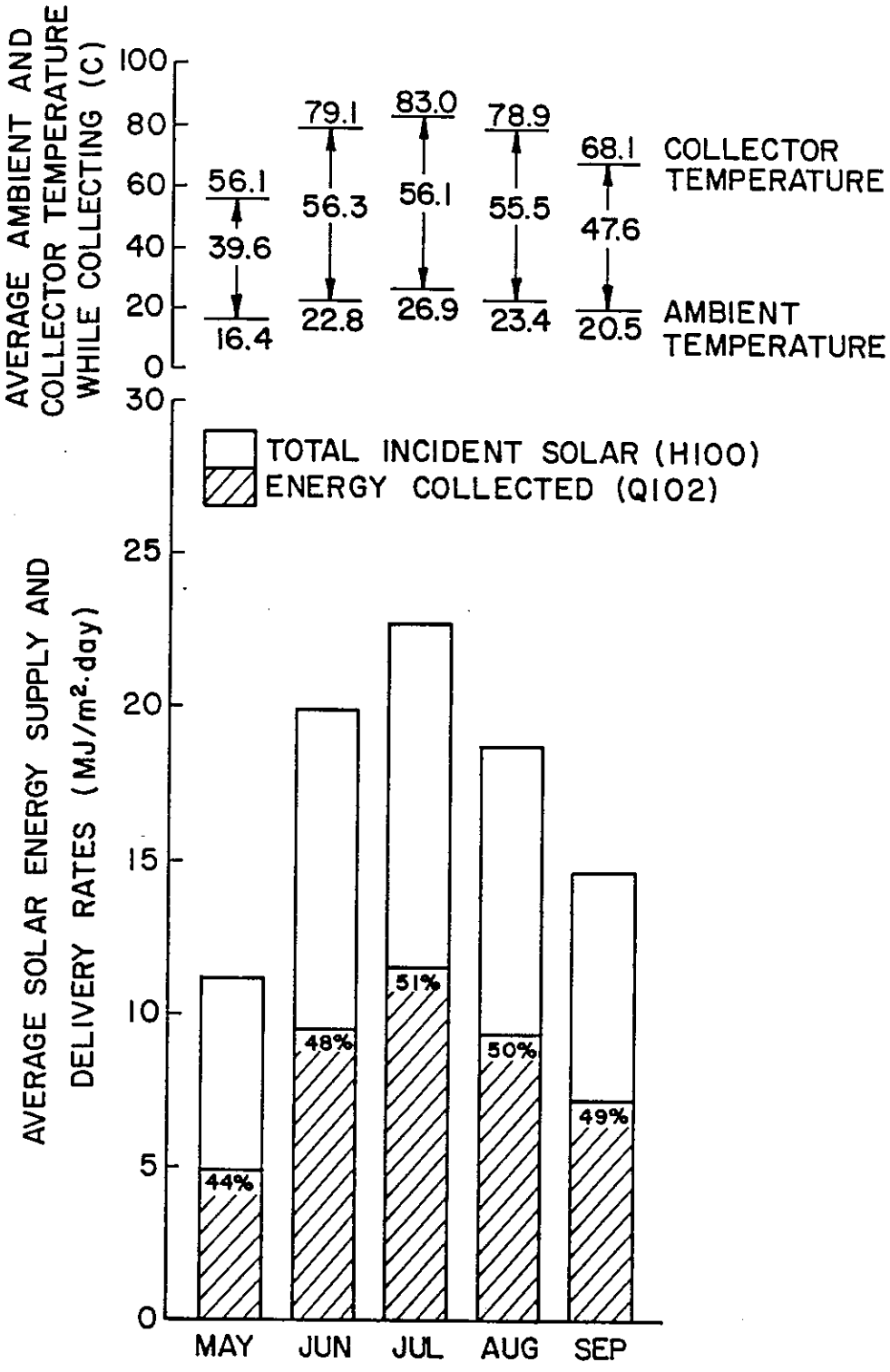

Figure 3 Average Energy Supply Rates for the Philips VTR 361 Collector at the Ispra Solar Laboratory in 1983.

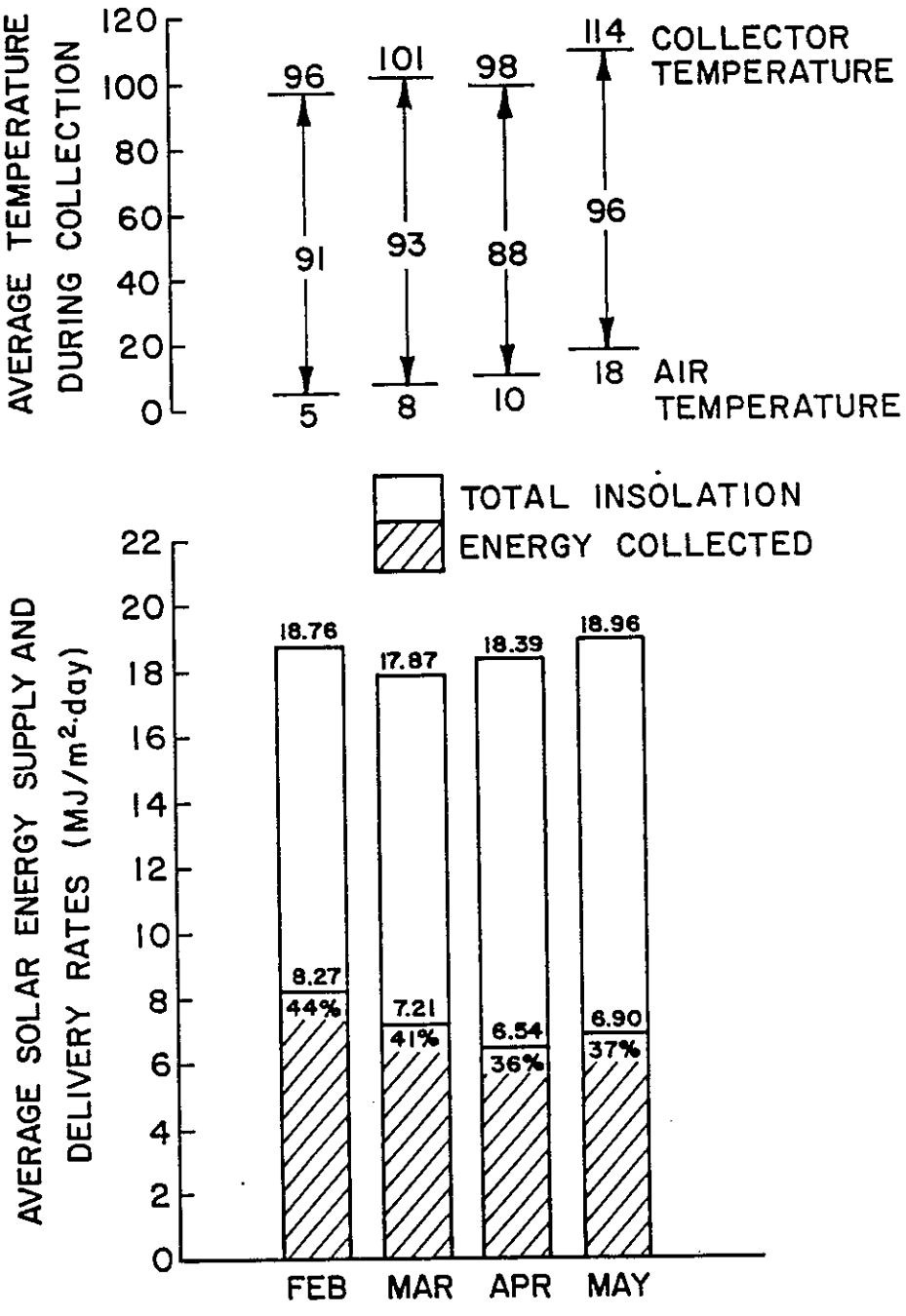

Figure 4 Monthly Average Energy Supply Rates for Colorado State University Solar House I in 1984.

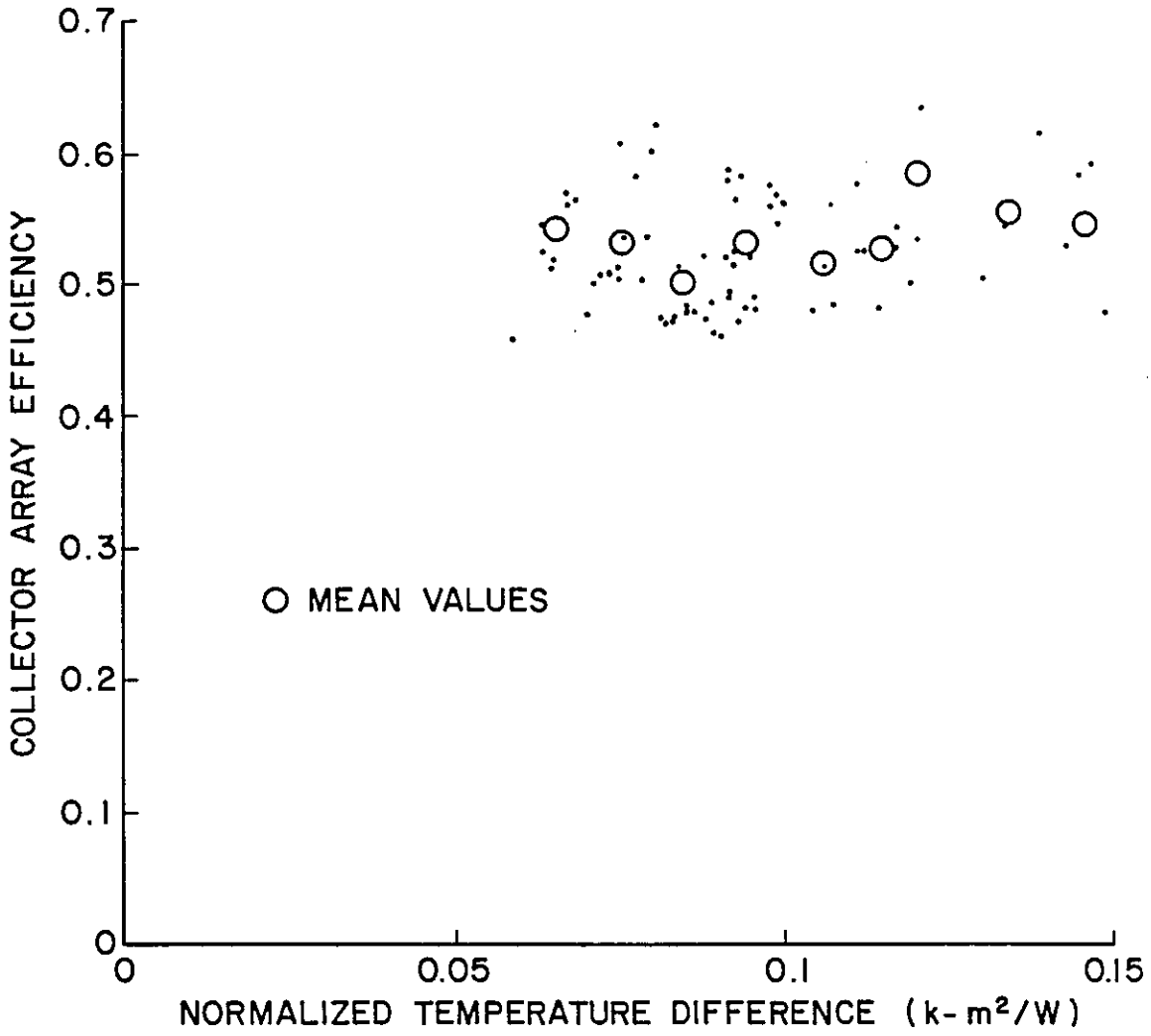

Figure 5 Collector Array Efficiency Diagram for Sydney University Evacuated Tubular Collector, 28 August to 28 September 1983.

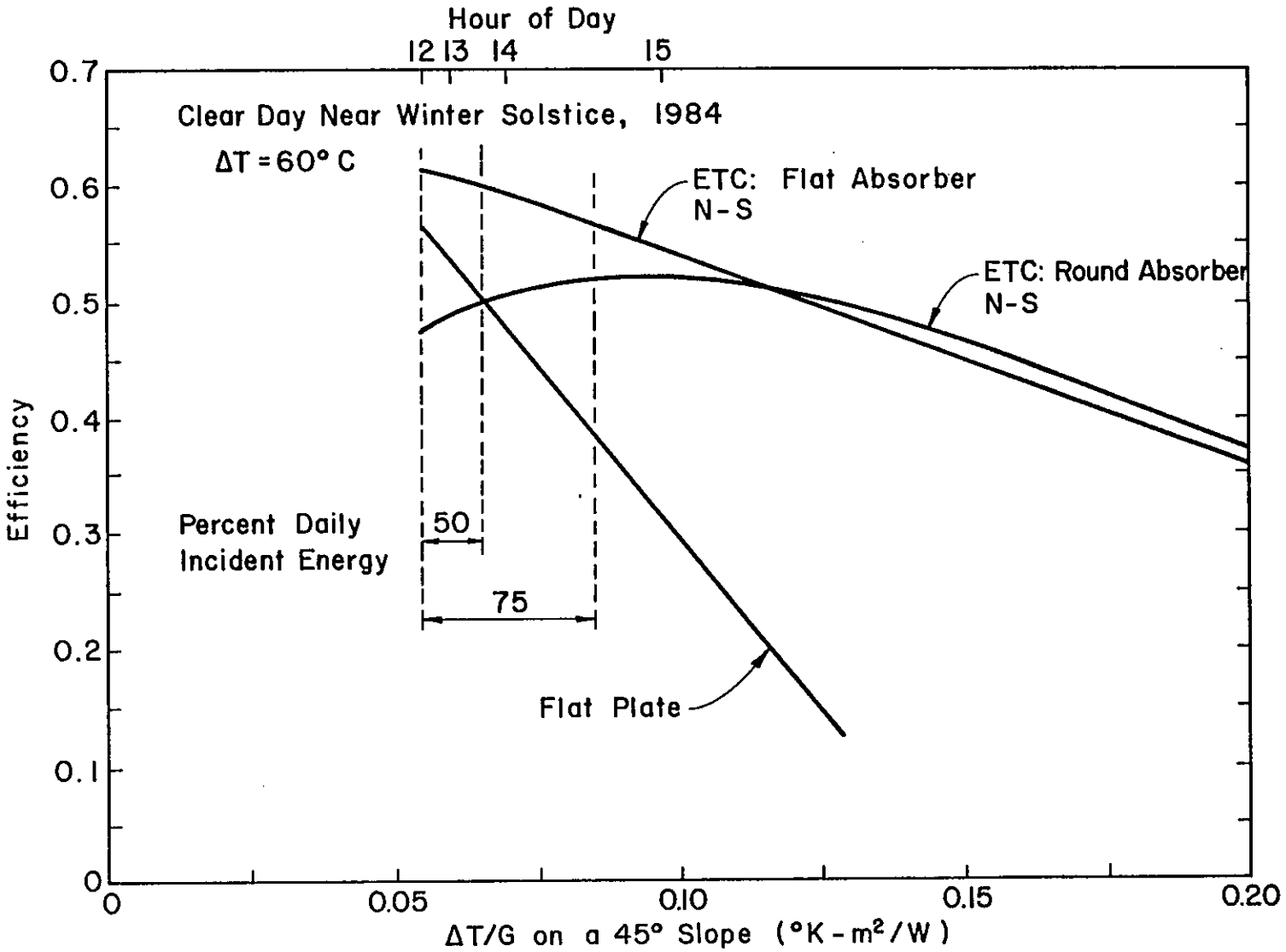

Figure 6 Calculated Effect of Incidence Angle on Collector Efficiency for a Clear Winter Solstice Day.

flat plate collectors at all but the lowest applications temperatures.

Figure 7 shows such a comparison for a set range of operating temperature differences. At these temperature differences the two best evacuated collectors outperform all the other collectors for every daily solar radiation level.

- **Long tube evacuated collectors exhibited significantly better performance than short tube evacuated collectors.**

Longer tubes reduce the manifold area needed and therefore reduce per unit collector area losses. In two instances both short and long tubes of basically the same design manufactured by essentially the same companies were used. In both cases lengthening the tubes substantially increased performance. One of these cases is shown in Figure 8.

- **Poor system design or installation was the most common cause of poor system performance, not the performance of the evacuated collectors.**

Reliability and Maintenance

- **In most cases no measurable loss of performance occurred during nearly seven years of operation.**

In one case there was no measurable loss of performance over almost thirteen years. A collector array began operation at Colorado State University over twelve years before, was dismantled and shipped to Germany three years later, and was reinstalled there. This collector continues to operate today.

- **Evacuated collectors required no maintenance in virtually all cases.**

- **Once shipped and installed in a properly functioning system tube vacuum loss and breakage from other than natural hazards has been on the order of one percent.**

Hail damage has occurred to one of the thinner-walled types where hail was over four cm in diameter. Breakage or loss of vacuum during shipping was about one and one-half percent, with most losses occurring in the small shipments. Breakage or vacuum loss during installation was not a problem except when a Dewar type was filled when hot. Precautions are necessary with this type during installation and operation to see that this does not occur.

- **In most collectors individual tubes, if damaged, can be replaced easily, often without draining the system or shutting it off.**

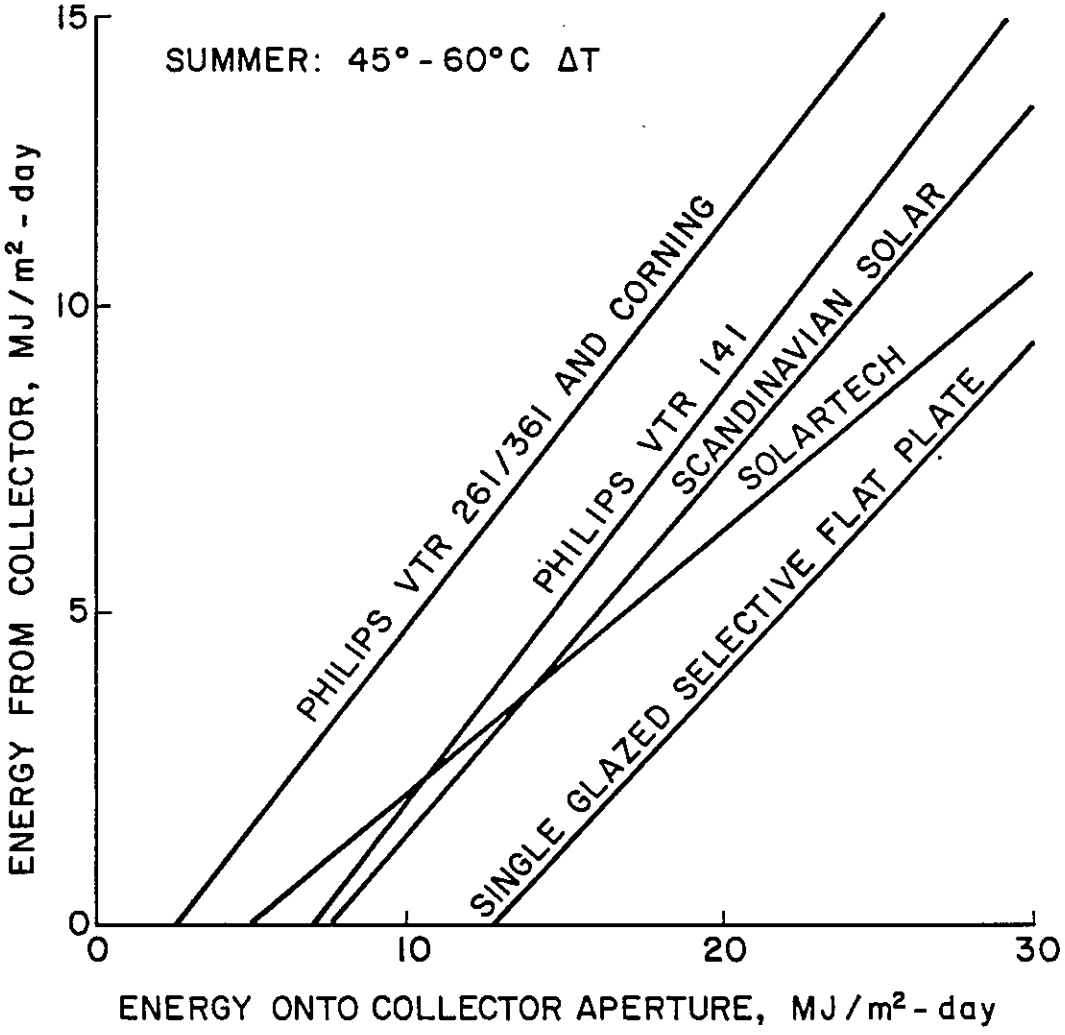

Figure 7 Comparison Between Evacuated and Flat Plate Collector Daily Performance.

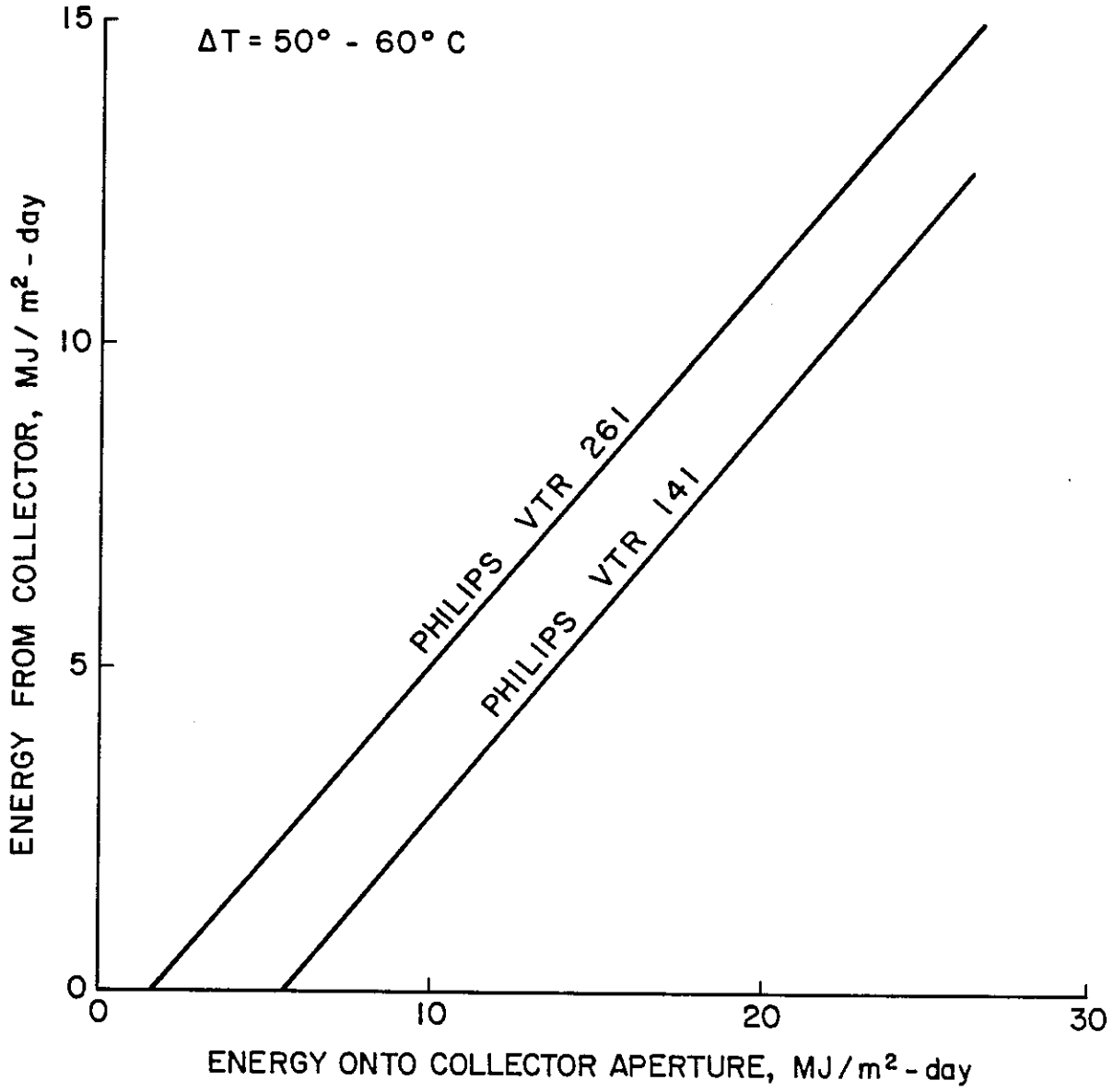

Figure 8 Comparison Between Philips Long and Short Heat Pipe Evacuated Tube Collectors.

Installation

- Horizontal mounting, possible with some evacuated collector designs, reduced interarray piping, mounting structure, installation labor, and thermal losses.

Collectors with close packed tubes, no reflectors, tiltable metal fins, and flow through heat removal were mounted nearly horizontally with little or no loss of individual module seasonal performance.

1. INTRODUCTION

This report provides experimental results and analyses of a multinational solar energy system research project on evacuated collector systems. For each of the eleven installations covered in this report, the thermal performance for essentially all operating periods during a four year span is presented as well as a great many particulars regarding system components, controls, loads, climate, installation, operation, maintenance, longevity, and snow cover.

Task VI of the International Energy Agency Solar heating and Cooling Programme was intiated in October 1979. The project objective was to further the understanding of the performance of evacuated collectors in solar heating, cooling, and hot water systems and to study, document, and compare the performance characteristics of such collectors in various systems and climates. To this end, research teams from ten countries performed experiments in well instrumented installations over a period of seven years. The applications ranged from single family residential heating and cooling to large scale industrial process heat and district heating. A report on eight of these installation covering the period 1979 through 1981 was published in November 1982 [1]. The eleven installations and periods covered in this report are shown in Table 1-1. Some supplemental installation results for 1985 and beyond are provided in Appendix E.

Each IEA task is managed by an Operating Agent. Professor William S. Duff of Colorado State University served as Operating Agent for Task VI on behalf of the United States Department of Energy.

1.1 RESEARCH APPROACH

1.1.1 Instrumentation

Each of the ten countries provided at least one well instrumented installation. Instrumentation was sufficient to calculate the primary reporting quantities to the high degree of accuracy specified in "Data Performance Requirements and Thermal Performance Evaluation Procedures for Solar Heating and Cooling Systems," published for the International Energy Agency by the United States National Bureau of Standards[157].

1.1.2 Staffing

Each country agreed to commit to the project at least two man years of scientific staff time each year as well as the equivalent of one full-time data engineer to be responsible for instrumentation and data acquisition equipment and the timely correction of system faults.

Table 1-1

Task VI Installations

Installation Type	End Use	Typical Solar Collector Temperatures in ^{o}C	Location	Period Covered in This Report
Industrial Process Heat	Bottle Washing	70-85	Edmonton, Canada	December 1982 to November 1984
Industrial Process Heat	Process Heat	50-110	Hallau, Switzerland	March 1984 to February 1985
District Heating	Space Heating, DHW, and IPH	50-60	Södertörn, Sweden	May 1982 to October 1984
District Heating	Space Heating and DHW	50-60	Knivsta, Sweden	September 1982 to June 1983
District Heating	Space Heating and DHW	80-120	Geneva, Switzerland	July 1982 to March 1984
Single Family Residential	Heating, Cooling and DHW	40-110	Colorado, USA	December 1982 to September 1983
Single Family Residential	Heating and DHW	40-80	Eindhoven, Netherlands	January 1984 to September 1984
Multifamily Residential	Heating and DHW	40-80	Freiburg, Germany	January 1982 to September 1983
Offices	Heating and Cooling	70-90	Sydney, Australia	December 1982 to February 1985
Laboratory	Cooling	80-90	Ispra, Italy	May 1982 to September 1984
Simulated Loads	Heating and DHW	30-60	Bracknell, UK	June 1981 to August 1983

1.1.3 Reporting

The adoption of a mandatory common reporting format[2] greatly enhanced the exchange of performance results within the Task. This format facilitated comparison of performance among different installations and allowed material to be conveniently assembled into Task wide reports. During the experimental part of the project a full report for each installation was written every year and number of Task wide reports on collector characterization, modeling, and so forth have been written. See [80-134] and [1-6].

1.2 EVACUATED TUBES

All evacuated collectors used in the Task installations consisted of a selective absorber surface enclosed in a vacuum and a means by which heat absorbed by the absorber surface can be removed from the collector tube.

Designs of currently available evacuated collectors can be categorized into two groups. One group is the Dewar type and the other the metal fin in vacuum type. Within each of these two basic designs many variations are possible.

1.2.1 Metal Fin in Vacuum Tubes

The metal fin in vacuum configuration uses a metal absorber plate in a single walled glass vacuum tube. Heat is removed from the absorber plate by circulating liquid through a metal tube bonded to the plate. Glass to metal seals are needed to pass the heat extraction tubes through the wall of the vacuum envelope. Collectors in this group differ mainly in the way that heat is transported out of the vacuum enclosure:

1. A U-tube heat removal design is shown in Figure 1-1.

2. An alternative configuration uses a straight through metal tube. In this design it is necessary to incorporate bellows in order to absorb the dimensional changes of the metal tube which result from temperature changes.

3. A third heat extraction technique shown in Figure 1-2 uses a heat pipe bonded to the metal absorber plate. Heat collected by the plate converts liquid in the heat pipe to vapor, the vapor flows to the condenser, it gives up its heat in converting back to a liquid, and the liquid then flows back down to the heat pipe.

4. Another variant uses two concentric metal tubes with the outer tube bonded to the metal absorber plate. Fluid flows in through the inner tube and out through the annulus between the tubes.

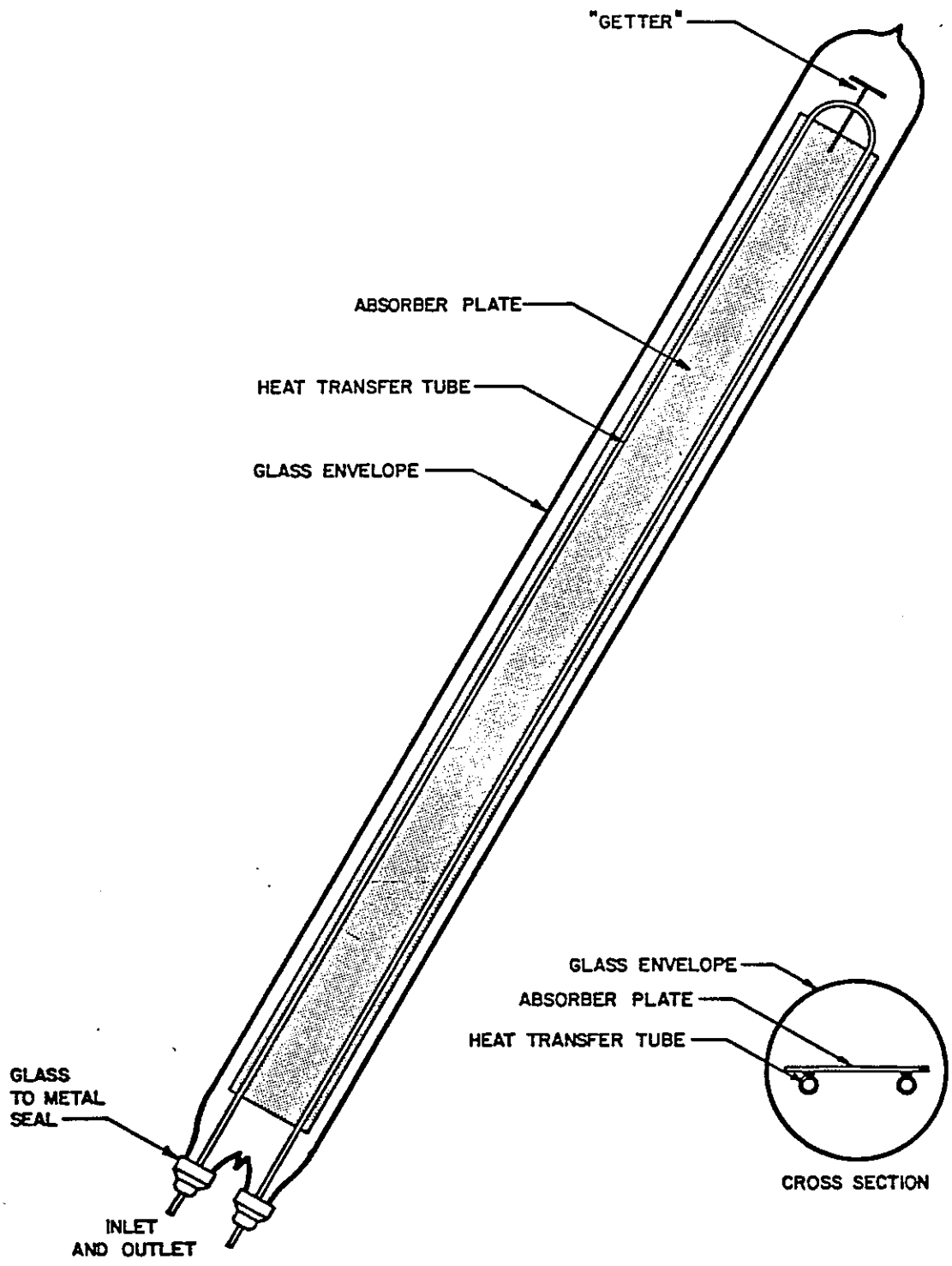

Figure 1-1 Metal Fin in Vacuum Tube Type -- U-tube Heat Extraction

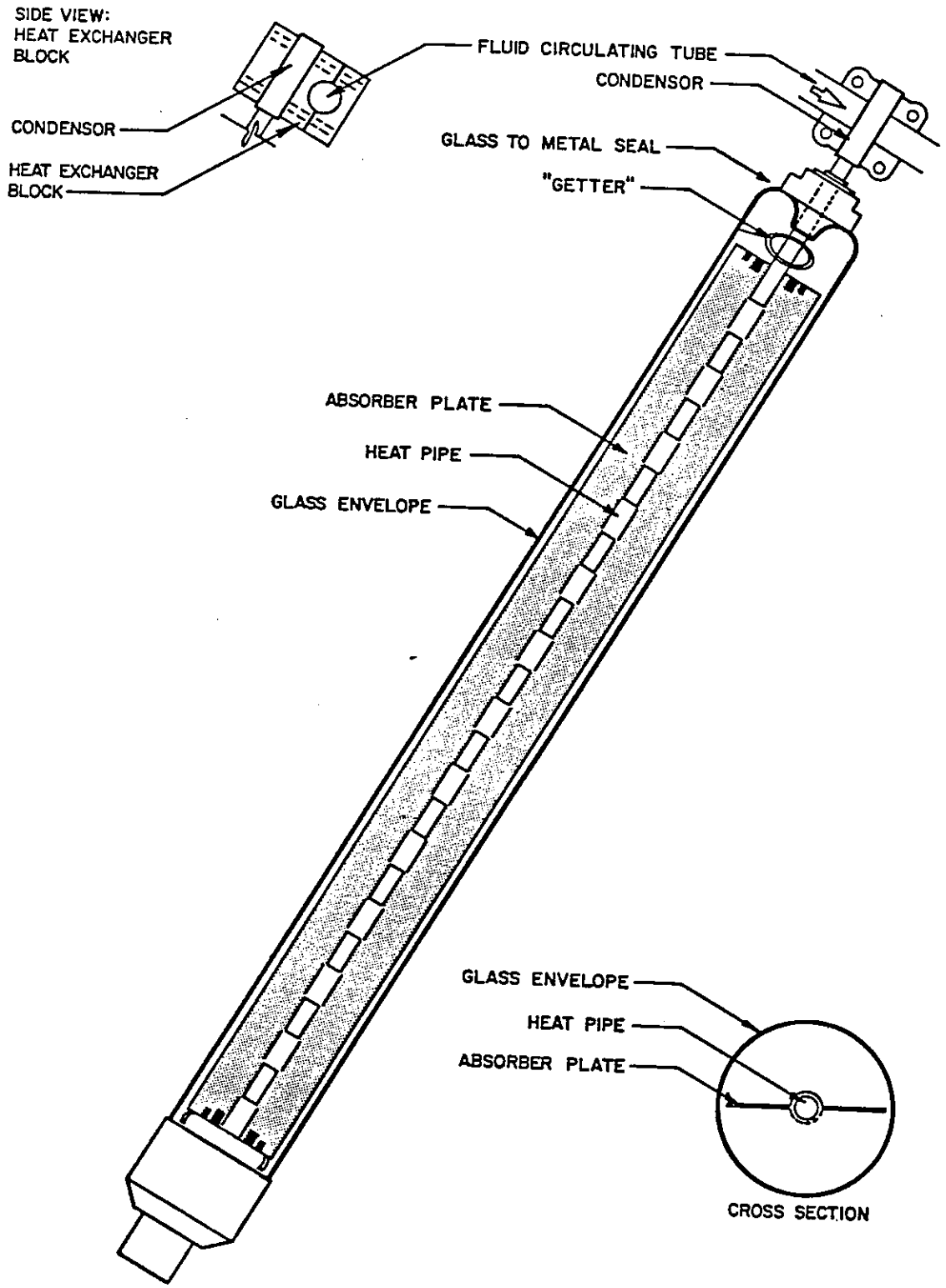

Figure 1-2 Metal Fin in Vacuum Tube Type -- Heat Pipe Heat Extraction

1.2.2 Dewar Tubes

The second type of evacuated tube construction is a Dewar flask. The selective surface is deposited on the outside of a domed glass tube. This tube is then inserted into a second larger domed glass tube and the tubes are joined at the open end. The space between the two tubes is then evacuated. It is not necessary to penetrate the glass envelope in order to extract heat from the tube. All methods of heat extraction involve circulating fluid into and out of the space inside the inner glass tube:

1. Heat can be extracted by using a liquid in contact with the inner glass tube. One way of doing this is shown in Figure 1-3. Liquid enters the inner Dewar tube through a constriction at the bottom. The tube fills and the liquid subsequently overflows into a drain down tube and then flows into a header pipe.

2. An alternative is to have the inner tube filled with liquid and connected directly to a header pipe. A natural thermosyphoning effect in the evacuated tube results in efficient heat extraction from the tube into the header.

3. A cylindrical metal fin attached to a U-tube design as shown in Figure 1-4 can be used. In such configurations the metal heat transfer fin enhances the heat transfer between the inner glass tube and the heat extraction piping, but satisfactory heat extraction will occur without it. The metal fin may be in contact with the inner glass tube, but heat transfer will be adequate even with no contact.

4. In addition, a heat pipe with or without the cylindrical metal fin can be used.

5. Another possibility is a single tube, with or without the cylindrical metal fin, with heat extraction by thermosyphoning.

1.2.3 New Designs

Some new evacuated collector tubes are being developed. A 125 mm wide tube with an internal mirror is expected to extend the temperature range where evacuated collectors achieve high seasonal collection efficiencies to about 200°C. A 150 mm wide tube with a storage tank internal to the tube is expected to be the basis for a high performance low cost DHW system. Other research focuses on evacuated receivers for line focus tracking concentrating collectors, where normal operating temperatures exceed those of current evacuated collectors.

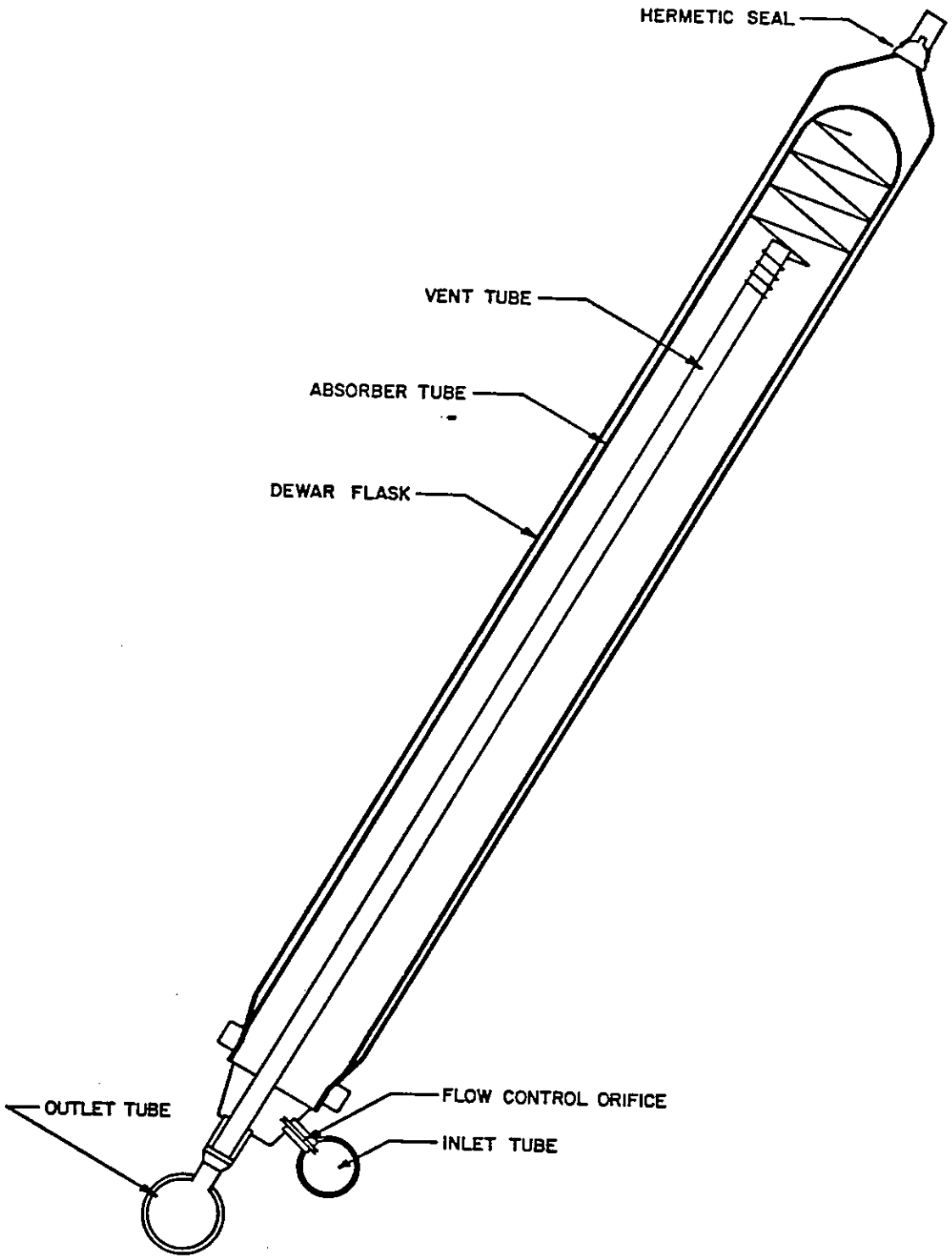

Figure 1-3 Dewar Tube Type -- Direct Liquid Contact and Overflow Heat Extraction

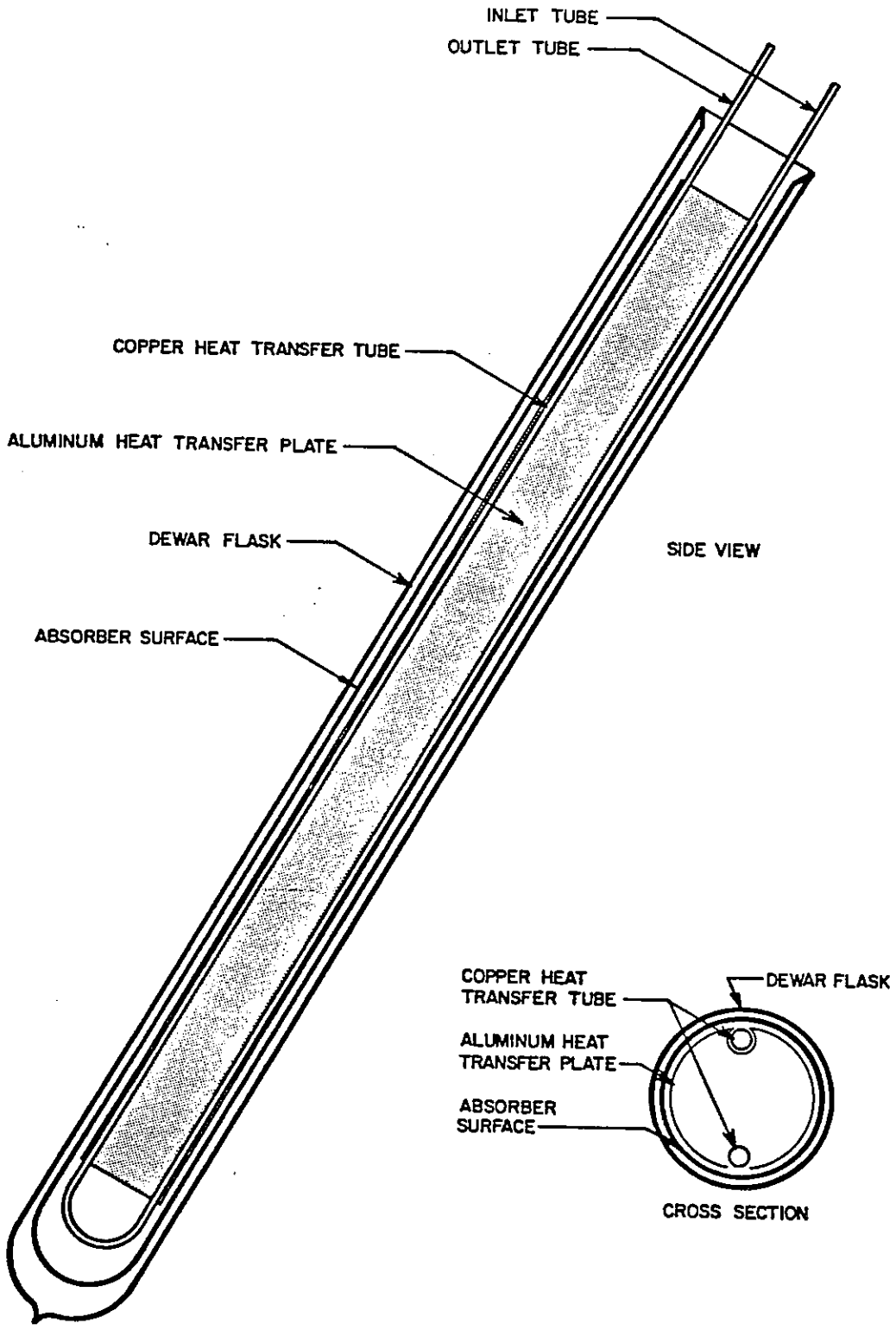

Figure 1-4 Dewar Tube Type -- U-Tube with Fin Heat Extraction

1.3 EVACUATED COLLECTOR MODULES

1.3.1 Absorber, Aperture, and Gross Collector Area

Throughout this report task collection performance results are stated on the basis of collector aperture area. The aperture area is the clear area between the support and manifold boxes at either end of the module's evacuated tubes. It includes tubes, spaces between tubes, and reflectors, if they are present. Absorber areas are always less since the absorbers are contained within the evacuated tubes.

To calculate gross area, the support and manifold boxes at either end of the module's evacuated tubes are included. Conversion of properties and performance of specific collectors from one area basis to another can easily be made by multiplying by the appropriate ratio. In some new evacuated collector designs the aperture area to gross area ratios run as high as 0.87, comparable to that of many flat plate collectors.

1.3.2 Incident Angle Effects

Solar collector performance data are most often quoted at an incidence angle normal to the plane of the collector. Such performance data may substantially understate overall evacuated collector performance because nearly all evacuated collector tube/module geometries result in collection performance increases compared with collection at normal incidence[3]. For some geometries this can be quite substantial, as much as 40 percent, during different times of the day and during different seasons. Thus, performance data at normal incidence should be treated as a lower limit for an evacuated collector. Experimental performance data in this report include incident angle effects.

1.4 EVACUATED COLLECTORS USED IN THE TASK VI INSTALLATIONS

Table 1-2 provides a cross reference between evacuated collector types and the Task VI installations. Listed for each different collector are the Task VI installations that have used it.

1.5 ORGANIZATION OF THE REPORT

Chapter 1 provides an introduction to the report. Chapter 2 provides photographs and descriptions of the installations, loads, and current activities. Chapter 3 describes the climate at each installation. Chapter 4 provides a detailed treatment of each component. The collectors are thoroughly described.

Table 1-2

Installations Using Different Evacuated Collector Types

Collector	Installations
Corning Cortec Metal Fin in Vacuum Type Long Tubes U-Tube Heat Removal Closely Packed Tubes Diffuse Reflector or None	Solarhaus Freiburg, Federal Republic of Germany SOLARCAD District Heating Project, Södertörn, Sweden SOLARIN Industry Project, Switzerland Solar House 1, Colorado State University, United States
General Electric TC-100 Dewar Type Short Tubes U-Tube Heat Removal Widely Spaced Tubes CPC Mirror Reflector	Osaka Sanyo Solar House, Japan Knivsta District Heating Project, Knivsta, Sweden Södortörn District Heating Project, Södertörn, Sweden
Owens-Illinois Sunpak Dewar Type Short Tubes Direct Contact Heat Removal Widely Spaced Tubes CPC Mirror Reflector	Knivsta District Heating Project, Knivsta, Sweden
Philips VTR141 Metal Fin In Vacuum Type Short Tubes Heat Pipe Heat Removal Closely Packed Tubes Diffuse Reflector or None	Knivsta District Heating Project, Knivsta, Sweden Södertörn District Heating Project, Södertörn, Sweden Evacuated Collector System Test Facility, United Kingdom Solar House 1, Colorado State University, United States
Philips VTR261 Metal Fin In Vacuum Type Long Tubes Heat Pipe Heat Removal Closely Packed or Moderately Spaced Tubes Diffuse Reflector or Ripple Mirror Reflector	Ispra Solar Heated & Cooled Laboratory, CEC Solarhaus Freiburg, Federal Republic of Germany Eindhoven Technological University Solar House, The Netherlands
Philips VTR361 Metal Fin In Vacuum Type Long Tubes Heat Pipe Heat Removal Moderately Spaced Tubes Ripple Mirror Reflector	Ispra Solar Heated & Cooled Laboratory, CEC Solar House 1, Colorado State University, United States
Philips Mark VI Non-Standard Tube/Module Short Tubes Non-Standard Heat Removal Closely Packed Tubes No Reflector	Solarhaus Freiburg, Federal Republic of Germany Solar House 1, Colorado State University, United States
Sanyo Metal Fin In Vacuum Type Long Tubes Flow Through Heat Removal Closely Packed Tubes Diffuse Reflector	Ispra Solar Heated & Cooled Laboratory, CEC Osaka Sanyo Solar House, Japan SOLARCAD District Heating Project, Switzerland
Sanyo Heat Pipe Metal Fin in Vacuum Type No Data Reported	Osaka Sanyo Solar House, Japan

Table 1-2
Installations Using Different Evacuated Collector Types

Collector	Installations
Solartech Dewar Type Short Tubes Direct Contact Heat Removal Widely Spaced Tubes CPC Mirror Reflector	Mountain Spring Bottle Washing Facility, Canada
Sunmaster (O-I tubes) Dewar Type Long Tubes Direct Contact Heat Removal Widely Spaced Tubes CPC Mirror Reflector	Solar House 1, Colorado State University, United States
Sydney University Dewar Type Short Tubes U-Tube Heat Removal Widely Spaced Tubes Diffuse Reflector	Sydney University Solar Heating & Cooling System, Australia

Chapter 5 describes the systems experiments. Included are the modes of operation and components involved, the ranges and average of the environmental conditions, the time period, the loads experienced, the systems schematics, and a written description for each experiment.

Chapter 6 presents the results of the experiments. Thermal performance is presented in many ways: instantaneous performance by means of efficiency curves, daily performance by means of energy input/output curves, monthly and seasonal performance by means of energy flow diagrams, energy supply and delivery bar charts, energy use bar charts, and system efficiency and solar fraction diagrams. Shipping, reliability, maintainability, and operation experiences are also provided in some detail.

Chapter 7 discusses the results and makes comparisons among the results. Instantaneous effects such as incident angle effects, snow cover, capacitance, performance temperature dependencies and other factors are seen to influence longer term performance in various installations. Daily performance graphics are used to show the performance consequences of the many differences among the collectors, climates, and installations. Among the factors showing up in the daily results are effects of tube size, evacuated collector type, reflectors and spacing, seasonal differences, preheating, capacitance, and snow cover. The differences between evacuated and flat plate collectors can also be easily seen. Monthly and annual performance is also discussed as is system efficiency and solar fraction. Comparisons of shipping, installation, and operation experiences are also given. Specifically, vacuum loss, thermal shock, stagnation, thermal cycling, outgassing, gas permeation, boiling, heat pipe operation, tube replacement, freezing, reflector degradation, hail, and design are covered.

Chapter 8 presents conclusions on thermal performance, shipping, reliability, maintenance, operation, and measurement.

Appendix A presents the detailed objectives, work plan and background of the Task. Appendix B provides the addresses of key Task researchers. Appendix C gives the meanings and structure of most of the nomenclature used in the report, Appendix D acknowledges the primary contributors to this report, and Appendix E provides supplemental installation results.

2. INSTALLATION DESCRIPTIONS

The Task VI installations comprise a wide range of evacuated collector applications. As of January 1984 there were two district heating systems in Sweden, a district heating system in Switzerland, a solar heated and cooled single family residence in the United States, a solar heated and cooled laboratory in Italy, a solar heated single family residence in the Netherlands, a solar heated multi-family residence emphasizing solar DHW production in West Germany, an industrial process heat application in Canada, an industrial process heat application in Switzerland, a domestic space heating system with simulated load in the United Kingdom, and a solar heating and cooling system for university offices in Australia.

Figures 2-1 through 2-11 are photographs of the installations. General installation descriptions are given in Table 2-1. Table 2-2 describes the installations' loads, and Table 2-3 outlines the current activities of the installations.

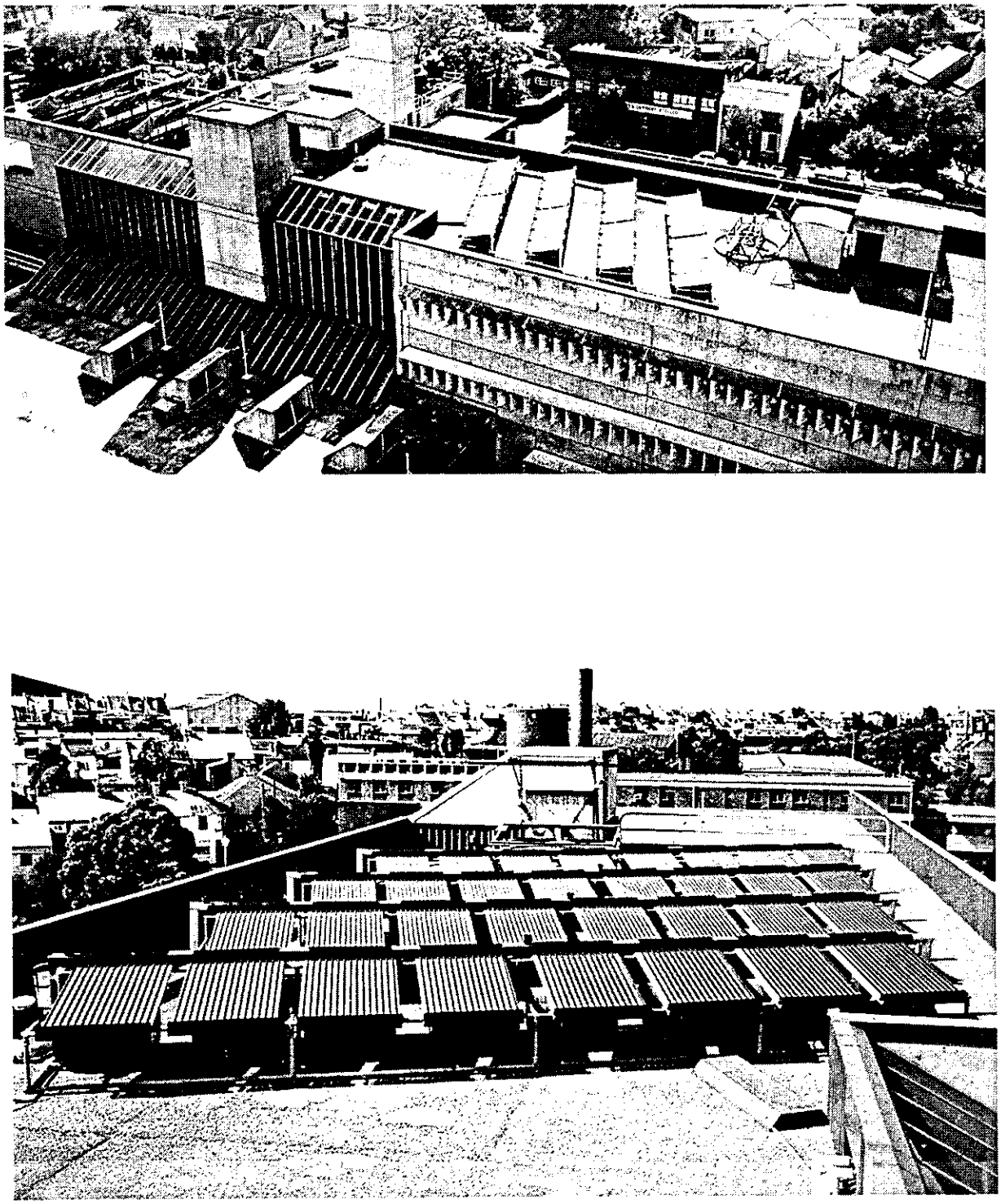

Figure 2-1. Sydney University Solar Heating and Cooling System Sydney, Australia.

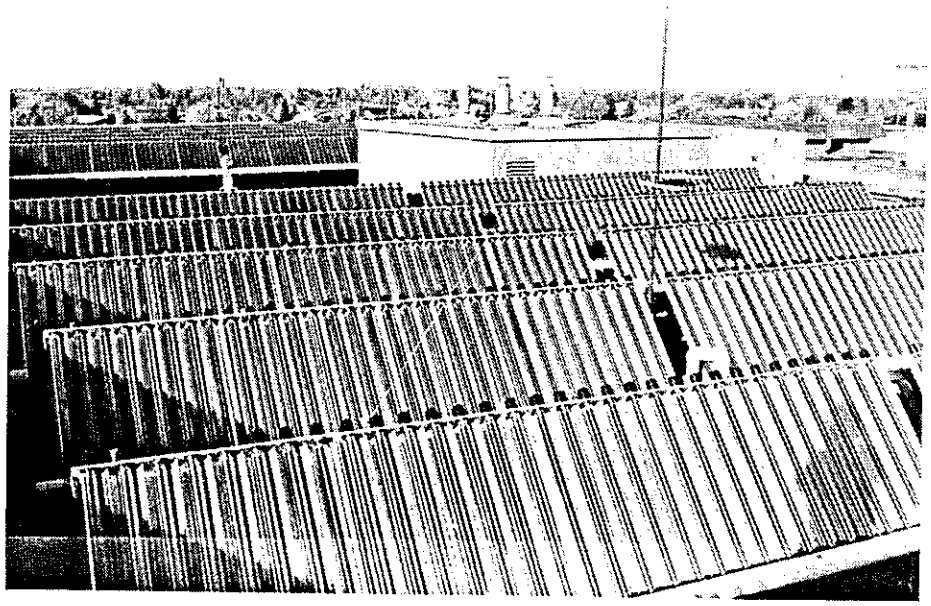

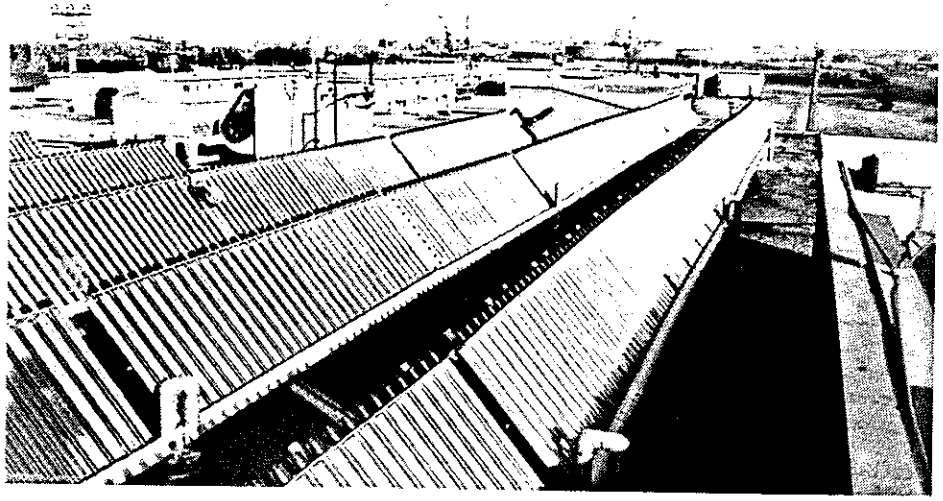

Figure 2-2. Mountain Spring Bottle Washing Facility Edmonton, Alberta, Canada.

Figure 2-3. Ispra Solar Heated and Cooled Laboratory Commission of European Communities.

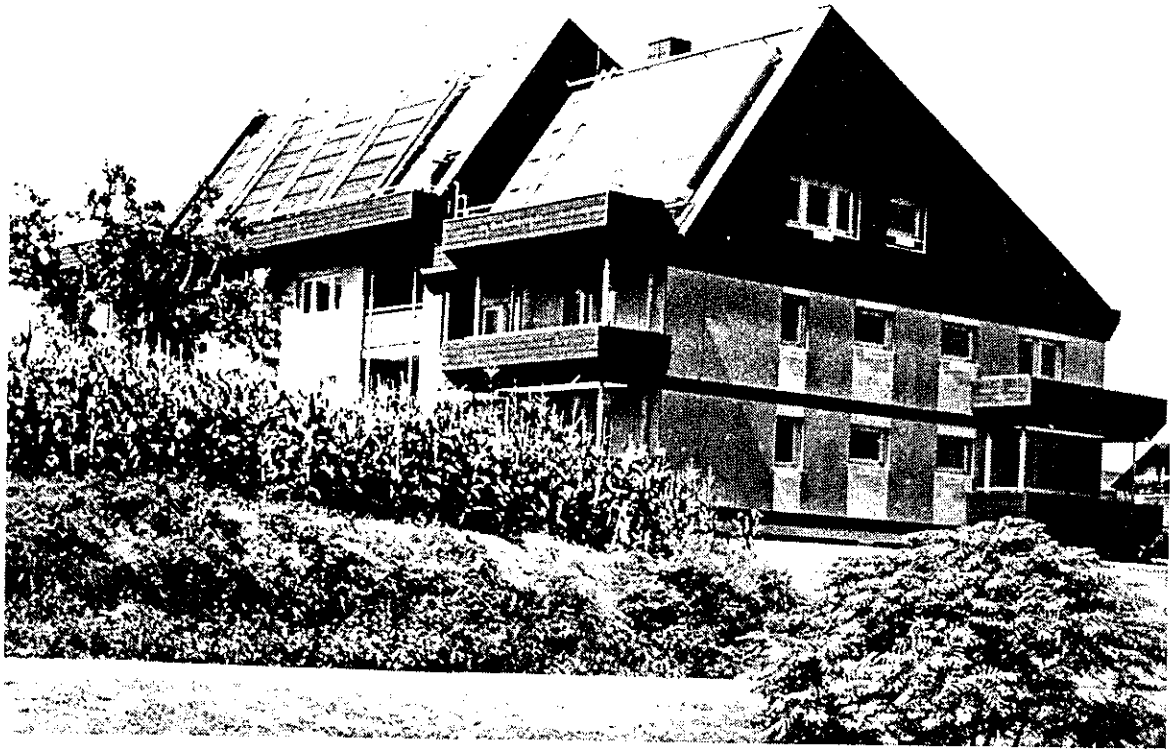

Figure 2-4. Solarhaus Freiburg, Federal Republic of Germany.

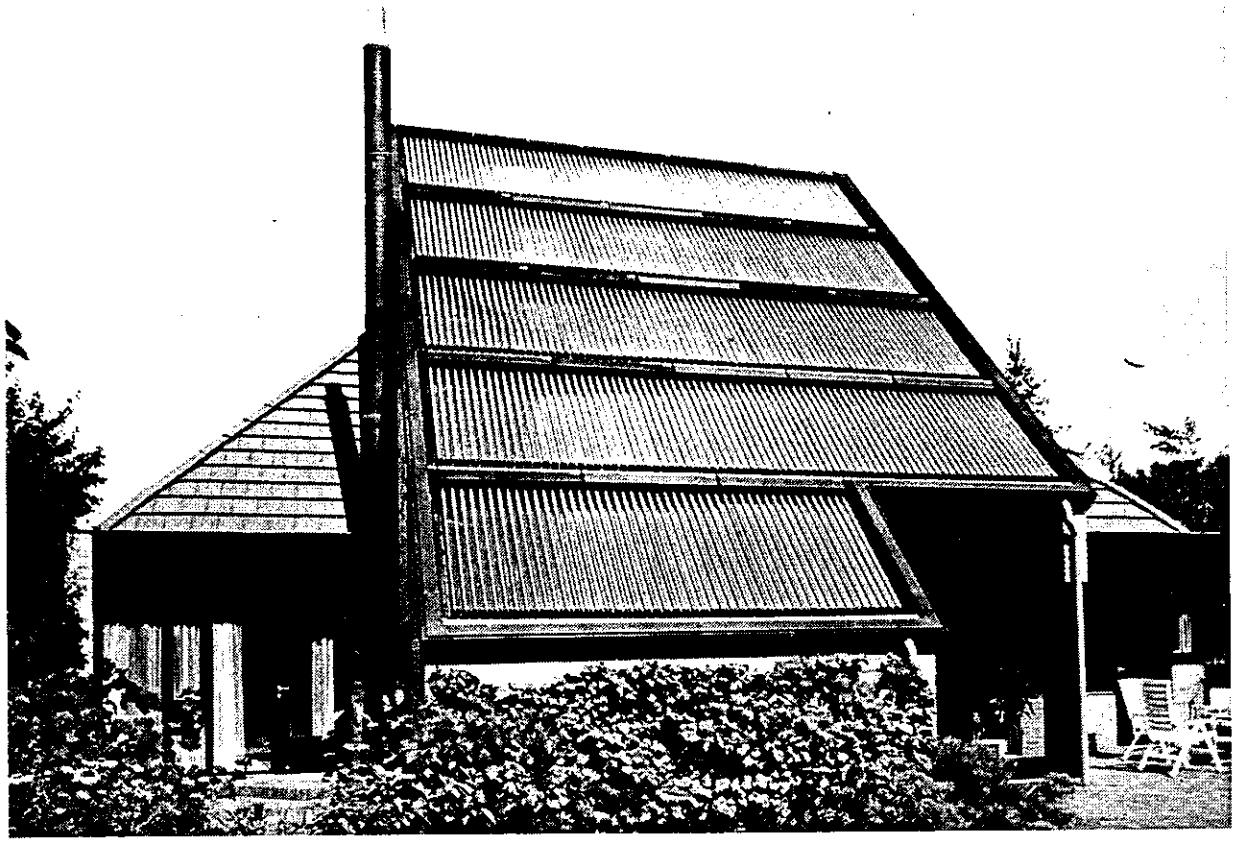

Figure 2-5. Eindhoven Technological University Solar House, Eindhoven, Netherlands.

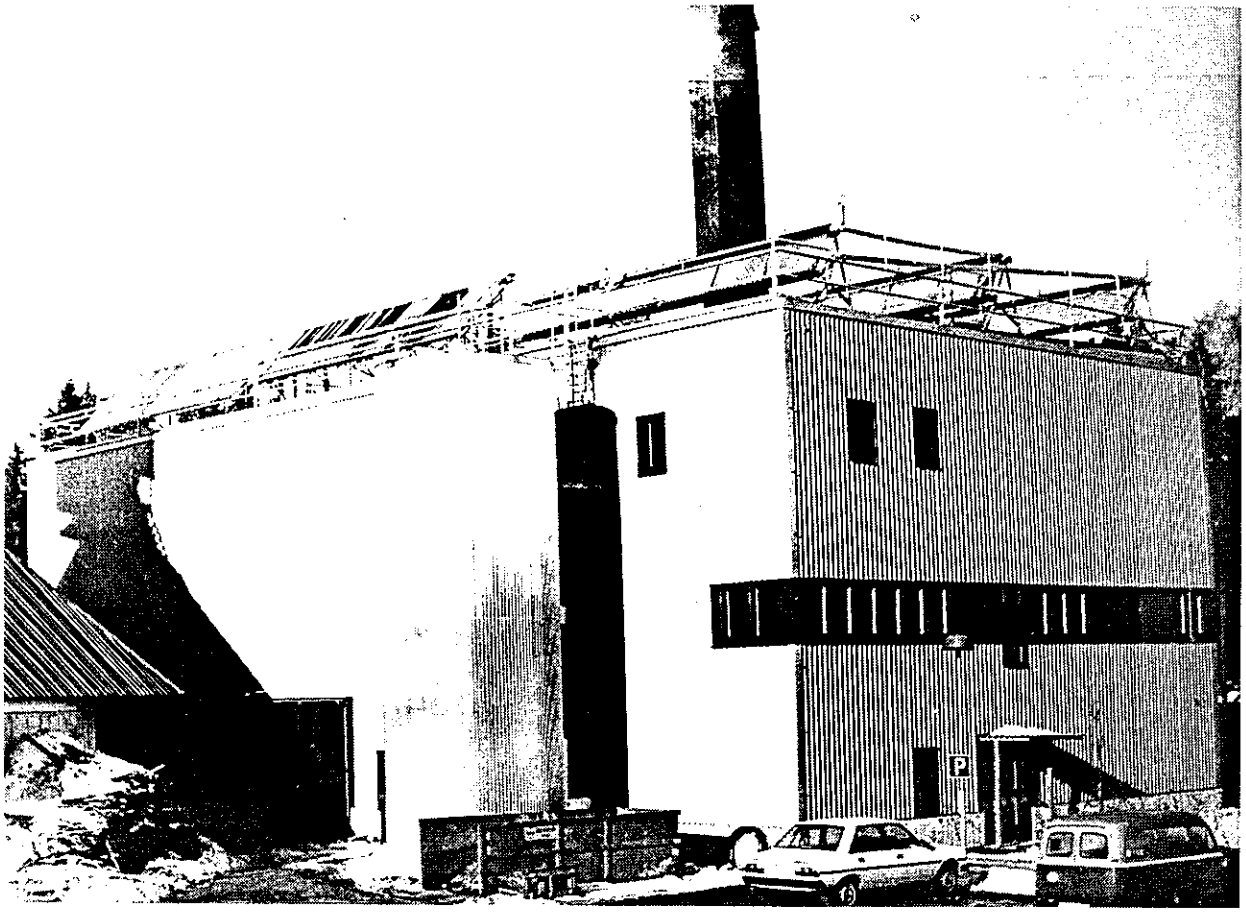

Figure 2-6. Knivsta District Heating Project, Knivsta, Sweden.

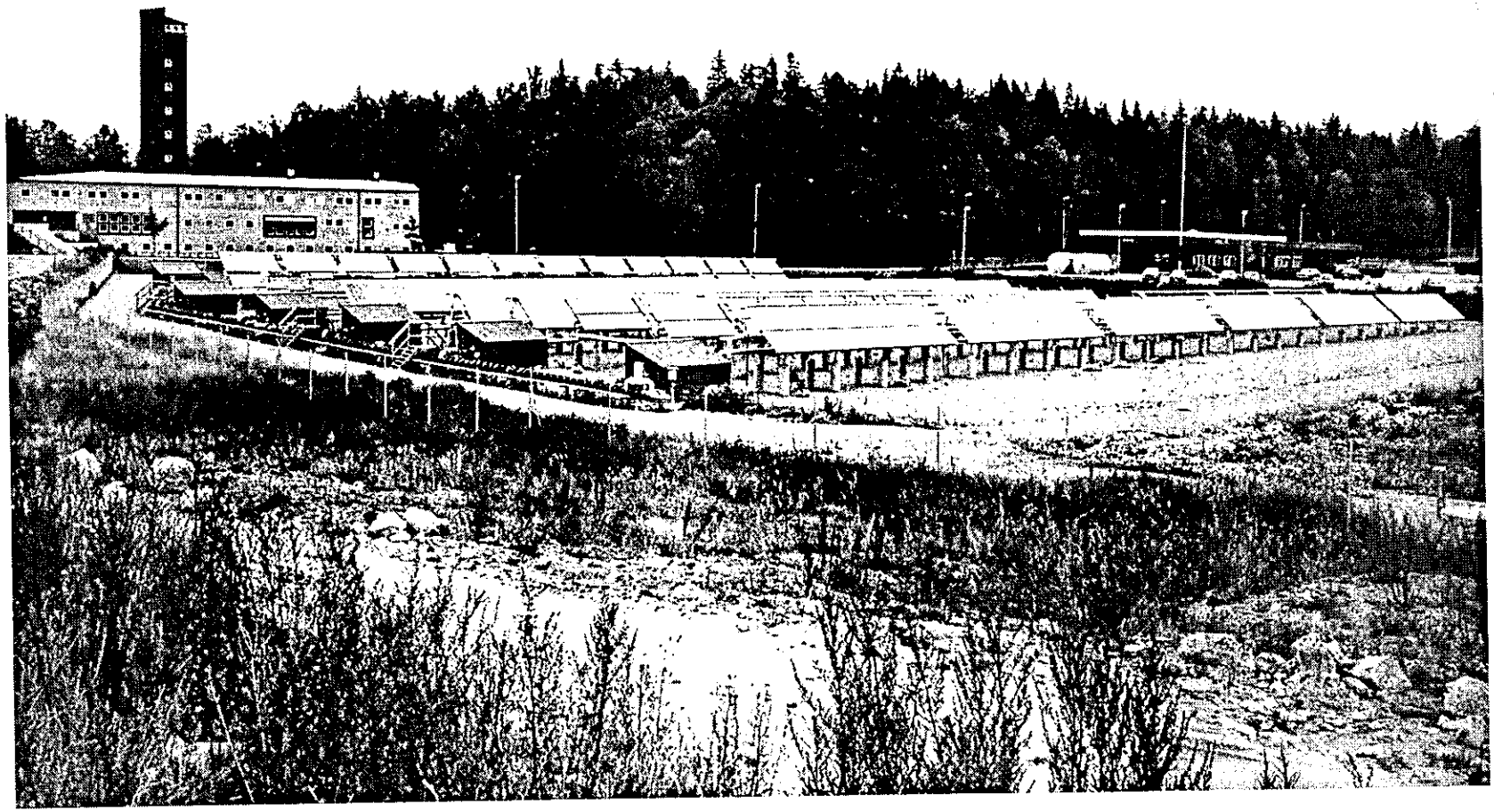

Figure 2-7. Södertörn District Heating Project, Södertörn, Sweden.

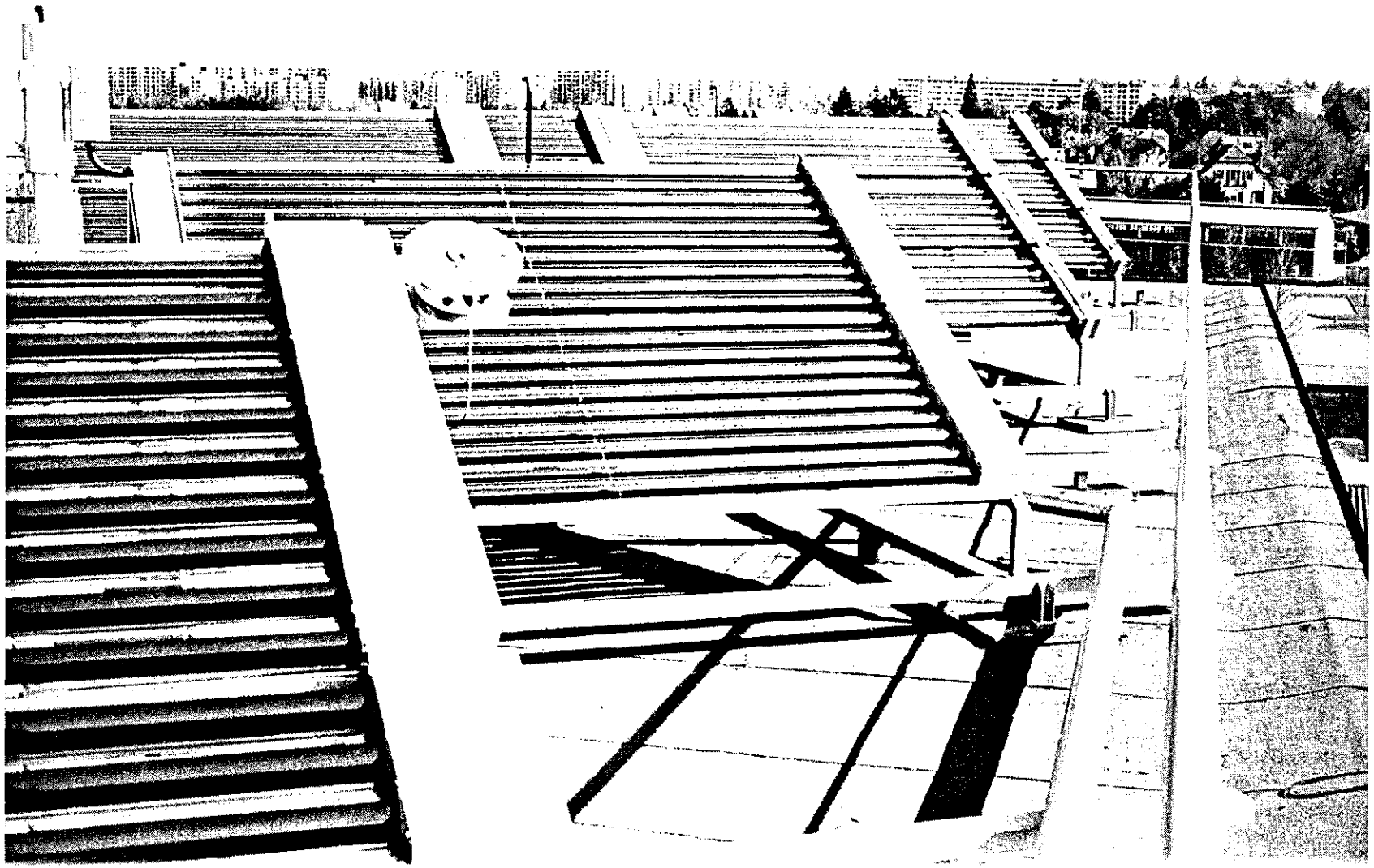

Figure 2-8. Solarcad District Heating Project, Geneva, Switzerland.

Figure 2-9. SOLARIN Project, Hallau, Switzerland.

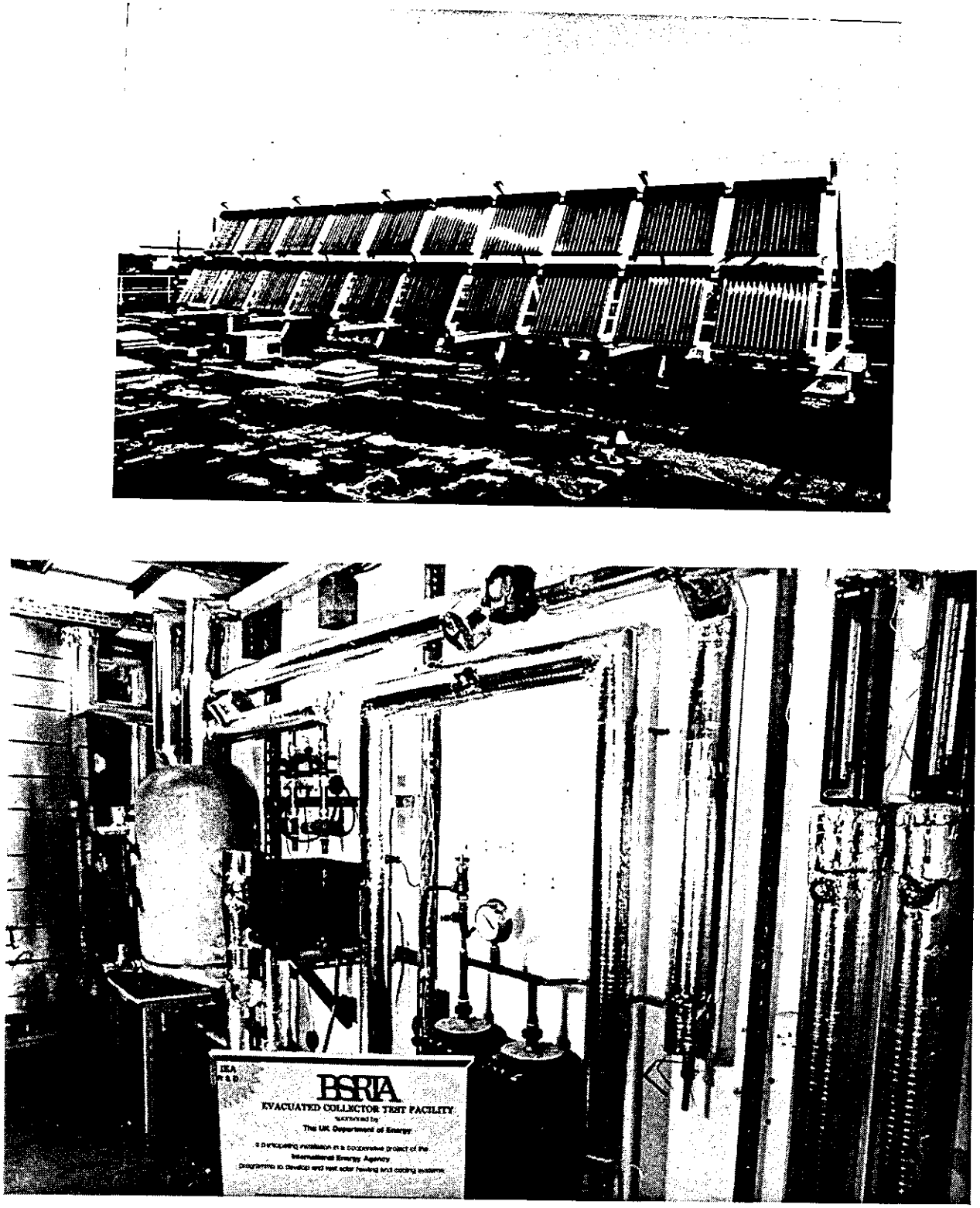

Figure 2-10. Evacuated Collector System Test Facility Bracknell, United Kingdom.

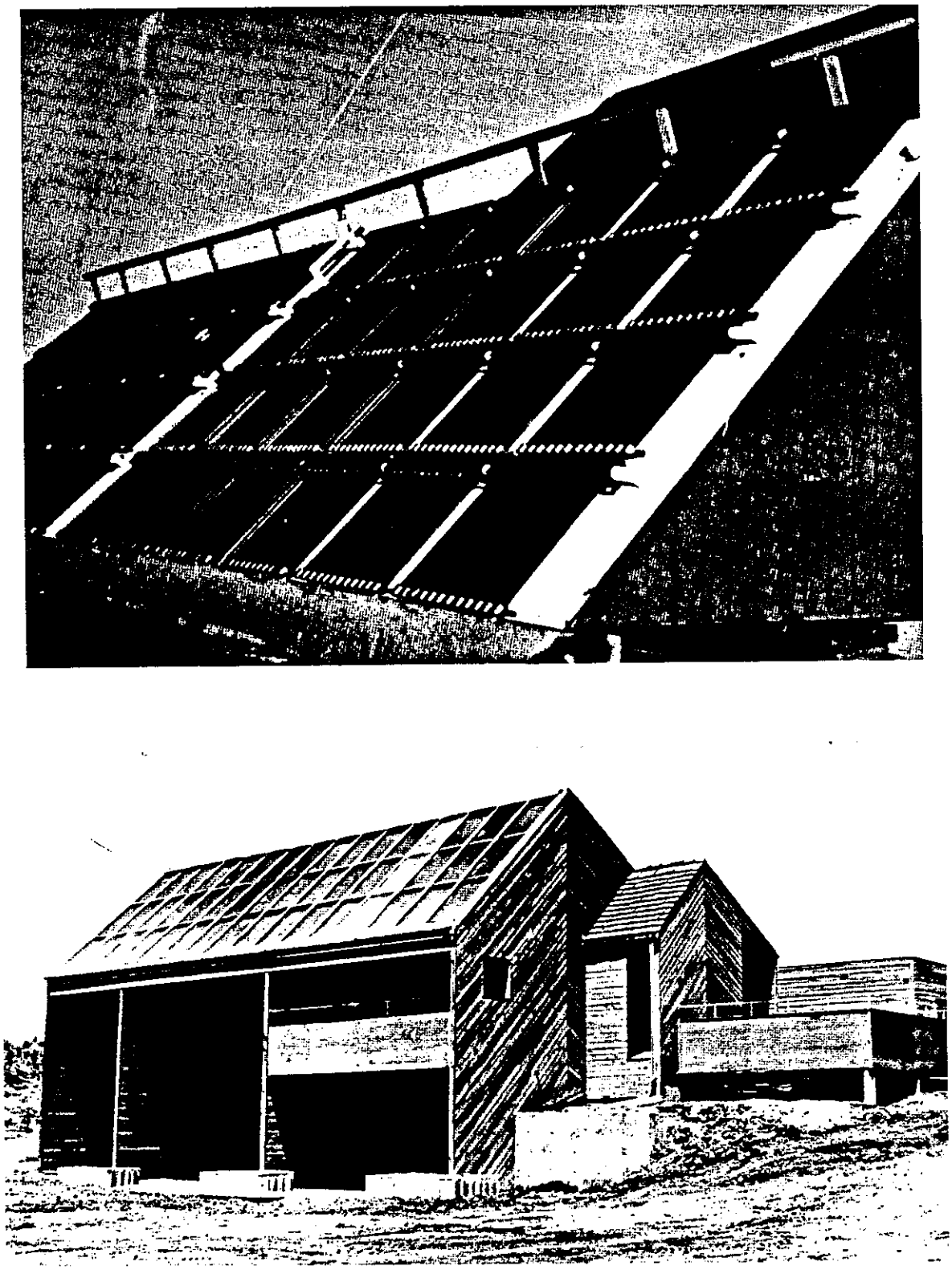

Figure 2-11. Colorado State University Solar House I Fort Collins, Colorado USA.

Table 2-1. Installation Descriptions

Sydney University Solar Heating and Cooling System, Department of Mechanical Engineering, University of Sydney Sydney, AUSTRALIA	Four offices located on the top floor of the Mechanical Engineering Building are cooled in summer using a heat driven absorption cooling cycle. Solar energy also used for space heating in winter. The total floor area of the air-conditioned space is 52 m^2.
Mountain Spring Bottle Washing Facility Edmonton, Alberta CANADA	The solar system, installed in a bottling plant, was designed to assist in maintaining the temperature of a caustic soda solution used for the washing of reusable empty soft drink bottles.
Ispra Solar Heated and Cooled Laboratory CEC	The Solar Laboratory was built for the study of active solar heating and cooling systems. It is a small office building with a floor area of 160 m^2. The solar cooling system is used for air-conditioning the building during the summer months. The heating is done with a separate solar heating system.
Solarhaus Freiburg FEDERAL REPUBLIC OF GERMANY	The solar house has a conditioned living area of 652 m^2. The three-story apartment building has approximately 25 permanent occupants in the 12 apartments. Solar energy is used for space heating and hot water.
Eindhoven Technological University Solar House THE NETHERLANDS	The solar house at the Eindhoven University of Technology, a rather spacious detached house, is situated in the outskirts of Eindhoven, some 4 km NNE of the city centre.
Knivsta District Heating Project Knivsta, SWEDEN	Knivsta is situated 45 kilometers north of Stockholm, Sweden, and 20 kilometers south of Uppsala. About 60 percent of the buildings are connected to a local heating network fed from a biomass-fired plant. The landscape in the area is rather flat, consisting mainly of open fields and some small areas of forest.
Sodertorn District Heating Project Sodertorn, SWEDEN	The Sodertorn plant is situated 20 km south of Stockholm. Seven different solar collector systems are connected directly to the local district heating system and can be compared under the same operating conditions.
SOLARCAD District Heating Geneva, SWITZERLAND	Two solar systems are connected directly, without intermediate storage, to the district heating network. The minimum heat demand is always much higher than the heat produced by solar. The district heating network supplies space heating and domestic hot water to surrounding buildings.
SOLARIN Industry Project Hallau, SWITZERLAND	Nearly 400 m^2 total area of evacuated collectors are installed on the roof of a food processing factory. They contribute to space heating and process heat. Hot water is stored in 2 tanks (10 m^3 and 23 m^3). Existing conventional burners provide auxiliary heating.
BSRIA Solar Test Facility with Simulated Loads Bracknell, UNITED KINGDOM	The solar domestic space and hot water heating system is installed at the laboratories of the Building Services Research and Information Association. The installation is a complete solar system including storages, but the loads are imposed by a subsystem which simulates the space heating and hot water requirements of a single family dwelling.
Colorado State University Solar House I Fort Collins, Colorado USA	Solar House I, completed in 1974, is a wood-frame, two story, three bedroom residential building utilized for offices. The conditioned living area is 249 m^2. Solar energy is used for space heating and space cooling.

Table 2-2. Description of Loads

Sydney University Solar Heating and Cooling System, Department of Mechanical Engineering, University of Sydney Sydney, AUSTRALIA	The cooling/heating system attempts to maintain office room temperatures between 21 and 25 C. As the four air-conditioned offices are located on top of a large 5 story building which is generally not air-conditioned, the load is relatively high and remains fairly constant compared to the size of the offices. Daily loads fluctuate between 120 to 150 MJ/day. During summer, the constant daily loads are significantly increased by solar gains through a large glass area along the western side of the building.
Mountain Spring Bottle Washing Facility Edmonton, Alberta CANADA	The load is composed of two components. Firstly, sensible heat required to heat the bottles for washing and sterilization purposes. Secondly, heat is required to overcome parasitic losses from the washing unit. The temperature of the caustic soda solution used for washing and sterilization is maintained between 72 C and 82 C by a gas-fired heater. The actual gas consumption from 1 May 1982 to 31 December 1983 for the washing process was 4055 GJ. The load for the same period was 2420 GJ. The gas consumption from 1 January 1984 to 31 December 1984 was 1685 GJ and the load was 1239 GJ.
Ispra Solar Heated and Cooled Laboratory CEC	During wintertime the indoor temperature is kept at 20 C. This requires about 240 MJ/day for 160 days. There is no DHW load in the building. The cooling season includes about 130 days with an average load of about 80 MJ/day. In the cooling season the room temperature is regulated as a function of outdoor temperature.
Solarhaus Freiburg FEDERAL REPUBLIC OF GERMANY	The indoor winter design conditions vary with each individual apartment, thus only the actual average daily heating loads are known. They ranged from 1341 MJ/day in 1980 to 1213 MJ/day in 1981. The average daily heating load has been reduced to 960 MJ/day (based on 214 days of heating period) due to a reduction of the ventilation rate to approximately 0.5 air cycles per hour. There is no summer cooling. The average daily energy consumption for the warm water supply was consistant with previous years (185 to 190 MJ/day), corresponding to daily hot water use of 1300 liters. Special energy saving designs include improved thermal insulation; triple-glazed windows, a better ventilation system and micro-computer control of the system.
Eindhoven Technological University Solar House THE NETHERLANDS	The load consists of the domestic hot water system (13 GJ/year) and the heating system of the house (83 GJ/year). The heated floor area amounts to 220 m^2, the volume is 810 m^3. The area of double glazed windows is 40 m^2 (theoretical heat transmission coefficient 3.2 W/m^2K). The total outside area is about 313 m^2 including the roof area. Both roof and walls have a theoretical heat transmission coefficient of 0.4 W/m^2 K. Ventilation and infiltration amounts to about 800 m^3/hr.
Knivsta District Heating Project Knivsta, SWEDEN	Three different types of evacuated solar collectors have been mounted on the roof of the district heating plant in Knivsta. The district heat load is always much larger than the energy production from the collectors, so the heat from the collectors is transferred to the return pipe of the district heating systems. There is no storage. The district heating plant is fired with biomass and the heating system has a peak demand of 15 MW.
Sodertorn District Heating Project Sodertorn, SWEDEN	The district heating load is always much larger than the energy production from the collectors so all the collector input can be used. The collectors are normally connected to the return pipe of the network where temperature levels around 50-60 C can be used most of the year.

Table 2-2 (cont). Description of Loads

SOLARCAD District Heating Project Geneva, SWITZERLAND	Three different networks jointly deliver heat to surrounding buildings for space heating and domestic hot water purposes. Separate loads cannot be identified. The test systems are connected to the return branch of one particular network (called Libellules). The load of this branch is characterized by the following: power capacity of the installed gas- fired furnace, 16 MW; delivered power ranging from 0.1 to 6 MWh/h; average daily load for the heating season 120 GJ/day; average daily load in summer (DHW only), 21 GJ/day. The solar systems usually operate above 80 C. The total district heating system (3 networks) is typically 15 times greater than the figures given.
SOLARIN Industry Project Hallau, SWITZERLAND	Hot water is needed for industrial processing and space heating. In the former case (i.e., pasteurization, bottle and case washing) the load is 2900 GJ/year ranging between 35 and 430 GJ/month with a peak demand in autumn; the required temperature is between 90 and 110 C. In the latter case and for the heating season, the load amounts to 640 GJ with a peak demand of 130 GJ/month; the temperature never exceeds 70 C. The total monthly load varies between 120 and 560 GJ/month, with a yearly average value of 290 GJ/month. The heat produced by solar is used for to industrial processing in summer, and space heating in winter. The load is divided into different and complicated loops for processing and heating, and thus is considered as a whole. It is possible to direct solar gains to low temperature uses.
BSRIA Solar Test Facility with Simulated Loads Bracknell, UNITED KINDGOM	The load on the solar system is imposed by a physical load simulator controlled by a computer, which calculates the required load from measured prevailing weather parameters every five minutes. The simulated house is maintained at 20 C provided the outside air temperature is less than 18 C. The house temperature may freely evolve above 18 C to a maximum of 25 C. The space heating load averages 146 MJ/day during the heating season with an annual total of 37 GJ. The domestic hot water load is 90 litres/day at 55 C distributed intermittently over 16 hours.
Colorado State University Solar House I Fort Collins, Colorado USA	The indoor winter design temperature of 21 C produces an average daily load ranging from 235 MJ/day to 305 MJ/day during the heating season. The summer indoor design temperature of 24 C produces an average daily load of about 445 MJ/day. Special energy saving features include a wall heat loss coefficient of 0.51 $W/m^2 \cdot C$ and ceiling heat loss coefficient of 0.30 W/m^2 C, triple-glazed windows and reduced infiltration by use of a vestibule entry. The calculated heat loss coefficient of the building is 390 W/C.

Table 2-3. Current Activities

Sydney University Solar Heating and Cooling System, Department of Mechanical Engineering, University of Sydney Sydney, AUSTRALIA	The current working programme includes the evaluation of a prototype evacuated collector using Sydney University's evacuated tubes and a "liquid-in-metal" type manifold. Long-term performance and durability in a heating/cooling application is of particular interest. The installation allows performance comparison between evacuated and flat plate collectors in the same system application. Investigations on the overall solar heating/cooling system performance are an on-going project task as well as identification of problems and limitations and methods for improvements. A new prototype ammonia/water absorption cycle incorporating a novel printed circuit heat exchanger design is being evaluated. Application and development of new computer simulation models and experimental validation is about to start.
Mountain Spring Bottle Washing Facility Edmonton, Alberta CANADA	During the commissioning process it was found that the system was deficient in several areas. The heat exchanger between the solar system and the caustic loop was found to have an operational effectiveness of 0.24. This low effectiveness was attributed to a low fluid flow rate on the caustic side and the determination that the heat exchanger was thermodynamically under-sized. The inability to transfer the required heat flux resulted in higher storage tank temperatures which often led to premature solar system shut down due to over-temperature of the storage tank. This problem has been remedied by the installation of a plate-type heat exchanger and a new pump in the caustic loop. The initial effectiveness of the plate-type heat exchanger was 0.65 to 0.7. However, due to fouling of the caustic side of the heat exchanger, the effectiveness is presently 0.54. Since November 1982, a number of changes have been made to the system. These include: 1. Replacement of the controller to improve heat transfer across the exchanger. The controller presently operates at 2.5 C on differential and 1.5 C off differential. 2. A timer was installed to control the time at which the gas-fired heater was activated. This minimized waste of auxiliary energy by stopping heater use under no load condition, i.e., weekends and nighttime. In October 1984, the southeast collector array composed of 16 Solartech ETC modules employing tubes four feet long was replaced by 12 new Solartech ETC modules employing tubes six feet long. As a result of these modifications, the performance of the systemis being monitored and analyzed in a continuous fashion. System analysis and simulation activities are continuing. It is expected that active monitoring of the system will be discontinued May 15, 1985.
Ispra Solar Heated and Cooled Laboratory CEC	The system will be operated during the summer of 1984 in the same way as it operated in 1983. Some improvements concerning the insulation of the storage systems will be made. The variations in collector performance compared to previous years will be studied in further detail. This will be done through monitoring, detailed analysis of data and scanning with infrared thermovision equipment. The replacement of the Sanyo collectors is foreseen for 1985. Modelling activities include detailed TRNSYS simulations of combined solar heating and cooling systems for Mediterranean climates and work on simplified models using a daily time step.

Table 2-3 (cont). Current Activities

Solarhaus Freiburg FEDERAL REPUBLIC OF GERMANY	After termination of the SOLARHAUS FREIBURG project, research activities on systems with evacuated collectors will include both experimental and theoretical investigations. Several kinds of simulation techniques are used to investigate the performance of these systems in fields ranging from domestic hot water (DHW) to industrial process heat (IPH) systems. The models used have been carefully validated with SOLARHAUS FREIBURG data. Complex models (with up to 90 temperature nodes) will be used to numerically investigate the range of confidence of simplified models, using the Input/Output relationship of the collector systems. In the area of DHW applications, simplified systems with thermosyphon circulation are being tested experimentally. System tests of Industrial Process Heat Applications with various types of ETC collectors with simulated load conditions are planned within the DFVLR laboratories at Stuttgart.
Eindhoven Technological University Solar House THE NETHERLANDS	The Solar House of the Eindhoven University of Technology has had flat plate collectors from 1976 to 1981, and evacuated tube collectors since 1981. Because of this it is possible to compare a flat-plate solar heating system with a second generation solar heating system using evacuated tube collectors under similar conditions. By extensive monitoring of the solar heating system the control strategy will be improved and simplified, step by step. System components such as the integrated auxiliary burner, the floating inlet and the swing arm, acting as feed line for the air heater, are tested under real conditions.
Knivsta District Heating Project Knivsta, SWEDEN and Sodertorn District Heating Project Sodertorn, SWEDEN	Present plans call for a national reduction in the dependence upon oil to 20 percent in 1985, and lower in the 1990's. This is to be accomplished through increased energy recovery from the incineration of garbage, use of biomass and heat pumps, instead of oil. Solar energy will give a rather insignificant contribution by 1985 but is expected to contribute approximately 10 percent in 1990 and 20 to 30 percent at a later stage. In Sweden solar energy can supply up to 10 percent of the demand for heating and domestic hot water by feeding directly into a district heating network. In order to reach a higher percentage, seasonal storage must be applied.
SOLARCAD District in operation since May 1982. Heating Project Geneva, SWITZERLAND	Corning collectors have been in operation since May 1982. Relevant data from precise measurements are available from July 1982. Sanyo collectors were mounted in 1980; they were equipped with accurate sensors in 1983 and relevant data are available from April 1983. Data is transmitted by phone line from site to the laboratory. Data have been carefully analyzed on the behaviour and the performances of the solar systems. Detailed studies on the Corning collector have been carried out, including determination of efficiency curves, stagnation temperature, and absorber emissivity. Working in conjunction with the manufacturer, improvements have been achieved. Thermal losses through insulation due to capacity effects are under investigation. The losses play an important role especially when dealing with high temperatures. Studies are continuing in all areas to improve simulation and modelling.
SOLARIN Industry Project Hallau, SWITZERLAND	The solar energy system has been in operation since July 1983. The initial, unimproved control system should be replaced by a microprocessor based controller by the end of 1983. All measuring equipment has been built, calibrated and installed. The 50 sensors are connected to a microprocessor data acquisition system, which can be controlled and read the University of Geneva (300 km away) by phone line. The analysis is carried out at the University.

Table 2-3 (cont). Current Activities

	Measurements and control are independent. Status signals from the controllers to the data acquisition system have not been incorporated yet so that some measured energy flows cannot be identified properly. This problem should be solved by the end of 1983. Nevertheless the measurement and data acquisition system has been debugged and preliminary figures on performance obtained. Good reliable results should become available starting in January 1984. Data handling and analysis programs are ready, but modifications and adaptations will probably still need to be made.
BSRIA Solar Test Facility with Simulated Loads Bracknell, UNITED KINGDOM	Dismantling of the system will follow withdrawal from task membership.
Colorado State University Solar House I Fort Collins, Colorado USA	During the summer of 1983, the Solar House I system was modified to include a 3600-litre high-temperature (120 C) phase-change storage unit and 590 kg of low-temperature (12.6 C) salt storage for the chiller. These storage units were integrated into a system comprised of Philips VTR 361 evacuated tube heat pipe collectors and a Carrier air-cooled absorption chiller. During May 1983 the original reflectors for the VTR 361 collectors, which were known to be malformed, were replaced with properly shaped reflectors. Since the high-temperature storage failed after only a few days of operation, the unit was taken out of service. The system will be operated as an indirect heating system for the winter using an ethylene-glycol solution as the heat transport medium.

3. CLIMATE

Long term average climate information for each Task location is given in Table 3-1. Climate varies substantially among installations. Elevations vary from sea level to almost 1600 meters. Heating loads vary from about 620 K-days to about 5200 K-days. Daily horizontal insolation for a mid-winter month varies from about 1.3 MJ/m^2 to about 10.7 MJ/m^2 and for a mid-summer month, from about 15.8 MJ/m^2 to about 23.3 MJ/m^2. Diffuse radiation varies from 30 percent to 79 percent. Average daily temperatures vary from -15°C to +22°C.

Table 3-1. Climate at the Task VI Locations

LOCATION	LATITUDE (degrees)	LONGITUDE (degrees)	ELEVATION (m)	HEAT DEGREE DAYS	HEATING MONTHS	COOLING MONTHS	AVERAGE WET BULB TEMP	AVERAGE RELATIVE HUMIDITY %	JANUARY DAILY INSOL. (Horizontal MJ/m²)	JULY DAILY INSOL. (Horizontal MJ/m²)	JANUARY DIFFUSE %	JULY DIFFUSE %	JANUARY AVG. DAILY TEMP (C)	JULY AVG. DAILY TEMP (C)	JANUARY AVG. MAX. DAILY TEMP (C)	JULY AVG. MAX. DAILY TEMP (C)	JANUARY AVG. MIN. DAILY TEMP (C)	JULY AVG. MIN. DAILY TEMP (C)	CLIMATE DESCRIPTION
AUSTRALIA	34 S	151 E	20	619	May-Sept	Oct-April	19.2	66	22.4	10.7	30	43	21.9	11.7	25.7	15.9	18.4	7.8	Temperate, hot/humid in February and March; mild and dry winters
CANADA	54 N	113 W	676	5201	NA	NA	NA	67	3.7	22.6	62	37	-15.0	17.4	-10.7	23.0	-19.2	11.8	Continental climate with dry winters, wetter summers
CEC	46	8 E	220	2445	Oct-April	June-Sept	17	72	4.5	21.0	30	40	1.9	21.2	6.4	26.8	-1.5	16.0	Humid mesothermal moderate
FEDERAL REPUBLIC OF GERMANY	48 N	7 E	220	3127	Sept-May	NA	NA	NA	2.6	16.7	71	53	0.7	18.5	12.8	32.8	-10.1	9.2	Mesothermal forest, moist, rainfall all year
NETHERLANDS	57 N	6 E	15	2785	Oct-April	NA	NA	75	2.1	15.8	70	62	1.6	17.1	4.9	22.0	0.3	13.4	Humid mesothermal marine
SWEDEN, N.	60 N	17 E	30	4180	Sept-May	NA	NA	NA	1.3	19.6	45	38	-4.1	16.4	-1.0	21.8	-4.7	14.0	Humid mesothermal marine, cool summers
SWEDEN, S.	60 N	17 E	30	4180	Sept-May	NA	NA	NA	1.3	19.6	45	38	-4.1	16.4	-1.0	21.8	-4.7	14.0	Humid mesothermal marine, cool summers
SWITZERLAND, G.	46 N	7 E	377	2740	Oct-May	NA	NA	NA	3.5	19.5	68	40	1.0	19.0	10.0	24.0	-2.0	13.0	Mesothermal forest, moist, rainfall all year
SWITZERLAND, H.	48 N	8 E	420	3270	Oct-May	NA	NA	NA	3.1	20.8	64	39	-1.7	17.4	8.0	24.0	-6.0	11.0	Mesothermal forest, moist, rainfall all year
UNITED KINGDOM	51 N	1 W	70	2700	Sept-May	NA	NA	NA	2.2	16.9	73	58	3.4	16.5	11.6	28.3	-6.8	6.8	Temperate oceanic
UNITED STATES	41 N	105 W	1585	3666	Oct-May	June-Oct			8.7	23.3	39	38	-3.3	21.9	4.8	29.9	-10.4	13.8	Steppe or semi arid

4. COMPONENTS AND SUBSYSTEMS

Since the focus of Task VI work is on systems using evacuated collectors, the evacuated collector itself is addressed in greater detail in this section than other components and subsystems. Even more information on collector characteristics such as incident angle modifiers, stagnation temperatures, flow rates, etc. and on other components and subsystems such as controls, site features, and energy conserving measures may be found in the Task VI collector and systems characterization report of Guisan et al[3] and in the individual Task VI installation reports[80-134]. These latter reports also contain information on instrumentation, sensor specifications, and calibration procedures.

4.1 COLLECTION

Task VI installations have used nearly every evacuated collector type that has reached commercial development, and many of those collector types are used in more than one installation. See Table 4-1 for collector types used.

A wide range of possibilities for evacuated collector designs, materials, and other characteristics result in many very different types of evacuated collectors. Collector specifications are noted in Table 4-2. Specific details for each application, such as tilt and total collector area, are given later in this section.

4.1.1 Definition of Collector Aperture Area

The task definition of collector aperture area is:

$$A001 = L \times W \times \cos \theta$$

Where L = exposed transparent part along the collector tubes (excluding boxes, black cups, headers, etc)

W = the width of the collector module. This is taken as:

$$W = n \times P$$

Where n = number of tubes, and p is the pitch of the tubes, or the distance between the centers of adjacent tubes.

θ = tilt angle of absorber surface with respect to the collector plane. For most Task VI evacuated collectors θ = 0 degrees and cos θ = 1.

Figure 4-1 illustrates several of these points.

Table 4-1. Evacuated Tube Collector -- Installation Reference

	Corning Corter	General Electric TC-100	Owens-Illinois Sunpak	Philips VTR 141 *	Philips VTR 261 *	Philips VTR 361 *	Philips Mark IV	Sanyo	Sanyo Heat Pipe	Solartech	Sunmaster (9-1 tubes)	Sydney University
Sydney University Solar Heating and Cooling System SYDNEY, AUSTRALIA												●
Mountain Spring Bottle Washing Facility CANADA										●		
Ispra Solar Heated and Cooled Laboratory CEC					●	●		●				
Solarhaus Freiburg FEDERAL REPUBLIC OF GERMANY	●				●		○					
Osaka Sanyo Solar House JAPAN		○						○	○			
Eindhoven Technological University Solar House THE NETHERLANDS					●							
Knivsta District Heating Project KNIVSTA, SWEDEN		●	●	●								
Sodertorn District Heating Project SODERTORN, SWEDEN		●		●								
SOLARCAD District Heating Project SWITZERLAND	●							●				
SOLAHIN Industry Project SWITZERLAND	●											
Evacuated Collector System Test Facility, UNITED KINGDOM				●								
Colorado State University Solar House I USA	○			○		●	○				●	

KEY:
● used during reporting period ○ previously used

* the numerical nature of the Philips collectors refers to tube type, not collector construction

Table 4-2. Specifications for Collectors Used In Task VI

ETC TYPE	# TUBES PER MODULE / PITCH	$F'\tau\alpha$ (7)(9)	$F'U_L$ (7)	APERTURE AREA PER MODULE	ABSORBER AREA PER MODULE	ABSORBER SURFACE MATERIAL	HEAT PIPE FLUID	LOCATION	FLUID VOLUME l/m^2	GLASS MATERIAL	REFLECTOR/ SHAPE/MATERIAL
Corning Cortec "A" French	6/113	0.71	1.38	1.45	1.12	Black Chrome front/back of absorber	NA	Switzerland	0.58	Pyrex	None
Corning Cortec "A" US	6/113	0.71	1.38	1.39	1.12	Black Chrome	NA	FRG	0.58	Pyrex	None
Corning Cortec "B" French	6/113	0.71	1.38	1.45	1.12	Black Chrome front/back of absorber	NA	Switzerland	0.58	Pyrex	None
Corning Cortec "D" French	6/113	0.85	1.30	1.45	1.12	Black Chrome front/back of absorber	NA	Switzerland	0.80	Pyrex	None
Geleral Electric TC-100	8/145	0.58	2.10	1.62(3)	1.38	GE Proprietary coating	NA	Japan, Sweden	1.20	Soda lime glass	Compound parabolic/ aluminum
Granges Al Sunstrip 80 FP	NA	0.79	3.50	NA	NA		NA	S. Sweden	0.00		NA
Miromit (FP) Model 210	NA	0.77	4.32	1.84	1.67	Black Nickel	NA	USA	2.22	White Water. 1 glass	None
Owens Illinois Sunpak	24/102	0.70	1.25	2.55(3)	2.55	O-I proprietary	NA	Sweden	11.50	Borosilicate glass	Compound parabolic/ aluminum
Philips Mark IV	108/65	0.71(8)	2.18(8)	7.37(4)	6.77	Cobalt sulphide oxide	NA	US, FRG	1.53	Soda lime glass	None
Philips VTR-141 (12 tube)	12/95	0.61*	1.80	1.15	0.67	Cobalt sulphide oxide	Isobutane	US	0.15	Soda lime glass	Diffuse
Philips VTR-141 (15 tube)	15/75	0.67(5)	2.21(5)	1.11	0.83	Cobalt black	Isobutane	UK	0.17	Soda lime glass	Flat/diffuse white
Philips VTR-141 (19 tube)	19/75	0.62	1.68	1.37	1.05	Cobalt sulphide oxide	Isobutane	Sweden	0.58	Soda lime glass	None
Philips VTR-261	16/82	0.65*	1.70	2.05	1.45	Cobalt sulphide oxide	Neopentane	Netherlands	0.13	Soda lime glass	Flat/tedlar coated aluminum
Philips VTR-261	12/104	0.68(8)	1.24(8)	1.95	1.09	Cobalt sulphide oxide	Neopentane	FRG	0.22	Soda lime glass	Ripple/aluminum
Philips VTR-261	19/75	0.66	1.70	2.22	1.72	Cobalt sulphide oxide	Neopentane	CEC	0.22	Soda lime glass	Aluminum flat
Philips VTR-361	14/104	0.67	1.30	2.27	1.27	Cobalt sulphide oxide	Water	USA,CEC	0.20	Soda lime glass	Ripple/aluminum
Sanyo	7/124	0.87(6)	3.50(6)	1.47	1.13	Chrome black	NA	Japan	0.00	Soda lime glass	Flat diffuse
Sanyo STC-U250	10/93	0.91(6)	3.00	2.42	1.75	Nickel base	NA	CEC	0.95	Soda lime glass	Flat diffuse
Scandinavian Solar (FP)	NA	0.71	3.40	12.00	NA	Selective	NA	S. Sweden	0.80	Toughened glass	NA
Solartech	8/152	.416(8)	1.01(8)	1.30	1.15	Copper chromium oxide	NA	Canada	6.92	Borosilicate glass	CPC/mylar coated aluminum
Sunmaster TRS81	8/152	0.63	1.08	2.14	1.89	Proprietary coating	NA	(5)	8.80	Borosilicate glass	CPC
Sydney University	15/60	0.58	1.74	1.25	1.97	Sputtered copper/metal carbide	NA	Australia	0.78	Borosilicate glass	Flat/diffuse white
Teknoterm FP (ETC cover)	NA	0.70	4.20				NA	S. Sweden	0.80	Soda lime glass	NA
Yazaki (FP)	NA	0.86	5.73	1.91	NA	Proprietary coating	NA	Australia	1.31	Soda lime glass	NA

* Calculated from solar simulator tests with 45 percent diffuse.
(1) Values are for one module based on aperture area and manufacturer information.
(2) Aperture area is based on the standard Task VI aperture area definition accepted at the May 1982 Geneva Meeting unless otherwise noted.
(3) Aperture area equals length of reflector area times width of reflector.
(4) Aperture area equals sum of the area of four front cover panes.
(5) Based on absorber area.
(6) Under consideration for several installations.
(7) These parameters are given for a collector fluid to ambient temperature differences of approximately 45°C.
(8) Based on array (including header, piping).
(9) The values which can be based on data or calculations, should not be compared.

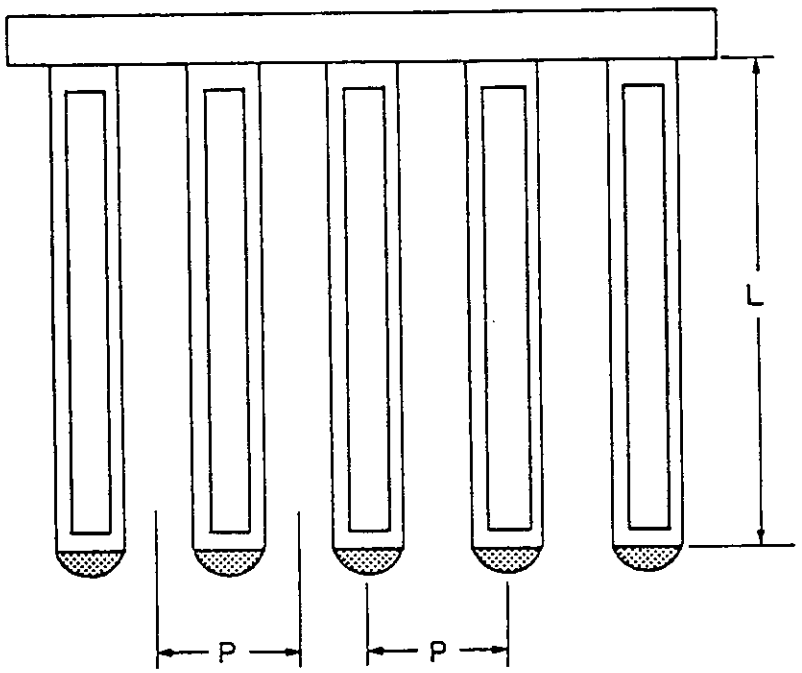

Area AOOI = $W \times L \cos \phi$

W = nP

n = 5 Tubes

ϕ = 0 (for horizontal planar absorbers)

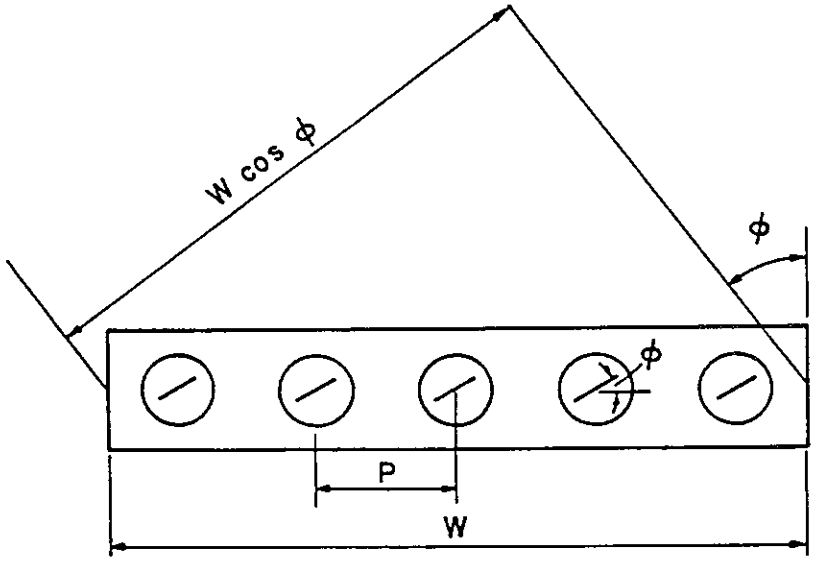

Figure 4-1. Aperture Dimensions

4.1.2 Aperture Areas Used by Each Installation

The aperture areas of each installation have been calculated using the definitions given in section 4.1.1. This definition was modified for subsequent Task work by replacing cos θ by 1 and incorporating the consequences of non-planer absorbers into the incidence angle modifier. See Guisan et al.[3, 47, 67].

4.1.3 Incident Angle Modifiers

The geometry of evacuated collectors is asymetric and thus incidence angle modifiers depend on collector orientation. In contrast to flat plate collectors, evacuated collector incident angle modifiers in the direction perpendicular to the tube axes are equal to one or are greater in nearly every instance. Thus, when performance data for solar collectors are quoted for a solar incidence angle normal to the plane of the collector, this should be considered a lower limit for evacuated collectors and an upper limit for flat plate collectors.

Complicating the issue of incidence angle modifiers is the possibility for non-planer orientation of the absorbers in the tubes, as seen in Figure 4-1. Incident angle modifiers have been measured for different collectors and detailed information is included in Guisan et al.[3].

4.1.4 Additional Collector Parameters

Figure 4-2 and Table 4-3 provide information on absorber surface properties and collector capacitance.

Whenever experimental conditions resulted in a wide range of collector fluid to ambient temperature differences (ΔT), non-linear behavior of collection efficiency as a function of $\Delta T/H100$ was observed. The non-linearity can easily be seen in many of the diagrams in Section 6.1. Because of this, the standard Hottel-Willier-Bliss characterization of collector performance based on a single line on the efficiency versus $\Delta T/H100$ diagram is inadequate for evacuated collectors. An alternate characterization is provided in Section 7.2. This characterization is further elaborated in Guisan[3].

If one is willing to use multiple curves, rather than a single line, then evacuated collector performance can be adequately characterized on the efficiency versus $\Delta T/H100$ diagram. Switzerland's experimental results were fit to:

$$\frac{Q112}{H100} = a + b\ \frac{\Delta T}{H100} + c\ \frac{\Delta T^2}{H100}$$

Table 4-3 Collector Array Capacitance

COUNTRY	INSTALLATION	LOCATION	COLLECTOR ARRAY CAPACITANCE kJ/K-m^2	COMPONENTS INCLUDED	METHOD OF CALCULATION
AUSTRALIA	Sydney University	Sydney	20	Collector hardware, piping and fluid	
CANADA	Solartech	Edmonton	6.40	Collector hardware, piping, insulation	Calculated
CEC	Ispra	Ispra	4.3	Collector hardware, piping, insulation	Multiple linear regression
FRG	Corning	Freiburg	3.6	Collector hardware, piping and fluid	Measured and calculated
	Philips VTR-261	Freiburg	5.6	Collector hardware, piping and fluid	Measured and calculated
NETHERLANDS	Eindhoven University	Eindhoven	2.55	Entire array, collector, piping, fluid	Measured
SWEDEN	Knivsta	Knivsta			
SWEDEN	Sodertorn	Sodertorn			
SWITZERLAND	Corning A	Geneva	9	Entire array, collector piping, fluid	Computer, measured, fitted
	Corning B	Geneva	10	Entire array, collector piping, fluid	Computer, measured, fitted
	Sanyo	Geneva	11	Entire array, collector piping, fluid	Computer, measured, fitted
	Corning B	Hallau	9.6	Entire array, collector piping, fluid	Computer, measured, fitted
UK	Bracknell	Bracknell	6.9	Entire array, collector piping, fluid	Calculated
USA	CSU Solar House I	Colorado			

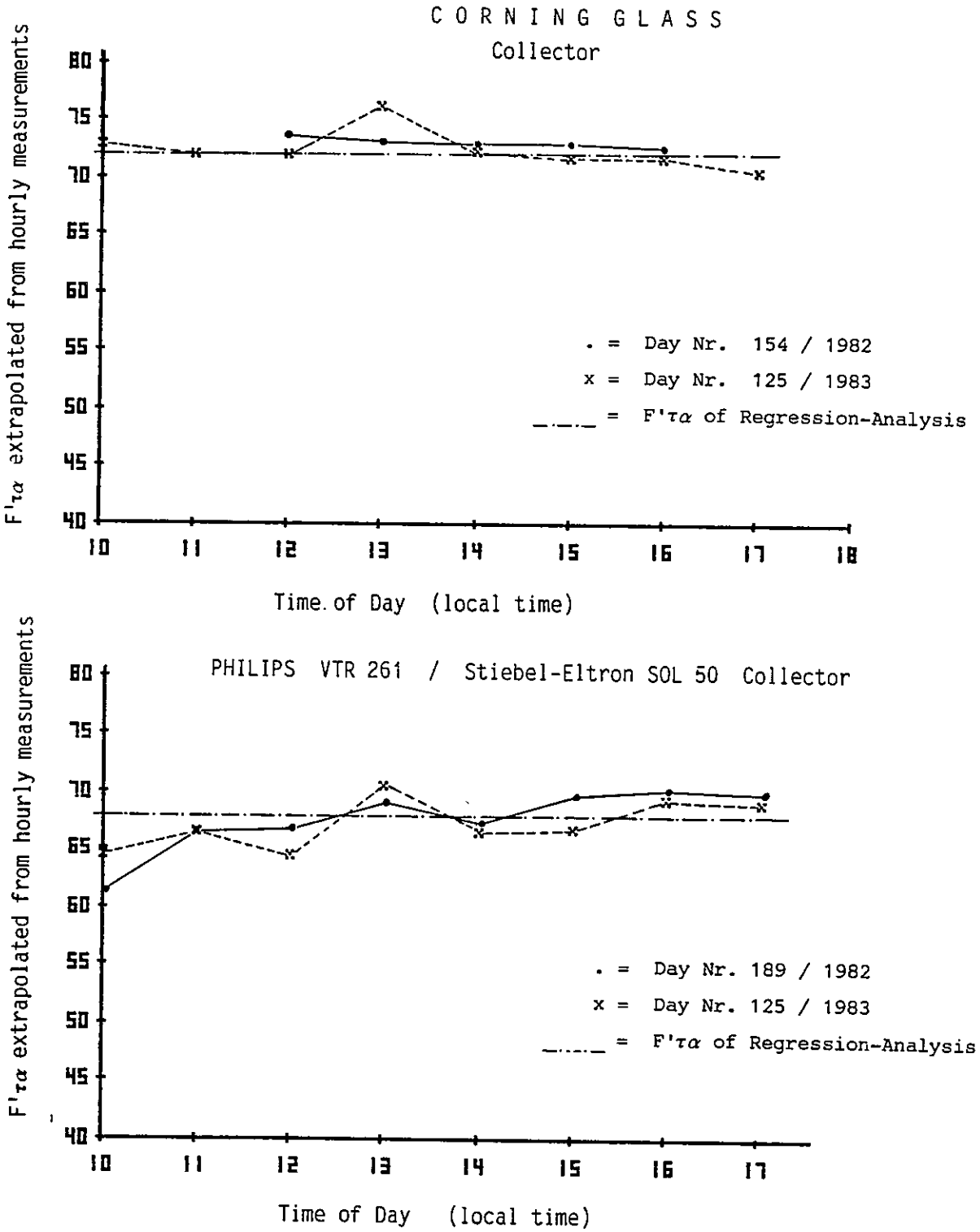

Figure 4-2. Extrapolated Transmittance-Absorptance-Product from Hourly Measurements Close to Ambient Temperature for the Corning Glass and Philips/Stiebel-Eltron collectors.

and U.S. experiment results were fit to:

$$\frac{Q112}{H100} = a + b\ \frac{\Delta T}{H100} + c\ \frac{\Delta T^2}{H100} + d\Delta T + e\ H100$$

4.1.5 Task VI Collector Designs

Subsequent figures provide more detailed information on the task collectors. Cross sections, photographs, isometrics and manufacturer efficiency curves are given.

4.1.5.1 Evacuated Tubes

An evacuated solar collector tube contains a selective surface surrounded by vacuum, and a mechanism to remove the heat which is absorbed by the selective surface. There are two basic configurations for the evacuated tubes themselves, and a large number of variations on these configurations. One configuration, illustrated in Figure 4-3 (a, b, and c), uses a metal absorber plate in a single walled glass vacuum tube. Heat is removed from the absorber plate by circulating liquid through a metal tube bonded to the plate.

In this construction, as in almost all metal-in-glass collectors, it is necessary to incorporate glass-to-metal seals in order to pass the heat extraction tubes through the wall of the vacuum envelope. A U-tube heat removal design is shown in Figure 4-3 (a).

An alternative configuration for single walled tubes, illustrated in Figure 4-3 (b) uses a straight through metal tube. In this design it is necessary to incorporate bellows in order to absorb the dimensional changes of the metal tube which result from the large temperature fluctuations.

A third heat extraction technique shown in Figure 4-3 (c) utilizes a heat pipe bonded to the metal absorber plate. Heat collected by the plate converts liquid in the heat pipe to vapor which is transported to the condenser, subsequently returning to the absorber end in liquid form.

The second basic form of construction for evacuated collector tubes, illustrated in Figure 4-3 (d) is essentially a Dewar flask. The selective surface is deposited on the outside of a domed glass tube. This tube is then inserted into a second glass tube and joined at the open end. The space between the two tubes is evacuated. In this construction, it is not necessary to penetrate the glass envelope in order to extract heat from the tube.

Various heat extraction techniques for Dewar flask tubes are illustrated in Figure 4-4. All methods involve circulating fluid into

(a)

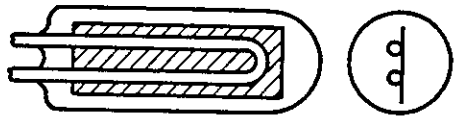

Metal Fin in Vacuum with U-Tube

(b)

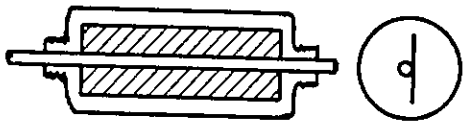

Metal Fin in Vacuum with Straight Through Tube

(c)

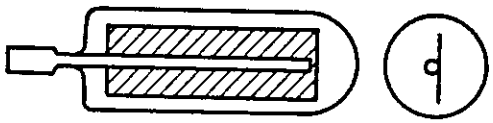

Metal Fin in Vacuum with Heat Pipe

(d)

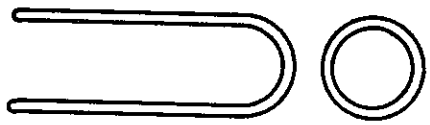

Dewar Flask Construction

(e)

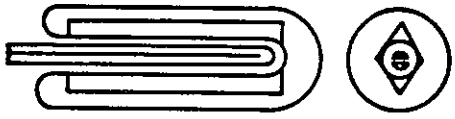

Dewar Flask with Metal-in-Vacuum Absorber

Figure 4-3. Different Configurations of Evacuated Tubular Collectors

(a)

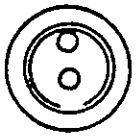

U-Tube Heat Extraction with a Metal Fin

(b)

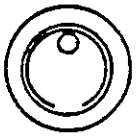

Single Tube Heat Extraction with a Metal Fin

(c)

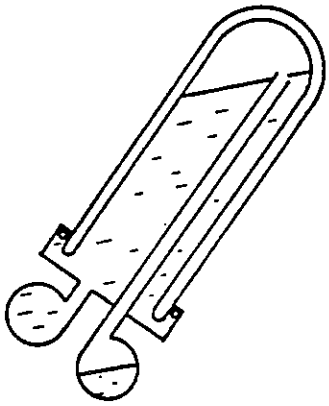

Overflow Extraction with Direct Liquid Contact

(d)

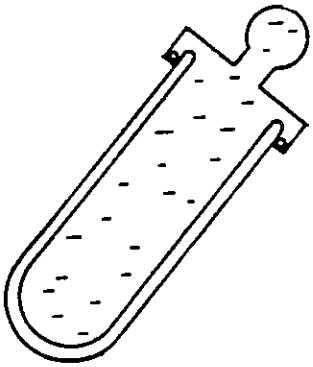

Thermosyphoning Heat Extraction with Direct Liquid Contact

Figure 4-4. Heat Extraction Methods for All-Glass Evacuated Collectors

and out of the space inside the tube. This fluid could be contained in a U-tube a shown in 4-4 (a), or in concentric tubes. In addition, a single liquid filled pipe, or a heat pipe as in Figure 4-4 (b) can be used. In such metal manifold configurations a metal heat transfer fin can enhance the heat transfer between the inner glass tube and the heat extraction piping.

Heat can also be extracted from the Dewar type evacuated tubes by using a liquid in contact with the inner glass tube. Two methods of doing this are shown in Figures 4-4 (c and d).

In Figure 4-4 (c) liquid enters the evacuated tube through a constriction at the bottom. The tube fills over a period of about 20 minutes and the liquid subsequently overflows into a drain down tube and then to an outlet header pipe. The constriction on the inlet side (of flow) is used to equalize flow through a multiplicity of parallel connected tubes. The design is drainable and this feature is used to provide freeze protection and to prevent excess heat being delivered into the thermal storage.

An alternative liquid-in-glass configuration is shown in Figure 4-4 (d). In this configuration the evacuated tube is filled with liquid and connected directly to a header pipe. A natural thermosyphoning effect in the evacuated tube results in efficient heat extraction from the tube into the header. However, the configuration is not drainable.

Many other configurations of evacuated collector tubes have been described in the literature and some of these have proceeded a certain distance towards commercialization. One design shown in Figure 4-3 (e) uses a metal absorber plate in vacuum but also incorporates the Dewar flask construction. Heat is absorbed by the metal plate and transferred by contact to the inner glass tube. It is then transferred to a metal heat extraction U-tube inside this glass tube and from there to the load.

Evacuated collector tubes are invariably built with cylindrical geometry because of the intrinsic mechanical strength of such a shape. The possibility of direct evacuation of a flat-plate collector construction has obvious attractions. There are, however, very great difficulties in realizing such a construction in practice, due primarily to the necessity for strengthening the glass cover plate and the difficulty of making a large rectangular vacuum seal to this plate. Despite many attempts, no evacuated flat plate collector has been constructed successfully on a commercial scale.

Evacuated tubes have been produced in a wide range of sizes. Dewar design tubes have been produced with outer diameters ranging from 30 to 53 mm and in lengths of 1.2 to 1.8 meters. Metal-in-vacuum designs have been produced in tube diameters ranging from 75 to 300 mm and lengths up to 8 meters, though commercial versions only range up to 2.4 meters.

Different types of glass have been used in evacuated tubes. Metal-in-vacuum tubes often utilize soda lime glass. In this configuration, the glass temperature remains close to ambient and is not subject to thermal shock except in the vicinity of the glass-to-metal seal. This latter effect can be minimized by suitable design. The types of seals used in such configurations include metal oxide-glass seals from conventional sealed beam headlight technology and glass frit seals. All-glass collector tubes of Dewar flask construction have been made using both soda lime glass and hard glass. Early installations using soda lime glass tubes experienced excessive tube breakage. This glass is susceptible to thermal shock since it is less strong than hard glass. One mechanism leading to breakage is damage to the inner tube which occurred during manufacture or during insertion of a metal heat transfer fin. Thermal stress results in propagation of cracks from this damage. All-glass collectors using liquid-in-glass heat extraction have invariably been made from hard glass such as Pyrex. Significant breakages were experienced during the early stages of development of such tubes. However, at this stage the breakage problem appears to have been largely solved provided that control subsystems work correctly. Should such controls fail, however, resulting in cold water entering stagnating tubes, glass breakage can occur.

Despite the very serious problems experienced with soda lime all-glass tubes, it is possible that the breakage problems associated with them could be overcome.

4.1.5.2 Selective Surfaces

Considerable advances have been made in selective surface technology over the past decade. A wide range of selective surfaces is available for evacuated tube and flat-plate collectors. These surfaces vary in their optical and thermal properties, and stability. Some early all-glass tubes utilized a chromium oxide-on-aluminum selective surface which was deposited by vacuum evaporation. More recently a three-layer surface consisting of an aluminum base layer, a graded chromium oxide intermediate layer and a magnesium fluoride top layer has been used. This surface has substantially improved optical properties and appears to be stable for extended periods at high temperature. A graded metal carbide cermet on copper selective surface has extremely good optical properties and is very stable for extended periods at high temperatures in vacuum. Electroplated chrome black is used as a selective surface for some metal fin in vacuum designs. A black anodized aluminum oxide selective surface has also been used as has an electro-deposited cobalt sulphide selective surface which has good optical properties and stability.

4.1.5.3 Vacuum Stability

Vacuum can be lost in an evacuated tube by tube breakage due to leaks in the vacuum envelope, or by outgassing of material in the vacuum.

All such problems have been experienced in evacuated tubes. Tube breakage and leakage, which have both been discussed above, can be virtually eliminated by proper tube and system design.

Some metal-in-glass collectors have exhibited problems with degradation of vacuum due to gas emission from the absorber plate. Gettering and other measures are used to eliminate this problem. Such degradation is also partially reversible. The performance of a degraded tube has been observed to improve after extended storage at low temperatures as a result of reabsorbtion of emitted gas by surfaces in the tube.

In the early stages of evacuated tube technology there was concern that vacuum degradation due to helium permeation of the glass envelope could have a significant effect on tube performance. It has been shown, however, that heat loss due to thermal conduction through the helium which accumulates in the tube results in only very small degradation in tube performance. Helium permeation is therefore known to not present a problem for long-term tube stability.

4.1.5.4 Reflectors

At the present time, the evacuated tubes represent the major cost component of an evacuated tubular collector. At high tube prices the cost-effectiveness of these collectors can be improved by reducing the number of tubes and using reflectors to concentrate the incident solar radiation. Several different reflector configurations have been used.

Figure 4-5 (a) shows a diffuse reflector which is mounted behind a spaced array of evacuated tubes. Such a construction increases the absorbed energy on each tube by 20 to 25 percent at normal incidence for absorber tubes spaced one tube diameter apart. Because of incidence angle effects, the net increase in energy absorbed by the collector over a full day relative to normal incidence is approximately 10 percent.

Greater enhancement per tube can be achieved by using specular reflectors. The most popular of these is the compound parabolic concentrator shown schematically in Figure 4-5 (b). Another variation is the circular configuration ripple reflector used by Philips.

Some prototype evacuated collectors have been built which eliminate reflector degradation by placing the reflector in the vacuum envelope. In one experiment design shown in Figure 4-5 (c) a CPC reflector was used in a cylindrical vacuum envelope. In another design, shown in Figure 4-5 (d), the outside glass envelope is shaped in the form of a CPC concentrator and the reflecting surface is deposited on the inside. Neither of these designs has proceeded beyond the laboratory stage although these designs promise a very high efficiency and extremely low loss.

(a)

Flat Diffuse Reflector

(b)

External Compound Parabolic Concentrator

(c)

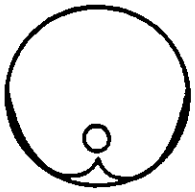

Internal Compound Parabolic Concentrator

(d)

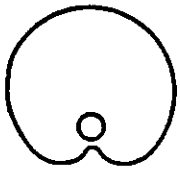

Tube with Draped Envelope

Figure 4-5. Reflectors Used with Evacuated Collectors.

4.1.5.5 Metal Fin In-Glass U-Tube Collectors

Figures 4-6 and 4-7 show the Corning US/Corning France collector. These collectors do not employ a reflector. Metal fin-in-glass U-tube collectors have also been manufactured by Nippon Electric Glass and Sharp of Japan.

4.1.5.6 Metal Fin In-Glass Collectors with Straight Through Tubes

Figures 4-8 and 4-9 show the Sanyo collector. These collectors do not employ a reflector.

4.1.5.7 Metal Fin-In-Glass Collectors with Heat Pipes

Figures 4-10 through 4-14 show the Philips collector. Philips has produced a number of versions of this collector, some with reflectors and some without. Other firms which have produced collectors of this basic design are Thermomax of the United Kingdom, Philco of Italy, and Nippon Electric Glass and Sanyo of Japan.

4.1.5.8 All-Glass Collectors with U-Tube Heat Extraction

Figure 4-15 shows the General Electric collector and 4-16 shows the Sydney University collector. These designs are also manufactured by Energy Design Corporation of the United States and Nitto Kohki of Japan.

4.1.5.9 All-Glass Collectors Using Overflow Extraction with Direct Liquid Contact

Figure 4-17 shows the Owens-Illinois collector and Figures 4-18 through 4-20 show the Solartech collector. Sunmaster in the U.S. manufactures a collector of the same design.

4.1.5.10 Flat Plate Collectors

Figures 4-21 through 4-23 show some flat plate collectors used in Task VI installation experiments. The Teknoterm collector of Figure 4-22 uses a second glazing of close packed evacuated tubes. The Scandinavian Solar collector of Figure 4-23 uses an outer glass and two teflon films as inner glazings. This latter collector has good optical performance combined with low losses.

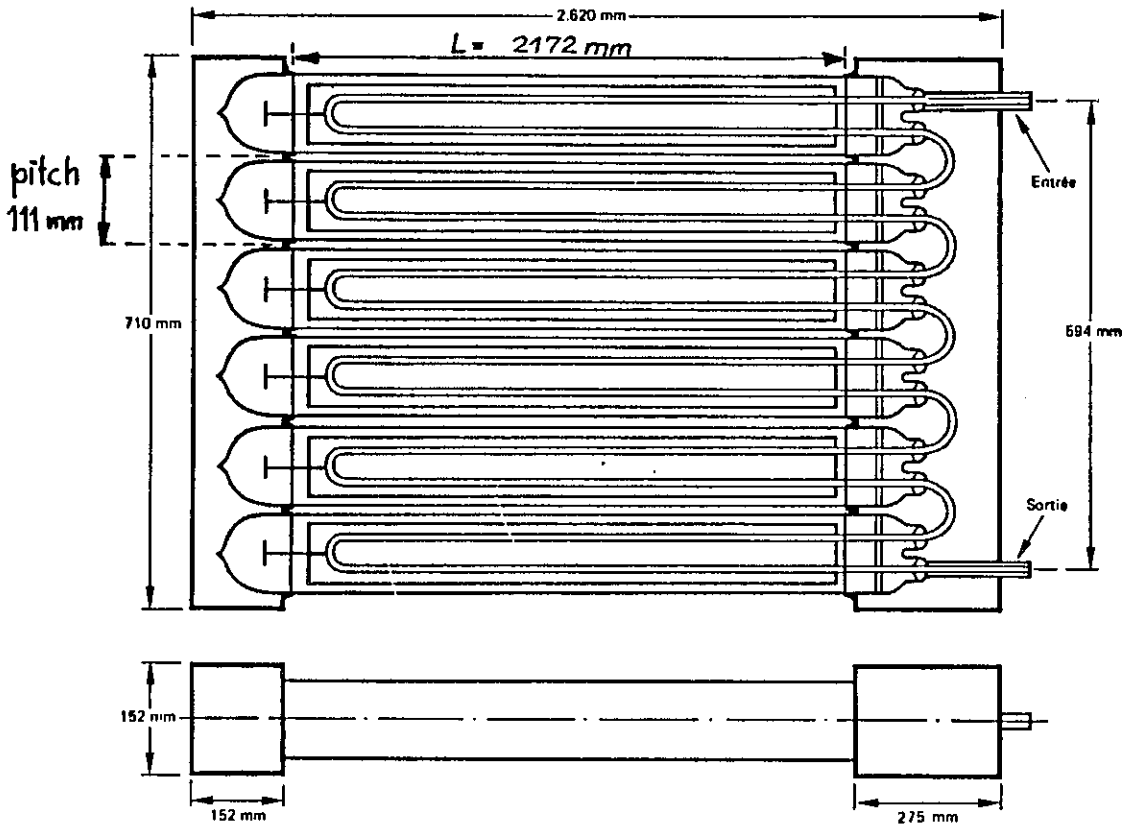

Cross section schematic of the Corning collector.

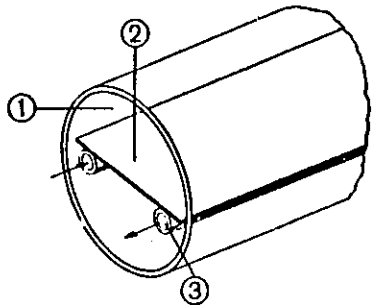

1. Evacuated glass tube.
2. Absorbing surface.
3. Fluid tube.

Aperture area : $6 \cdot 111.3 \cdot 2172\ mm^2 = 1.45\ m^2$

Corning Cortec 'A','B','D' collector

CH-HTG-1 , CH2-HTG-1

Figure 4-6. Cross Section Schematic of the Corning Cortec "A", "B" and "D" Collector, Geneva, Switzerland.

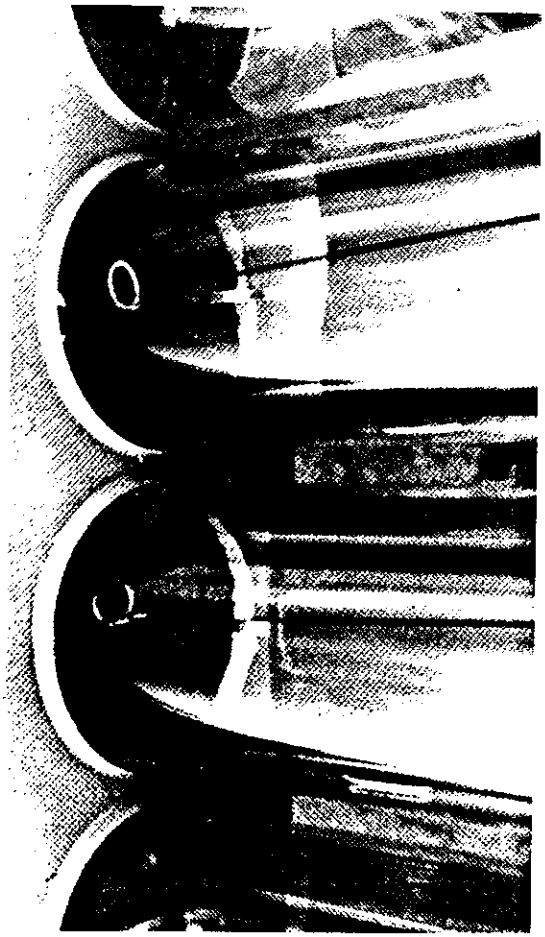

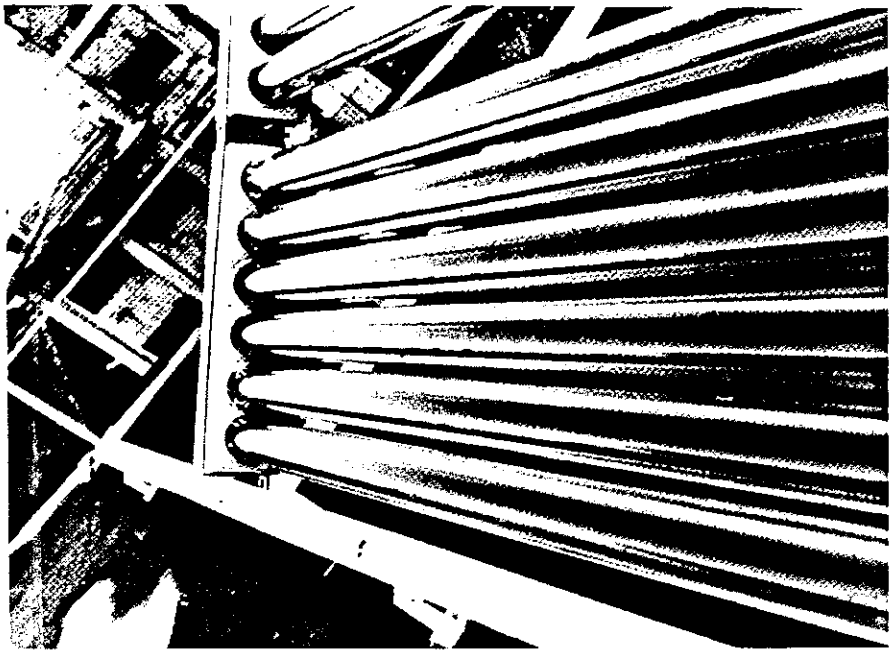

Figure 4-7. View of the Corning Cortec ("A" and "B") Tubular Collector.

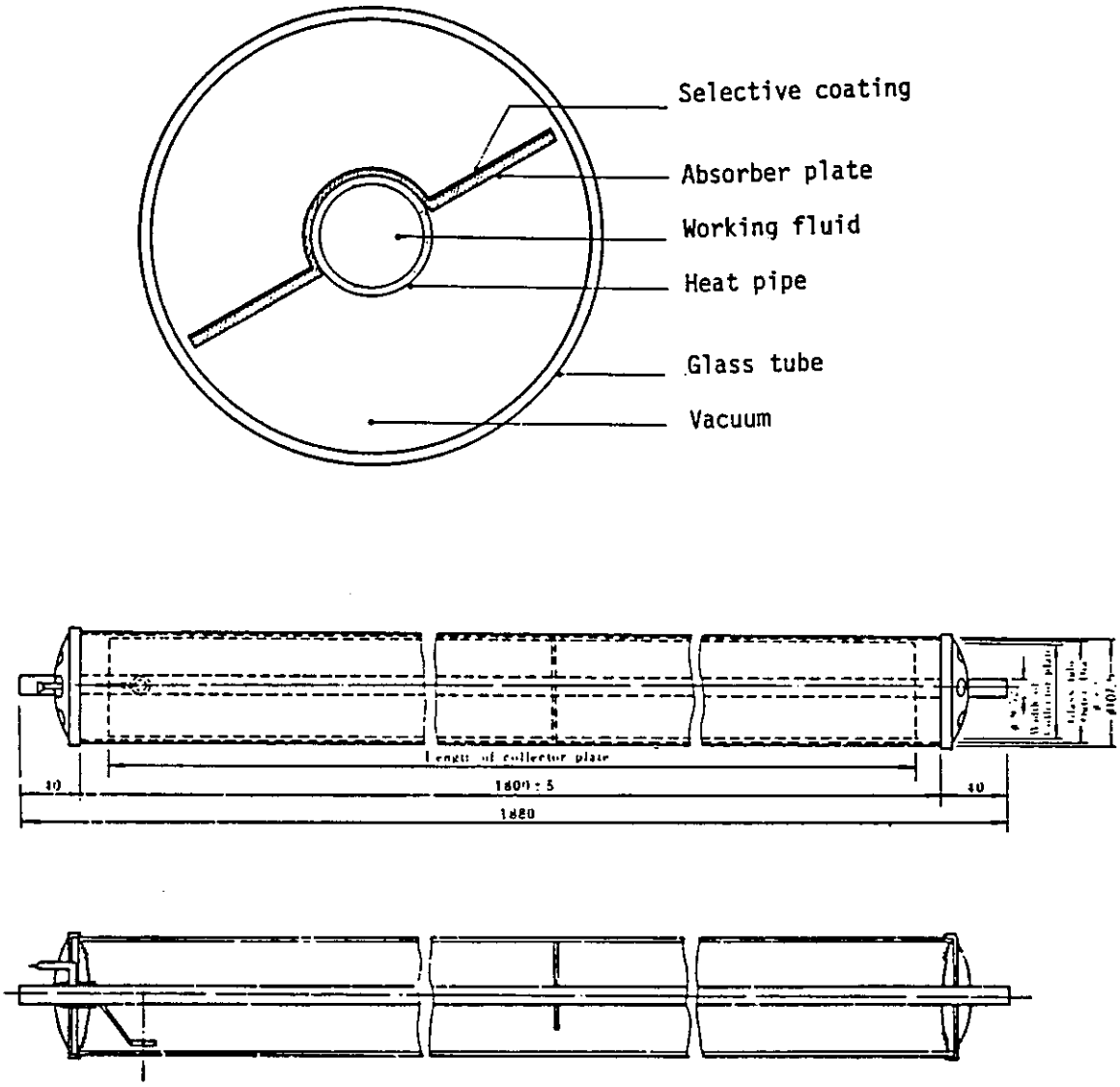

Figure 4-8. Structure of the Sanyo Collector (STC-CU250), Geneva, Switzerland.

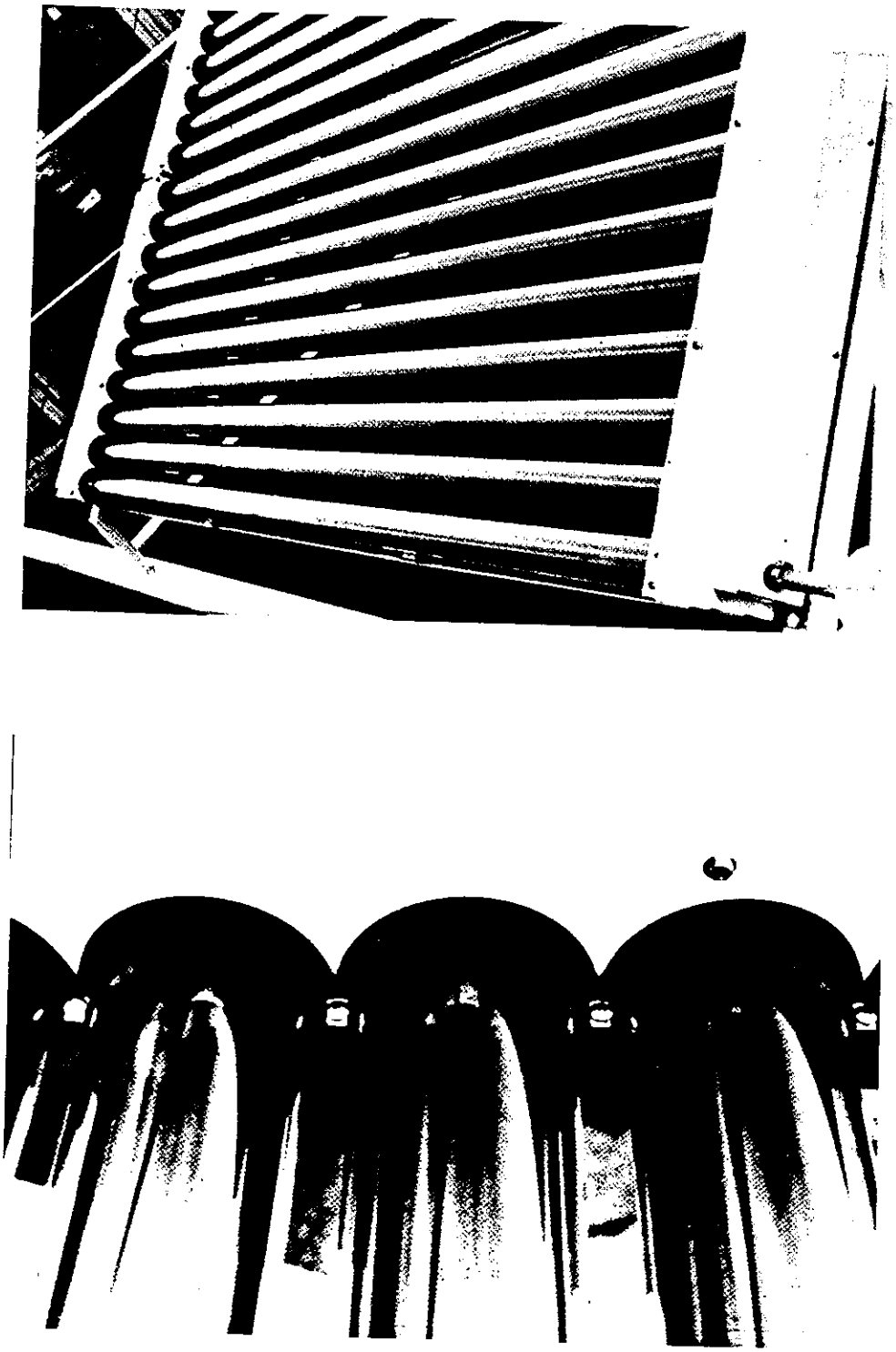

Figure 4-9. View of the Sanyo STC-CU250 Tubular Collector, Geneva, Switzerland.

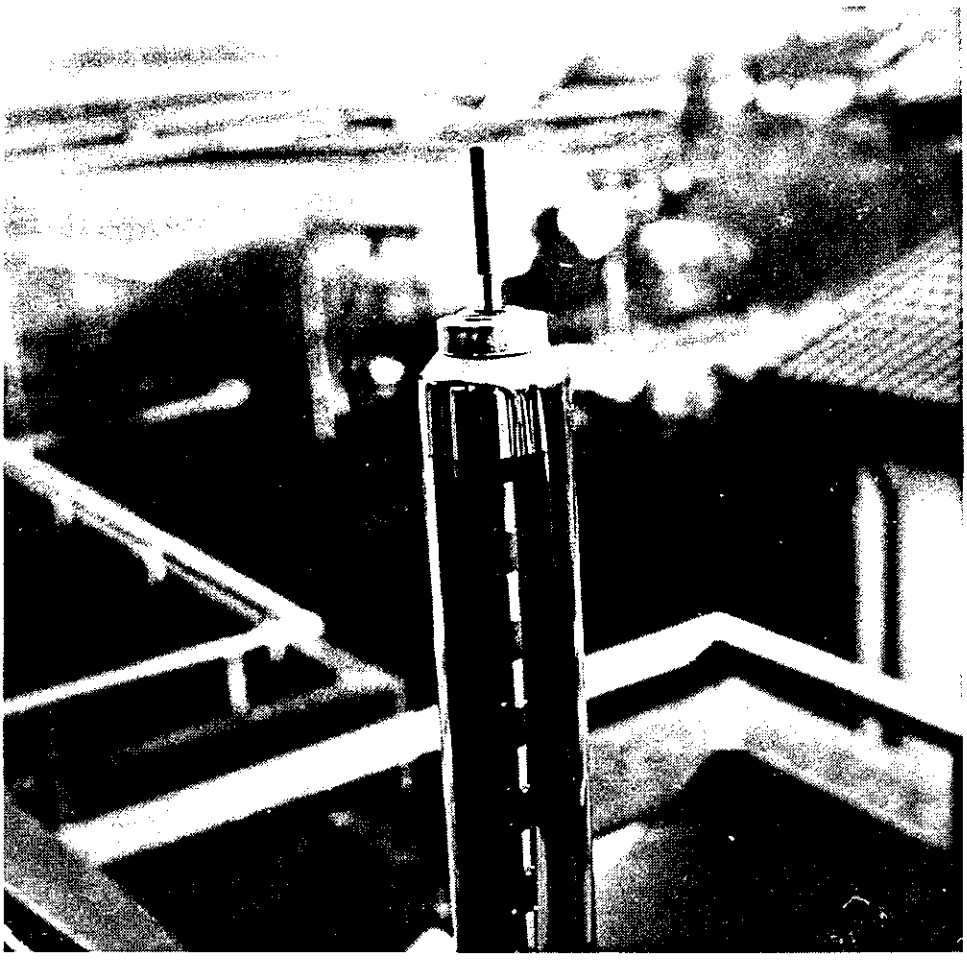

Figure 4-10. Individual Philips VTR 261 Collector Tube and Condenser, Federal Republic of Germany.

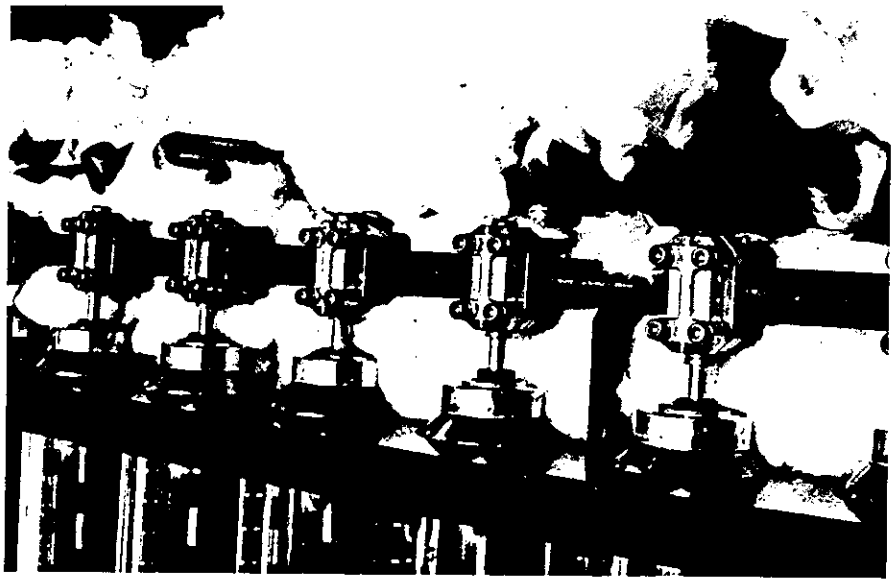

Figure 4-11. Aluminum Clamps Transfer Heat from the Condenser to the Heat Transport Pipe, Colorado State University.

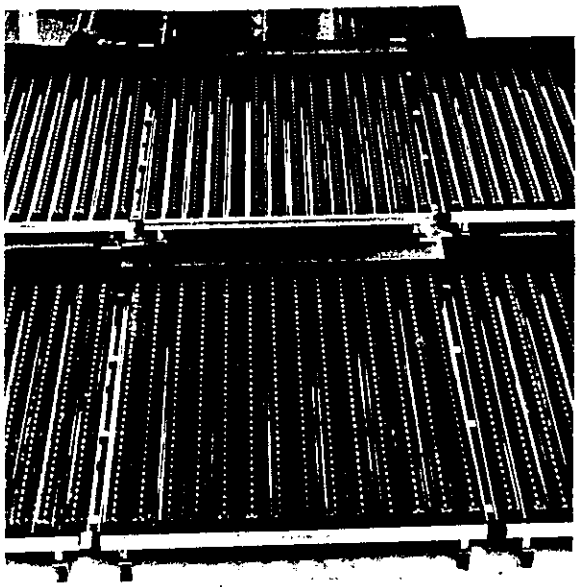

Figure 4-12. A Collector Module of Philips VTR 361 Evacuated-Tube Heat Pipe Collectors, Colorado State University.

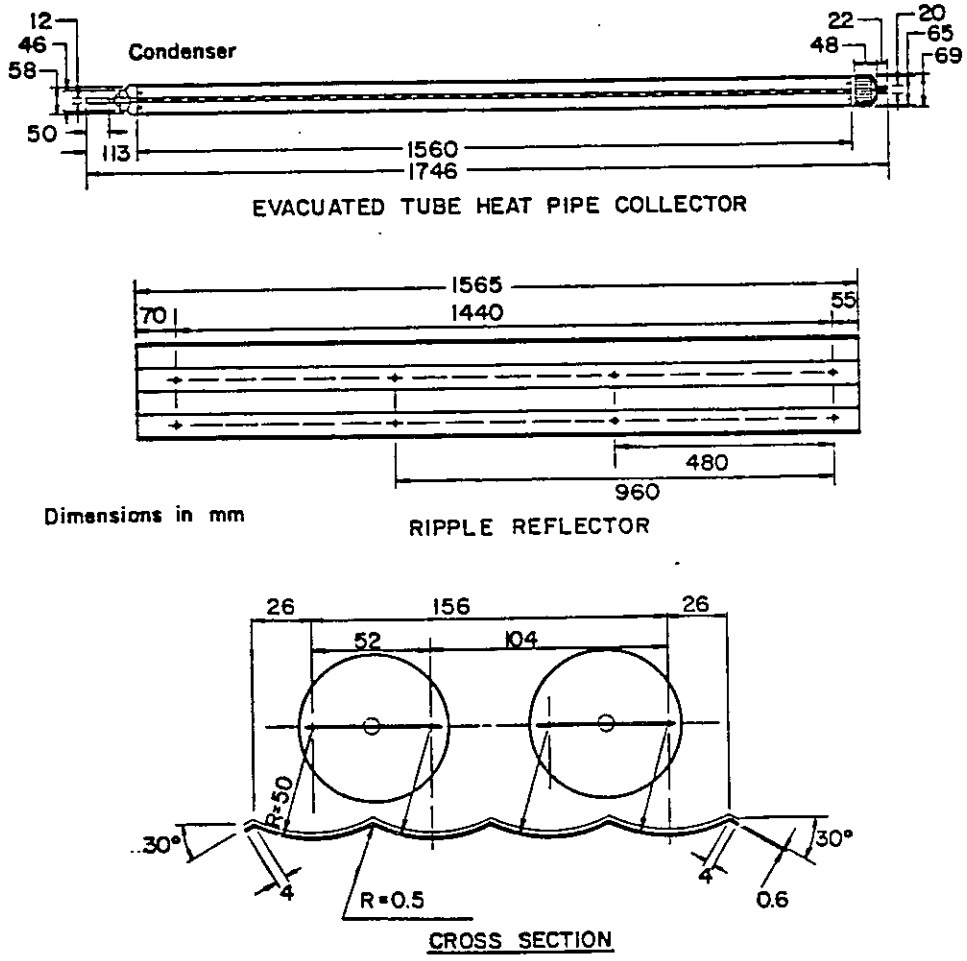

Figure 4-13. Dimensions of Typical Philips VTR-361 Heat Pipe Collector and Ripple Reflector Position, Colorado State University.

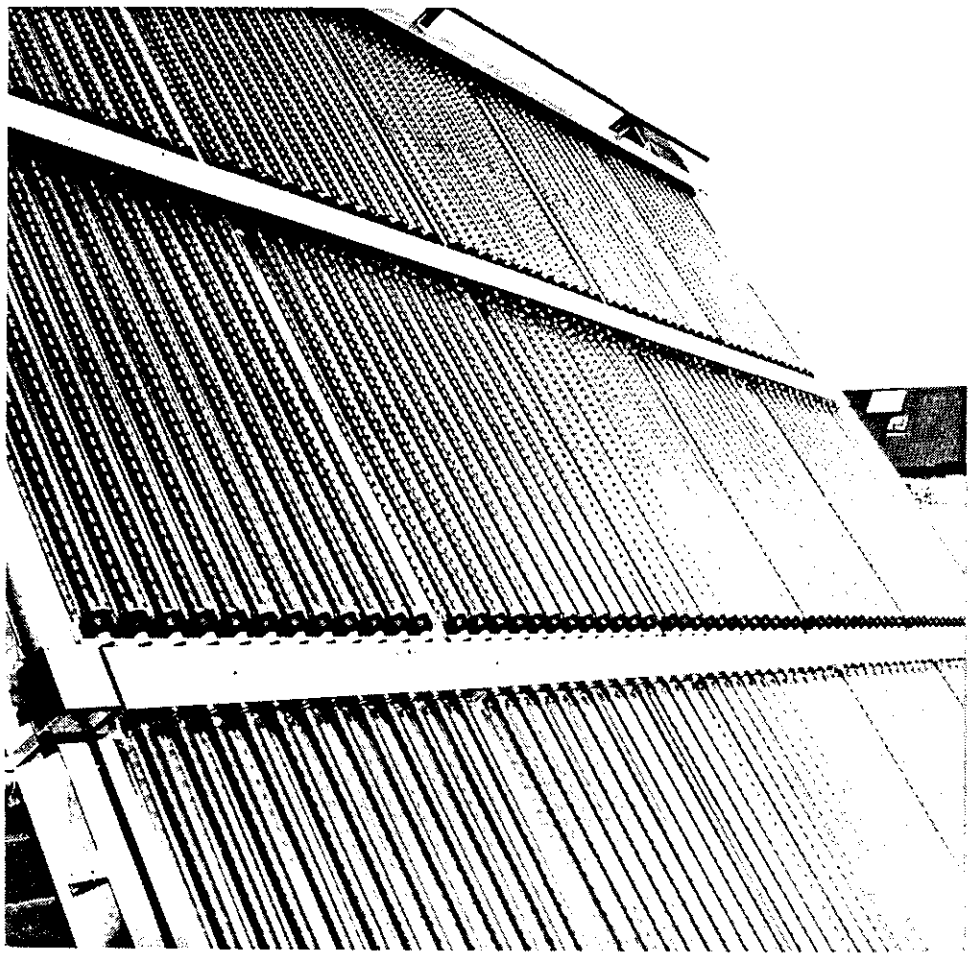

Figure 4-14. Philips/Stiebel-Eltron VTR 261 Collector Array, Federal Republic of Germany.

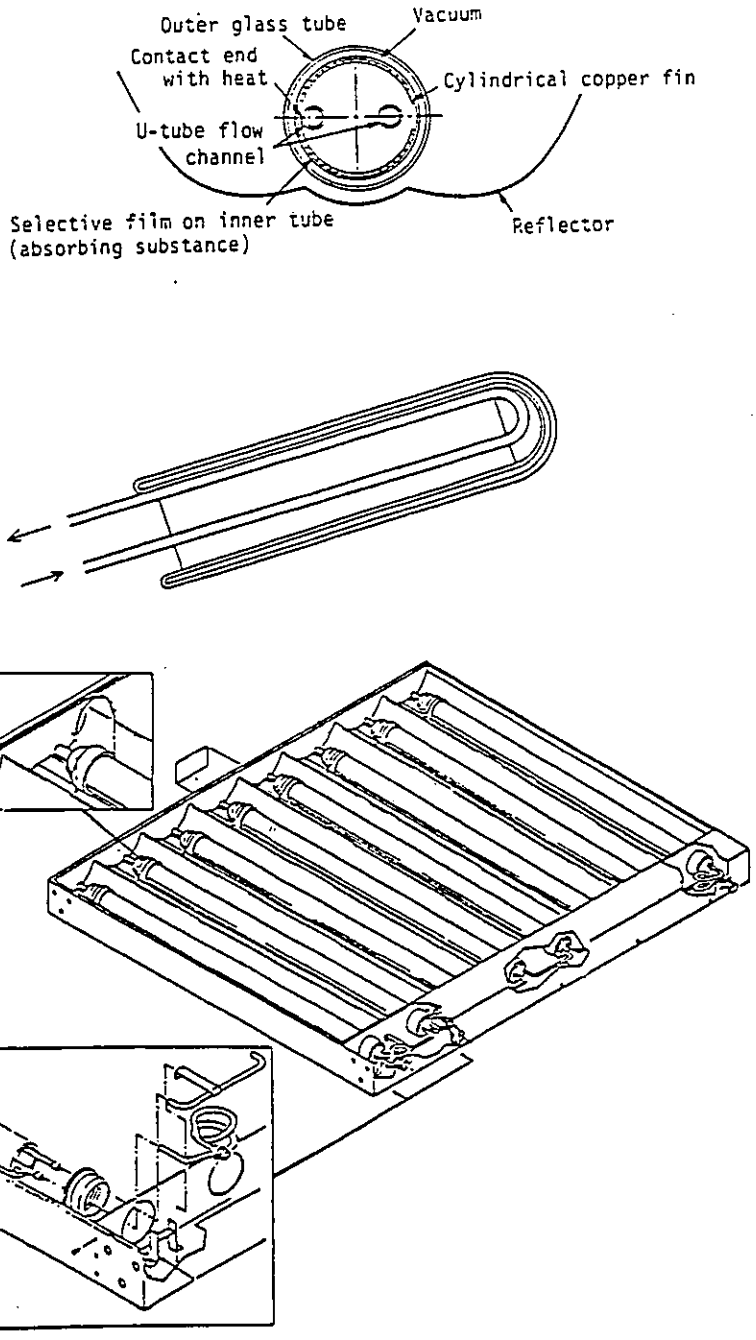

Figure 4-15. General Electric Collector.

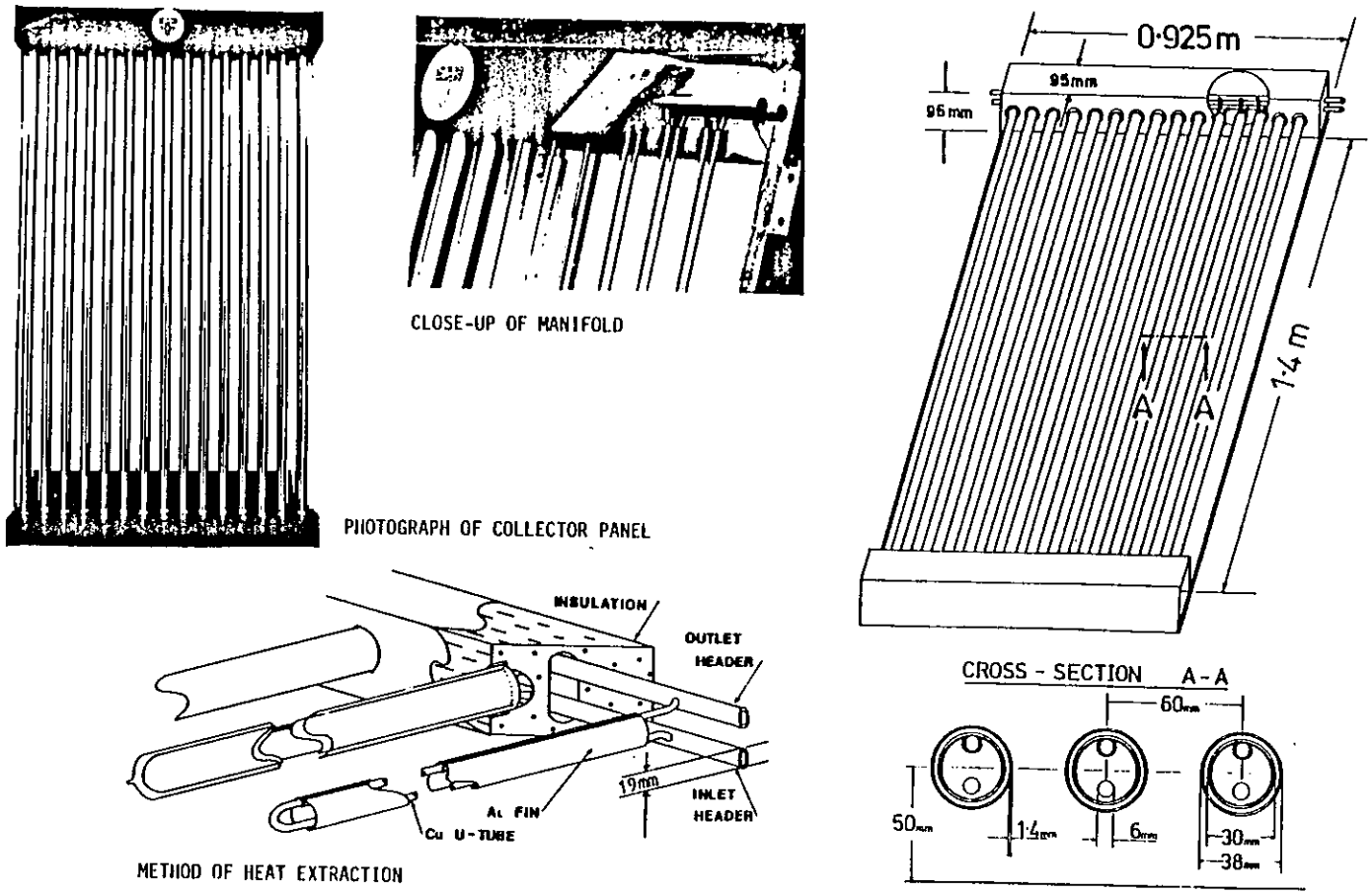

Figure 4-16. Sydney University Evacuated Tubular Collector ("Liquid-in-Metal" manifold), Australia.

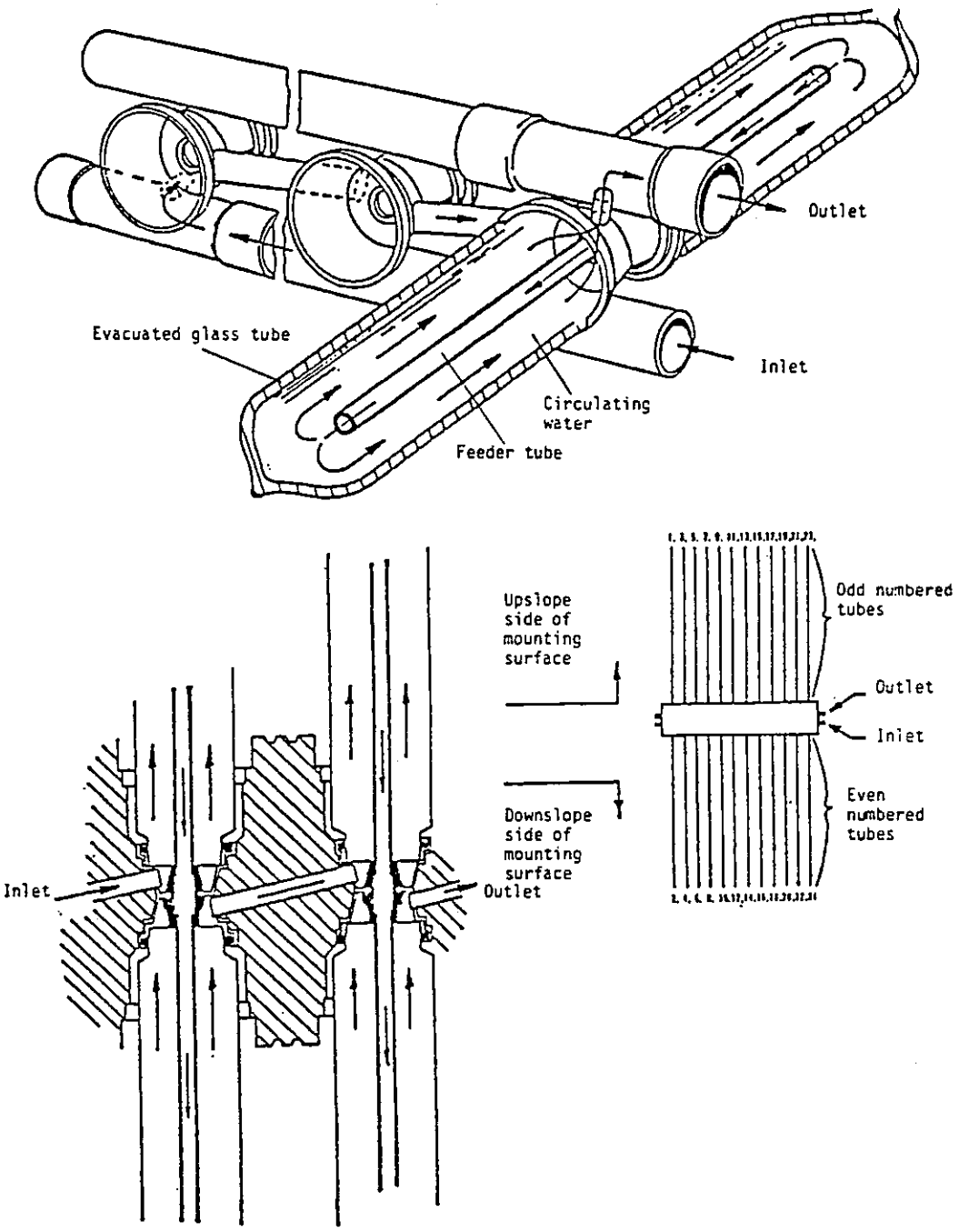

Figure 4-17. Owens-Illinois Collector.

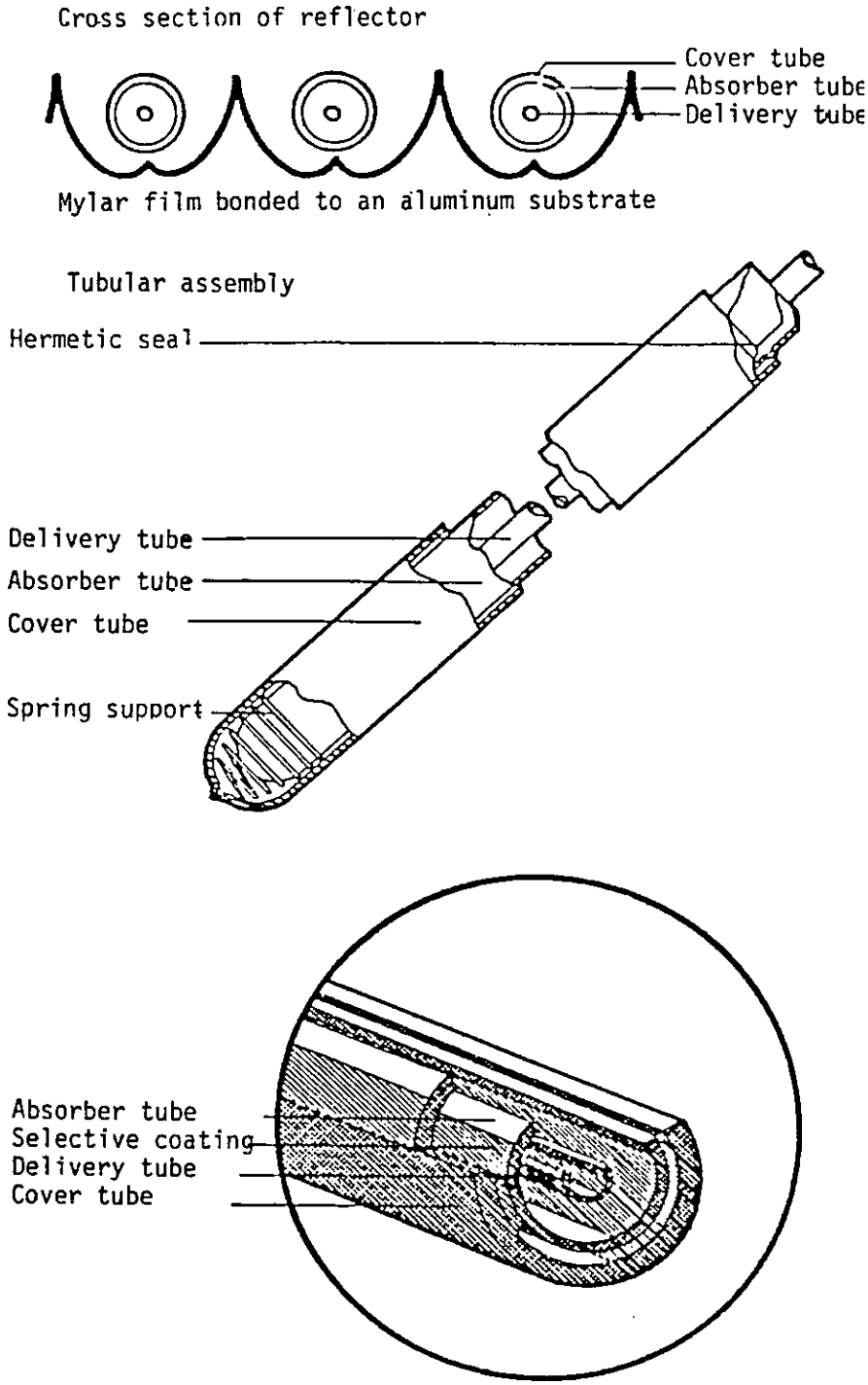

Figure 4-18. Cross Section of the Solartech Collector, Mountain Spring Bottle Washing Facility, Canada.

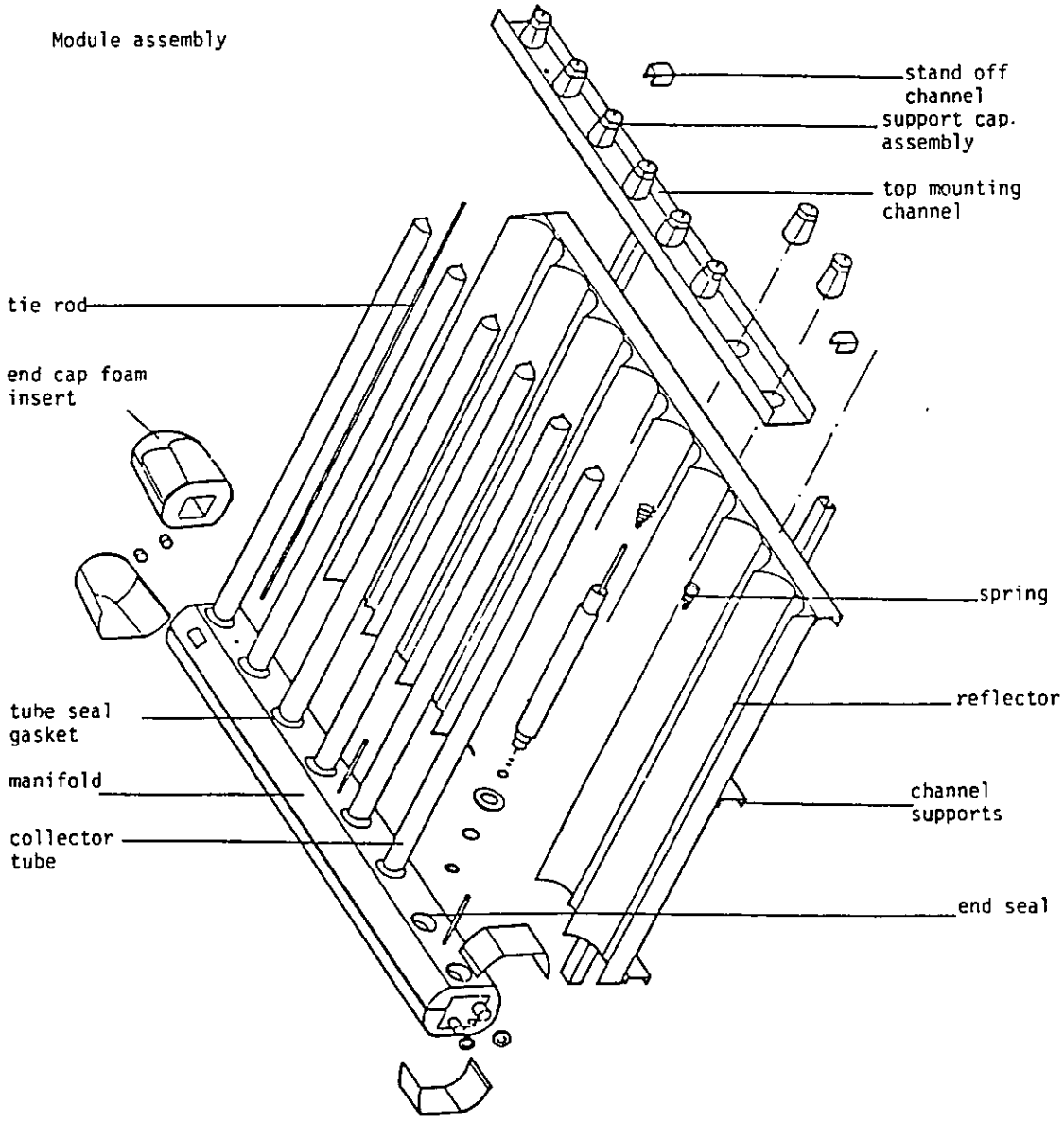

Figure 4-19. Module Assembly of the Solartech Collector, Mountain Spring Bottle Washing Facility, Canada.

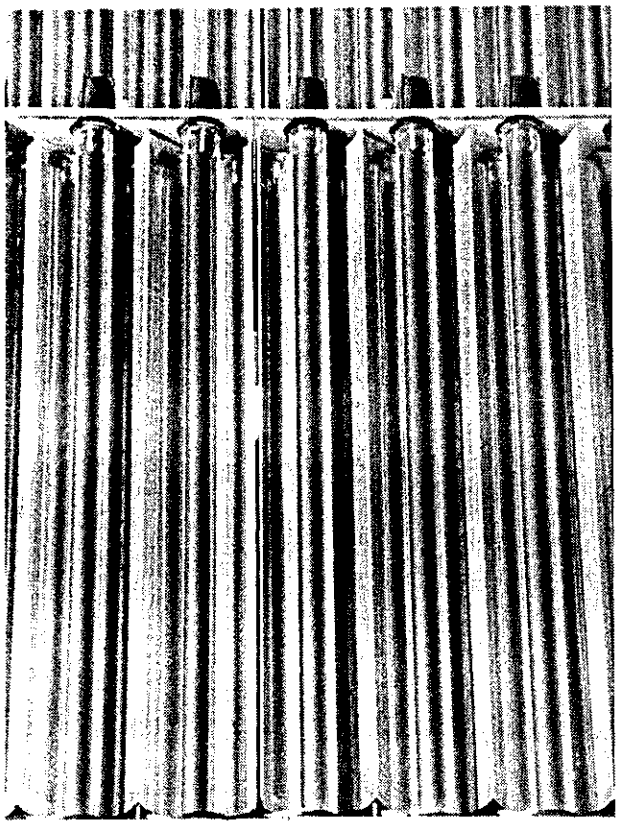

Figure 4-20. Close-up Photograph of Solartech Collector, Mountain Spring Bottle Washing Facility, Canada.

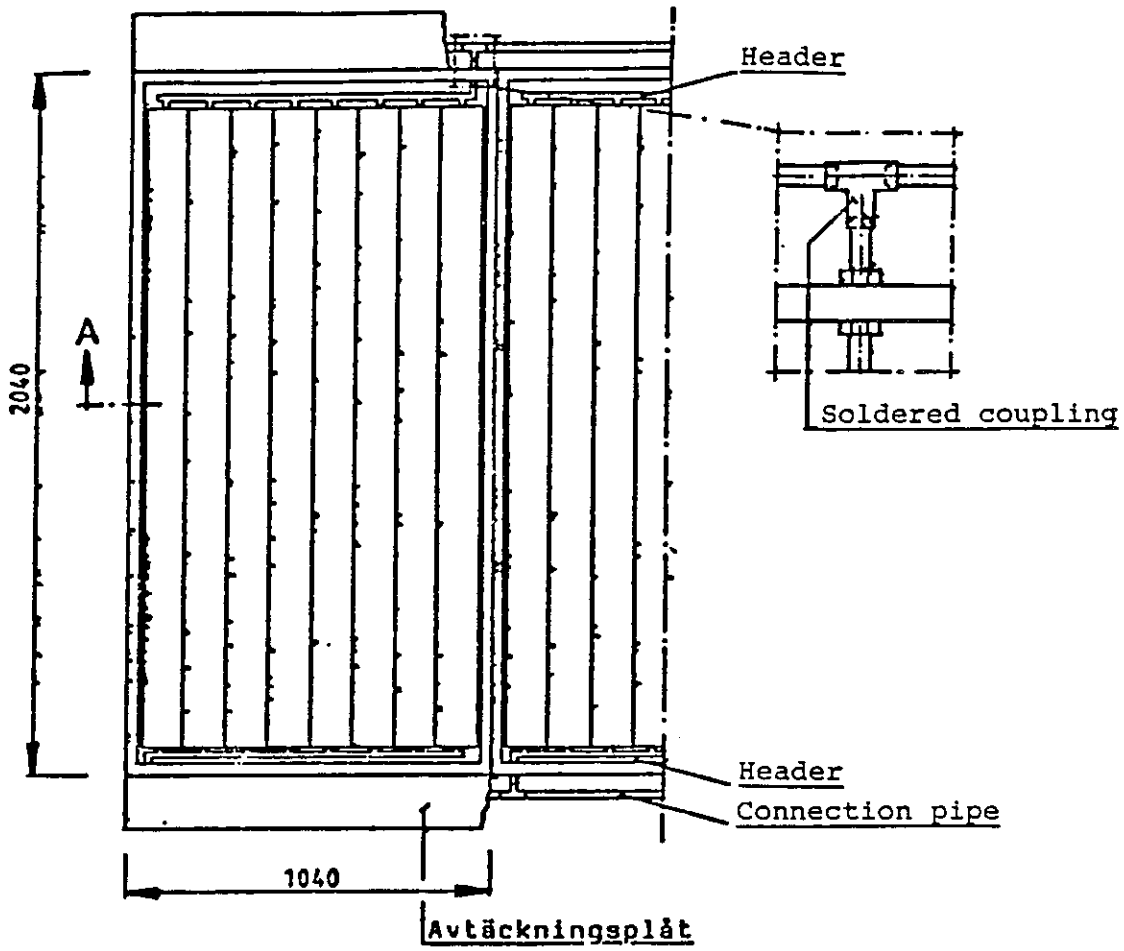

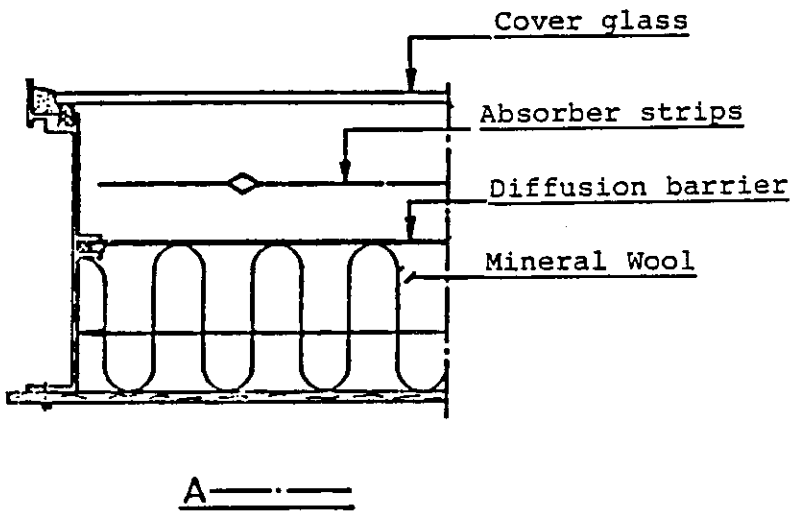

Figure 4-21. Granges Aluminum Collectors.

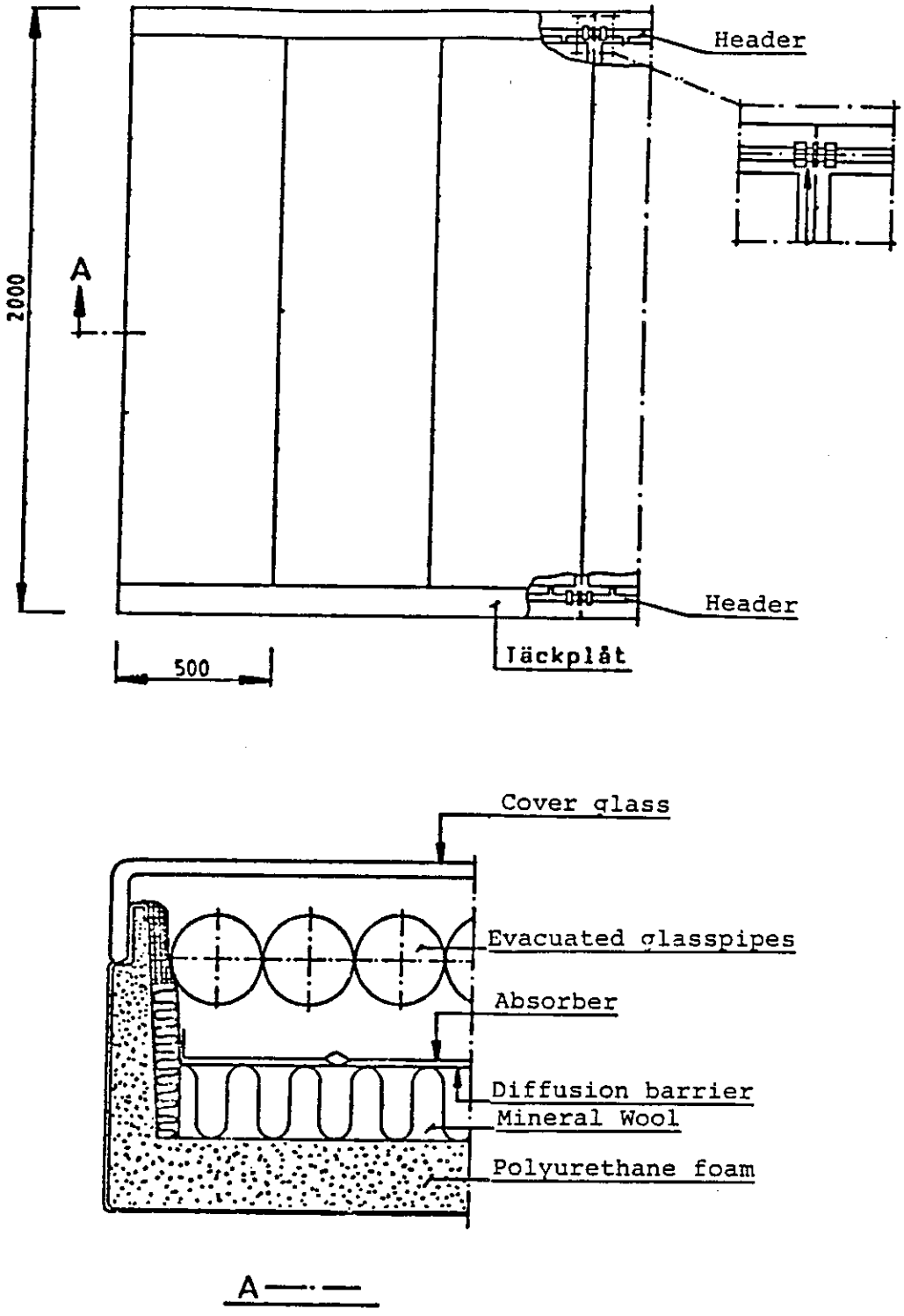

Figure 4-22. Teknoterm Collector.

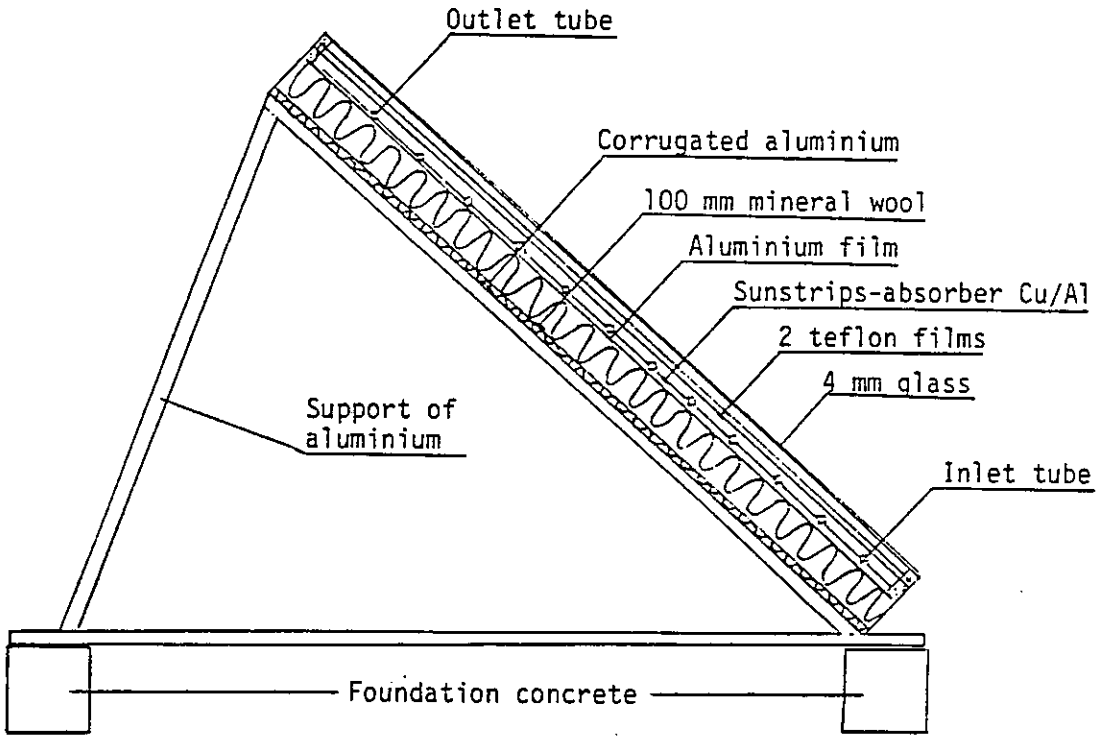

Figure 4-23. The Solar Collector from Scandinavian Solar, Scandinavian HT.

4.2. STORAGE

Storage is the next most important subsystem in most solar energy systems. This section gives descriptions of the storage systems used by each of the installations. The range is from no storage to multi-tank systems. Any additional storage features, such as stratification enhancement devices, are also described.

4.2.1 Sydney University Solar Heating and Cooling System, Sydney, Australia

Hot Water Storage: The storage capacity of the corrugated copper hot water tank is 3.2 m^3. The vessel is open to atmosphere and heavily insulated (300 mm polyurethane foam). Weather protection is accomplished with a second outer shell of corrugated iron. The tank does not have a heat exchanger. Connecting pipework is steel reinforced high temperature rubber hose. The theoretical overall loss coefficient is 0.053 W/m^2K yielding a loss factor of 1.15 W/K.

Chilled Water Storage: A chilled water tank can be used as a buffer between the absorption cooling machine and the load. The storage capacity is 1.35 m^3. The inner and outer skins are galvanized iron, separated by 100 mm of polyurethane insulation. The theoretical overall loss coefficient is 0.159 W/m^2K, the overall loss factor 1.79 W/K.

4.2.2 Mountain Spring Bottle Washing Facility, Edmonton, Alberta, Canada

Due to the nature of this application in which the load occurred concurrently with available solar energy, a storage tank was not needed. Instead, an accumulator tank of 5.7 m^3 (gross volume) was utilized. The capacity of this tank was adequate to fill the entire collector loop and still have sufficient fluid inventory so that the heat exchanger circulating pump operated satisfactorily. During periods when the bottle washing facility was not operating, as on weekends, and solar energy was available, heat could be transferred from the accumulator tank to the soaker tank, effectively increasing the storage capacity of the system by the soaker tank's 14 m^3 volume.

The accumulator tank is a steel tank lined with dense concrete, i.e., alcrete, precrete. The heat capacity is 4190 J/kg-K with maximum and minimum operating temperatures of 93°C and 71°C respectively. The overall heat loss coefficient is 9.43 W/K. Stratification is insignificant. All losses from the accumulator tank are non-useful.

4.2.3 Ispra Solar Heated and Cooled Laboratory, CEC

The cooling system has two heat storages: a hot water storage of 0.5 m^3 and a chilled water storage of 50 m^3.

HOT Water Storage: Hot water storage is used to stabilize the inlet temperature of the absorption chiller. Its function is not to provide cooling capacity during the evening or night, but to permit the chiller to continue operation when short interruptions in solar radiation occur. The cylindrical storage tank, is 0.85 m high and 0.75 m in diameter. The insulation is 0.7 m thick. The inlet and outlet connections have been designed to enhance stratification. The heat capacity is 2.1 MJ/K.

Chilled Water Storage: During May and part of June in ISPRA, there is excellent insolation with rather low outdoor temperatures. On the other hand during July and August the cooling load is high and there is less sunshine than previous months. There was a large underground storage tank available in the Solar Laboratory, therefore, it was decided to store the overcapacity of cooling available at the end of the spring for use during the summer. The storage consists of a 50 m^3 water-filled concrete vessel built under the Solar Laboratory. The inlet and outlet connections are designed to achieve maximum stratification. As the temperature in the storage is close to the ground temperature, the heat losses in the storage are almost negligible.

4.2.4 Solarhaus Freiburg, Federal Republic of Germany

Domestic Hot Water Storage: A storage capacity of 2.5 m^3 of water has been determined as optimal by computer simulation runs. This storage capacity has been separated into 1.5 m^3 of preheat storage and 1.0 m^3 of hot water storage, to increase system efficiency. The storage tanks are connected in series to the cold water mains. Both are cylindrical pressurized steel tanks with a height of about 2.0 m and a diameter of 1.1 and 0.9 m respectively. They are insulated with 20 cm of rock wool and covered with a thick galvanized sheet-steel envelope, giving loss factors of 9.0 and 5.86 W/K respectively. Delivery of solar energy occurs via immersed tubular heat-exchangers in the bottom of each tank. A 12 kW resistance electric heater, located in the upper half of the hot water tank, is used to supply electrical auxiliary energy. It should be noted that solar energy is directly used in the drinking water system. There is no danger of contamination by the collector fluid because of the higher static pressure in the DHW system.

Solar Heating Storage: The storage capacity of the solar heating system is subdivided into two parts: a 15 m^3 of low temperature storage and 5 m^3 of conventional heating storage, as a buffer tank. There is storage for 7-10 days of heating when the average heating load is 100 kWh/day, which is typical for May or October. The 15 m^3 storage tank is a cube 2.5 m on a side insulated with 10 cm of mineral wool. It has a loss coefficient of 25-35 W/K, depending on storage tank temperature. The time constant is about 25-30 days. The tank is made of welded 3 mm sheet-steel and withstands only the static pressure of its contents. Solar energy is delivered through two internal tubular heat exchangers at the bottom part of the tank, and heat is withdrawn through another heat exchanger inside the top part of the storage.

The other heating storage tank of 5 m^3 capacity is designed for daily storage or direct use of solar energy. It is a cylindrical pressurized tank, insulated with 15 cm of mineral wool, has a loss coefficient of 15 W/K and a time constant of about 15 days. Energy input is either from solar or thermal energy from the oil burner. The energy output is shared between heating and auxiliary energy for the DHW system.

4.2.5 Eindhoven University of Technology Solar House, The Netherlands

Mass of working medium	3700 kg
Heat capacity	15.54 MJ/K
Maximum temperature	80°C
Minimum temperature	12°C
Heat loss factor	6.2 W/K (theoretical)
Stratification	Enhanced by floating inlet, bottom to top heating of domestic hot water, and swing arm

There is a nitrogen-filled expansion tank in the top of the vessel, serving both the collector loop and the heater circuit.

4.2.6 Knivsta District Heating Project, Knivsta, Sweden

No storage is used.

4.2.7 Södertörn District Heating Project, Södertörn, SWEDEN

No storage is used.

4.2.8 SOLARCAD District Heating Project, Geneva, Switzerland

No storage is used. Heat is transferred through heat exchangers directly to the district heating system.

4.2.9 SOLARIN Industry Project, Hallau, Switzerland

Two horizontal steel cylinders filled with water and insulated with 150 mm of mineral wool are used for heat storage. Their volumes are 10 and 23 m^3. They correspond typically to one day and one weekend of heat storage. Heat losses are theoretically 14 and 28 W/K, but experimental values are twice as large. For processing needs (summer time) the temperature ranges from 90°C to 120°C. For space heating (winter time) temperatures down to 15°C can still be useful (preheating of air taken from outside).

Two tanks allow more flexibility than one for control of heat storage strategy. Although natural stratification occurs, it is not important due to frequent mixing and small temperature differences. Nevertheless, ten temperature sensors per tank are used to give a detailed thermal picture.

4.2.10 BSRIA Solar Test Facility with Simulated Loads, Bracknell, United Kingdom

The system contains two storage tanks, one for the space heating system with a working mass of 1400 kg and the other for the hot water heating system with a working mass of 117 kg.

The space heating storage consists of a vertical steel tank filled with water. It contains a helical copper coil the full height of the tank through which the hot fluid from the collectors is pumped. The coil has connections at top and bottom and also at the center to permit investigation of the effect of using only the lower part of the coil. The storage has connections at top and bottom for flow to and return from the space heating distribution subsystem. Expansion of the contents of the storage is accommodated by connecting it to an open expansion tank at a high level. The storage has a height of 2.35 m, a diameter of .90 m and a volume of 1.40 m^3. The heat loss coefficient is about 10 W/K. No losses are useful losses. The domestic hot water storage consists of a vertical copper cylinder, the lower half of which contains a copper heating coil through which the solar collector fluid is pumped. The cylinder is fed at the base with cold water from a storage cistern at high level and the preheated water is drawn off from the top. The cylinder has a height of 0.90 m, a diameter of 0.45 m and a volume of 0.118 m^3. It has an overall heat loss coefficient of about 6 W/K. No losses are useful losses.

4.2.11 Colorado State University Solar House I, Fort Collins, Colorado, USA

A 3600-litre cylindrical pressure storage tank filled with approximately 2400 kg of high density polyethylene (HDPE) pellets was intended for use during the summer of 1983. The pellets are generally 6 mm in diameter and have a heat capacity of about 209 KJ/kg at a phase-change temperature of about 130°C. The material is stable to a temperature of 150°C, at which point melting occurs.

Although water temperature was kept below 135°C, the plastic pellets fused together after a few cycles of operation. This reduced the porosity of the mass and its overall capability for heat storage. The material also fused to the filters and as water expanded, the mass moved vertically within the tank and sheared off the filters and clogged the system. A standard 4000-litre pressurized water storage tank was used for the balance of the season.

4.3 SITE SPECIFIC COLLECTOR INFORMATION AND DETAILS OF OTHER COMPONENTS AND SUBSYSTEMS

This section provides collector information that is specific to each installation and details of other components and subsystems. Unusual features of an installation are also presented.

4.3.1 Sydney University Heating and Cooling System, Sydney, Australia

Collection: Two types of collectors are used in this installation, a good quality flat plate collector incorporating low iron glass and a selectively coated stainless steel absorber and a prototype Sydney University evacuated collector using "liquid-in-metal" tube and fin heat removal. The two collector types can be operated independently or jointly.

	YAZAKI FLAT PLATE	S.U. EVACUATED TUBE
No. of Modules	18	32
Total Aperture Area	34.4 m^2	40.0 m^2
Collector Tilt	33.5^o	12.5^o
Surface Azimuth	12.5^o East of North	0^o
Working Fluid	Water	Water
Module Connections	3 rows of 6 modules	4 rows of 8 modules (per row: two sets of 60 tubes in parallel)

Cooling: A Yazaki water/lithium bromide absorption chiller (WFC 600) has been used during the reporting period. The chiller has a nominal cooling capacity of 7 kW for a chilled water temperature of 8^oC and a generator inlet temperature of 88^oC. The required heat input is 11.6 kW and heat rejection is via a wet cooling tower at 29.5^oC. The resulting coefficient of performance (COP) is 0.6.

Heat supply to the absorption chiller is from a 3200 litre hot water tank. The tank acts as a buffer for periods of inadequate solar supply (mainly early morning and late afternoon).

If the generator inlet temperature drops below 75^oC a back-up instantaneous electric heater (13 kW) is turned on. During the auxiliary mode the hot water tank is by-passed.

The cooling system can be operated with or without chilled water storage (manual changeover). The chilled water storage has a capacity of 1350 litres and plumbing to and from the tank is designed to enhance stratification.

Heating: Space heating is accomplished via circulating water from the hot water tank to the air handling units within the air-conditioned

offices and back to the energy storage. The auxiliary heater is turned on if supply water temperatures drop below 40°C. The hot water tank is then by-passed.

Controls: System control uses conventional electronic controllers. The collector pumps are activated by differential temperature controllers (adjustable set-points and switching differentials).

A time-switch governs operation of the air conditioning plant. The offices are air-conditioned during day-time only (e.g., 09.00 to 18.00), seven days a week. A room thermostat is connected to a 2-stage controller and to a proportional controller. Depending on the set conditions and the actual room temperature, the system will operate in one of the three modes: cooling, neither cooling nor heating, or heating. Chiller, pumps, motorized valves, auxiliary heater, etc., are controlled by separate thermostats and component interlocking is via control wiring and relays in the main control switch box.

4.3.2 Mountain Spring Bottle Washing Facility, Edmonton, Canada

Collection: Three collector loops, consisting of 24, 86, and 106 Solartech evacuated tube collectors (equivalent to the Sunmaster, DEC-8A model) are mounted on the flat roof of the soft drink bottling plant. The collectors are fitted with CPC reflectors. During the winter months (November to February), there is considerable mutual shading among some of the collector rows.

SOLARTECH	
Number of Modules	216
Absorber Area	284 m^2
Total Aperture Area	281 m^2
Array Capacitance per m^2 of aperture area (kJ/m^2-K)	45.8 (includes fluid)
Fluid Volume per m^2 of aperture area (l/m^2)	9.30 (collectors and array piping)
Working Fluid	Deionized water
Fluid flow rate per m^2 of aperture area ($l/hr\text{-}m^2$)	30
Piping Material	Copper in collector headers; steel in array piping
Module Connections	All in parallel
Collector Tilt Angle	50°
Surface Azimuth	0°
Tube Orientation	North-South

Heat Transfer: The three collector loops are connected to a central solar accumulator tank. A separate transfer loop transfers heat from the solar tank (when demanded and available) via a heat exchanger to the

caustic loop, which maintains the temperature of the bottle washing tank near 65°C.

Controls: Both the collection loop and the transfer loop are controlled by differential temperature controllers.

COLLECTOR On-Differential, 13°C; Off-Differential, 3°C
TRANSFER On-Differential, 2.5°C; Off-Differential, 1.5°C

4.3.3 Ispra Solar Heated and Cooled Laboratory

Collection: Three different types of collectors were used during the reporting period. The Sanyo collectors are used with and without reflectors. The different arrays are connected in parallel at the same storage.

	SANYO	PHILIPS VTR 261	PHILIPS VTR 361
No. of Modules	12	5	3
Total Aperture Area	29.04 m^2	11.1 m^2	6.81 m^2
Collector Tilt	30°	30°	30°
Surface Azimuth	0°	0°	0°
Working Fluid	water	water	water
Fluid Flowrate	1700 kg/h	1080 kg/h	680 kg/h
Module Connections	2 rows of 6 modules (one row with flat reflectors in front)	1 row	1 row

Cooling: The hot water from the collectors goes through a small buffer storage to the generator of the absorption chiller. The chiller cools the large chilled water storage. The Laboratory is cooled with the chilled water from the storage. No auxiliary boiler is provided.

Controls: Each collector type has its own differential controller with a sensor in the buffer storage and in the collector itself. The chiller is switched on when the temperature in the buffer storage is 85°C and switched off when the temperature drops below 77°C.

4.3.4 Solarhaus Freiburg, Federal Republic of Germany

In the period from January 1982 to May 1983 the following four solar systems were operating in SOLARHAUS FREIBURG with the DHW and Heating systems.

Philips MK IV - Heating System:	January 1982 - May 1982
Corning Glass - DHW System:	January 1982 - May 1982
Philips VTR 261/Stiebel-Eltron DHW System:	June 1982 - May 1983
Corning Glass - Heating System:	June 1982 - May 1983

Collection: Four different solar systems have been tested by the alternative coupling of the two collector systems (Corning and Philips), with two DHW and heating systems. As there is no principal change of the solar system design, the energy flows are affected by these experiments only in magnitude. The heat capacity of one Corning collector module has been estimated at about 5 kJ/K per module and 300 kJ/K for the entire array including piping etc. This is considered low as the collector reaches system temperature within a rather short time. The Philips collector field has a thermal capacity of 947 kJ/K causing a pronounced heatup phase in the morning and cooldown phase in the afternoon.

	CORNING GLASS	PHILIPS MARK VI	PHILIPS VTR 261 STIEBEL-ELTRON
No. of Modules	24	4	15
Aperture Area	33.3 m^2	29.45 m^2	29.2 m^2
Collector Tilt	55^0	55^0	55^0
Surface Azimuth	12^0	12^0	12^0
Working Fluid	*	*	*
Fluid Flow Rate	32 l/min	32 l/min	32 l/min
Module Connect.	4 rows of 6 modules	1 row of 4 modules	3 rows of 5 modules

* 38% by Volume Propylene Glycol-Water solution

Heating: The space heating system utilizes oversize radiators. This is because solar heating is usually at a lower temperature than conventional heating. For an external ambient temperature of -12^oC, this system operates at 50^oC rather than 90^oC. The radiator operating temperature is centrally controlled so that it decreases linearly with rising ambient temperature. Additionally, all radiators are equipped with thermostatic valves to prevent overheating of the living space by external or internal loads.

Domestic Hot Water Heating: The major component of the DHW system is the 1 m^3 hot water buffer tank. A conventional circulation loop maintains most of the hot water distribution network at the design temperature for 16 hours of the day, even when there is no hot water consumption. The losses due to this circulation are approximately 20 percent of the net hot water load. The losses are outside the insulated enclosure in the house's attic, and so they are not useful.

Storage capacity is 2.5 m^3. This volume was determined from computer simulation to be the optimum for the system. The storage

consists of a 1.5 m^3 preheat tank and a 1 m^3 hot water storage tank. The purpose of dual storage vessels was to improve system efficiency. The preheat tank has the cold mains water inlet. Collector outlet water is returned into the preheat tank at the appropriate temperature level, between mains temperature and 67°C, by a floating return pipe. The 1 m^3 hot water storage tank receives the solar preheated water in the lower half of the tank. The upper half of the hot water storage tank is constantly maintained within the design temperature range of 48-50°C by using auxiliary energy.

Solar energy may be delivered in both storage tanks via tubular heat exchangers built into the bottom of each tank. Actual solar energy delivery will depend on the control strategy of each experiment. Auxiliary energy is fed only into the hot water storage tank, either by a 12 kW electric resistance heater inside the tank, or by an external heat exchanger connected to the control heating system. It should be noted that solar energy is directly used in the drinking water system. Both of the storage tanks are insulated all around with 20 cm of mineral wool.

Controls: A microprocessor operated control system was installed in the Solarhaus Freiburg, with a conventional control system as standby. In order to investigate the influence of modified control on the dynamics and the energy consumption of the various systems, several control strategies for the solar, DHW, and the heating system have been developed and tested.

The collector pump is switched on for at least ten minutes when the radiation level exceeds 130 W/m^2. Collector operation stops when the collector temperature rise falls below 0.5K. Collected solar energy may be delivered to either the hot water or preheat storage tank, depending on their temperatures, and the insolation intensity. Any excess energy collected in the DHW system (i.e., storage tanks at maximum temperature) may be fed into the heating system storage, in parallel with the output from the heating system collectors.

For an electrical auxiliary control of DHW, a standard thermostat is used for the electric element in the 1 m^3 hot water storage tank. An 'energy-hysteresis' control strategy is used for the supply of auxiliary thermal energy. Two temperature sensors, located in different parts of the storage tank, provide the necessary signals.

4.3.5 Eindhoven Technological University Solar House, The Netherlands

The collector array consists of 23 modules of 16 evacuated tubular collectors each:

Characteristics	Working fluid in heat-pipe; neopentane Selective surface; Cobalt-oxide
Vacuum	10^{-2} Pa
Module Aperture Area	2.05 m^2
Module Gross Area	2.37 m^2
Array Aperture Area	47.15 m^2
Array Gross Area	57.66 m^2
System Fluid	Water from the mains, no additives
Flowrate	Variable 5-22 kg/(m^2 hr)
Orientation (Azimuth)	7° West from South
Tilt	48°
Maximum Outlet Temp.	90°C
Reflectors	Behind the tubes is a Tedlar-coated Aluminum film (manufactured by Solar Usage Now)
Freeze Protection Method	Flushing in case of freeze risk

Domestic Hot Water Subsystem: The heat exchanger in the storage vessel consists of 11.5 m of finned copper tube, half of which is concentrated in the upper part of the tank.

Make	Trufin
Type	W/H 35-11-14 100 01
External Heat Exchanging Surface	2.42 m^2

Heat Distribution Subsystem: Energy is transferred from the storage vessel to a water-to-air heat exchanger (made by Holland Heating). This heat exchanger is designed to heat the air up to 50°C at an outdoor temperature of -15°C and has a theoretical transfer capacity of 1500 W/K. The water flow in the heat exchanger amounts to 300 kg/hr making the throughputs of collector array and distribution system essentially equal. The garage is heated by waste ventilating air, drawn from bath rooms and toilets.

Control System Hardware: The control system hardware consists of a control unit and sensors for temperature, pressure and fluid level.

All setpoints in the control unit are adjustable, providing great flexibility of the control system. This flexibility permits convenient experimentation with the control strategy. The aims of these experiments are

- To eliminate superfluous operating modes and hardware parts
- To simplify intricate operating modes, or control functions
- To optimize the control strategy.

A diagram showing the location of sensors and control devices is given in Figure 5-6. For temperature measurements Pt 100 resistance thermometers are used. Temperature and current transmitters are all Philips transmitters, type E. Temperature setpoints are adjustable using Philips Witromats. The collector pump is a Wilo RS 25/70 V. This pump is controllable for a variable flow of 200 - 800 /hr by means of a frequency controller, type Electroproject EPFC-1.5kW. The motorized valves are made by Landis and Gyr.

4.3.6 Knivsta District Heating Project, Knivsta, Sweden

Collection: Four collectors have been tested in this installation, three evacuated tube collectors, and one flat-plate collector.

	GENERAL ELECTRIC TC100	OWENS ILLINOIS SUNPAK	PHILIPS VTR 141	SCANDINAVIAN SOLAR HT (FP)
No. of Modules	8	24	19	2
Total Aperture Area (m^2)	38.36	35.64	24.62	24
Collector Tilt	45^0	45^0	60^0	45^0
Fluid Flow Rate	27	22	10	6 (litres/min)

The collector heat transfer medium is a water glycol mixture.

Heating: The collectors are connected via a heat exchanger directly to the district heating network without any storage.

Controls: The pumps in the collector loop are run 24 hours per day. When the temperature in the loop is warmer than the return temperature of the network, the network loop side of the heat exchanger is activated. To prevent freezing in the heat exchanger network side, a bypass is opened on the collector side when temperatures are less than a few degrees centigrade about zero.

No preheating of the collector loop with energy from the district heating network has been applied except for a few instances for freeze protection and system experiments. This will not have a significant influence on the reported data.

Measurements: Q112 does not include the preheating energy delivered from the collectors to the piping system outside the array in the morning. For direct comparison of Q112 for Knivsta with other results, the daily energy input/output, curves have to be shifted upwards and parallel (except for the General Electric T100) by 0.3 MJ/m^2d for the Owens Illinois; $0.5MJ/m^2d$ for the Scandinavian Solar; and 1.1 MJ/m^2d for the Philips VTR 141 collectors.

4.3.7 Sōdertōrn District Heating Project, Sōdertōrn, Sweden

Collection: Seven collector systems are being tested in the Södertörn plant. Two evacuated tube collectors, four standard flat-plate collectors, and one second generation flat-plate collector with anti-convection glazing. Three of the flat-plate collectors are presented.

	GENERAL ELECTRIC TC100	PHILIPS VTR 141	SCANDINAVIAN SOLAR HT	GRANGES ALUMINUM SUNSTRIP 80	TEKNOTERM HT
No. of Modules	48	88	78	100	192
Total Aperture Area (m^2)	150	120.6	216	191	144
Collector Tilt	40^o	60^o	43^o	40^o	40^o
Fluid Flowrate (litres/min)	97	72-216	59	200	192

The collector loop is filled with a water glycol mixture.

Heating: The collectors are connected via a heat exchanger directly to the district heating network without any storage.

Controls: The circulation in the collector loop starts when the collectors reach a temperature of about 45^oC. The heat transfer to the network is controlled by valves on both sides of the heat exchanger. These are opened when the collector loop is warmer than the network return temperature.

No preheating of the collector loop by the district heating network has been applied except for a few weeks to evaluate system dynamic effects.

Measurements: Q112 does not include the preheating energy delivered from the collectors to the piping system outside the array during the morning. However, as this piping system is very small compared to the aperture area, no correction is needed for direct comparison with other results.

4.3.8 SOLARCAD District Heating Project, Geneva, Switzerland

Collection: The collectors are mounted on a flat roof with the absorber plates parallel to the collector plane. Each row slightly shades part of the next one. Three separate loops for the Corning "A" and "B" and Sanyo collectors allow for separate performance measurements.

	CORNING CORTEC "A"	CORNING CORTEC "B"	SANYO STC CU 250
No. of Modules	6	6	8
Absorber Area (m^2)	6.72 x 2	6.72	14.0
Aperture Area	8.7	8.7	19.5
Array Capacitance per m^2 of aperture area ($kJ/m^2{}^oC$)	10.9	12.3	14.0
Fluid Volume per m^2 of aperture area (l/m^2)	1.33	1.53	1.72
Working Fluid	Glycolen in water 0% summer 30% winter	Glycolen in water 0% summer 30% winter	Glycolen in Water, 0% Summer, 30% winter
Fluid Flow Rate (l/h) array input/ output	350	350	550
through one module	58	58	137
Tube Material (piping)	iron	iron	iron
Module Connections (series/parallel)	6 modules in parallel	6 modules in parallel	4 parallel branches of 2 in series
Collector Tilt Angle	30^o to hor.	30^o to hor.	30^o to hor.
Azimuth Faced by Array	4^o (W)	4^o (W)	4^o (W)
Reflector/ Background	white plates	none	none
Tube Orientation	E-W	E-W	E-W

Heating: The same load (district heating network) applies to all three systems.

Controls: The solar radiation level is monitored to control collector circulation pumps. Three-way valves allow for the preheating of the closed collector loop until the temperature is higher than the district heating return line. The pump connecting the heat exchangers to the district heating network was operated continuously up to March 1983; since April 1983 it has been operated only when at least one collector pump was running. Preset times prevent fast operating mode oscillations.

4.3.9. SOLARIN Industry Project, Hallau, Switzerland

Collection: Corning Cortec "D" collectors are used. They are mounted 0.5 m above the flat roof of the factory. The roof is covered by

white painted gravel. The collector plane is tilted 2^{o} from horizontal. Absorbers are tilted 30^{o} with respect to the collector plane. Shadowing effects from one absorber to the next can be important in the winter. Provision is made for testing other collectors (focusing type).

	CORNING CORTEC "D" *
No. of Modules	280
Absorber Area (m^2)	362
Aperture Area (m^2)	406.0
Array Capacitance per m^2 of aperture area (kJ/m^2 K)	9.6
Fluid Volume per m^2 of aperture area ($/m^2$)	approximately 1.4
Working Fluid	32% glycolen in water
Fluid Flow Rate (l/h)	
array input/output	approximately 10,000
through one module	7 litres
Tube Material (piping)	iron
Module Connections	7 branches in parallel; (series/parallel) 20 series per branch of 2 in parallel
Collector Tilt Angle	2^{o} to Horizontal
Azimuth Faced by Array	0^{o} South
Reflector/Background	clear roof
Tube Orientation	E-W

* Same as Corning Cortec "A" except absorbers tilted by 30o to the collector plane

Heating: Solar gains contribute to processing needs in summer and space heating in winter. Auxiliary heating is provided by existing conventional burners. Low temperature heat use is sometimes possible, for example, preheating of outside air through a heat exchanger, for space heating.

Controls: The solar radiation level is used to control the collector pump. Temperatures in different parts of the system are used to determine the position of valves and operation of pumps. A rather complicated control strategy is achieved utilizing a microprocessor in order to allow different operating options: direct use of solar, solar to storage, storage to load, choice of storage, choice of load, partial and/or combined operations. All together 12 sensors act on 3 pumps and 8 valves. Manual operation of the system is possible.

4.3.10. Evacuated Collector System Test Facility, United Kingdom

Collection: The solar circuit subsystem has a common return from all the collectors to the plant area. The flow can be directed just through or past the heating coil in the space heating storage, then

through or past the coil in the domestic hot water storage. There are two separate flow pipes from the plant area to the collectors, each serving ten collector modules.

	PHILIPS VTR 151 (15 TUBE)
Number of Modules	20
Total Aperture Area	21.6 m^2
Collector Tilt	61.5^o
Surface Azimuth	0^o
Working Fluid	30% propylene glycol-water
Fluid Flow Rate	6 l/min
Module Connection	2 rows of 10 modules

Heating: The space heating load simulator subsystem draws off water from the space heating storage at a controlled temperature. It is controlled by the system computer, according to the prevailing weather conditions. Heat is rejected to ambient through a series of heat exchangers. The present configuration of the system has a maximum water flow rate to and from the space heating storage of 0.061 /sec and an overall effectiveness of 0.31.

Domestic Hot Water Heating: The domestic hot water subsystem draws off water at either 0.15 or 0.30 /sec for a variable length of time. The flow rate and length of each draw off are selected by the computer according to the time of day. At present the total domestic hot water load is 90 l/day.

Controls: The controller starts up in the idle mode. In this mode no part of the solar system is activated and the controller continuously interrogates the collector thermostat.

As soon as the collector temperature reaches the collector thermostat set point (currently 60^oC) the controller enters the start up mode and sets the solar system in the "collector pump on" mode.

After a delay (4 minutes), the controller enters the run mode. It interrogates the two storage differential thermostats and, if a storage differential thermostat is on, the fluid in the collector circuit is directed through the heating coil in the appropriate storage.

Each storage has its own differential thermostat. The thermostats are independent of each other. A storage differential thermostat switches on when the fluid in the collector circuit before the branch to the heating coil is warmer than the water in the appropriate storage. According to which storage differential thermostats are on, the solar system operates in the "solar to domestic hot water" or "solar to space heating store" or "solar to space heating storage and domestic hot water" mode.

Each storage has a high limit thermostat. When the temperature in a storage reaches its high limit thermostat set point the controller behaves as if the appropriate storage differential thermostat were off. This function is provided by a hardware thermostat for the domestic hot water storage and by computer software for the space heating storage.

4.3.11 Colorado State University Solar House I, USA

Collection: The collectors used during the reporting period were the Philips VTR 361 collectors mounted on a test bed located south of Solar House I.

	PHILIPS
Number of Modules	24
Total Aperture Area	54.513 m^2
Collector Tilt	45^o
Surface Azimuth	0^o
Working Fluid	water
Fluid Flow Rate	37 litres/minute
Module Connections	2 rows of 12 modules each

Heating: Space heating is accomplished by use of the main load pump circulating water from storage through a water-to-air heating coil, back to the bottom of the storage tank. Simultaneously, the blower in the duct is activated, drawing air through the coil and delivering heat through duct work to the rooms. Auxiliary heating is provided by an off-peak electric thermal energy storage unit.

Off-Peak Electric Heat Storage Unit: This device is an assembly of refractory bricks contained in an insulated metal cabinet manufactured by the TPI Corporation. Electric heating elements supply heat to the bricks during the off-peak demand period at night. In normal operation, without auxiliary, air heated in the solar coil by-passes the off-peak electric unit. When auxiliary heat is needed, air leaving the solar heating coil is routed through the brick work by motorized dampers. If auxiliary space heating is needed during the night off-peak cycle, the air stream by-passes the bricks and is heated by direct resistance heating. The storage capacity is 200 kWh with 28.9 kW charging load at 208 volts, and 121 amps.

Cooling: A Carrier prototype air-cooled lithium-bromide water chiller, Model SAM-3A, was used during the reporting period. The chiller is an experimental unit under development with DOE assistance. Intended for use in arid regions, heat is rejected directly from the absorber and condenser to the atmosphere through finned tubes. Although designed for an operating temperature of 110^oC, a reasonable working range is from 80 to 120^oC. Capacity decreases with increasing ambient temperature, and decreasing hot water supply temperature. The operating COP is in the range from 0.7 to 0.8.

Domestic Hot Water: There was no DHW heating during this period when many experimental changes were made and separate components were being evaluated.

Controls: A microprocessor-based controller is used to control the system. The Carrier chiller has its own internal controls for protection against crystallization, freezing, etc. Collector flow is initiated by a temperature difference between a heat transfer block at the condenser of one collector tube and bottom of storage, but is terminated when the collector outlet fluid temperature is $1^{o}C$ greater than bottom of storage temperature. There is heat rejection to the atmosphere when collector outlet fluid temperature reaches a preset temperature. During the summer, the preset temperature was $135^{o}C$ and during winter it was lowered to $120^{o}C$.

Space heating and cooling are controlled by switch closures at the thermostat. Set temperature, although controllable in the microprocessor, is manually adjustable to suit the comfort level desired by occupants.

5. SYSTEMS EXPERIMENTS

Many of the Task VI installations run multiple experiments or experiments with multiple systems. Colorado State University Solar House I, for example, sequentially tested eight different systems during the two-year period of the previous interim report and the Knivsta District Heating Project simultaneously tests three different collector systems.

Even with multiple experiments or experiments with multiple systems, an experimental project can only directly produce results for a very limited number of design points. This limitation is due to the expense of altering the design, to the weeks or months required to thoroughly debug an altered operating and data acquisition system, and to the need for a minimum of a few weeks or perhaps even a season of data from one design to achieve a significant confidence level in the results.

The Task has also developed both simplified methods and specialized simulation models and carefully validated these models against data so that results may be extended to other design points and climates. Such extensions are included in Gemmell et al[5] and Schreitmüller[6].

The system experiments of this Task provide not only validation data sets for the eventual generalization of results but, more importantly, operating experience and data that can only be gained from a real system. Many real problems in system and subsystem design, in component selection and matching, in reliability and longevity and in controls and operating strategies can only be discovered by actual system operation. In addition, simulations of complex systems, such as the systems in this Task, inevitably have numerous unanticipated deficiencies which must be identified and corrected prior to any final validation against real data. Thus, the systems described in this section are providing important input for the improvement of real systems and for the development of realistic predictive models.

The experiments of this Task, including those covered in the previous Task VI interim report [1], are given in Table 5-1. The experiments described in the body of this report cover the period October 1981 through September 1985.

Actual climate data for the experimental period for each of the installations which have reportable data are provided in Table 5-2. These data may be compared with the long-term average climate information given in Table 3-1. The individual experiment descriptions also note whether or not the experiment period was typical.

Further details of individual experiments and systems are provided below and in the Task interim reports[80-134].

Table 5-1. Experiment Descriptors, Modes, Components and Operating Dates

COUNTRY	MODE	DATES	COLLECTOR	CHILLER	AUXILIARY	MAIN TANK	DOMESTIC HOT WATER	CONTROLS
AUSTRALIA	Space cooling	24 Dec 1982 to 20 Jan 1983	SU Evacuated collector	Yazaki WFC 600 absorption chiller	Electric instantaneous heater	3.2 m^3 corrugated copper tank outside cooled space	NA	Conventional
	Space heating	9 Jul 1983 to 26 Jul 1983	Yazaki Flat-plate collector	NA	Electric instantaneous heater	3.2 m^3 corrugated copper tank outside heated space	NA	Conventional
	Space heating	28 Aug 1983 to 28 Sep 1983	SU Evacuated collector	NA	Electric instantaneous heater	3.2 m^3 corrugated copper tank outside heated space	NA	Conventional
	Space cooling	1 Nov 1983 to 30 Apr 1984	SU Evacuated collector	Yazaki WFC 600 absorption chiller	Electric instantaneous heater	3.2 m^3 corrugated copper tank outside cooled space	NA	Conventional
	Space heating	1 May 1984 to 30 Oct 1984	SU Evacuated collector	NA	Electric instantaneous heater	3.2 m^3 corrugated copper tank outside heated space	NA	Conventional
	Space cooling	1 Nov 1984 to 31 Mar 1985	SU Evacuated collector	Yazaki WFC 600 absorption chiller	Electric instantaneous heater	3.2 m^3 corrugated copper tank outside cooled space	NA	Conventional
CANADA	Industrial water	1 Apr 1981 to 30 Apr 1982	Solartech	NA	Gas fired burner	5.7 m^3 concrete lined steel tank	NA	Conventional
	Industrial water	1 May 1982 to 31 Dec 1982	Solartech	NA	Gas fired burner	5.7 m^3 concrete lined steel tank	NA	Conventional
	Industrial water	1 Jan 1983 to 31 Dec 1983	Solartech	NA	Gas fired burner	5.7 m^3 concrete lined steel tank	NA	Conventional
	Industrial water	1 Jan 1984 to 31 Dec 1984	Solartech	NA	Gas fired burner	5.7 m^3 concrete lined steel tank	NA	Conventional
CEC	Space cooling	15 July to 15 Dec 1982	Sanyo and Philips VTR261	ARKLA WF36	None	50 m^3 concrete	NA	Conventional
	Space cooling	11 May 1983 to 23 Sep 1983	Sanyo and Philips VTR261/ VTR361	ARKLA WF36	None	50 m^3 concrete	NA	Conventional
FEDERAL REPUBLIC OF GERMANY	DHW	Mar to May and Aug 1979	Corning	NA	Electric and/or central heat storage	1.5 m^3 cylindrical tank outside heated space	Internal HX two tank	Microprocessor with conventional back-up
	Space heating	Mar to May and Aug 1979	Philips MK IV	NA	Oil burner	15 m^3 cylindrical tank outside heated space	Internal HX two tank	Microprocessor with conventional back-up
	DHW	June, July Philips Sept-Dec 1979	MK IV	NA	Electric and/or central heat storage	1.5 m^3 cylindrical tank outside heated space	Internal HX two tank	Microprocessor with conventional back-up
	Space heating	June, July Sept-Dec 1979	Corning	NA	Oil burner	15 m^3 cylindrical tank outside heated space	Internal HX two tank	Microprocessor with conventional back-up
	DHW	Jan to May 1980	Philips MK IV	NA	Electric and/or central heat storage	1.5 m^3 cylindrical tank outside heated space	Internal HX two tank	Microprocessor with conventional back-up
	Space heating	Jan to May 1980	Corning	NA	Oil burner	15 m^3 cylindrical tank outside heated space	Internal HX two tank	Microprocessor with conventional back-up
	DHW	June to Dec 1980	Corning	NA	Electric and/or central heat storage	1.5 m^3 cylindrical tank outside heated space	Internal HX two tank	Microprocessor with conventional back
	Space heating	June to Dec 1980	Philips MK IV	NA	Oil burner	15 m^3 cylindrical tank outside heated space	Internal HX two tank	Microprocessor with conventional back-up
	DHW	Jan to Dec 1981	Corning	NA	Electric and/or central heat storage	1.5 m^3 cylindrical tank outside heated space	Internal HX two tank	Microprocessor with conventional back-up
	Space heating	Jan to May 1981	Philips MK IV	NA	Oil burner	15 m^3 cylindrical tank outside heated space	Internal HX two tank	Microprocessor with conventional back-up
	Space heating	Jan to May 1982	Philips MK IV Corning	NA	Oil burner	15 m^3 cylindrical tank outside heated space	Internal HX two tank	Microprocessor with conventional back-up
	DHW	Jan to May 1982	Corning Philips/Stieble	NA	Electric and/or central heat storage	1.5 m^3 cylindrical tank outside heated space	Internal HX two tank	Microprocessor with conventional back-up
	DHW	June 1982 to May 1983	Philips/Stieble	NA	Electric and/or central heat storage	1.5 m^3 cylindrical tank outside heated space	Internal HX two tank	Microprocessor with conventional back-up
	Space heating	June 1982 to May 1983	Corning	NA	Oil burner	15 m^3 cylindrical tank outside heated space	Internal HX two tank	Microprocessor with conventional back-up

Table 5-1 (cont).

COUNTRY	MODE	DATES	COLLECTOR	CHILLER	AUXILIARY	MAIN TANK	DOMESTIC HOT WATER	CONTROLS
NETHERLANDS	Space heating and DHW	Sept 1982 to Sept 1983	Philips VTR-261	NA	Gas fired burner	3.7 m^3 multi-featured tank in heated space	No storage, but HX in main tank	MP-87A microcomputer
SWEDEN	District, space heating and DHW	Aug 1981 to Dec 1981	GE	NA	Biomass fired plant	NA	NA	Conventional differential thermostats
	District, space heating and DHW	Aug 1981 to Dec 1981	O-I	NA	Biomass fired plant	NA	NA	Conventional differential thermostats
	District, space heating and DHW	Aug 1981 to Dec 1981	Philips VTR-261	NA	Biomass fired plant	NA	NA	Conventional differential thermostats
	District, space heating and DHW	Feb 1983 to Dec 1983	Scand. Solar HT	NA	Biomass fired plant	NA	NA	Conventional differential thermostats
	District, space heating and DHW	May 1982 to Dec 1983	Technotherm HT	NA	Coal fired plant	NA	NA	Conventional differential thermostats
	District, space heating and DHW	May 1982 to Dec 1983	Philips VTR 141	NA	Coal fired plant	NA	NA	Conventional differential thermostats
	District, space heating and DHW	May 1982 to Dec 1983	Granges Aluminum	NA	Coal fired plant	NA	NA	Conventional differential thermostats
	District, space heating and DHW	May 1982 to Dec 1983	General Electric TC 100	NA	Coal fired plant	NA	NA	Conventional differential thermostats
	District, space heating and DHW	April 1983 to Dec 1983	Scand. Solar HT	NA	Coal fired plant	NA	NA	Conventional differential thermostats
SWITZERLAND	District, space heating and DHW	July 1982 to March 1984	Corning	NA	Gas fired plant	NA	NA	Conventional control
	District, space heating and DHW	Apr 1983 to March 1984	Sanyo	NA	Gas fired plant	NA	NA	Conventional control
UK	Space heating and simulated DHW	Sept 1981 to June 1982	Philips VTR-141	NA	NA	1.4 m^3 vertical cylindrical steel tank internal HX lower half	0.12 m^3 internal HX in cylindrical copper tank	Computer, simulated fan coil, to 20 C
	Space heating and simulated DHW	June 1982 to Aug 1982	Philips VTR-141	NA	NA	1.4 m^3 tank, internal HX coil from top to bottom	0.12 m^3 internal HX cylindrical copper tank	Computer, simulated fan coil, to 35 C
	Space heating and simulated DHW	Oct 1982 to May 1983	Philips VTR-141	NA	NA	1.4 m^3 tank, internal HX coil from top to bottom	0.12 m^3 internal HX cylindrical copper tank	Computer, simulated fan coil, to 20 C
USA	Space heating and DHW	5 Feb 1980 to 6 Mar 1980	Miromit	NA	Electric off-peak thermal storage	4.4 m^3 rectangular steel tank in cooled space	External HX, two tank electric auxiliary	ATOP, MECA I and conventional
	Space cooling and DHW	10 June 1980 to 30 July 1980	Miromit	Arkla WF36 LiBr absorption	Electric boiler	4.4 m^3 rectangular steel tank in cooled space	External HX, two tank electric auxiliary	Conventional
	Space cooling and DHW	11 Aug 1980 to 8 Sept 1980	Philips VTR-141	Arkla WF36 LiBr absorption	Electric boiler	4.4 m^3 rectangular steel tank in cooled space	External HX, two tank electric auxiliary	Conventional
	Space cooling and DHW	18 Sept 1980 to 30 Sept 1980	Philips VTR-141	Arkla XWF3600 LiBr absorption	Electric boiler	4.4 m^3 rectangular steel tank in cooled space	External HX, two tank electric auxiliary	Conventional
	Space heating and DHW	8 Nov 1980 to 14 Jan 1981	Philips VTR-141	NA	Electric boiler	4.4 m^3 rectangular steel tank in heated space	External HX, two tank electric auxiliary	Conventional
	Space heating and DHW	14 Jan 1981 to 1 Feb 1981	Philips VTR-141	NA	Electric boiler	4.4 m^3 rectangular steel tank in heated space	External HX, single tank electric auxiliary	Conventional
	Space heating and DHW	12 Feb 1981 to 31 March 1981	Philips VTR-141	NA	Electric off-peak thermal storage	4.4 m^3 rectangular steel tank in heated space	External HX, single tank electric auxiliary	ATOP, MECA I
	Space cooling and DHW	1 July 1981 to 17 Sept 1981	Philips VTR-141	Arkla XWF3600 LiBr absorption	Electric boiler	4.4 m^3 cylindrical steel pressurized tank out cooled space	Internal HX, single tank electric auxiliary	MECA II
	Space heating	1 Dec 1982 to 19 Apr 1983	Philips VTR-361	NA	Electric off-peak	4.4 m^3 pressurized water outside heated space	None	Microprocessor
	Space cooling	1 Sept 1983 to 14 Oct 1983	Philips VTR-361	Carrier air-cooled	Electric boiler	3.6 m^3 HDPE 4.4 m^3 water	None	Microprocessor

TABLE 5-2. CLIMATE DATA FOR EXPERIMENTAL PERIODS

COUNTRY	EXPERIMENT DATES	DEGREE DAYS	AVERAGE DAILY INSOLATION (MJ/m2)	AVERAGE DAILY AMBIENT TEMP(C)	AVERAGE DAILY MAX TEMP (C)	AVERAGE DAILY MIN TEMP (C)
Australia	24 Dec 82 to 20 Jan 83	NA	20.22	23.8	35.0	17.8
Australia	9 July 83 to 26 July 83	53	13.98	14.7	15.1	7.9
Australia	28 Aug 83 to 28 Sept 83	36	18.53	17.0	21.8	12.4
Australia	1 Nov 83 to 30 Apr 84	NA	17.13	20.6	23.9	17.2
Australia	1 May 84 to 31 Oct 84	528	12.72	14.3	18.4	10.9
Australia	1 Nov 84 to 31 Mar 85	NA	21.79	21.0	24.7	18.7
Canada	1 April 81 to 30 April 82					
Canada	1 May 82 to 31 Dec 82	NA	14.0	8.8	NA	NA
Canada	1 Jan 83 to 31 Dec 83	NA	12.7	3.9	NA	NA
Canada	1 Jan 84 to 31 Dec 84	NA	13.5	4.2	NA	NA
CEC	July 82 to Sept 82	---	17.0	20.5	25.7	15.7
CEC	May 83 to Sept 83	---	19.0	20.7	26.2	15.8
FRG	March to May and Aug 79	NA	12.5	12.9	---	---
FRG	March to May and Aug 79	NA	12.5	12.9	---	---
FRG	June, July, Sept to Dec 79	NA	11.2	12.5	---	---
FRG	June, July, Sept to Dec 79	NA	11.2	12.5	---	---
FRG	Jan to May 80	NA	9.4*	6.2	---	---
FRG	Jan to May 80	NA	9.9	6.2	---	---
FRG	June to Dec	80	NA	11.9	11.7	------
FRG	June to Dec	80	NA	11.2*	11.7	------
FRG	Jan to Dec 81	NA	10.7	9.8	---	---
FRG	Jan to Dec 81	NA	10.7	9.8	---	---
FRG	Jan to May 82	2891	11.8	10.3	---	---
FRG	Jan to May 82	NA	11.8	10.3	---	---
FRG	June 82 to May 83	NA	10.9	10.6	---	---
FRG	June 82 to May 83	2798	10.9	10.6	---	---

* Collector was periodically shaded

TABLE 5-2 (cont).

COUNTRY	EXPERIMENT DATES	DEGREE DAYS	AVERAGE DAILY INSOLATION (MJ/m2)	AVERAGE DAILY AMBIENT TEMP (C)	AVERAGE DAILYMAX TEMP (C)	AVERAGE DAILY MIN TEMP (C)
Netherlands	Planned (Interim Report)					
Sweden	Aug 81 to Nov 83	NA	9.9	5.7	NA	NA
Sweden	Aug 81 to Dec 83	NA	9.9	5.7	NA	NA
Sweden	Aug 81 to Dec 83	NA	9.9	5.7	NA	NA
Sweden	Feb 83 to Dec 83		10.8	6.0	NA	NA
Sweden	May 82 to Dec 83		10.4	6.6	NA	NA
Sweden	May 82 to Dec 83		10.4	6.6	NA	NA
Sweden	May 82 to Dec 83		10.4	6.6	NA	NA
Sweden	May 82 to Dec 83		10.4	6.6	NA	NA
Sweden	April 83 to Dec 83		11.5	8.0	NA	NA
Switzerland	July 82 to Mar 84	4498	12.0	12.4	29.9	-3.6
Switzerland	April 83 to Mar 84	2795	13.4	13.2	29.9	-3.3
UK	1 Oct 81 to 2 June 82	326*	3.4*	4.84*	NA	NA
UK	Jun 82 to Aug 82	112	14.6	16.0	NA	NA
UK	Oct 82 to May 83	1596	7.6	7.2	NA	NA
USA	5 Feb 80 to 8 Mar 80	1082	17.5	-1.5	7.4	-6.7
USA	10 June 80 to 30 July 80	360	21.0	21.7	30.6	13.5
USA	11 Aug 80 to 8 Sept 80	111	19.8	20.4	27.8	11.5
USA	18 Sept 80 to 30 Sept 80	13	25.7	16.7	26.0	8.2
USA	8 Nov 80 to 14 Jan 81	1813	14.2	3.1	11.0	-4.7
USA	14 Jan 81 to 1 Feb 81	568	17.5	0.9	8.9	-7.7
USA	12 Feb 81 to 31 Mar 81	1245	18.9	3.2	10.8	-3.8
USA	1 July 81 to 17 Sept 81	382	19.0	20.8	28.3	12.9
USA	1 Dec 82 to 19 April 83	1220	14.57	2.1	13.6	-9.1
USA	1 Sept 83 to 14 Oct 83	NA	21.36	15.2	23.8	6.0

* Data relates to period 1 October 1981 to 23 December 1981.

5.1 SYDNEY UNIVERSITY SOLAR HEATING AND COOLING SYSTEM SYDNEY, AUSTRALIA

5.1.1 24 December 1982 to 20 January 1983

Sydney University evacuated collectors were used during the entire cooling season of 1982/1983 to power the Yazaki absorption cooling machine. Since data acquisition was not yet fully automated during November 1983 to April 1983, the data shown is restricted to a few weeks, where system information could be stored on cassette tapes.

Manual records from heat meters and integrated data logger information confirm that the system performed very well as was later indicated during the rest of the cooling period.

A system diagram of the space cooling mode without chilled water storage is given in Figure 5-1.

5.1.2 July 9 to July 26, 1983

The space heating period in Sydney covers the months May through September. System operation and monitoring during this period was frequently interrupted by minor system modifications and maintenance work, sensor calibration, and debugging of computer software.

During the first part of the heating season Yazaki flat-plate collectors were used.

5.1.3 August 28 to September 28, 1983

One month's experimental data was obtained during the latter part of the heating season using the Sydney University evacuated tubular collectors. The system diagram for the heating mode is given in Figure 5-2.

5.1.4 November 1 1983 to April 30, 1984

Sydney University evacuated collectors were being monitored during this reporting period. The system operated smoothly and reliably. Unfortunately, the data acquisition system was not fully reliable.

5.1.5 May 1 to October 31, 1984

Sydney University evacuated collectors were used for the supply of energy for heating between May 1, 1984 and October 31, 1984. Relatively small loads resulted in frequent collector boiling and necessitated energy dumping.

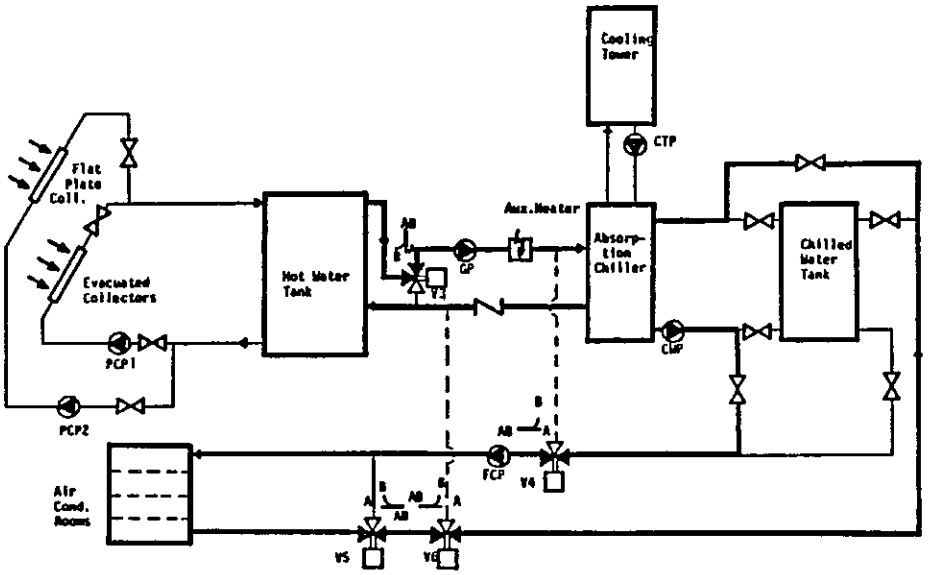

Figure 5-1. System Schematic - Cooling Mode, Sydney University, Australia.

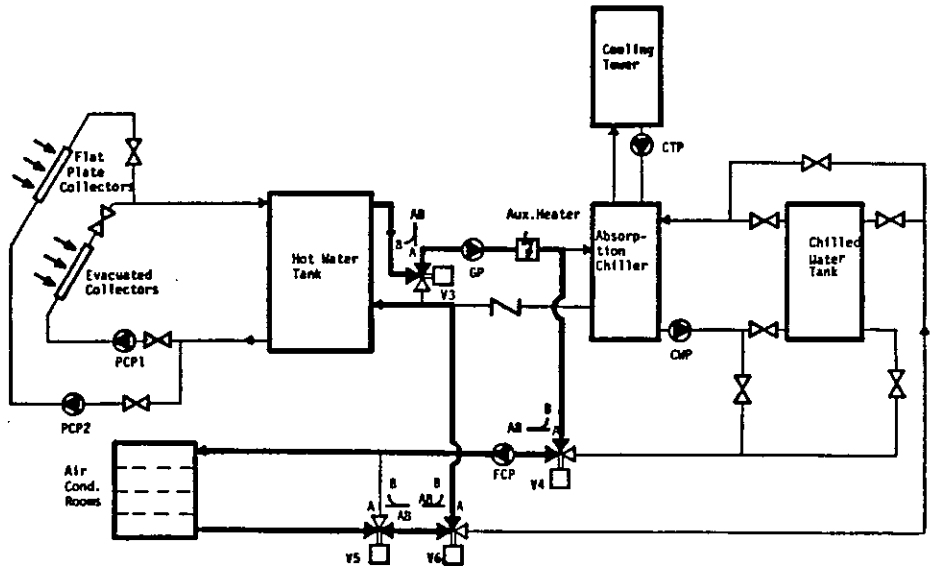

Figure 5-2. System Schematic - Heating Mode, Sydney University, Australia.

5.1.6 November 1, 1984 to March 31, 1985

There were no system operation problems worthwhile noting during the 1984/85 cooling season. The Sydney University evacuated collectors continued to perform very well. Insulation of pipes is deteriorating rather rapidly which has some effect on the overall system performance. The Yazaki absorption chiller worked maintenance free, but COP's were rather poor.

5.2 MOUNTAIN SPRING BOTTLE WASHING FACILITY, EDMONTON, CANADA

The objective is to determine areas in which costs in future installations may be reduced or eliminated. This is done by replacing or upgrading subsystem components where practical, or by simulation to maximize performance. A system diagram is given in Figure 5-3.

5.2.1 1 May 1982 to 31 December 1982, 1 January 1983 to 31 December, 1983

The collector loop has two temperature sensors to monitor and control the system. One is mounted in a wall near the bottom of the solar tank and the other is located inside a specially equipped control solar collector. The collector operates in two modes:

Normal operation: The collector turns on at a ΔT of $3^{o}C$.

Overtemperature: If the solar tank temperature is greater than $95^{o}C$, the solar collection loops shuts off. If the collector control temperature exceeds $150^{o}C$, the operation of the collection loop ceases. This is to prevent the breakage of hot tubes by thermal shock. There are two modes of operation for the heat transfer loop. First, if heat is demanded by the soaker tank and the accumulator temperature is $2.5^{o}C$ greater than the inlet temperature to the heat exchanger, the circulation pump between the accumulator and the heat exchanger is activated, thus initiating heat transfer. The system turns off at a ΔT of $1.5^{o}C$. Second, if the accumulator temperature reaches $90.5^{o}C$ and if no heat is demanded by the soaker tank, (i.e., weekends), both the soaker tank pump and the heat exchanger circulation pump are activated in order to dump heat into the 14,000 litre soaker tank. This effectively increases the storage capacity of the system by 14000 litres.

5.3 ISPRA SOLAR HEATED AND COOLED LABORATORY, COMMISSION OF EUROPEAN COMMUNITIES

The purpose of the experiments is to study the operation and understand the performance of a solar cooling system with evacuated tubular collectors under the climatic conditions of Ispra.

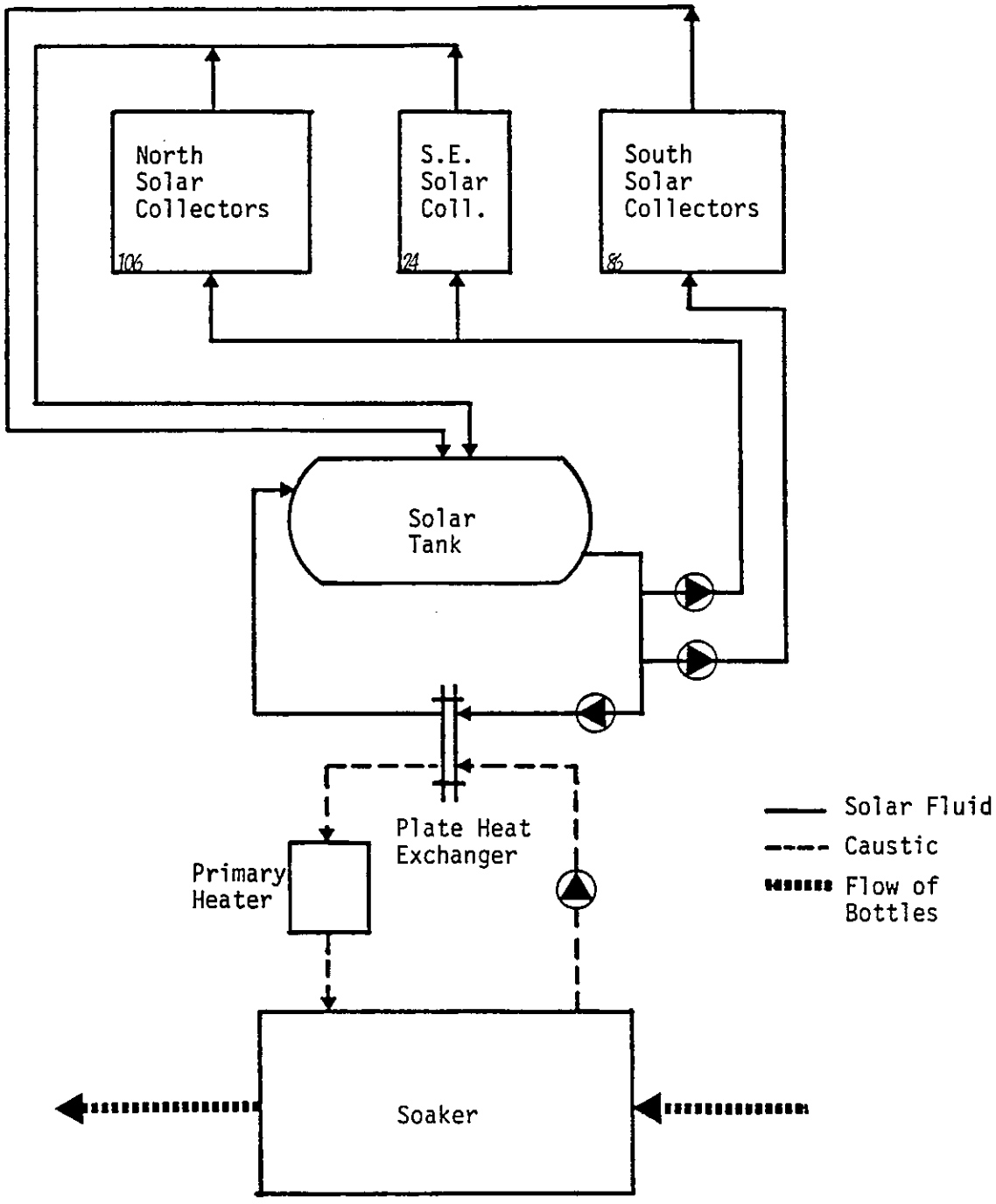

Figure 5-3 System Schematic, Mountain Spring Bottle Washing Facility, Edmonton, Canada.

5.3.1 15 July 1982 to 15 September 1982

The system is schematically shown in Figure 5-4. It consists essentially of

- o 29.04 m^2 of Sanyo evacuated tube collectors (two arrays of 6 modules);
- o 17.9 m^2 of Philips evacuated tube collectors;
- o a hot water storage of 0.5 m^3;
- o a $LiBr/H_2O$ absorption chiller;
- o a large storage of chilled water;
- o fan-coil units

The collector array D, three modules of the Philips VTR 361, were not utilized in this experiment. The collector subsystem has two differential controllers, one for the Sanyo collectors and one for the Philips collecftors. The collector pump is switched on if one of the collector temperatures is 5^oC higher than the bottom of the hot storage. Simultaneously, the corresponding motorized valve is opened. When the other collector array starts operating the pump will change speed and the appropriate valve will be opened.

When the temperature at the outlet of one system is less than 2^oC higher than the temperature at the bottom of the hot storage, the corresponding motorized valve closes the circuit and the pump will change speed. When both the valves are closed, the pump stops.

The use of a large chilled water storage tank permits the chiller to be operated continuously if there is sufficient sunshine. This allows for a rather simple control strategy. The chiller is started when the temperature in the hot storage reaches 85^oC. It is stopped when the temperature in the buffer drops below 77^oC.

A room thermostat switches on the pump of the distribution system when the room temperature reaches 23^oC. The pump is stopped when the temperature drops below 22.5^oC.

A proportional controller regulates the temperature at the outlet of the fancoil units as a function of the outdoor temperature.

5.3.2 11 May 1983 to 23 September 1983

This experiment is essentially the same as the 15 July 1982 to 15 September 1982 experiment. The only difference is that the Philips VTR 361 array D, was installed and operating.

5.4 SOLARHAUS FREIBURG, FEDERAL REPUBLIC OF GERMANY

Table 5-1 shows the experiments in the period from January 1982 to May 1983 when the following solar energy systems were supplying the

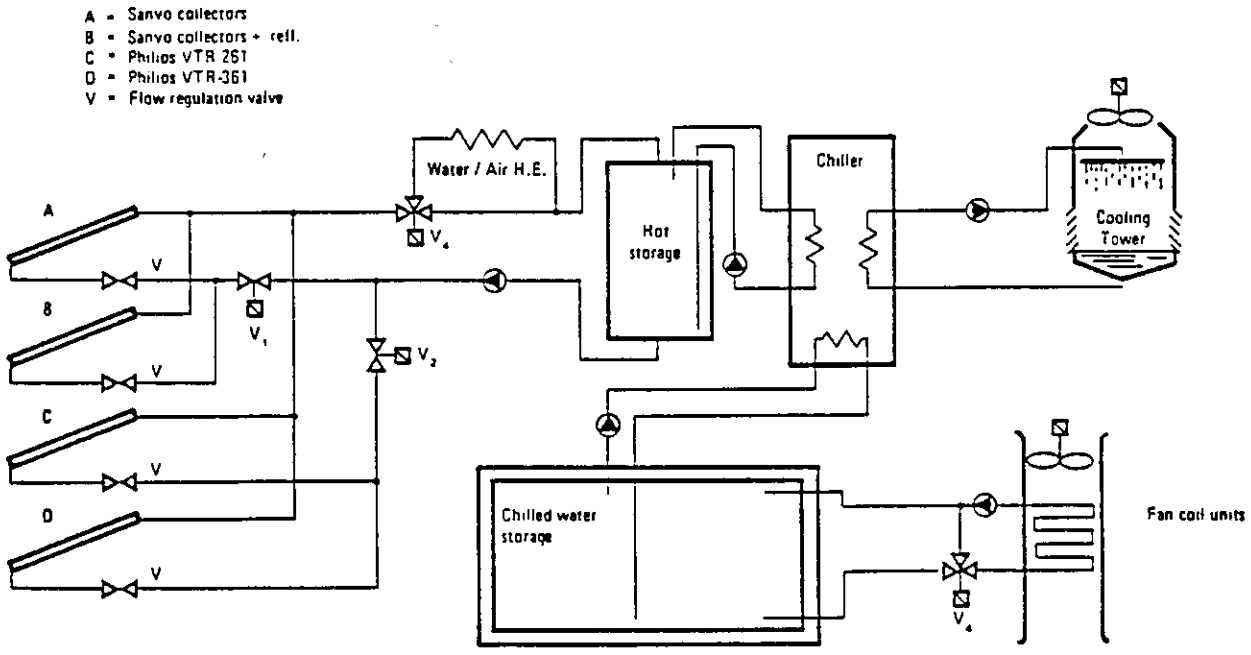

Figure 5-4 Schematic View of the Solar Cooling System at the Ispra Solar Laboratory. DHW and heating load in the

SOLARHAUS FREIBURG installation. The system is schematically shown in Figure 5-5.

Philips MK IV - Heating System:	January 1982 to May 1982
Corning Glass - DHW System:	January 1982 to May 1982
Philips VTR-261/Stiebel-Eltron DHW System:	June 1982 to May 1983
Corning Glass - Heating System:	June 1982 to May 1983

Except for the replacement of the Philips IV collectors with the Philips/Stiebel-Eltron collectors, the experiments are identical with the experiments in preceding periods.

As in the preceding report, primary experiments are based on yearly periods in order to give meaningful performance parameters.

There was a load-oriented analysis in 1982, with the operating periods of the Philips IV and the Philips/Stiebel-Eltron collectors being differentiated. The Philips MK IV collectors were exchanged for the Philips/Stiebel Eltron collectors in 1982.

The next experiment ia a load-oriented DHW and heating system analysis in the annual operating period of the Philips/Stiebel-Eltron collector from June 1982 to May 1983.

The effects of modified control-strategies (one-storage tank or two-storage tank strategies) cannot be addressed in the experimental data, because system performance is affected by too many stochastic influences (e.g., weather, load, season etc.).

5.5 EINDHOVEN TECHNOLOGICAL UNIVERSITY SOLAR HOUSE, THE NETHERLANDS

The system investigated in the Solar House at EUT is schematically shown in Figure 5-6 and encompasses:

- a collector array consisting of 23 Philips VTR 261 collectors with an array aperture of 47.15 m^2
- a storage vessel with a working mass of 3700 kg and a heat capacity of 15.54 MJ
- variable collector flow
- a real load of a spacious detached dwelling in Dutch climatic conditions.

The objectives are

- to gain performance and operational data for the Philips VTR 261 evacuated tubular collectors under real conditions
- to establish a well validated basis for the comparison of conventional and ETC system performances

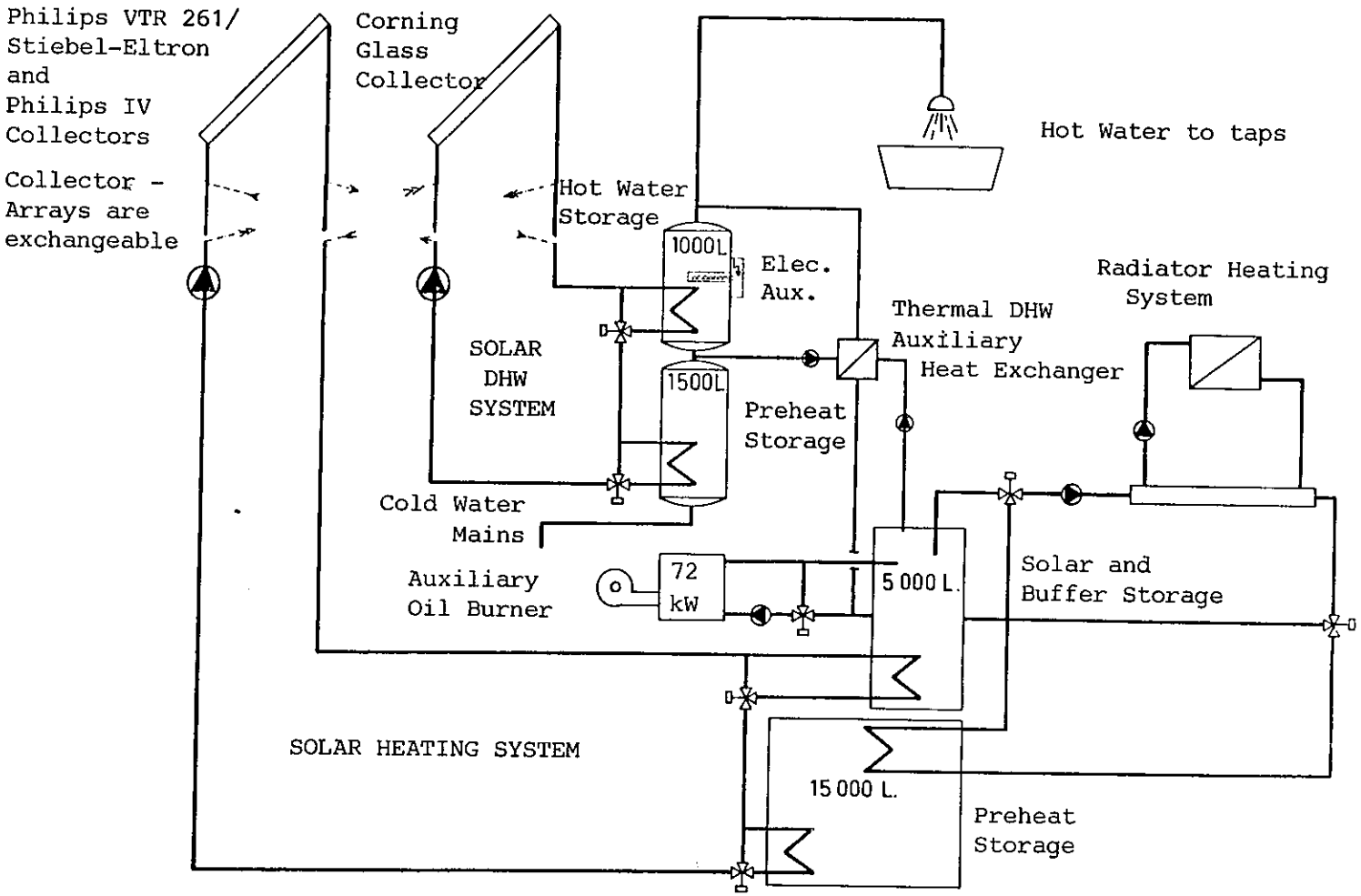

Figure 5-5. Solar System Schematic for Solarhaus Freiburg.

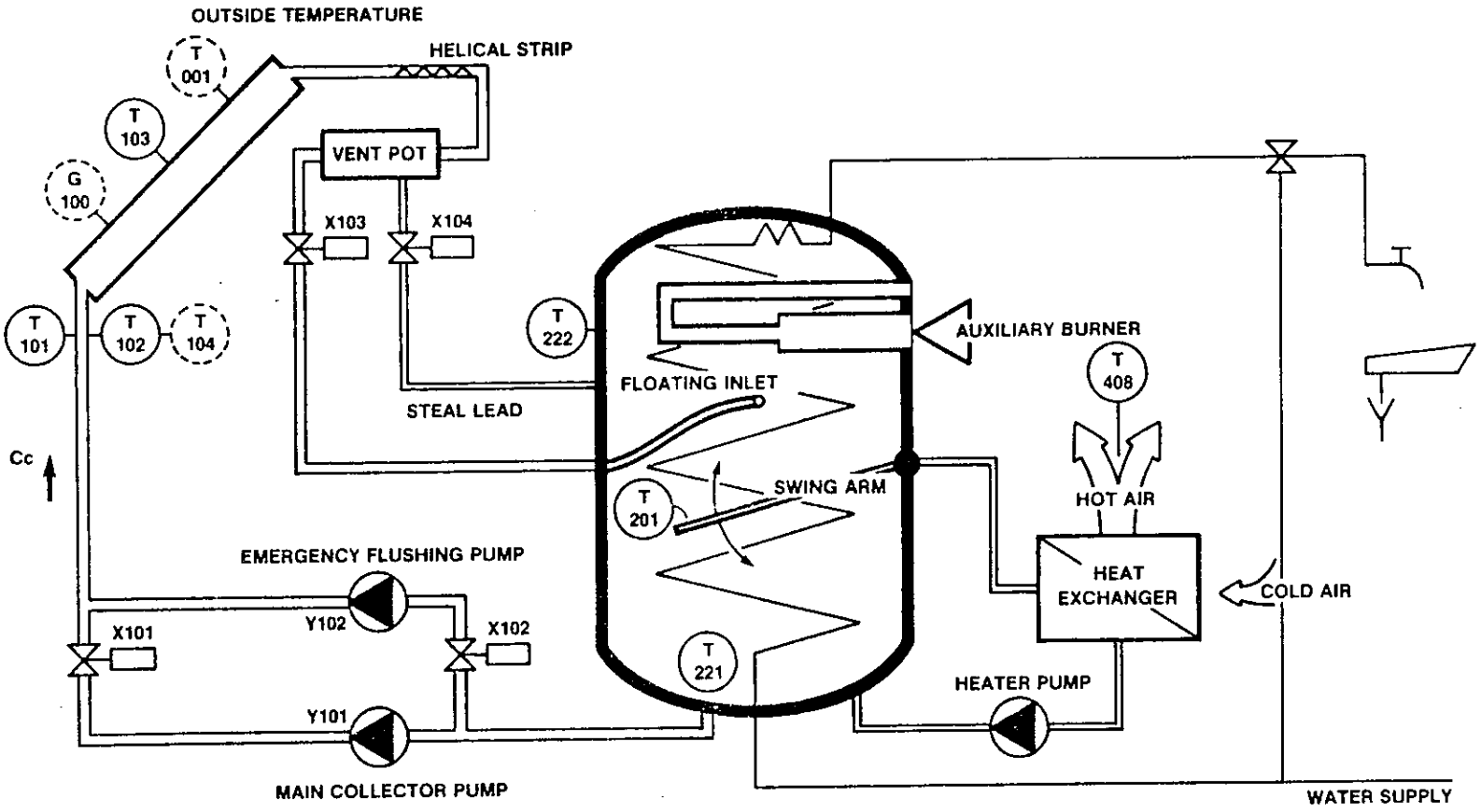

Figure 5-6. System Schematic for the Eindhoven University of Technology Solar House, The Netherlands.

- o to prove the novel control strategy, which implies roughly equal daily throughputs for the collector loop and the load circuits
- o to test the concept of the integrated heater-stratified storage designs.

The monitoring system encompasses 29 temperature probes, 6 mode indicators, a pyronometer and a wind speed and direction meter. Data are taken each minute and subsequently processed to 5 minute averages and daily and weekly performance records. Final yearly performance calculations and collector characterization are executed with the EUT Burroughs 7900 computer. Occasionally, special measuring equipment is installed to obtain detailed information on the behavior of components.

Control Strategy:

- o Roughly equal throughputs for the collector loop and the load circuits
- o Collector flow dependent on the irradiation
- o Using the stratified storage, the temperature of the water delivered to the air heater is dependent on the ambient temperature.

Protection:

- o Freeze protection by means of flushing the collector array
- o Protection against super-heating by boiling dry

5.6 KNIVSTA DISTRICT HEATING SYSTEM, KNIVSTA, SWEDEN

5.6.1 Basic Experiments

The long-term goal of Swedish solar energy activities is to reduce Sweden's oil dependence. The main purpose of the Knivsta project is to gain experience in handling this new technology and to find out how the collector systems work outside the laboratory environment. The three solar energy systems all operate as shown on Figures 5-7 and 5-8. Four different experiments have been conducted, corresponding to four different collectors.

Each collector type has its own closed system with expansion tanks and circulation pumps. The heat from each solar array is transferred to the return pipes of the district heating system by means of flat-plate heat exchangers. Circulation in the district heating system is powered by the main pump in the district heating network.

The pumps in the solar circuit have worked continuously whereas the flow on the district heating side is regulated by a motor valve which opens or closes at a $4^{o}C$ difference between the solar and district heating circuits. There are also other possibilities to control the pumps of the solar collector circuits. For example, General Electric

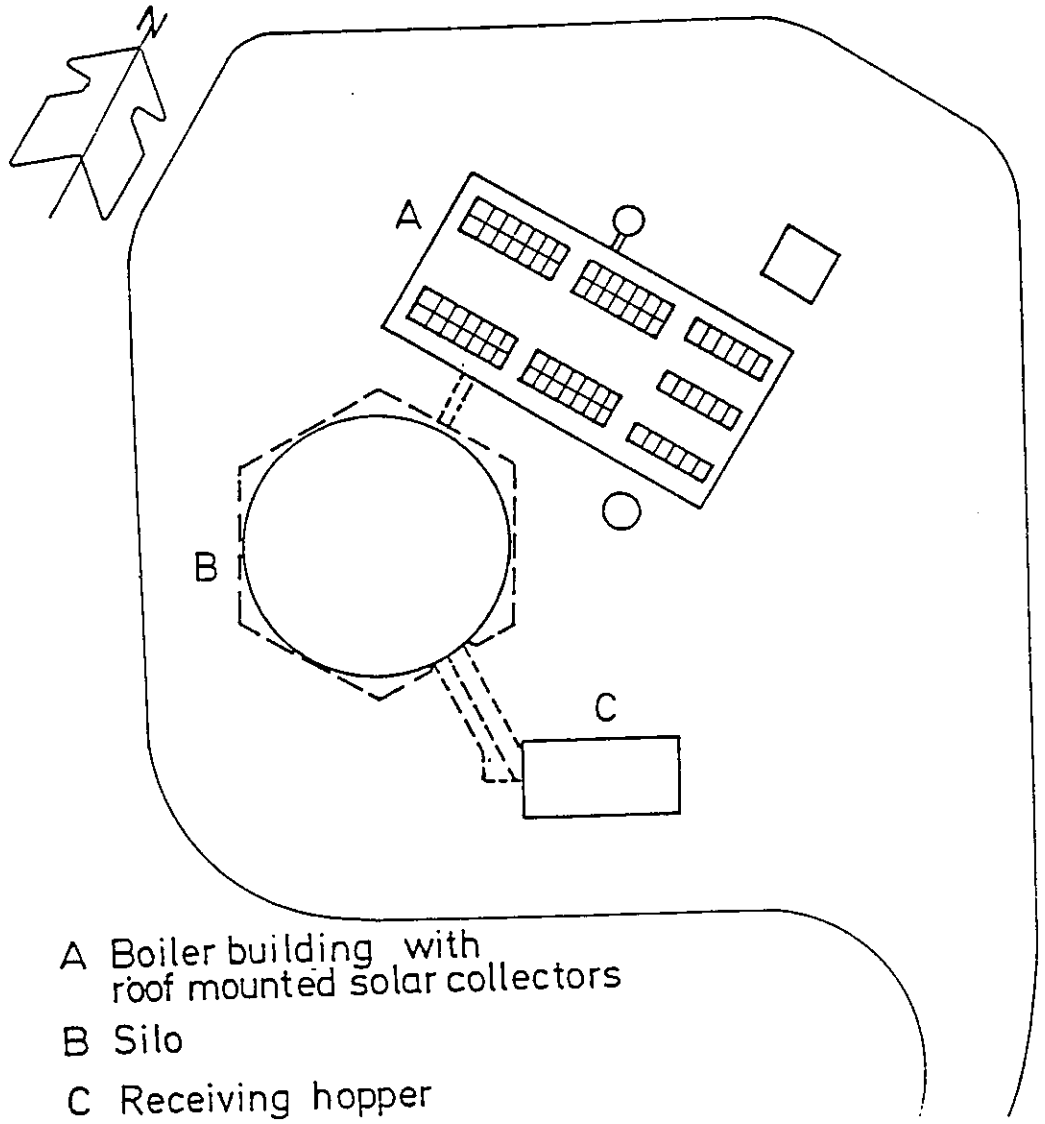

SOLAR COLLECTOR INSTALLATION

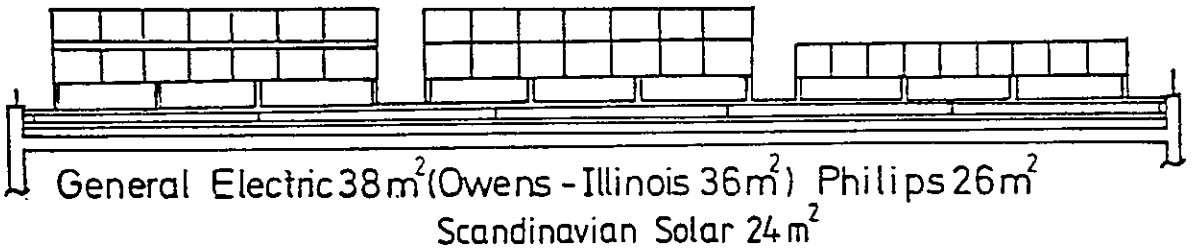

Figure 5-7. Layout of the Knivsta Plant, Knivsta, Sweden.

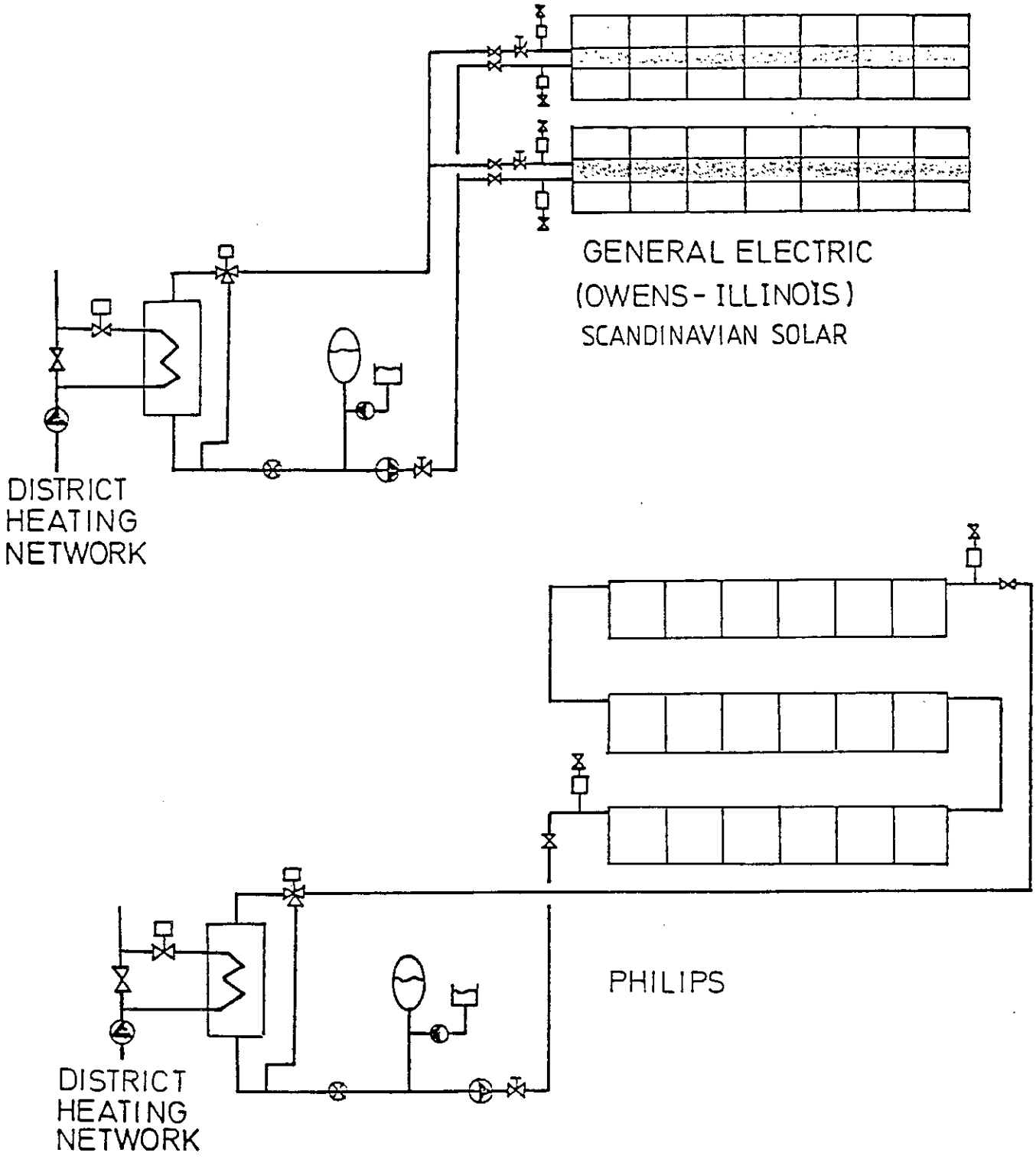

Figure 5-8. Schematic of the Installation in the Knivsta Plant, Knivsta, Sweden. makes a controller that integrates

solar radiation over time. Fast cycling due to short duration cloudiness may be avoided by choosing a suitable integration period.

In the Philips solar circuit the pump can be started and stopped at an adjustable temperature difference between the solar collector and district heating temperatures.

It is also possible that the pumps may be controlled by a timer. The pumps may then, for example, work continuously for a certain time during the day.

In January 1983 the Owens Illinois collectors were exchanged for flat-plate collectors from Scandinavian Solar. This makes the comparison between evacuated collectors and flat-plate collectors possible.

5.6.2 Related Experiments

One of the technical experiments to be conducted is an investigation into the effects of heat capacity. The Knivsta installation comprises systems with both high and low heat capacity and hence its role and impact on energy production in large collector fields can be studied readily. Both measurements and studies are planned.

One experiment was conducted in September 1981 when the system operation was changed from differential temperature control to continuous operation. This meant that the solar collectors were always heated with the district heating water to avoid frost problems.

5.7 THE SÖDERTÖRN DISTRICT HEATING PROJECT, SÖDERTÖRN, SWEDEN

5.7.1 Basic Experiment

The demonstration plant allows for operating experience to be gained with larger solar collector fields using different collector types. For this reporting period, 7 subgroups are under operation, the size of each unit being between 120 and 216 m^2. There are two ETC collectors, four selective surface flat-plate collectors and one flat-plate collector with an evacuated glass tube cover. A location map of the systems in the installation is given in Figure 5-9.

Each unit is separately connected to the district heating return pipe by means of a heat exchanger. Each solar system is operated with a water-glycol mixture. Figure 5-10 shows a simplified scheme of the solar collector circuit. All circulation components (shunts, pumps, heat exchanger, valves) are installed in a small (wintersafe) operating hut. Five experiments are presented corresponding to long-term operation of five different collectors.

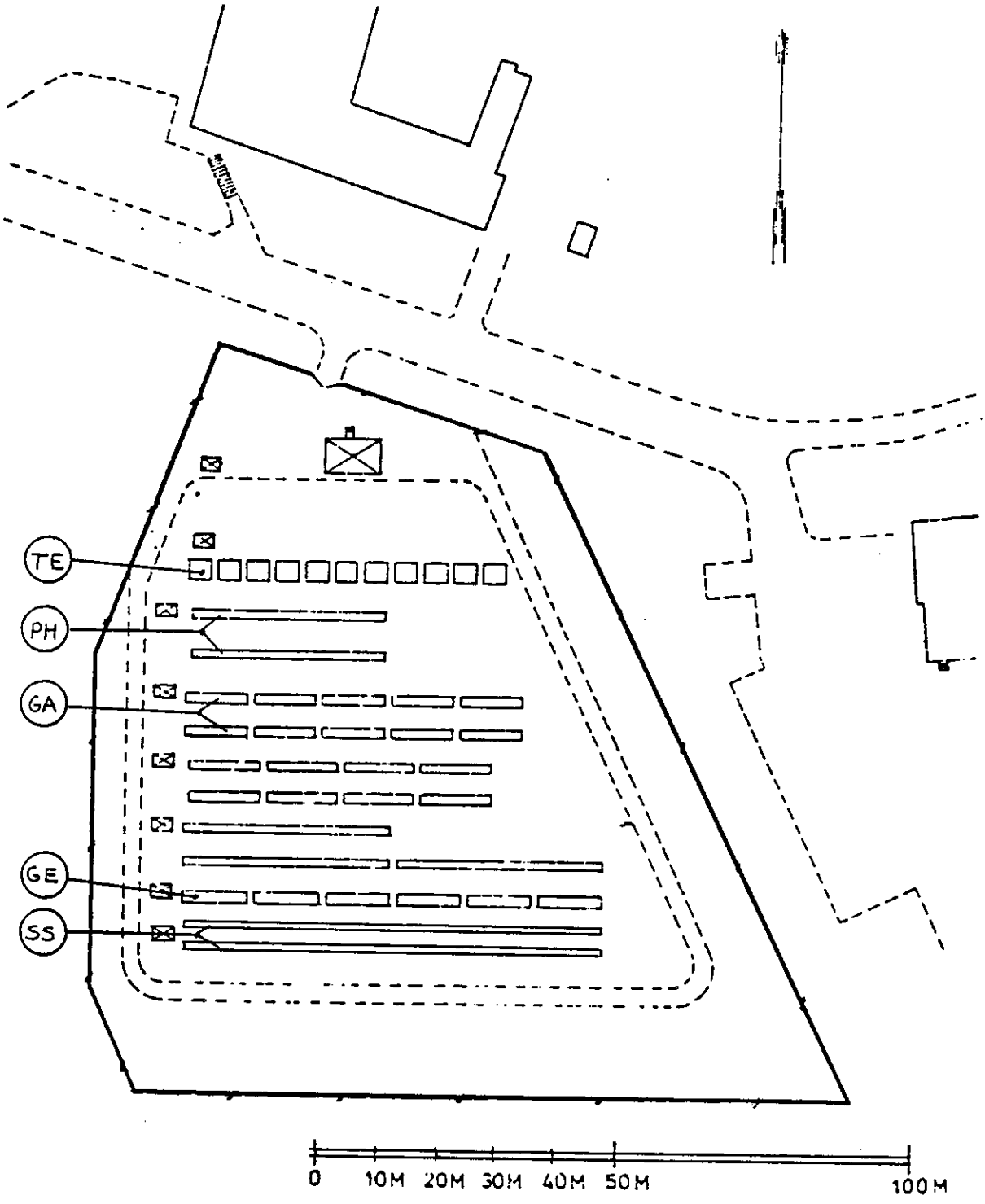

Figure 5-9. Layout of the Södertörn District Heating Project, Södertörn, Sweden.

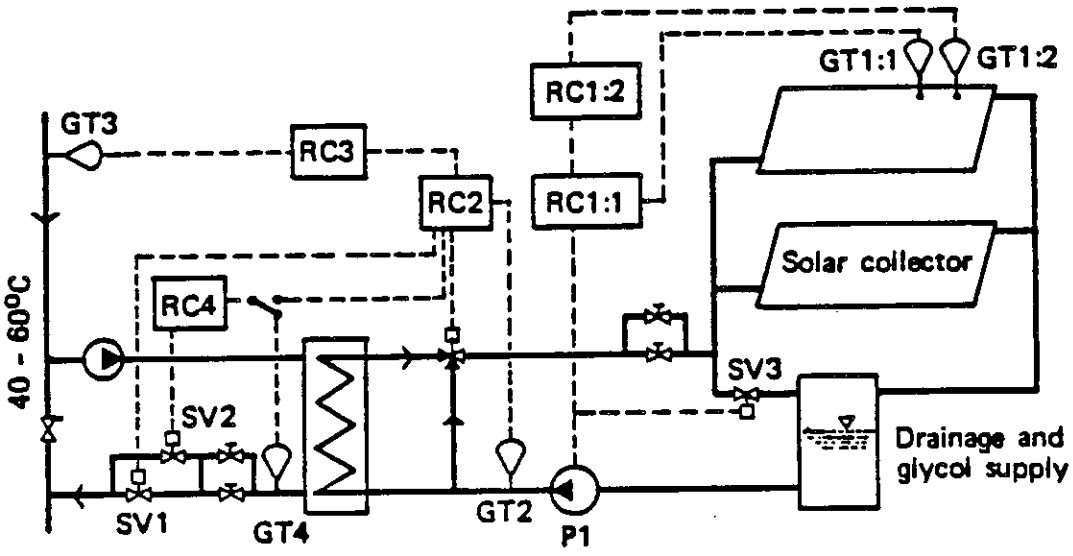

Figure 5-10. Schematic for One of the Seven Solar Collector Subunits at the Södertörn Installation, Södertörn, Sweden.

5.7.2 Related Experiments

The effect of back irradiation onto the Philips array is investigated and the influence of the operating ΔT on a longterm basis is tested by changing the ΔT each year. The system dynamic effects on a daily basis are investigated by preheating the collector arrays for short periods and comparing the results with normal operation.

5.8 SOLARCAD DISTRICT HEATING PROJECT, GENEVA, SWITZERLAND

The system diagram is shown separately on Figure 5-11. The collector loops are connected through heat exchangers to the district heating network. Accurate sensors allow evaluation of all energy flows, especially at the output of the collector arrays and at the output of the heat exchangers. The collectors and heat exchangers are considered as the test systems. No measurements are taken from the heat exchangers to the district heating system. The heat exchanger energy output is evaluated and corresponds to the net solar gain from the system (negative energy output can be involved when pump 3 is working while pump 1 and 2 are not).

5.8.1 July 1982 to September 1983

Evaluate the performances of both Corning Cortec collector systems ("A" and "B" separately). Identify all collector system losses (thermal losses, capacity effects, etc.). Understand physical behavior of both systems. Validate simulations or design procedures.

5.8.2 April 1983 to August 1983

Evaluate the performance of the Sanyo collector system (STC-CU250). Identify all collector system losses (thermal losses, capacity effects, etc.). Understand physical behavior of both systems. Validate simulations or design procedures.

5.8.3 1985-1986

A new 1000 m^2 system has been carefully designed and built with improved Corning Cortec collectors. Experiment implies monitoring, performance evaluation and detailed analysis of the whole system.

5.9 SOLARIN INDUSTRY PROJECT, HALLAU, SWITZERLAND

The main objective of the project is to evaluate the performance of evacuated collectors for industrial purposes in Swiss climatic conditions.

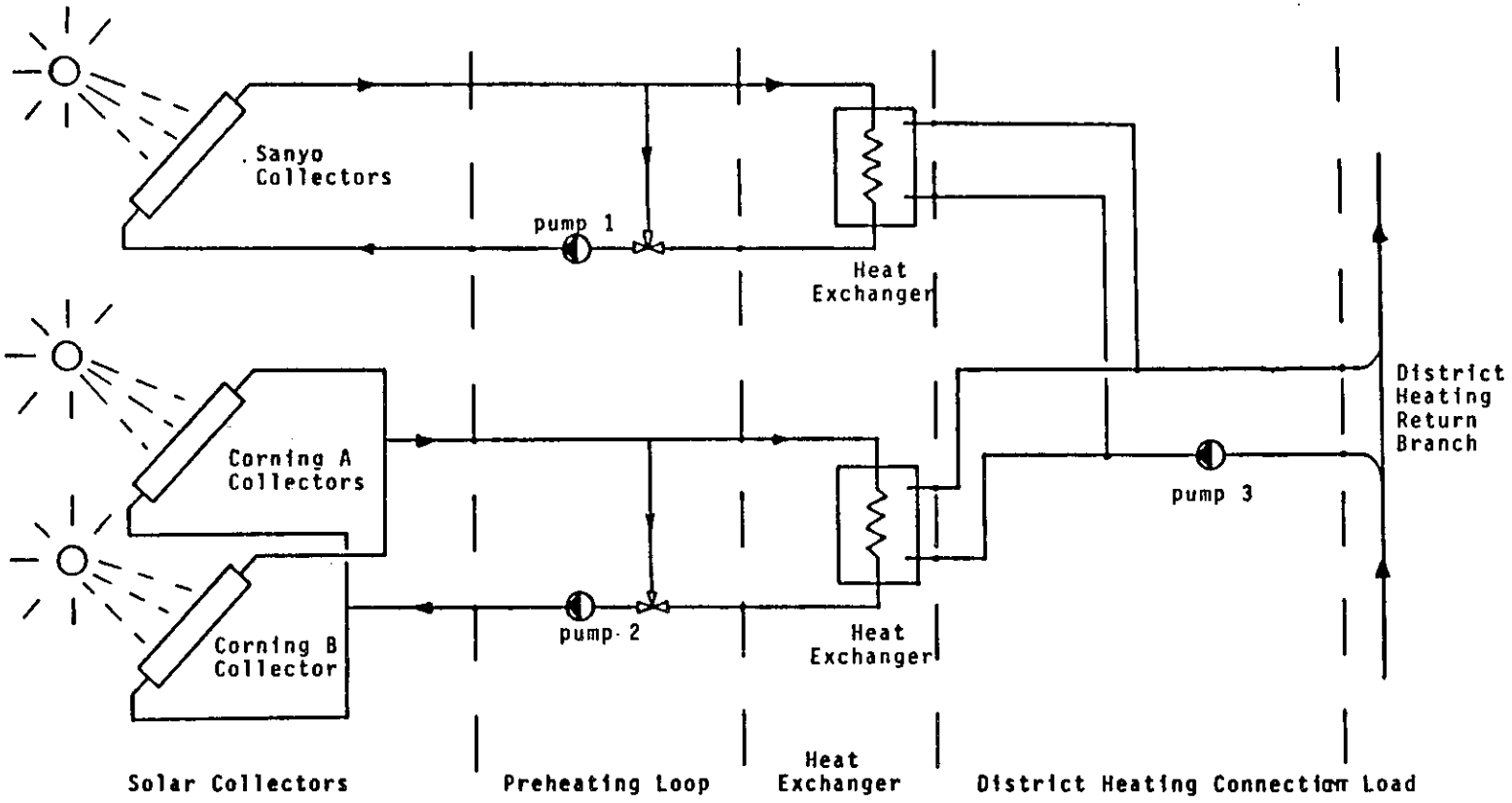

Figure 5-11. Solar System Schematic, Solarcad District Heating Project, Geneva, Switzerland.

Based on previous experiments (see [26, 27]) the Corning Cortec collector has been chosen. Other collectors types may be included, such as a focusing collector.

The system diagram is shown in Figure 5-12. The solar loop is connected through a heat exchanger to the main loop which is connected to both storage tanks. Several accurate sensors allow evaluation of all energy flows (especially solar radiation, collector output, heat exchanger input/output, storage inputs and outputs, storage internal energies, heat to load energy flows) as well as piping losses.

5.9.2 March 1984 to February 1985

Evaluate the performance of the Corning Cortec "D" collectors and of the whole system. Identify all collector and system losses (thermal losses, capacity effects,). Understand physical and thermal behavior of the system. Validate simulation or design procedures.

A full year of data is obtained from March 1984 to February 1985. This period is characterized by a control problem with the system and by almost continuous failures of some flowmeters. Nevertheless, the solar loop has been accurately monitored and heat gains from collectors properly evaluated. Results are therefore presented only for the collection subsystem and not for the rest of the system.

Monitoring will continue through 1985, and problem areas will be treated. Further details of the system are published in Appendix E.

5.10 EVACUATED COLLECTOR SYSTEM TEST FACILITY, UNITED KINGDOM

The purpose of the project was to gather data on the performance of solar heating systems using evacuated collectors with emphasis on validation of mathematical modelling of the system. Some of the system experiments were thus biased to the requirements of the latter. The system is schematically shown in Figure 5-13.

5.10.1 September 1981 to May 1982

The operating modes of the system are designed so that when the collector temperature reaches the setting of the collector thermostat ($60^{o}C$), the solar circuit pump is turned on and the fluid bypasses the heating coils in the storage tank. After a delay (3 minutes) the differential thermostats are interrogated. Each thermostat senses the temperature of the circulating fluid immediately before the branch to the heating or DHW storage tank and the temperature of water in that tank. If the differential exceeds the on differential ($5^{o}C$) the circulating fluid is directed through the coil in the storage. When the differential drops below the off differential ($2^{o}C$), the fluid is directed past the coil in the storage. If the temperature in either storage exceeds the high limit ($90^{o}C$ for the space heating storage and

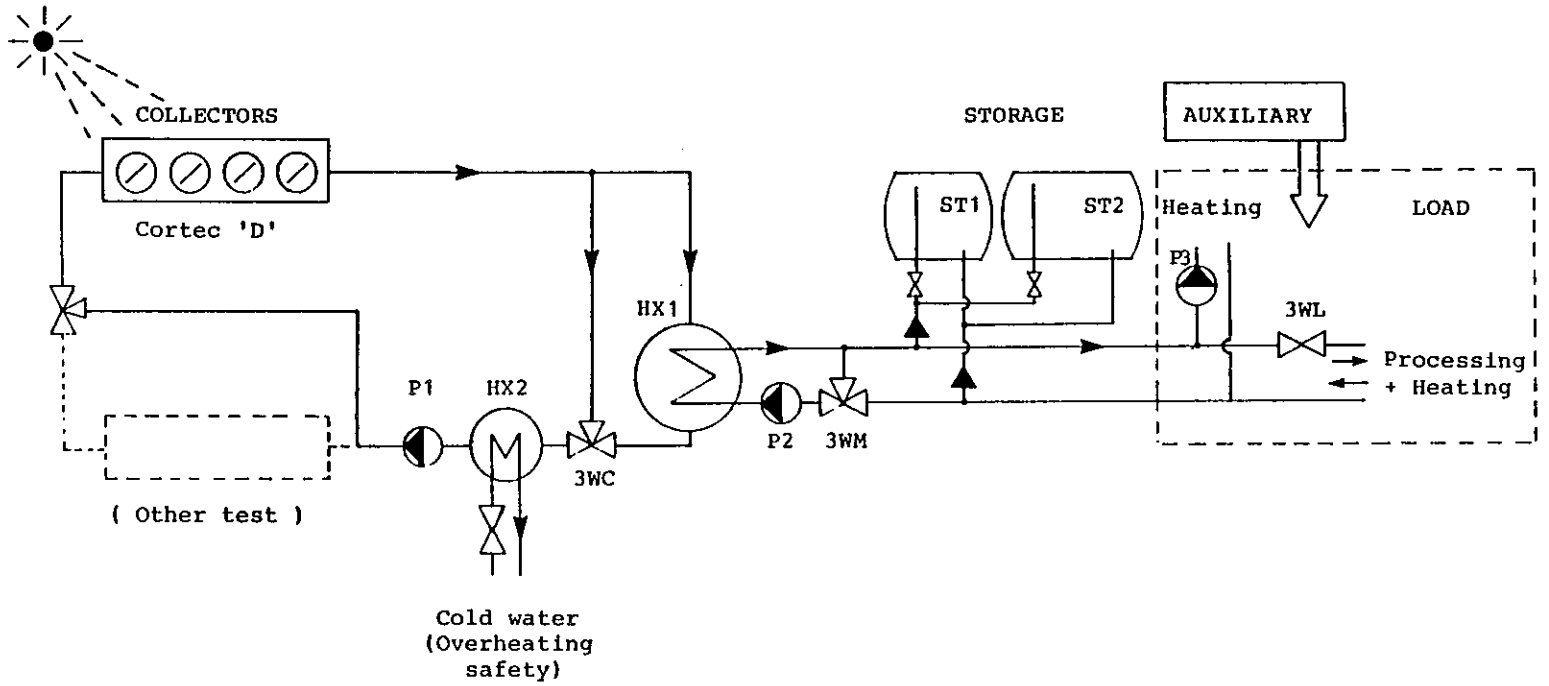

Figure 5-12. Solar System Schematic, Hallau, Switzerland.

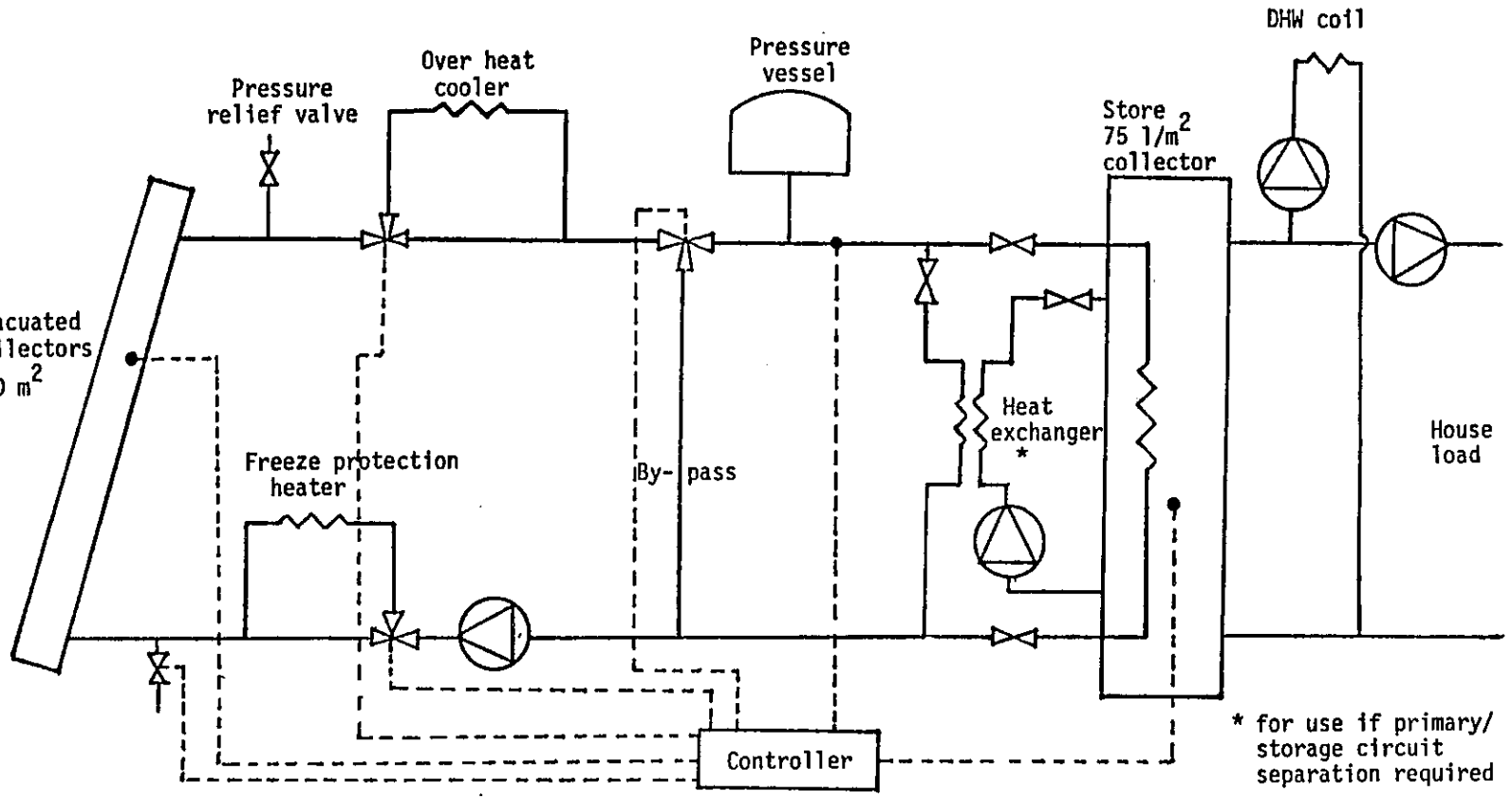

Figure 5-13. System Schematic for the Evacuated Collector System Test Facility, United Kingdom.

55°C for the domestic hot water storage), the fluid is directed past the appropriate coil. If the collector fluid bypasses both coils the pump is stopped and restarting is inhibited for eleven minutes.

This first experiment provided space heating with a requested interior temperature of 20°C and domestic hot water. Only the lower half of the heating coil in the space heating storage was used. A fan coil heating system was simulated.

5.10.2 June 1982 to August 1982

The required interior temperature of the simulated house was increased to 35°C with a fan coil heating system. All of the heating coil in the space heating storage was utilized in this and subsequent experiments. These changes were undertaken primarily to provide additional data for model validation purposes at higher operating temperatures.

5.10.3 October 1982 to May 1983

The same simulated house and hot water load was used as before but the dwelling heating system was changed to an air heating system, resulting in lower system operating temperatures.

5.11 COLORADO STATE UNIVERSITY SOLAR HOUSE I, UNITED STATES

Although the collector remained the same (Philips VTR 361) from the 1982-83 winter season through the summer of 1983, the system configuration was different. An indirect heating system was used during the winter with ethylene glycol as the collector fluid, while during summer, the experiment involved high temperature (130°C) pressurized water and phase-change storage. After abandoning the phase-change unit, pressurized water storage was used for the balance of summer (starting in late August). Because of difficulties with the phase-change storage unit, there was no chiller operation during the hottest months of summer, July and August.

5.11.1 December 1, 1982 to April 14, 1983

Figure 5-14 shows a sketch of the space heating system arrangement. The objectives of the experiment were to determine performance of the Philips VTR 361 collectors in a solar heating system and to evaluate overall system performance.

Collector fluid circulation and heat storage starts when the heat transfer block temperature of the Philips collector is 12°C higher than bottom of storage. After starting, the collection pumps remain on for five minutes regardless of temperature differences, but after the five

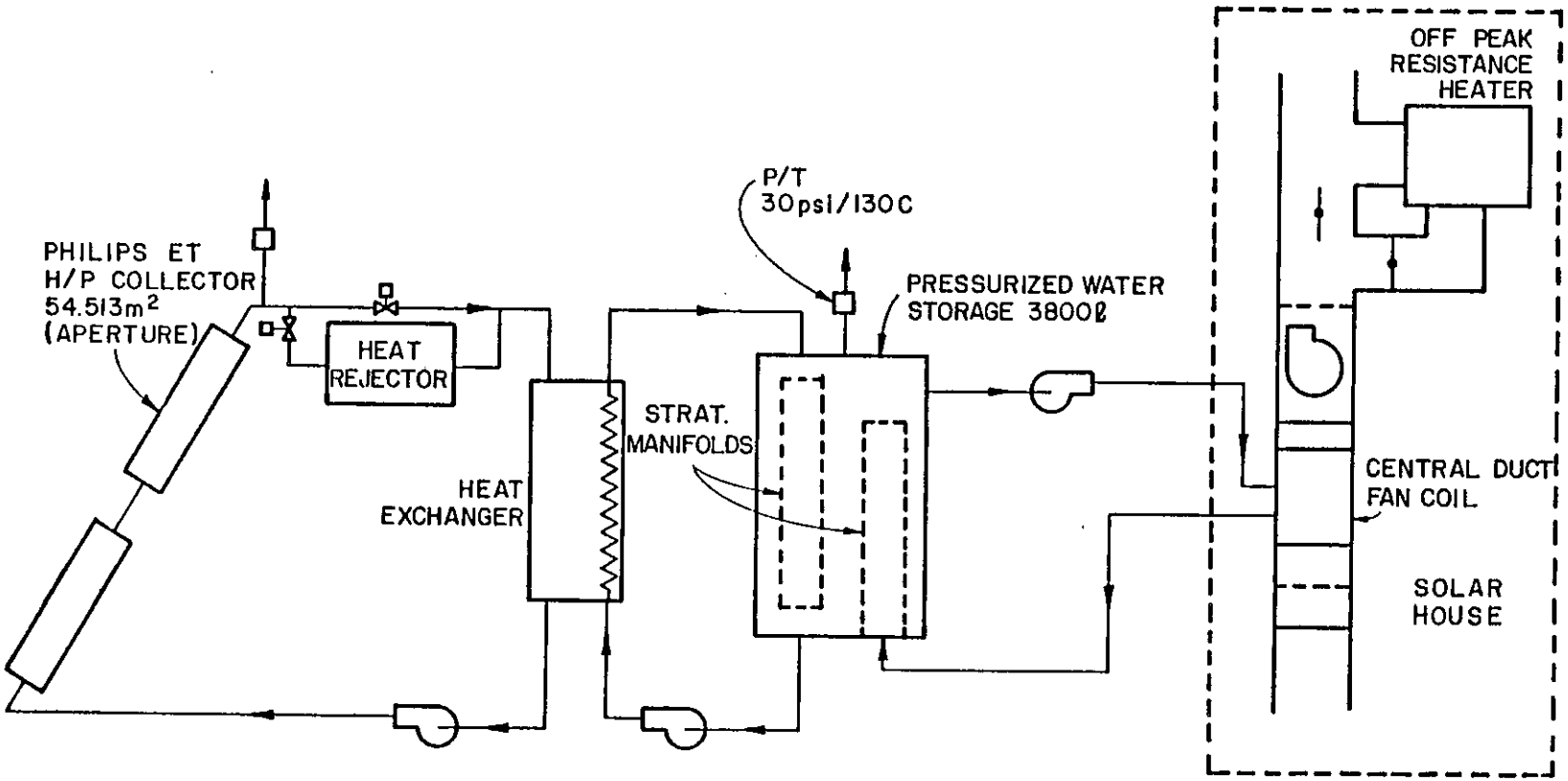

Figure 5-14. Space Heating System Arrangement for Heating Season 1982-1983, Colorado State University Solar House I.

minute period temperature difference between collector outlet and bottom of storage determines when the pumps shut off. The system operates satisfactorily with a shut-off temperature difference of 2°C. Space heating is controlled by a traditional room thermostat. When solar heated water is above 30°C, preference is to use the central duct coil to heat room air. However, should room temperature continue to drop to a second set poin, the circulating room air is diverted through the off-peak storage unit.

Unlike previous years, the off-peak unit was operated only with its internal control referenced to ambient outdoor temperature. The level of electrical heating of the ceramic blocks is inversely related to outdoor temperature. As the experiment progressed it became increasingly evident that the solar system would provide a substantial portion of the space heating load as storage temperatures remained high. In March 1983, the collector array was reduced to one-half the original area (27.26 m^2) by removing the lower row of tubes on the test bed. There was, however, no measurable increase of collector efficiency as a result of lower storage temperatures.

5.11.2 September 1, 1983 to October 14, 1983

Figure 5-15 shows a drawing of the space cooling solar system. The objectives of the experiment were to determine the influence of new specular reflectors (with proper shape) on collector performance, to determine the influence of phase-change storage units on collector and chiller performance, and to evaluate overall system performance.

The hot-side storage unit consisted of 2400 kg of high density polyethylene (HDPE) pellets. The material was developed by Monsanto Research Corporation and is suitable for storage of heat at 130°C with a solid-solid phase-change heat storage capacity of 209 kJ/kg. Radiation cross-linking of HDPE enables the material to be self-encapsulated in pellets of about 6 mm diameter. With pellets of this size, there is a high surface-to-volume ratio for heat transfer. With a large cross-sectional area of the storage tank and liquid flowing through the tank, the pellets, which are lighter than water, remain suspended and offer no resistance to flow within the storage unit. Design difficulties arise in containing the pellets within the tank and minimizing pressure drop at the tank outlets.

Cold-side storage was provided by a commercially available salt storage unit purchased from CalMac Manufacturing Company. The phase-change salt is a mixture of sodium sulfate and magnesium chloride to give a phase-change temperature of 12.5°C and heat of fusion of 140 kJ/kg. A spirally-wound plastic heat exchanger with 1500 m of tubing is imbedded in the salt tank with the tubes arranged so that the fluid flows in alternate directions in adjacent tubes. Vertical headers are provided both at the center and outside edge of the circular tank. Flow is unidirectional from header to header. The chiller can be operated with

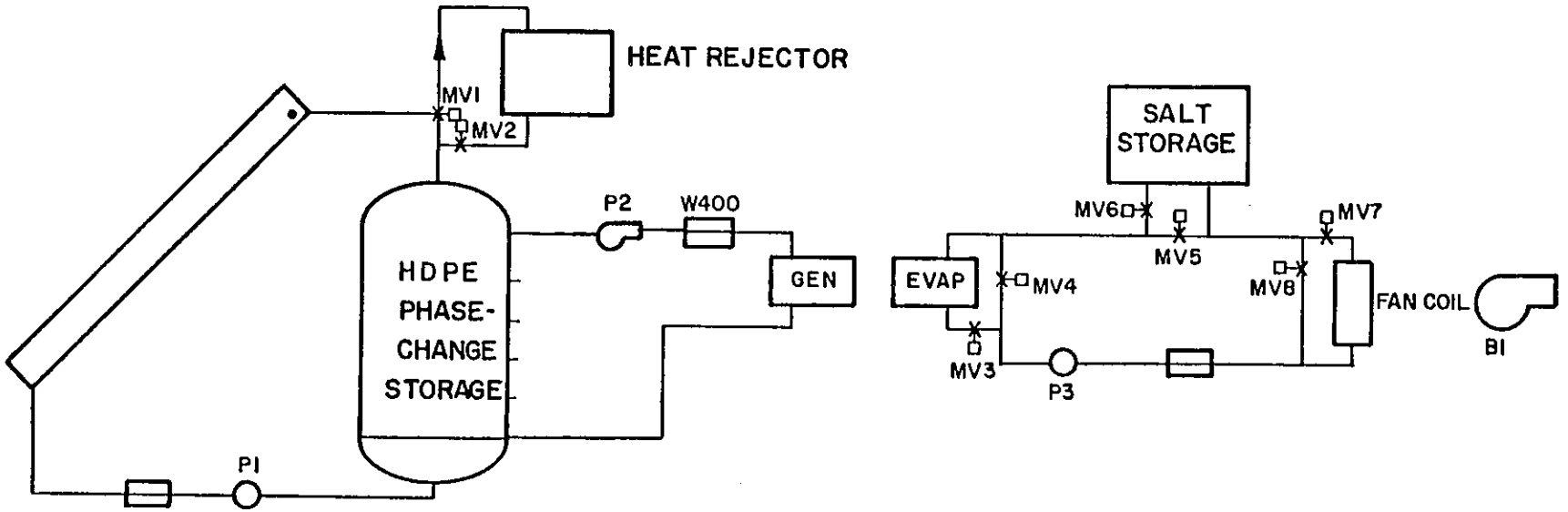

Figure 5-15. Space Cooling System Arrangement for Cooling Season 1983, Colorado State University Solar House I.

or without cold storage, and the room can be cooled with the chiller or by using cold storage.

6. RESULTS

Six different types of graphic representations are used in this section. Formats follow the IEA Task VI format of Appendix C. See also Chandrashekar[2]. These formats have been further standardized so that one installation's results may be readily compared with those of another. Axes on most types of plots are identically dimensioned and labelled so that overlays of several installation's plots can be made.

The graphs consist of:

- collector system efficiency diagrams
- energy input/output plots
- energy flow diagrams
- energy supply and delivery bar charts
- energy use bar charts
- system efficiency and solar fraction diagrams.

6.1 COLLECTOR EFFICIENCY DIAGRAMS

Normally there is one efficiency plot for each experimental period. However, if appropriate, several experimental periods are combined for these plots. The efficiencies plotted are for steady-state operation between the hours of 11 a.m., and 2 p.m. In some cases, steady-state efficiencies throughout the day are also plotted.

The efficiencies are corrected for capacitance effects. Capacitance effects are calculated by multiplying the difference in average collector temperature at the beginning and end of the data collection time interval by the effective capacitance of the system between the temperature difference sensor locations. The effective capacitance can be estimated in several ways, as suggested in Chandrashekar and Vanoli[2].

The abscissa in these figures is the temperature difference between the average collector fluid temperature and the average ambient temperature divided by the solar incident energy on the aperture plane per unit aperture area of the collector, (T100-T001)/G100. The ordinate is the solar energy collected, corrected for capacitance effects, divided by the incident solar energy on the aperture plane, (Q112 + Q105)/H100. Performance is shown in the form of the regression lines which are based on up to 1000 data points per experiment. Data points are divided into three groups with regard to three ranges of (T100-T001)/G100. A vertical bar and dot is drawn for each range. In many of these figures the location of the dot provides the mean value of the group and the length of the bar shows one standard deviation on either side of the mean.

An energy histogram showing the distribution of collected energies as a function of N108, the normalized temperature difference, is also included in most diagrams.

6.1.1 The Sydney University Solar Heating and Cooling System, Sydney, Australia

A total of eighteen efficiency plots are shown covering different time spans during the reporting period. It is worthwhile noting that the bulk of the data points usually concentrates around a fairly narrow band on the ($\Delta T/G$)-axis; this is particularly evident in the 11 a.m. to 2 p.m., graphs. The reason for the data point concentration lies in the requirement for continuous collector pump operation which is met predominantly during noon operation at high solar radiation.

Figure 6.1-1 presents efficiencies from 11 a.m., to 2 p.m., and Figure 6.1-2 presents efficiencies taken at various points throughout the day.

Figures 6.1-1, 6.1-2, 6.1-5, and Figure 6.1-6 show array efficiencies of the Sydney University evacuated tubular collector during cooling (December 1982 and January 1983) and heating (August and September 1983). The performance of the Yazaki flat-plate collector while operating in a winter month (July 1983) is given in Figures 6.1-3 and 6.1-4.

The evacuated tubular collector plots clearly indicate that a single straight line efficiency characterization as derived from instantaneous collector tests is inadequate to fully describe the performance of the S.U. evacuated collector. Angle of incidence modifier effects which are inherent to this type of collector with a curved absorber geometry, operating temperatures, level of insolation, diffuse solar energy fractions, etc., influence the location of actual data points significantly.

Agreement between efficiency information derived from array measurements and results from single panel tests is reasonable for a good quality flat-plate collector operating at low temperatures (Figures 6.1-3 and 6.1-4. However it has been observed that at the elevated collector temperatures required to drive an absorption cooling cycle, array performance of the Yazaki flat-plate collector is 10 to 20 percent below the anticipated performance as derived from an instantaneous collector test.

Figures 6.1-7 and 6.1-8 show collector array efficiency during typical summer operation (December 1983). Array efficiencies (11 a.m. to 2 p.m.) are in reasonable agreement with single panel test data. On an all-day basis, significant incidence angle modifier effects which are an important design feature of the S.U collector become apparent.

During mid-season months (i.e., April) the collectors usually work at very high temperatures since the loads are very small. System

operation is often near boiling point. Figure 6.1-9 and 6.1-10 typically represent a mid-season situation.

Collector performance during winter is given in Figures 6.1-11 and 6.1-12. The bulk of the 11 a.m., to 2 p.m., data is still in reasonable agreement with single panel test information. However, data scatter has become larger.

The reason for the increased data scatter during winter is related to fluctuating pipe losses in the interconnecting array pipework. The protective paint of the rockwool pipe insulation has deteriorated during the monitoring period and depending on weather conditions the insulation may be partially wet. Insulation dryout takes 2 to 3 days and is significantly influenced by the collector loop operating temperature.

Figures 6.1-13 and 6.1-14 show efficiency plots for a typical Sydney spring month (September 1984) and Figures 6.1-15 and 6.1-16 contain December 1984 data.

The last two graphs, Figures 6.1-17 and 6.1-18, represent collector efficiency for March 1985. Here, array performance data is above single panel test information presumably due to months of fine, sunny weather.

6.1.2 Mountain Spring Bottle Washing Facility Edmonton, Canada

Figure 6.1-19 presents measured collector array efficiencies from 11:00 - 14:00 hours on days in which clear sky conditions prevailed. The points plotted are points resulting from one hour of steady state solar energy system operation. The bar chart represents the percentage of total energy collected as a function of N108. It should be noted that this energy collected applies to the points in question and not to the entire reporting period.

The single panel test curve obtained from the National Solar Test Facility (NSTF) is above the points as the losses from the collector array are higher due to the inter array piping.

6.1.3 Ispra Solar Heated and Cooled Laboratory Commission of European Communities

In Figure 6.1-20 to 6.1-23 the array efficiency plots for the four different collector arrays are given. The Sanyo (I) collector is the array Sanyo collectors without reflectors and the Sanyo (II) collector is the array with reflectors.

From Figure 6.1-20 it can be seen that the Sanyo collectors did show a considerable decrease in performance. In Figure 6.1-21 the points of the array efficiency are close to the measured efficiency curve, this is due to the fact that the reflectors compensate for the decrease in collector efficiency.

In all four plots it can be seen that the points are closely grouped together. This is a result of the rather constant operation conditions of the system. The bar-chart for the energy delivery is omitted from this figure since almost all the energy is delivered in a very narrow band on the normalized temperature scale.

6.1.4 Solarhaus Freiburg Federal Republic of Germany

The results of collector system efficiency regression analysis is shown in Figures 6.1-24 through 6.1-27 for the Corning Glass and Philips/ Stiebel-Eltron collectors. The corresponding regression parameters for the measurement period June 1982/May 1983 are shown in the following table:

	Transmittance-Absorptance-Coefficient %	Heat-Loss Coefficient $W/m^2 \cdot K$
PHILIPS/STIEBEL-ELTRON	67.7	1.24
CORNING GLASS	72.0	1.68

The figures show the hourly efficiency points of the entire collector field from 11 a.m, to 2 p.m., during the annual period June 1982/May 1983. This presentation implies, that the heat loss parameters correspond to the total heat loss of the collector modules and the piping between them. Therefore, these values may not be compared with test values of individual collectors unless the associated piping heat loss is taken into account.

The dotted line in Figure 6.1-24 gives the manufacturer's efficiency regression for the Corning Glass Collector. With an aperture area of 33.3 m^2, the difference in the over-all heat loss parameter corresponds to 10 W/K for the whole collector field piping.

Figure 6.1-25 shows the efficiency of the new Philips/Stiebel-Eltron Heat Pipe collector. A comparison with the values of the previous Philips IV collector shows the enormous improvement of the new collector concept.

The efficiency points at the extreme left side of the diagrams for both collectors were obtained with special experiments in order to measure the collector efficiency at operating temperatures close to the ambient temperature for a thermal determination of the $F'\tau\alpha$ value. Because of the very high solar radiation at these measurements, the overall accuracy is about 3 percent. Figures 6.1-26 and 6.1- 27 show the extrapolated transmittance-absorptance product for both collectors. As a result, the $F'\tau\alpha$ value of this experiment is nearly identical with the value obtained by the regression analysis.

Furthermore, a second experiment 11 months after the installation of the Philips/Stiebel-Eltron collector showed no measurable degradation of the reflectivity of the specular aluminum ripple-reflector in this first year of operation, although a certain visual dullness is observed.

Both diagrams, Figures 6.1-24 and 6.1-25 show histograms of the distribution of the incident solar radiation over the operating conditions of the collectors. The shape of the distributions is nearly identical for the Corning Glass (operating with the heating system) and the Philips/Stiebel-Eltron Collector (operating with the domestic hot water system).

However it is noteworthy, that more than 90 percent of the incident radiation over the mid-day hours of a year is delivered at operating conditions N108 less than .09 $K \cdot m^2/W$; only about 10 percent of the radiation arrives in the long right hand tail of the distribution and is associated with the wide cloud of efficiency points, which consists in these applications mostly of insignificant operating conditions.

This situation is remarkable, because these "low-energy" points may cause a certain "rotation of the efficiency curve", which is indicated by a combined increase or decrease of both the $F'\tau\alpha$ and $F'U_L$ values.

For comparison, the following table summarizes the efficiency parameters of previous measurement periods:

	PHILIPS MK IV		CORNING GLASS	
MEASUREMENT PERIOD:	$F'\tau\alpha$	F'UL W/m^2K	$F'\tau\alpha$	F'UL W/m^2K
1979	67.6%	2.58	70.3	1.52
1980	62.1%	2.04	66.4	1.24
1981	68.5%	2.47	67.2	1.31

6.1.5 Eindhoven Technological University Solar House, The Netherlands

In Figure 6.1.28 the collector array efficiency diagram for the solar house of the Eindhoven echnological University is given. The presentation of the efficiency curves deviates somewhat from the other curves presented here because this collector array is operated with a variable low flow rate, dependent on the insolation. A long time base would not suffice and a five minute interval was used.

Because of the dependency of the flow rate on the insolation and thus on the temperature difference between collector and bottom of storage, the usual temperature dependent collector array efficiency regression cannot be assessed. Instead the collector efficiency has been

shown to be dependent on the insolation. See comment on the efficiency hypothesis in Veltkamp[75].

Efficiency points are not only corrected for heat capacitance but, what is more important in this installation, for the time delay induced by the flow.

6.1.6 Knivsta District Heating System, Knivsta, Sweden

Figures 6.1-29 through 6.1-32 show measured noon collector array efficiency for the four collectors tested at Knivsta. The lines represent either single module tests or manufacturer's information. The results from 1982 and 1983 are separated. No significant degradation can be detected from these results and this corresponds to the other results presented. A slight seasonal variation in efficiency has been observed for the Philips array both 1982 and 1983. The variation is probably due to different amounts of back radiation depending on the solar declination.

At these operating conditions, the Owens-Illinois collectors show the highest instantaneous collector efficiency followed by the Philips VTR 141, Scandinavian Solar and General Electric collectors.

6.1.7 The Södertörn District Heating Project, Södertörn, Sweden

Figures 6.1-33 through 6.1-37 show the measuring points presented as hourly average noon time values and each includes 40 individual measuring point. No regression lines are presented as the operating conditions give such a small range of points along the y-axis and this is also the reason that the energy histogram is excluded. The points are sparse but carefully selected for stable operating conditions. Teknoterm HT and Philips VTR 141 show good agreement to the single module curve. The deviation for Granges Aluminum Sunstrip 80 is caused by uneven flow in the absorbers which reduces performance distribution. The points for General Electric collector fall onto the manufacturer's curve, as was the case in the Knivsta installation.

The Scandinavian Solar HT array shows higher performance than the single module test but the test module was reduced in size from 12 m^2 normally to about 2 m^2. Therefore, higher heat losses could be expected for the single module compared to the full size module.

6.1.8 SOLARCAD Project, Geneva Switzerland

Efficiency plots, Figures 6.1-38 through 6.1-40, are corrected for capacitance effects the array thermal capacity results by computation and is checked experimentally. The scattering of the points is due to other dynamic effects, such as mixed parameters in the definition of the abscissa (temperature difference and insolation not being considered as

separate parameters), changes made during test periods, etc. The linear fit through the points is not very sensitive to the capacitance, when considered as a variable parameter.

The curves correspond to efficiency measurements made on a single module using a specialized testing facility by H. Van Kuijk of the Ecol Polytechnique, Lausanne, Switzerland. They clearly show the dependence on both the temperature difference and the insolation.

Efficiency plots, Figures 6.1-41 through 6.1-47 are given for 3 periods; 2 starting periods involving changes and a full year period as noted below:

I. July 1 1982 to November 4, 1982: Corning A, Corning B
II. November 5, 1982 to March 31, 1983: Corning A, Corning B
III. April 1, 1983 to March 31, 1984: Corning A, Corning B, Sanyo

Efficiency measurements made on single modules are given elsewhere.

Dynamic array efficiencies and stationary single module efficiencies can differ for several reasons. These include significant differences from one module to another, additional losses due to plumbing involved in an array and different test conditions.

The French-made Corning Cortec collectors should be considered as production prototypes. Not all problems have been corrected. Collector "A" improved from period one to period two, because a white background was added behind the collectors. Collector "B" deteriorated from period two to period three (loss of vacuum for a few tubes). It cannot be concluded that a selective surface on both sides of the absorber is better than on only the front side (opposite effects have been observed in separate tests). Performance reported has to be considered as performance averaged over the entire test period, which includes defects and modifications. Better performance is now observed with the new Cortec collector.

6.1.9 SOLARIN Project, Hallau, Switzerland

Figure 6.1-48 shows hourly efficiencies for the one year period considered: March 6, 1984 to February 28, 1985, excluding one month from September 5, 1984 to October 12, 1984.

Some points rejected with respect to the following criteria are

- The pump should be "on" at least 6 minutes before the considered hour
- No switching of valves is allowed during the considered hour (it may induce large temperature variations and then significant dynamic effects)

- o Capacitance correction (Q105) has to be smaller than one third of the delivered heat (Q112)

- o Snow cover, as measured at the closest meteorological station, must not exceed 1 cm.

For the Corning Cortec evacuated tubular collector the absorber is tilted by 30 degrees with respect to the collector plane (also tilted by 2 degrees from horizontal). The poor collector orientation is compensated by tilting the absorber, resulting in a better collector efficiency as compared to normal conditions. Solar radiation is measured in the collector plane and tilting the absorber contributes to improving the "incidence angle modifier" factor. With respect to normal conditions we have less solar energy but almost the same heat gains. Also refer to comments in Section 5.9.2.

6.1.10 BSRIA Solar Test Facility with Simulated Loads, Bracknell, United Kingdom

An efficiency diagram for the Philips VTR-141 collectors is provided in Figures 6.1-49 and 6.1-50 for 320 full hours of operation between 11.00 and 14.00 hours, solar time. Even though capacitance effects have been taken into account, a derived $F'(\tau\alpha)$ of 0.56 is not as high as the manufacturer's quoted figure of 0.67. The reason for this discrepancy has not been explained. During an investigation into seasonal variations in daily efficiency the hourly data was replotted taking the ambient and collector fluid temperature to the fourth power. Assuming the fluid temperature is not too dissimilar from the absorber temperature, the radiative heat loss parameters provide a very similar set of r^2 values on the regression analysis.

6.1.11 Colorado State University Solar House I, United States

The instantaneous efficiency of the evacuated-tube heat pipe collector is not adequately represented by a single parameter as is the normal flat-plate collector.

Instantaneous collector efficiencies during specific days are shown in Figure 6.1-51. Clearly it is difficult to "fit" a single curve through the data. Efficiency curves and a regression equation using 1982-83 data are shown in Figure 6.1-52. To compare how collector performance in 1983-1984 compares with performance in 1982-1983, "measured" efficiencies for 1983-1984 are compared with calculated efficiencies in Figure 6.1-53. Although scatter of data on Figure 6.1-53 is about 10 percent on both sides of the match line, there is no indication that a collector efficiency for the two years are significantly different.

It should be noted that the reflectors of the collectors were changed in May 1983. Curvature is greater for the new reflector. The

only notable difference with the improved reflector shape is an increase of efficiency about the noon period and a slight decrease in the early morning and late afternoon periods.

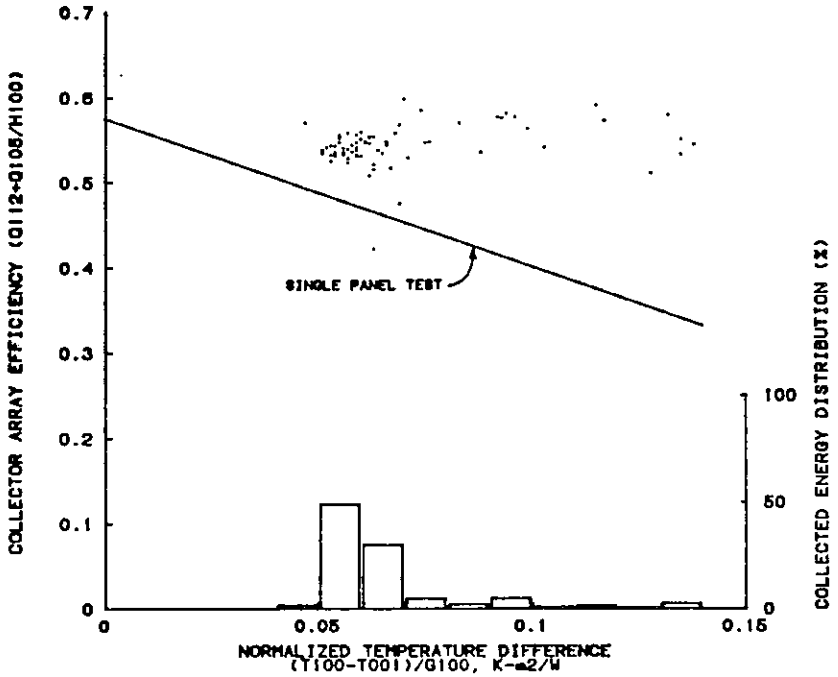

Figure 6.1-1. Collector Array Efficiency Diagram for Sydney University Evacuated Tubular Collector, 11 a.m., to 2 p.m., Australia, 24 December 1982 to 20 January 1983.

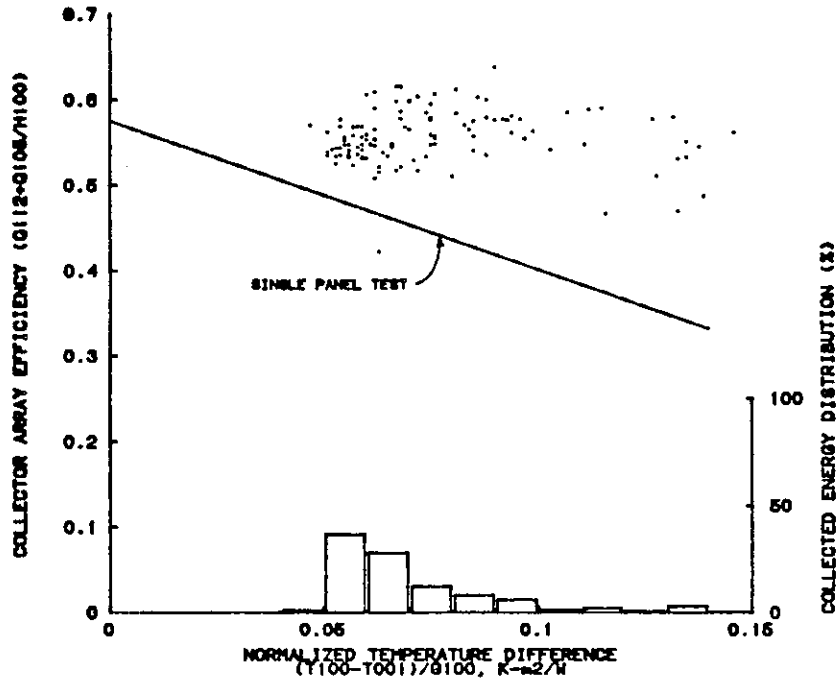

Figure 6.1-2. Collector Array Efficiency Diagram for Sydney University Evacuated Tubular Collector, All Day, Australia, 24 December 1982 to 20 January 1983.

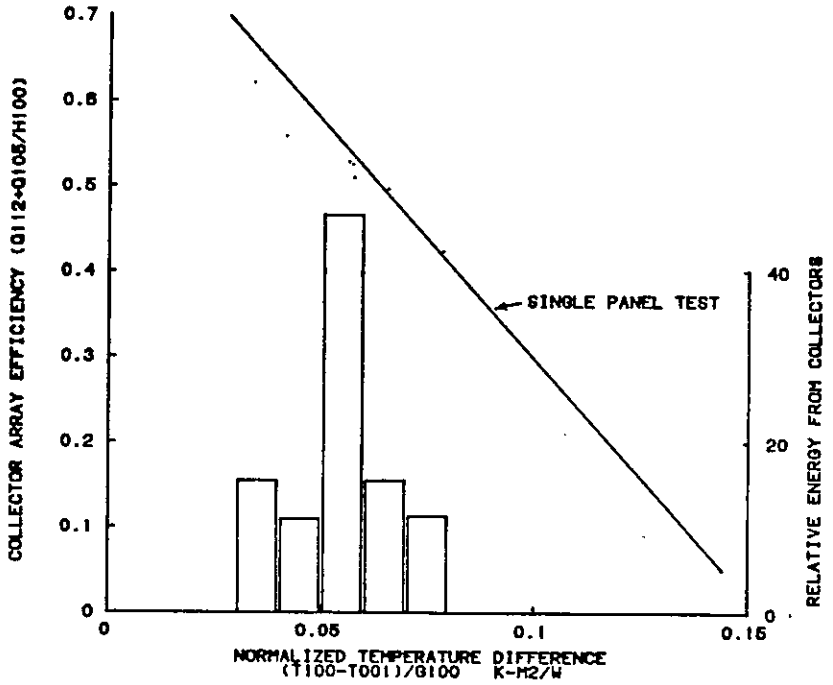

Figure 6.1-3. Collector Array Efficiency Diagram for Yazaki Flat-Plate Collector, 11 a.m., to 2 p.m., Australia, 9 July 1983 to 26 July 1983.

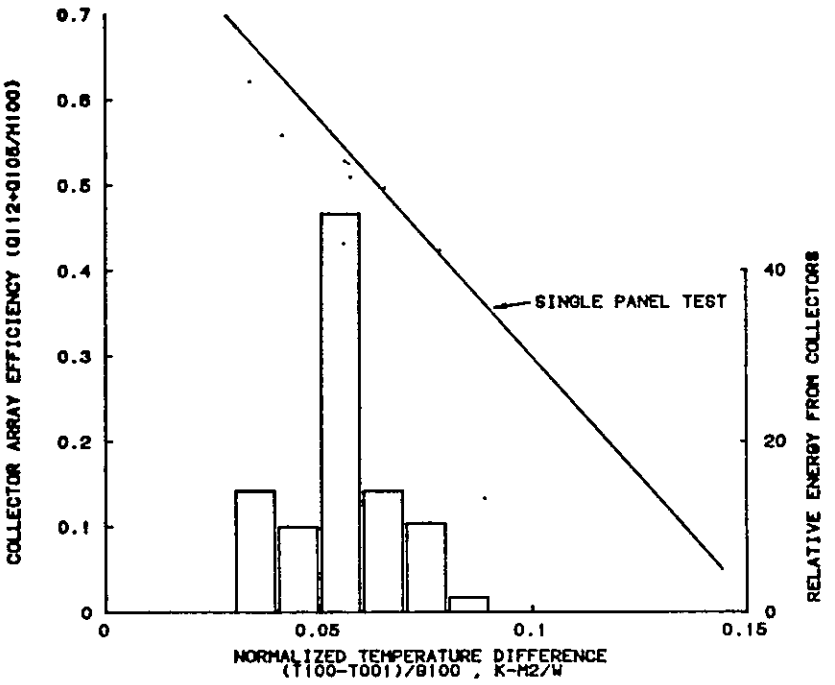

Figure 6.1-4. Collector Array Efficiency Diagram for Yazaki Flat-Plate Collector, All Day, Australia, 9 July 1983 to 26 July 1983.

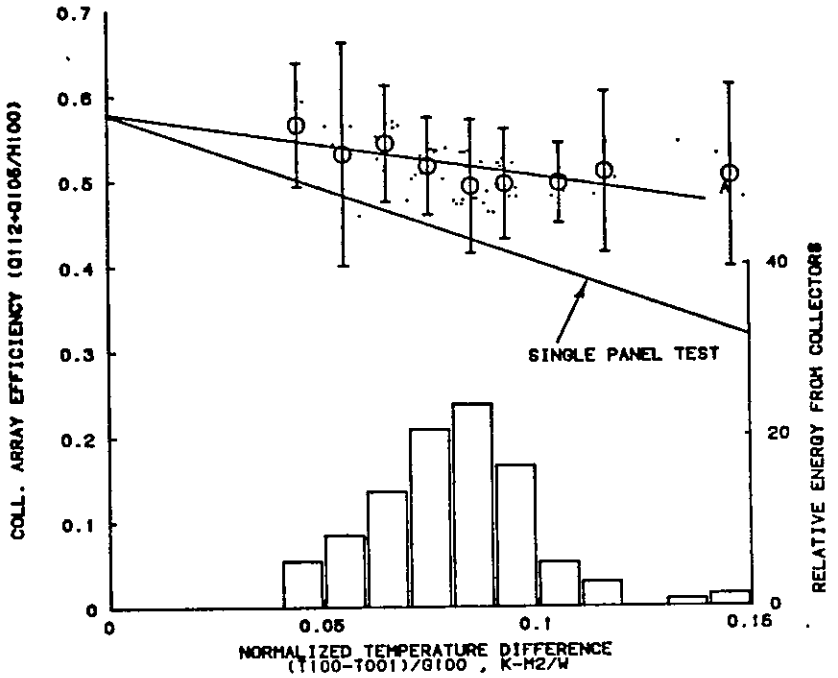

Figure 6.1-5. Collector Array Efficiency Diagram for Sydney University Evacuated Tubular Collector, 11 a.m., to 2 p.m., Australia, 28 August 1983 to 28 September 1983.

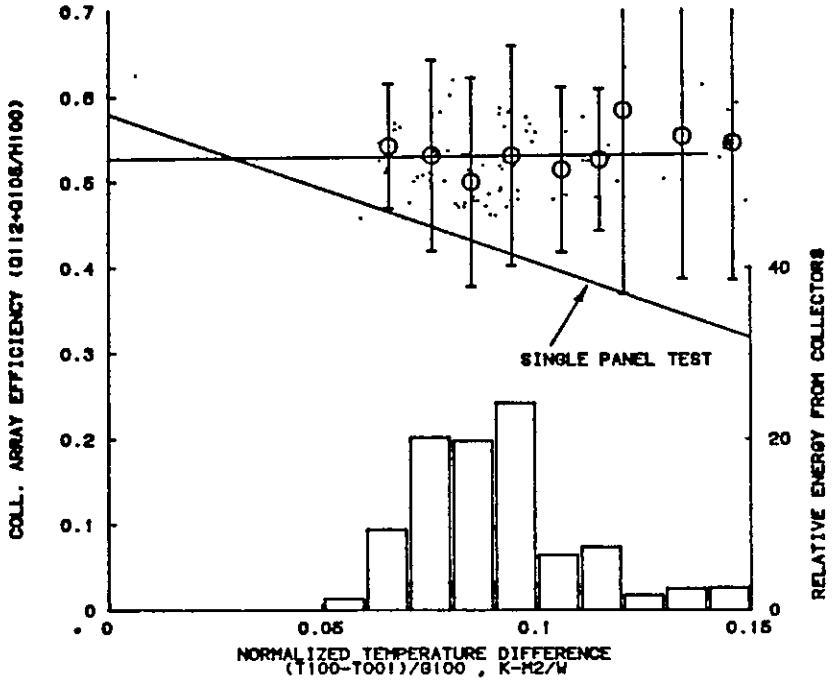

Figure 6.1-6. Collector Array Efficiency Diagram for Sydney University Evacuated Tubular Collector, All Day, Australia, 28 August 1983 to 28 September 1983.

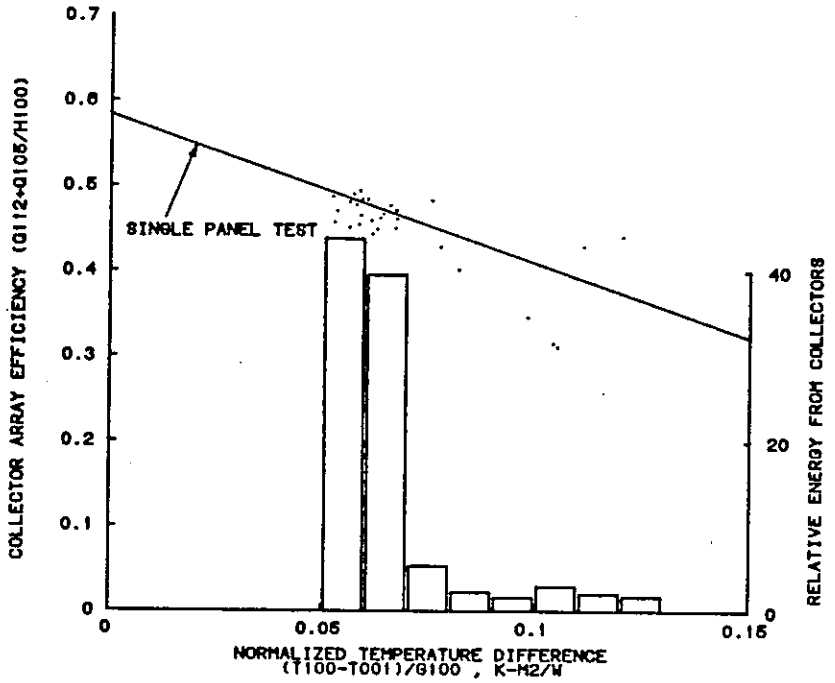

Figure 6.1-7. Collector Array Efficiency Diagram for Sydney University Evacuated Tubular Collector, 11 a.m., to 2 p.m., Australia, 1 December 1983 to 31 December 1983.

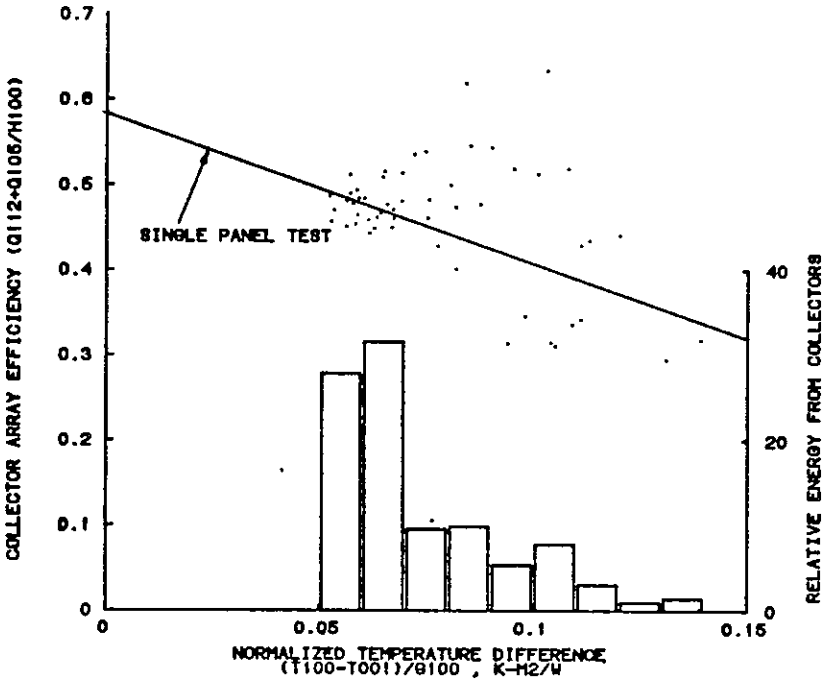

Figure 6.1-8. Collector Array Efficiency Diagram for Sydney University Evacuated Tubular Collector, All Day, Australia, 1 December 1983 to 31 December 1983.

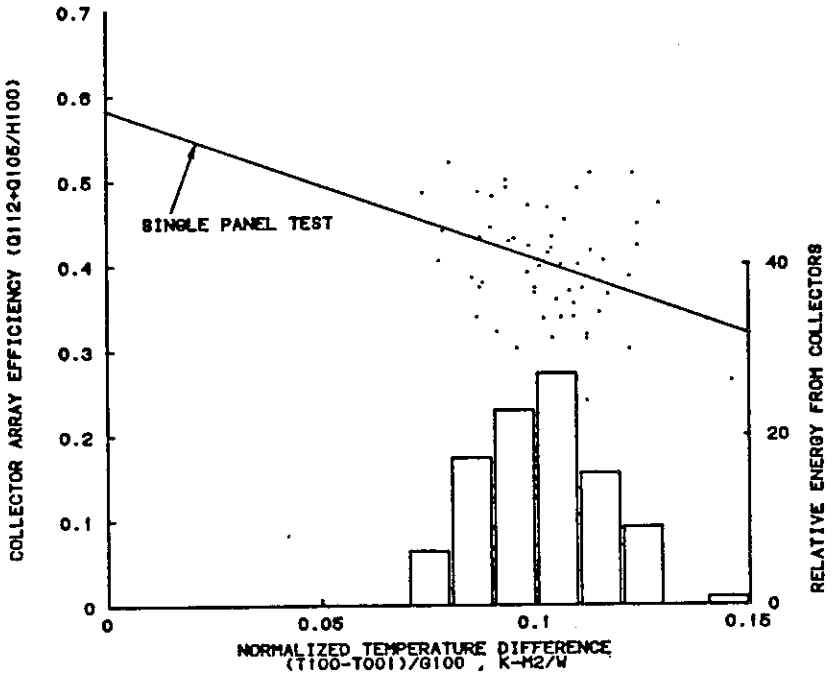

Figure 6.1-9. Collector Array Efficiency Diagram for Sydney University Evacuated Tubular Collector, 11 a.m., to 2 p.m., Australia, 1 April 1984 to 30 April 1984.

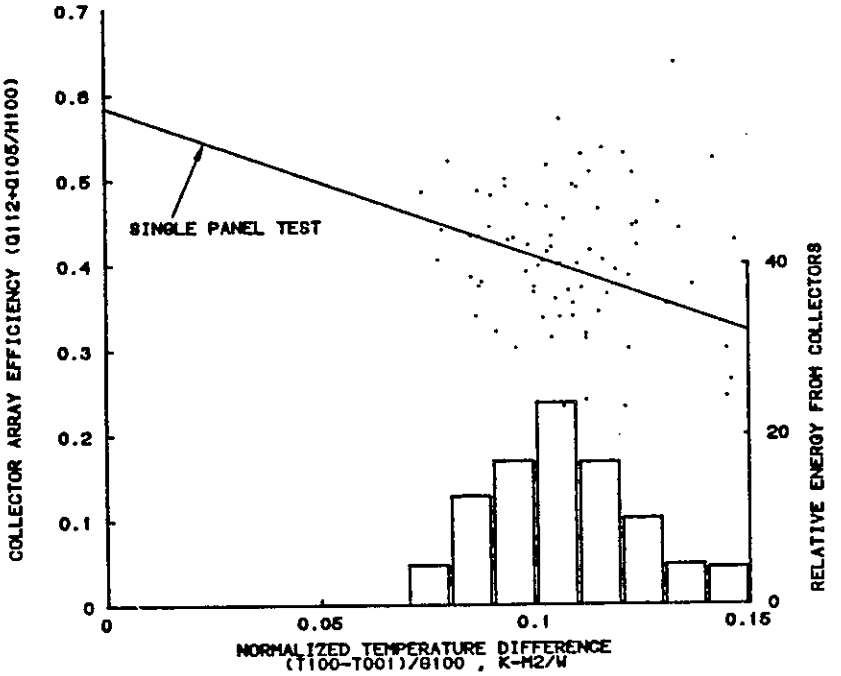

Figure 6.1-10. Collector Array Efficiency Diagram for Sydney University Evacuated Tubular Collector, All Day, Australia, 1 April 1984 to 30 April 1984.

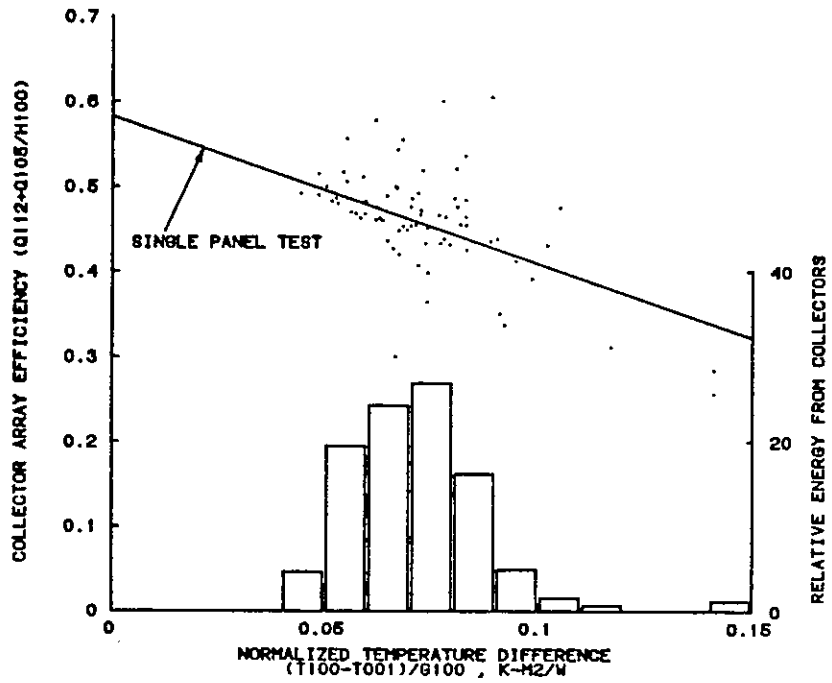

Figure 6.1-11. Collector Array Efficiency Diagram for Sydney University Evacuated Tubular Collector, 11 a.m., to 2 p.m., Australia, 1 June 1984 to 30 June 1984.

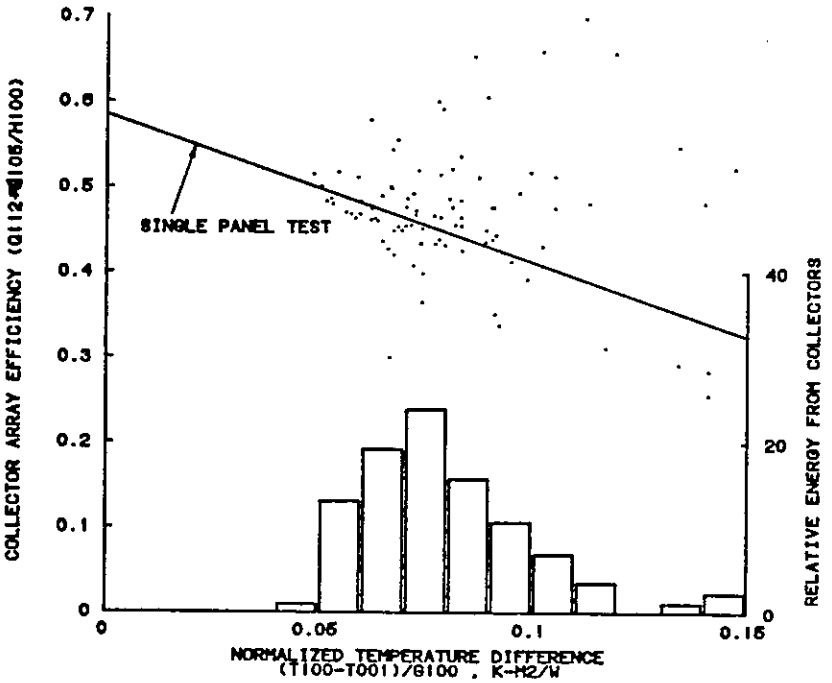

Figure 6.1-12. Collector Array Efficiency Diagram for Sydney University Evacuated Tubular Collector, All Day, Australia, 1 June 1984 to 30 June 1984.

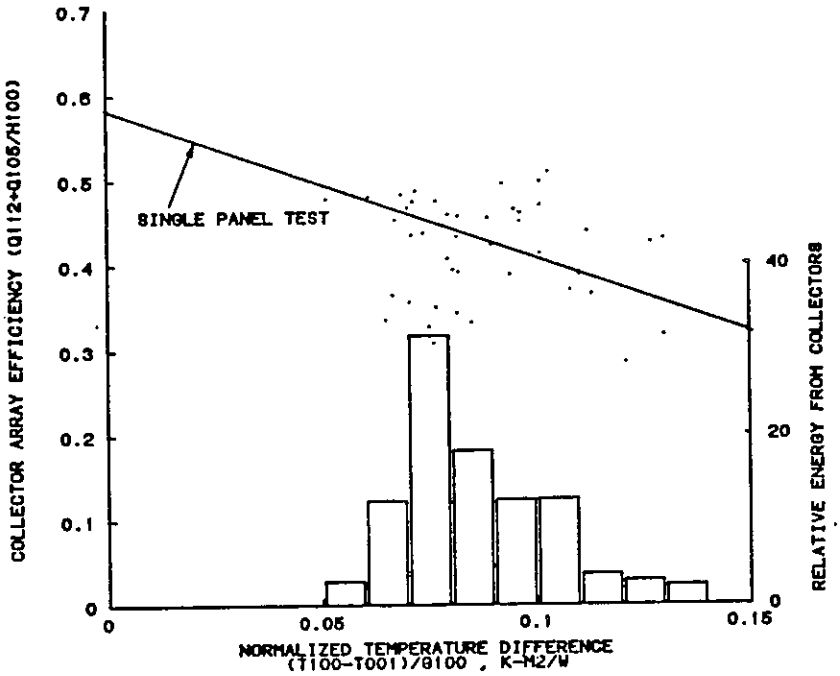

Figure 6.1-13. Collector Array Efficiency Diagram for Sydney University Evacuated Tubular Collector, 11 a.m., to 2 p.m., Australia, 1 September 1984 to 30 September 1984.

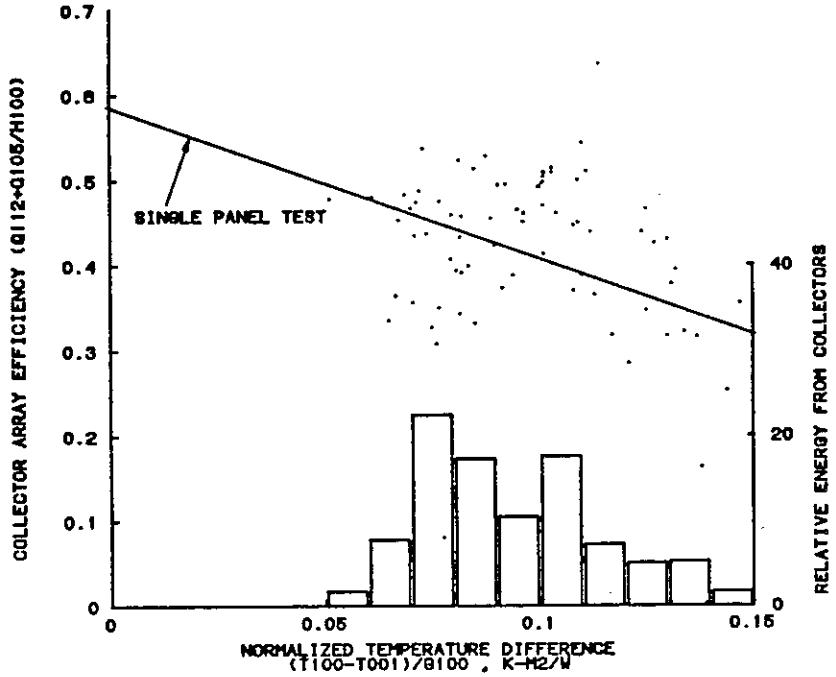

Figure 6.1-14. Collector Array Efficiency Diagram for Sydney University Evacuated Tubular Collector, All Day, Australia, 1 September 1984 to 30 September 1984.

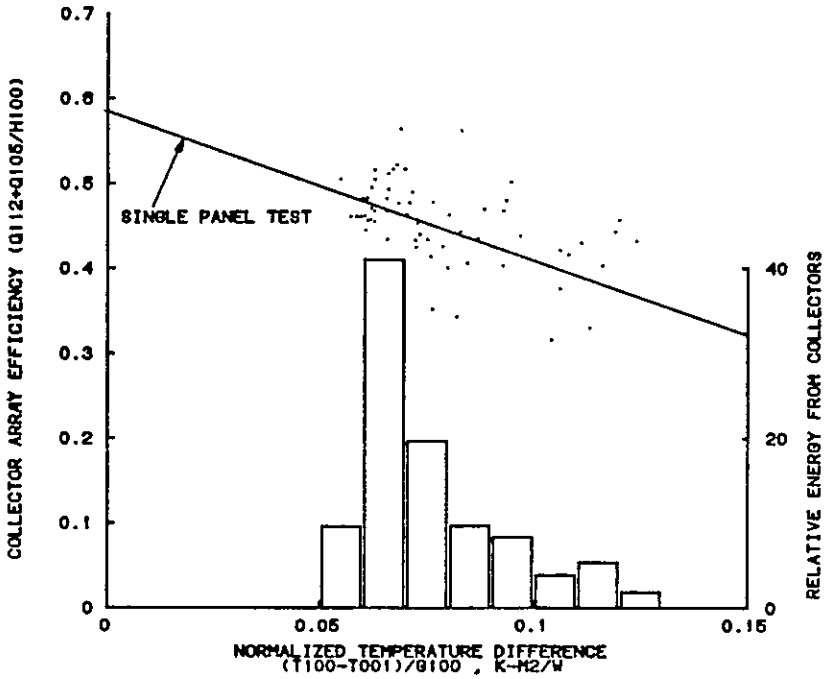

Figure 6.1-15. Collector Array Efficiency Diagram for Sydney University Evacuated Tubular Collector, 11 a.m., to 2 p.m., Australia 1 December 1984 to 31 December 1984.

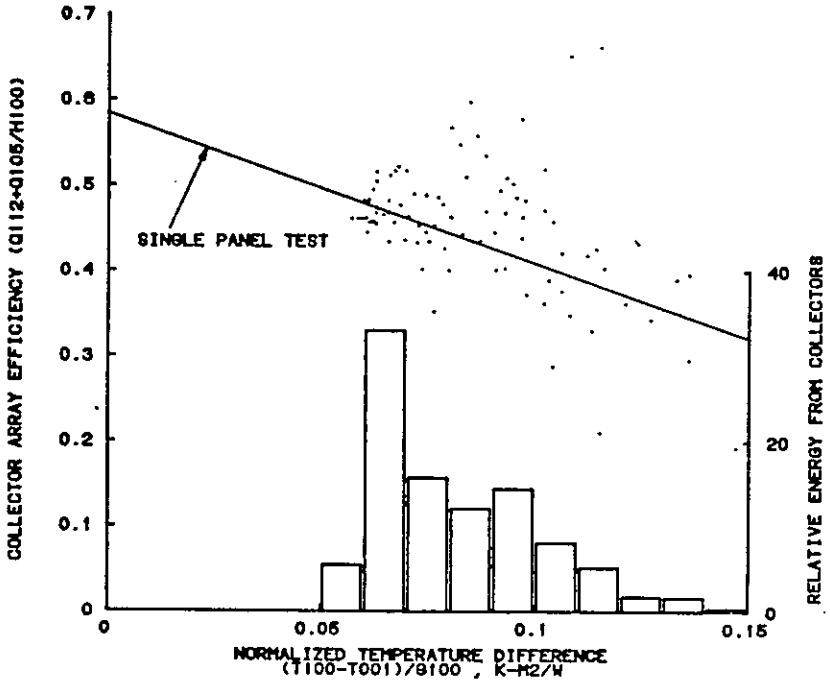

Figure 6.1-16. Collector Array Efficiency Diagram for Sydney University Evacuated Tubular Collector, All Day, Australia, 1 December 1984 to 30 December 1984.

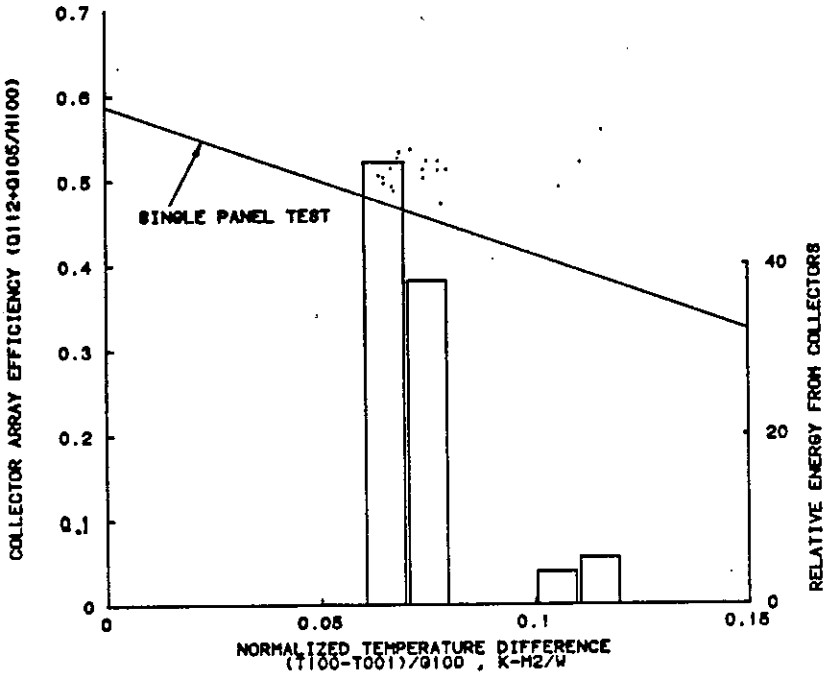

Figure 6.1-17. Collector Array Efficiency Diagram for Sydney University Evacuated Tubular Collector, 11 a.m., to 2 p.m., Australia, 1 March 1985 to 31 March 1984.

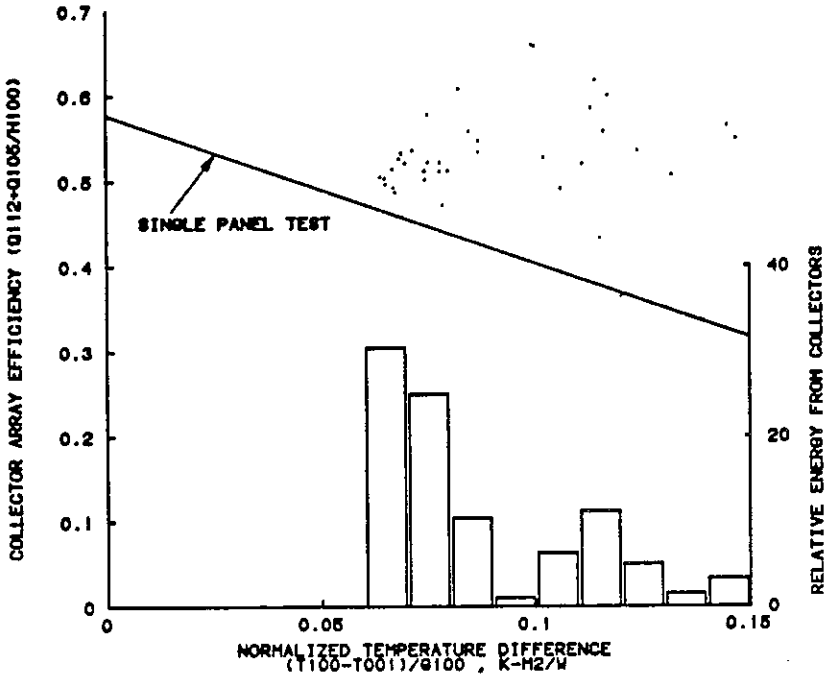

Figure 6.1-18. Collector Array Efficiency Diagram for Sydney University Evacuated Tubular Collector, All Day, Australia, 1 March 1985 to 31 March 1985.

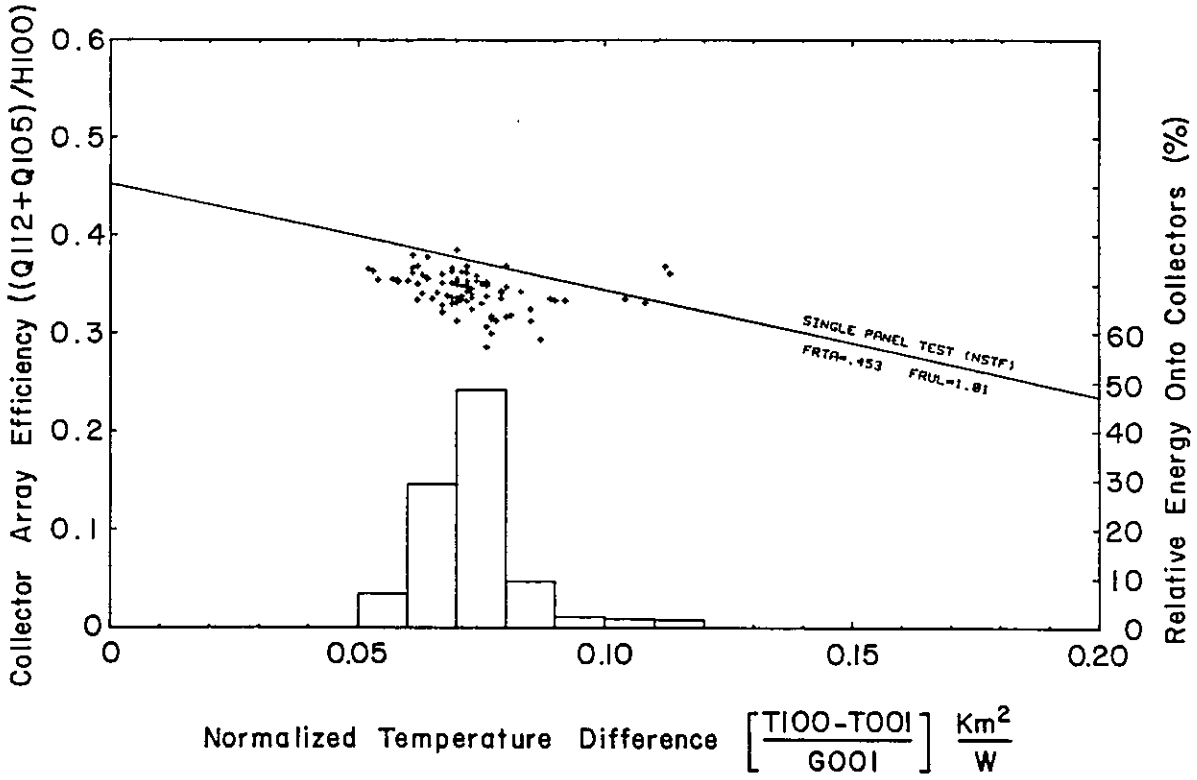

Figure 6.1-19. Collector Array Efficiency for Mountain Spring Bottle Washing Facility, Canada.

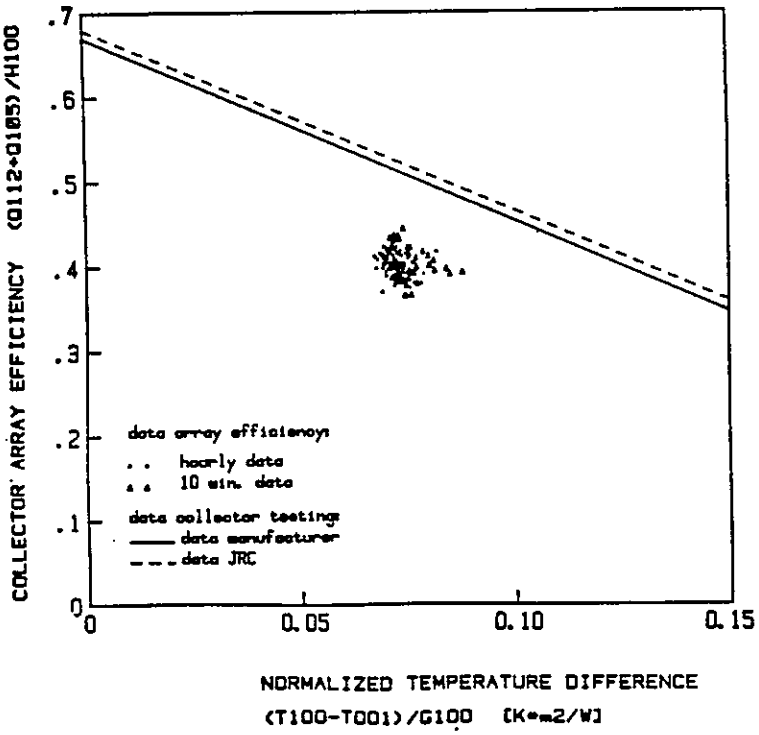

Figure 6.1-20. Collector Array Efficiency Diagram for the Sanyo (I) Collector, 11 a.m., to 2 p.m., Ispra Solar Laboratory, May to September 1983.

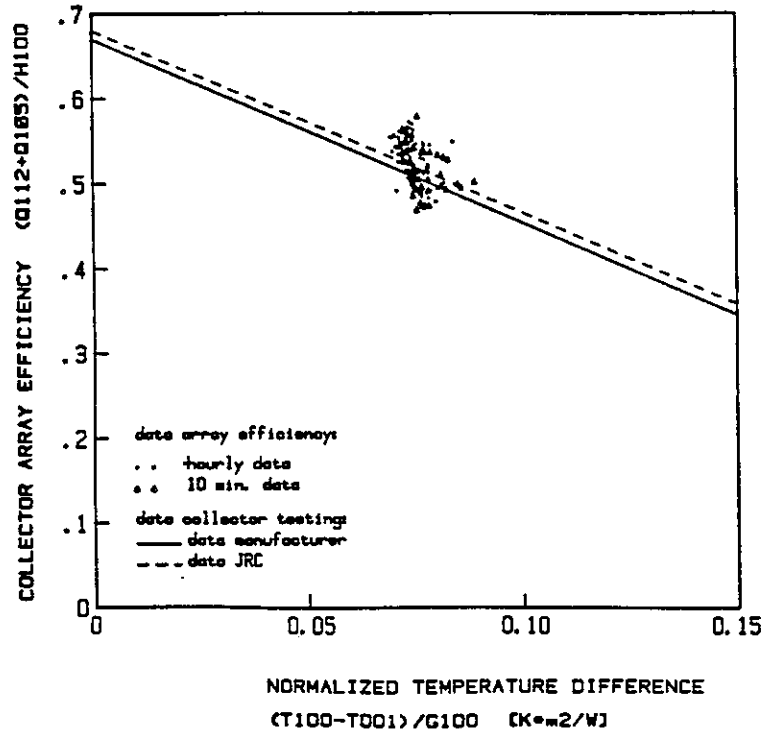

Figure 6.1-21. Collector Array Efficiency Diagram for the Sanyo (II) Collector, 11 a.m., to 2 p.m., Ispra Solar Laboratory, May to September 1983.

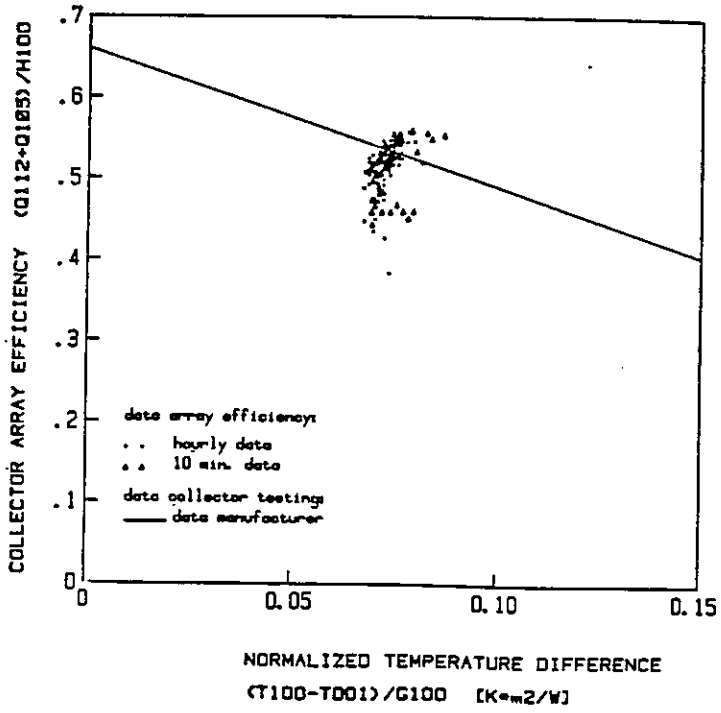

Figure 6.1-22. Collector Array Efficiency Diagram for the Philips VTR 261 Collector, 11 a.m., to 2 p.m., Ispra Solar Laboratory, May to September 1983.

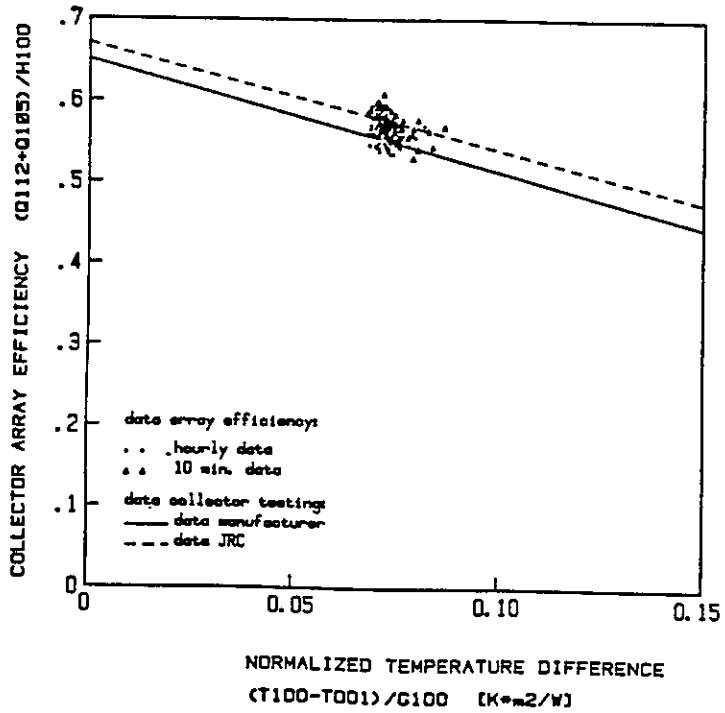

Figure 6.1-23. Collector Array Efficiency Diagram for the Philips VTR 361 Collector, 11 a.m., to 2 p.m., Ispra Solar Laboratory, May to September, 1983.

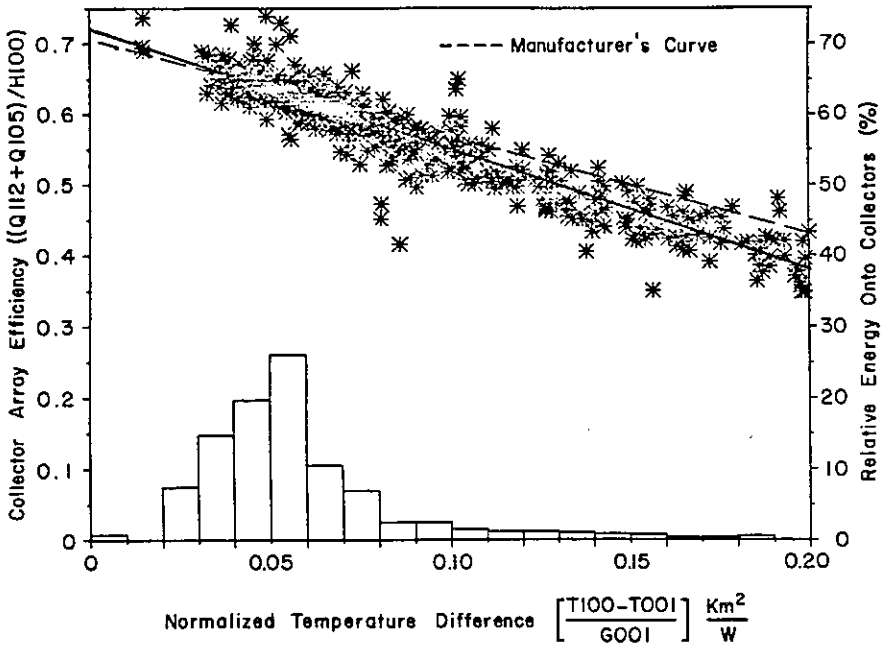

Figure 6.1-24. Collector Array Efficiency Diagram for the Corning Glass Collector at Solarhaus Freiburg, 11 a.m., to 2 p.m., Federal Republic of Germany, June 1982 to May 1983.

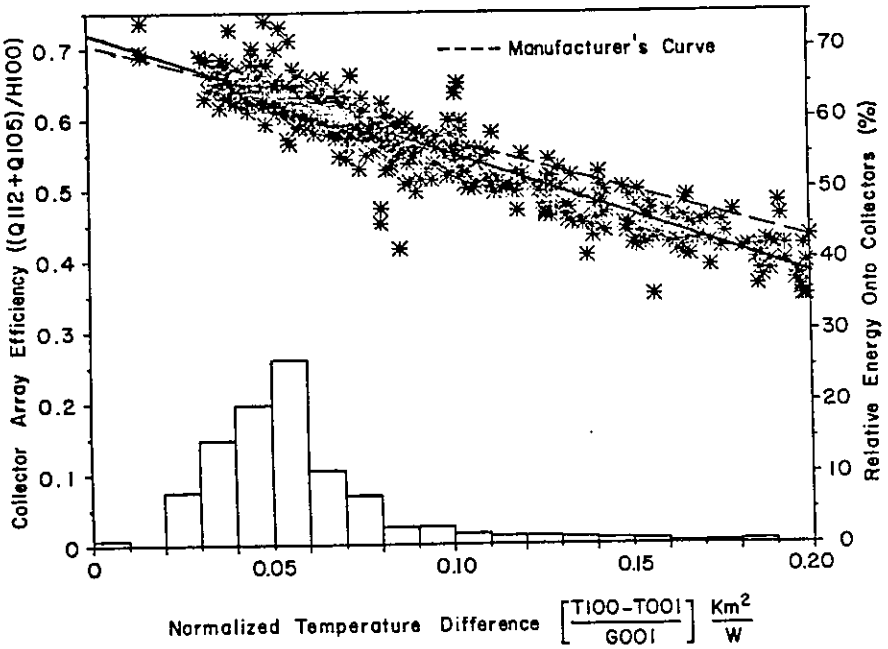

Figure 6.1-25. Collector Array Efficiency Diagram for the Philips/ Stiebel-Eltron Collector at Solarhaus Freiburg, 11 a.m., to 2 p.m., Federal Republic of Germany, June 1982 to May 1983.

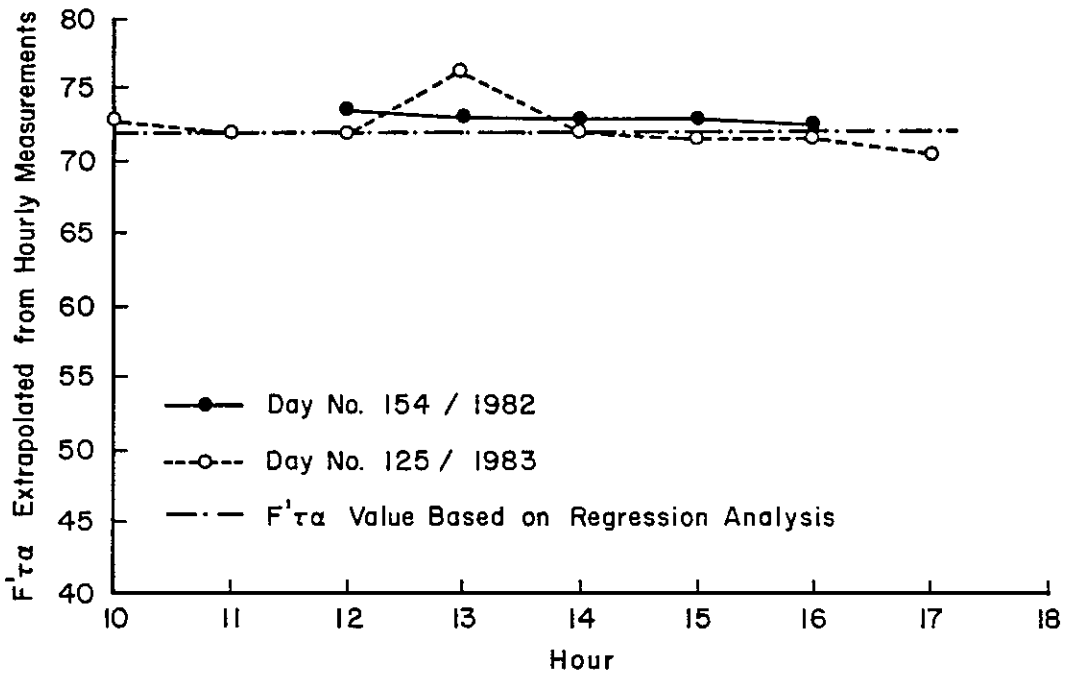

Figure 6.1-26. Extrapolated Transmittance-Absorptance Product for the Corning Glass Collector at Solarhaus Freiburg, Federal Republic of Germany.

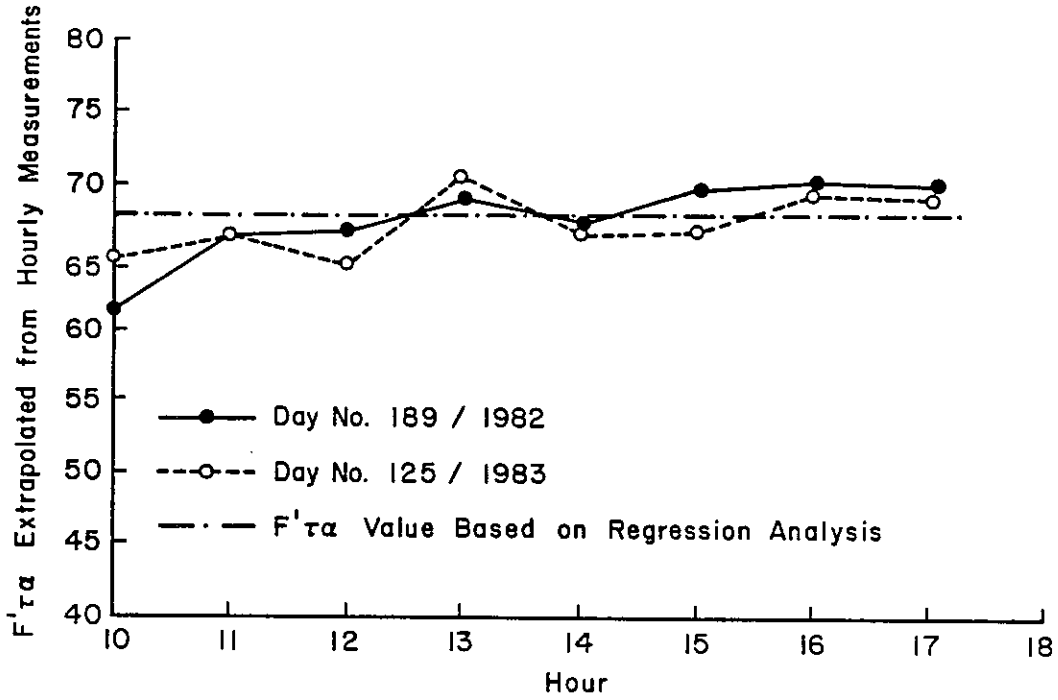

Figure 6.1-27. Extrapolated Transmittance-Absorptance Product for the Philips/Stiebel- Eltron Collector at Solarhaus Freiburg, Federal Republic of Germany.

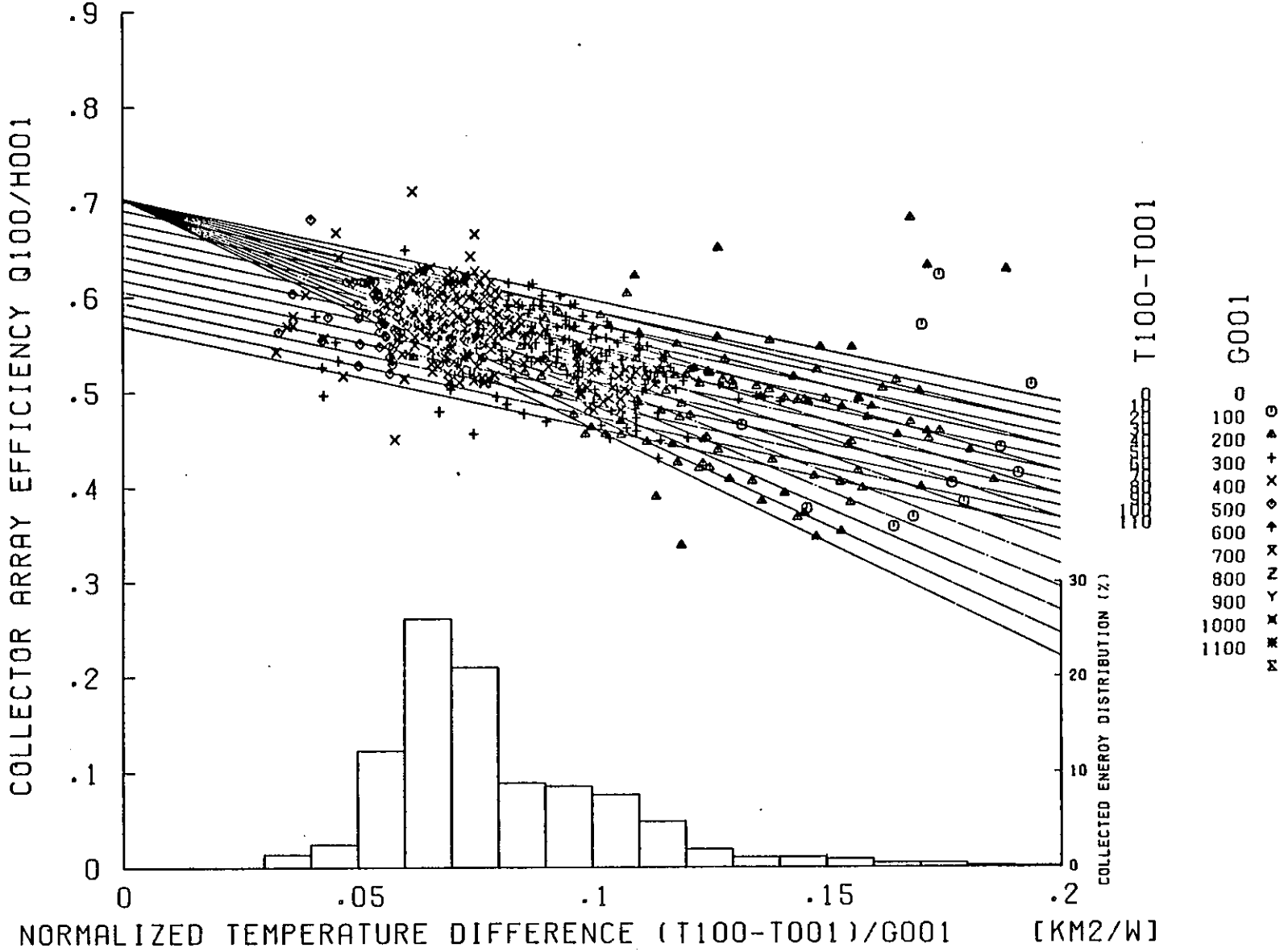

Figure 6.1-28. Collector Array Efficiency Diagram 10 a.m. to 5 p.m. for the Eindhoven University of Technology, The Netherlands.

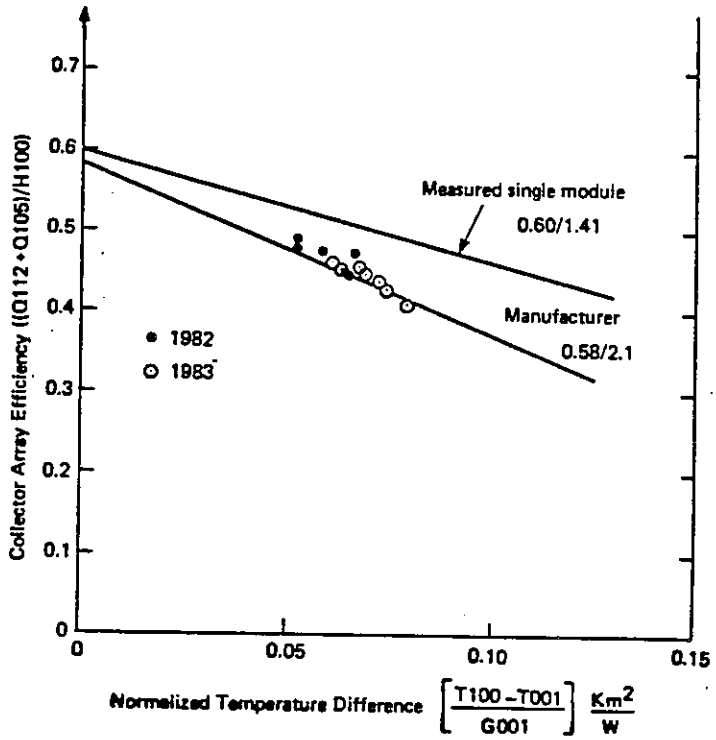

Figure 6.1-29. Collector Array Efficiency Diagram for the General Electric Collector, Knivsta, Sweden.

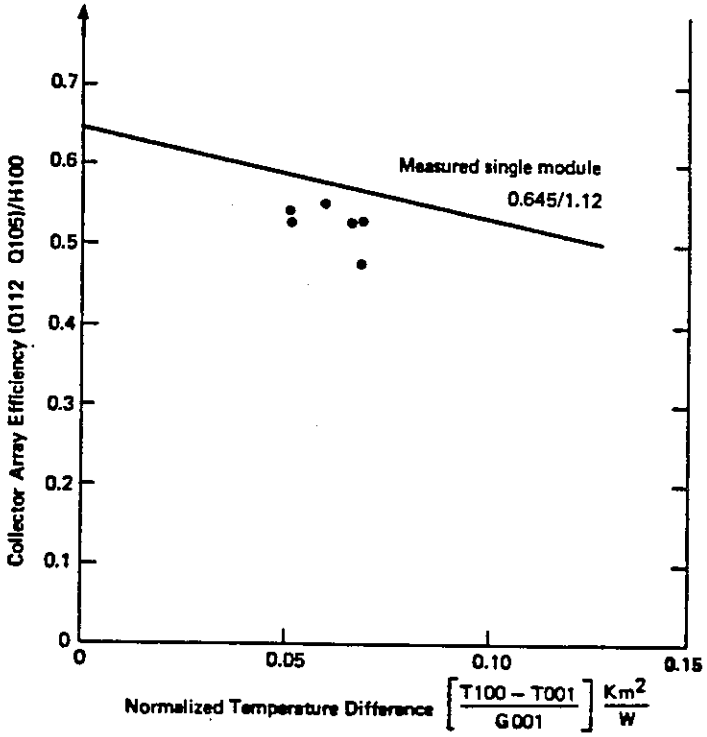

Figure 6.1-30. Collector Array Efficiency Diagram for the Owens-Illinois Collector, Knivsta, Sweden.

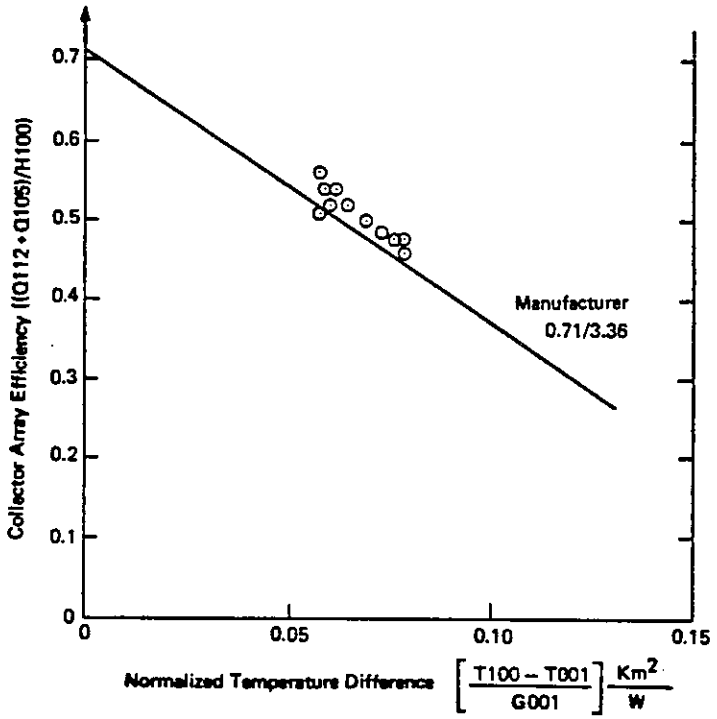

Figure 6.1-31. Collector Array Efficiency Diagram for the Scandinavian Solar HT Collector, Knivsta, Sweden.

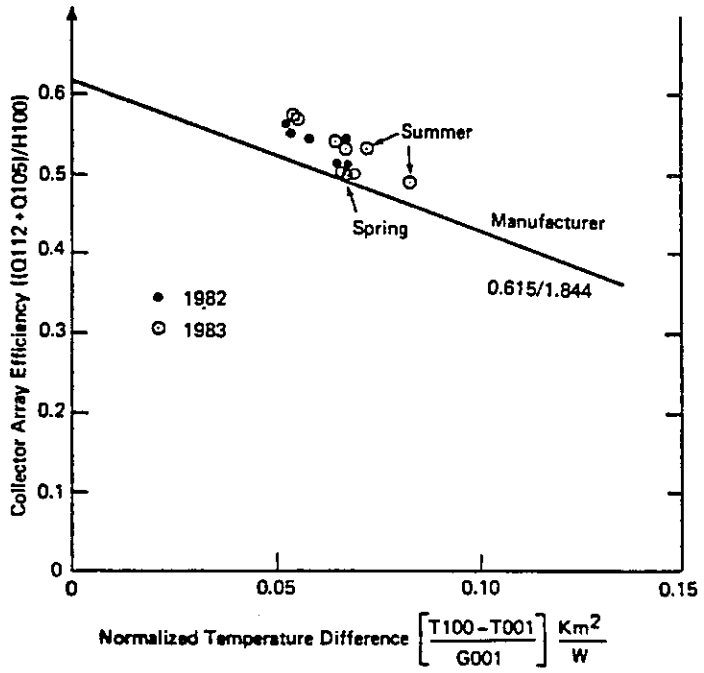

Figure 6.1-32. Collector Array Efficiency Diagram for the Philips Collector, Knivsta, Sweden.

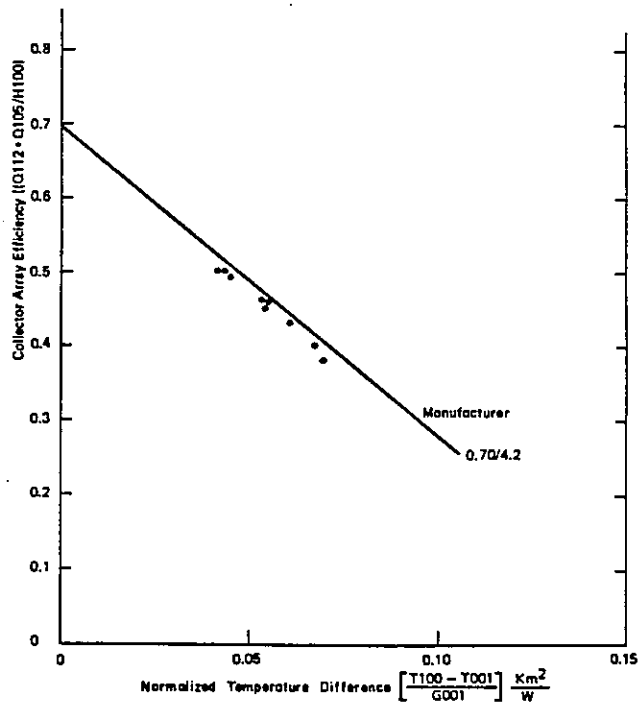

Figure 6.1-33. Collector Array Efficiency Diagram for the Teknoterm HT Collector, 11 a.m., to 2 p.m., Södertörn, Sweden, 1983.

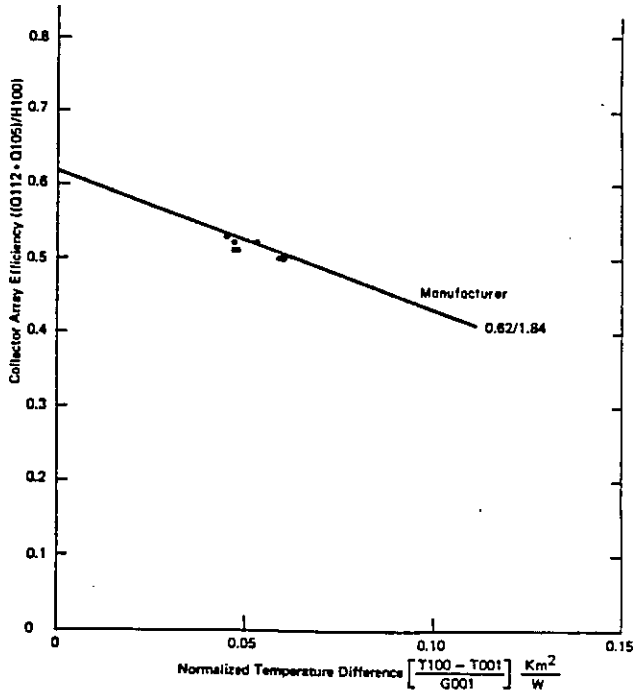

Figure 6.1-34. Collector Array Efficiency Diagram for the Philips VTR Collector, 11 a.m., to 2 p.m., Södertörn, Sweden, 1983.

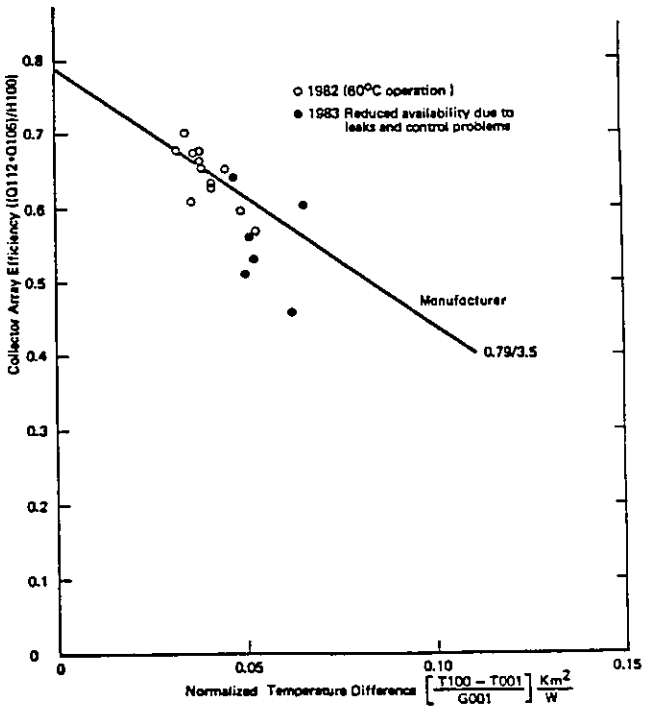

Figure 6.1-35. Collector Array Efficiency Diagram for the Granges Aluminum Collector, 11 a.m., to 2 p.m., Södertörn, Sweden, 1983.

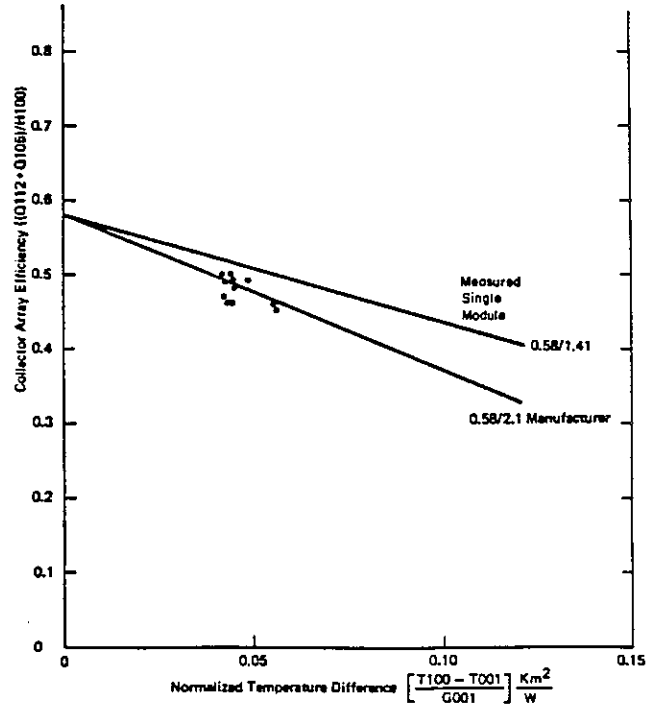

Figure 6.1-36. Collector Array Efficiency Diagram for the General Electric TC 100 Collector, 11 a.m., to 2 p.m., Södertörn, Sweden, 1983.

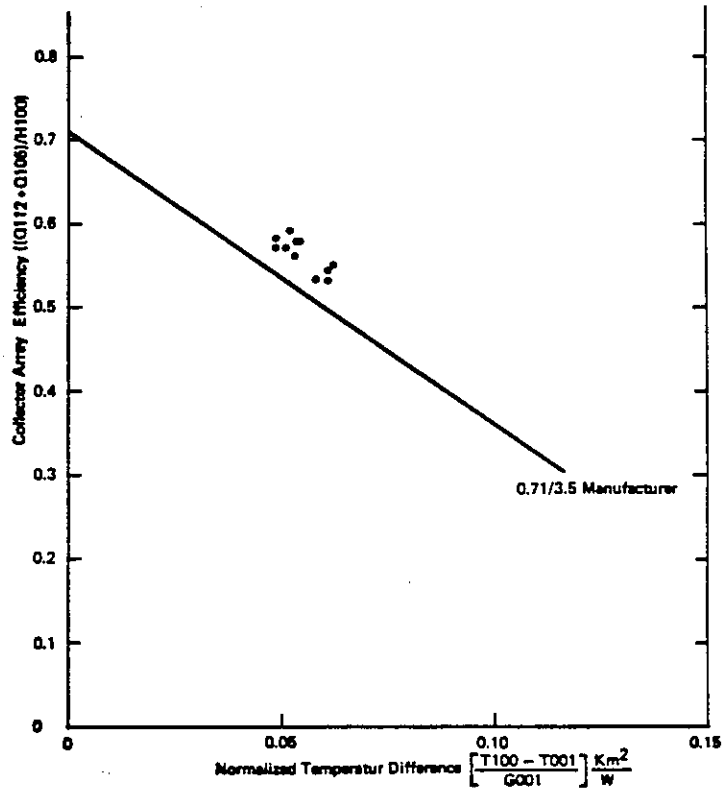

Figure 6.1-37. Collector Array Efficiency Diagram for the Scandinavian Solar HT Collector, 11 a.m., to 2 p.m., Södertörn, Sweden, 1983.

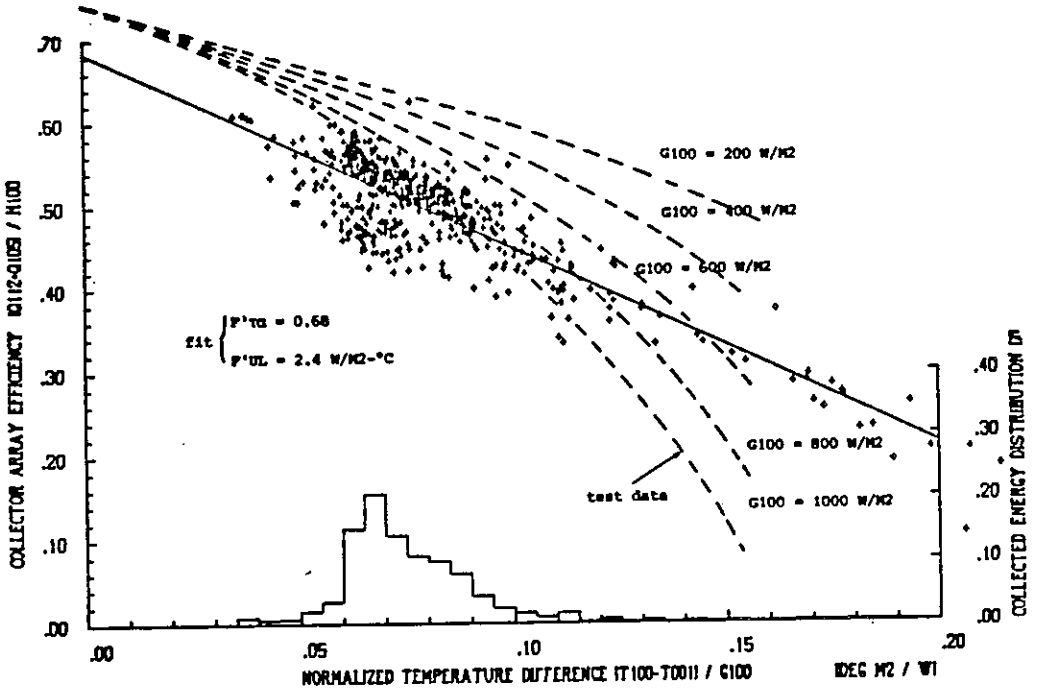

Figure 6.1-38. Collector Array Efficiency Diagram for the Corning Cortec "A" Collector, 11 a.m., to 2 p.m., Geneva, Switzerland, January 7, 1982 to September 30, 1983.

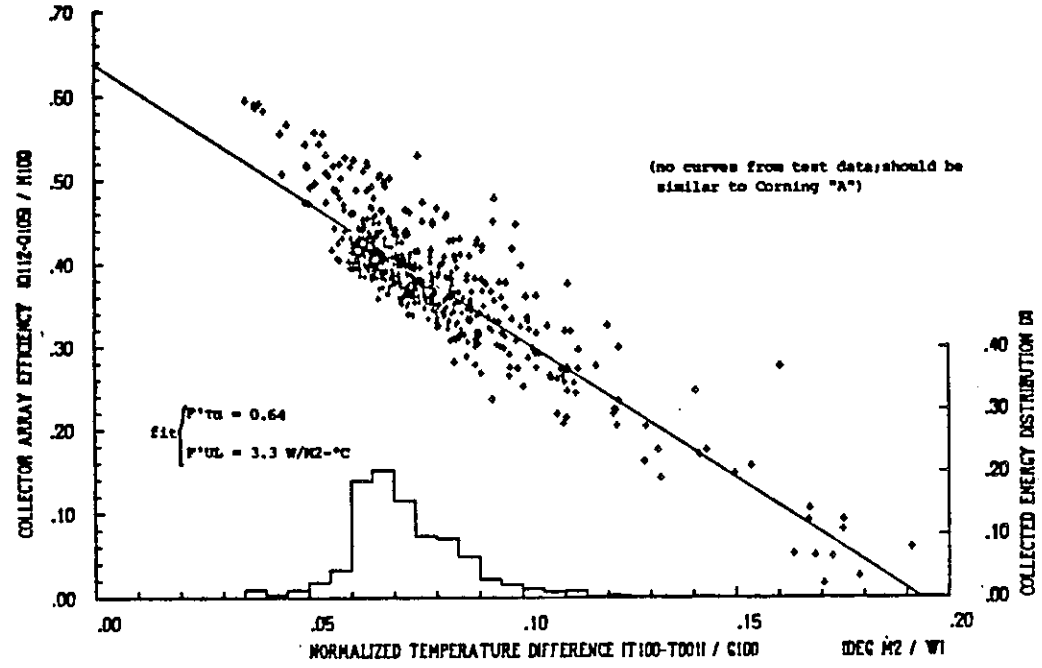

Figure 6.1-39. Collector Array Efficiency Diagram for the Corning Cortec "B" Collector, 11 a.m., to 2 p.m., Geneva, Switzerland, January 7, 1982 to September 30, 1983.

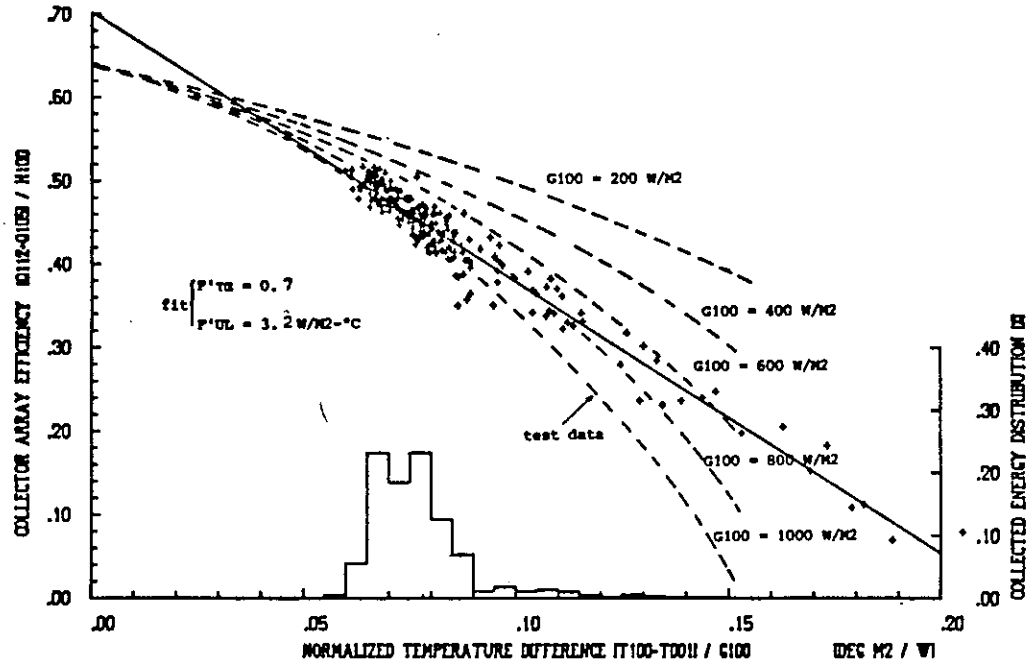

Figure 6.1-40. Collector Array Efficiency Diagram for the Sanyo STC-CU250 Collector, 11 a.m., to 2 p.m., Geneva, Switzerland, January 4, 1982 to August 25, 1983.

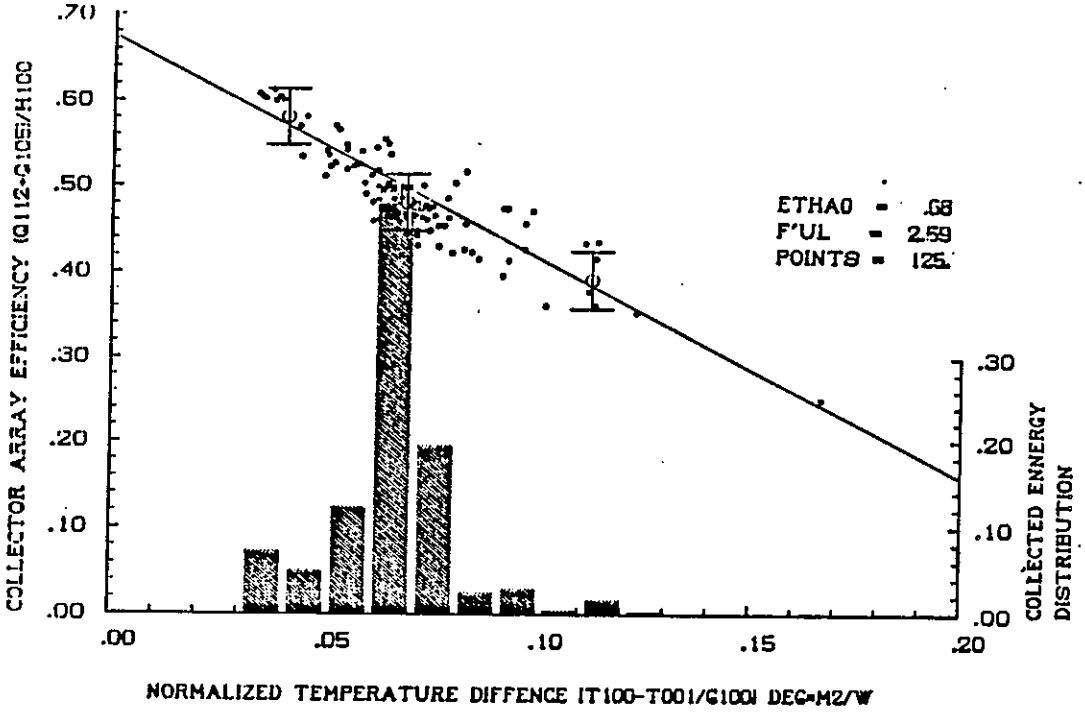

Figure 6.1-41. Collector Array Efficiency Diagram for the Corning Cortec "A" Collector, 11 a.m., to 2 p.m., Geneva, Switzerland, July 1, 1982 to November 4, 1982.

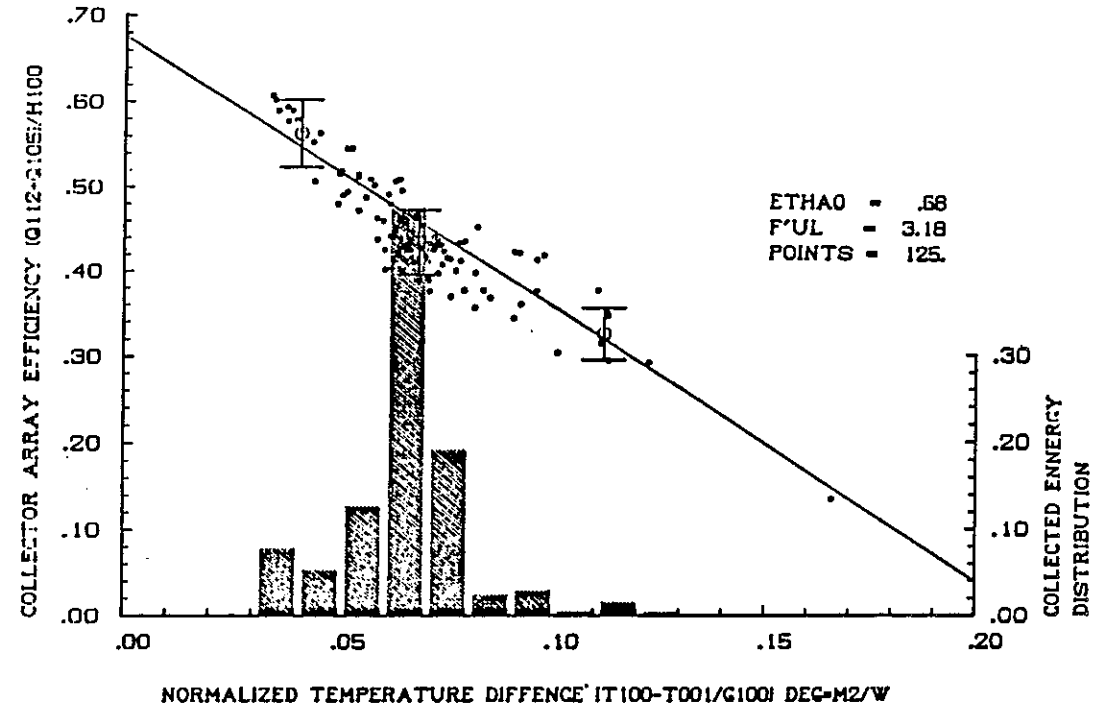

Figure 6.1-42. Collector Array Efficiency Diagram for the Corning Cortec "B" Collector, 11 a.m., to 2 p.m., Geneva, Switzerland, July 1, 1982 to November 4, 1982.

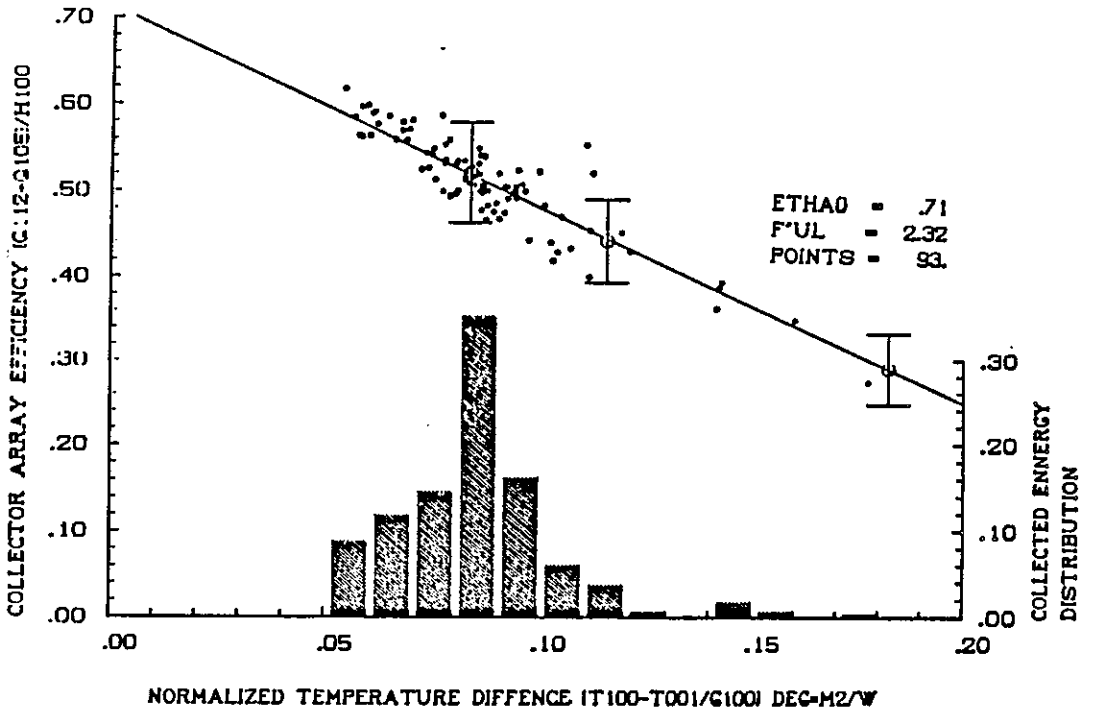

Figure 6.1-43. Collector Array Efficiency Diagram for the Corning Cortec "A" Collector, 11 a.m., to 2 p.m., Geneva, Switzerland, November 4, 1982 to March 31, 1983.

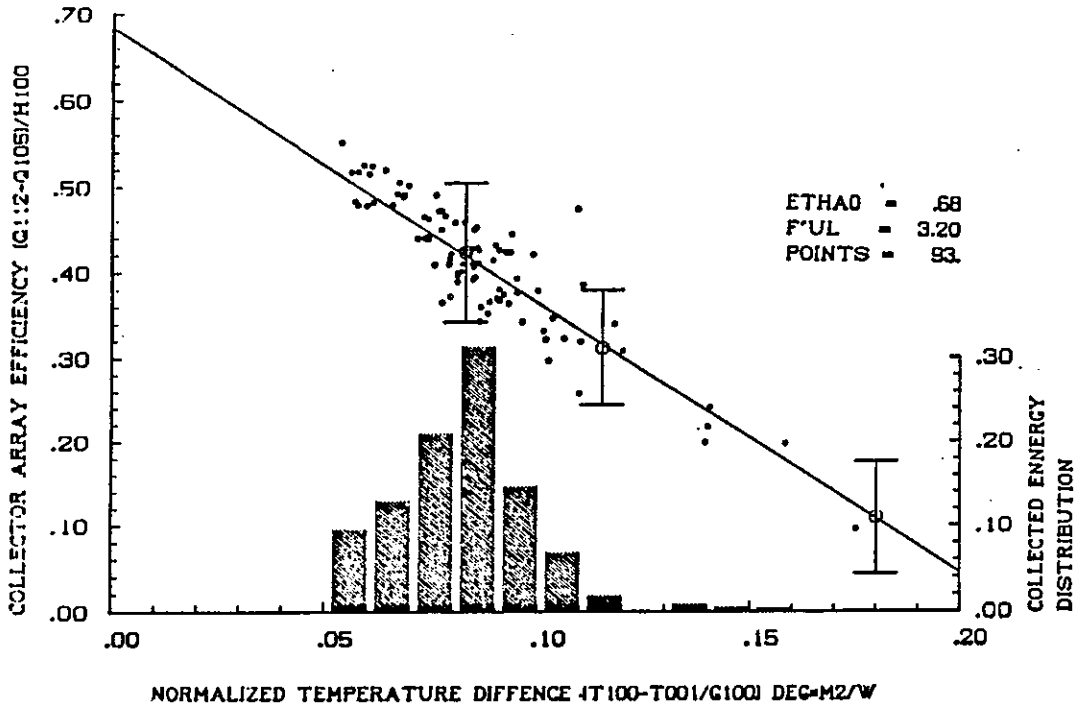

Figure 6.1-44. Collector Array Efficiency Diagram for the Corning Cortec "B" Collector, 11 a.m., to 2 p.m., Geneva, Switzerland, November 4, 1982 to March 31, 1983.

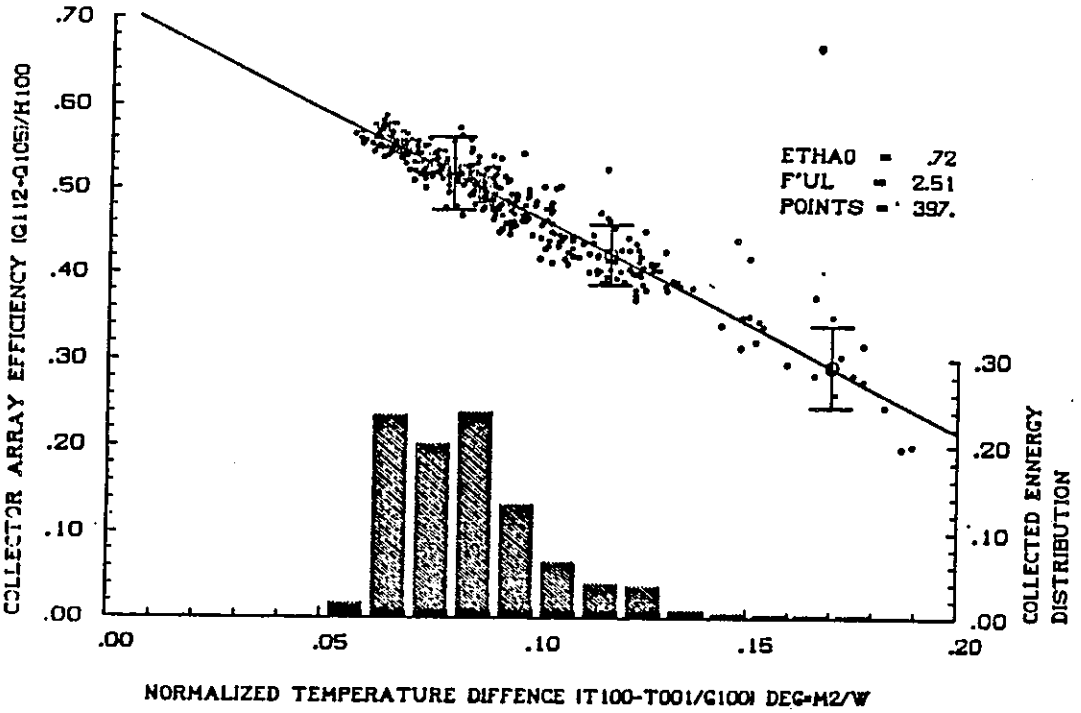

Figure 6.1-45. Collector Array Efficiency Diagram for the Corning Cortec "A" Collector, 11 a.m., to 2 p.m., Geneva, Switzerland, April 1, 1983 to March 31, 1984.

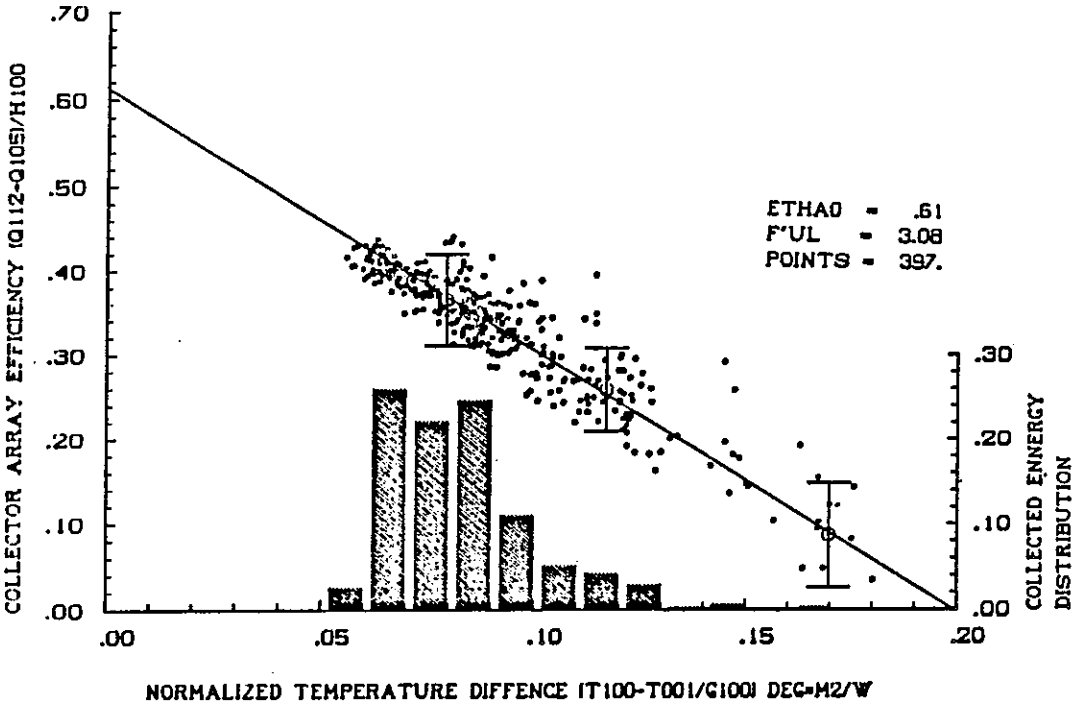

Figure 6.1-46. Collector Array Efficiency Diagram for the Corning Cortec "B" Collector, 11 a.m., to 2 p.m., Geneva, Switzerland, April 1, 1983 to March 31, 1984.

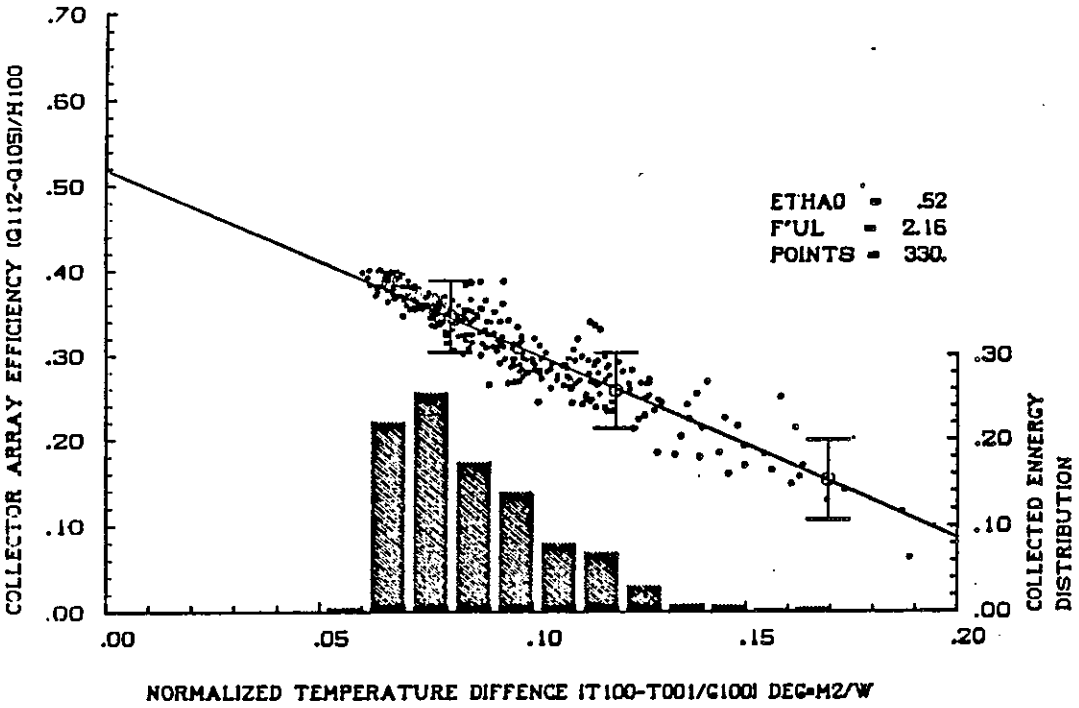

Figure 6.1-47. Collector Array Efficiency Diagram for the Sanyo STC-CU250 Collector, 11 a.m., to 2 p.m., Geneva, Switzerland, April 1, 1983 to March 31, 1984.

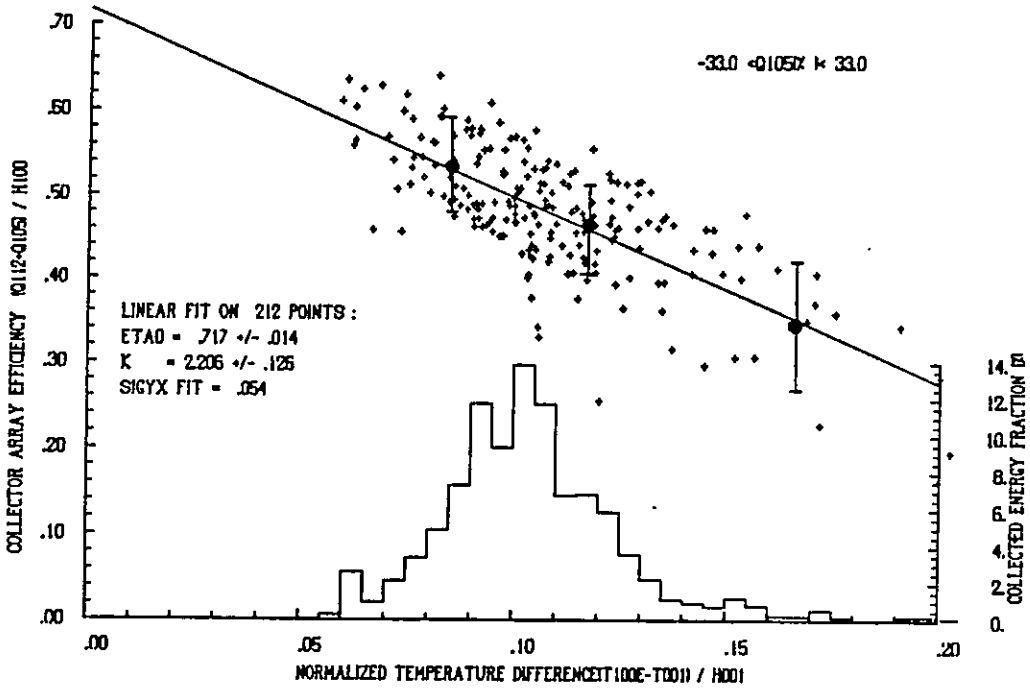

Figure 6.1-48. Cortec ETC Array Efficiency Diagram, 11 a.m. to 2 p.m., Hallau, Switzerland, March 3, 1984 to February 28, 1985.

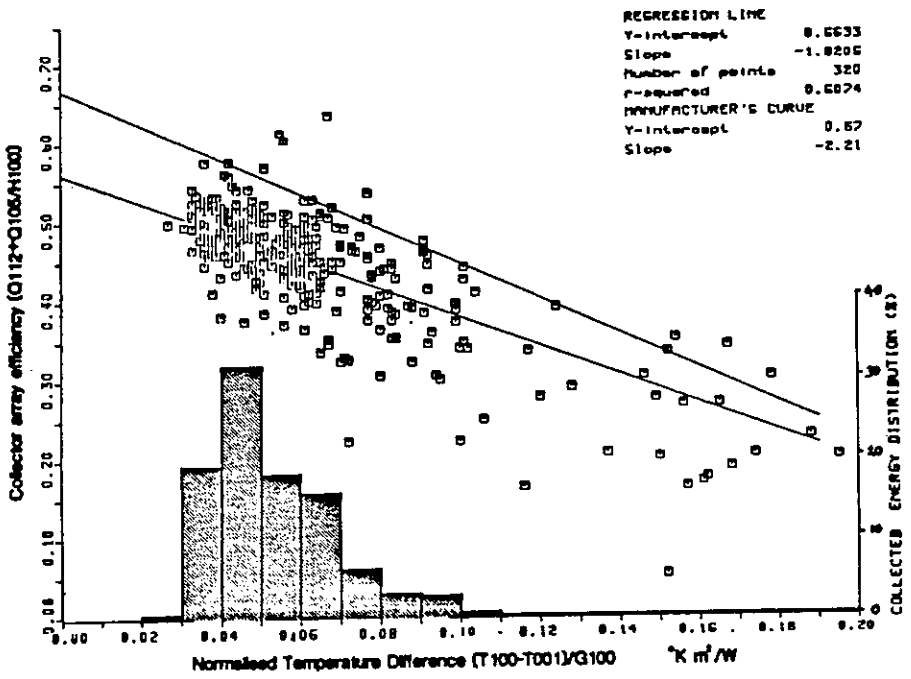

Figure 6.1-49. Collector Array Efficiency Diagram for the Philips VTR151 Collector, 11 a.m. to 2 p.m., Bracknell, United Kingdom, September, 1981 to May 1983.

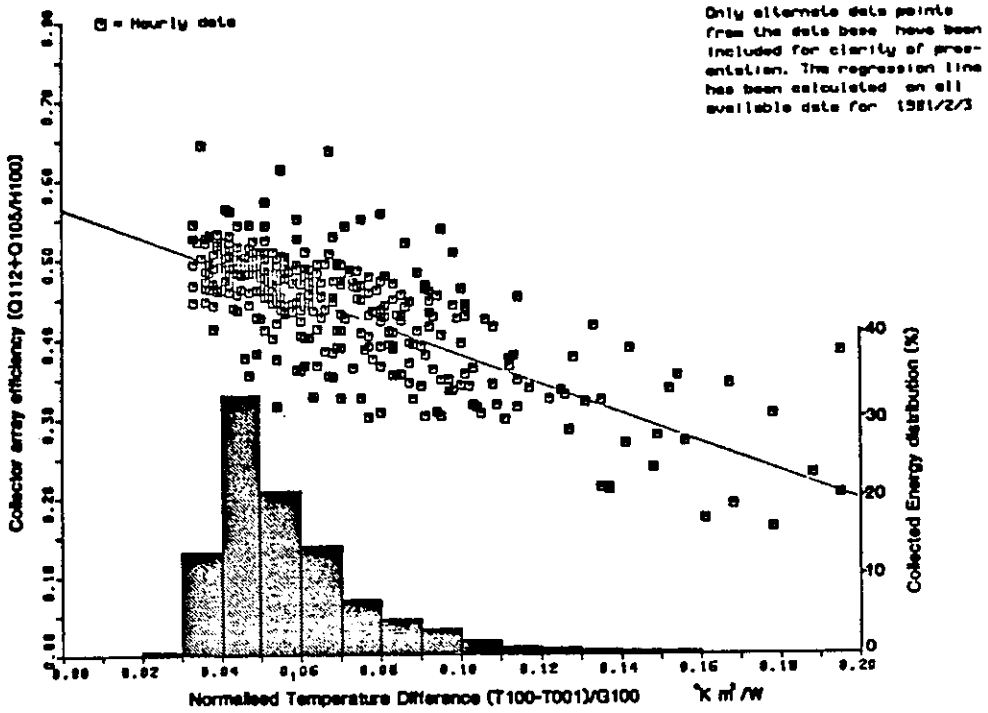

Figure 6.1-50. Collector Array Efficiency Diagram for the Philips VTR151 Collector, All Day, Bracknell, United Kingdom, September, 1981 to May 1983.

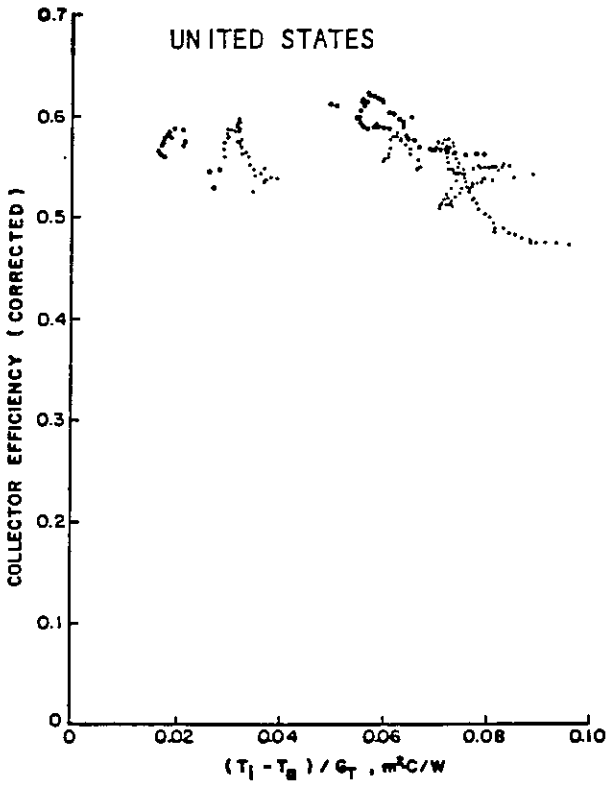

Figure 6.1-51. Instantaneous Efficiency for Selected Days, CSU Solar House I, United States, 1983-1984.

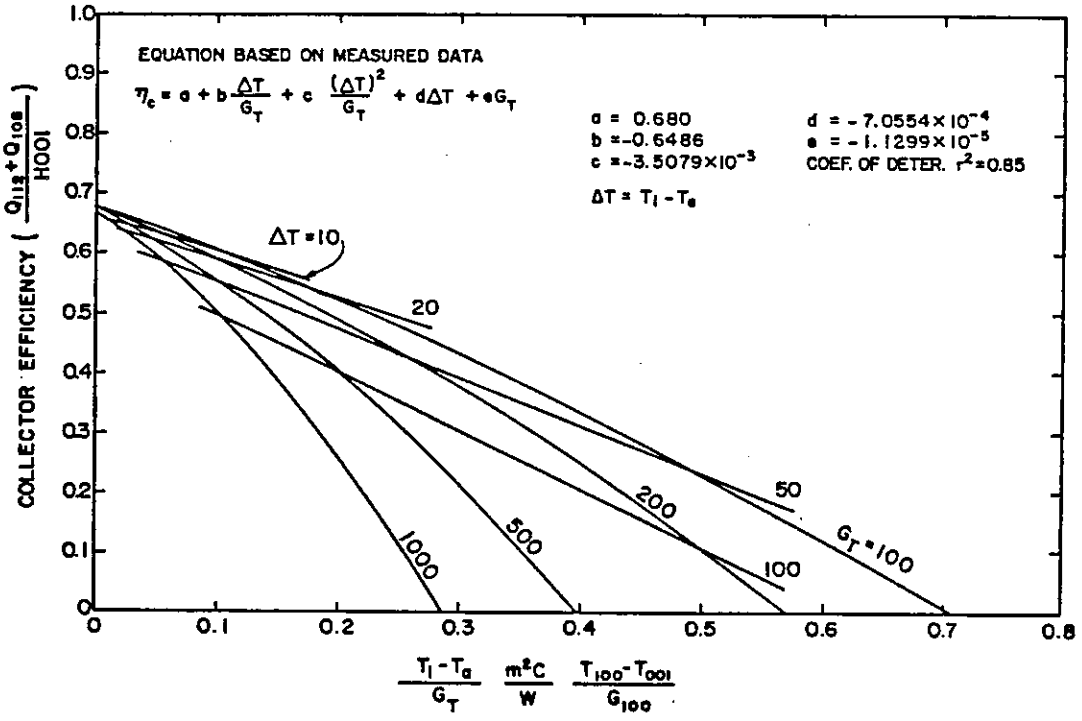

Figure 6.1-52. Instantaneous Efficiency for Philips VTR 361 Collectors on CSU Solar House I, United States, 1982 to 1983.

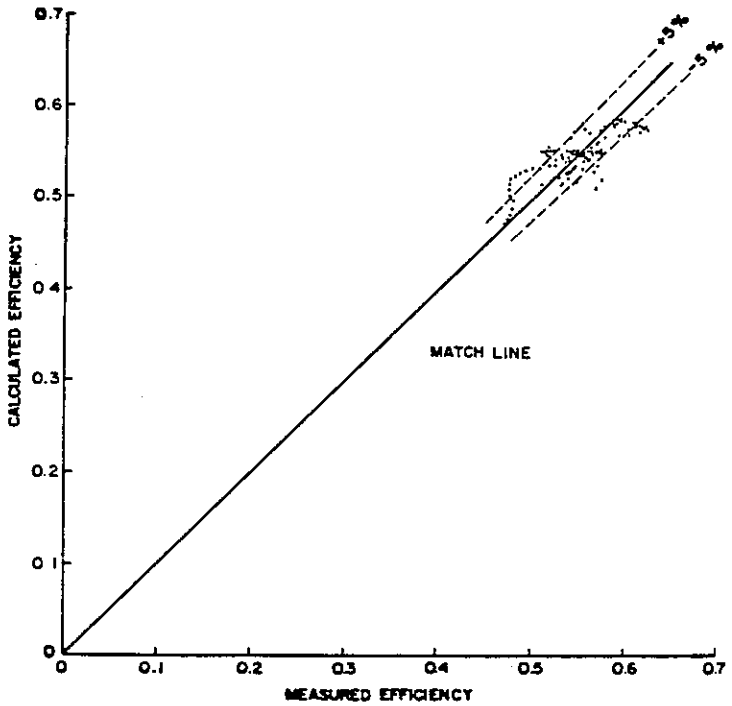

Figure 6.1-53. Comparison of Measured and Calculated Efficiencies, CSU Solar House I, United States.

6.2 DAILY ENERGY INPUT/OUTPUT PLOTS

Daily energy input/output plots are generated by fitting a least squares regression line to daily collection performance data. As can be seen in the figures, the points, when aggregated into average collector to average ambient temperature difference ranges, closely fit a linear curve. The ordinate in these plots is the daily total solar energy collected per unit collector aperture area, Q112/A100. The abscissa is the daily total solar energy incident on the aperture plane per unit of collector aperture area, H100/A100.

Normally one daily energy input/output plot is included for each experimental period. If appropriate, however, several experimental periods are combined. Only monthly regression lines are shown for the various temperature difference ranges in order that differences among systems and operating conditions can be clearly seen. The number of points used in the regression and the variance, or coefficient of determination, are also shown.

6.2.1 The Sydney University Solar Heating and Cooling System Sydney, Australia

Eight daily energy input/output plots are shown. The first input/output diagram, Figure 6.2-1, gives an indication of the average daily collector output of the Sydney University evacuated tubular collector during the summer months 1982/83. The information presented is based on heat meter readings of energy collection at the tank and thus includes pipe losses.

Figure 6.2-2 covers the winter mode operating period of the Yazaki flat-plate collector during July 9-23, 1983. The third input/output diagram, Figure 6.2-3, is again for the Sydney University evacuated tubular collector during spring 1983 where, due to the small load, the collectors operated at very high temperatures with correspondingly high ΔT (collector minus ambient temperature). Nevertheless, the array performance of the evacuated tubular collectors is very good, with an average daily energy yield of 8.8 MJ/m^2 at a solar incidence of 20.0 MJ/m^2-day at ΔT's ranging between 60 and 75^{o}C.

Figure 6.2-4 shows an input/output diagram for October/November 1983 for two different ΔT ranges, 45-60^{o}C and 60-75^{o}C. Figure 6.2-5 covers the period December 1983 to April 1984 yet for only one ΔT group 45-60^{o}C.

The input/output diagram for typical winter operation (May to July 1984) is given in Figure 6.2-6. A seasonal shift of input/output lines of constant ΔT is noticeable. As a result of shorter days in winter, input/output lines move to the left. Figure 6.2-6 shows a solar radiation threshold of 3 MJ/m^2d for the ΔT-range 45-60^{o}C whereas during summer the threshold value is approximately 5 MJm^2d. The slope of input/output lines of constant ΔT remains approximately constant.

Figures 6.2-7 and 6.2-8 are input/output diagrams for September/October 1984 and December 1984 to February 1985. The input/output line for $\Delta T=60-75^{o}C$ in Figure 6.2-7 shows a slightly different slope compared with the input/output line for the smaller ΔT-group. The apparent change is more a result of a lack of data points for low solar fluxes rather than a real collector behavior.

The information given in Figure 6.2-8 for the period December 1984 to February 1985 is almost identical to the results obtained from measurements during the same period in 1983/84. There has not been any measurable change in collector performance during the two year system operation using S.U. evacuated collectors.

6.2.2 Mountain Spring Bottle Washing Facility Edmonton, Canada

Daily energy input/output curves are shown in Figures 6.2-9 through 6.2-19. The figures are generated by fitting a linear least squares curve to daily data points of total daily energy in the collector plane (HI00) versus the energy collected (Q112). Energies are normalized by the aperture area. Both yearly and monthly input/output curves are given.

Figures 6.2-9 and 6.2-11 are yearly input/output curves for the periods May through December 1982, January through December 1983 and January through November 1984. The number of points on each graph is not equal to the number of days in each of the periods in question as a result of the filtering of the data to remove any days in which the solar system or data acquisition system operated in an unsatisfactory manner (i.e., snow on collectors, unserviceable flow meters). The yearly input/output curves show remarkable repeatability. In 1982, the X-intercept and slope were 4.3 and 0.37, respectively, while in 1983 they were 4.6 and 0.39. In 1984, the X-intercept and slope were 4.6 and 0.38.

Figures 6.2-12 through 6.2-18 are monthly input/output curves for the months of December 1982, February 1983, July 1983, February 1984, April 1984, July 1984 and October 1984. Note that for the production of these curves all monthly daily points are used except outlyers resulting from solar system or data acquisition malfunction. Table 6.2-1 gives pertinent input/output data (month, slope, X-intercept, number of points, and ΔT) for 1983 and 1984.

As expected, there is great variation in the input/output curves between winter and summer months. In the winter months, X-intercept and slope range from 1.56 to 4.52 and from 0.16 to 0.373 respectively, while in the non-winter months, the X-intercept ranges from 3.12 to 7.32 and the slope ranges from .349 to .459. The small X-intercept in the winter months is explained largely by shorter collector operating hours, while the smaller slope value (which is largely an expression of collector optical efficiency) is explained by factors such as snow cover and shading effects.

TABLE 6.2.1 INPUT/OUTPUT DATA FOR 1983/1984 FOR SOLARTECH ETC MOUNTAIN SPRING, EDMONTON, CANADA

YEAR	MONTH	SLOPE	X-INTERCEPT (MJ/m^2-day)	No. of Points	ΔT (K)	CORRELATION COEFFICIENT
1983	Jan.	0.160	3.84	31	64	0.916
	Feb.	0.269	3.48	22	63	0.941
	March	0.313	4.52	21	66	0.940
	April	0.381	4.63	25	63	0.977
	May	0.403	5.29	31	56	0.990
	June	0.392	4.53	26	54	0.989
	July	0.414	4.65	31	53	0.990
	Aug.	0.416	4.56	29	54	0.984
	Sept.	0.377	3.30	27	57	0.990
	Oct.	0.367	3.12	29	57	0.992
	Nov.	0.310	3.16	5	49	0.960
	Dec.	0.063	8.04	14	27	0.841
1984	Jan.	0.238	1.56	15	27	0.993
	Feb.	0.335	4.03	29	64	0.966
	March	0.373	4.15	25	70	0.987
	April	0.404	4.23	30	60	0.993
	May	0.388	4.39	30	59	0.984
	June	0.405	5.29	26	57	0.992
	July	0.433	6.09	30	56	0.990
	Aug.	0.459	7.32	31	55	0.982
	Sept.	0.351	5.22	29	63	0.977
	Oct.	0.349	4.58	25	57	0.982
	Nov.	0.172	3.07	19	58	0.760
	Dec.	N/A	N/A	N/A	N/A	N/A

Includes all points except outlyers and Q112 = 0

The fact that some of the points in the winter are indicative of negative values of collected energy is worth commenting on. It appears to be a peculiarity of data collected from a system possessing large piping capacitance and operating in the drainback mode. As a result of this combination of factors, there will be a number of days during the winter months when the collector system is turned on and the capacitance heat loss to the piping will not be made up by the collected solar energy, thus giving an overall negative output for the day. In a non-drained system, on the other hand, such negative energy collection data will not occur. However, because start-up losses are higher, there will be more non-operational days in a non-drained system and therefore its overall energy delivery will often be lower.

A 1984 all-year input/output plot is shown in Figure 6.2-19. It is interesting to note the curvature suggested by the data points near the origin of the plot corresponding to the winter months, namely November through February. The data points, near the origin of the plot,

correspond to periods of solar system operation with low solar altitude, shading of the collector array and possible snow accumulation on the collector modules. Thus analyses of the input/output plots from the winter months can lead to erroneous results. An analysis using only clear-day points is now used for the purpose of studying the seasonal differences.

6.2.3 Ispra Solar Heated and Cooled Laboratory Commission of European Communities

Figures 6.2-20 to 6.2-43 display the daily energy input/output diagrams for the four collector arrays.

Figure 6.2-20 refers to the Sanyo collectors without reflectors, for the years 1981 and 1982. Also in this figure a performance decrease can be observed. The regression line given in this figure refers to the data of 1982.

The decrease in performance of the Sanyo collectors that was evident in the efficiency plots may also be seen in the daily energy input/output diagrams. It is also seen that the Philips VTR 361 collectors outperform the VTR 261 collectors.

6.2.4 Solarhaus Freiburg Federal Republic of Germany

Collector system input/output diagrams are shown in Figures 6.2-44 and 6.2-45 for the Corning Glass Collector and in Figures 6.2-46 and 6.2-47 for the Philips/Stiebel-Eltron heat-pipe collector. Generally, both collectors display the strong linear relationship which has already been found in previous operating periods.

The daily radiation threshold value of the new Philips/Stiebel-Eltron heat-pipe collector is in the same order of magnitude as the value for the Corning Glass collector and less than half the value of the old Philips Mark IV collector. This is certainly due to the lower heat loss coefficient and the lower capacitance of the heat-pipe collector.

A comparison of the slope and x-intercept values of the Corning Glass collector with values of preceding years shows a slight variation. The Corning Glass collector has higher x-intercepts in 1979 and 1982/83 when it was operating with the heating system, than from 1980 to 1981 when it was operating with the domestic hot water system. One reason for this behavior is certainly the difference of the typical daily temperature profiles of the solar heating system and the solar domestic hot water system. That is, at the end of the day the collector temperature in the heating system approaches the storage tank temperature which is normally close to the daily maximum collector temperature. However, in a domestic hot water system, the late afternoon warm water load causes the end-day collector temperature to decrease towards the cold water inlet temperature of the storage tank. Thus, the different

daily temperature profiles show the impact of a specific load type on the parameters of input/output curves.

The slope of the Corning Glass collector input/output curve is higher in 1979 and in 1982/83. The reason for this variation is probably the change of the southern surroundings of the Solarhaus during the measurement periods, which caused the following effects. In 1980 and 1981, a construction crane was slightly shading the collectors. Since the end of 1981, the vitrified roof-tiles of a new residence placed immediately south of the Solarhaus is probably slightly enhancing the incident radiation over a major part of the collectors, and this radiation is not measured by the pyranometer which is mounted near the extreme west part of the collectors.

During several summer nights, the collectors were continuously operated at temperatures above 70°C in order to measure the thermal loss factor of the collector field. The experiment gave a heat loss parameter of 1.34 $W/m^2.K$ for the Corning Glass collector, which is very close to the value of the regression analysis of the efficiency diagram. In the case of the Philips/Stiebel-Eltron heat-pipe collector, because of the one-way heat transfer of the heat-pipe, the measured heat loss in this experiment of 0.8 $W/m^2.K$ corresponds only to the part of the installed piping and of the header. If the heat loss factor of the efficiency curve is assumed for the total installation, the heat loss of an individual tube would amount to 0.07 W/K per tube.

6.2.5 Eindhoven Technological University Solar House, The Netherlands

Collector array input/output diagrams are shown in Figures 6.2-48 through 6.2-51, for January, March, and September 1984 and for the whole year 1984.

The data from days on which the flow through the collector array is stopped because of overheating of the storage, from days without collector operation, or from days with monitoring errors are not displayed and not included in the regression analysis. Mainly due to overheating, only a few data points are left in summer. The input/output curves by month are displayed without grouping them into ΔT ranges because the numbers of points in the separate ranges was too low to give a meaningful regression. As can be seen in the input/output curves by year, the regression curves for the different ΔT ranges are very close and in fact the spacing is insignificant.

The regression curves are calculated for a function of one variable with both a measuring error in the function and the variable in the following way:

Slope $\quad (\Sigma x\ \Sigma y/n - \Sigma(x\ y))/((\Sigma x)^2/n - \Sigma x^2)$

y-intercept $\quad (\Sigma y - \text{slope}\ \Sigma x)/n$

x-intercept	-y intercept/slope
correlation coefficient	slope $((\Sigma x^2/n-(\Sigma x/n)^2)\cdot.5 \; / \; (\Sigma y^2/n-(\Sigma y/n)^2))\cdot.5$

6.2.6 Knivsta District Heating System, Knivsta, Sweden

The input/output diagram of Figure 6.2-52 shows regression lines for daily sums from two periods with nearly constant operating conditions. The first one from March until September 1982 and the second one from February until June 1983. The change between the two periods for General Electric collectors and Philips collectors, shows no significant degradation in performance. The flat-plate Scandinavian Solar collector shows some intermediate performance compared to the evacuated tubular collectors. The operating ΔT has been around $60^{o}C$ for all collectors.

The daily points giving the lines for the second period are presented in Figures 6.2-53 through 6.2-55. The correlation coefficient is surprisingly high for such a long period containing both winter and summer days. The Scandinavian Solar collector shows the largest spread but this is partly caused by deaeration problems during the first operating period.

6.2.7 The Södertörn District Heating Project, Södertörn, Sweden

The daily average input/output performance for four of the collector systems is shown in Figure 6.2-56. The lines are long-term regression lines for the period May to October 1982. The operating ΔT has been very stable and the variance indicates that the single line presentation could be meaningful even for such long periods in this system application. The Philips collectors show the highest performance for all daily insolation levels. The flat-plate collectors require higher threshold insolation but the slopes are similar to the Philips collectors. General Electric collectors show an intermediate characteristic.

For the $80^{o}C$ operation period there are the input/output diagrams for June, July and August, Figures 6.2-57 through 6.2-59. The difference between the normal flat-plate and evacuated tube collectors has increased. The Scandinavian Solar Energy array still performs well compared to the evacuated tubular collectors. In August, the array was out of operation during 16 days for corrective maintenance and the curve is excluded. When comparing the two test periods one can see the expected parallel shift of the input/output curves. The shift is smallest for the PH collectors.

Figures 6.2-60 through 6.2-67 are daily energy input/output regression lines for some of the systems in Södertörn. The winter months are excluded due to frequent snow cover. During October 1982 preheating operation was conducted and the curves show unusual shifts, but all other lines are from normal operation.

During the period April 1983 to October 1983 operation was tested at 80°C for some periods giving an apparent scatter of the lines, especially for the Philips collector.

The other two periods June 1982 to May 1983 and April 1984 to October 1984 have very constant operating conditions, except for seasonal and climatic conditions. The control mode differs slightly for the two periods giving the smallest T100 variation for the 1982/1983 period and the most constant T100 for the 1984 period.

6.2.8 SOLARCAD Project, Geneva, Switzerland

Separate plots are shown in Figures 6.2-68 through 6.2-83 for the following three periods:

I: Corning A, Corning B;
II: Corning A, Corning B;
III: Corning A, Corning B, Sanyo.

Subperiods:	summer months:	May, June and July
	winter months:	November, December and January
	fall months:	August, September, October,
	spring months:	February, March, April

The subperiods allow investigation of seasonal effects.

Points with $0 < \Delta T < 15^{o}C$ usually correspond to very cloudy days. The fits are restricted to days involving a pump operating time of at least 2 hours. The same remarks as for the efficiency plots also apply here.

6.2.9 SOLARIN Project, Hallau, Switzerland

Figure 6.2-84 is a plot for the one year period considered. Also see the comments listed in Section 6.1.9. Some daily data were rejected because of snow or control problems. Figures 6.2-85 to 6.2-87 split the same information so that seasonal effects could be investigated. Seasons are defined by:

winter months:	November, December, January
summer months:	May, June, July
spring months:	February, March, April
fall months:	August, September, October

Linear fits involve only those points characterized by an abcissa larger than 5 MJ/m^2 (3 MJm^2 for winter).

6.2.10 Evacuated Collector System Test Facility, Bracknell, United Kingdom

Daily energy input/output diagrams are provided in Figures 6.2-88 through 6.2-90, representing summer and winter conditions. Although not dramatic the seasonal shift in performance is evident and is more apparent when data are plotted on a month by month basis. The input/output diagram for all the data from the experiments is given in the figure and all points for summer operation are below the mean regression line. The reasons for this are due principally to higher radiative heat loss and also increased number of daily operating hours.

6.2.11 Colorado State University Solar House I, United States

Total energy delivered from collectors during a day is a function of the optical, and thermal properties of the collector, its orientation and tilt, the physical condition of the array, and total insolation. Physical condition of the collector refers to such items as dust and snow cover, number of defective tubes in the array, and condition of the specular reflector.

Graphs of energy delivery from the collector as a function of total insolation are given in Figures 6.2-91 through 6.2-95. Each graph is for a narrow range of average fluid temperature difference from ambient air temperature. According to procedures set forth by the International Energy Agency Task VI group, input/output relations are determined for each $15^{o}C$ temperature increment starting from $0^{o}C$. Points near the horizontal axis in Figure 6.2-91 and 6.2-92 are a consequence of complete snow cover of the collectors. On days with snow cover during part of the day, or partial snow cover all day, the points lie between the regression line and the horizontal axis. This may be seen in Figure 6.2-91. Data for days with complete or partial snow cover were not included in establishing the regression lines, although they are indicated on the figures.

A composite graph which includes only the regression lines is shown in Figure 6.2-96. The ratio of energy output to energy input is progressively less with increasing ΔT.

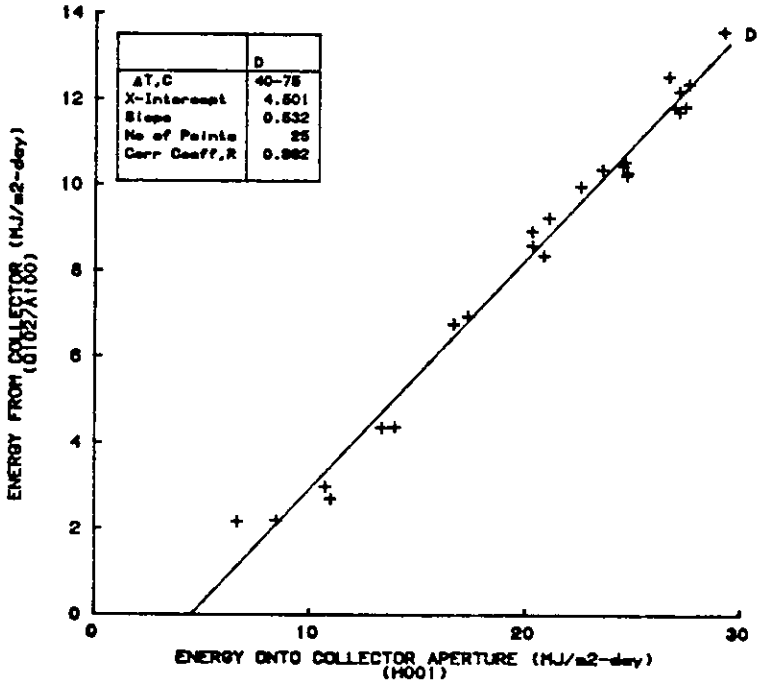

Figure 6.2-1. Daily Energy Input/Output Diagram for S. U. Evacuated Tubular Collector at Sydney, Australia, 24 December 1982 to 20 January 1983,

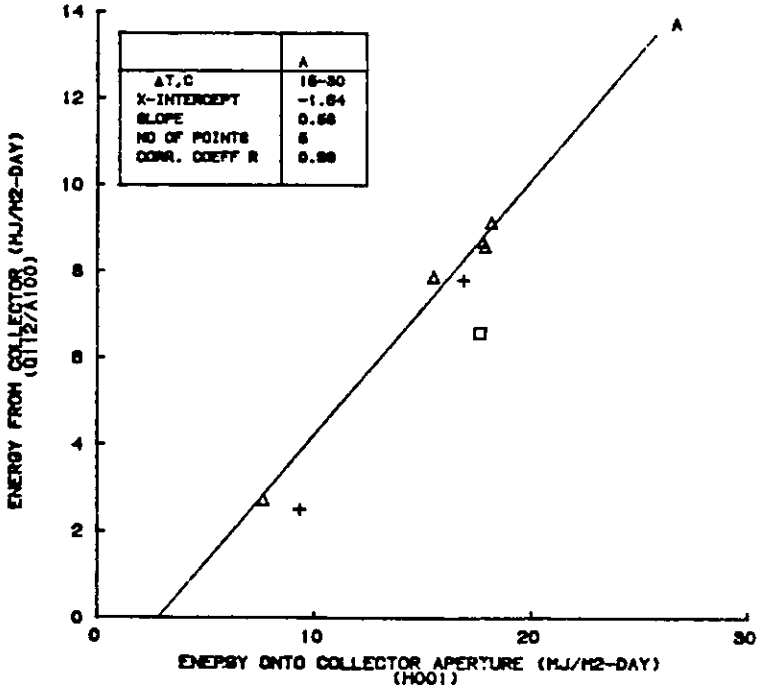

Figure 6.2-2. Daily Energy Input/Output Diagram for Yazaki Flat-Plate Collector, Sydney, Australia, 9 July 1983 to 8 August 1983.

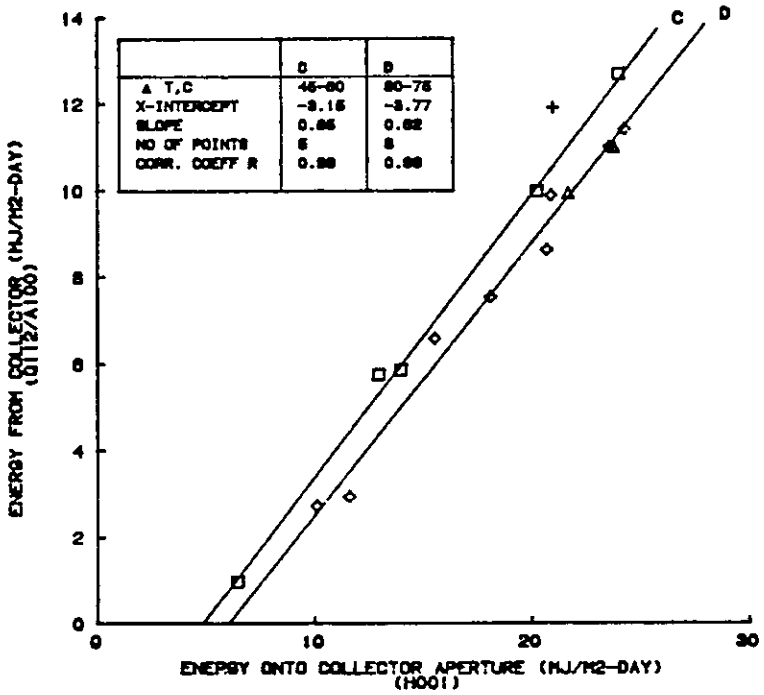

Figure 6.2-3. Daily Energy Input/Output Diagram for S. U. Evacuated Tubular Collector at Sydney, Australia, 28 August 1983 to 28 September 1983.

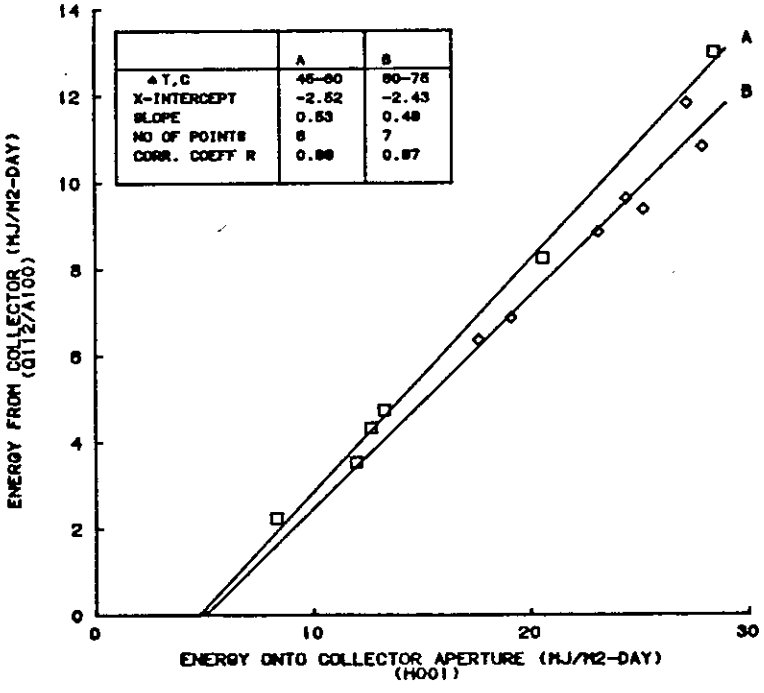

Figure 6.2-4. Daily Energy Input/Output Diagram for S. U. Evacuated Tubular Collector at Sydney, Australia, 1 October 1983 to 30 November 1983.

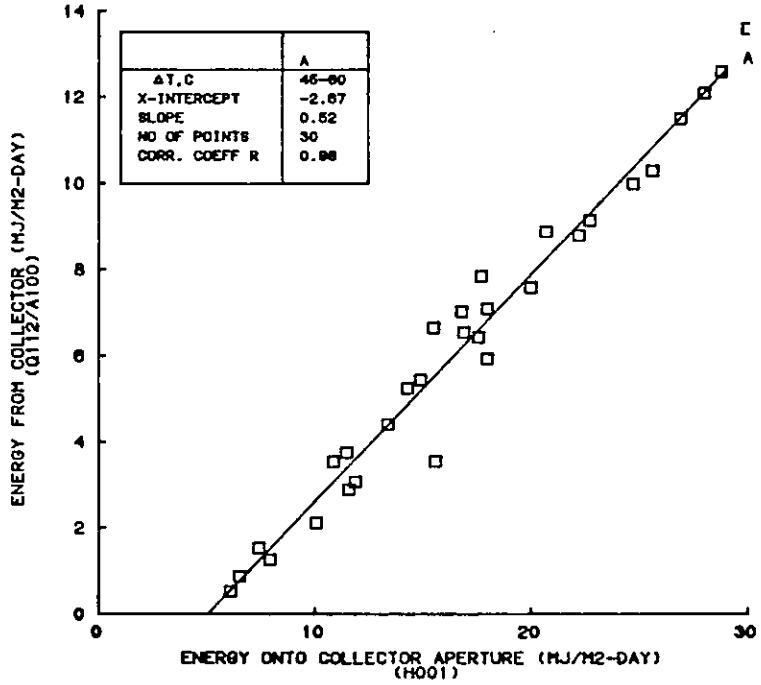

Figure 6.2-5. Daily Energy Input/Output Diagram for S. U. Evacuated Tubular Collector at Sydney, Australia, 1 December 1983 to 30 April 1984.

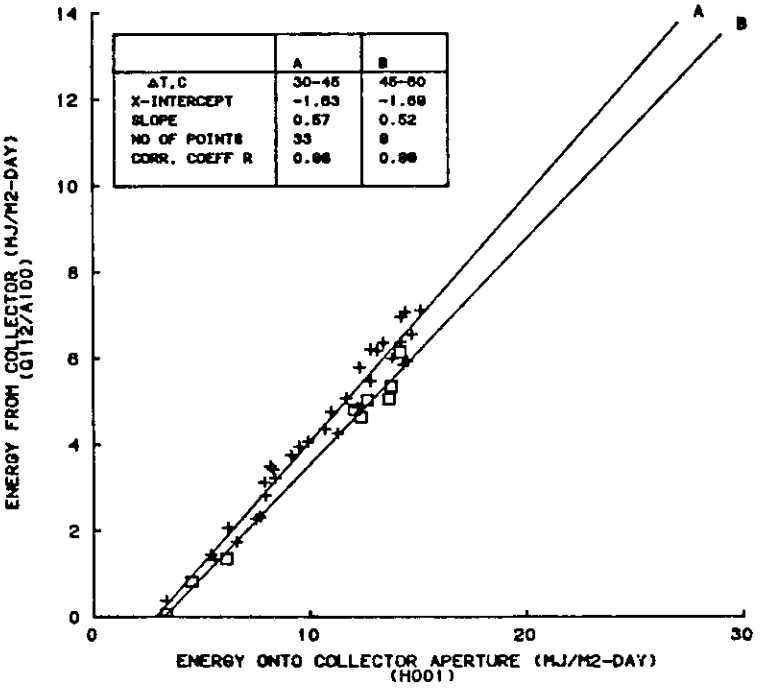

Figure 6.2-6. Daily Energy Input/Output Diagram for S. U. Evacuated Tubular Collector at Sydney, Australia, 1 May 1984 to 31 July 1984.

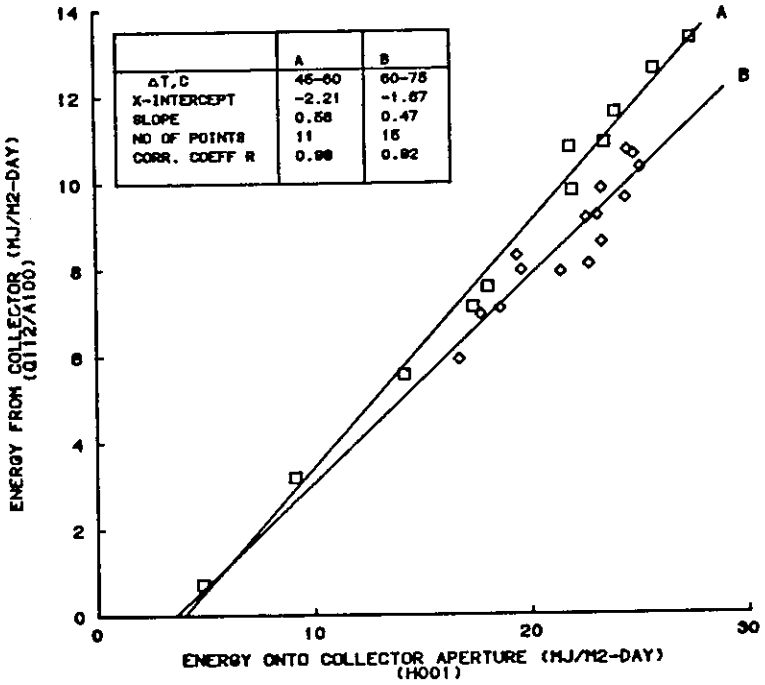

Figure 6.2-7. Daily Energy Input/Output Diagram for S. U. Evacuated Tubular Collector at Sydney, Australia, 1 September 1984 to 31 October 1984.

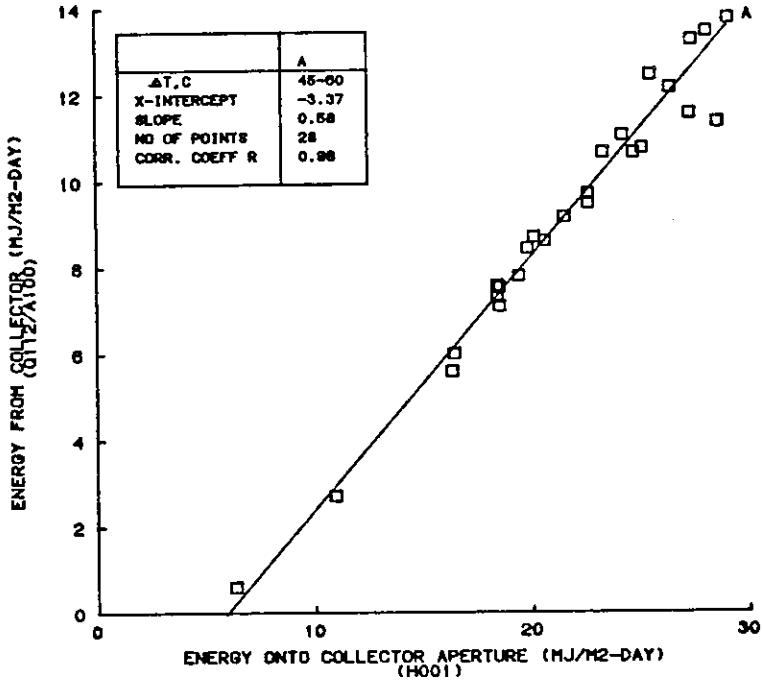

Figure 6.2-8. Daily Energy Input/Output Diagram for S. U. Evacuated Tubular Collector at Sydney, Australia, 1 December 1984 to 28 February 1985.

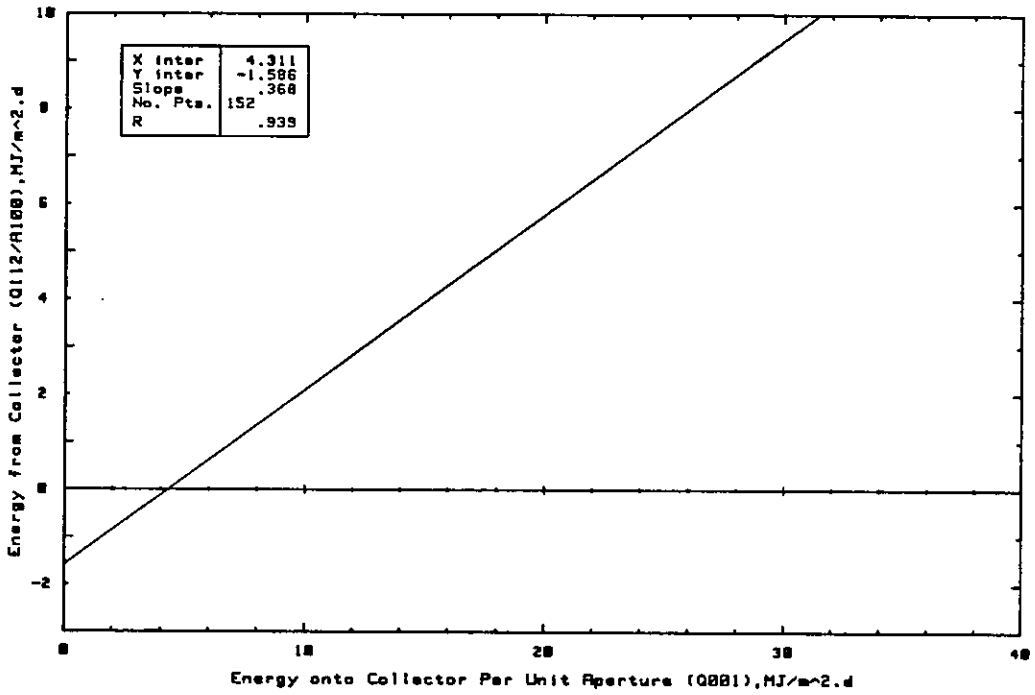

Figure 6.2-9. Daily Energy Input/Output Diagram for Solartech ETC at the Mountain Spring Bottle Washing Facility, Canada, May to December 1982.

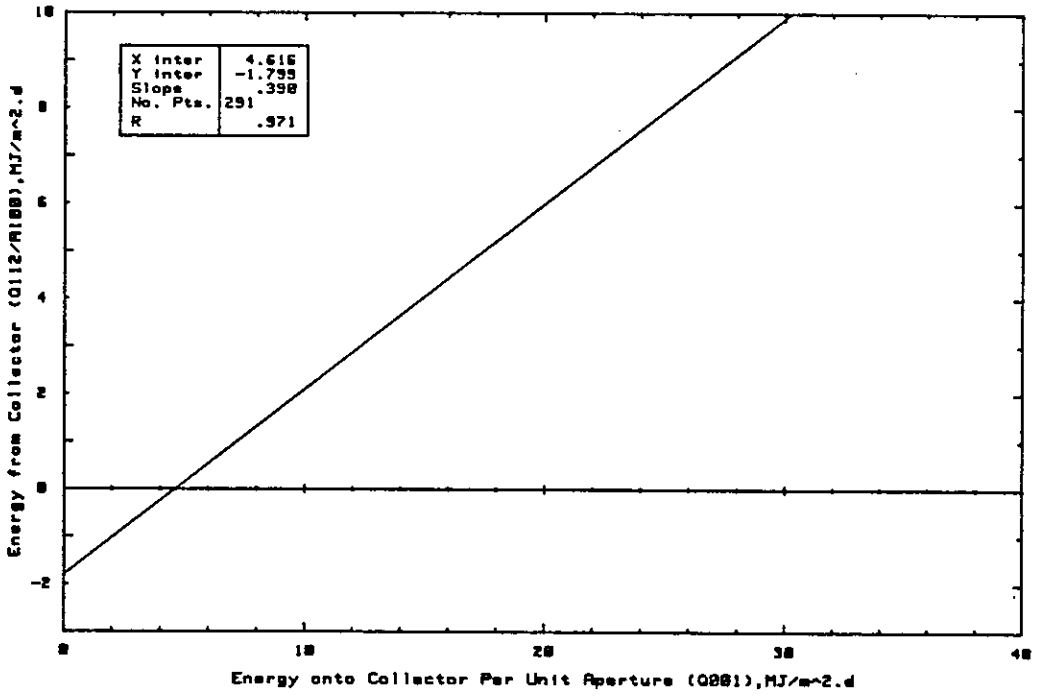

Figure 6.2-10. Daily Energy Input/Output Diagram for Solartech ETC at the Mountain Spring Bottle Washing Facility, Canada, January to December 1983.

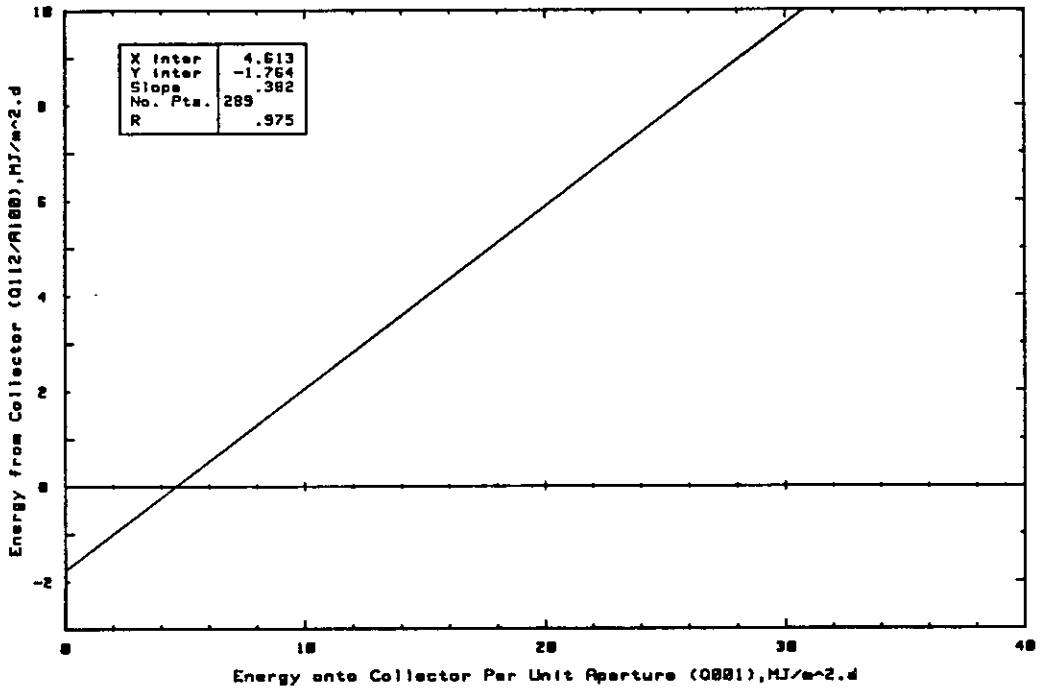

Figure 6.2-11. Daily Energy Input/Output Diagram for Solartech ETC at the Mountain Spring Bottle Washing Facility, Canada, January 1984 to November 1984.

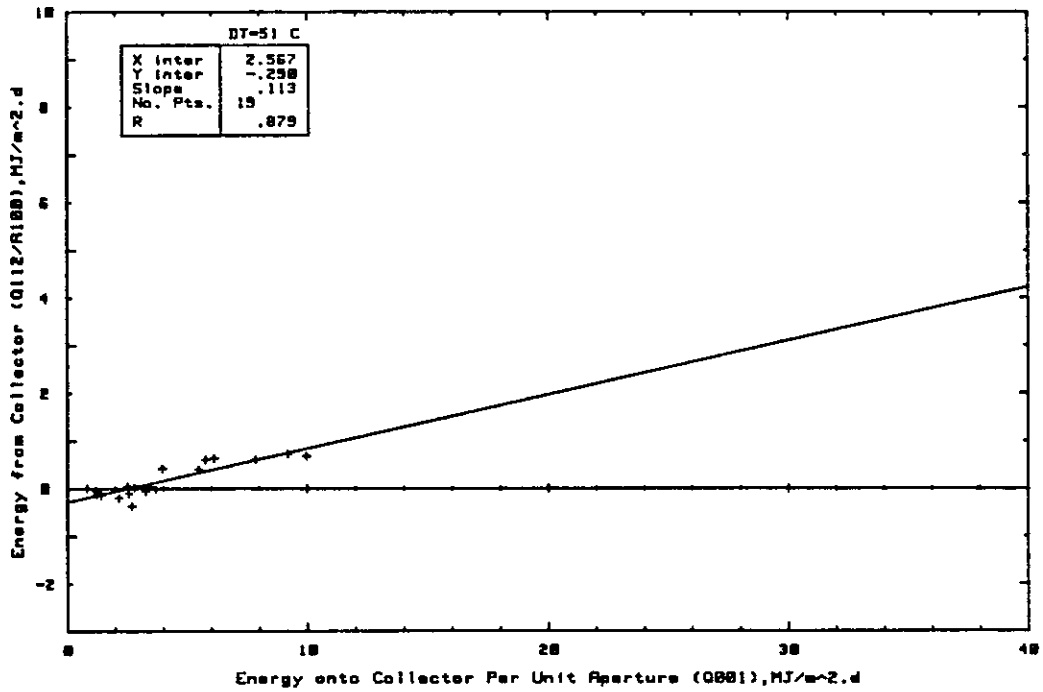

Figure 6.2-12. Daily Energy Input/Output Diagram for Solartech ETC at the Mountain Spring Bottle Washing Facility, Canada, December 1982.

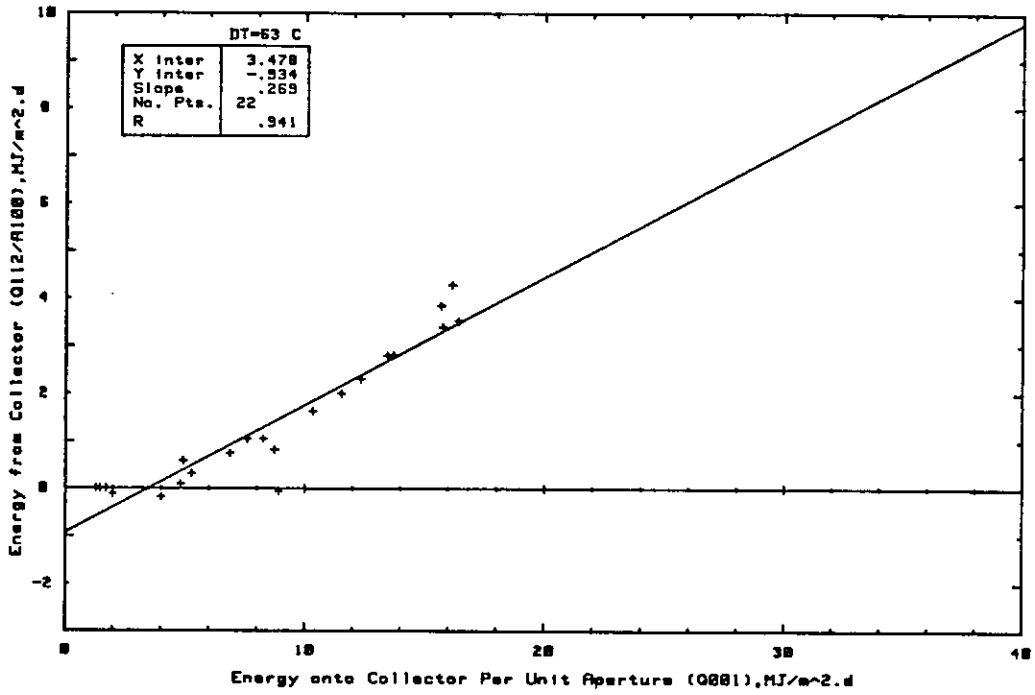

Figure 6.2-13. Daily Energy Input/Output Diagram for Solartech ETC at the Mountain Spring Bottle Washing Facility, Canada, February, 1983.

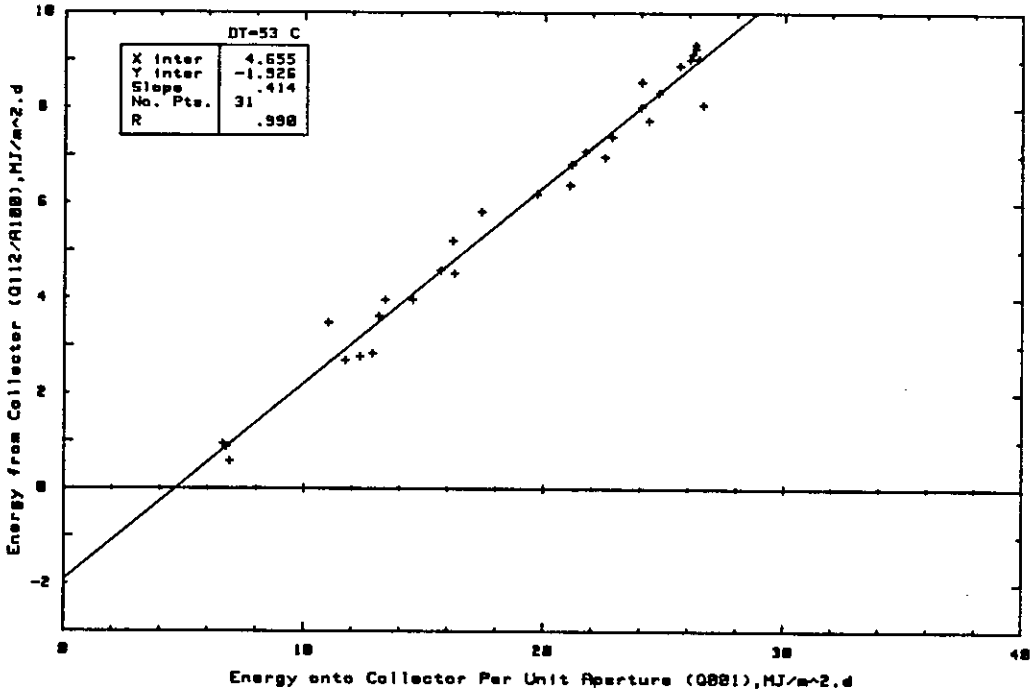

Figure 6.2-14. Daily Energy Input/Output Diagram for Solartech ETC at the Mountain Spring Bottle Washing Facility, Canada, July, 1983.

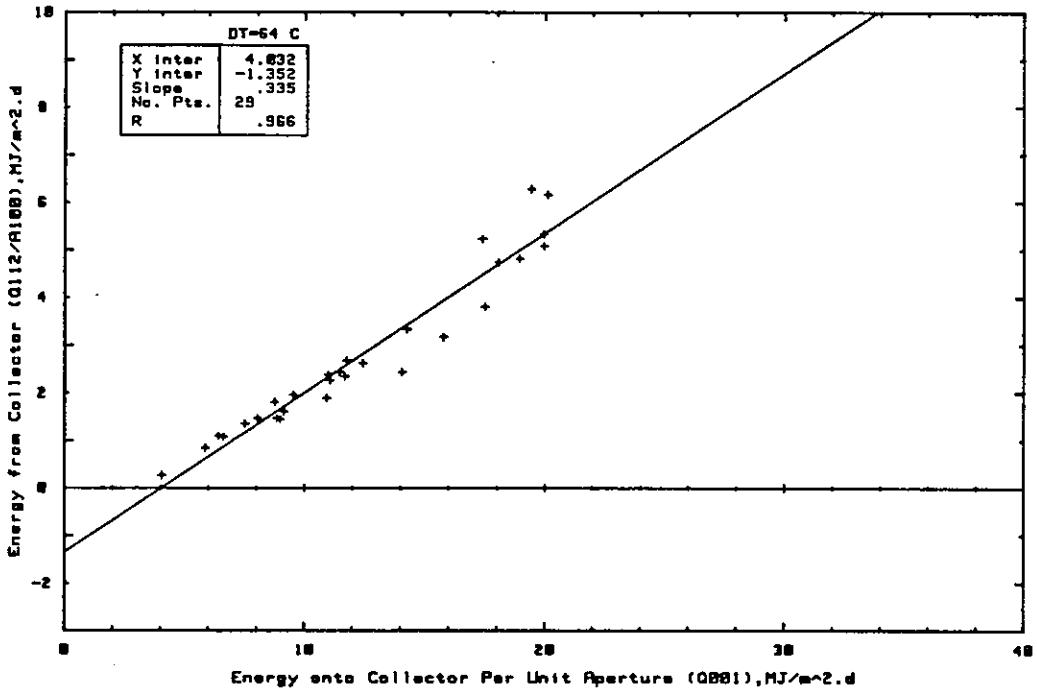

Figure 6.2-15. Daily Energy Input/Output Diagram for Solartech ETC at the Mountain Spring Bottle Washing Facility, Canada, February, 1984.

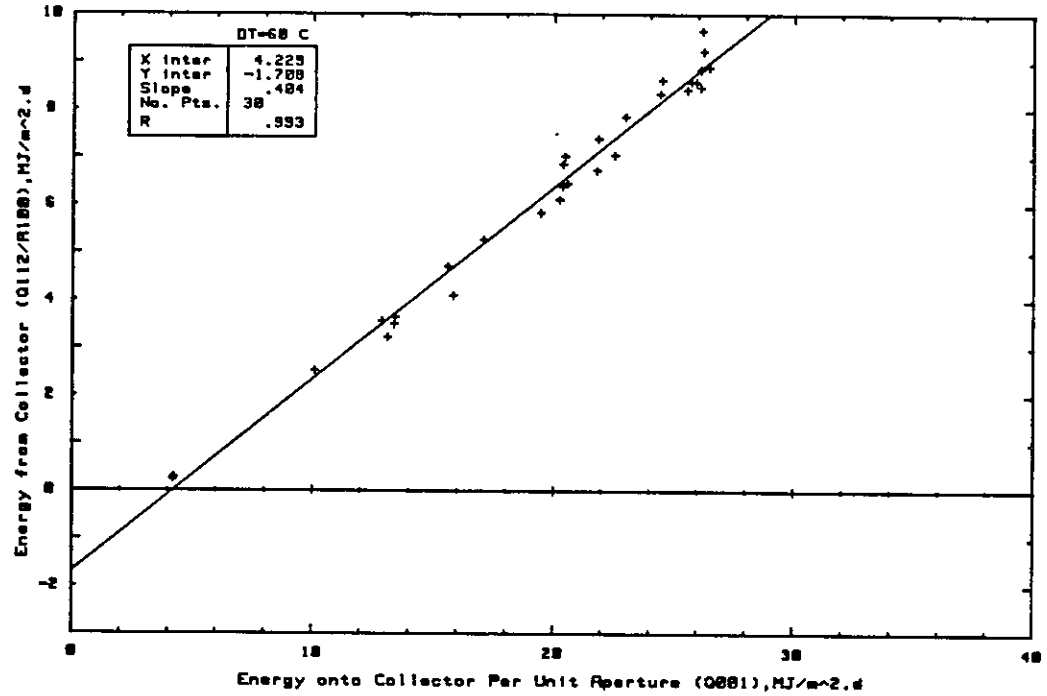

Figure 6.2-16. Daily Energy Input/Output Diagram for Solartech ETC at the Mountain Spring Bottle Washing Facility, Canada, April, 1984.

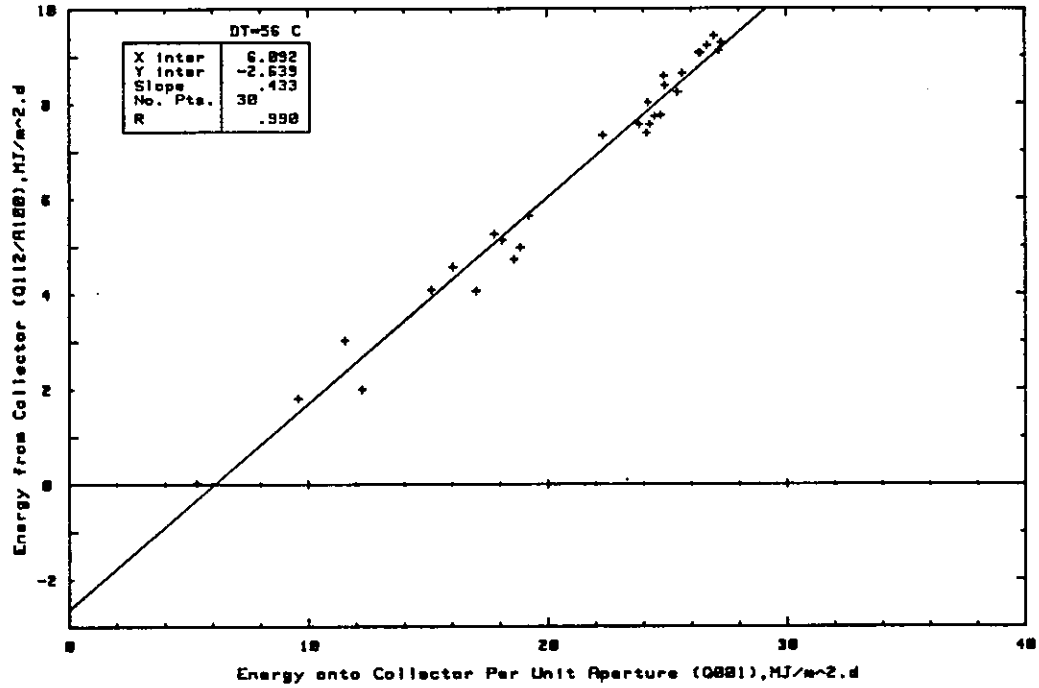

Figure 6.2-17. Daily Energy Input/Output Diagram for Solartech ETC at the Mountain Spring Bottle Washing Facility, Canada, July, 1984.

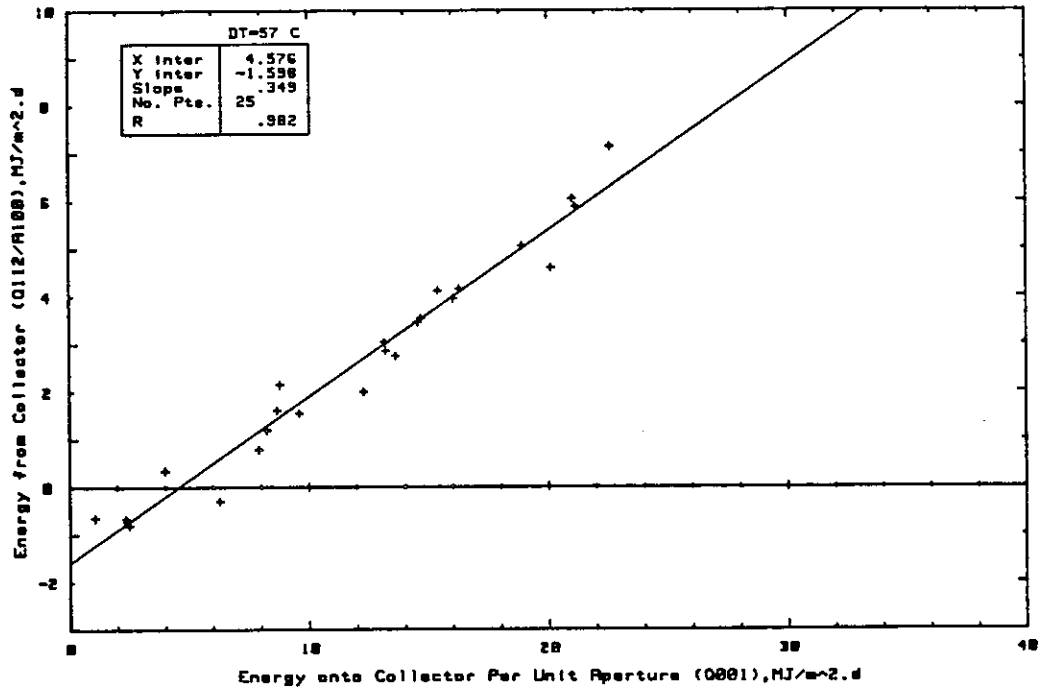

Figure 6.2-18. Daily Energy Input/Output Diagram for Solartech ETC at the Mountain Spring Bottle Washing Facility, Canada, October, 1984.

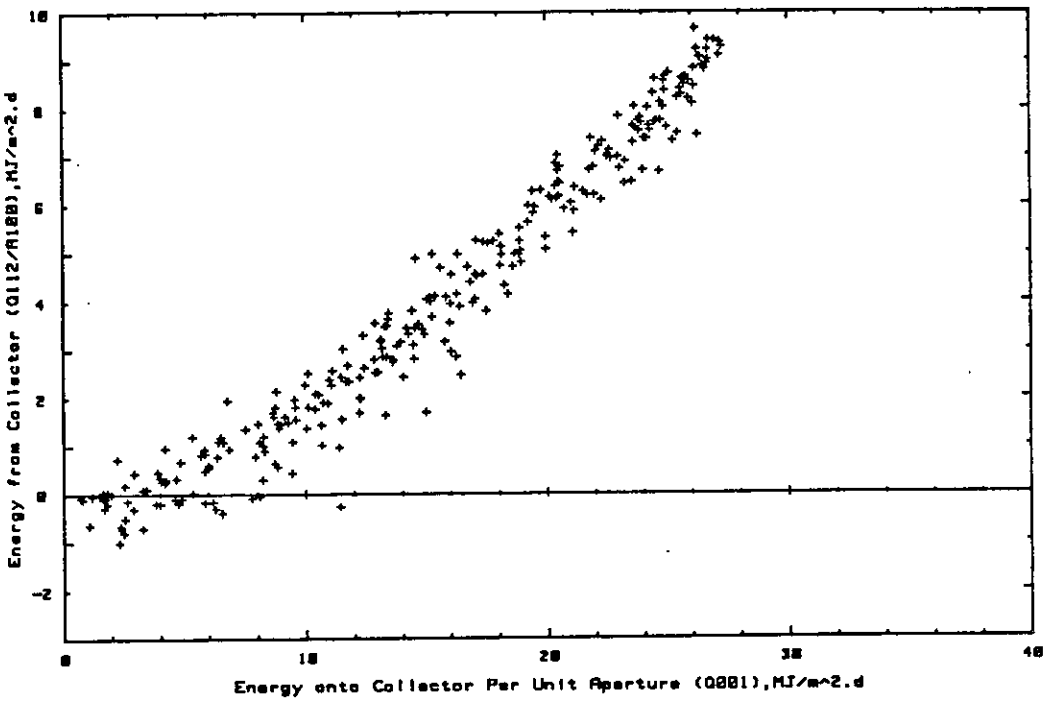

Figure 6.2-19. Daily Energy Input/Output Diagram for Solartech ETC at the Mountain Spring Bottle Washing Facility, Canada, January to November, 1984.

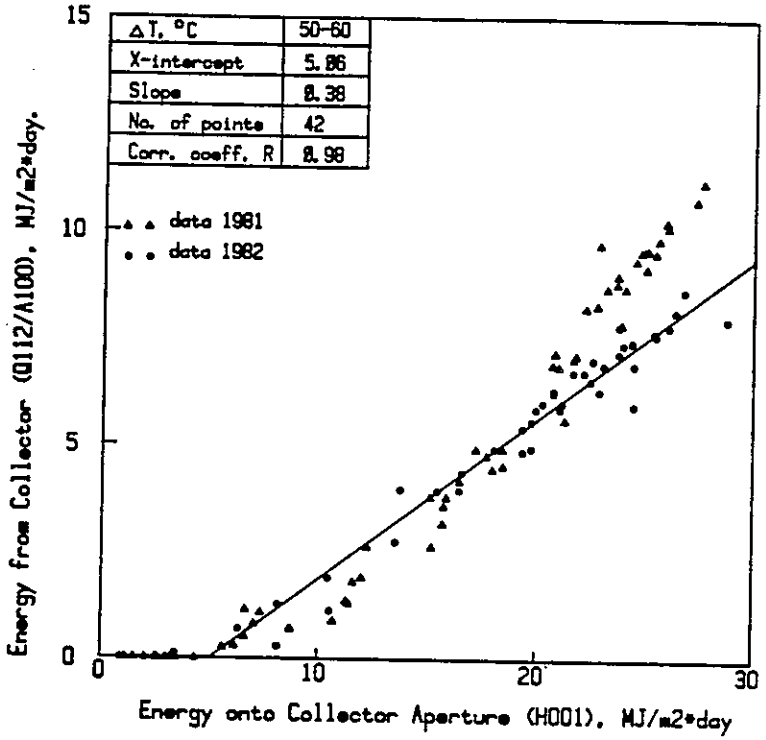

Figure 6.2-20. Daily Energy Input/Output Diagram for Sanyo (I) Collector for the Ispra Solar Laboratory, May to September, 1982.

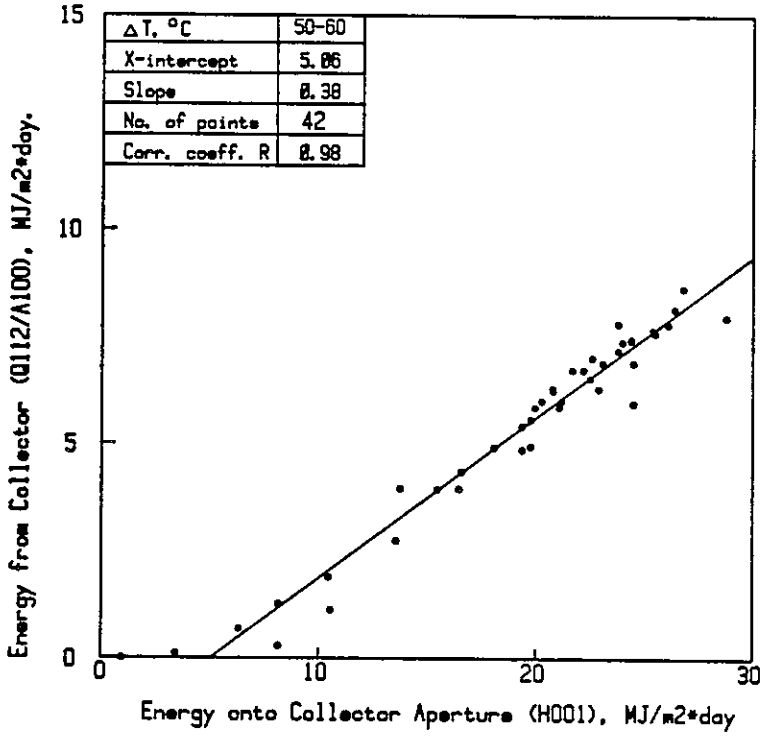

Figure 6.2-21. Daily Energy Input/Output Diagram for Sanyo (I) Collector for the Ispra Solar Laboratory, July to September, 1982.

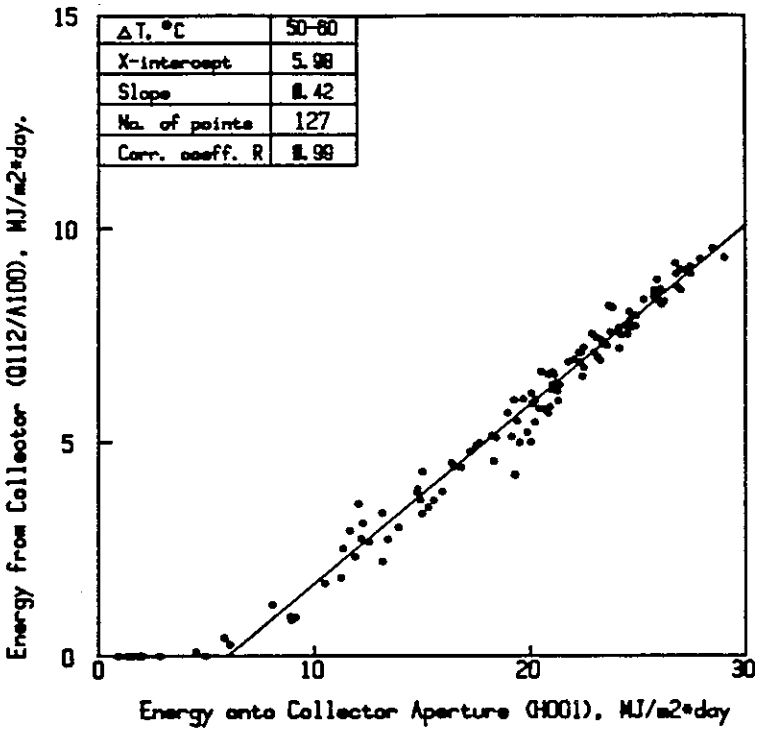

Figure 6.2-22. Daily Energy Input/Output Diagram for Sanyo (I) Collector for the Ispra Solar Laboratory, May to September, 1983.

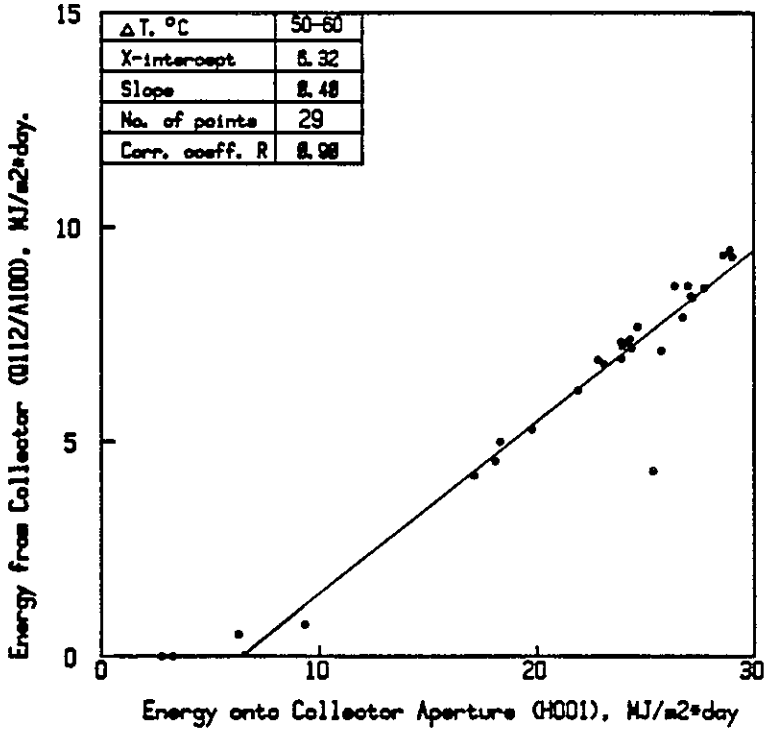

Figure 6.2-23. Daily Energy Input/Output Diagram for Sanyo (I) Collector for the Ispra Solar Laboratory, June, 1984.

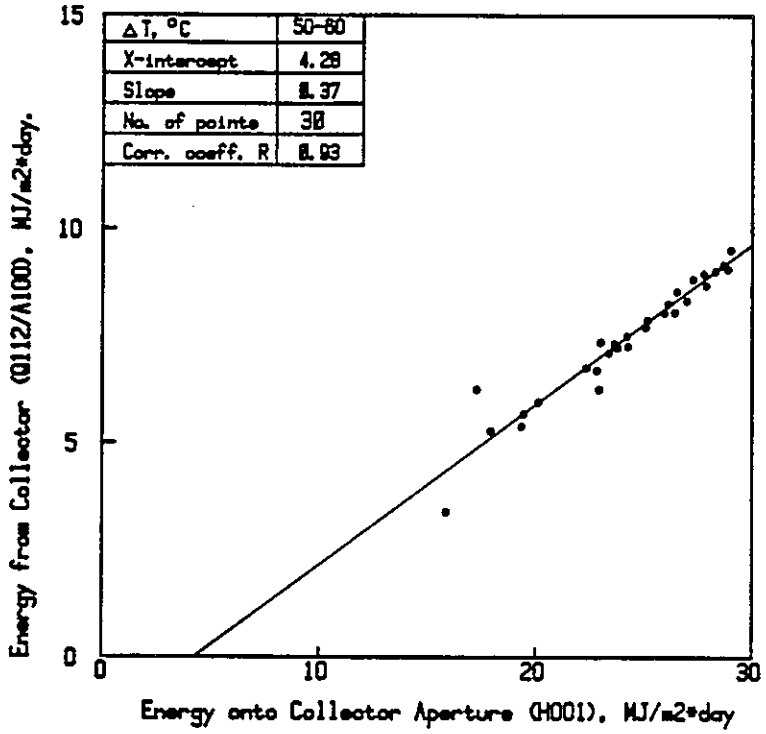

Figure 6.2-24. Daily Energy Input/Output Diagram for Sanyo (I) Collector for the Ispra Solar Laboratory, July, 1984.

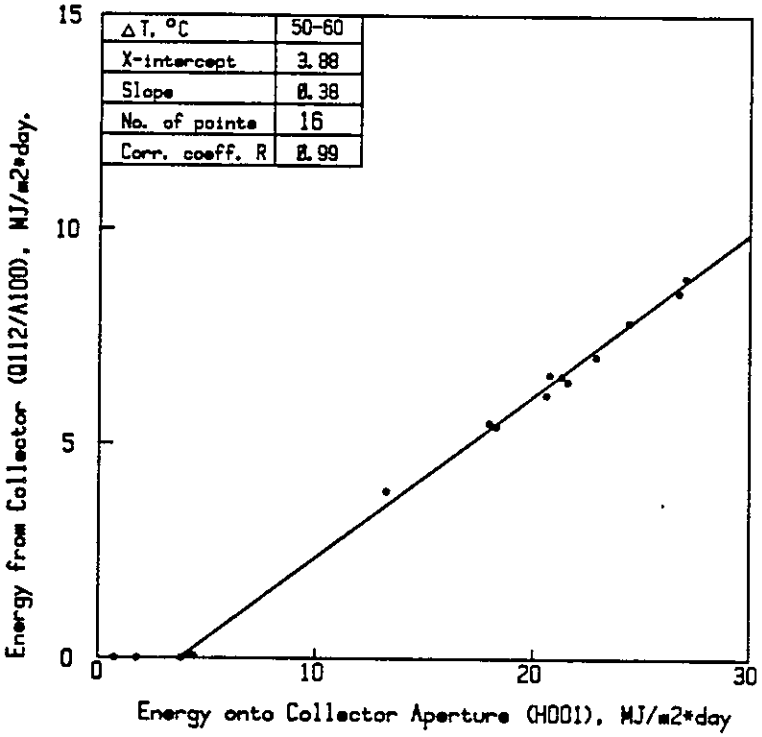

Figure 6.2-25. Daily Energy Input/Output Diagram for Sanyo (I) Collector for the Ispra Solar Laboratory, August, 1984.

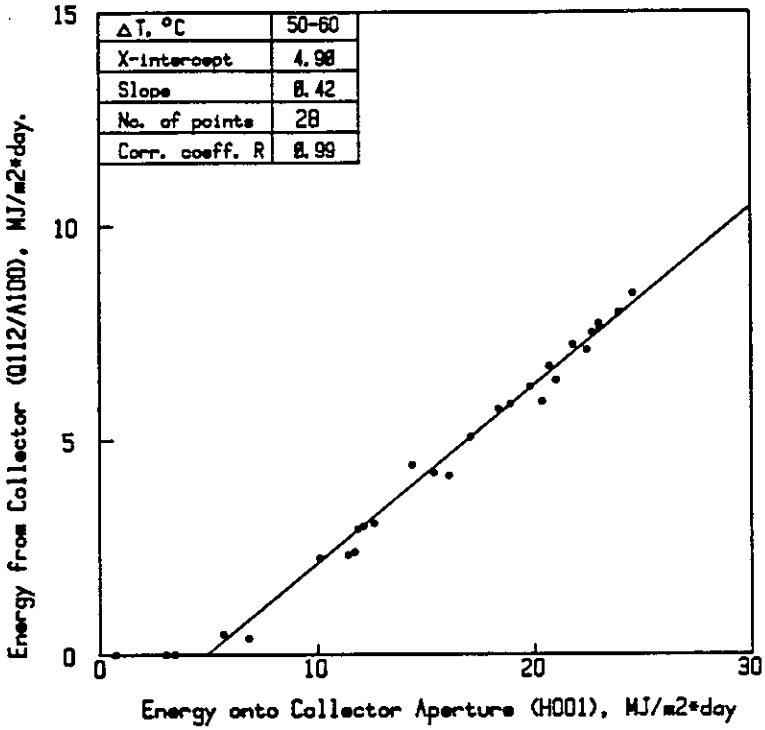

Figure 6.2-26. Daily Energy Input/Output Diagram for Sanyo (I) Collector for the Ispra Solar Laboratory, September, 1984.

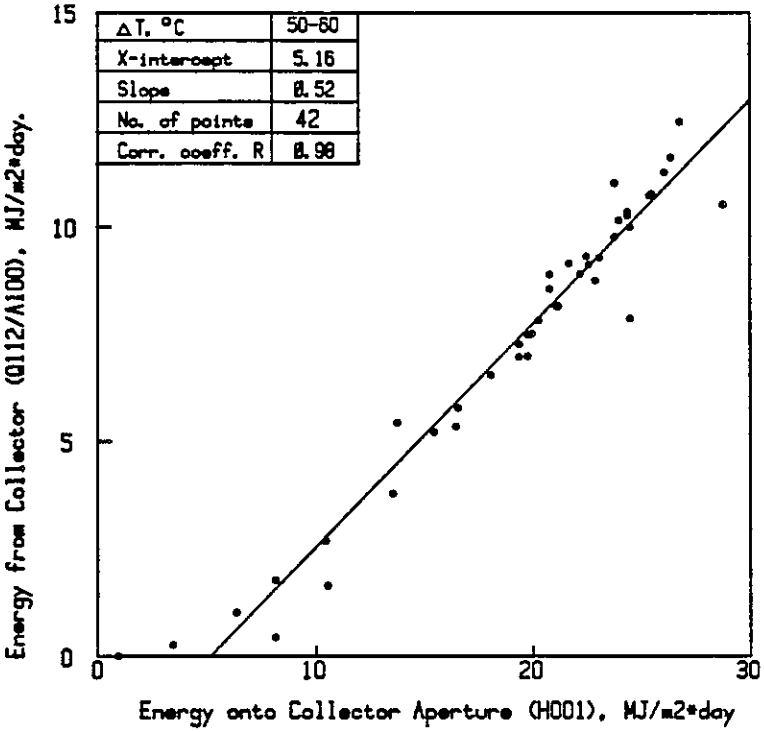

Figure 6.2-27. Daily Energy Input/Output Diagram for Sanyo (II) Collector for the Ispra Solar Laboratory, July to September, 1982.

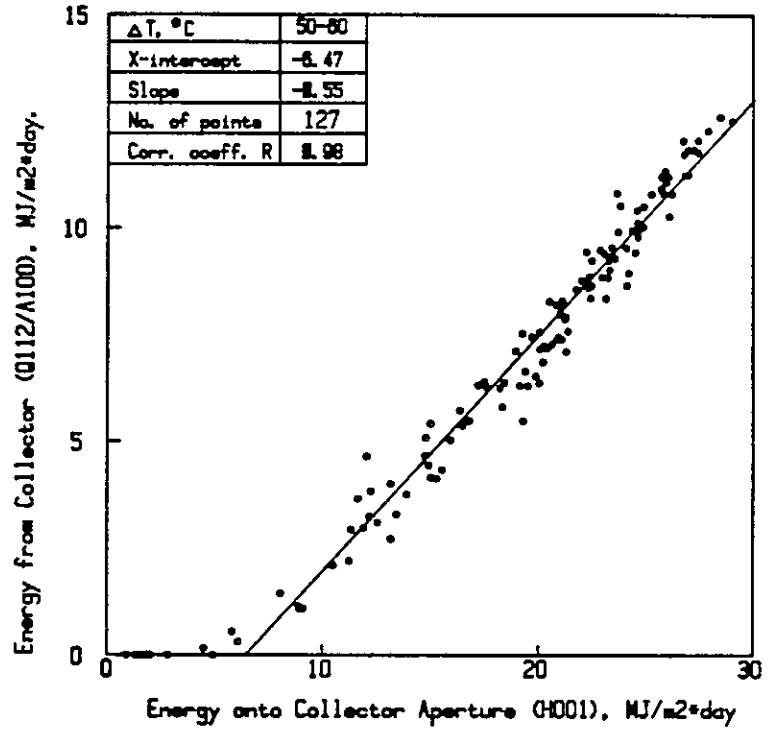

Figure 6.2-28. Daily Energy Input/Output Diagram for Sanyo (II) Collector for the Ispra Solar Laboratory, May to September, 1983.

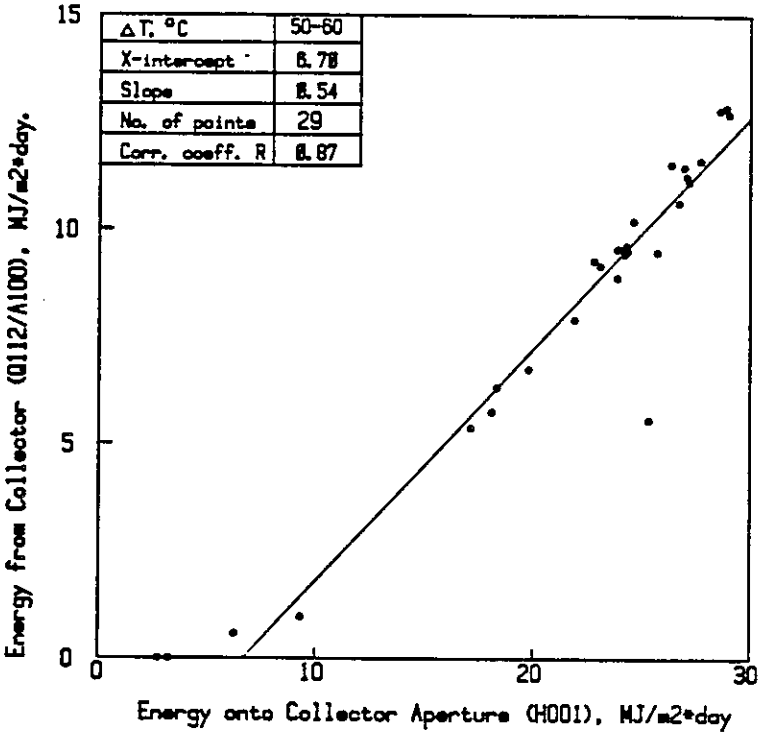

Figure 6.2-29. Daily Energy Input/Output Diagram for Sanyo (II) Collector for the Ispra Solar Laboratory, June, 1984.

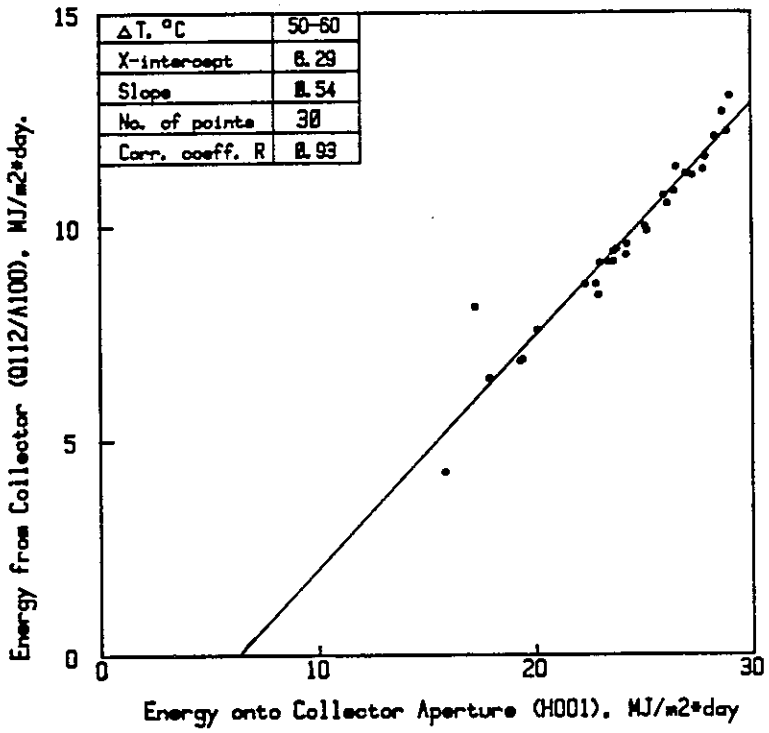

Figure 6.2-30. Daily Energy Input/Output Diagram for Sanyo (II) Collector for the Ispra Solar Laboratory, July, 1984.

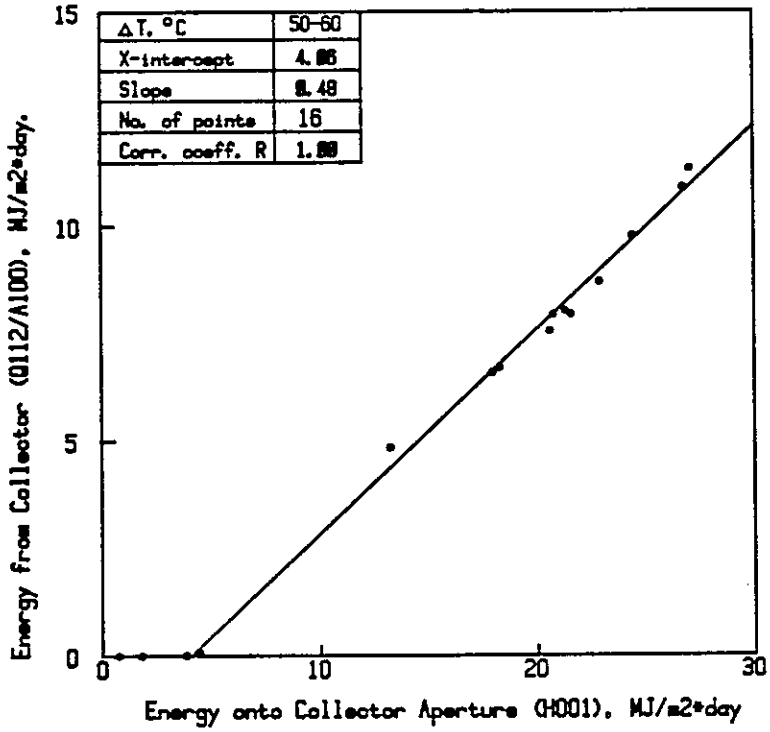

Figure 6.2-31. Daily Energy Input/Output Diagram for Sanyo (II) Collector for the Ispra Solar Laboratory, August, 1984.

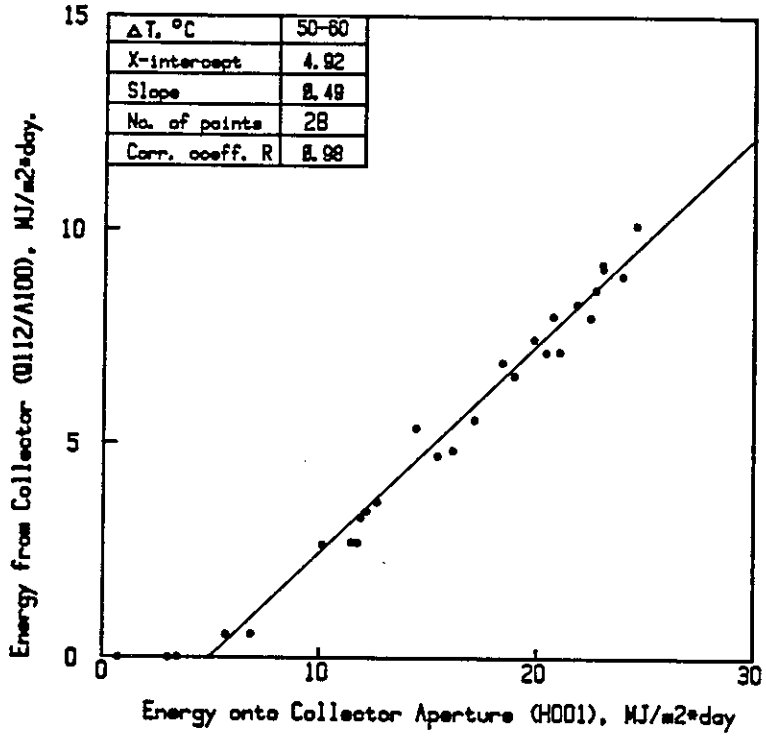

Figure 6.2-32. Daily Energy Input/Output Diagram for Sanyo (II) Collector for the Ispra Solar Laboratory, September, 1984.

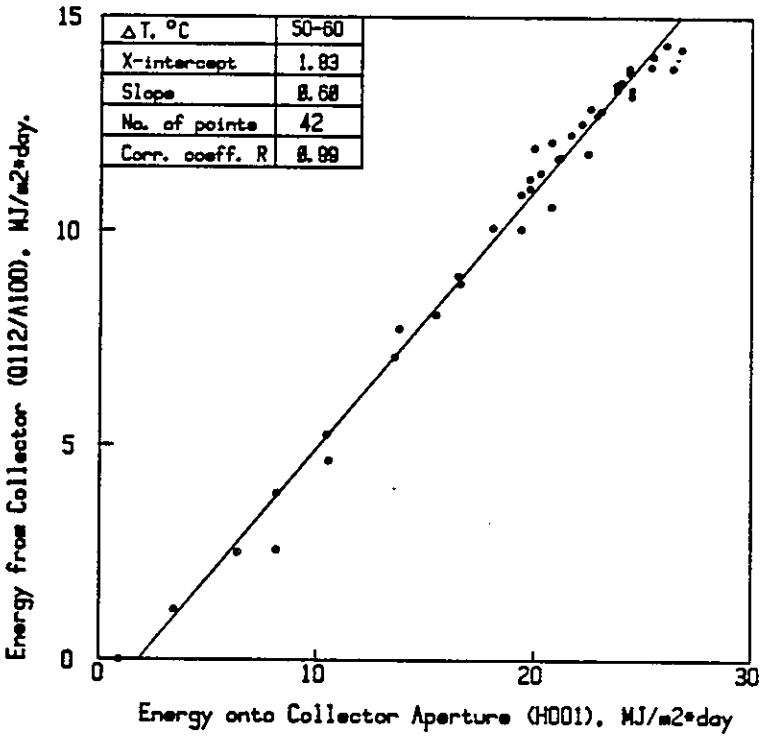

Figure 6.2-33. Daily Energy Input/Output Diagram for Philips VTR 261 Collector for the Ispra Solar Laboratory, July to September, 1982.

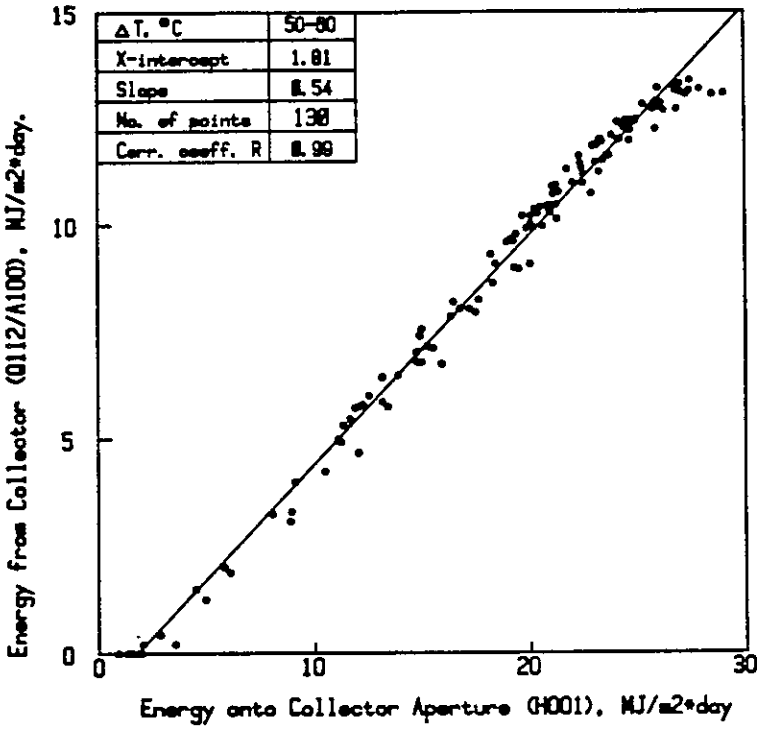

Figure 6.2-34. Daily Energy Input/Output Diagram for Philips VTR 261 Collector for the Ispra Solar Laboratory, May to September, 1983.

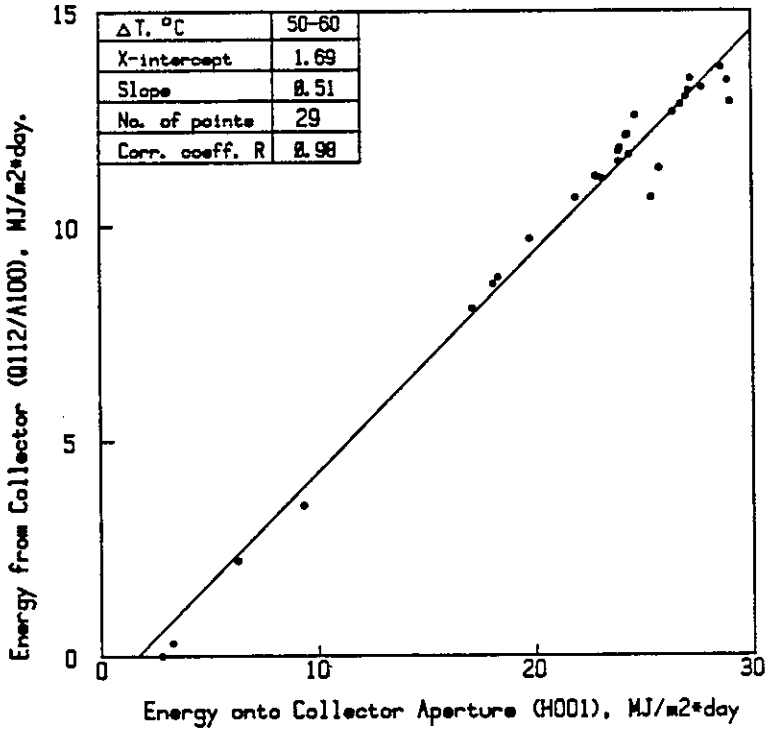

Figure 6.2-35. Daily Energy Input/Output Diagram for Philips VTR 261 Collector for the Ispra Solar Laboratory, June, 1984.

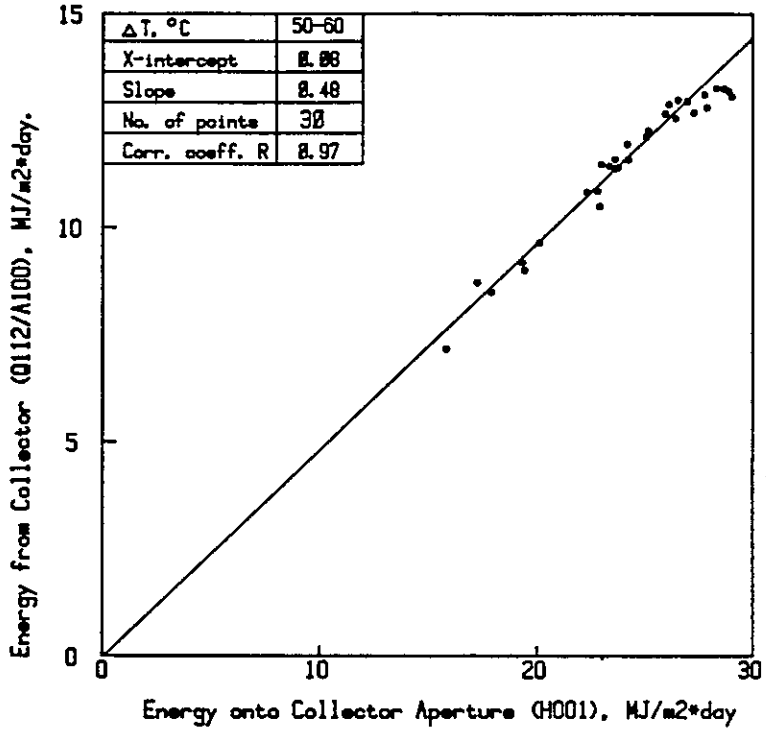

Figure 6.2-36. Daily Energy Input/Output Diagram for Philips VTR 261 Collector for the Ispra Solar Laboratory, July, 1984.

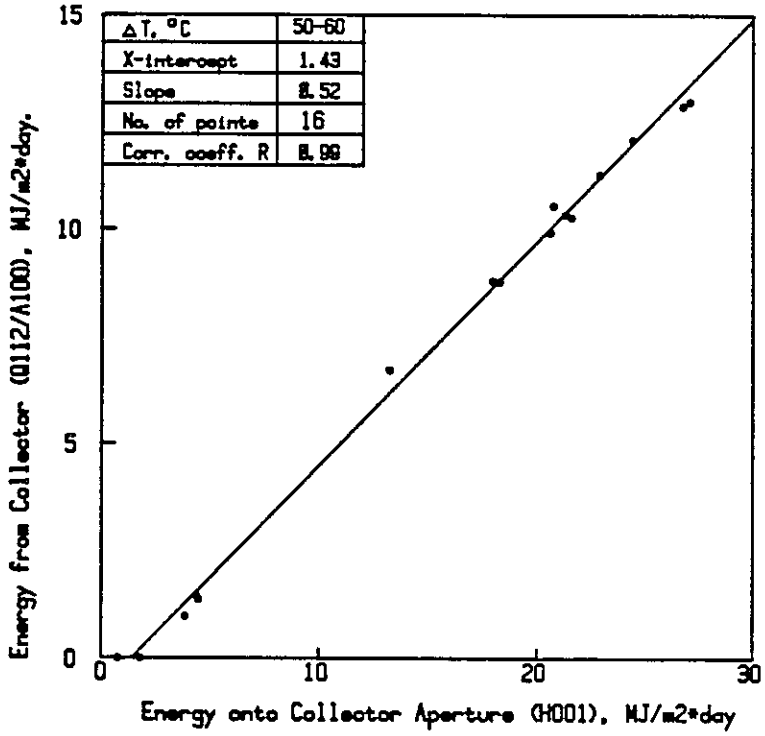

Figure 6.2-37. Daily Energy Input/Output Diagram for Philips VTR 261 Collector for the Ispra Solar Laboratory, August, 1984.

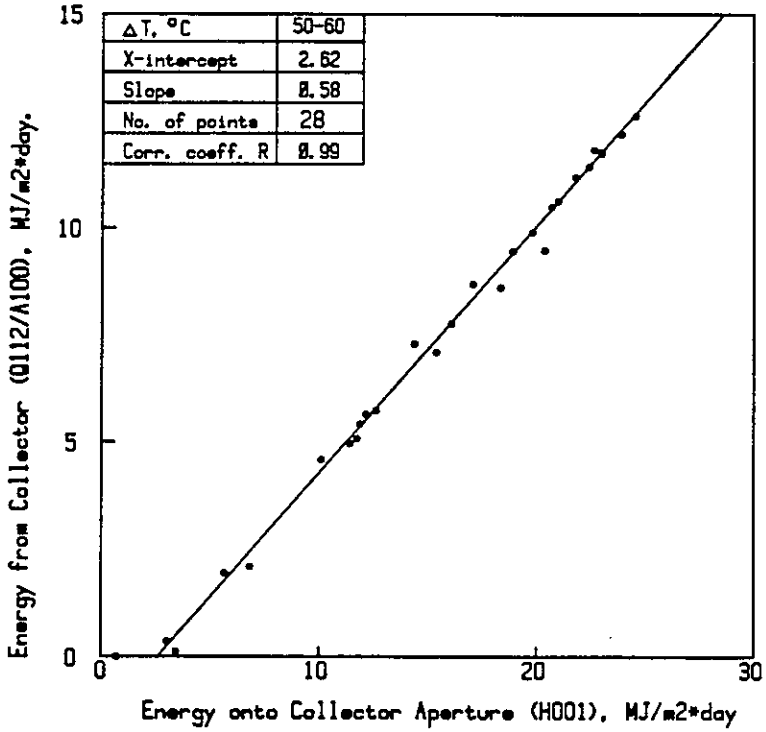

Figure 6.2-38. Daily Energy Input/Output Diagram for Philips VTR 261 Collector for the Ispra Solar Laboratory, September, 1984.

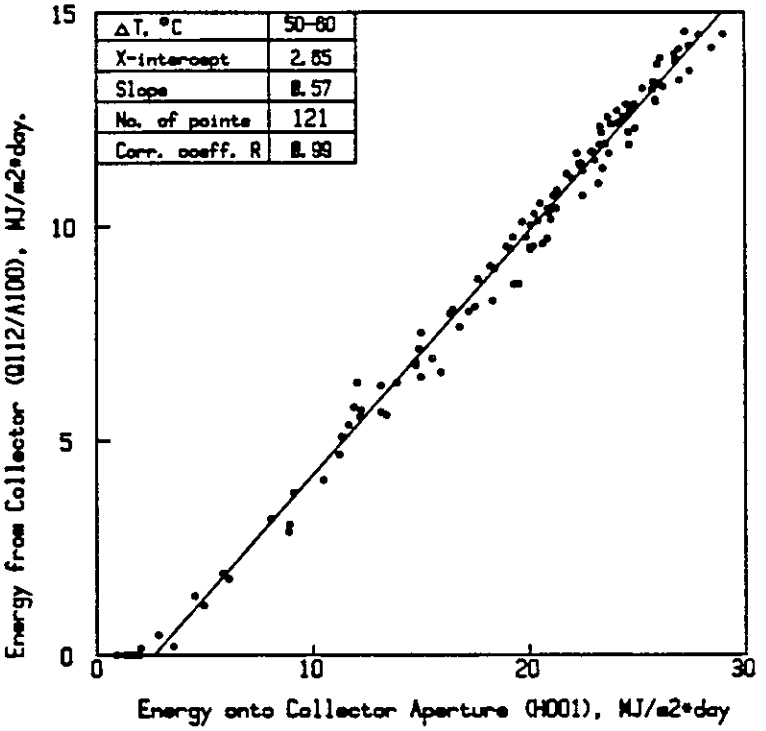

Figure 6.2-39. Daily Energy Input/Output Diagram for Philips VTR 361 Collector for the Ispra Solar Laboratory, May to September, 1983.

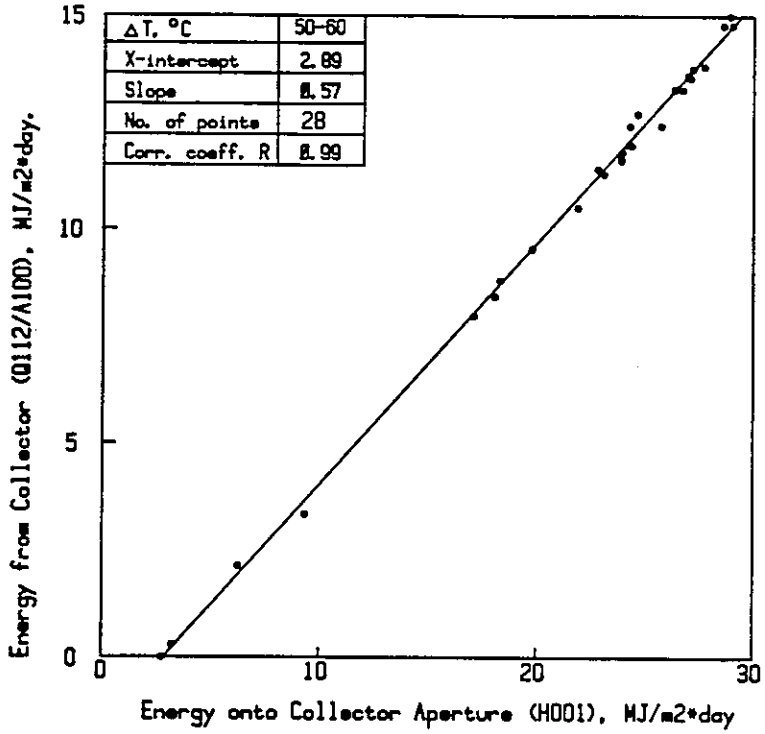

Figure 6.2-40. Daily Energy Input/Output Diagram for Philips VTR 361 Collector for the Ispra Solar Laboratory, June, 1984.

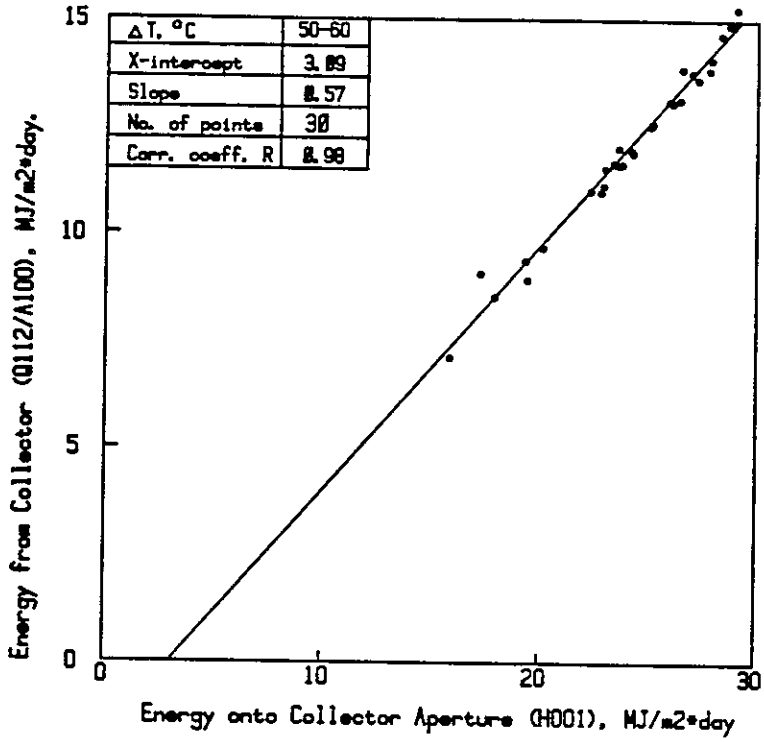

Figure 6.2-41. Daily Energy Input/Output Diagram for Philips VTR 361 Collector for the Ispra Solar Laboratory, July, 1984.

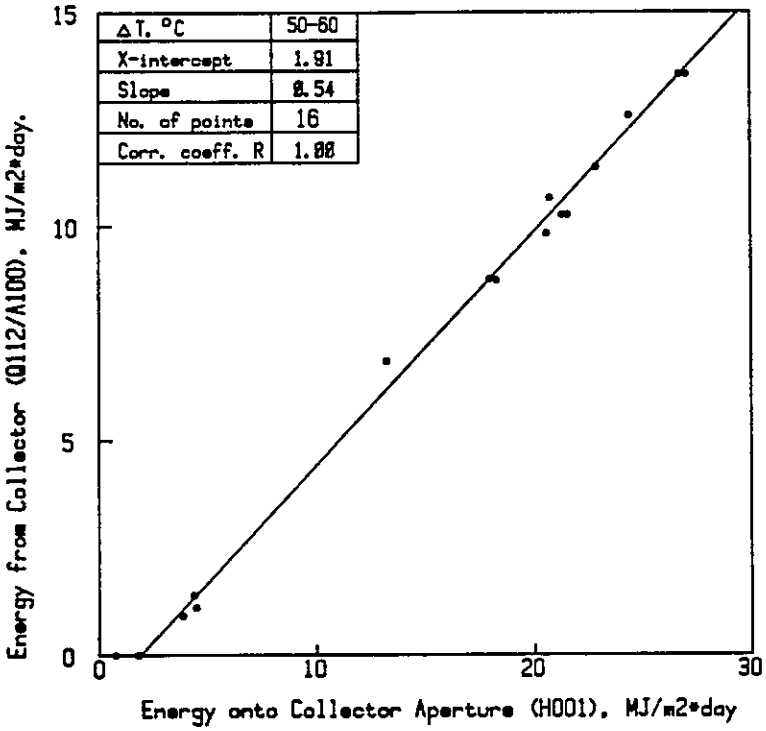

Figure 6.2-42. Daily Energy Input/Output Diagram for Philips VTR 361 Collector for the Ispra Solar Laboratory, August, 1984.

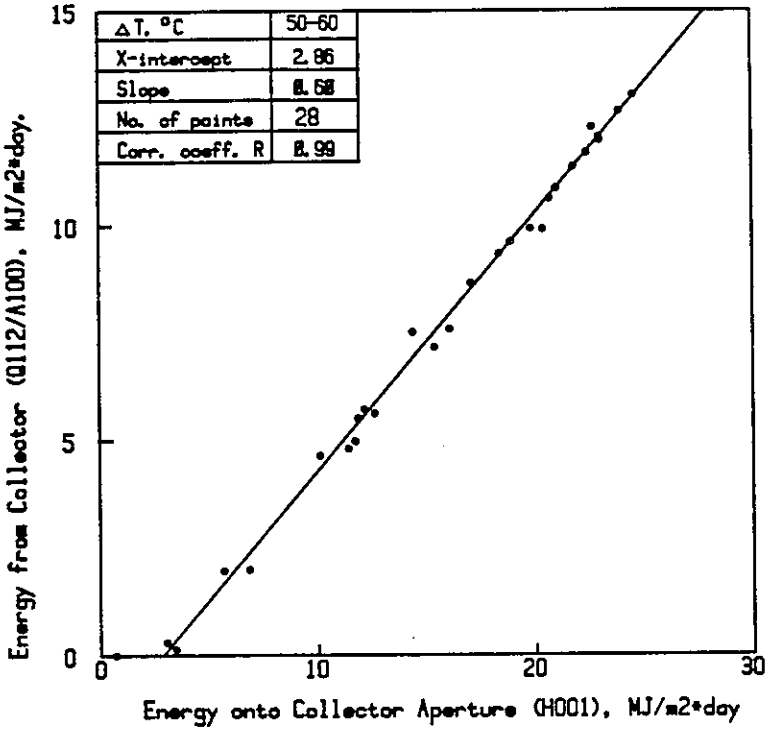

Figure 6.2-43. Daily Energy Input/Output Diagram for Philips VTR 361 Collector for the Ispra Solar Laboratory, September, 1984.

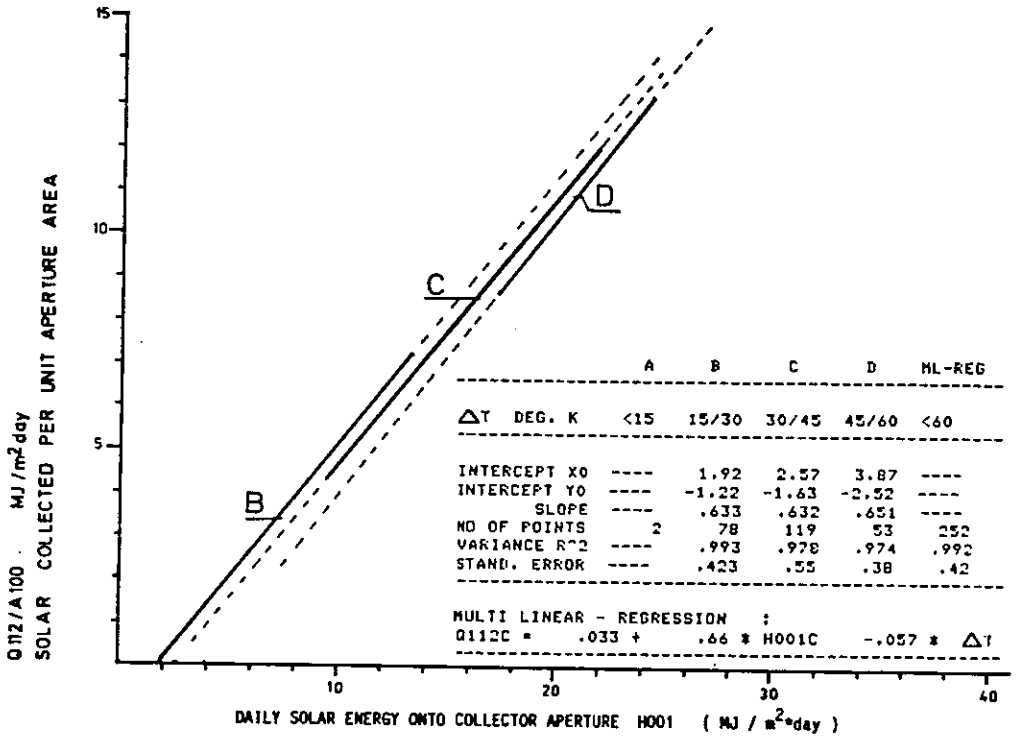

Figure 6.2-44. Daily Energy Input/Output Diagram for the Corning Glass Collector, Solarhaus Freiburg, Federal Republic of Germany, June 1982 to May 1983.

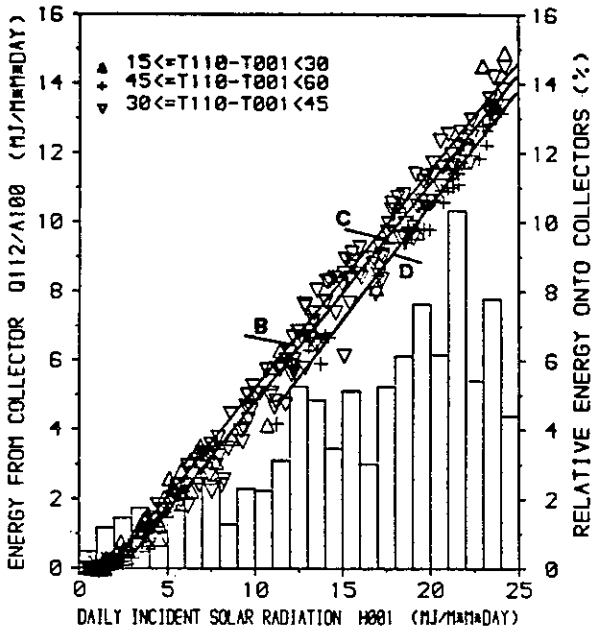

	B	C	D
Temperature Band ΔT (K)	15 - 30	30 - 45	45 - 60
x - Intercept	1.76	2.46	4.3
slope	0.63	0.63	0.66
Number of Days	85	152	36
Correlation Coeff. R^2	0.97	0.98	0.97

Figure 6.2-45. Daily Energy Input/Output Diagram for the Corning Glass Collector, Solarhaus Freiburg, Federal Republic of Germany, 1982.

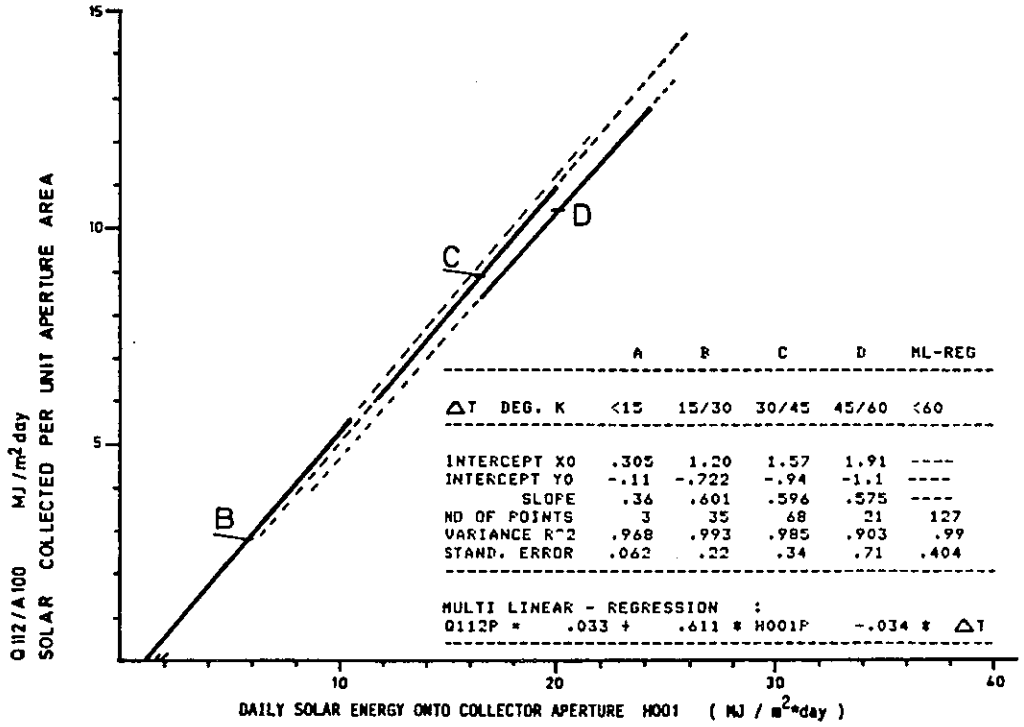

Figure 6.2-46. Daily Energy Input/Output Diagram for the Philips/ Stiebel-Eltron Collector, Solarhaus Freiburg, Federal Republic of Germany, June 1982 to December 1983.

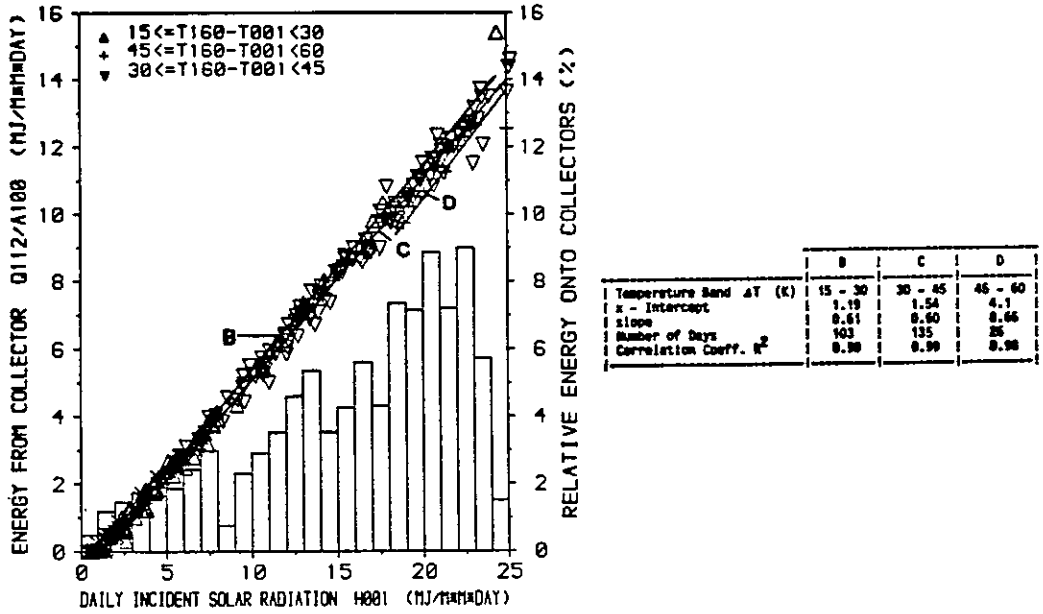

Figure 6.2-47. Daily Energy Input/Output Diagram for the Philips/Stiebel-Eltron Collector, Solarhaus Freiburg, Federal Republic of Germany, June 1982 to May 1983.

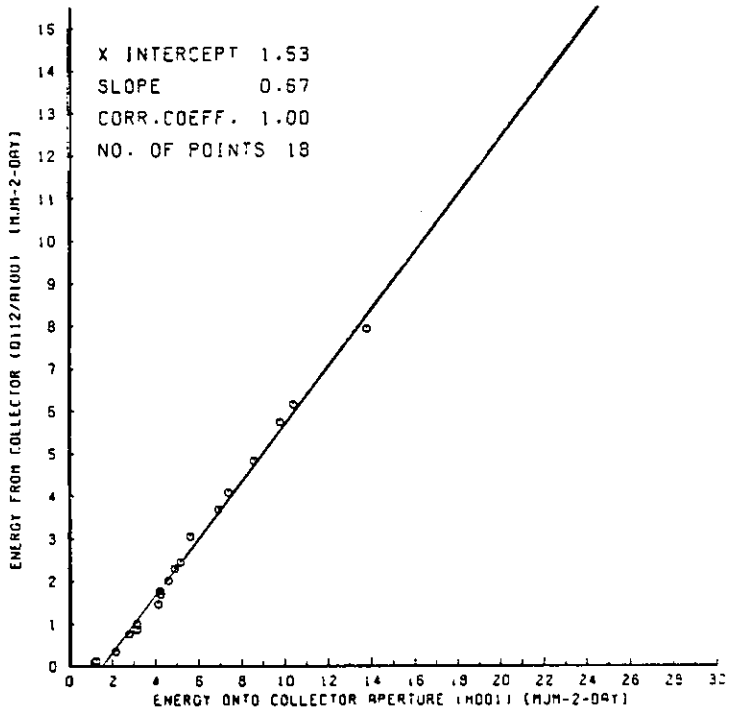

Figure 6.2-48. Daily Energy Input/Output Diagram for the Philips VTR 261, EUT Solar House, January, 1984.

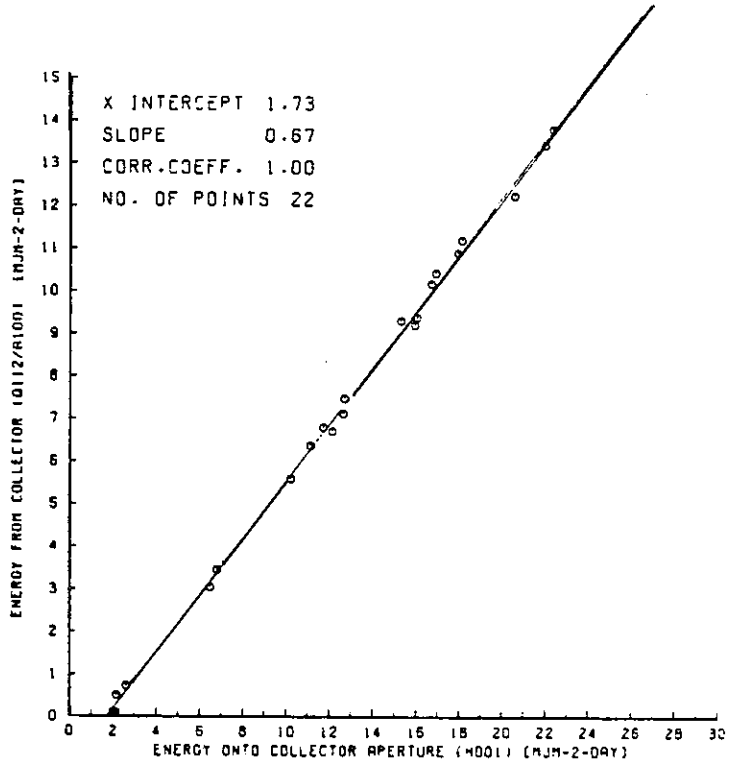

Figure 6.2-49. Daily Energy Input/Output Diagram for the Philips VTR 261, EUT Solar House, March, 1984.

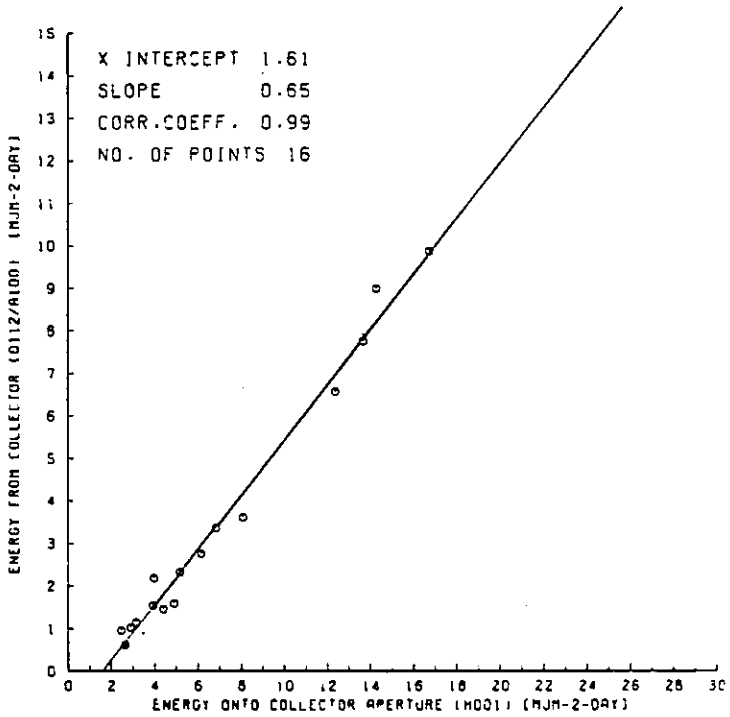

Figure 6.2-50. Daily Energy Input/Output Diagram for the Philips VTR 261, EUT Solar House, September, 1984.

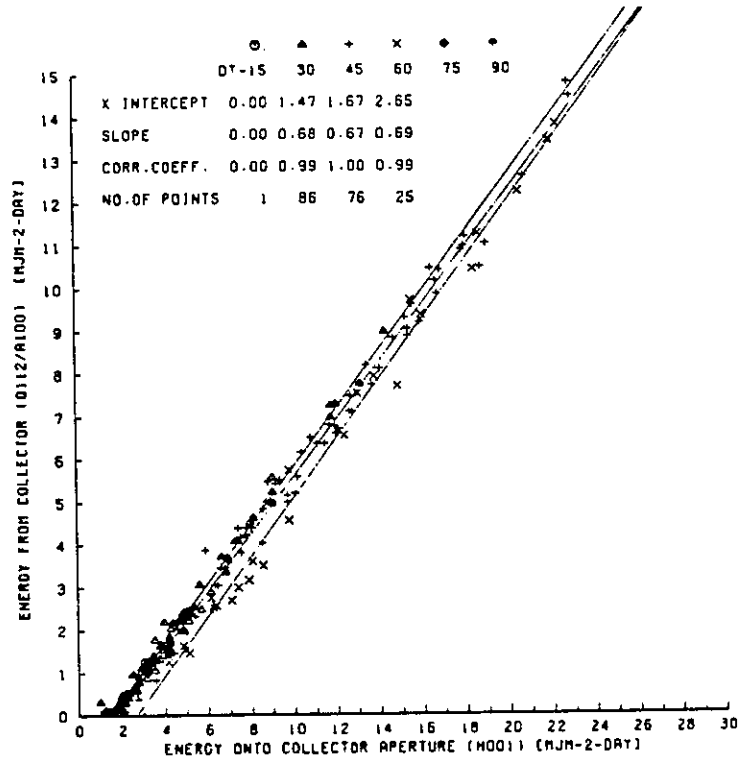

Figure 6.2-51. Daily Energy Input/Output Diagram for the Philips VTR 261, EUT Solar House.

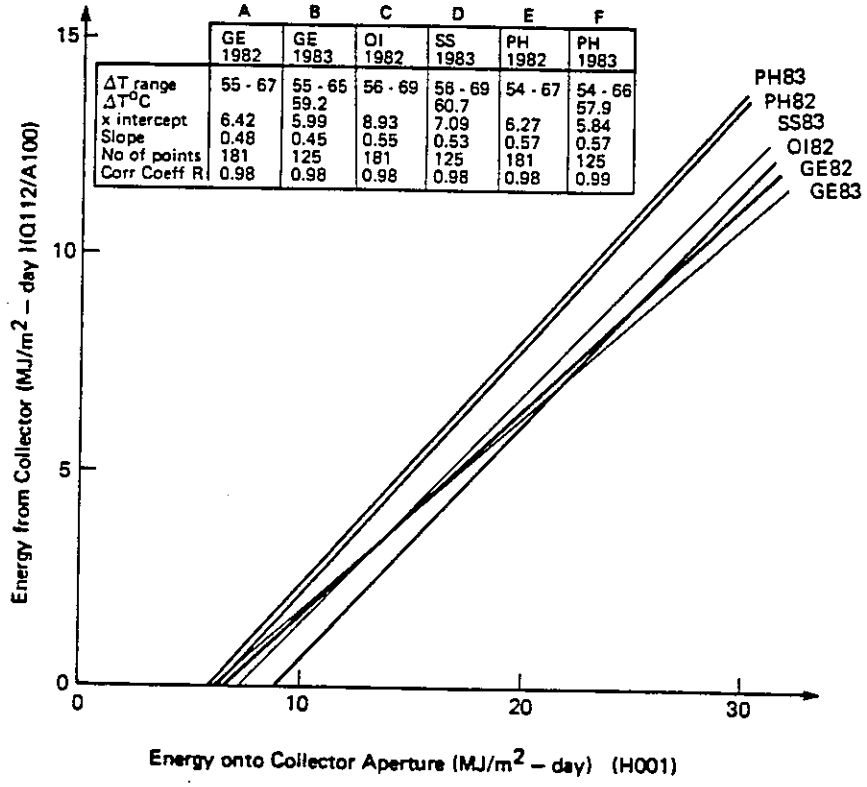

Figure 6.2-52. Daily Energy Input/Output Diagram for Knivsta, Sweden, March to September 1982 and February to June 1983.

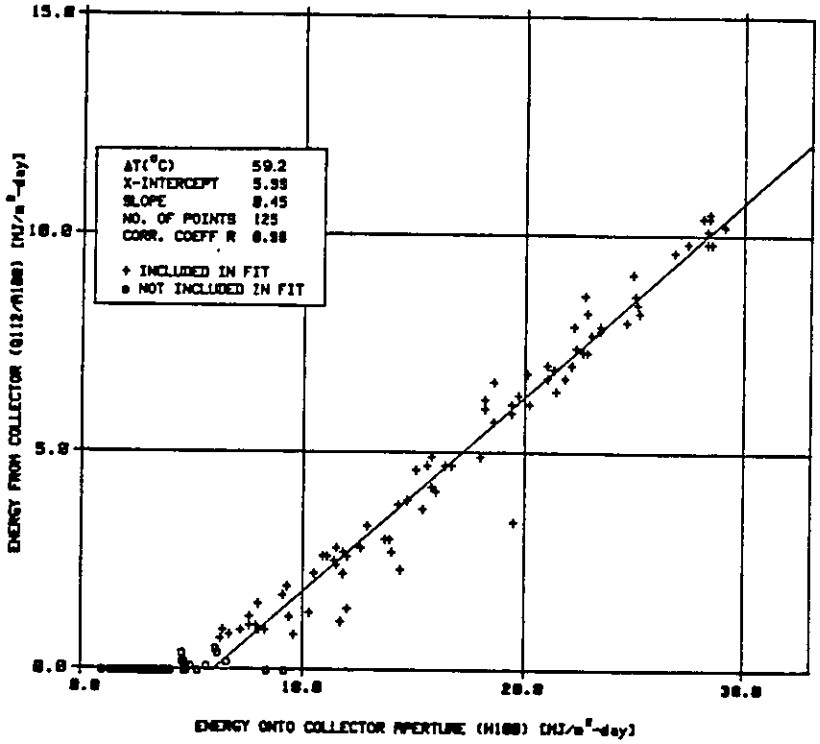

Figure 6.2-53. Daily Energy Input/Output Diagram for the General Electric TC100, Collector, Knivsta, Sweden, February to June 1983.

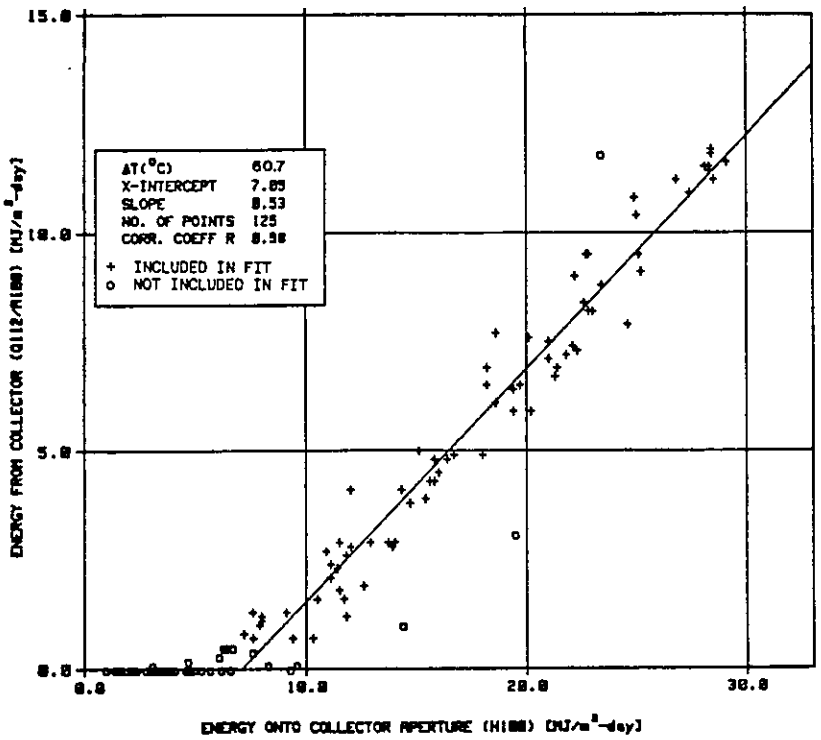

Figure 6.2-54. Daily Energy Input/Output Diagram for the Scandinavian Solar HT Collector, Knivsta, Sweden, February to June 1983.

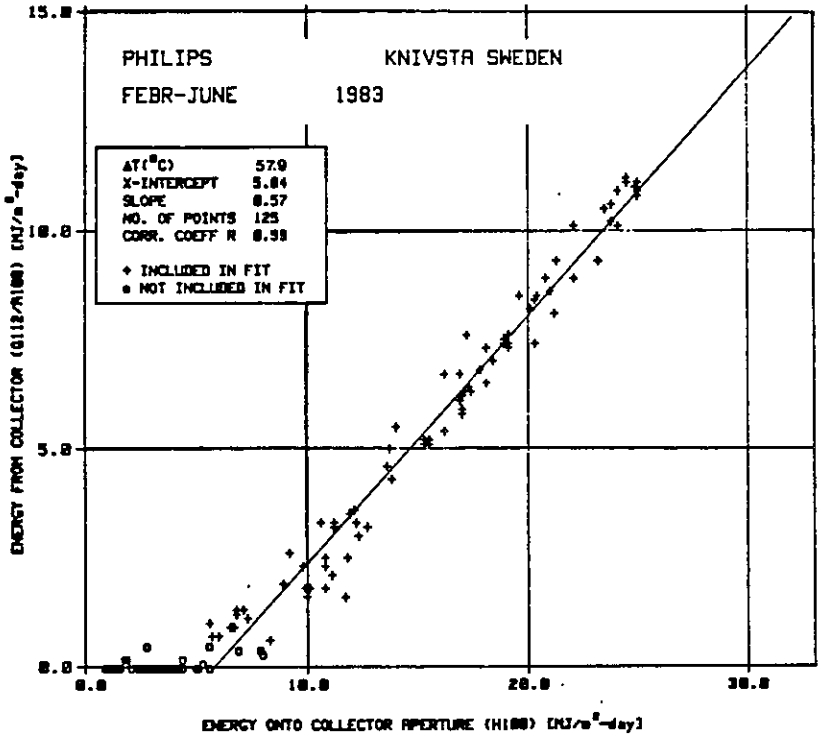

Figure 6.2-55. Daily Energy Input/Output Diagram for the Philips VTR 141 Collector, Knivsta, Sweden, February to June 1983.

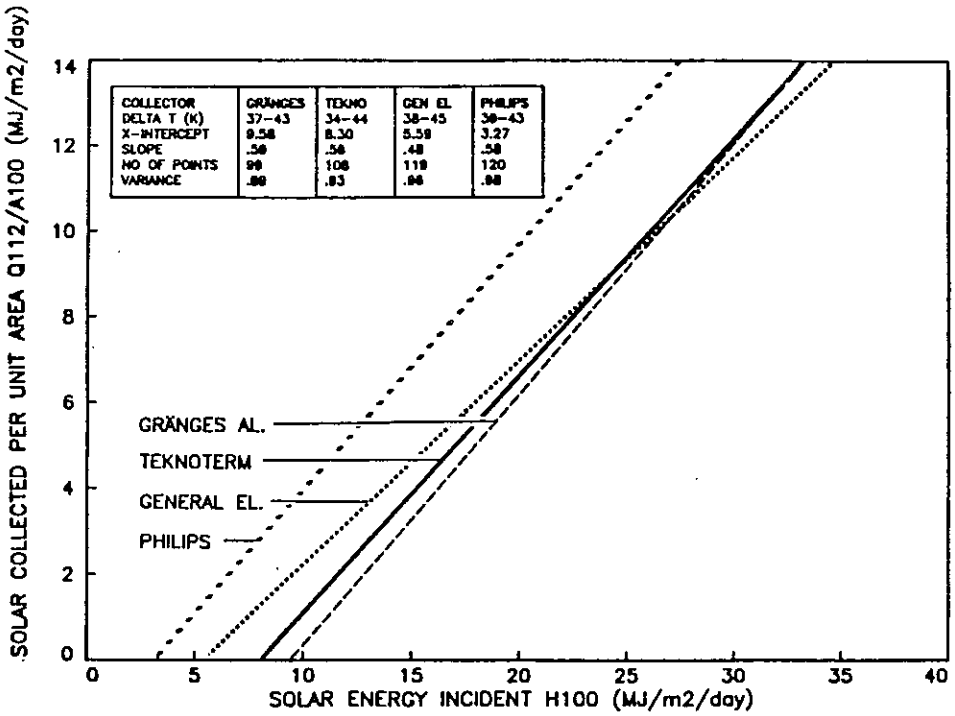

Figure 6.2-56. Daily Energy Input/Output Regression Lines Diagram, Södertörn, Sweden, May to October 1982.

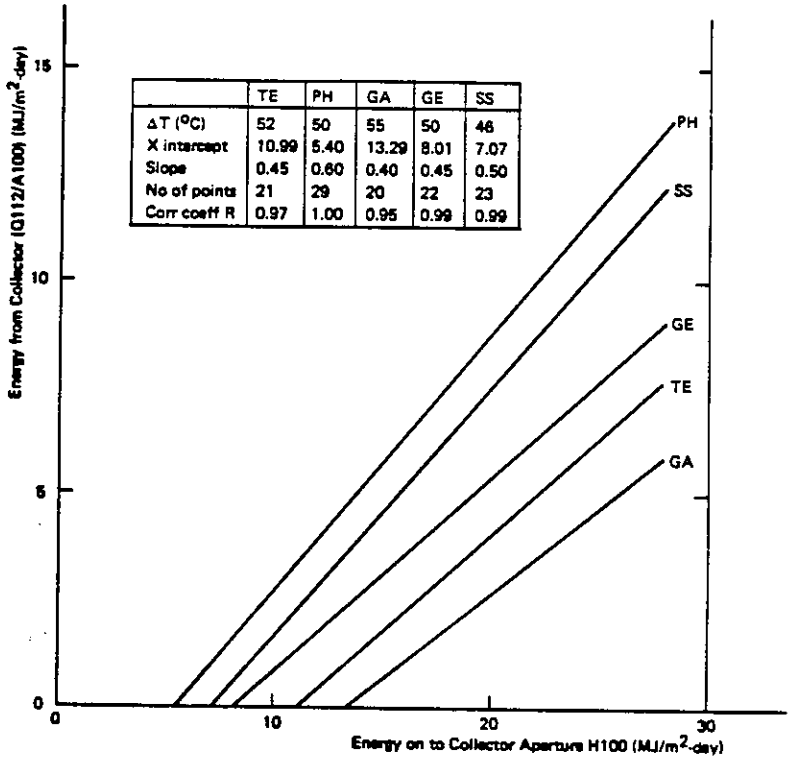

Figure 6.2-57. Daily Energy Input/Output Diagram, 80°C Operation, Södertörn, Sweden, June 1983.

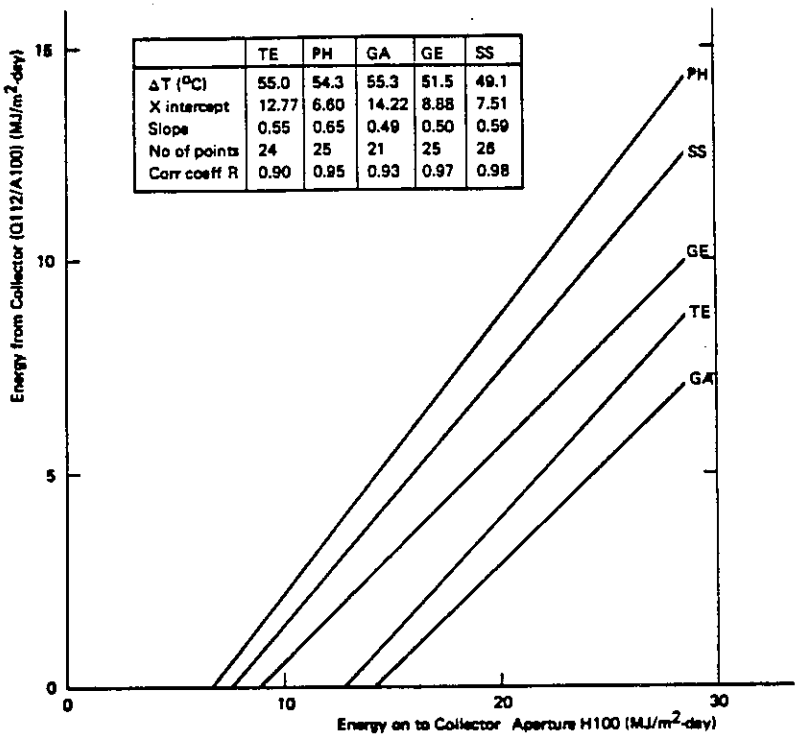

Figure 6.2-58. Daily Energy Input/Output Diagram, 80°C Operation, Södertörn, Sweden, July 1983.

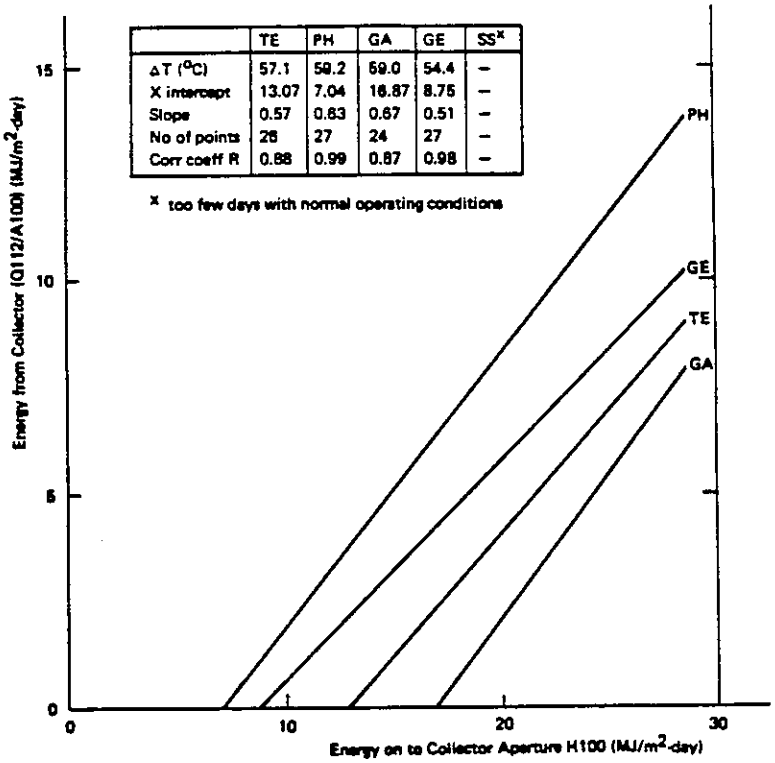

Figure 6.2-59. Daily Energy Input/Output Diagram, 80°C Operation, Södertörn, Sweden, August, 1983.

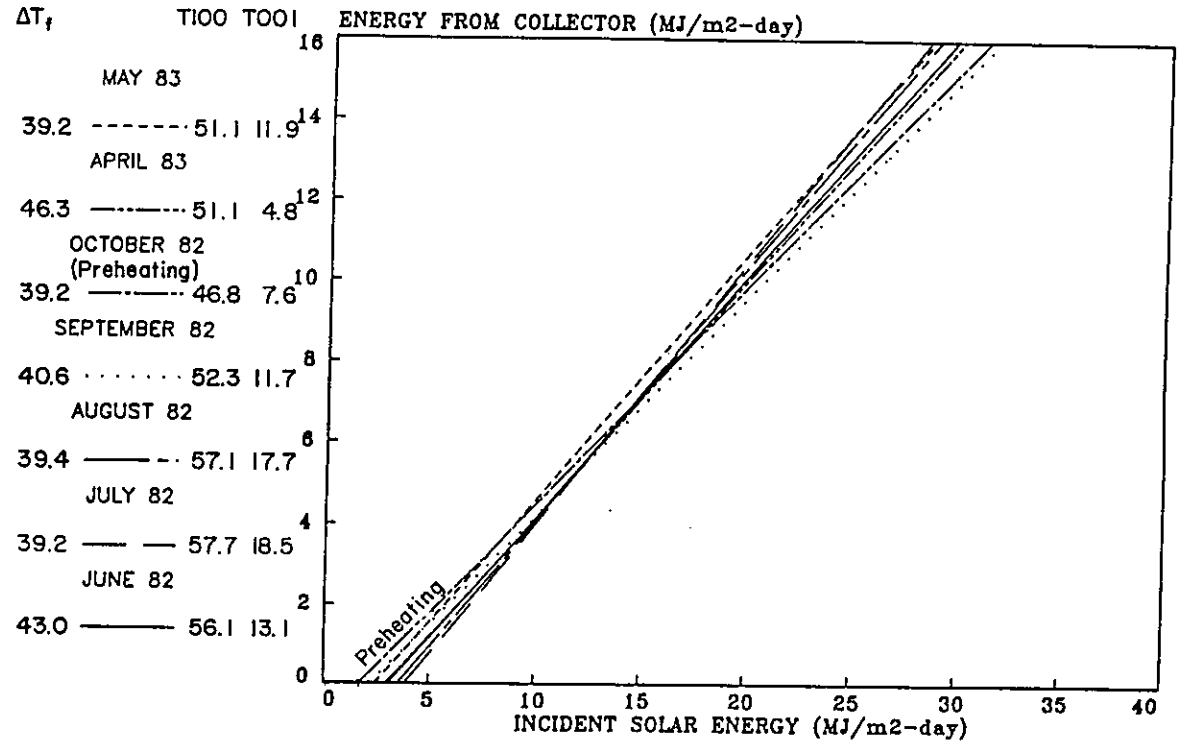

Figure 6.2-60. Daily Energy Input/Output Diagram for the Philips Collector, Södertörn, Sweden, June 1982 to May 1983.

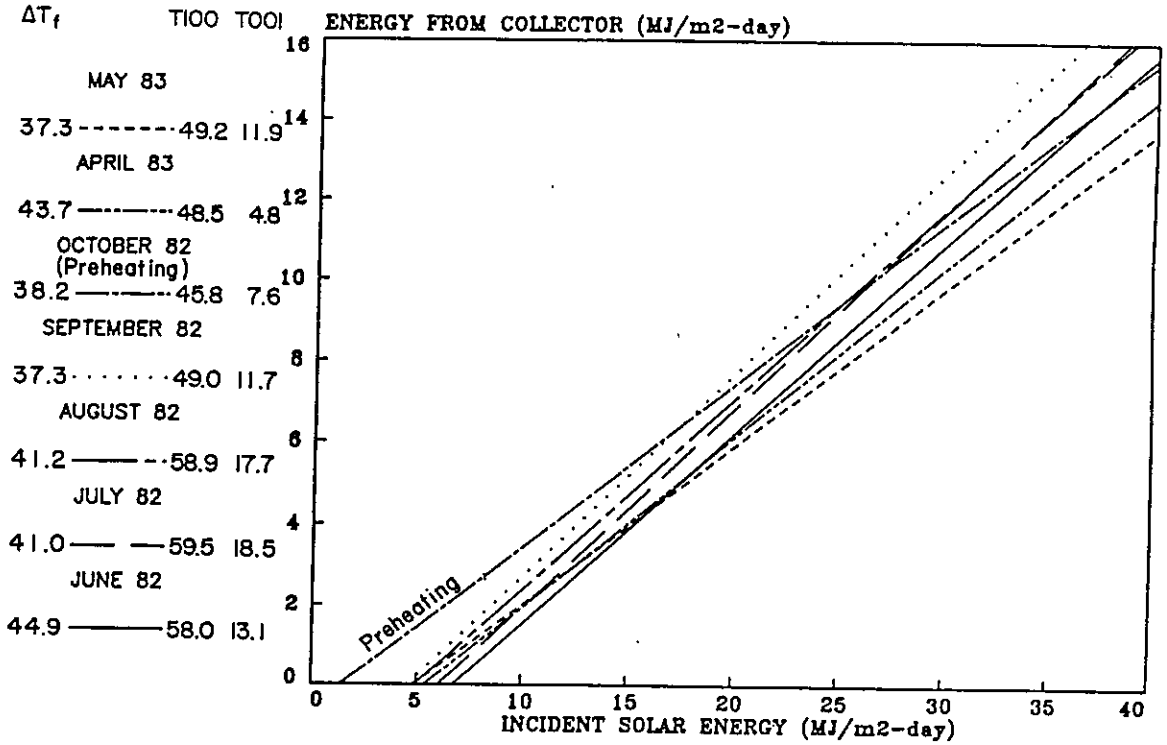

Figure 6.2-61. Daily Energy Input/Output Diagram for the General Electric Collector, Södertörn, Sweden, June 1982 to May 1983.

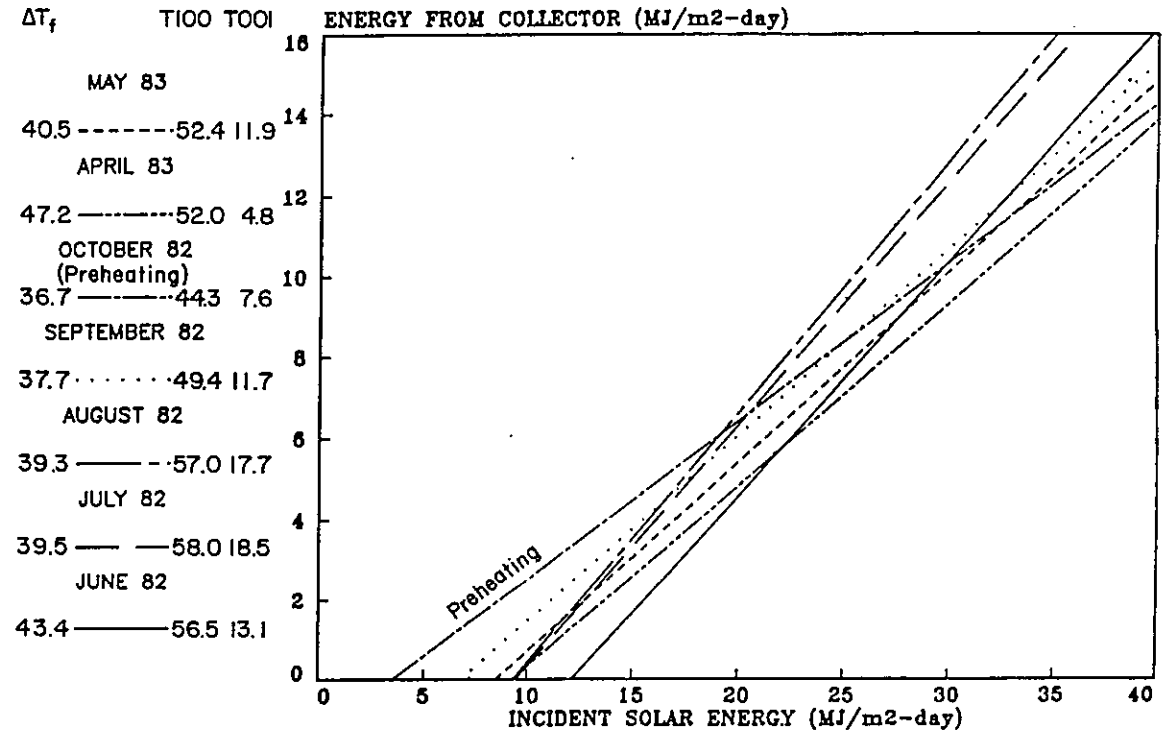

Figure 6.2-62. Daily Energy Input/Output Diagram for the NYBY Collector, Södertörn, Sweden, June 1982 to May 1983.

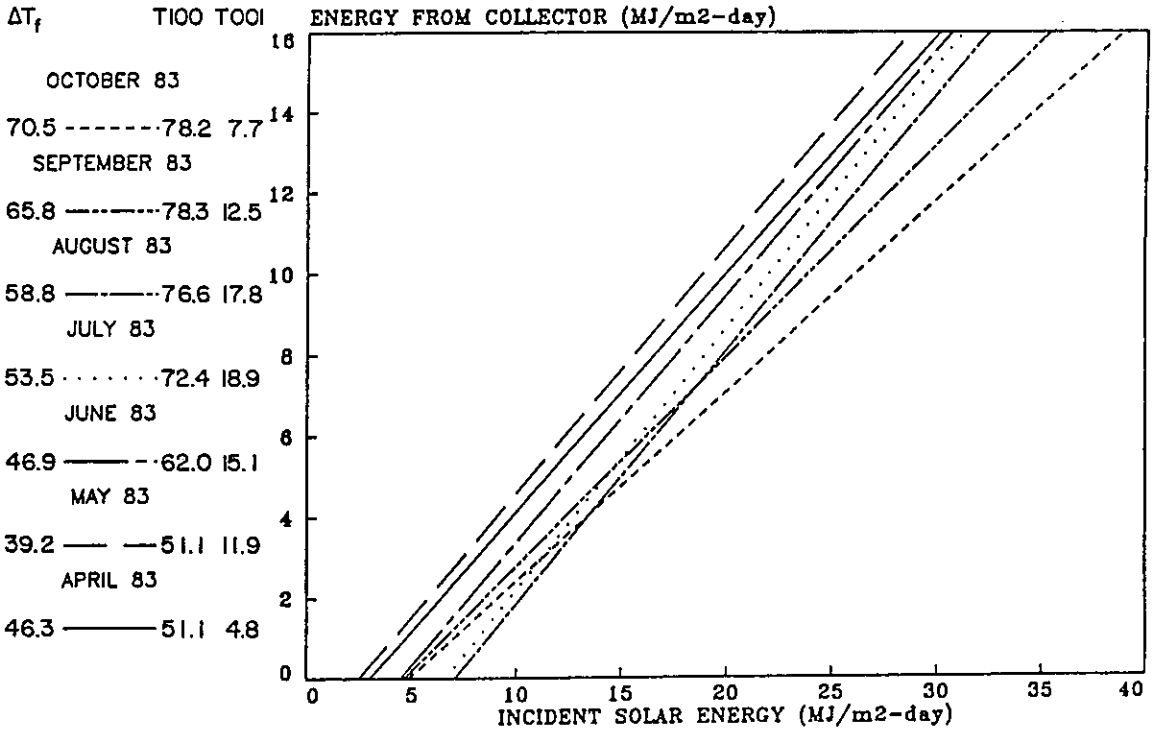

Figure 6.2-63. Daily Energy Input/Output Diagram for the Philips Collector, Södertörn, Sweden, April 1983 to October 1983.

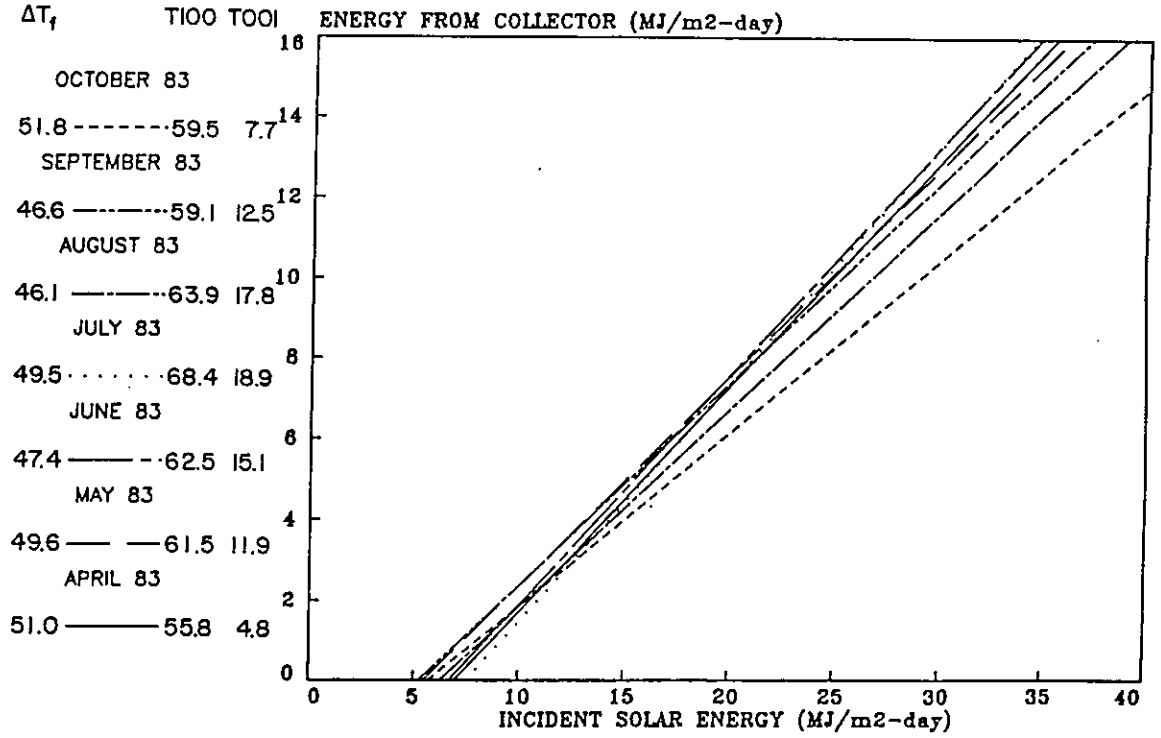

Figure 6.2-64. Daily Energy Input/Output Diagram for the Scandinavian Solar Collector, Södertörn, Sweden, April 1983 to October 1983.

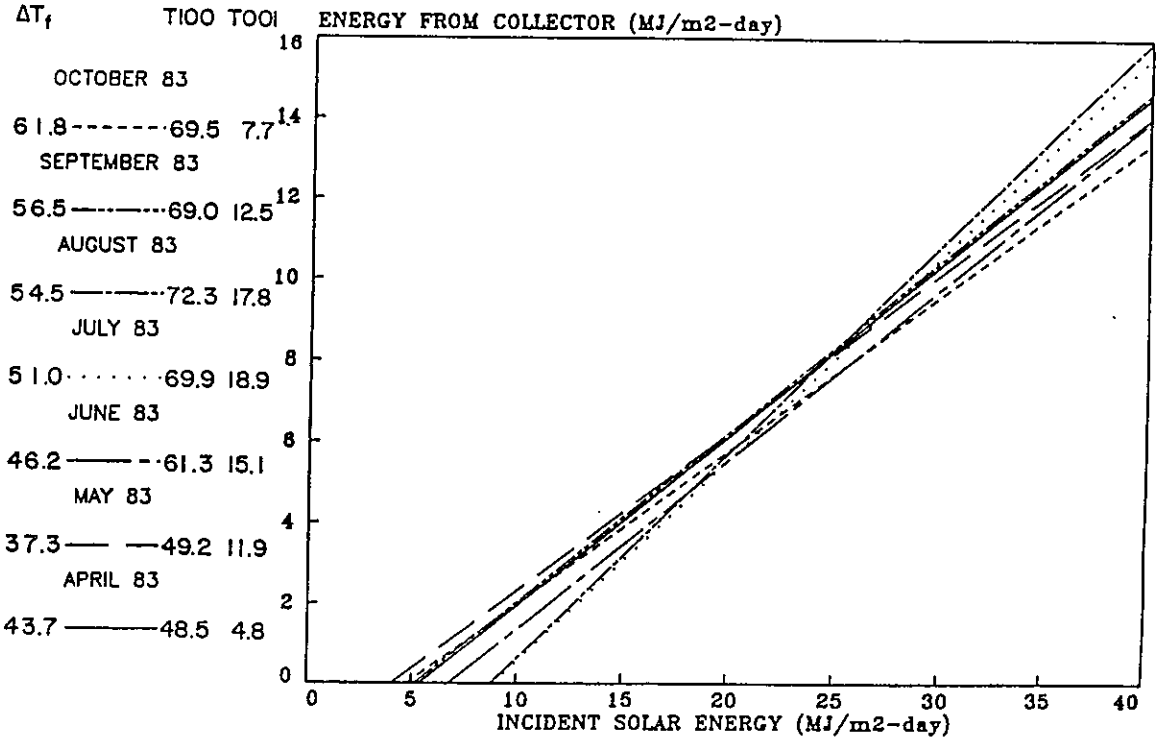

Figure 6.2-65. Daily Energy Input/Output Diagram for the General Electric Collector, Södertörn, Sweden, April 1983 to October 1983.

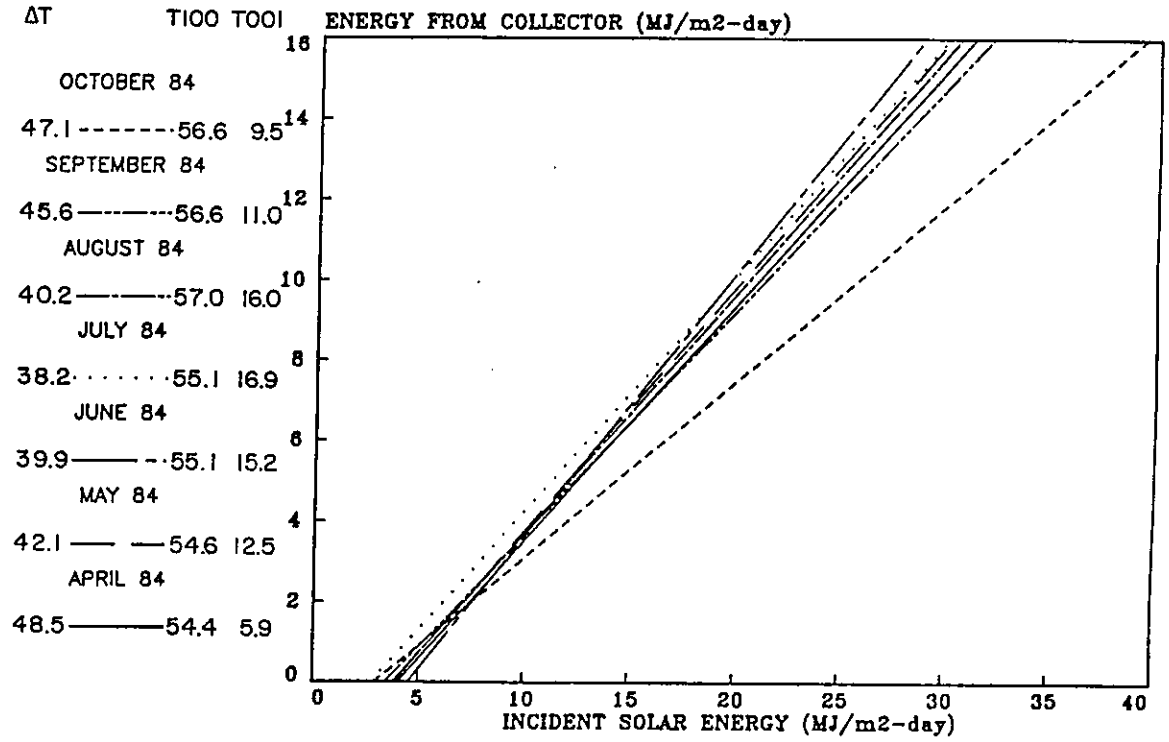

Figure 6.2-66. Daily Energy Input/Output Diagram for the Philips Collector, Södertörn, Sweden, April 1984 to October 1984.

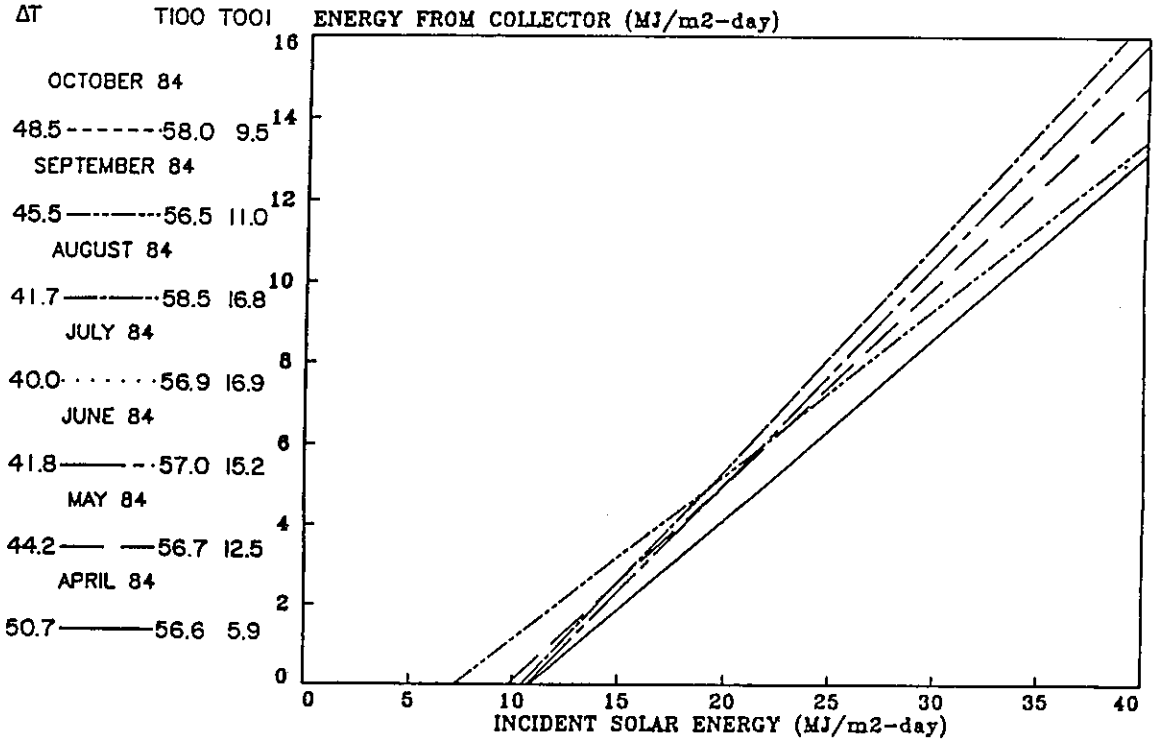

Figure 6.2-67. Daily Energy Input/Output Diagram for the NYBY Collector, Södertörn, Sweden, April 1984 to October 1984.

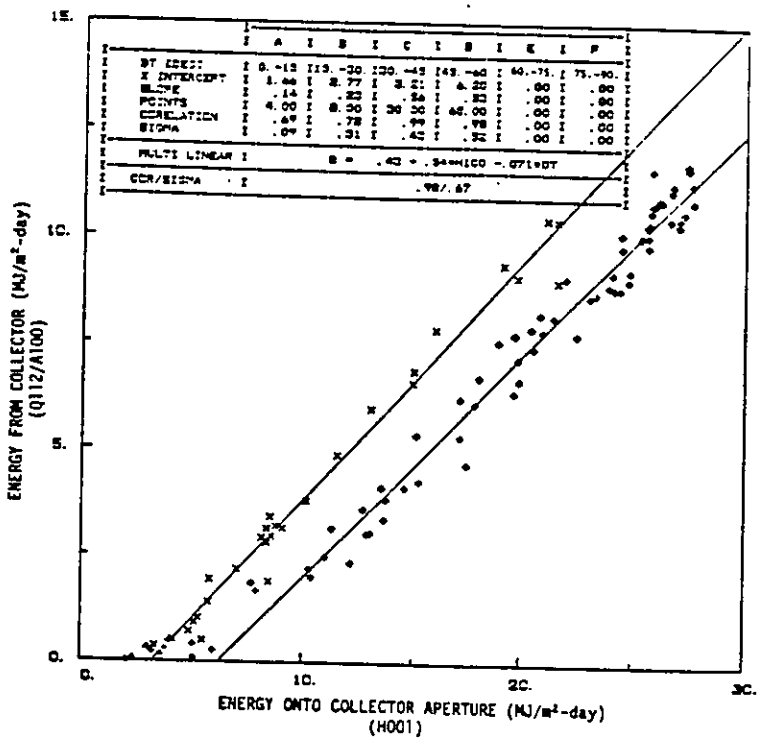

Figure 6.2-68. Daily Energy Input/Output Diagram for Corning Cortec "A" Geneva, Switzerland, July 1, 1982 to November 4, 1982.

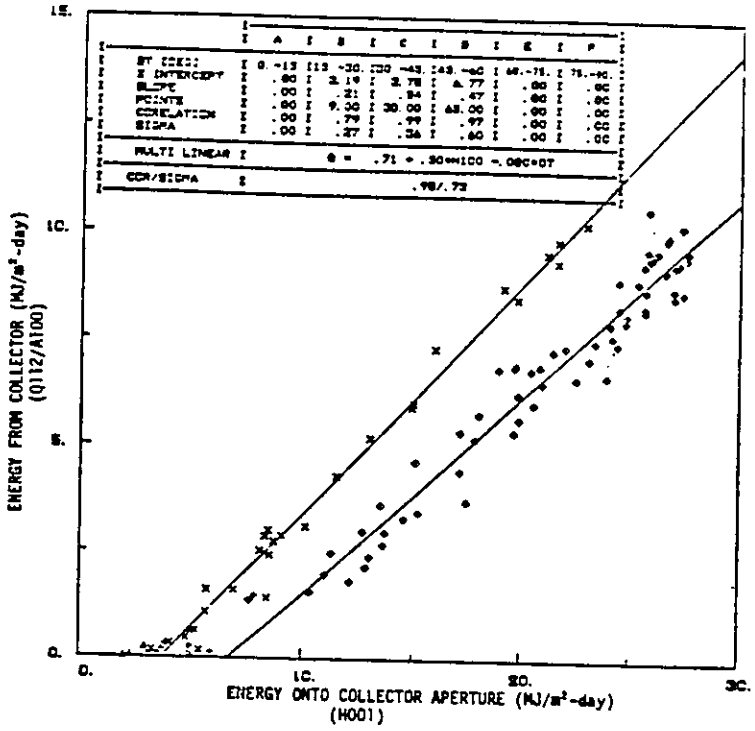

Figure 6.2-69. Daily Energy Input/Output Diagram for Corning Cortec "B" Geneva, Switzerland, July 1, 1982 to November 4, 1982.

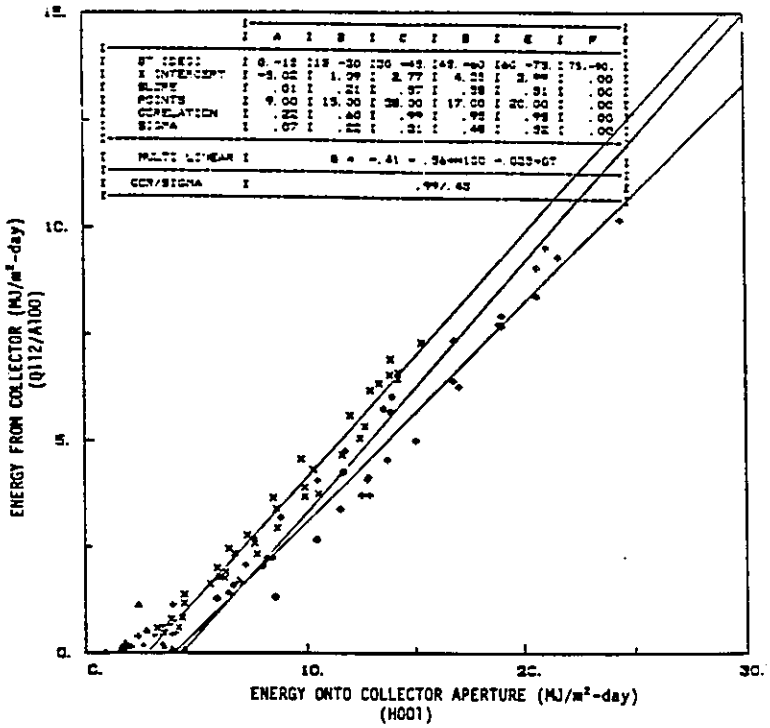

Figure 6.2-70. Daily Energy Input/Output Diagram for Corning Cortec "A" Geneva, Switzerland, November 4, 1982 to March 31, 1983.

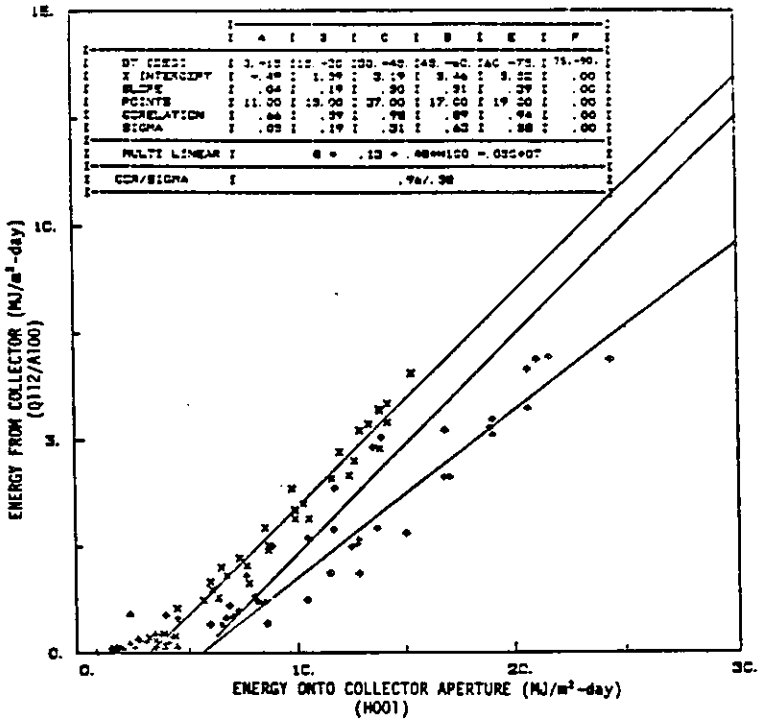

Figure 6.2-71. Daily Energy Input/Output Diagram for Corning Cortec "B" Geneva, Switzerland, November 4, 1982 to March 31, 1983.

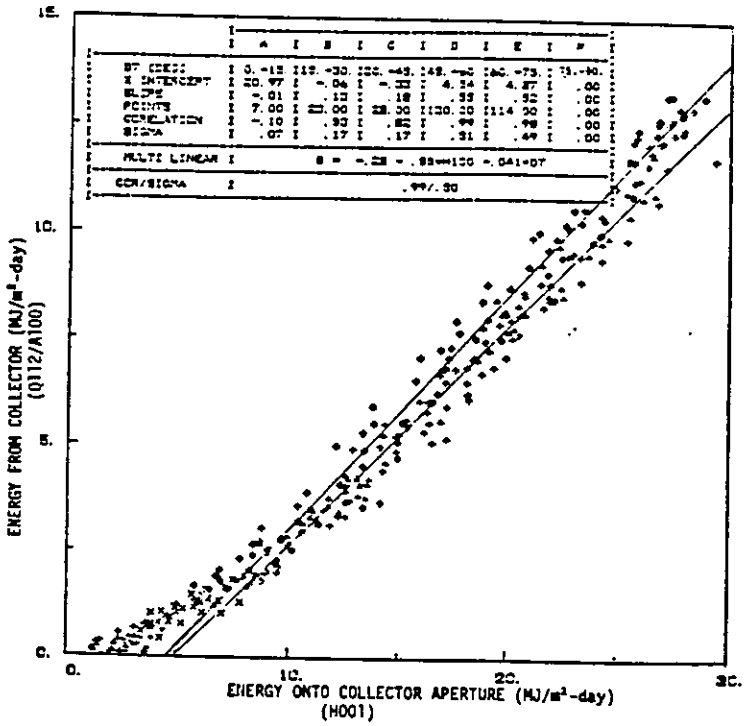

Figure 6.2-72. Daily Energy Input/Output Diagram for Corning Cortec "A" Geneva, Switzerland, April 1, 1983 to March 31, 1984.

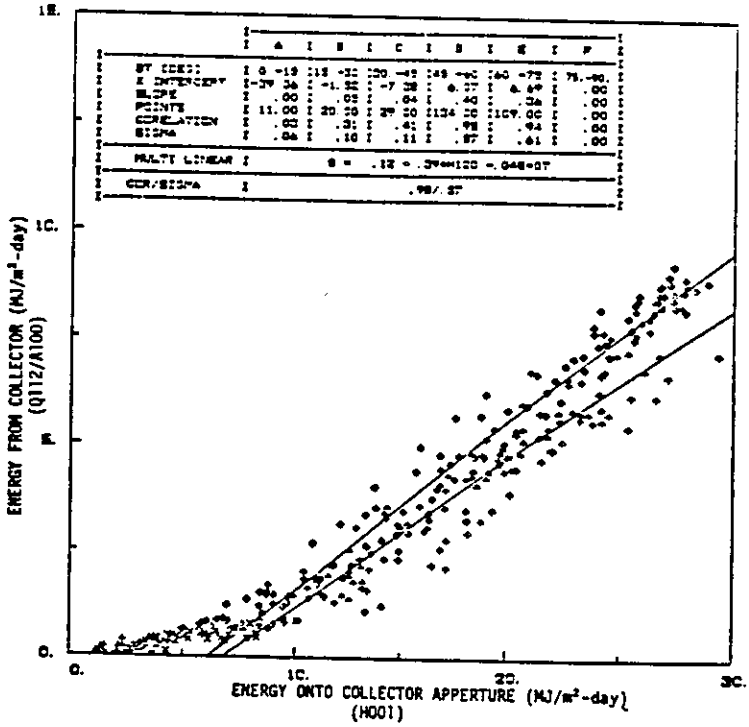

Figure 6.2-73. Daily Energy Input/Output Diagram for Corning Cortec "B" Geneva, Switzerland, April 1, 1983 to March 31, 1984.

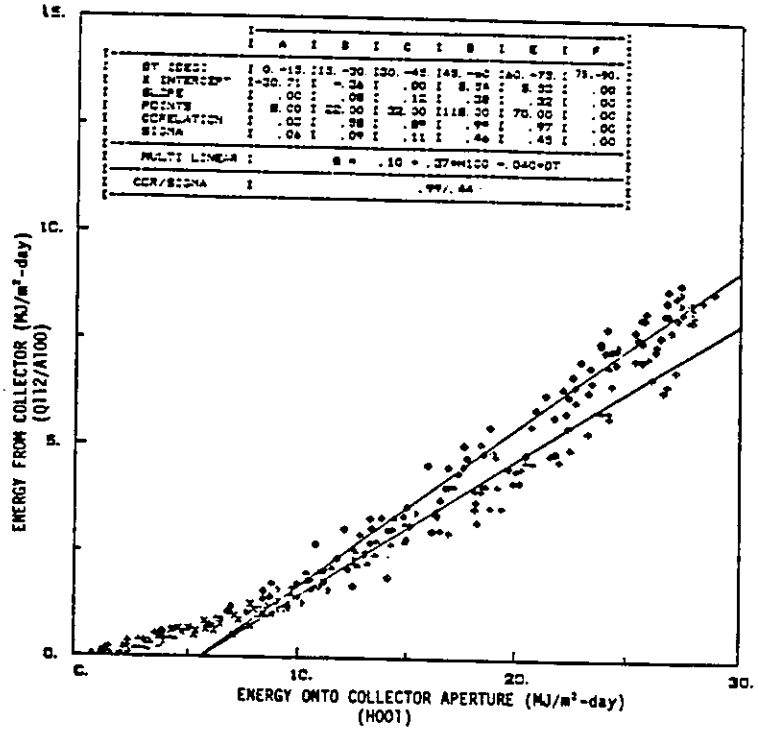

Figure 6.2-74. Daily Energy Input/Output Diagram for Sanyo STC-CU250 Geneva, Switzerland, April 1, 1983 to March 31, 1984.

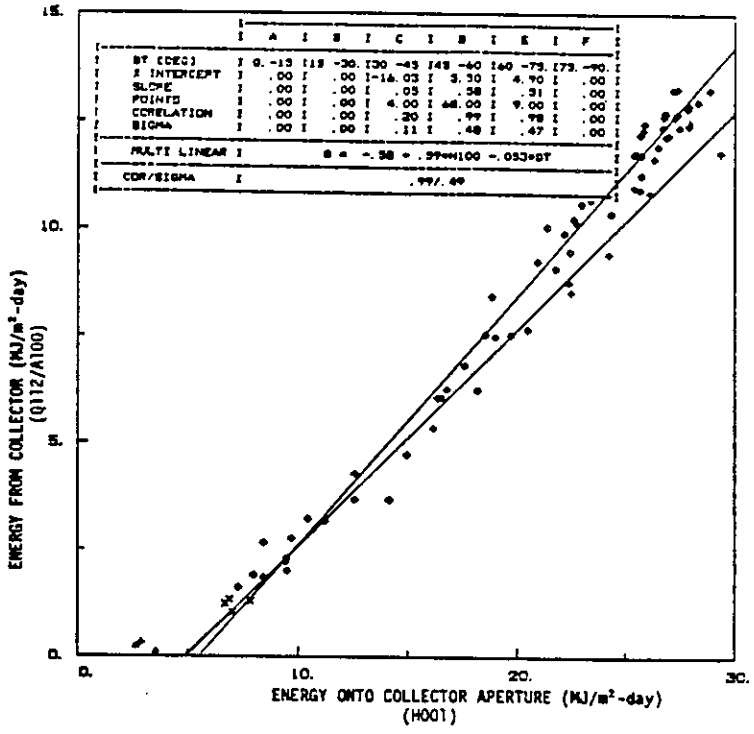

Figure 6.2-75. Daily Energy Input/Output Diagram for Corning Cortec "A" Geneva, Switzerland, May 1, 1983 to July 31, 1983.

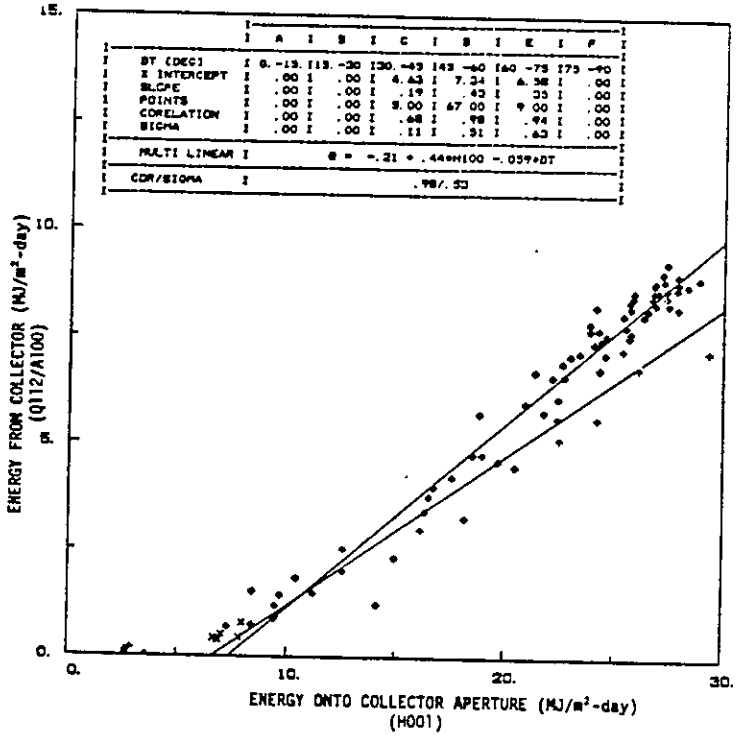

Figure 6.2-76. Daily Energy Input/Output Diagram for Corning Cortec "B" Geneva, Switzerland, May 1, 1983 to July 31, 1983.

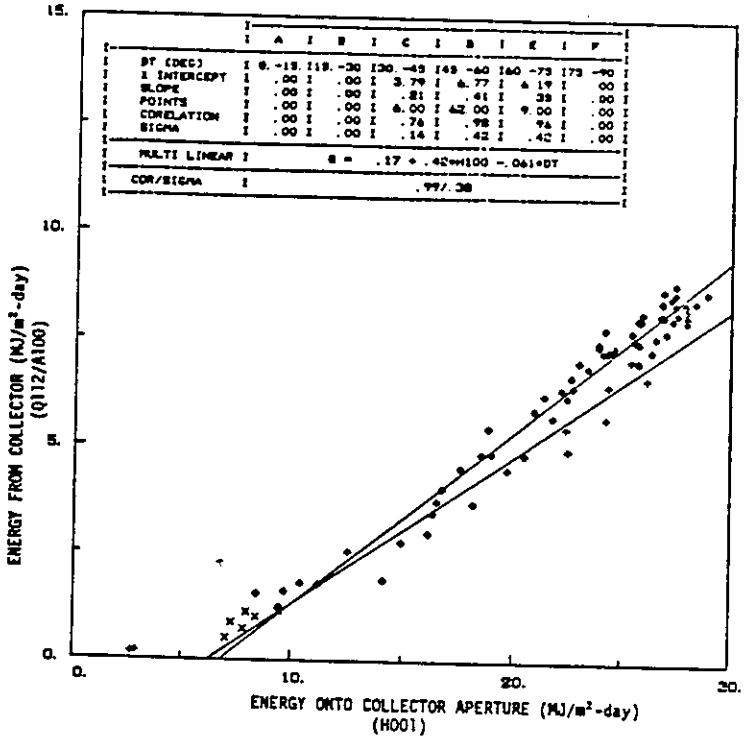

Figure 6.2-77. Daily Energy Input/Output Diagram for Sanyo STC-CU250 Geneva, Switzerland, May 1, 1983 to July 31, 1983.

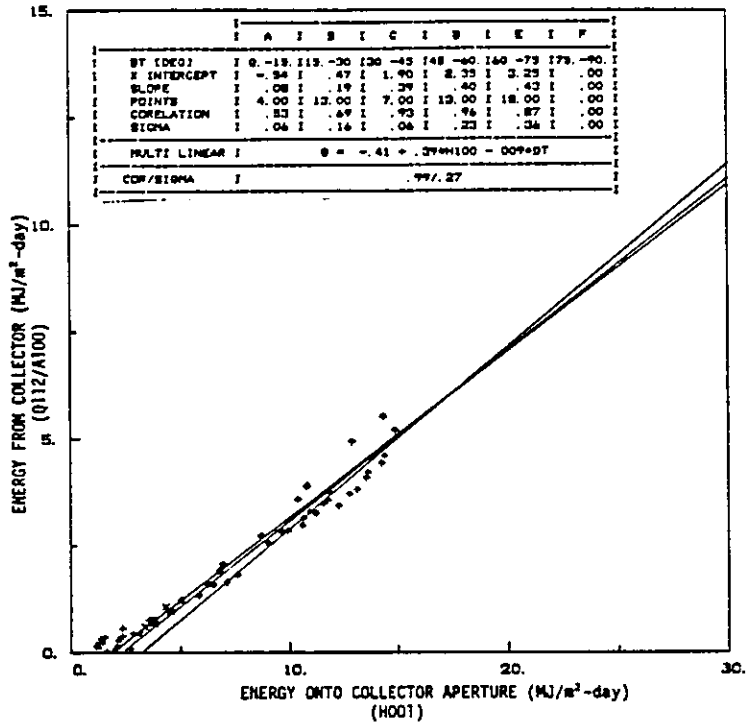

Figure 6.2-78. Daily Energy Input/Output Diagram for Corning Cortec "A" Geneva, Switzerland, November 1, 1983 to January 31, 1984.

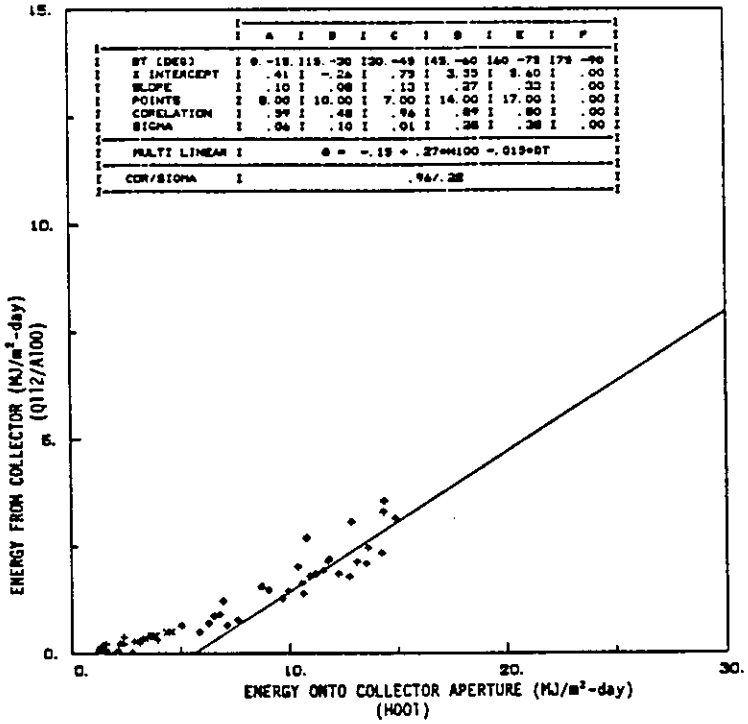

Figure 6.2-79. Daily Energy Input/Output Diagram for Corning Cortec "B" Geneva, Switzerland, November 1, 1983 to January 31, 1984.

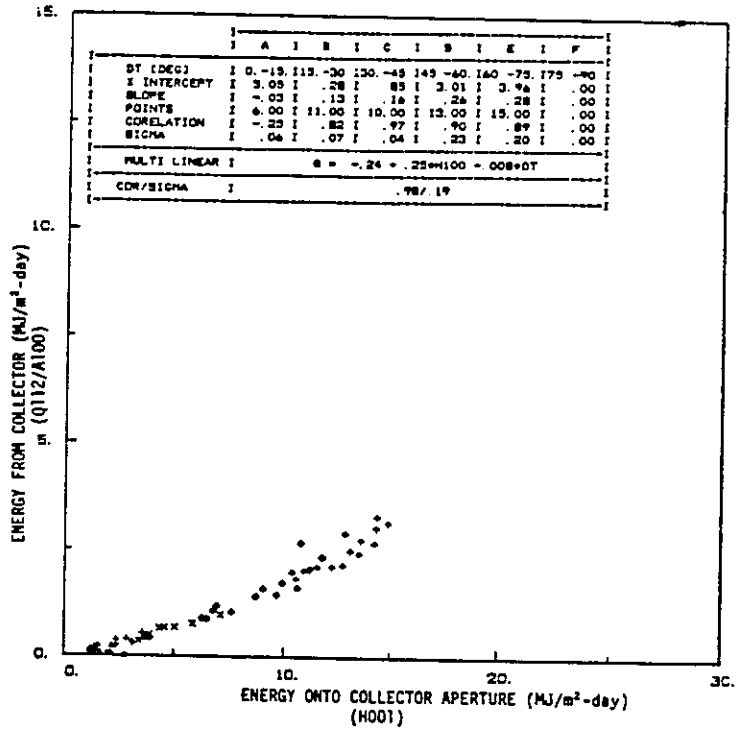

Figure 6.2-80. Daily Energy Input/Output Diagram for Sanyo STC-CU250 Geneva, Switzerland, November 1, 1983 to January 31, 1984.

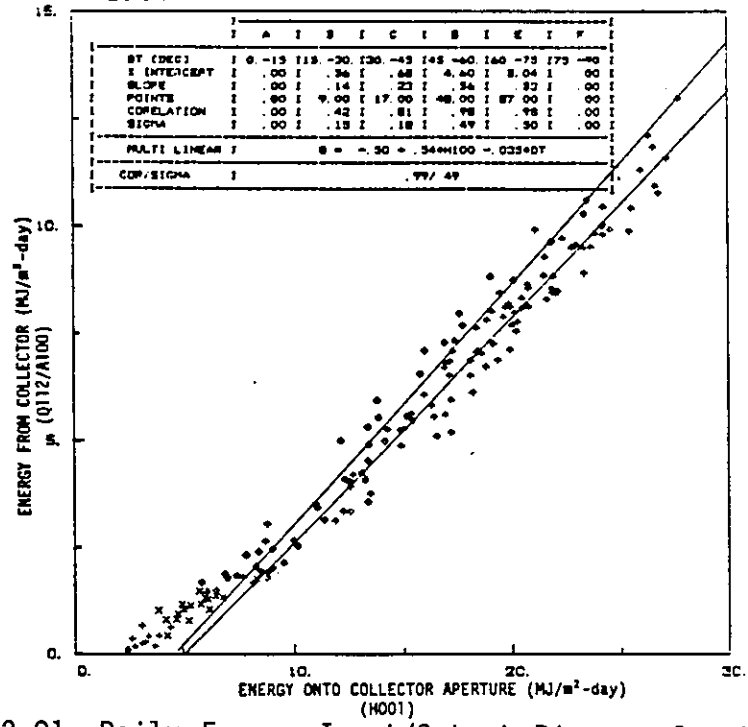

Figure 6.2-81. Daily Energy Input/Output Diagram for Corning Cortec "A" Geneva, Switzerland, April 1, 1983 to April 30, 1983 August 1, 1983 to October 31, 1983, February 1, 1984 to March 31, 1984.

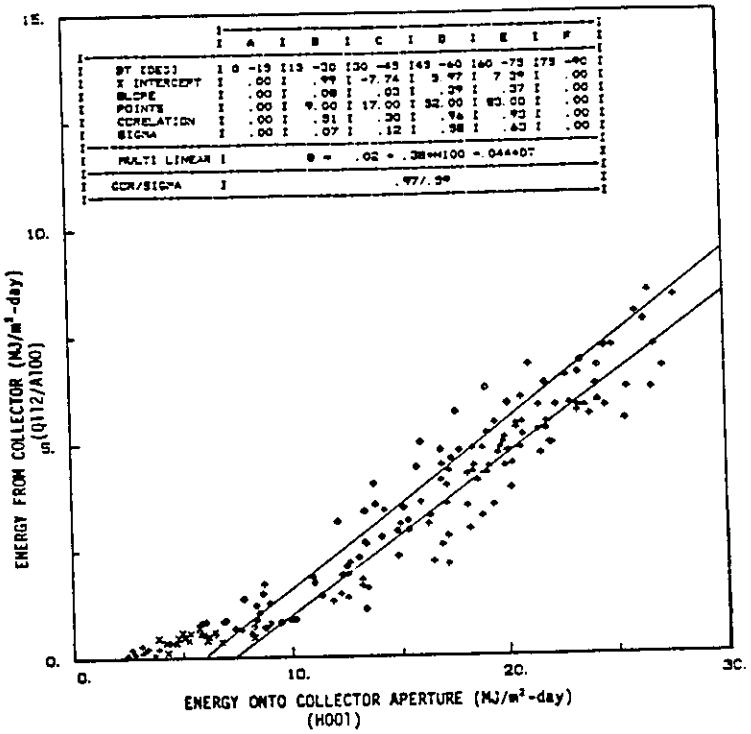

Figure 6.2-82. Daily Energy Input/Output Diagram for Corning Cortec "B" Geneva, Switzerland, April 1, 1983 to April 30, 1983 August 1, 1983 to October 31, 1983, February 1, 1984 to March 31, 1984.

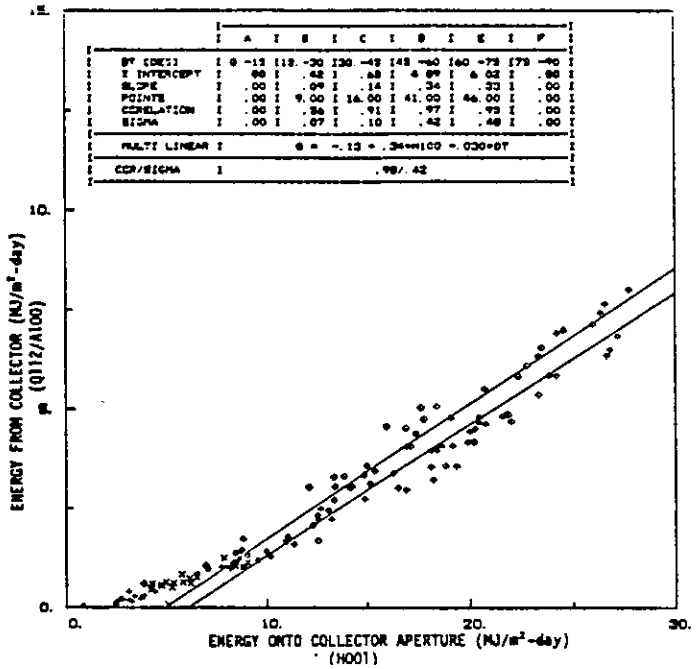

Figure 6.2-83. Daily Energy Input/Output Diagram for Sanyo STC-CU250 Geneva, Switzerland, April 1, 1983 to April 30, 1983, August 1, 1983 to October 31, 1983, February 1, 1984 to March 31, 1984.

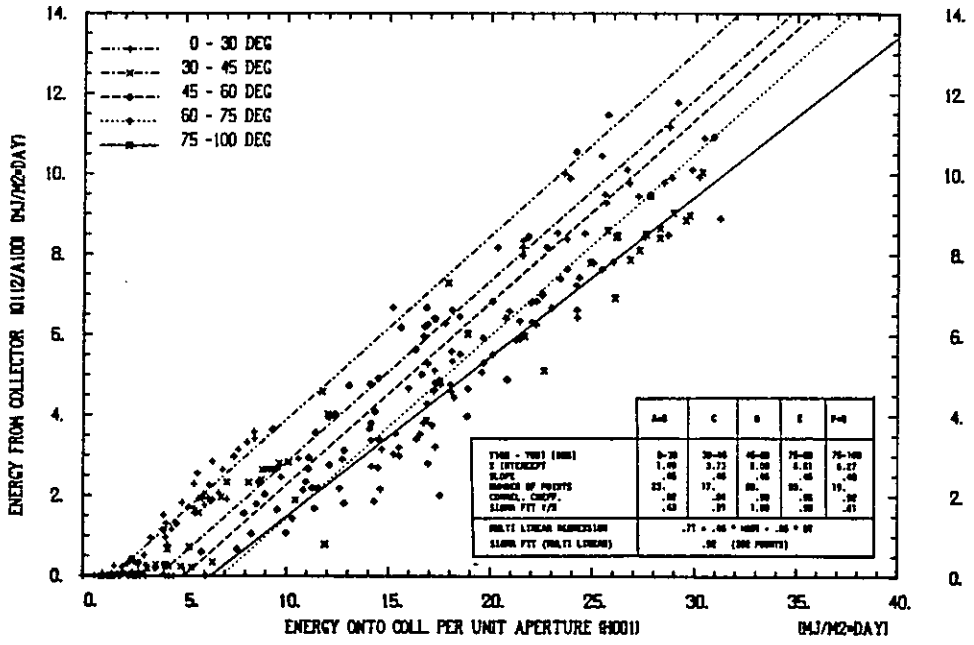

Figure 6.2-84. Daily Energy Input/Output Diagram for Cortec ETC, Hallau, Switzerland, March 6, 1984 to February 28, 1985.

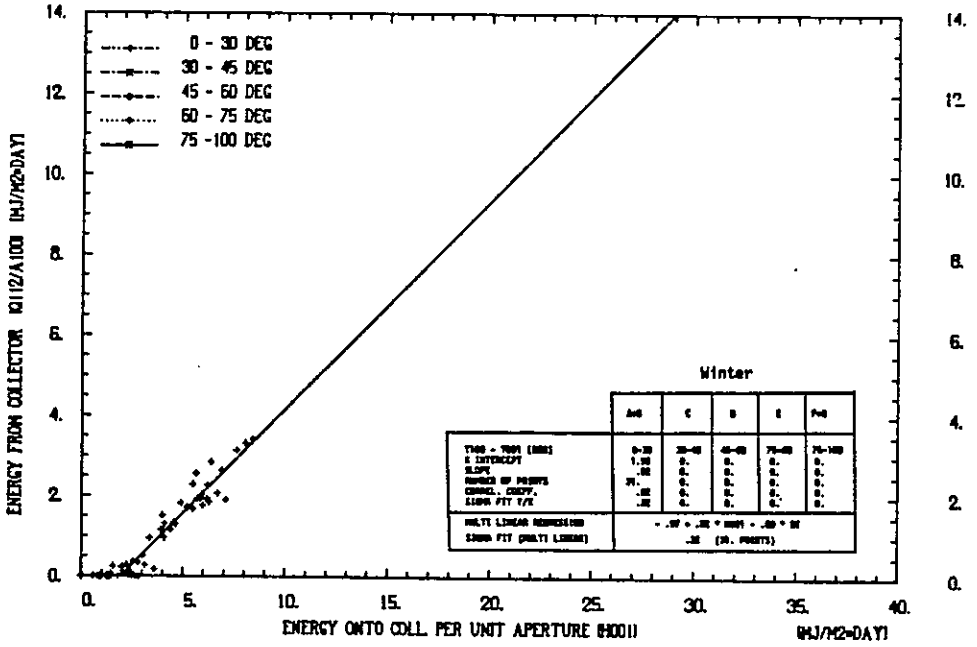

Figure 6.2-85. Daily Energy Input/Output Diagram for Cortec ETC, Hallau, Switzerland, November 1, 1984 to December 31, 1984.

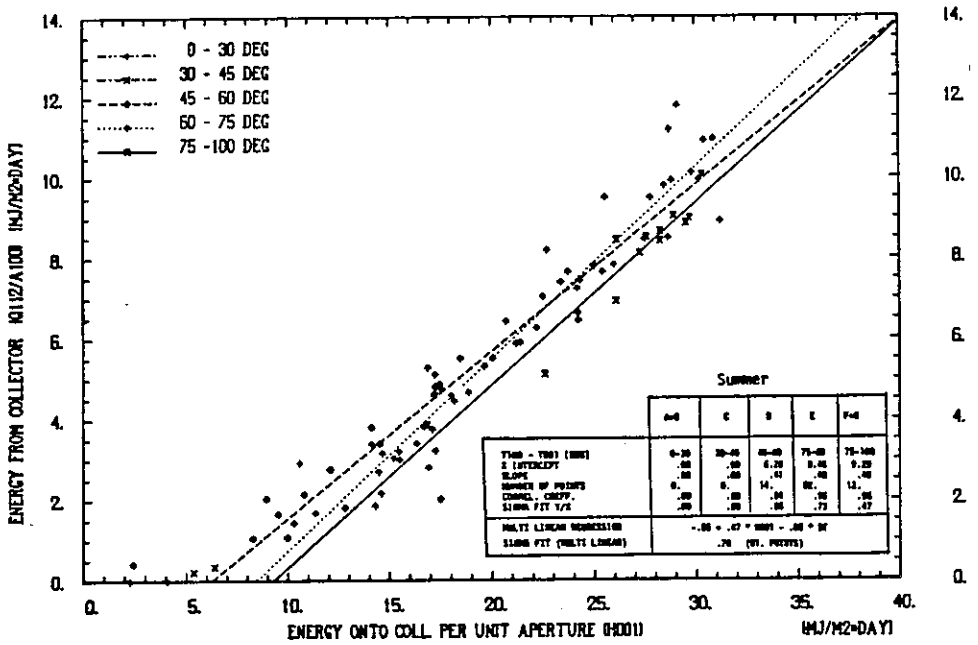

Figure 6.2-86. Daily Energy Input/Output Diagram for Cortec ETC, Hallau, Switzerland, May 1, 1984 to July 31, 1984.

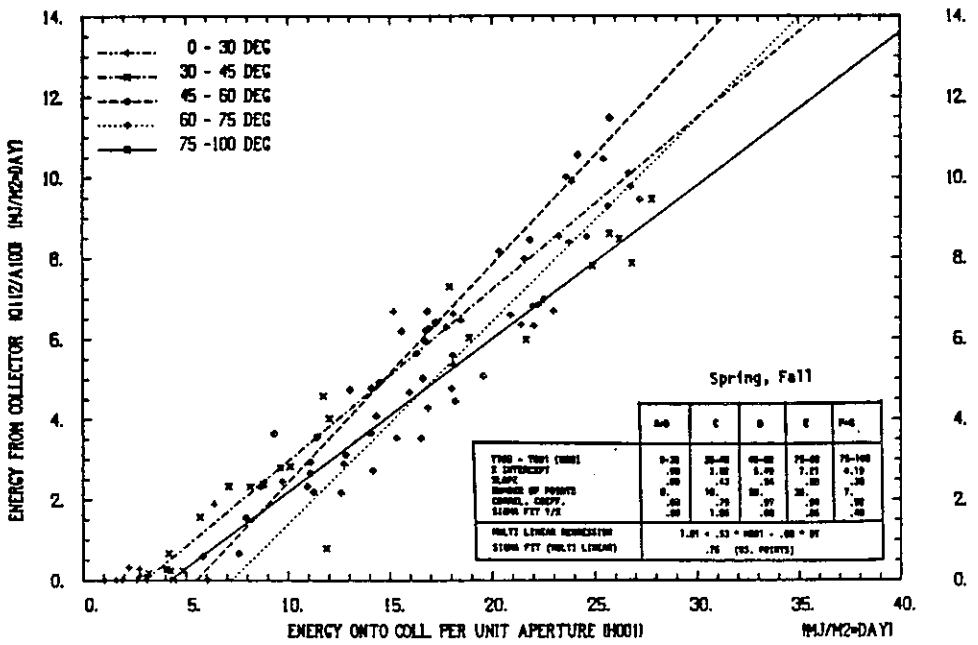

Figure 6.2-87. Daily Energy Input/Output Diagram for Cortec ETC, Hallau, Switzerland, March 6, 1984 to February 28, 1985.

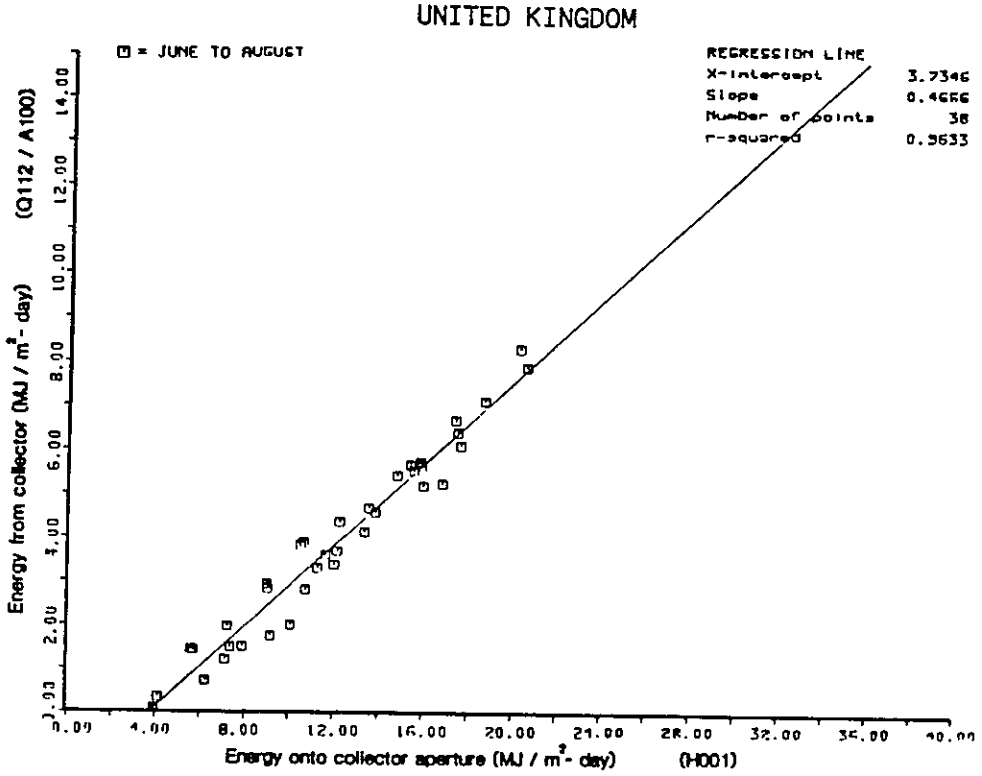

Figure 6.2-88. Daily Energy Input/Output, Philips VTR141, BSRIA Solar Test Facility with Simulated Loads, Bracknell, United Kingdom, June 1981 to August 1983.

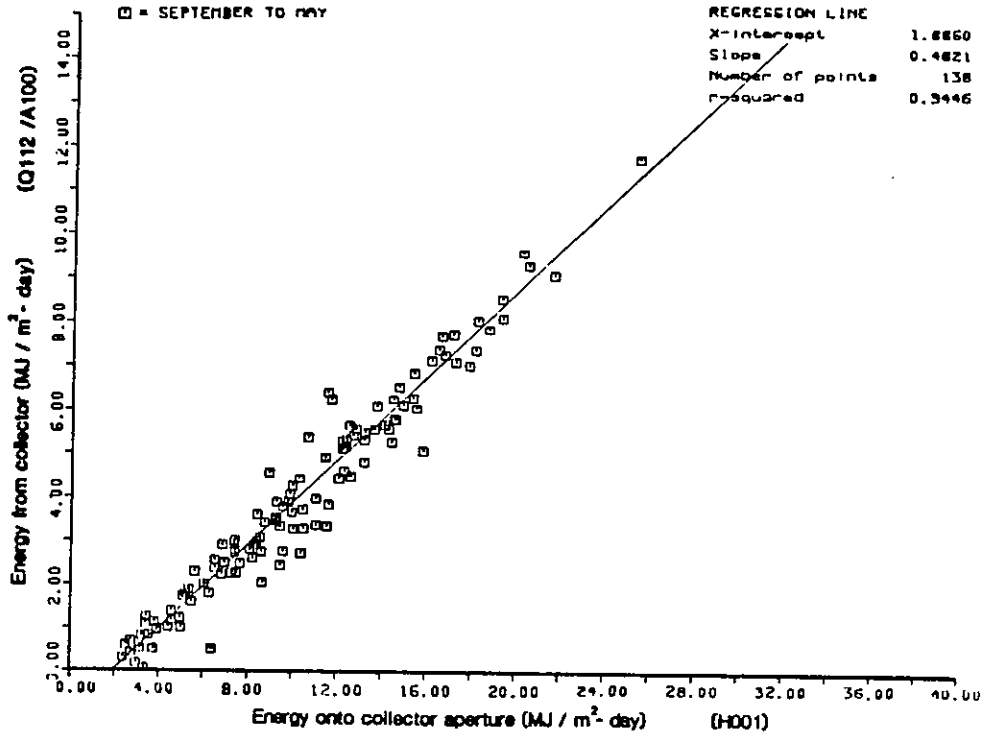

Figure 6.2-89. Daily Energy Input/Output, Philips VTR141, BSRIA Solar Test Facility with Simulated Loads, Bracknell, United Kingdom, September to May.

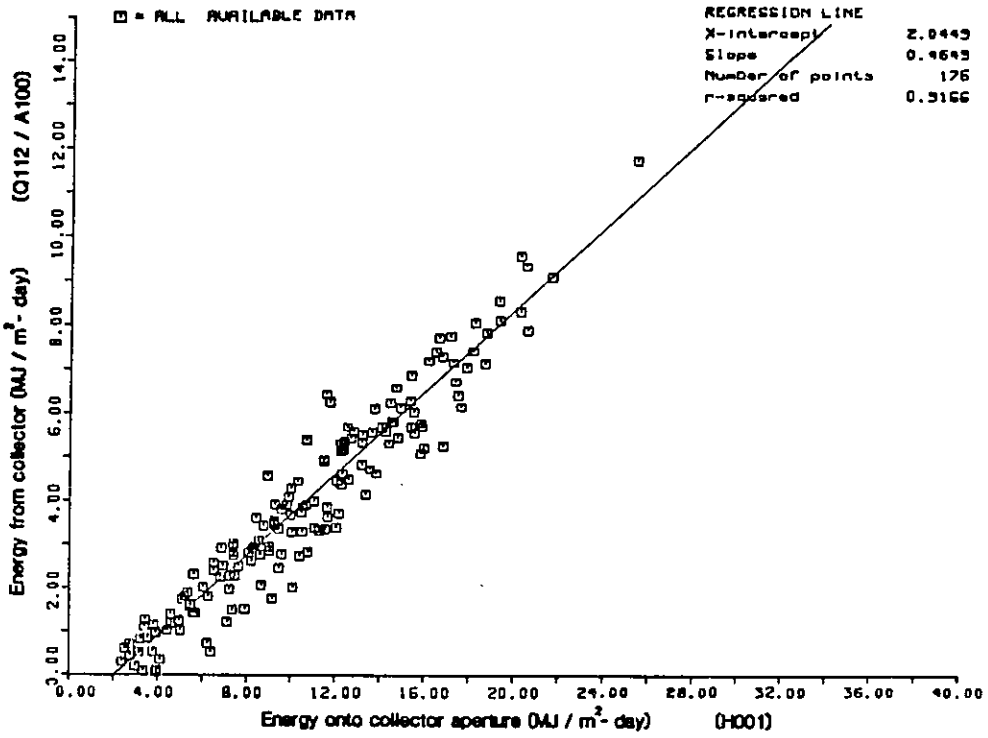

Figure 6.2-90. Daily Energy Input/Output, Philips VTR141, BSRIA Solar Test Facility with Simulated Loads, Bracknell, United Kingdom, All Available Data.

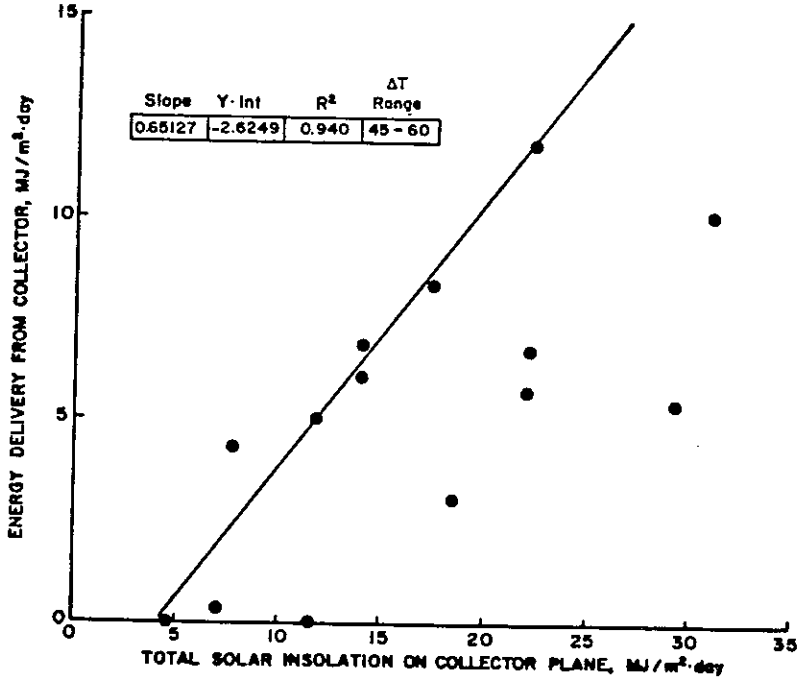

Figure 6.2-91. Daily Energy Input/Output from Philips VTR-361 Collectors, ΔT Range 45-60°C, Colorado State University, United States, December 1982 to September 1983.

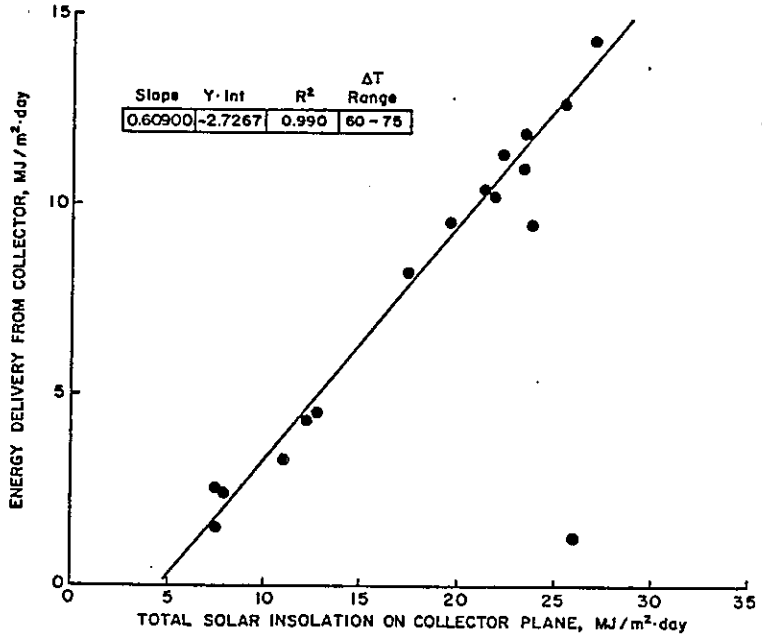

Figure 6.2-92. Daily Energy Input/Output from Philips VTR-361 Collectors, ΔT Range 60-75°C, Colorado State University, United States, December 1982 to September 1983.

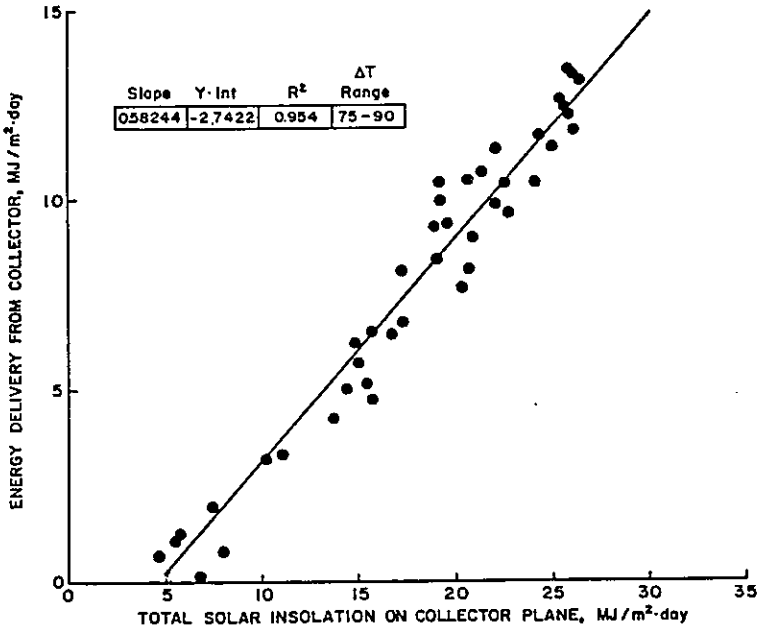

Figure 6.2-93. Daily Energy Input/Output from Philips VTR-361 Collectors, ΔT Range 75-90°C, Colorado State University, United States, December 1982 to September 1983.

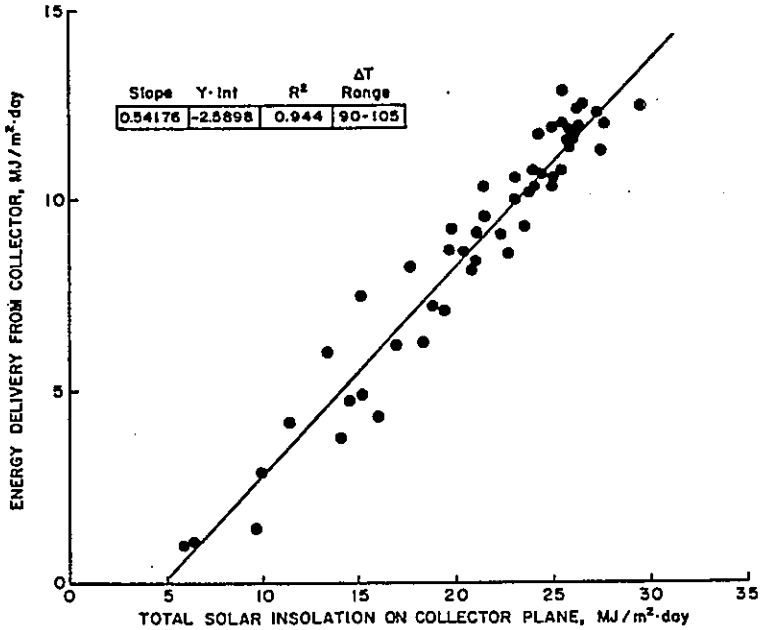

Figure 6.2-94. Daily Energy Input/Output from Philips VTR-361 Collectors, ΔT Range 90-105°C, Colorado State University, United States, December 1982 to September 1983.

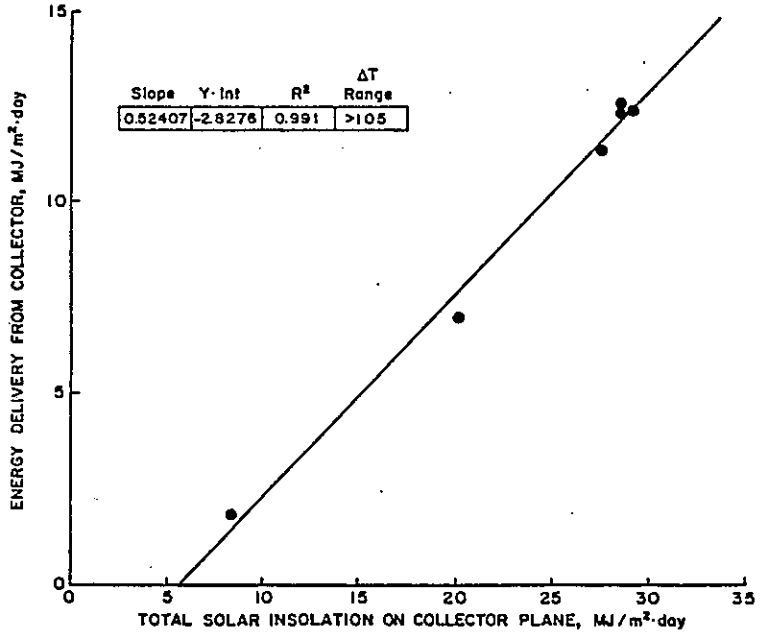

Figure 6.2-95. Daily Energy Input/Output from Philips VTR-361 Collectors, ΔT Range > 105°C, Colorado State University, United States, December 1982 to September 1983.

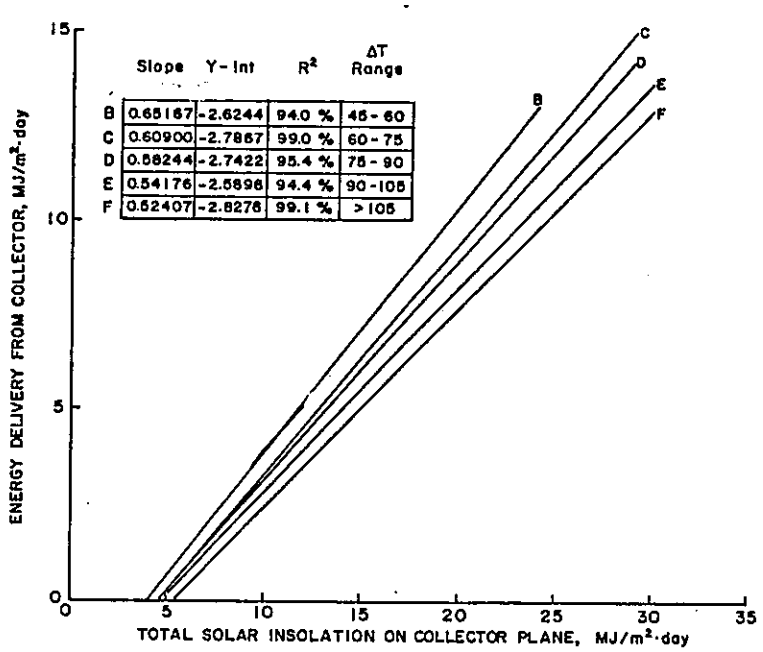

Figure 6.2-96. Composite Daily Energy Input/Output from Philips VTR-361 Collectors, Colorado State University, United States, December 1982 to September 1983.

6.3 ENERGY FLOW DIAGRAM

The qualitative interaction of energy flows between different subsystems and their quantitative values are displayed in one diagram, called an energy flow, or arrow, diagram. Each diagram starts with the total energy incident on the collector aperture during the appropriate period, including the time when the collector is non-operational, and displays graphically, as well as numerically, how different portions of the energy are used or lost.

Normally one energy flow diagram is included for each experiment. If appropriate, however, several experimental periods are combined.

6.3.1 The Sydney University Solar Heating and Cooling System Sydney, Australia

Figure 6.3-1 shows a typical situation of energy flows during cooling. While approximately 40 percent of the incident solar energy is supplied to the hot water tank, only approximately 15 percent of the available energy is converted into cooling and supplied to the load. The relatively inefficient use of heat in absorption cooling machines is clearly demonstrated.

An energy flow diagram during typical winter operation is given in Figure 6.3-2. More than 30 percent of the incident solar energy ends up as useful energy for heating purposes. Yazaki flat-plate collectors were used in this period and at relatively low operating temperatures their conversion efficiency from solar to thermal exceeded 46 percent.

The third arrow diagram, Figure 6.3-3, is for a period of low load during which the Sydney University evacuated tubular collectors frequently operated near boiling point. Energy dumping at night was introduced to lower system temperatures. The graph however highlights a system problem; extremely high pipe losses in the collection system are encountered (more than 30 percent of the collected energy). Higher pipe losses are expected at operating temperatures approaching 100^{o}C, but they are made worse by deterioration of the collector loop pipe insulation.

Figure 6.3-4 shows the energy flow diagram for the period December 1983 to April 1984, which in essence is the cooling season in Australia. The diagram draws attention to the rather poor energy conversion efficiency of the absorption chiller which is manifest in a poor overall system efficiency.

As seen in Figure 6.3-5, the situation improves significantly during winter since solar heated water is directly pumped through the air handling units in the offices. There are no intermediate heat exchangers required and thus a significant portion of the collected solar energy ends up as useful energy to cover the heating load.

One month's cooling performance for January 1985 is summarized in Figure 6.3-6. The graph reflects the same trends as indicated for Figure 6.3-4.

6.3.2 Mountain Spring Bottle Washing Facility, Edmonton, Canada

Energy flow diagrams for the periods 1 May 1982 to 31 December 1982 and 1 January 1983 to 31 December 1983 are presented in Figures 6.3-7 and 6.3-8 respectively. In both diagrams it can be seen that significant energy losses occur from the piping and storage tank. These losses amount to 22.5 percent and 16.7 percent for 1982 and 1983 respectively. The 1983 losses are less due to the new heat exchanger and controls governing the transfer of energy (Q202) from the solar system and the caustic loop.

6.3.3 Ispra Solar Heated and Cooled Laboratory, Commission of European Communities

The Energy Flow diagram for the system of the Ispra Solar Laboratory is given in Figures 6.3-9. The data are from the period May to September, 1983. It should be mentioned that the storage plus heat transport losses indicated in the diagram also include the heat dumped via the air heat exchanger, for cases where temperatures in the hot storage system were too high. The amount of heat dumped in this way is on the order of 2000 MJ. The monthly energy flows for each collector array are given in Table 6.3-1.

6.3.4 Solarhaus Freiburg, Federal Republic of Germany

For both system types, energy flow diagrams are produced for two representative periods:

- the calendar year 1982 with combined operation of the Corning and Philips/Stiebel-Eltron collectors with the DHW system, and operation of the Philips IV and Corning Collectors with the heating system. See Figures 6.3-10 and 6.3-11.
- the period from June 1982 to May 1983 with operation of the Philips/Stiebel-Eltron with the DHW system and the Corning collector with the heating system. See Figures 6.3-12 and 6.3-13.

Since the solar and conventional systems are basically identical with the systems in previous reports, the associated energy flows remain unchanged as well.

However, in 1982 a solar contribution of the DHW system of 66.6 percent was measured. This is a record for a project that has been operating since the beginning of 1979. This solar fraction corresponds

TABLE 6.3-1. MONTHLY ENERGY FLOWS OF THE COLLECTOR SUBSYSTEM ISPRA SOLAR LABORATORY

		JUNE		JULY		AUGUST		SEPTEMBER		SUMMER	
		MJ	%	MJ	%	MJ	%	MJ	%	MJ	%
Sanyo I	Collected	2652	30	3243	32	2351	29	801	27	9163	30
	On Losses	4375	50	5646	55	3953	48	1287	43	15592	50
	Off Losses	1695	20	1357	13	1870	23	891	30	6199	20
Sanyo II	Collected	3320	38	4160	41	2955	36	977	33	11672	38
	On Losses	3618	42	4729	46	3349	41	1111	37	13082	42
	Off Losses	1695	20	1357	13	1870	23	89	30	6199	20
Philips VTR 261	Collected	3142	48	3867	49	3093	50	1099	48	11523	49
	On Losses	3875	43	3526	45	2427	38	746	33	9823	41
	Off Losses	582	9	440	6	729	12	432	19	2318	10
Philips VTR 361	Collected	1943	48	2440	51	1913	50	687	49	7173	49
	On Losses	1749	43	2095	43	1473	38	445	32	5923	41
	Off Losses	357	9	270	6	447	12	265	19	1422	10
Total of 4 Arrays	Collected	10967	39	13710	42	10312	39	3564	37	39530	40
	On Losses	12617	45	15996	48	11202	42	3589	37	44422	44
	Off Losses	4330	16	3424	10	4915	19	2479	26	16138	16

to 499 kWh per year of useful delivered solar energy per square meter of collector area. This solar contribution was realized together with a solar collection system efficiency of 41.4 percent. The main reason for this improvement was the combined operation of the two high performance ETC collectors of Corning Glass and Philips/Stiebel-Eltron during a period with both a rather even DHW load together with a continuous availability of solar radiation.

The combined energy flow diagrams for the heating and DHW systems are shown in Figures 6.3-12 and 6.3-13. As a result of the relatively small collector area of the solar heating system (less than 5 percent of the heated floor area), the solar heating fraction remains at about 11 percent and 11.6 percent, about the same as in the previous years.

Although the investigation of the independent operation of the solar DHW system remains the primary objective of the Solarhaus Freiburg project, this diagram suggests the definition of a global solar fraction of the total DHW and heating load. As compared to the previous values, 22 and 24 percent in 1980 and 1981, this global solar fraction reached a maximum value of 27.6 percent in 1982, together with a solar system efficiency of 31.7 percent, corresponding to a specific amount of useful solar energy of 380 kWh/m^2 per year, based on the collector aperture area.

6.3.5 Eindhoven Technological University Solar House, The Netherlands

Because of the integration of the storage and the auxiliary natural gas burner it is virtually impossible to discern the solar and the auxiliary energy flows to hot water and space heating from measured data. A deduction of these energy flows will be given when the energy balance in the storage is better assessed.

6.3.6 Knivsta District Heating System, Knivsta, Sweden

The total energy flows for the systems are shown in the energy flow arrow diagrams, Figures 6.3-14 through 6.3-20. The diagrams are divided into several periods, October 1981 to September 1982, June 1982 to May 1983 and February to October 1983. The second period is chosen for easy comparison with the second installation, Södertörn. For the Scandinavian Solar collector, the first nine months of operation, February to October 1983, are shown. Notice especially the high piping losses and the large pumping energy added to the system. Indirectly the large piping losses also affect H101 and Q112 by prolonging the warming up period in the morning. The Philips collectors system is also presented for the same period for comparison. See Figure 6.3-20. The efficiencies for the General Electric and Philips collectors show no significant change between the periods.

6.3.7 The Södertörn District Heating Project Södertörn, Sweden

The total energy flows for the systems are shown in the energy flow diagrams of Figures 6.3-21 through 6.3-30. Notice the low collector off losses for the Philips VTR 141 collector. This is partly because, for this latitude and collector slope, the collectors are being significantly irradiated on the back side. Energy measurements have been started to investigate how much influence this can have on the performance. The measurements so far indicate that the back insolation can amount to 10 to 20 percent of the front aperture area insolation. Twenty percent during summer and 10 percent during winter time for the Philips VTR 141 array. The piping losses are small for all systems due to the short distances between the collectors and the district heating network.

6.3.8 SOLARCAD Project, Geneva, Switzerland

Arrow diagrams for two experiments are shown in Figures 6.3-31 and 6.3-36. The two diagrams involve only those days with good recorded data.

It is noticed that significant losses take place between the collector outlet and system (or heat exchanger) outlet. "Off" losses due to capacity effects play an important role. All losses are increased when working at higher temperatures.

The same remarks made for the efficiency plots also apply here.

6.3.9 SOLARIN Project, Hallau, Switzerland

The arrow diagram shown in Figure 6.3-37 involves only the collection subsystem and applies to the subject one year period. It can be seen that heat losses between the array and the rest of the system are reasonably low, but excess heat rejected amounts to roughly 10 percent of the delivered heat. This is due partly to poor control.

From other partial measurements we know that for the rest of the system, including the two storages, other losses should amount to roughly 50,000 MJ, which leads to a final system efficiency around 21 percent. Due to some improvements we expect this last figure to rise to 25 percent for the year 1985.

Also see sections 5.9.2, 6.1.9 and 6.2.9.

6.3.10 BSRIA Solar Test Facility with Simulated Loads, Bracknell, United Kingdom

An energy flow diagram is provided in Figure 6.3-38 in which the collector off losses were 16 percent, i.e., no collector pump operation. As a percentage of the total incident radiation, 37 percent was collected. The system supplied 33 percent of the space heating load and, because of the system operating control bias, only supplied 2.4 percent of the domestic hot water load during this heating season. Nevertheless, 36 percent of the incident solar energy was used for heating.

6.3.11 Colorado State University Solar House I, United States

An inventory of energy flows for the winter period, for the system shown in Figure 5-14, is shown in Figure 6.3-39. A sizable portion of the total energy collected is shown as heat rejection to the atmosphere, and is a consequence of a collector array over-sized for the load. There was also no domestic water heating for the period.

An energy flow diagram for the last few days of summer is shown in Figure 6.3-40. Difficulties with the hot-side phase-change storage unit during most of the summer prevented chiller operation.

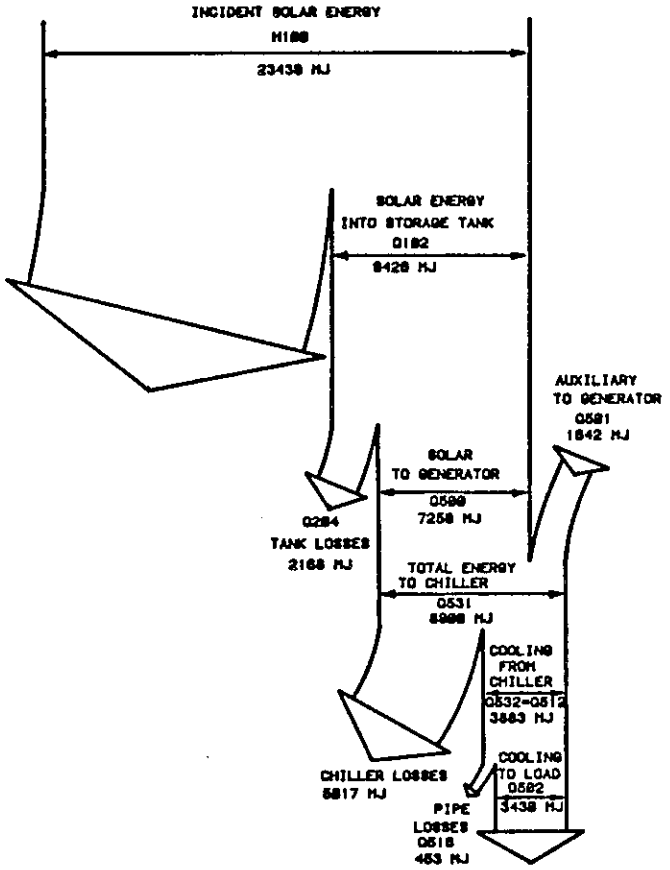

Figure 6.3-1. Energy Flow Diagram for S.U. Evacuated Tubular Collectors at Sydney, Australia, 25 December 1982 to 20 January 1983.

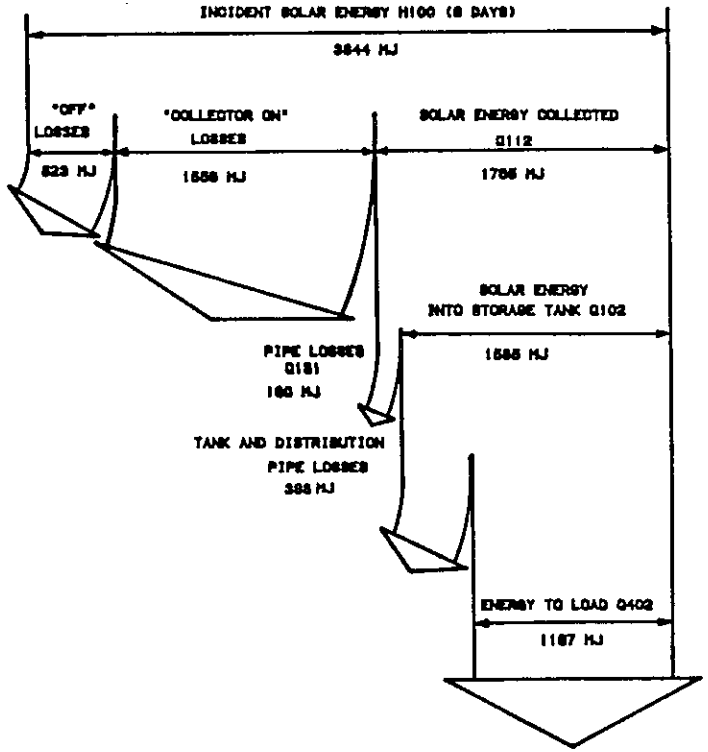

Figure 6.3-2. Energy Flow Diagram for Yazaki Flat-Plate Collectors at Sydney, Australia, 9 July to 26 July 1983.

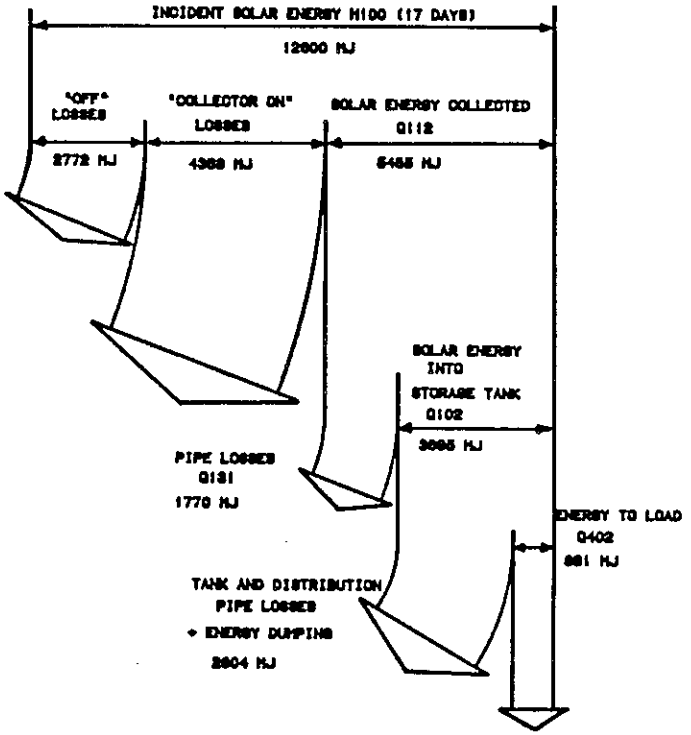

Figure 6.3-3. Energy Flow Diagram for S.U. Evacuated Tubular Collectors at Sydney, Australia, 28 August to 28 September 1983.

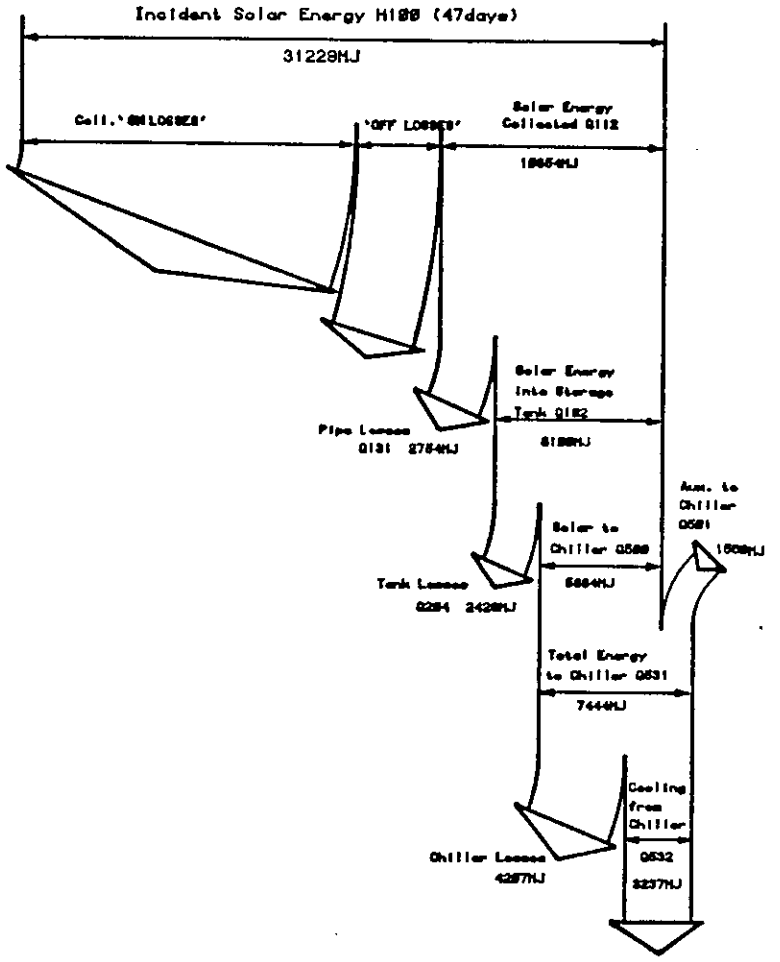

Figure 6.3-4. Energy Flow Diagram for S.U. Evacuated Tubular Collectors at Sydney, Australia, 1 December 1983 to 30 April 1984.

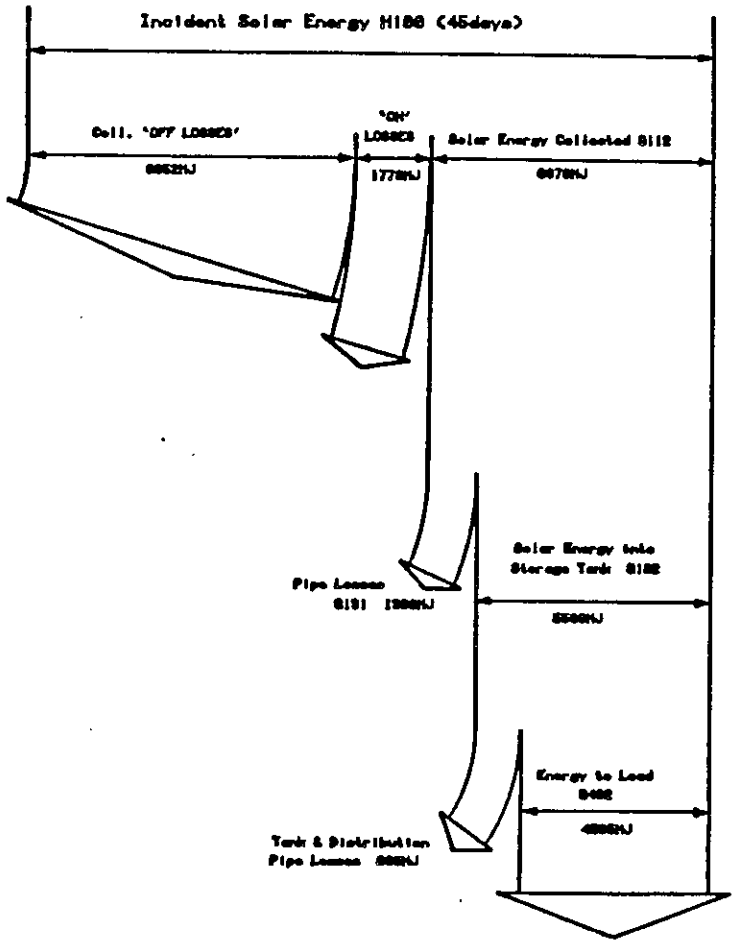

Figure 6.3-5. Energy Flow Diagram for S.U. Evacuated Tubular Collectors at Sydney, Australia, 1 June 1984 to 31 July 1984.

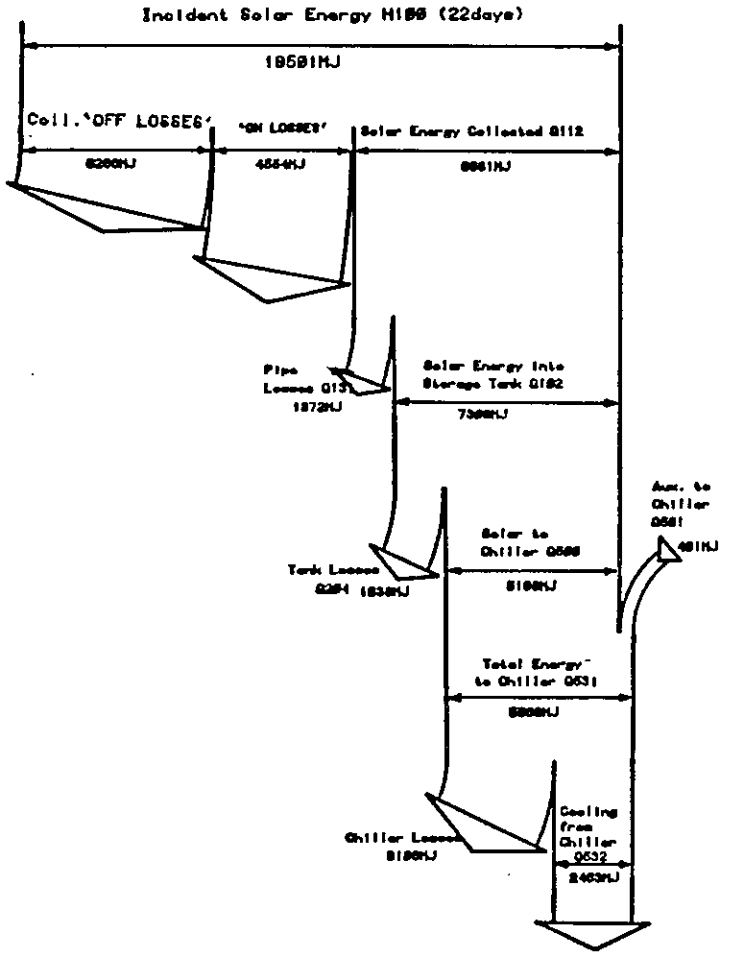

Figure 6.3-6. Energy Flow Diagram for S.U. Evacuated Tubular Collectors at Sydney, Australia, 1 January 1985 to 31 January 1985.

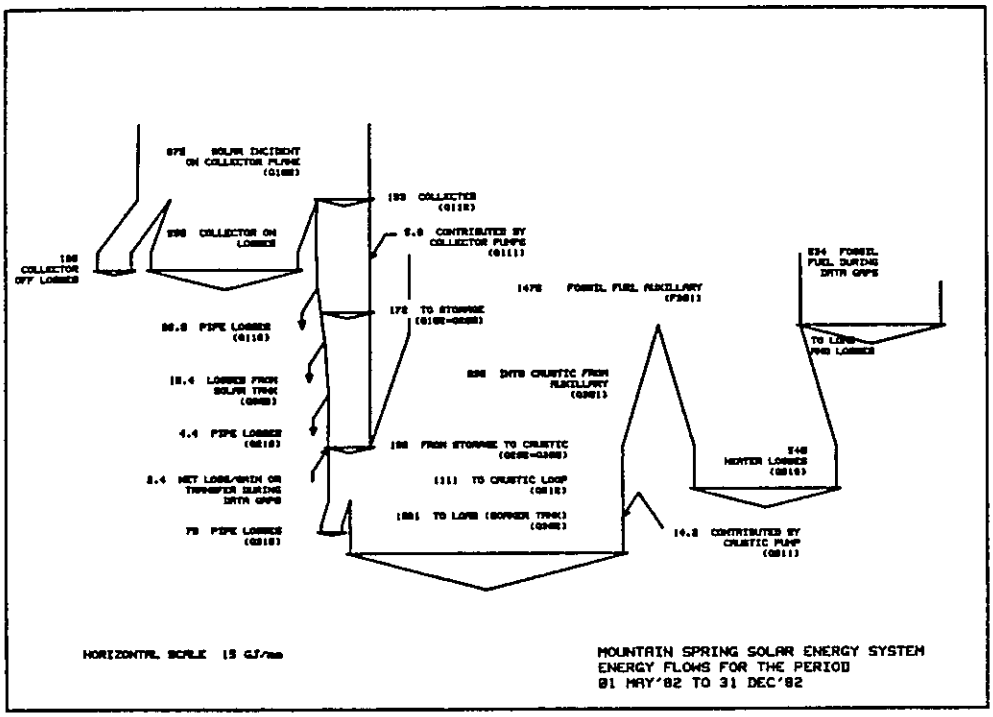

Figure 6.3-7. Energy Flows for Solartech ETC's at the Mountain Spring Bottle Washing Facility, Canada, 1 May 1982 to 31 December 1982.

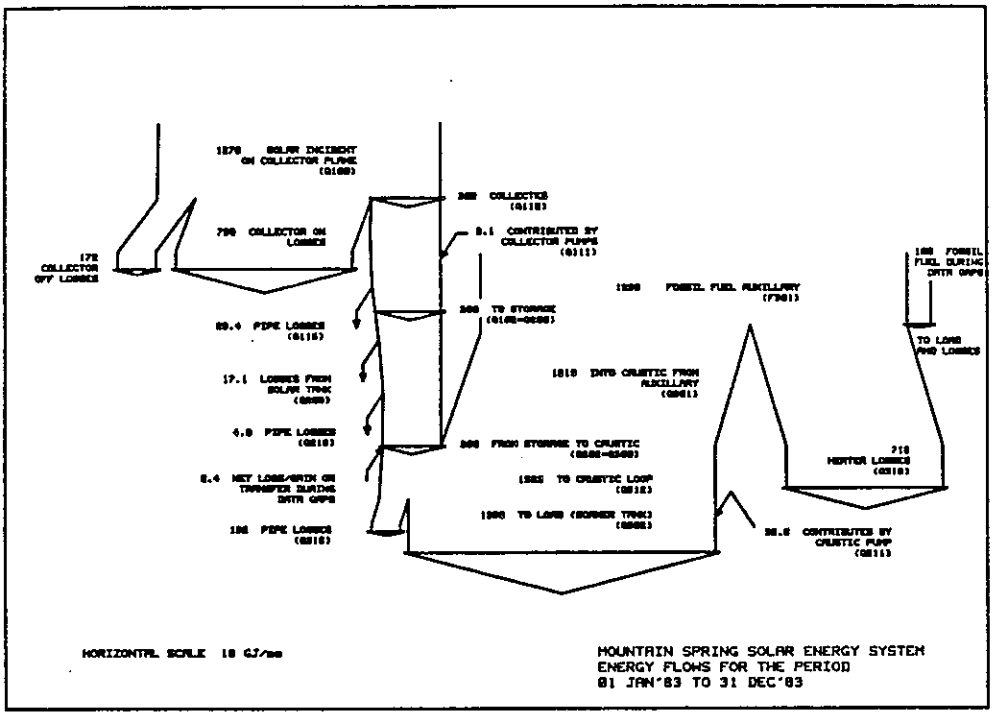

Figure 6.3-8. Energy Flows for Solartech ETC's at the Mountain Spring Bottle Washing Facility, Canada, 1 January 1983 to 31 December 1983.

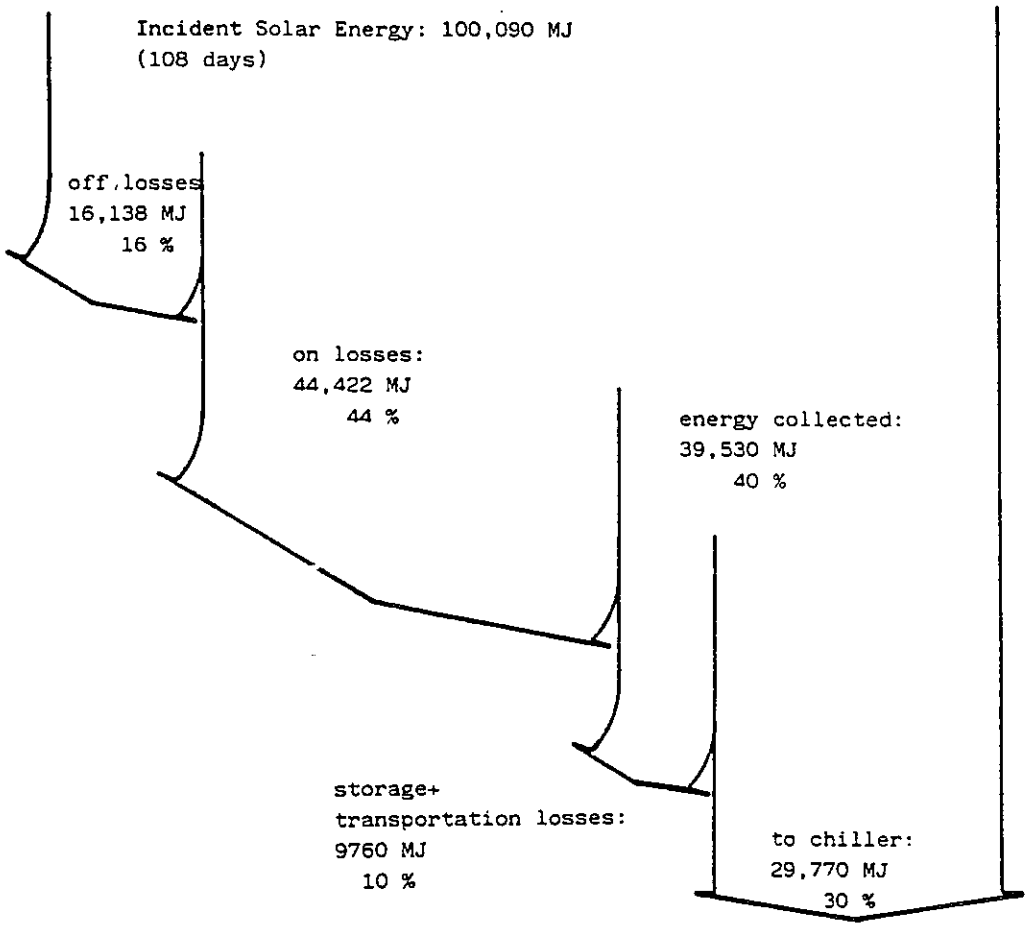

Figure 6.3-9. Energy Flow Diagram at the Ispra Solar Laboratory.

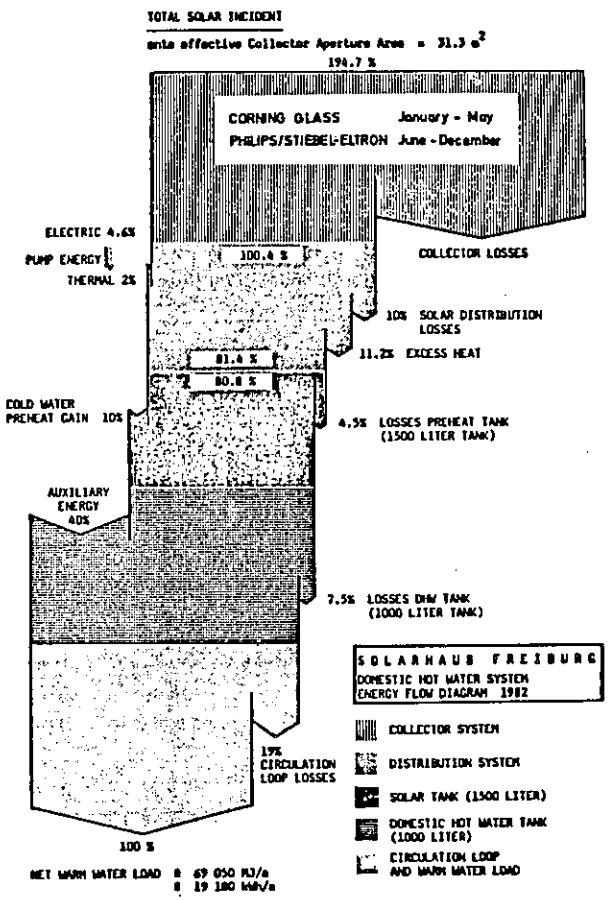

Figure 6.3-10. Energy Flow Diagram of the Domestic Hot Water System at Solarhaus Freiburg, Federal Republic of Germany, (with subsequent operation of the Corning Glass and Philips/Stiebel-Eltron Collectors), 1982.

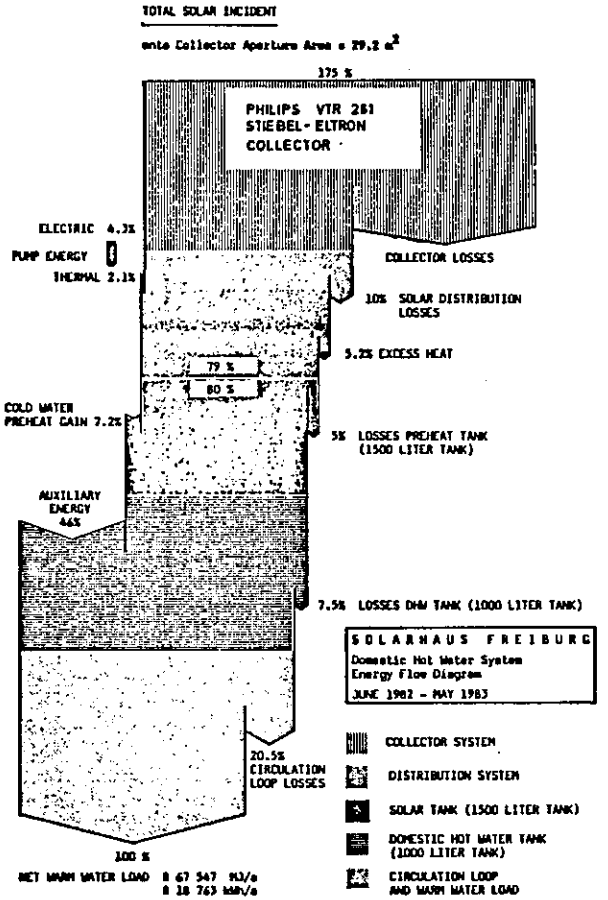

Figure 6.3-11. Energy Flow Diagram of the Domestic Hot Water System at Solarhaus Freiburg, Federal Republic of Germany, June 1982 May 1983.

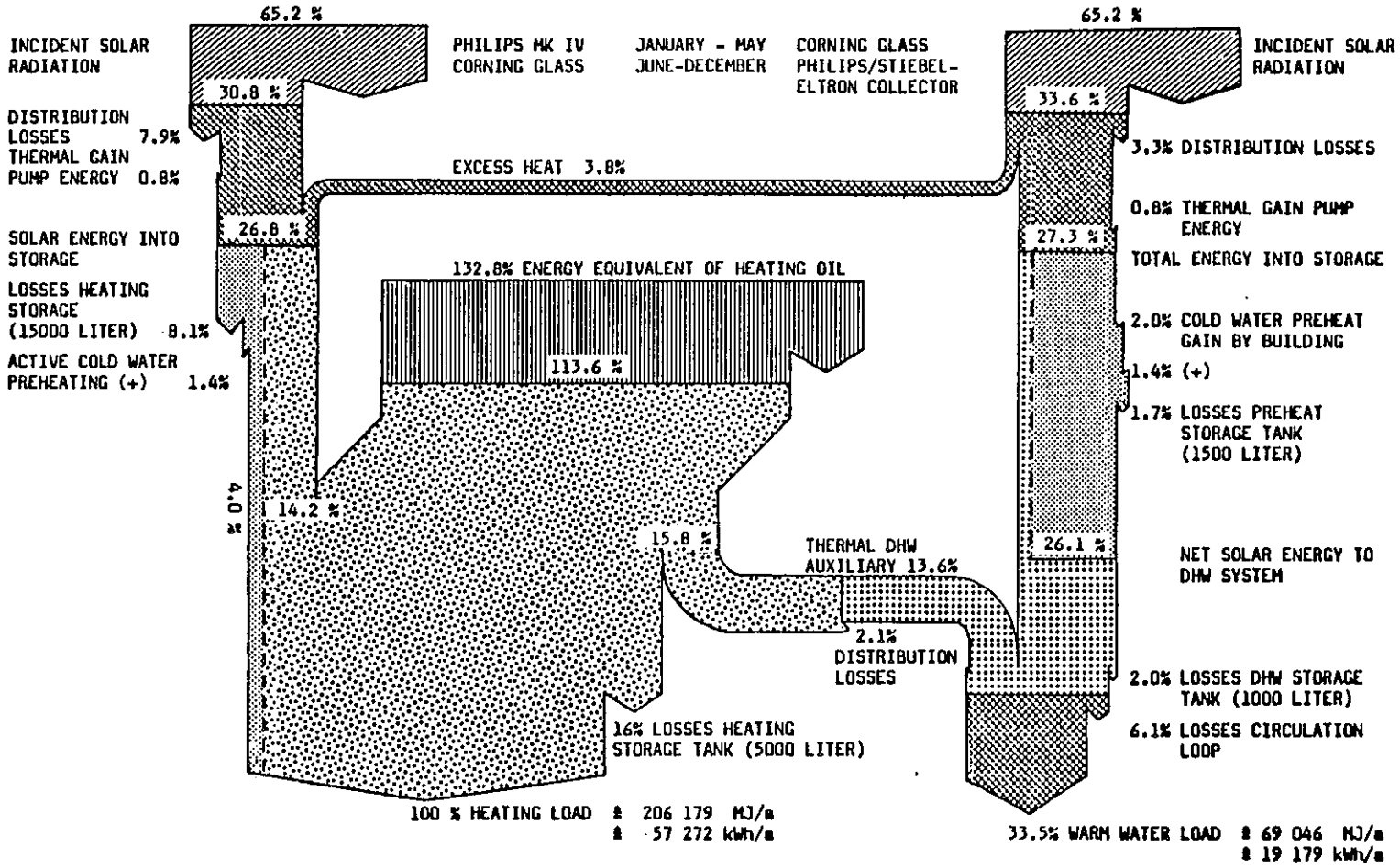

Figure 6.3-12. Energy Flow Diagram of the Domestic Hot Water System and Heating Systems at Solarhaus Freiburg, Federal Republic of Germany (with operation of the Corning Glass and Philips/Stiebel-Eltron Collectors), 1982.

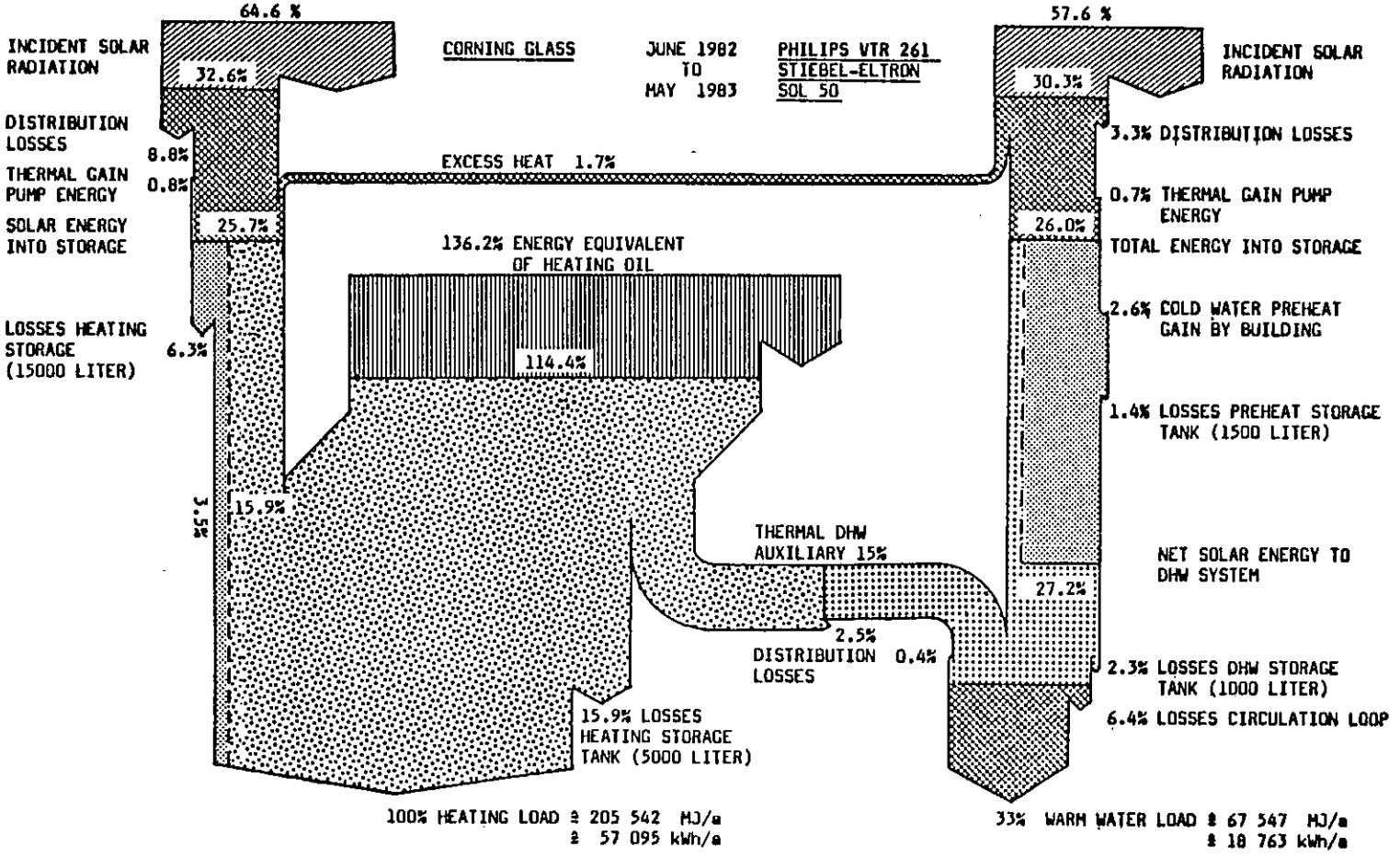

Figure 6.3-13. Energy Flow Diagram of the Domestic Hot Water System and Heating Systems at Solarhaus Freiburg, Federal Republic of Germany, June 1982 to May 1983.

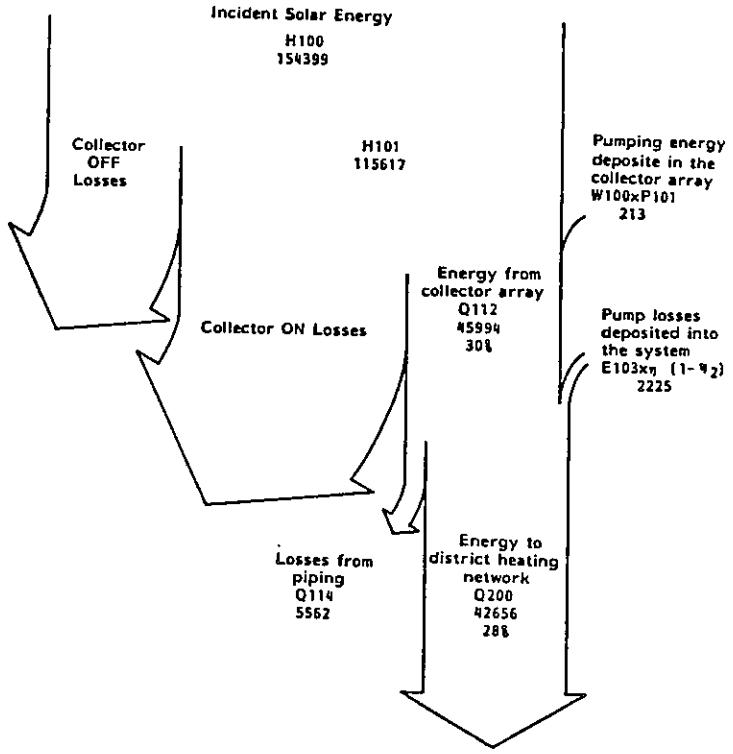

Figure 6.3-14. Energy Flow Diagram for General Electric TC100 Collector Knivsta, Sweden, October 1981 to September 1982.

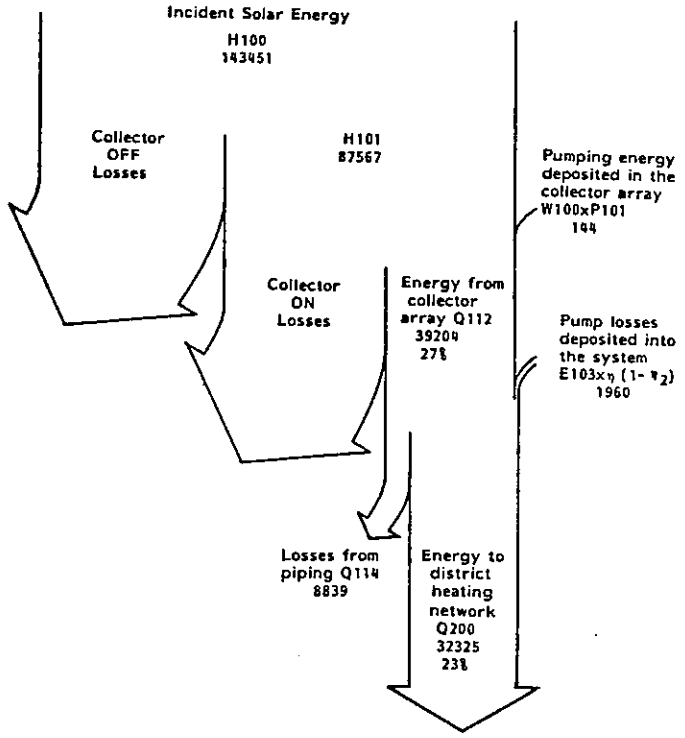

Figure 6.3-15. Energy Flow Diagram for Owens Illinois Electric Collector, Knivsta, Sweden, October 1981 to September 1982.

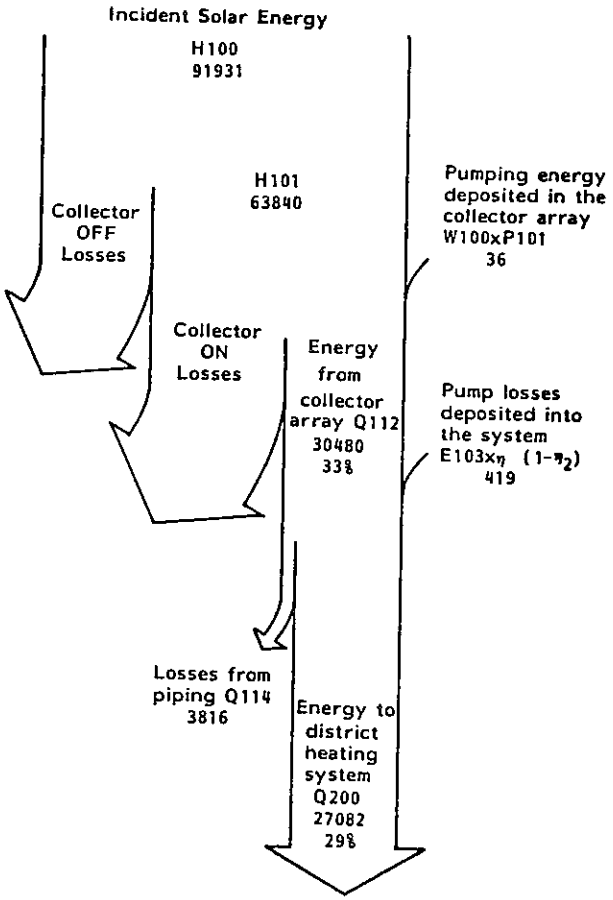

Figure 6.3-16. Energy Flow Diagram for Philips VTR 141 Collector, Knivsta, Sweden, October 1981 to Septembar 1987.

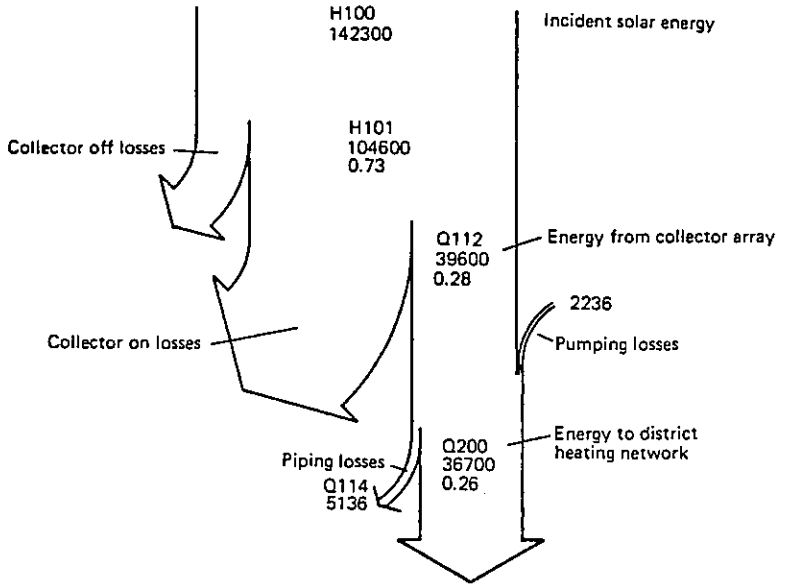

Figure 6.3-17. Energy Flow Diagram for General Electric TC100, Knivsta, Sweden, June to September 1982.

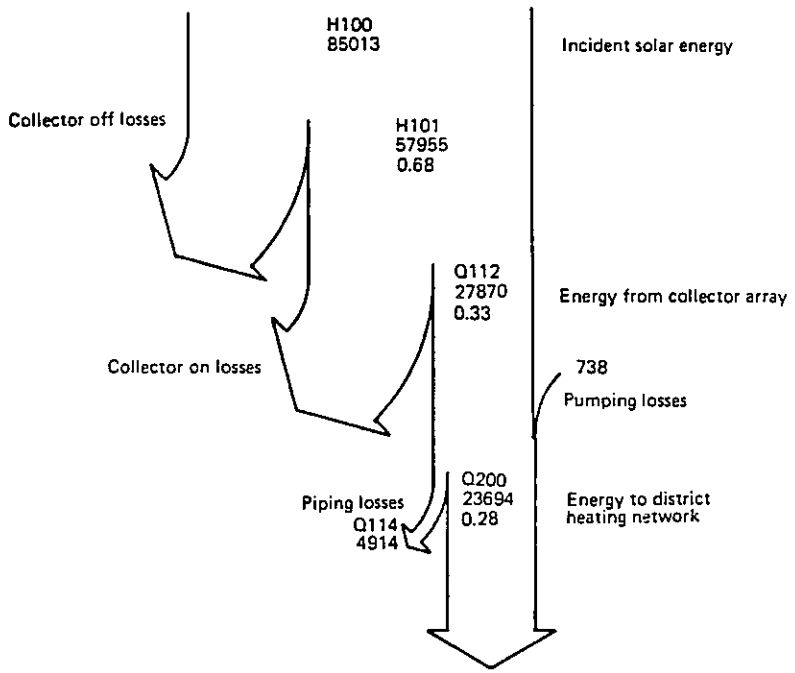

Figure 6.3-18. Energy Flow Diagram for Philips VTR 141 Collector, Knivsta, Sweden, June 1982 to May 1983.

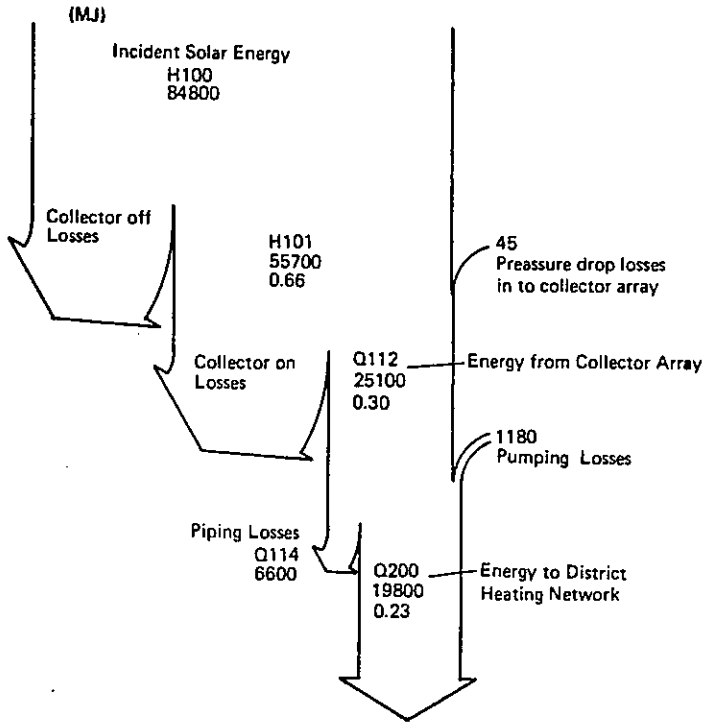

Figure 6.3-19. Energy Flow Diagram for Scandinavian Solar HT Collector, Knivsta, Sweden, February to October 1983.

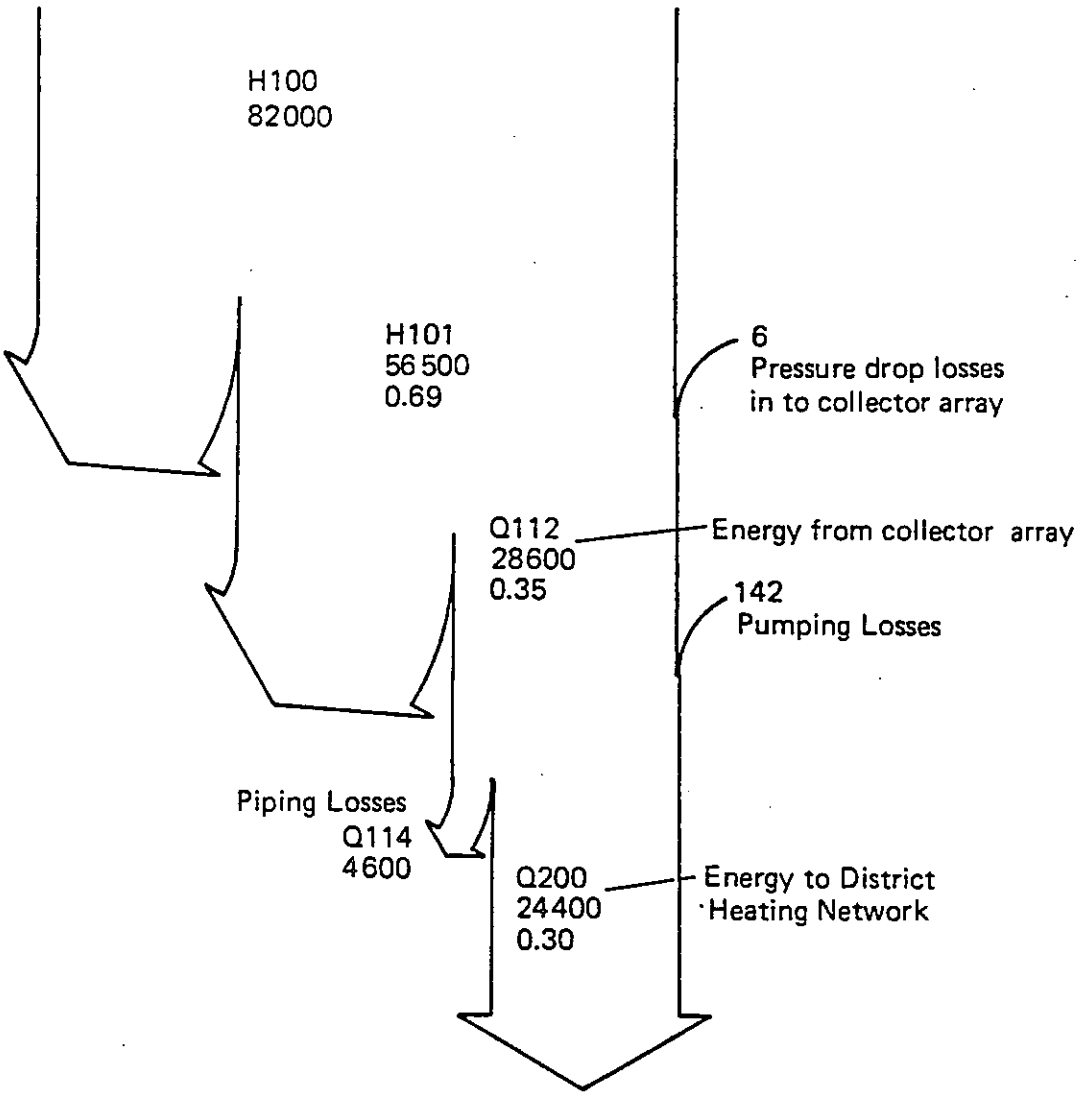

Figure 6.3-20. Energy Flow Diagram for Philips VTR 141 Collector, Knivsta, Sweden, February to October 1983.

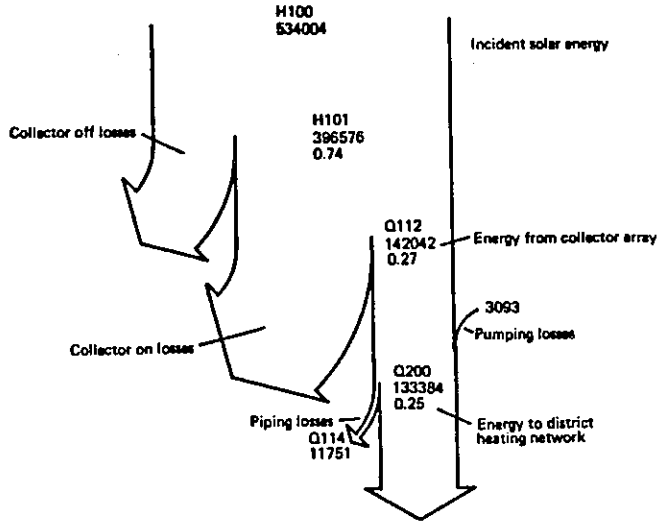

Figure 6.3-21. Energy Flow Diagram for Teknoterm Collector, Södertörn, Sweden, 60°C Operation, June 1982 to May 1983.

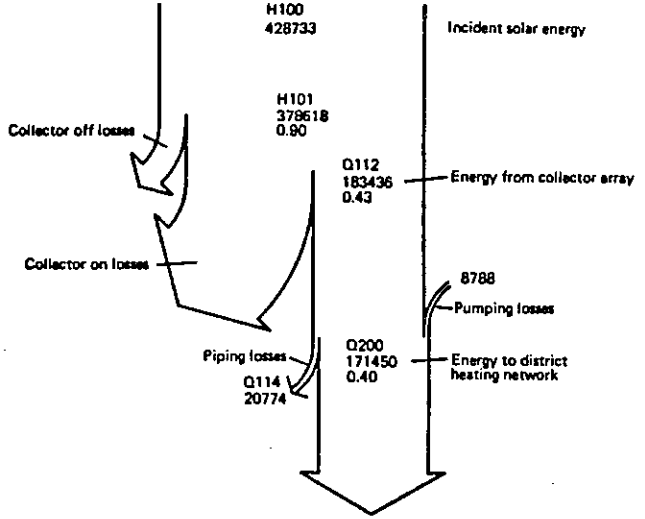

Figure 6.3-22. Energy Flow Diagram for Philips VTR 141 Collector, Södertörn, Sweden, 60°C Operation, June 1982 to May 1983.

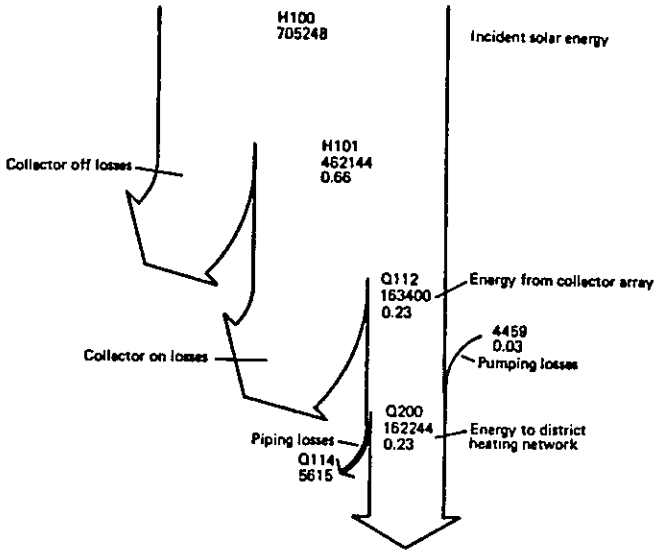

Figure 6.3-23. Energy Flow Diagram for Granges Aluminum Collector, Södertörn, Sweden, 60°C Operation, June 1982 to May 1983.

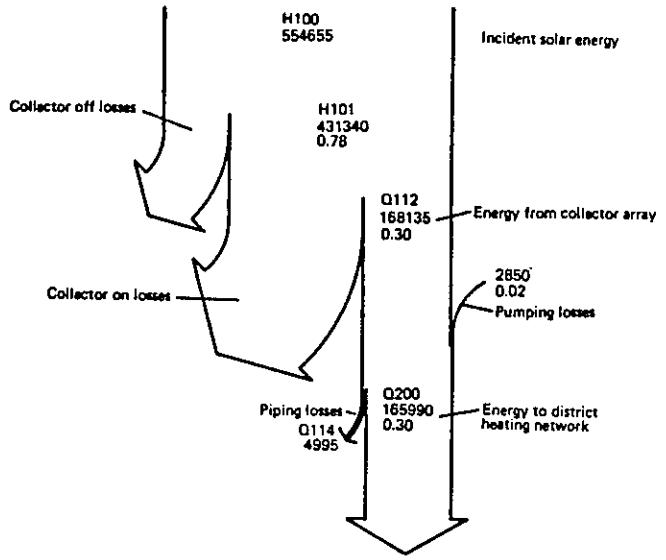

Figure 6.3-24. Energy Flow Diagram for General Electric TC100 Collector, Södertörn, Sweden, 60°C Operation, June 1982 to May 1983.

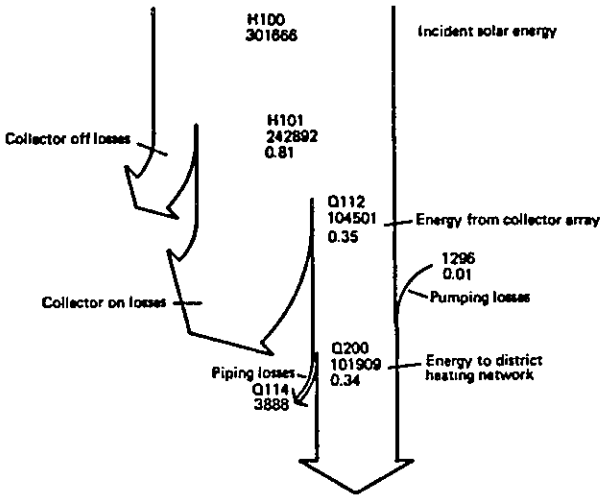

Figure 6.3-25. Energy Flow Diagram for Scandinavian Solar HT Collector, Södertörn, Sweden, 60°C Operation, June 1983.

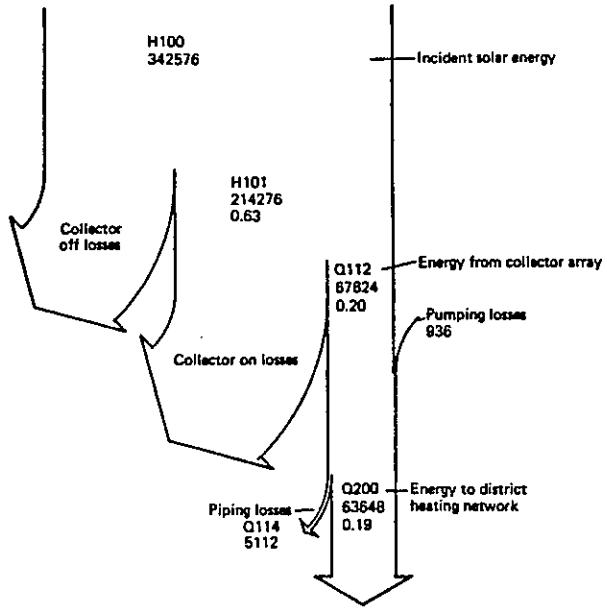

Figure 6.3-26. Energy Flow Diagram for Teknoterm Collector, Södertörn, Sweden, 80°C Operation, June to October, 1983.

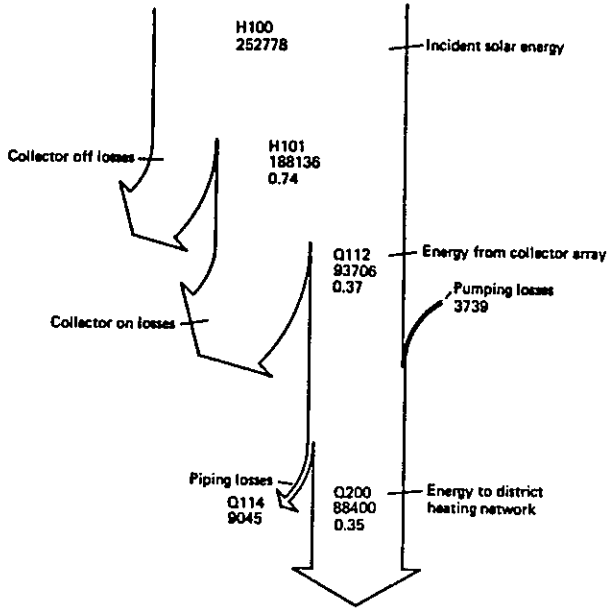

Figure 6.3-27. Energy Flow Diagram for Philips VTR 141 Collector, Södertörn, Sweden, 80°C Operation, June to October, 1983.

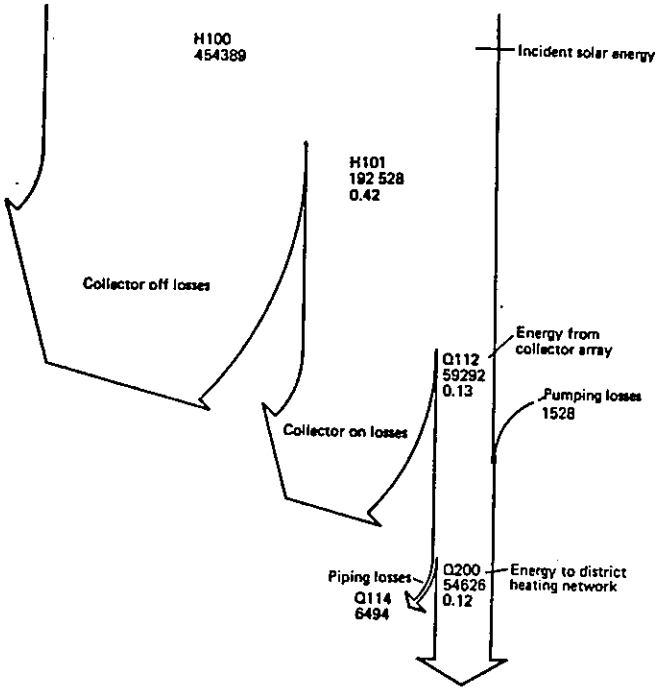

Figure 6.3-28. Energy Flow Diagram for Granges Aluminum Sunstrip 80, Södertörn, Sweden, 80°C Operation, June to October, 1983.

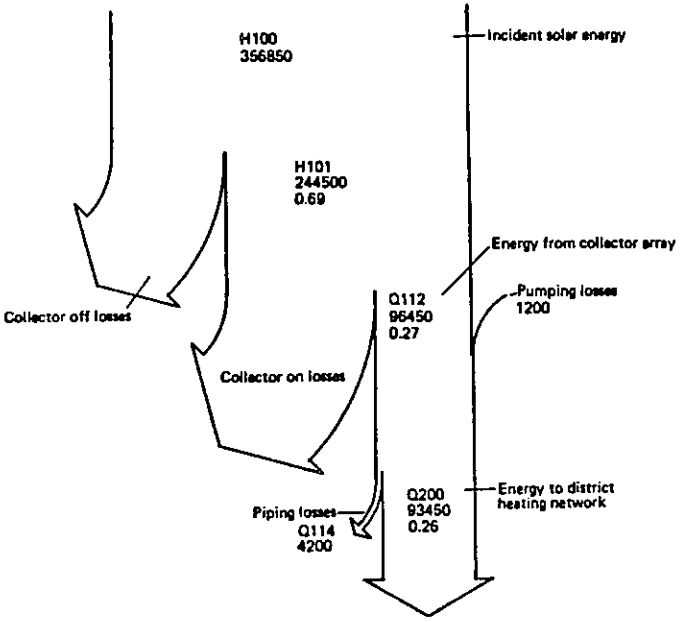

Figure 6.3-29. Energy Flow Diagram for General Electric TC100 Collector, Södertörn, Sweden 80°C Operation, June to October, 1983.

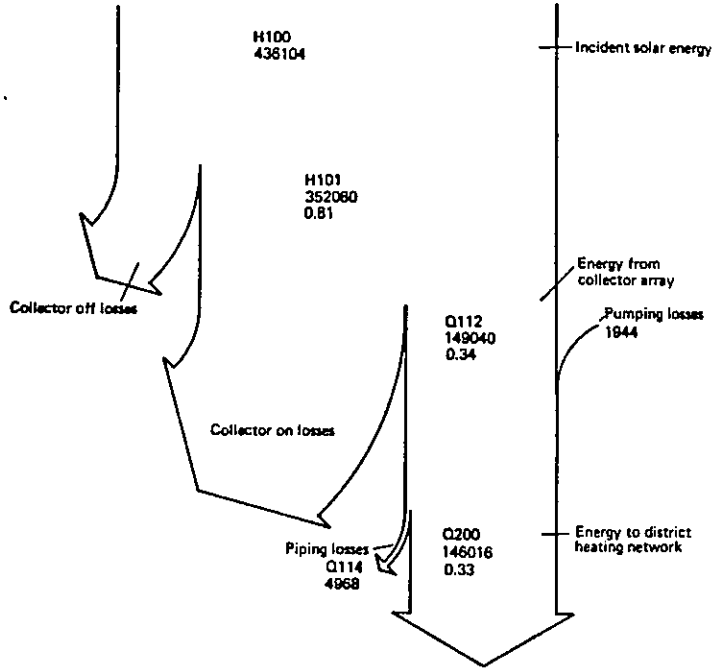

Figure 6.3-30. Energy Flow Diagram for Scandinavian Solar HT Collector, Södertörn, Sweden, 80°C Operation, June to October, 1983.

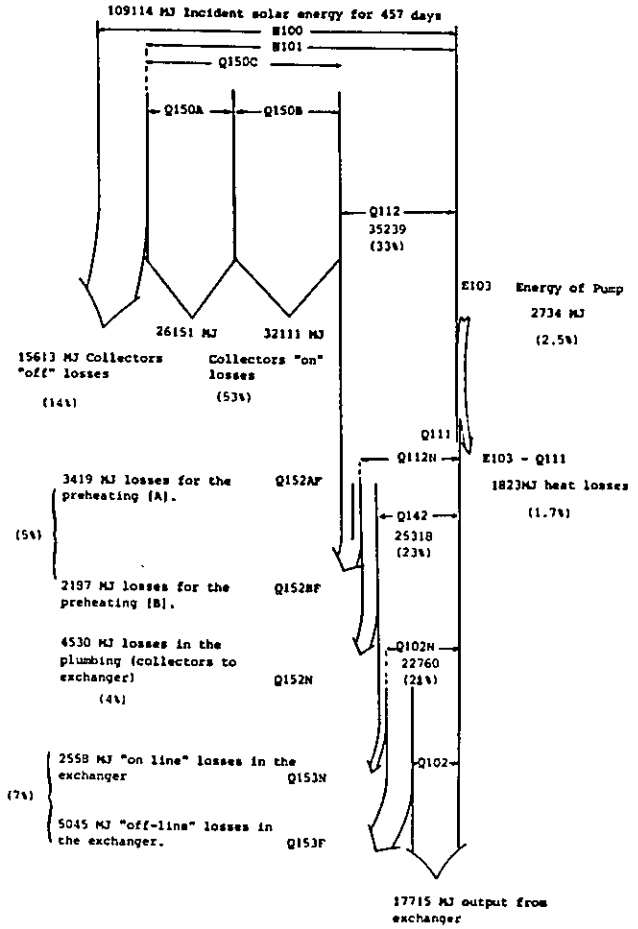

Figure 6.3-31. Energy Flow Arrow Diagram for Corning A+B, Geneva, Switzerland, July 1982 to September 1983.

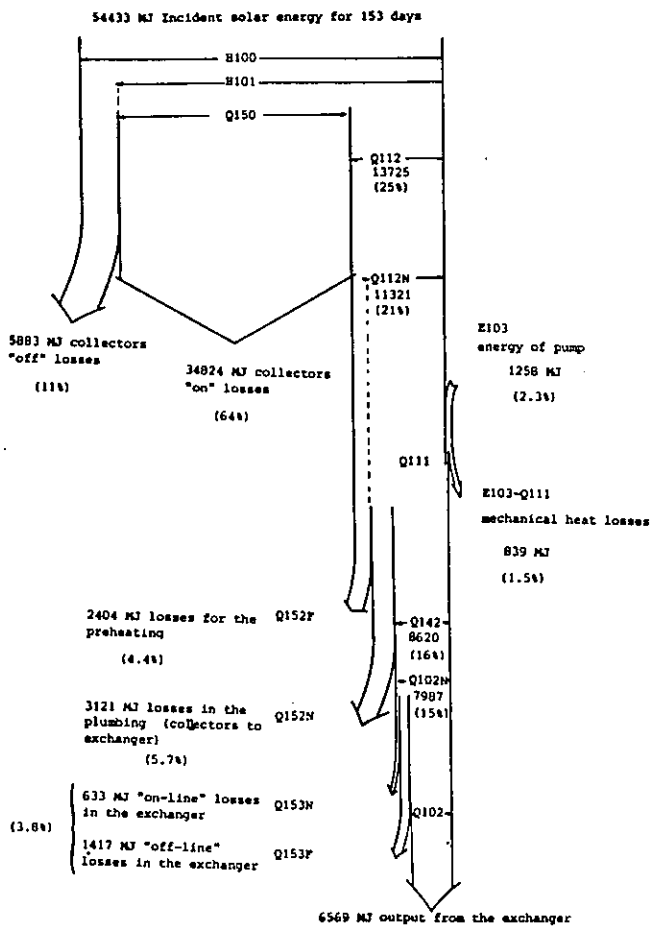

Figure 6.3-32. Energy Flow Arrow Diagram for Sanyo SCT-CU250, Geneva, Switzerland, April to August 1983.

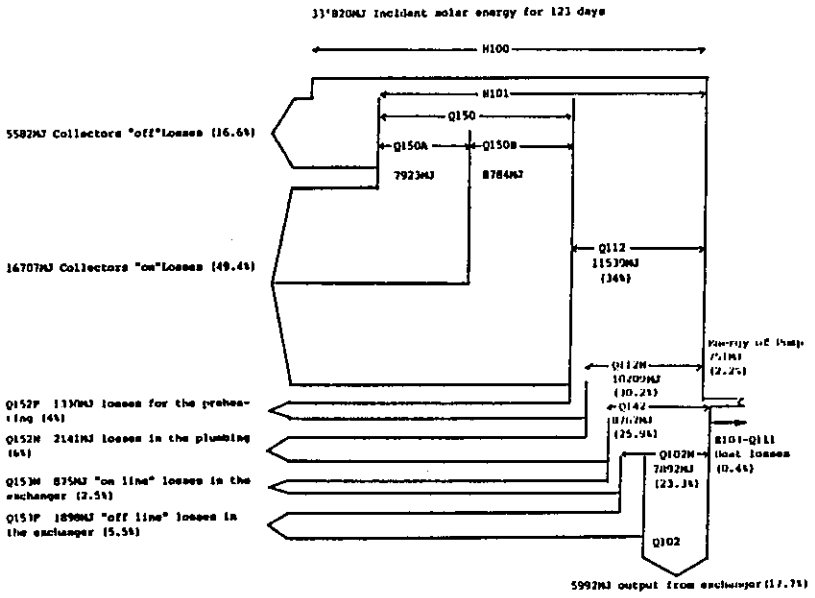

Figure 6.3-33. Energy Flow Arrow Diagram for Corning A+B, Geneva, Switzerland, July 1982 to October 1982.

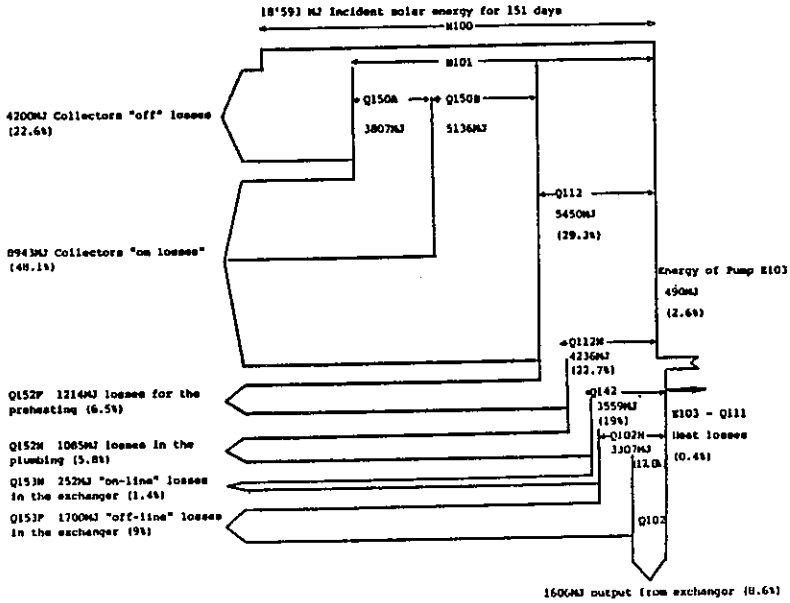

Figure 6.3-34. Energy Flow Arrow Diagram for Corning A+B, Geneva, Switzerland, November 1982 to March 1983.

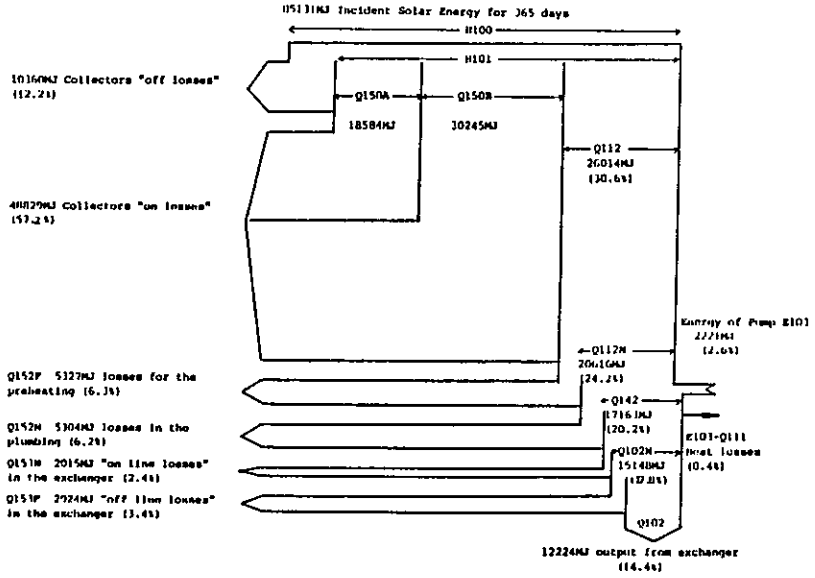

Figure 6.3-35. Energy Flow Arrow Diagram for Corning A+B, Geneva, Switzerland, April 1983 to March 1984.

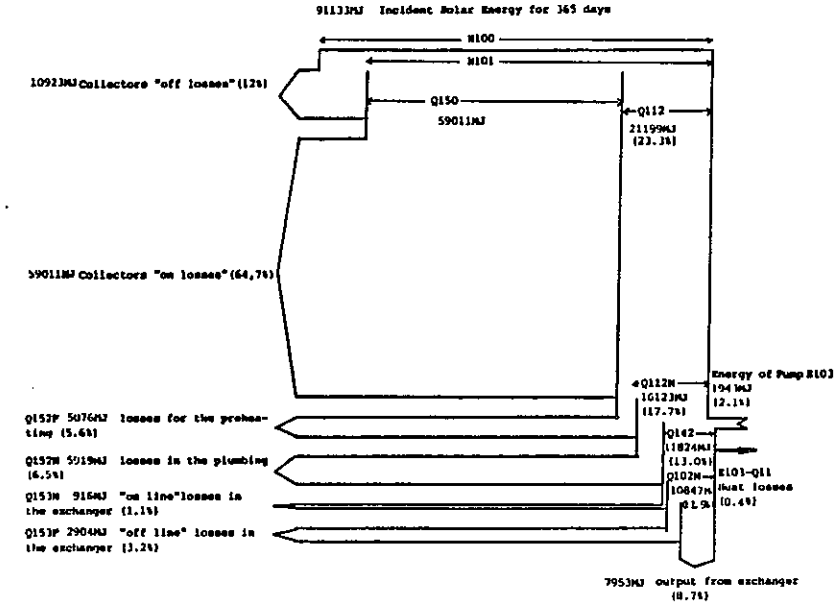

Figure 6.3-36. Energy Flow Arrow Diagram for Sanyo SCT-CU250, Geneva, Switzerland, April 1983 to March 1984.

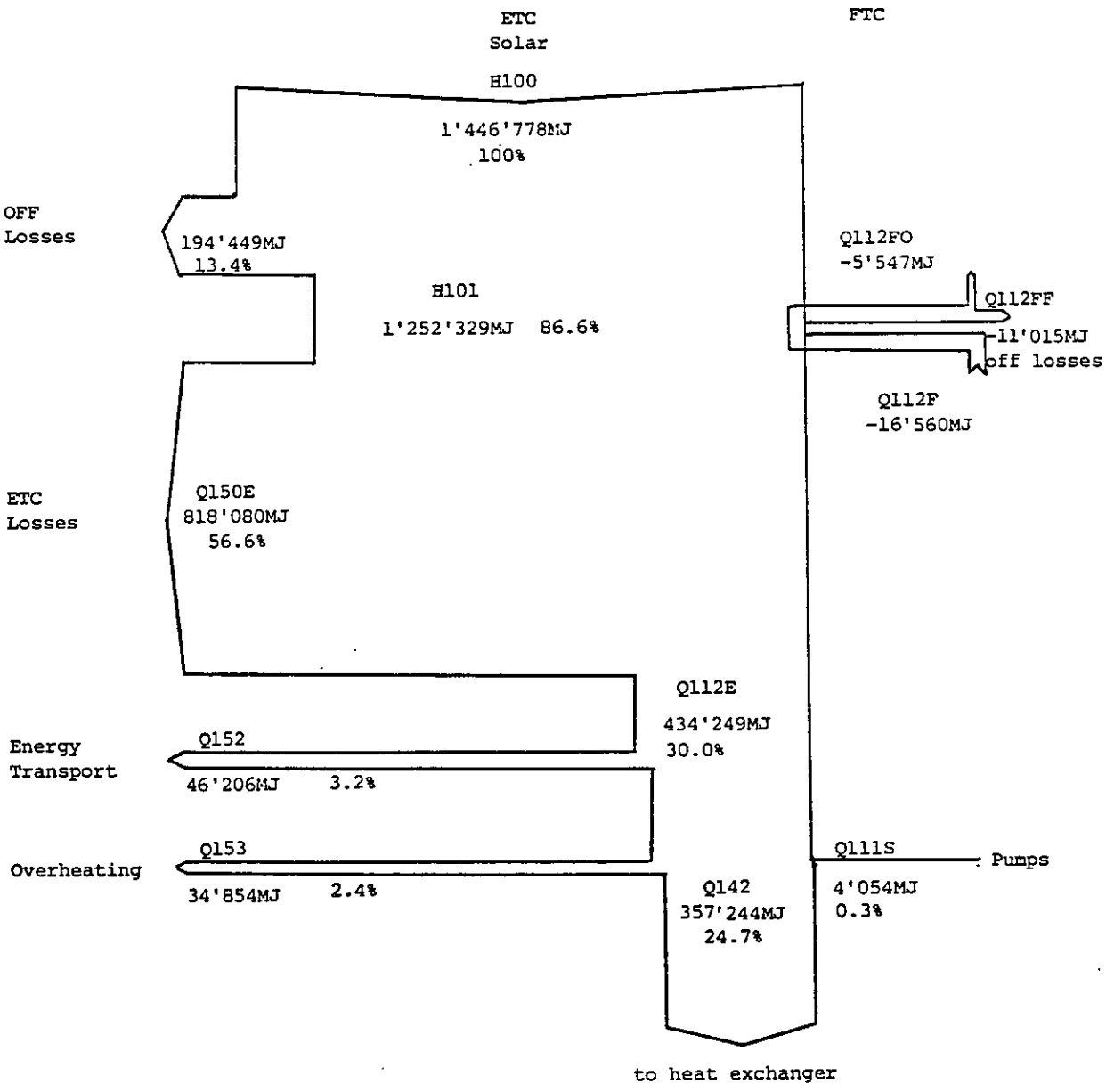

Figure 6.3-37. Energy Flow Arrow Diagram for Corning "D", Solarin, Hallau, Switzerland, 6 March 1984 to 28 February 1985.

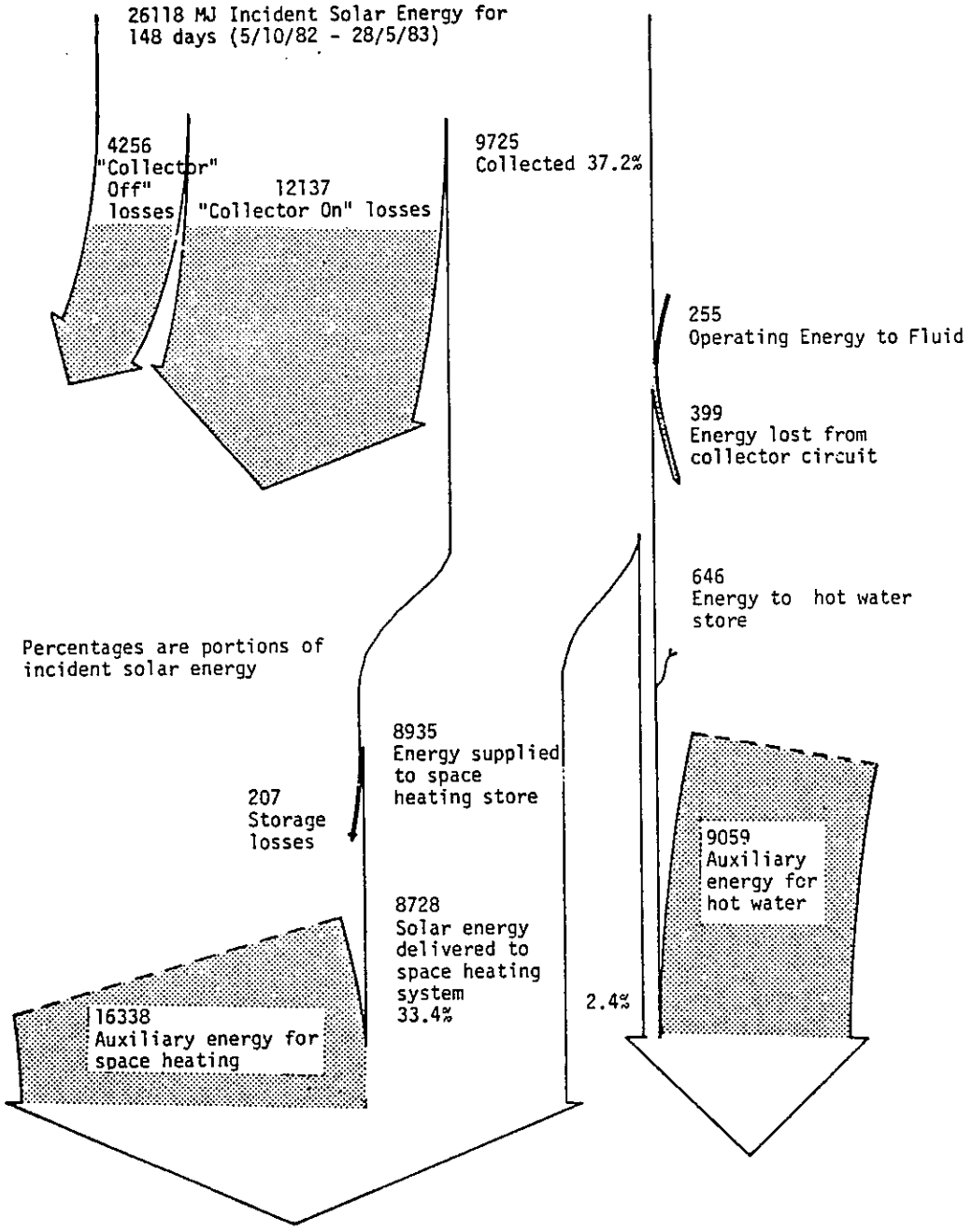

Figure 6.3-38. Energy Flow Diagram for Philips VTR151 Collector at BSRIA Solar Test Facility with Simulated Loads, United Kingdom, 5 October 1982 to 28 May 1983.

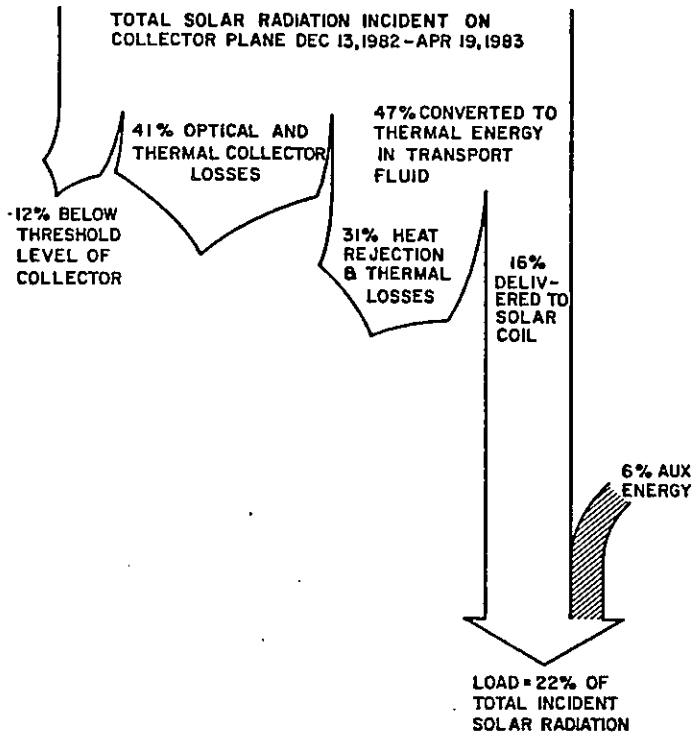

Figure 6.3-39. Energy Flows Diagram for the Philips VTR 361 Collector at CSU Solar House I, United States, Winter 1982-83.

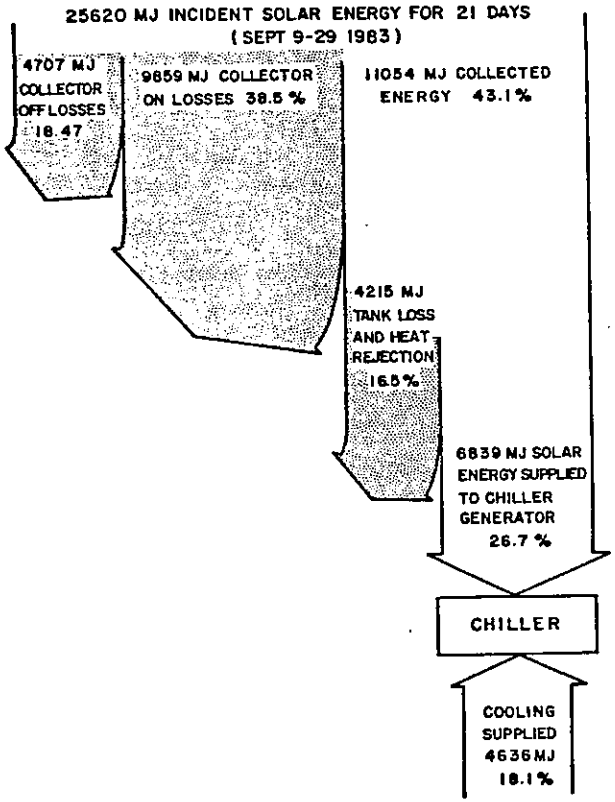

Figure 6.3-40. Energy Flows Diagram for the Philips VTR 361 Collector at CSU Solar House I, United States, September 1983.

6.4 ENERGY SUPPLY AND DELIVERY BAR CHART

Month-to-month system performance is easily interpreted from energy supply and delivery bar charts. These charts may be used to compare the effectiveness of different systems and to ascertain other system performance characteristics, such as the ability of the collection system to supply energy at low insolation levels.

6.4.1 The Sydney University Solar Heating and Cooling System, Sydney, Australia

Figures 6.4-1 and 6.4-2 indicate average energy supply rates during system cooling operation (December 1982 to January 1983) as well as during heating (July 1983 to September 1983). During the cooling season the Sydney University evacuated tubular collector was used exclusively. The energy supply bar charts indicate a typical collection efficiency on the order of 40 percent during cooling operation. Because of instrument difficulties at the time, Figure 6.4-1 shows information of energy collected which is supplied to the tank rather than energy collected at the collector.

During system heating operation, two different types of collectors have been used, though only during a short period. Figure 6.4-2 shows energy supply rates of the Yazaki flat-plate collector for the period July 9-26, 1983 as well as that of the Sydney University evacuated tubular collector during the period August 28, 1983 to September 28, 1983.

It is noted that a significant proportion of the data for many months is absent. This is mainly due to planned interruptions to system operation or data acquisition or failure of data acquisition equipment, rather than failure of the solar system or air-conditioning hardware. The amount of data available should not therefore be taken as an indication of system reliability.

Figures 6.4-3 through 6.4-5 show energy supply rates for three different periods between November 1983 and March 1985.

It is interesting to note that during periods of low loads and collector operating temperatures near the boiling point (April/May 1984), situations occur where the solar energy incident on the collectors while the collector pump is running is smaller than the actual produced useful energy. This is a result of pump cycling. A substantial amount of energy is collected and stored in the collector loop during the pump "off time" yet the incident solar flux is not accounted for. This capacitively stored energy ends up in the storage tank as useful and metered energy during every pump "on" cycle.

Average monthly collector efficiency has remained high at 40 percent or above, except during the month with small loads where boiling occurred

in the collectors. Collector performance information during those periods must not be to assess the Sydney University evacuated collectors.

6.4.2 Mountain Spring Bottle Washing Facility, Edmonton, Canada

Energy supply bar charts for the periods 1 May 1982 to 31 December 1982 and 1 January 1983 to 31 December 1983 are shown in Figure 6.4-6 and 6.4-7 respectively.

Though the solar energy system was designed for continuous operation throughout the year, it is readily apparent that operation during the months of November through March is not practical. This is due to two reasons: first, the low solar altitude (13 degrees on December 21) and second, snow fouling the collector array.

6.4.3 Ispra Solar Heated and Cooled Laboratory, Commission of European Communities

The monthly average supply rates are shown in Figures 6.4-8 to 6.4-11. The weather during the month of May was very bad and this results in lower collection efficiencies, especially for the Sanyo collectors. Days on which a collector array did not operate correctly have been omitted. Therefore, the month of May includes only 3 days for the Philips VTR 261 collectors.

The performance of the Philips VTR 261 and the VTR 361 collector is almost the same. This is remarkable since the VTR 361 has only 14 tubes per module and the VTR 261 has 19 tubes for an equal aperture area module.

6.4.4 Solarhaus Freiburg, Federal Republic of Germany

Energy supply bar charts in Figures 6.4-12 and 6.4-13 show the annual distribution of the incident radiation and of the thermal collector output for the Corning Glass collector, and in Figures 6.4-14 and 6.4-15 for the Philips IV and Philips/Stiebel-Eltron heat pipe collector.

The annual variation of the daily operating collector temperature and of the ambient air temperature is displayed. Results are shown for the two years 1982 and 1982/83 in order to present meaningful seasonal quantities.

The annual insolation onto the collector plane was 4304 MJ/m^2 in 1982, and 3989 $MJ/m^2 \cdot a$ in the 1982/83 period, due to a very rainy and atypical spring in 1983.

Although the Corning Glass collector was operating with the heating system, the annual collection efficiencies of 50.9 percent and 50.4

percent did not change as compared with preceding years. In Figure 6.4-14, the improvement of collection efficiency after the replacement of the Philips IV with the Philips/Stiebel-Eltron collector has to be pointed out. The average daily efficiency changed from 38.5 percent in May 1982 (Philips IV) to a value of 53.7 percent in June 1982 (Philips/Stiebel-Eltron heat pipe collector). The collection efficiency during the period from June 1982 to May 1983 was 52.7 percent.

The two annual profiles of the average daily operating temperatures show a slightly higher temperature of the Corning Glass collector when operating with the heating system (44.1°C Corning: 41.5°C Philips/Stiebel-Eltron).

6.4.5 Eindhoven Technological University Solar House, The Netherlands

The average energy supply and delivery rates for the Philips VTR 261 EUT Solar House are given in Figure 6.4-16.

6.4.6 Knivsta District Heating System, Knivsta, Sweden

The monthly average energy supply is shown in Figures 6.4-17 and 6.4-18. Four months in the diagrams overlap. Figure 6.4-17 contains some information in addition to that specified in the Task VI format requirements. The difference in energy output from collectors Q112 is surprisingly low during the summer, but in the winter the Owens-Illinois collectors suffer because of their high heat capacity. During November to January, hardly any energy is collected due to the low daily irradiation, which seldom reaches the threshold value, even when preheating is used. Snow cover also influences the results.

The even energy output from the collectors is somewhat misleading as the Philips collectors are tilted at 60 degrees. The measured irradiation onto the aperture area of the Philips collectors is lower than the others, which are tilted 45 degree planes. Hence the Philips collectors operate at higher efficiency. This is partly due to the additional irradiation falling on the bach side of the collectors. This energy is better utilized, partly because of a higher incidence angle modifier during morning and evening, which also compensates for the long piping system relative to the aperture area.

The Scandinavian Solar flat-plate collector, put into operation in February 1982, has shown surprisingly good results compared to the ETC collectors. The off losses H100 and H101 are higher due to higher $F'U_L$ value but also due to the higher piping losses per unit of aperture area of the three systems. The piping system is designed for the Owens-Illinois collector array which had 50 percent larger aperture area. Looking at the "on" efficiency instead, compensates for that and this collector efficiency is somewhere between General Electric and Philips

collectors. The system efficiency is drastically decreased by the large piping losses.

6.4.7 The Södertörn District Heating Project, Södertörn, Sweden

The monthly average energy supply is shown in Figures 6.4-19 and 6.4-20. The first diagram shows the Teknoterm collectors compared to General Electric and Phillips collectors. The Philips collectors perform best in spite of the 60 degree slope which gives less irradiated energy to the collector front aperture. The second diagram shows the Philips collector compared to Grandges Aluminum and Scandinavian Solar collectors. The efficiency of the Philips collectors is outstanding but the energy output from the Scandinavian Solar collectors is comparable, due to a more favorable collector slope. The operating ΔT of the Scandinavian Solar collectors is about $10^{o}C$ higher for that period.

The seasonal variation of the monthly energies is very pronounced due to the high latitude (59 N). Figures 6.4-21 through 6.4-25 show the monthly average energy supply from the collector arrays during 1983. In June the controls are changed so that $80^{o}C$,rather than $60^{o}C$, outlet temperature fluid is provided to the network. The availability of the Granges Aluminum collectors has been quite low so the results are somewhat misleading and should not be used to evaluate the potential of these collectors. The Scandinavian Solar collector has also had reduced availability during August.

6.4.8 SOLARCAD Project, Geneva, Switzerland

As noted in Figure 6.4-26, the bar chart includes both Corning "A" and "B" collectors with energy outputs that are distinguished by Q112 A and B. The percent quoted for Q112 includes A and B together. The B collectors have degraded since March 1983 due to the loss of vacuum for a few tubes.

Also shown in Figure 6.4-27 is the energy collected Q102 at the from the entire collection system, including the heat exchanger. Figure 6.4-28 gives the Sanyo collector performances.

Also shown in these Figures is the energy collected Q102 at the outlet of the system, considered as the heat exchanger outlet.

This energy can be close to zero in the winter months. The positive output of collectors is insufficient to overcome losses of the system, usually heat losses and thermal capacity effects, or "on" and "off" losses.

Dynamic effects combined with a poor control may even lead to negative system output. See also remarks about efficiency plots and arrow diagrams in Sections 6.1.8 and 6.3.8.

6.4.9 SOLARIN Project, Hallau, Switzerland

In Figure 6.4-29 the last item plotted corresponds to the heat delivered by the solar loop at the inlet of the heat exchanger Q142 and not at the outlet Q102. The difference between the values is small. Note the comments in Sections 5.9.2, 6.1.9, 6.2.9 and 6.3.9.

Snow in January and part of February leads to very low performance. Heat losses between the collector array and the heat exchanger are mainly due to the rejection of excess heat. This can be due to defects in the control, i.e. winter control is correct, but summer control (May up to August 1984) was not optimized, as is seen on Figure 6.4-29.

6.4.10 Evacuated Collector System Test Facility, Bracknell, United Kingdom

The total incident solar energy, incident energy while collecting, and energy collected are given in bar charts on Figures 6.4-30 and 6.4-31. Only the first three months have been analyzed in this form. The conversion of incident energy to collected energy varied between 32 percent in December 1982 to 40 percent in April 1983, with an average of just over 35 percent.

6.4.11 Colorado State University Solar House I, United States

Average energy supply and delivery rates from the Philips VTR 361 collectors for the winter and summer periods are shown in Figures 6.4-32 and 6.4-33. A high percentage of available insolation is utilized by the collectors and because collector efficiency is high, monthly average delivery rates are also high. Although temperature data are not shown on the winter bar graph, storage temperatures are high in the spring months because heating loads are small.

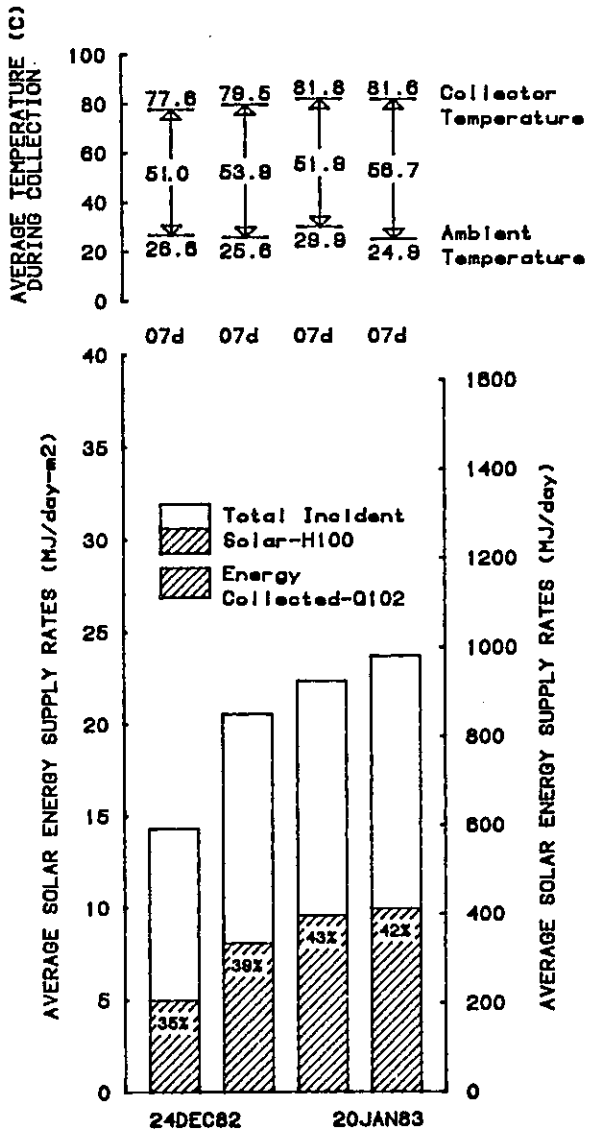

Figure 6.4-1. Average Energy Supply Rate for Sydney University Evacuated Tubular Collector at Sydney, Australia, 24 December 1982 to 20 January 1983.

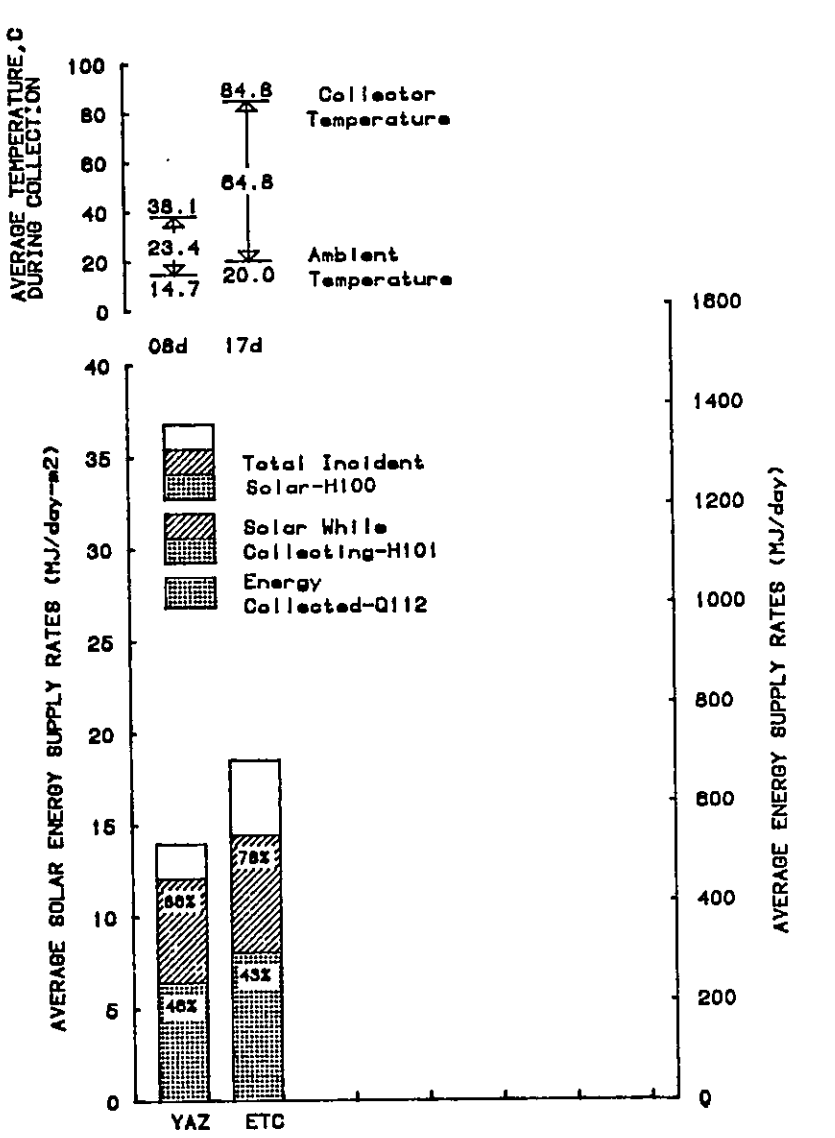

Figure 6.4-2. Average Energy Supply Rate for Sydney University Flat Plate and Sydney University Evacuated Collector at Sydney, Australia, 8 July 1983 to 28 September 1983.

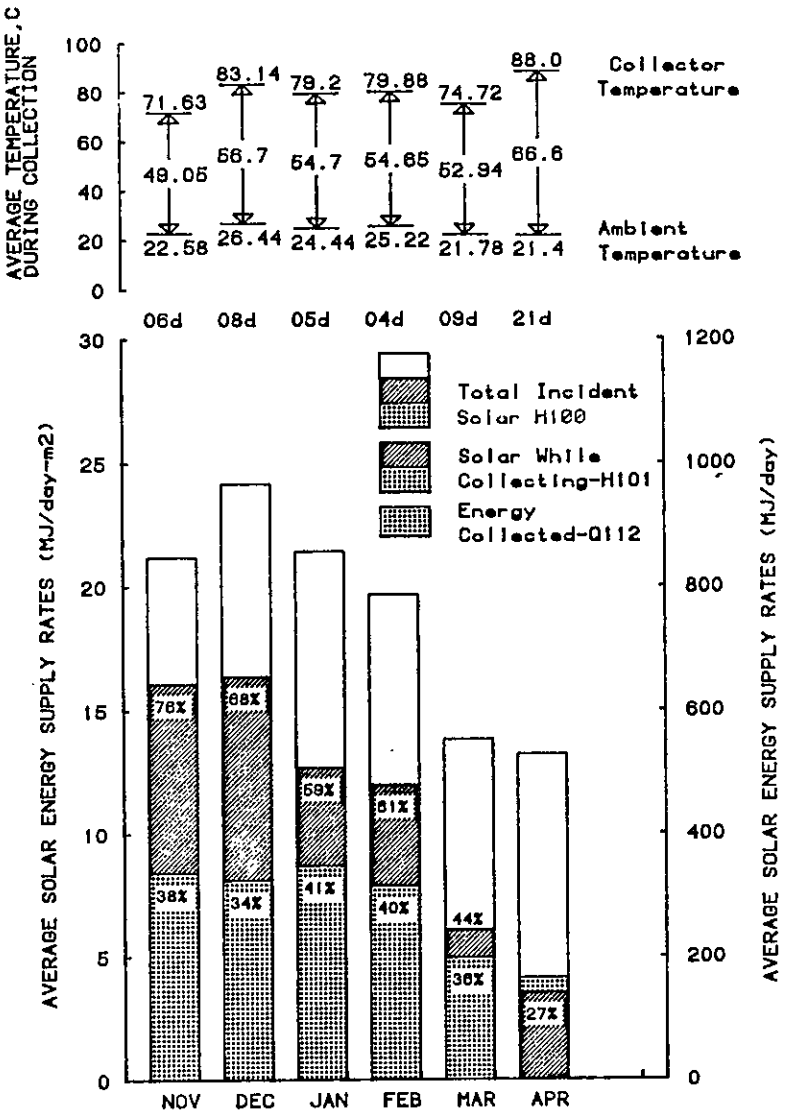

Figure 6.4-3. Average Energy Supply Rate for Sydney University Evacuated Collector at Sydney, Australia, 1 November 1983 to 30 April 1984.

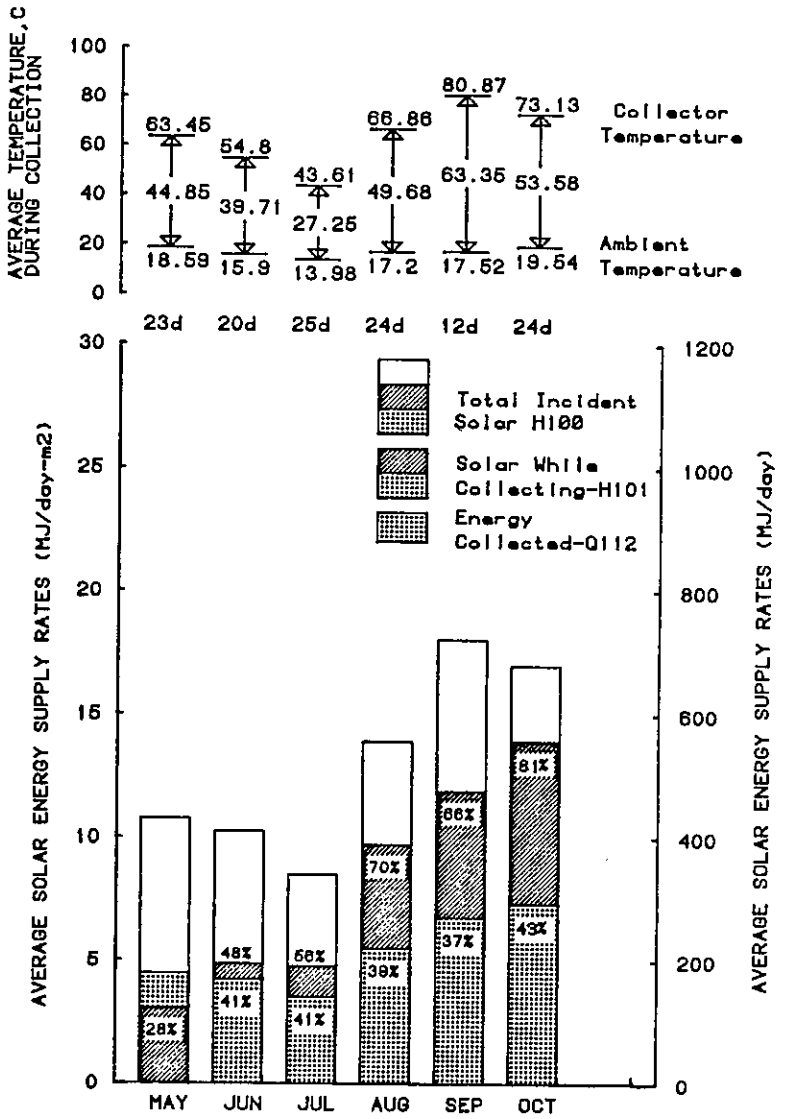

Figure 6.4-4. Average Energy Supply Rate for Sydney University Evacuated Collector at Sydney, Australia, 1 May 1984 to 30 October 1984.

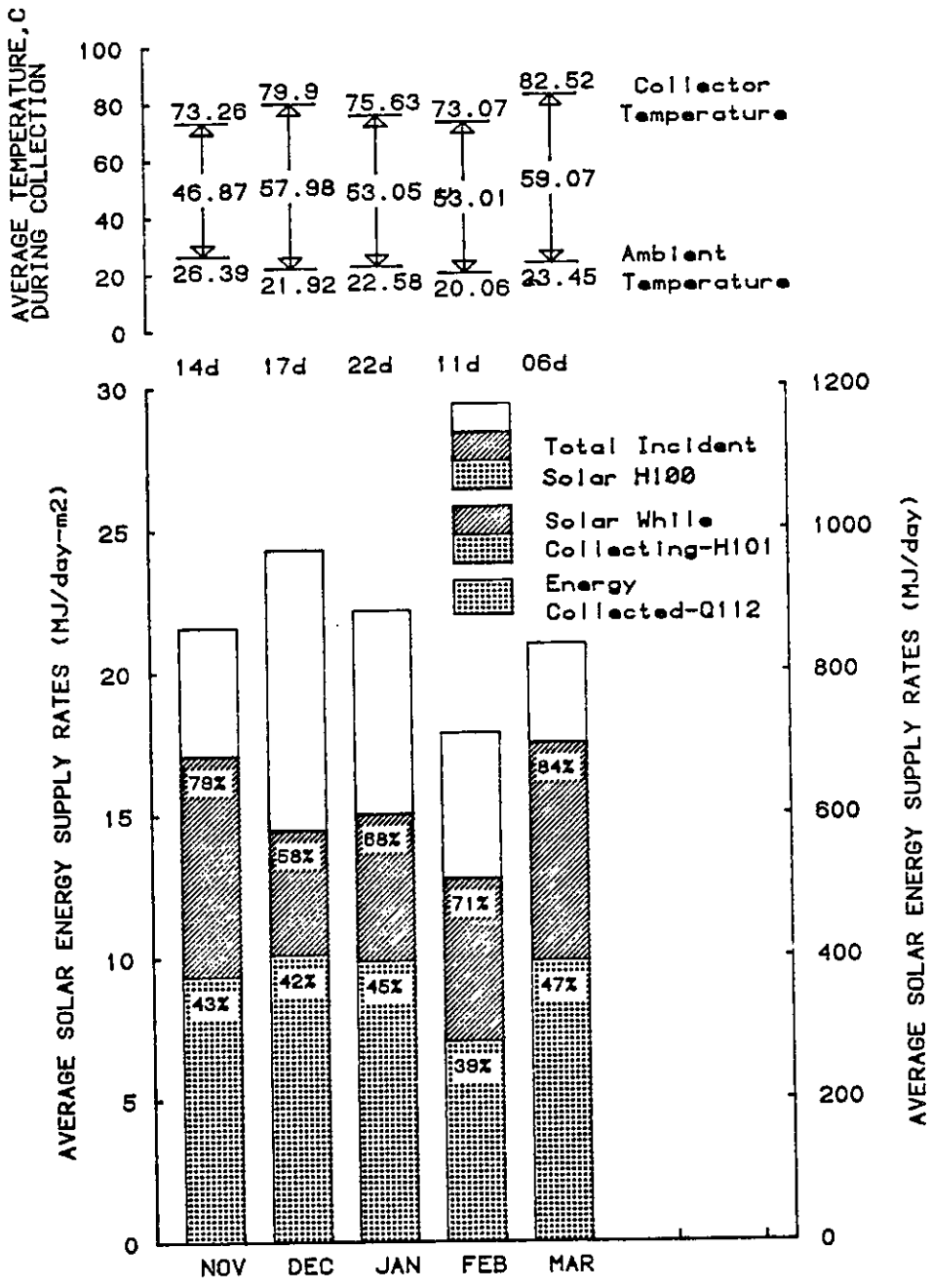

Figure 6.4-5. Average Energy Supply Rate for Sydney University Evacuated Collector at Sydney, Australia, 1 November 1984 to 31 March 1985.

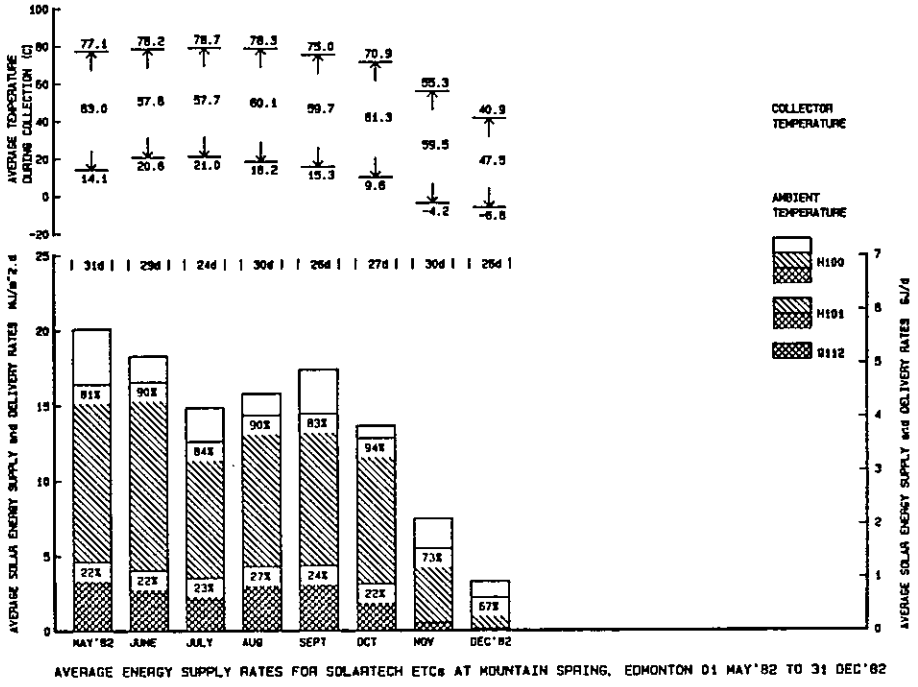

Figure 6.4-6. Average Energy Supply Rates for Solartech ETC's at the Mountain Spring Bottle Washing Facility, Canada, 1 May 1982 to 31 December 1982.

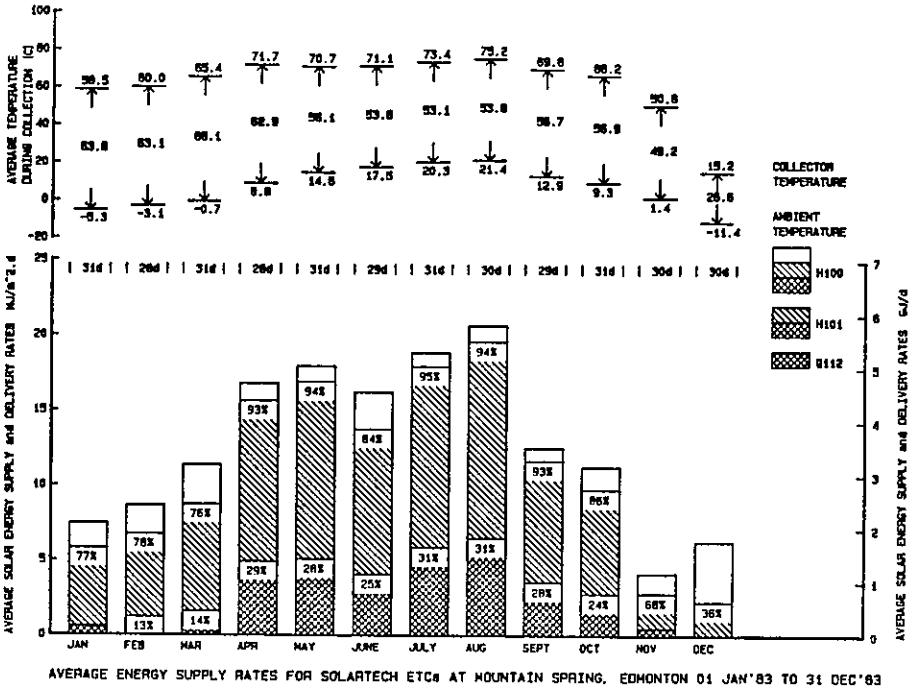

Figure 6.4-7. Average Energy Supply Rates for Solartech ETC's at the Mountain Spring Bottle Washing Facility, Canada, 1 January 1983 to 31 December 1983. CEC

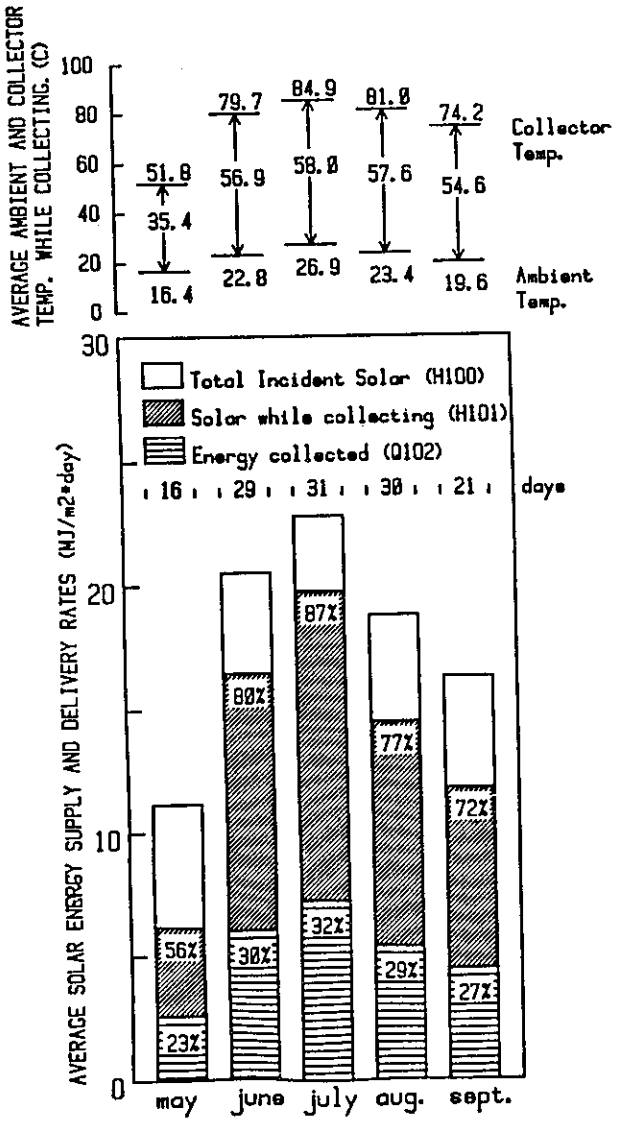

Figure 6.4-8. Average Energy Supply Rates for Sanyo (I) Collector, Ispra Solar Laboratory, 1983.

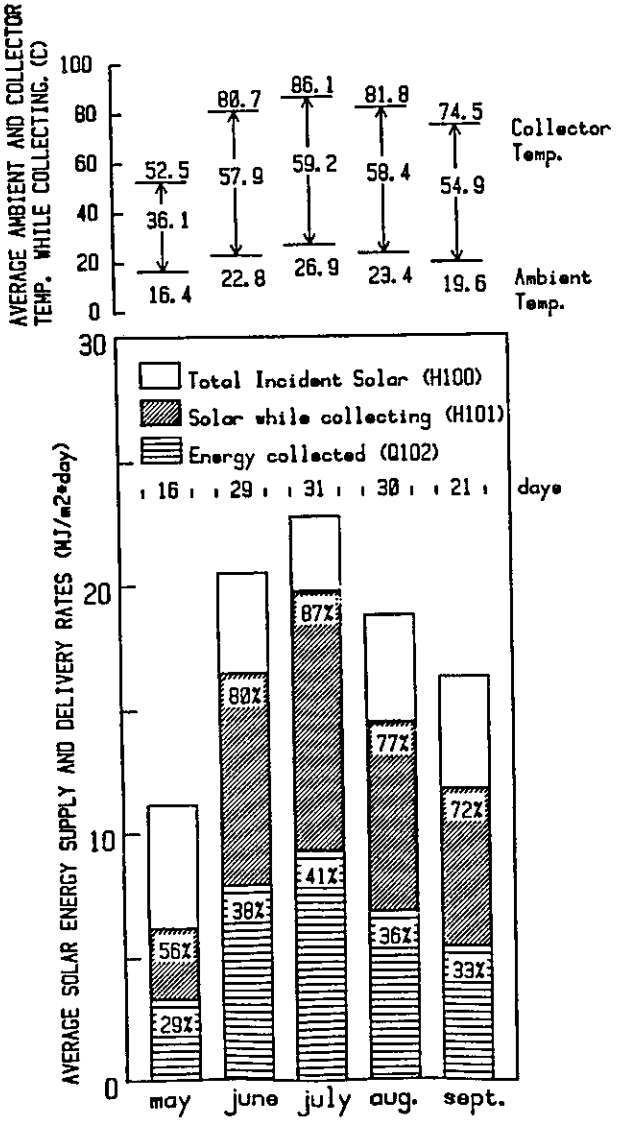

Figure 6.4-9. Average Energy Supply Rates for Sanyo (II) Collector, Ispra Solar Laboratory, 1983.

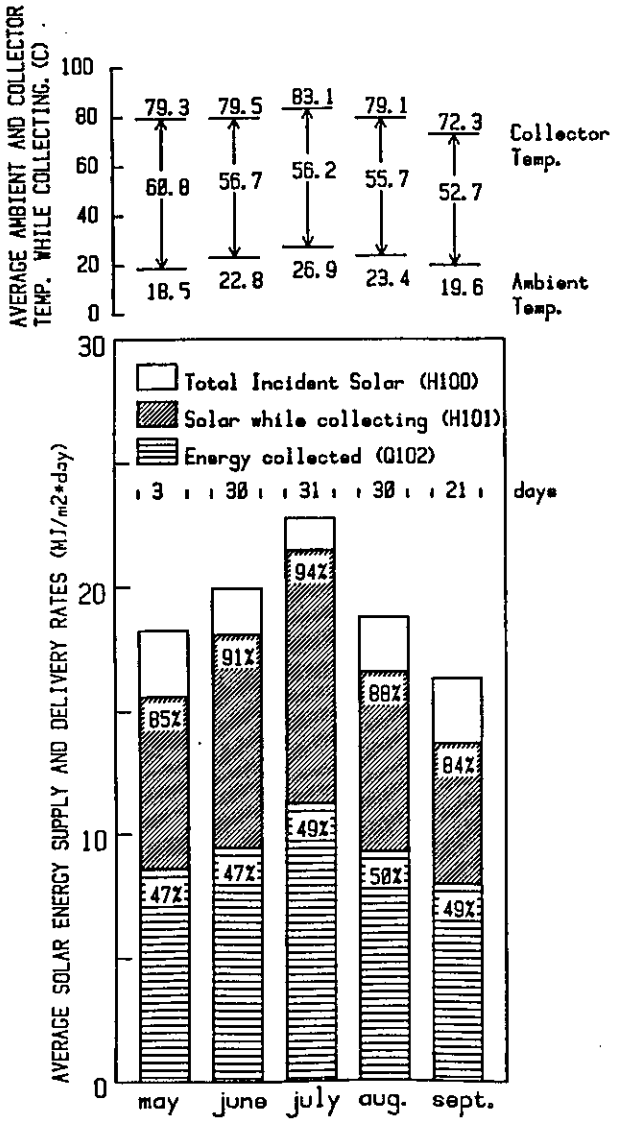

Figure 6.4-10. Average Energy Supply Rates for Philips VTR 261 Collector, Ispra Solar Laboratory, 1983.

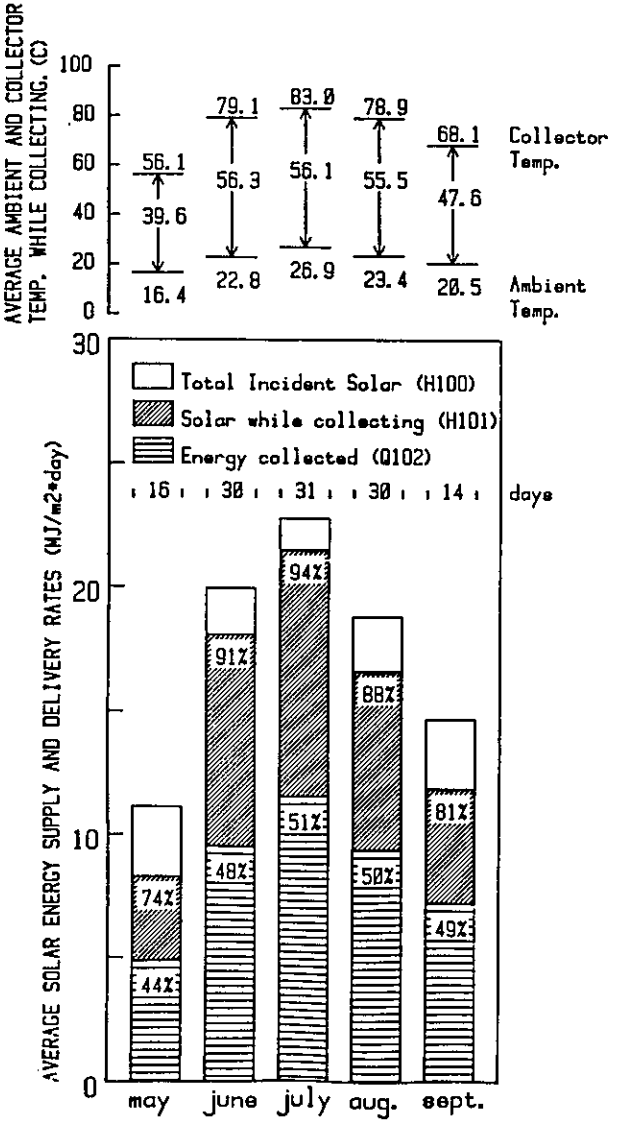

Figure 6.4-11. Average Energy Supply Rates for Philips VTR 361 Collector, Ispra Solar Laboratory, 1983.

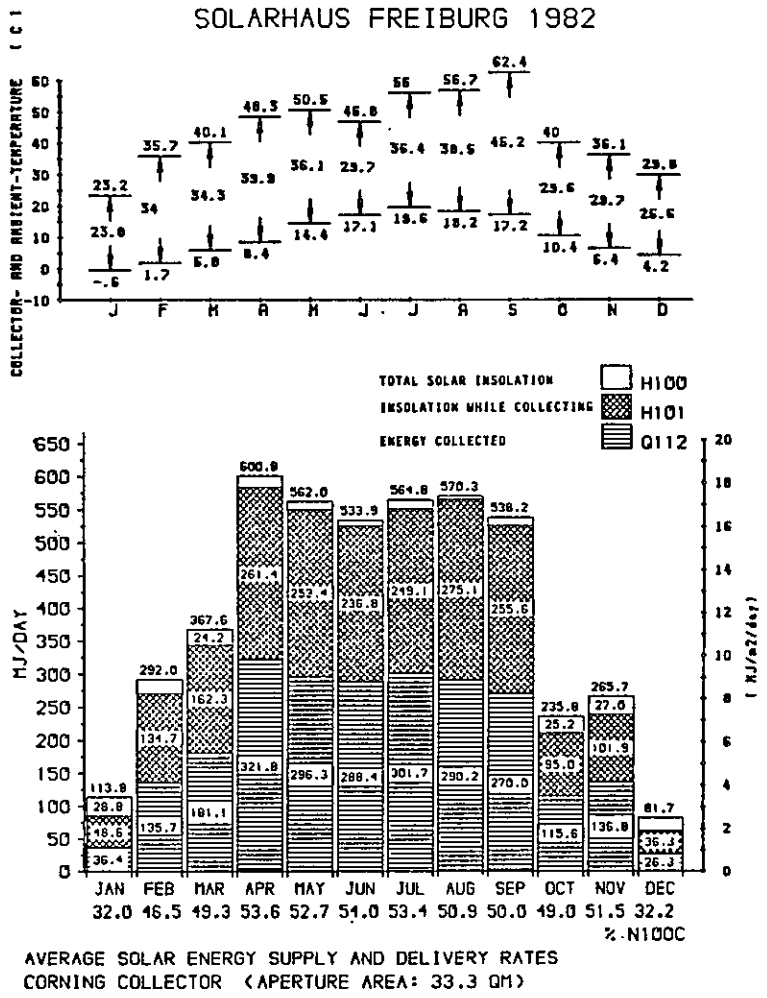

Figure 6.4-12. Average Energy Supply Rates for the Corning Glass Collector, Solarhaus Freiburg, Federal Republic of Germany, 1982.

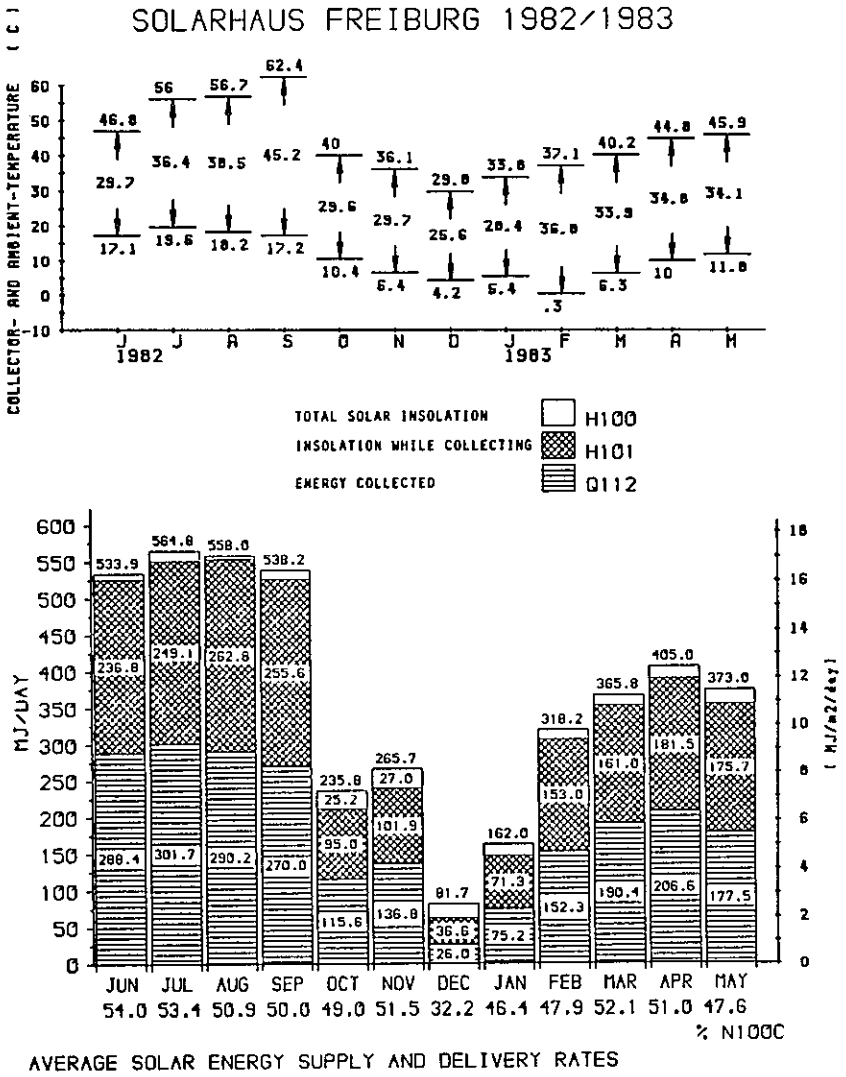

Figure 6.4-13. Average Energy Supply Rates for the Corning Glass Collector, Solarhaus Freiburg, Federal Republic of Germany, June 1982 to May 1983.

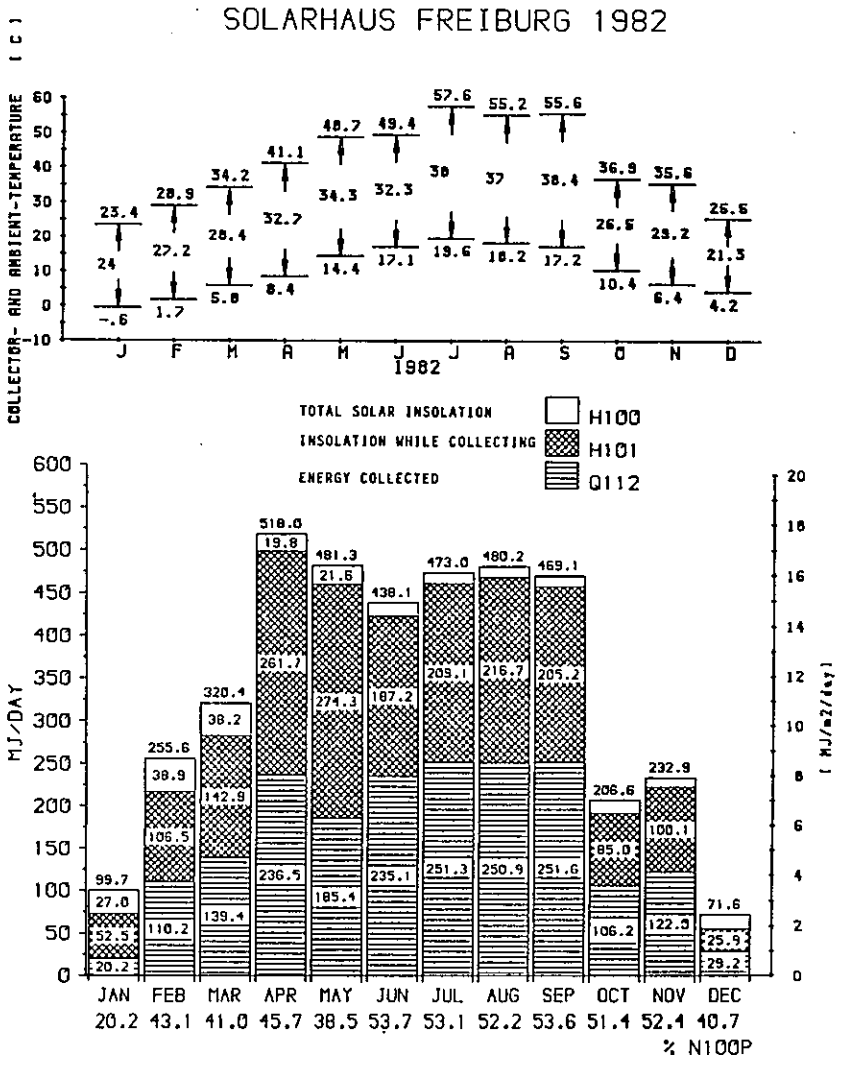

Figure 6.4-14. Average Energy Supply Rates for the Philips MK IV and Philips/Stiebel-Eltron Collectors, Solarhaus Freiburg, Federal Republic of Germany, 1982.

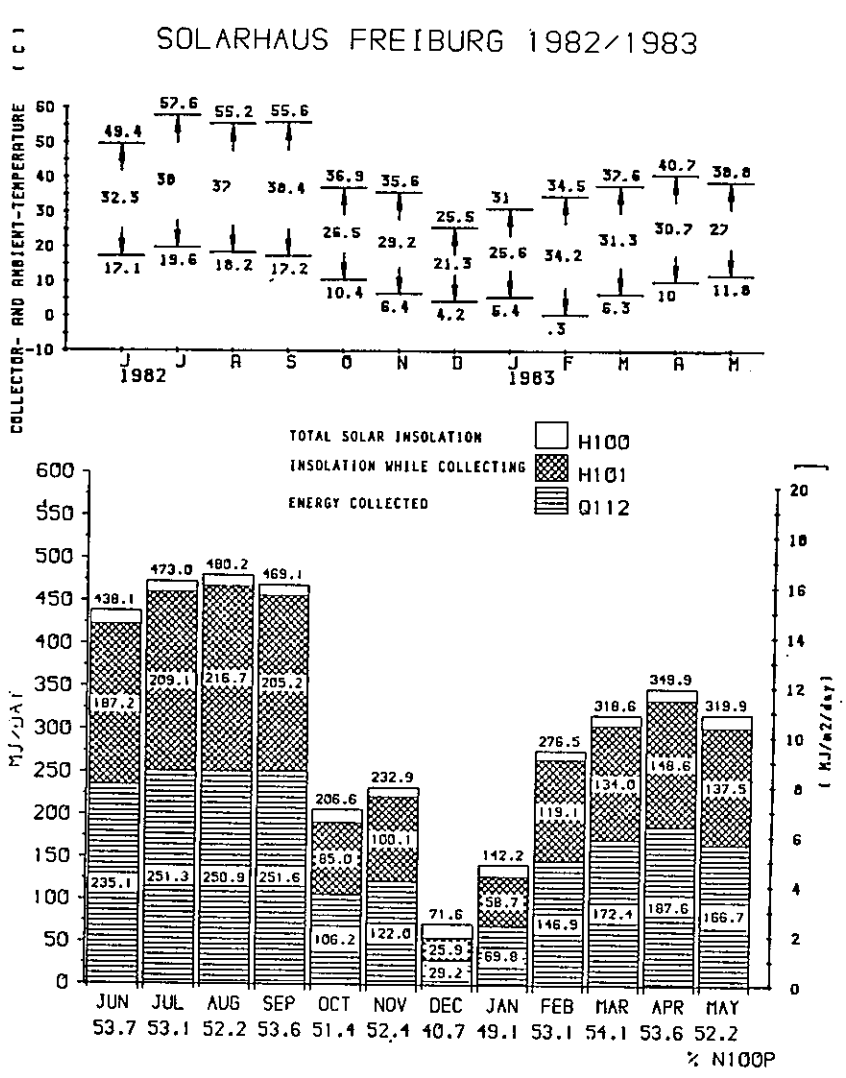

Figure 6.4-15. Average Energy Supply Rates for the Philips/ Stiebel-Eltron Collector, Solarhaus Freiburg, Federal Republic of Germany, June 1982 to May 1983.

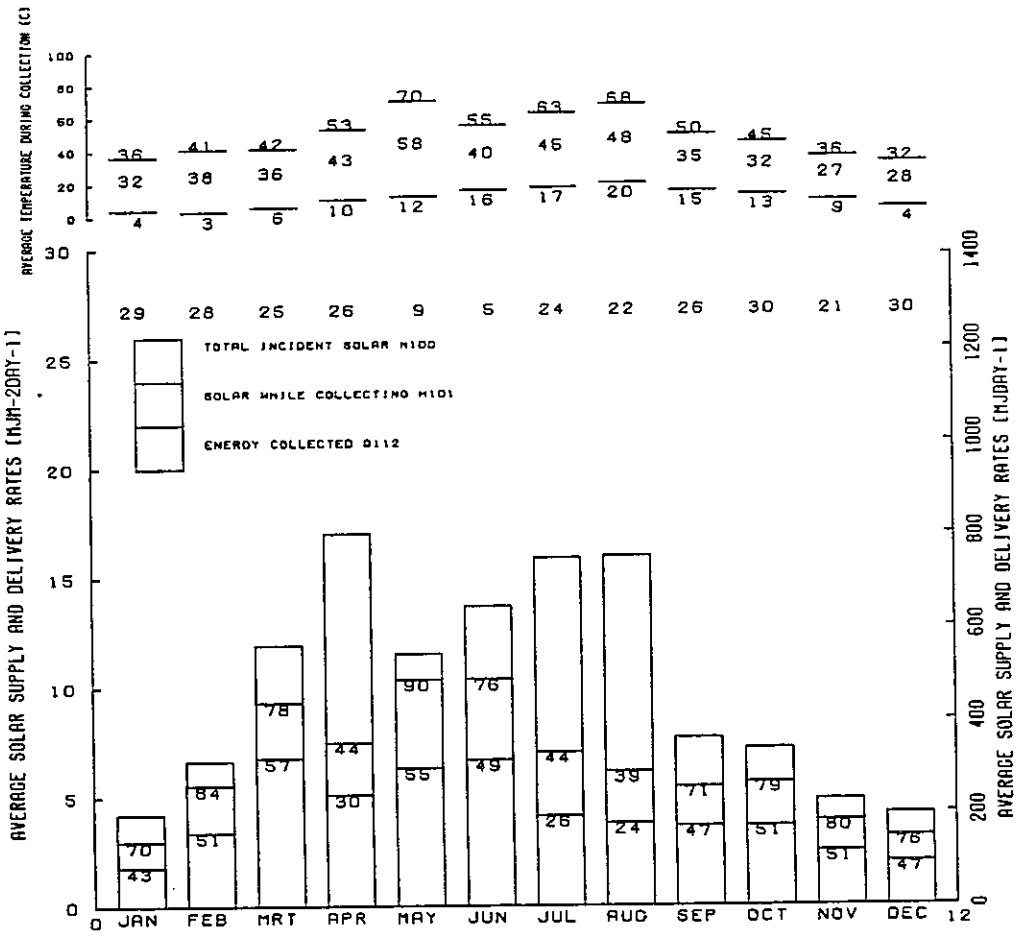

Figure 6.4-16. Average Supply and Delivery Rates for the Philips VTR 261, EUT Solar House, 1984.

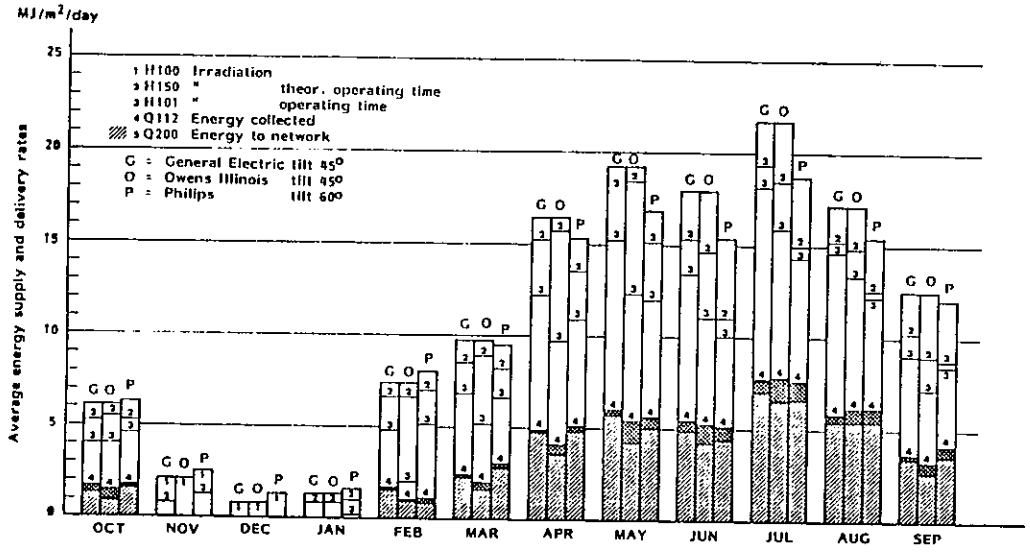

Figure 6.4-17. Average Energy and Delivery Rate for the Knivsta District Heating System, Knivsta, Sweden, October 1981 to September 1982.

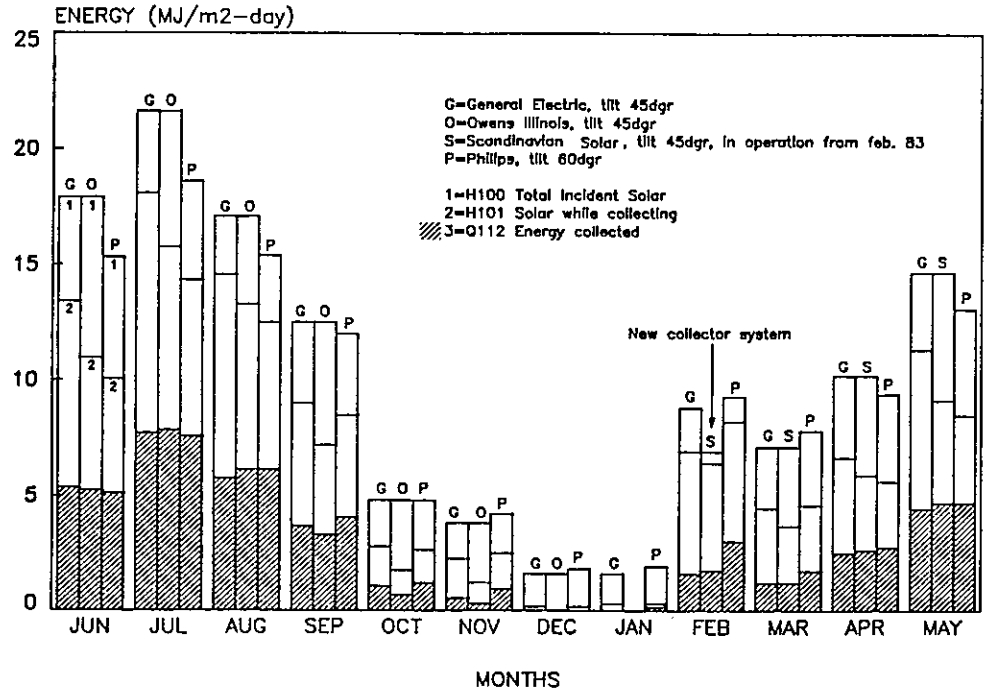

Figure 6.4-18. Average Energy Supply Bar Chart for the Knivsta District Heating System, Knivsta, Sweden, June 1982 to May 1983.

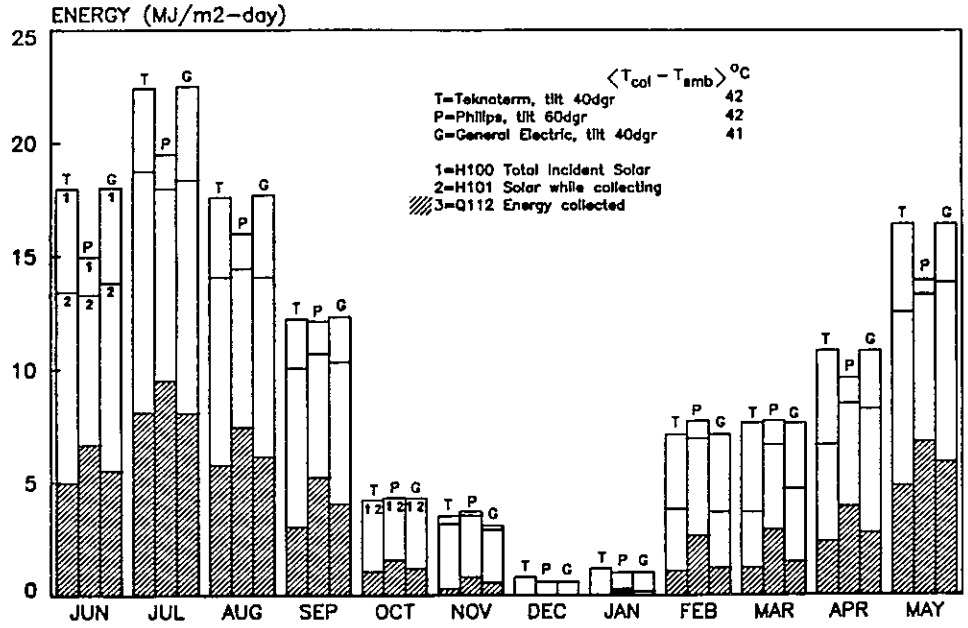

Figure 6.4-19. Average Energy Supply Bar Chart for Teknoterm, Philips VTR 141 and General Electric TC 100, Södertörn, Sweden, June 1982 to May 1983.

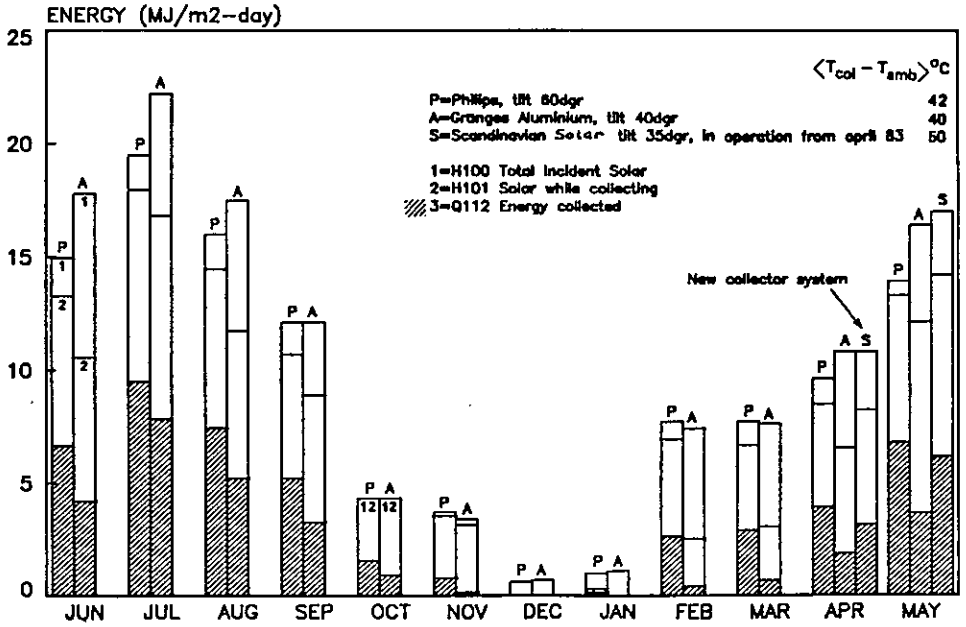

Figure 6.4-20. Average Energy Supply Bar Chart for Philips VTR 141, Granges Aluminum and Scandinavian Solar HT, Södertörn, Sweden, June 1982 to May 1983.

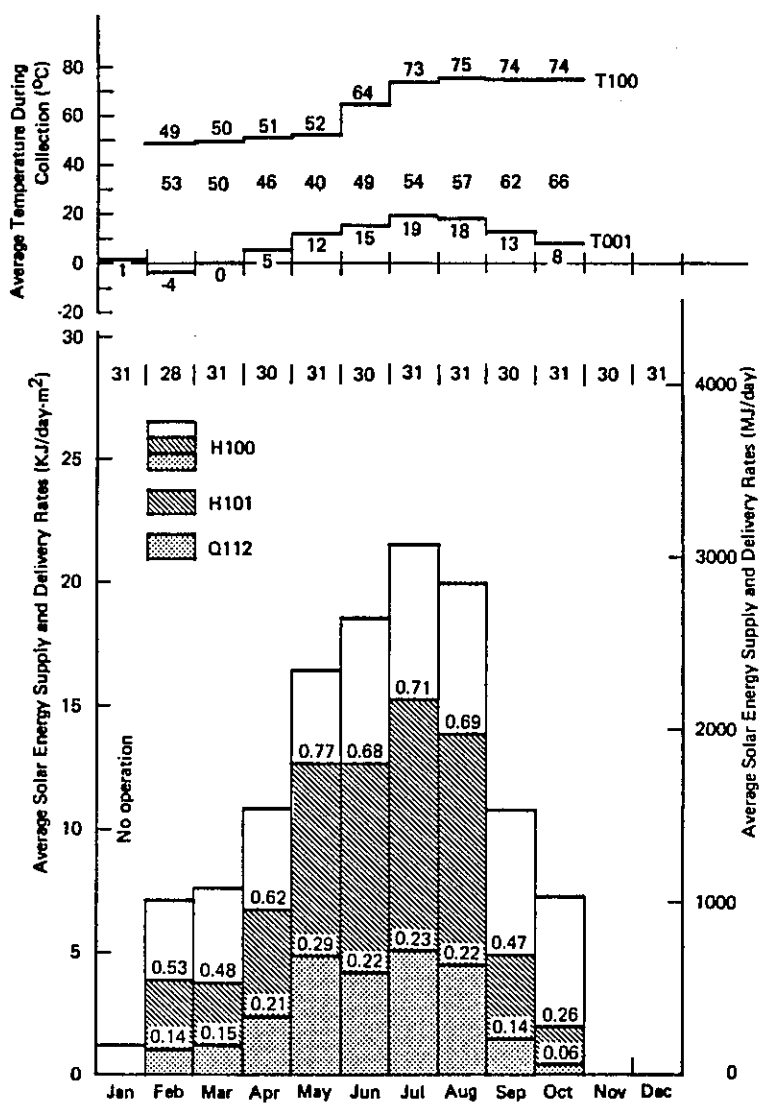

Figure 6.4-21. Average Energy Supply Rates for Teknoterm, Södertörn, Sweden, 1983.

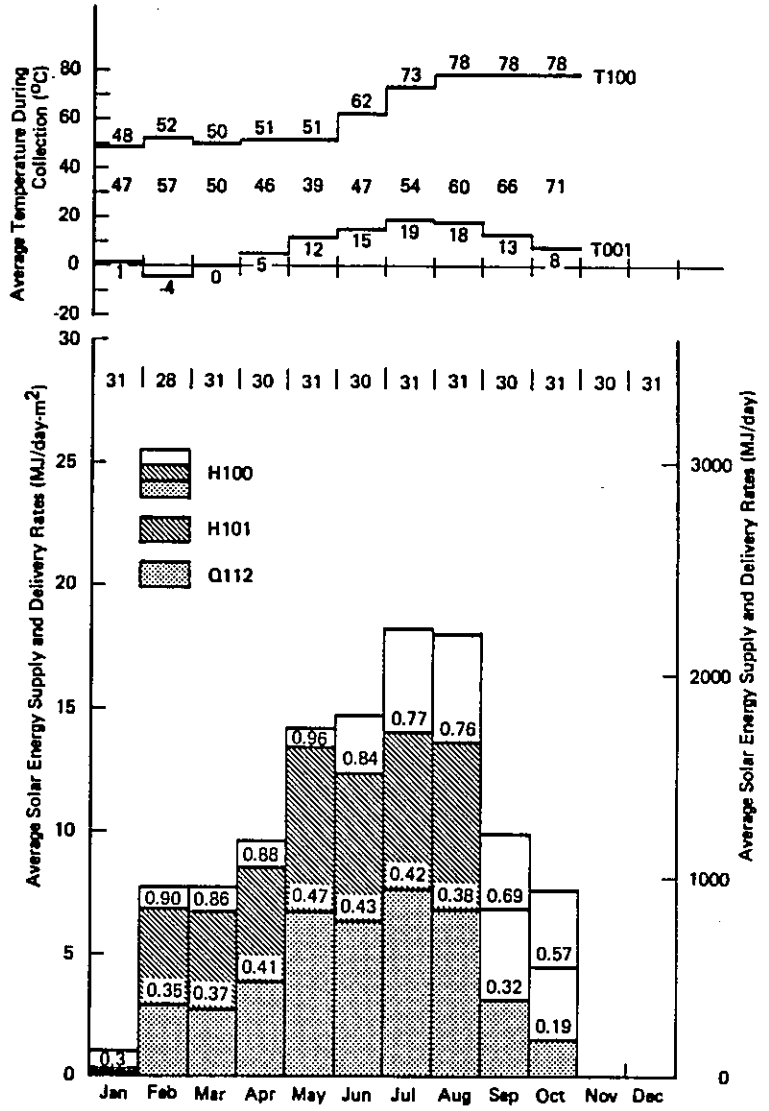

Figure 6.4-22. Average Energy Supply Rates for Philips VTR 141, Södertörn, Sweden, 1983.

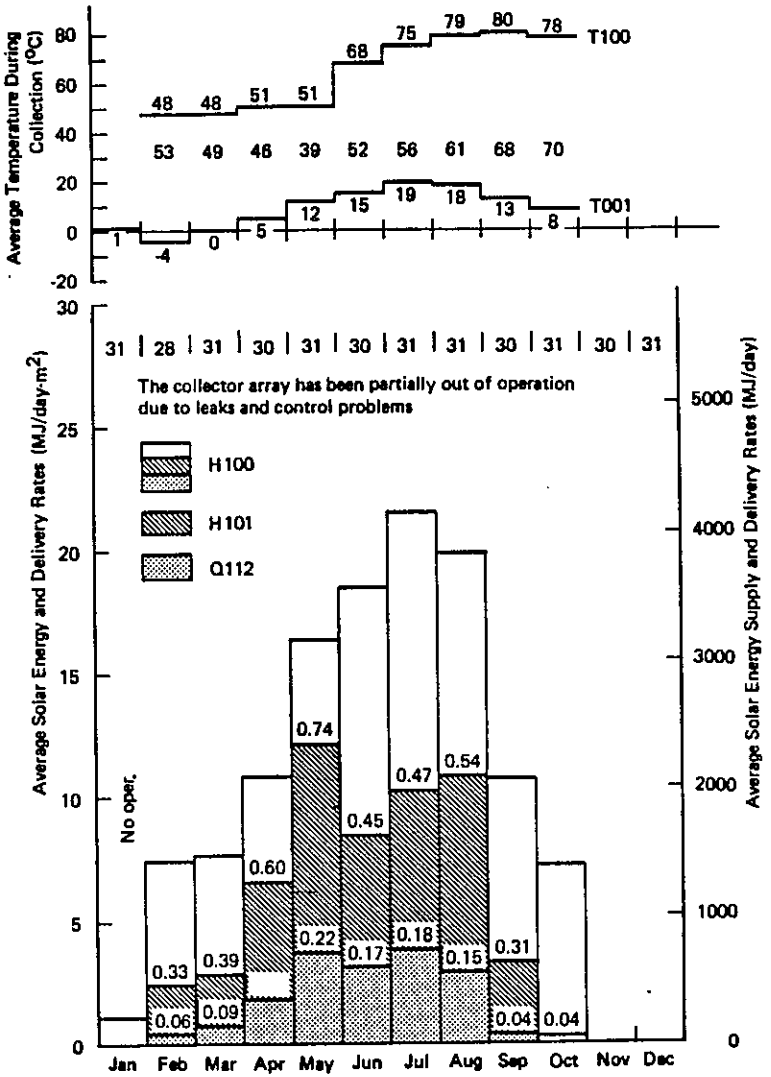

Figure 6.4-23. Average Energy Supply Rates for Granges Aluminum, Södertörn, Sweden, 1983.

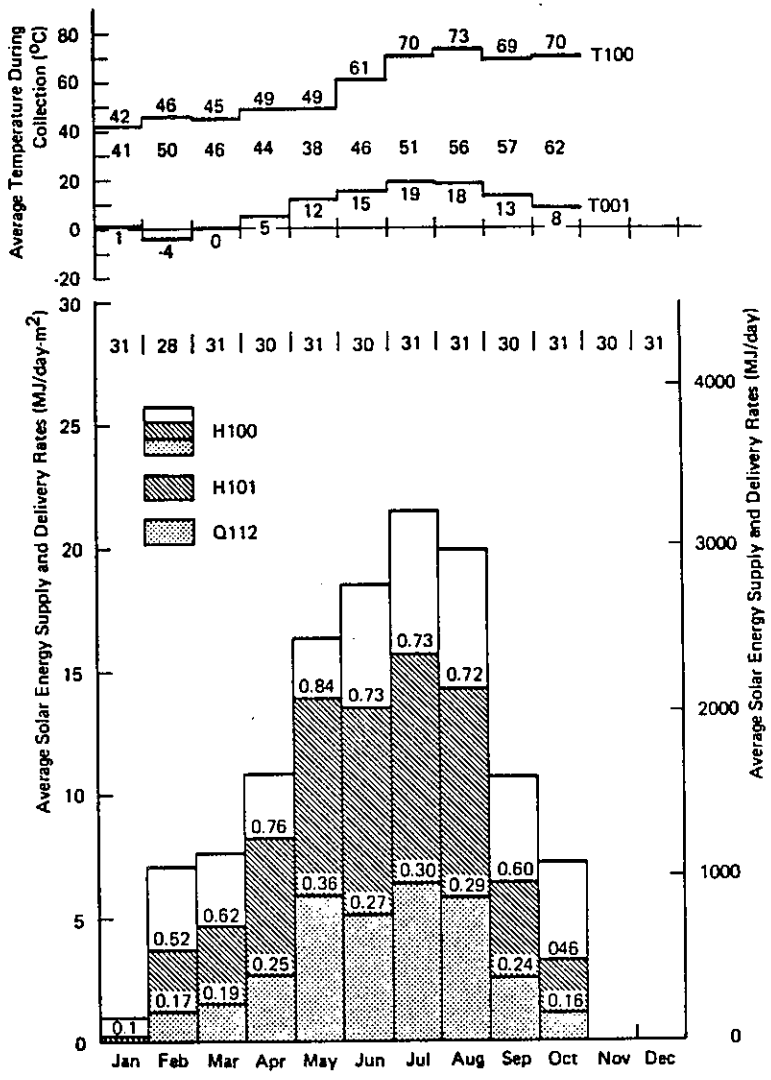

Figure 6.4-24. Average Energy Supply Rates for General Electric TC 100 Collector, Södertörn, Sweden, 1983.

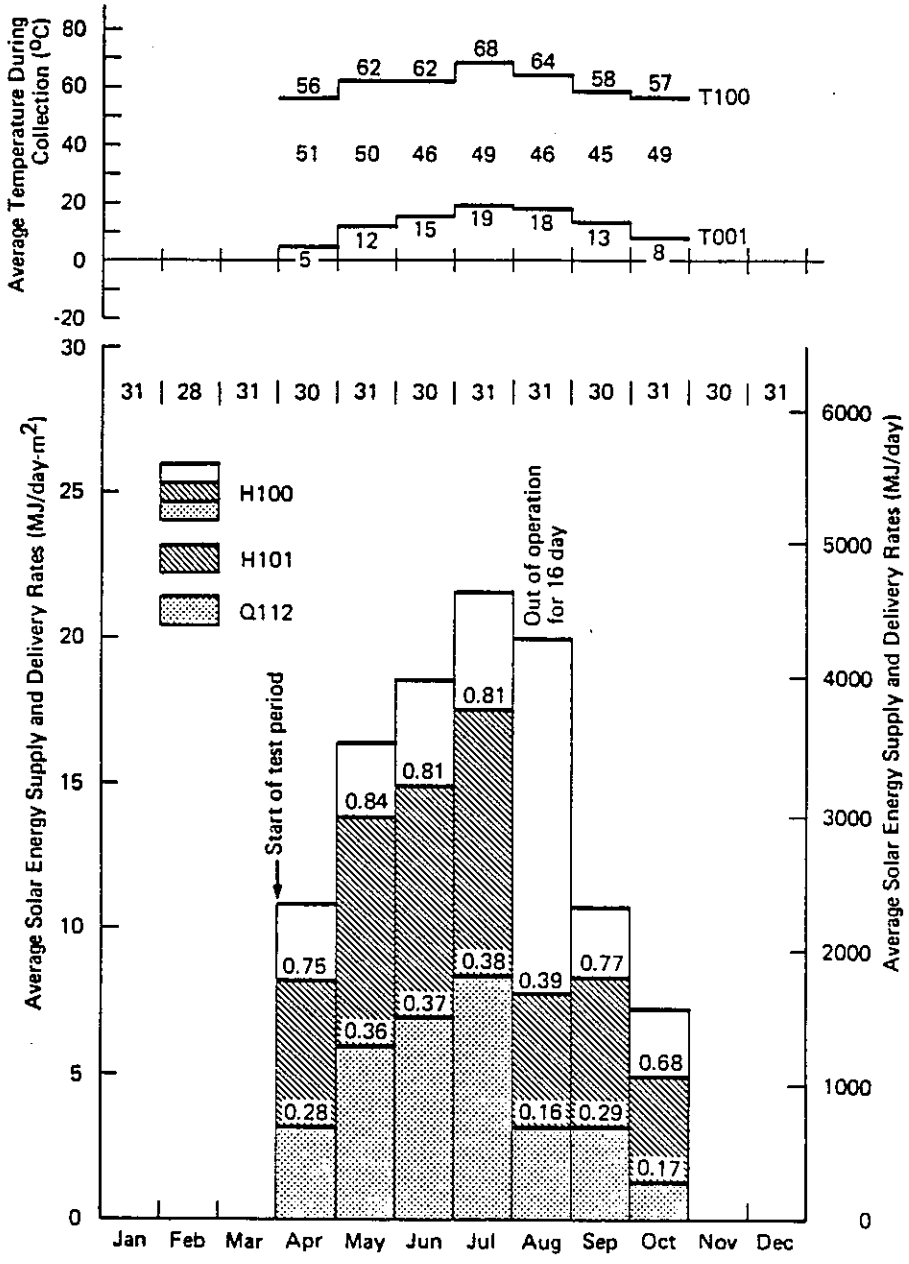

Figure 6.4-25. Average Energy Supply Rates for Scandinavian Solar HT Collector, Södertörn, Sweden, 1983.

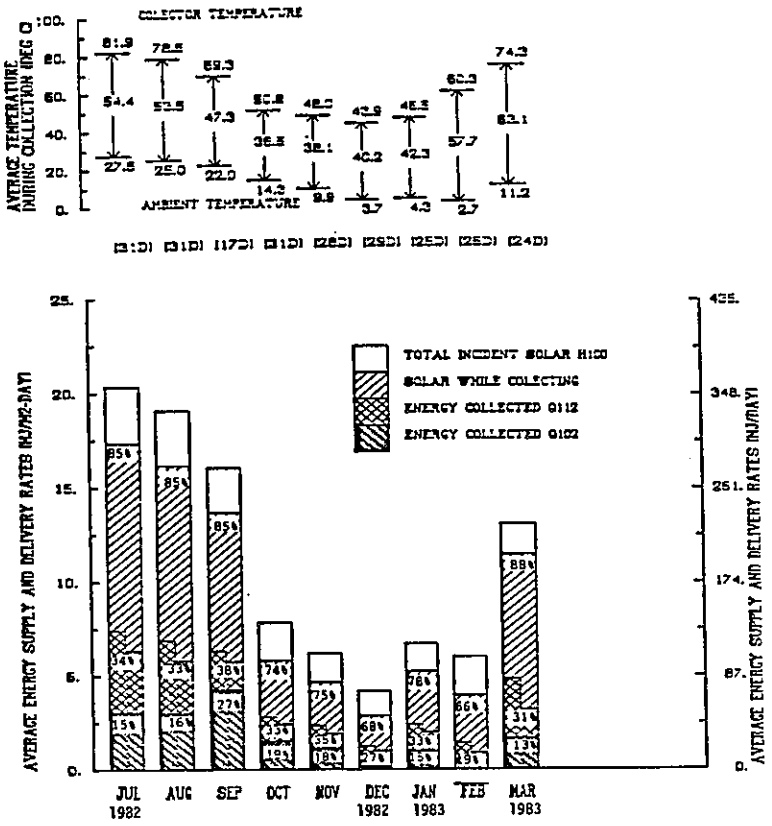

Figure 6.4-26. Average Energy Supply Rates for Corning A+B from Geneva, Switzerland, July 1982 to March 1983.

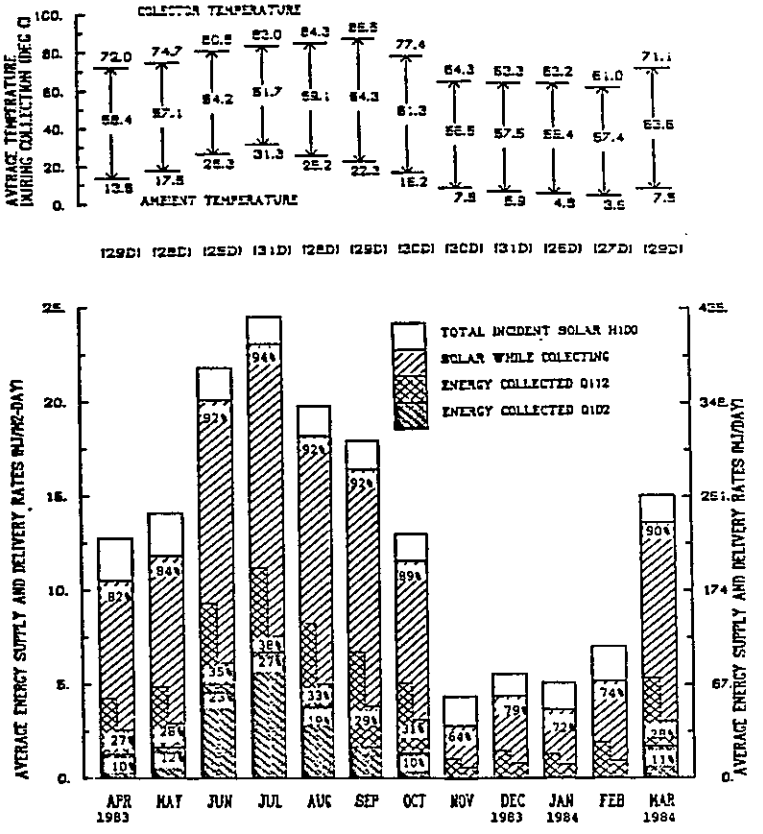

Figure 6.4-27. Average Energy Supply Rates for Corning A+B from Geneva, Switzerland, April 1983 to March 1984.

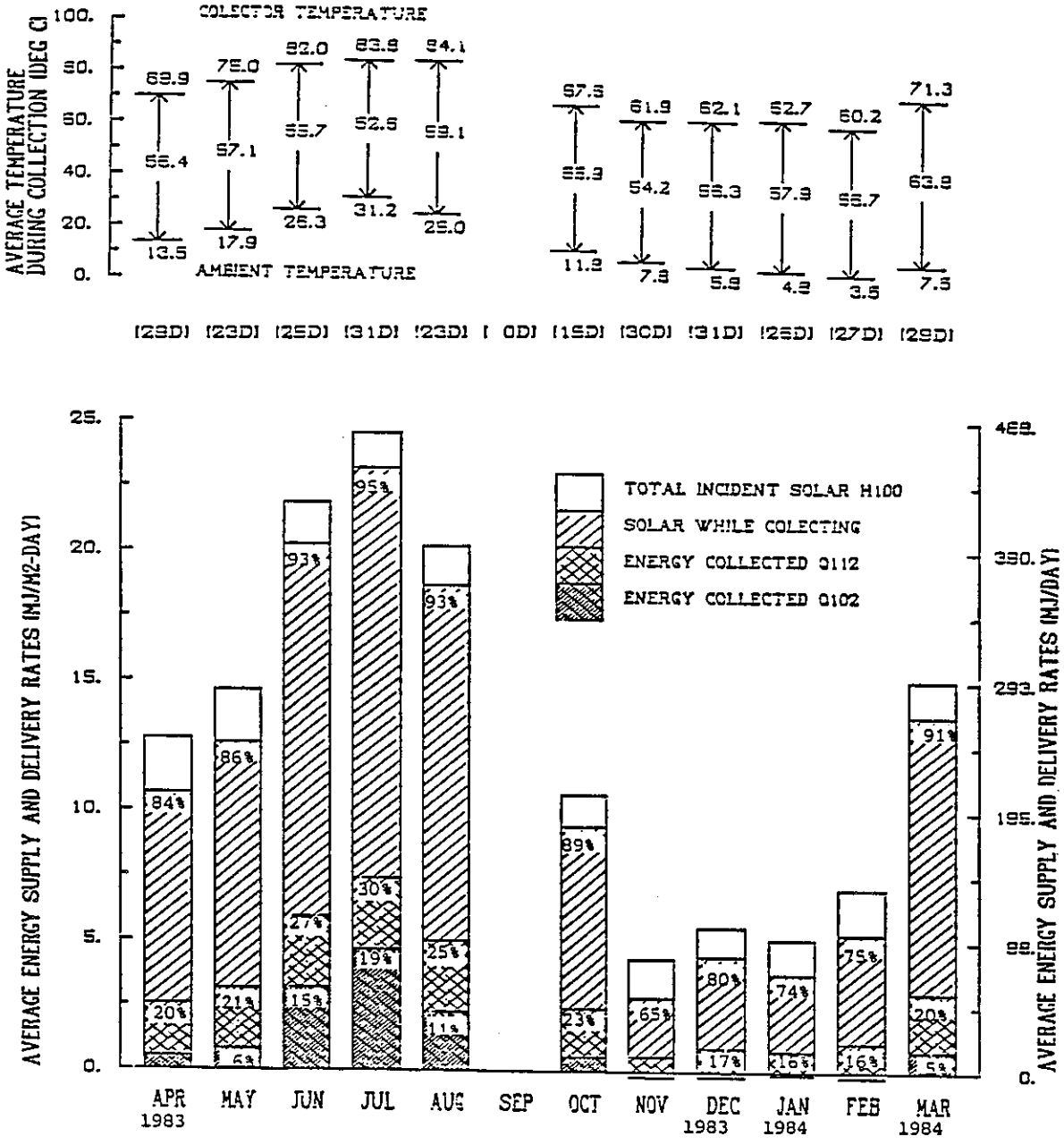

Figure 6.4-28. Average Energy Supply Rates for Sanyo Collector from Geneva, Switzerland, April 1983 to March 1984.

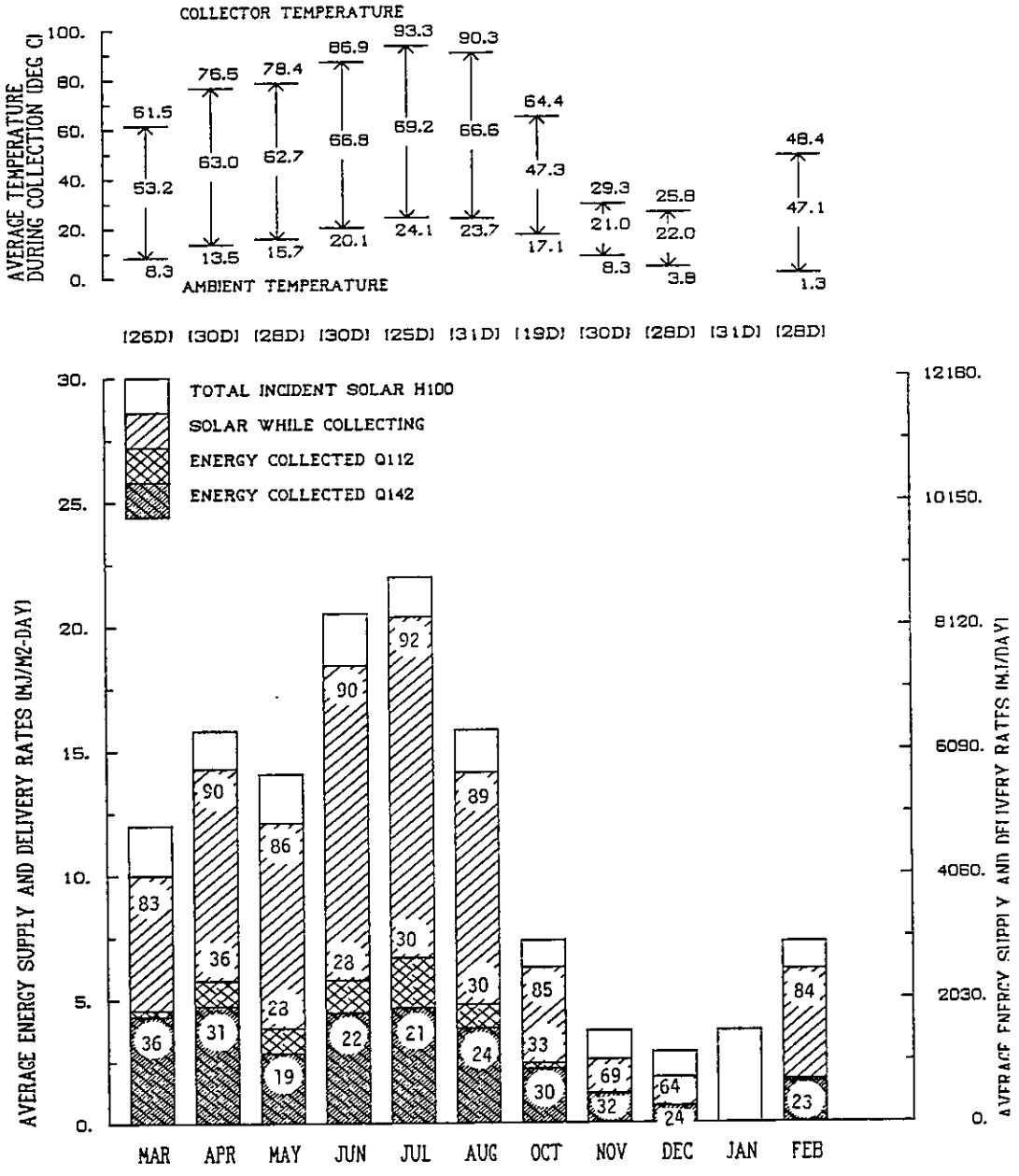

Figure 6.4-29. Average Energy Supply Rates for Cortec "D" Collector at Solarin, Hallau, Switzerland, 6 March 1984 to 28 February 1985.

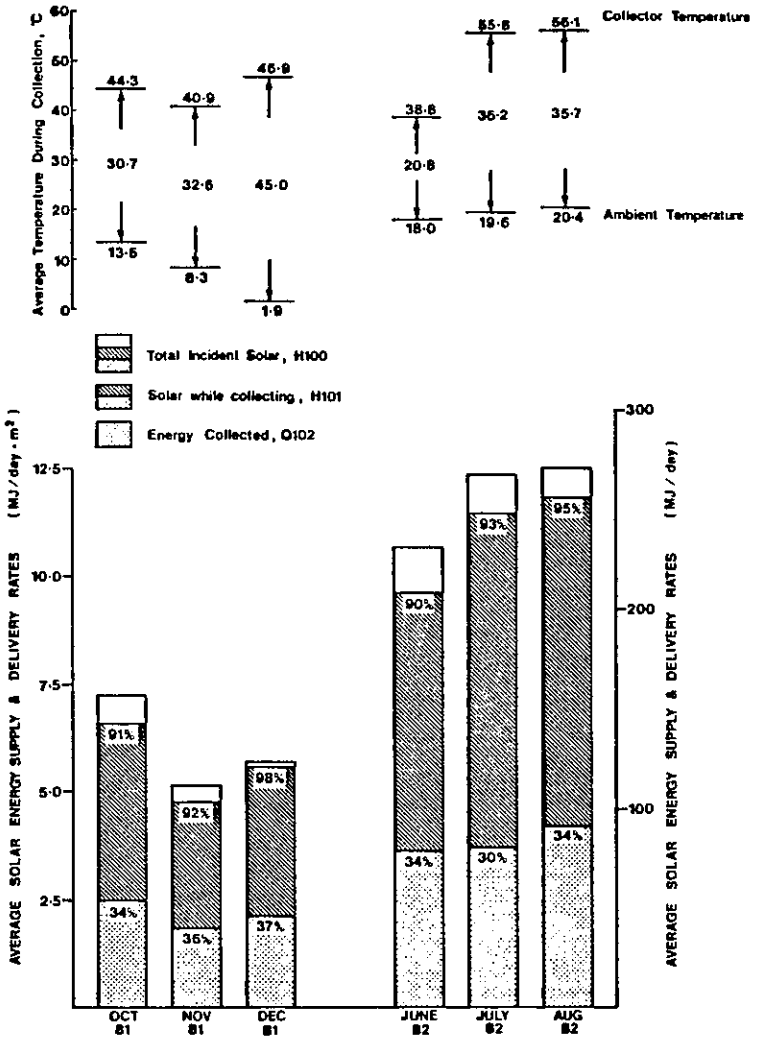

Figure 6.4-30. Average Energy Supply Rates for Philips VTR141 Collectors at BSRIA Solar Test Facility with Simulated Loads, United Kingdom, October 1981 to August 1982.

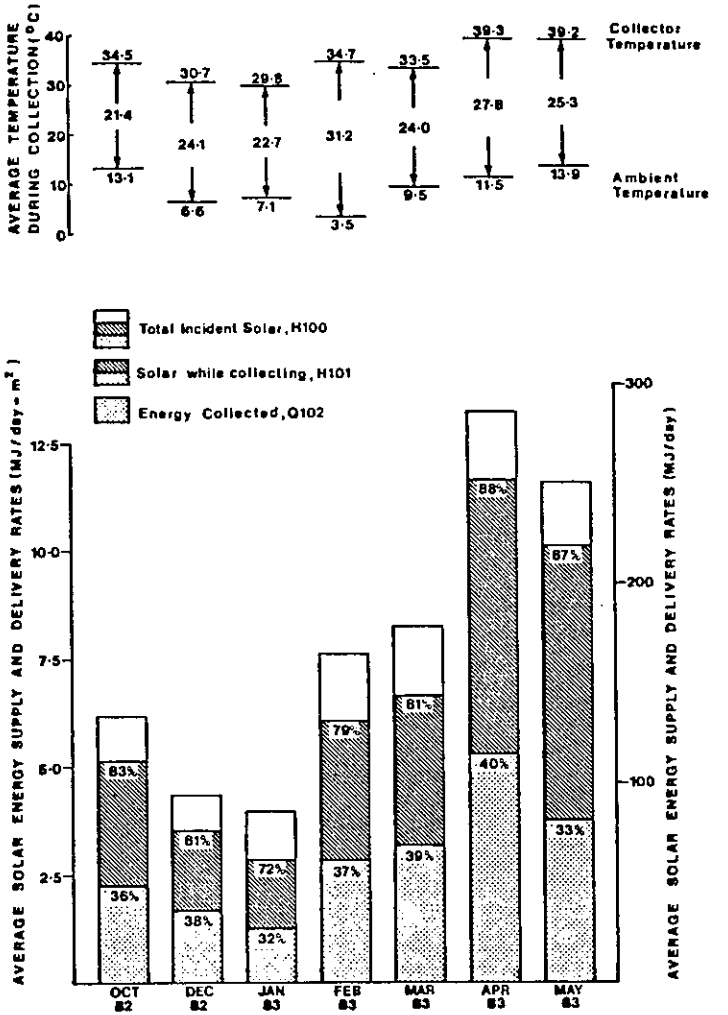

Figure 6.4-31. Average Energy Supply Rates for Philips VTR141 Collectors at BSRIA Solar Test Facility with Simulated Loads, United Kingdom, October 1982 to May 1983.

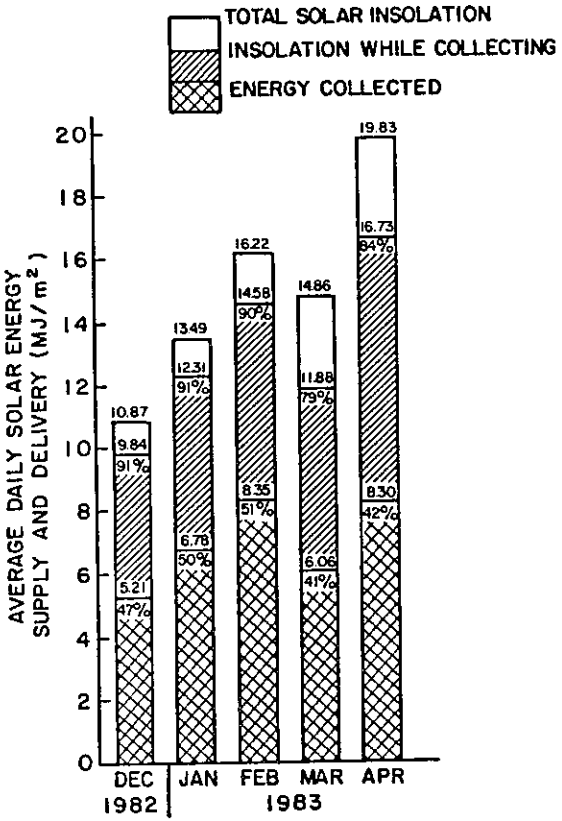

Figure 6.4-32. Average Energy Supply Rates for the Philips VTR 361 Collector at CSU Solar House I, December 1982 to April, 1983.

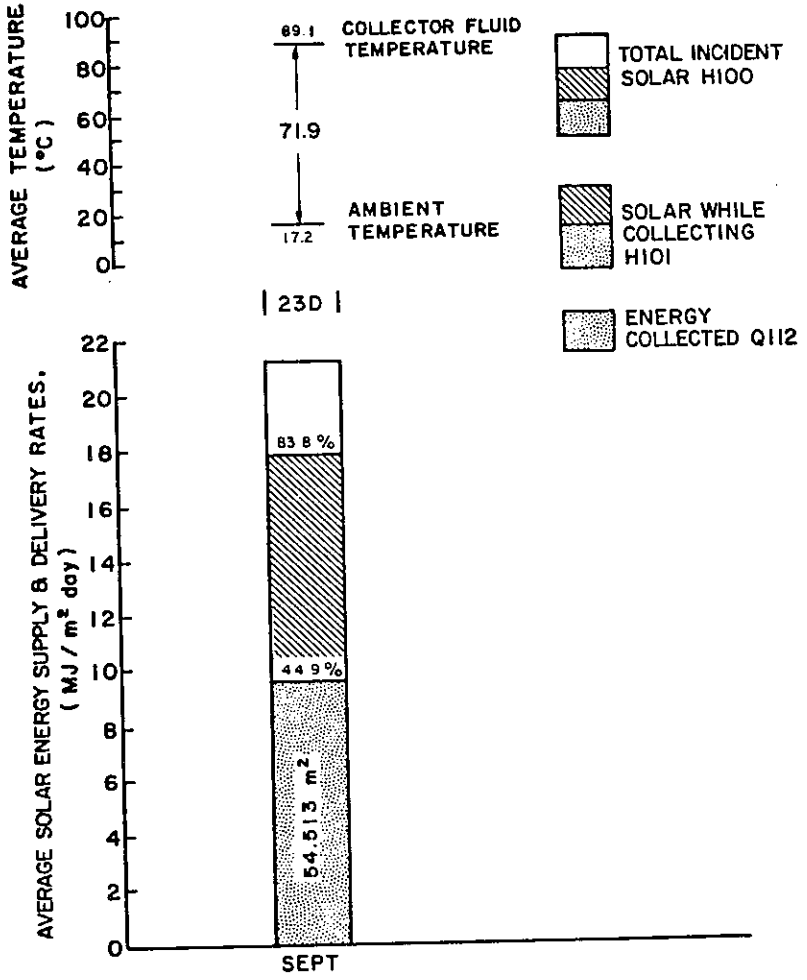

Figure 6.4-33. Average Energy Supply Rates for the Philips VTR-361 Collector at CSU Solar House I, December 1982 to CSU Solar House I, September 1983.

6.5 ENERGY USE BAR CHART

The energy use bar chart shows the solar and auxiliary energies which have met the space heating, cooling, and hot water demands.

6.5.1 The Sydney University Solar Heating and Cooling System, Sydney, Australia

Energy usage for the Sydney University system is shown in Figures 6.5-1 through 6.5-3. During cooling (December 1982 to January 1983) a high proportion of the energy driving the absorption cooling machine could be supplied by solar. 100 percent coverage of the heating load was achieved during July to September 1983. While the heating load during system operation using Yazaki flat-plate collectors is fairly typical (148 MJ/d), the low load in September coincides with spring weather conditions in Sydney with an almost negligible demand for heating.

Figures 6.5-3 through 6.5-5 show monthly energy use summaries for the period November 1983 to March 1985. Figure 6.5-3 indicates typical energy use rates during system cooling operation. Average daily energy use rates during the hottest months, December through February are between 250 to 300 MJ/d. The load drops off sharply in April. A very similar load pattern is shown for the 1984/85 cooling season (Figure 6.5-5).

Energy use rates during winter are given in Figure 6.5-4. The period May through October 1984 is characterized by relatively low energy use. The reasons are two-fold in that Sydney had a relatively mild winter in 1984 and the occupants in the air-conditioned rooms prefer colder working conditions. The amount of heat delivered to each room can be controlled by each room occupant by means of selecting the fan speed of the room's air-handling unit. Three of the four offices use a "low" fan speed setting and in some situations the fans are turned off altogether. The winter load of approximately 100 MJ/d is well below the average energy use during winter of around 150 MJ/d.

In order to avoid system operation near the boiling point during intermediate months with small loads (April, May, September, October), energy is dumped via the collectors at night. Dumped energy, however, is not accounted for in the energy use bar charts.

6.5.2 Mountain Spring Bottle Washing Facility, Edmonton, Canada

Energy use bar charts for the period 1 May 1982 to 31 December 1982 and 1 January 1983 to 31 December 1983 are shown in Figure 6.5-6 and 6.5-7 respectively.

Once again the operation of the solar system from November through March is not practical. The improved system performance during 1983 is readily apparent by the improved values of Q300.

The seasonal nature of the load is shown with peaks in June and December. The June peak reflects the increase in inventory to meet the additional consumption of soft drinks over the summer holiday. The December peak results from the Christmas season. Additionally, from November through March there is an increase in the load reflecting the necessity in heating the bottles from the cold outdoor ambient temperature to 65°C.

6.5.3 Ispra Solar Heated and Cooled Laboratory, Commission of European Communities

Since the only energy demand in the system of the Ispra Solar Laboratory is space cooling, the solar fraction is always equal 1 (no auxiliary energy is provided for) and thus these figures have been omitted.

6.5.4 Solarhaus Freiburg, Federal Republic of Germany

In Figures 6.5-8 and 6.5-9, the profile of the annual DHW load is displayed by monthly averages of the daily solar energy delivery and the daily auxiliary energy use. In the year 1982, the sequential operation of the Corning Glass collectors (January-May) and the Philips/Stiebel-Eltron collectors (June-December) resulted in a yearly solar contribution of 66.6 percent. This energy corresponds to a specific amount 1796 MJ/m^2 (499 kWh/m^2) of useful solar energy, based on a weighted aperture area of 31.1 m^2.

Although this specific value increased in the June 1982 to May 1983 period to 1847 MJ/m^2 (513 kWh/m^2), the solar fraction in this period was 63.4 percent due to poor radiation conditions in early 1983.

6.5.5 Eindhoven Technological University Solar House, The Netherlands

Because of the integration of the storage with the auxiliary natural gas burner, it is virtually impossible to discern the energy flows to hot water and space heating from measured data. A calculated chart will be given when the energy balance in the storage is better understood.

6.5.6 Knivsta District Heating System, Knivsta, Sweden

The load in the Knivsta district heating system is so much larger than the collector array energy output that the energy use bar chart will not be meaningful and will not br presented.

6.5.7 The Södertörn District Heating Project, Södertörn, Sweden

The load in the Södertörn district heating system is so much larger than the collector array energy output that the energy use bar chart will not be meaningful and will not be presented.

6.5.8 SOLARCAD Project, Geneva, Switzerland

Because the heat produced by solar is much smaller than the load of the Libellules district heating network, different scales are used in Figures 6.5-10 through 6.5-12. The scales differ by a factor of 100. Space heating and domestic hot water contributions cannot be distinguished in the district heating system.

The Sanyo and Corning collectors are presented separately even though they supply the same load. Average energy use rates expressed in MJ/day can be added up for overlapping periods.

The system output temperature is also the user (or the load) temperature.

Also see remarks on the efficiency plot, arrow diagram and bar charts in sections 6.1.8, 6.3.8, and 6.4.8.

6.5.9 SOLARIN Project, Hallau, Switzerland

Due to flowmeter failures, results are available only for the solar loop and not for the entire system. See section 5.9.2.

6.5.10 Evacuated Collector System Test Facility, Bracknell, United Kingdom

The energy use bar charts for the three experimental periods are given in Figures 6.5-13 and 6.5-14 and present the percentage solar contribution to the load subdivided into space and hot water heating categories. Some loads were not representative of a realistic space heating load profile, but the data was used for mathematical model validation exercises. However, most load profiles and weather conditions are fairly typical for a small family house in the UK with the hot water load perhaps a little too low. The solar contribution varied from 12 percent in December 1982 to 51 percent and 53 percent in April and May 1983 respectively. Only mean midnight storage temperatures are given as mean storage temperatures are not readily available. Midnight storage temperatures are likely to be an average of the minimum storage temperatures and thus somewhat depressed from the average.

6.5.11 Colorado State University Solar House I, United States

Energy used for winter and summer periods for heating and cooling Solar House I are shown in Figures 6.5-15 and 6.5-16. The high percentage of solar heating in December, January, and February indicate that collector area is too large for the load experienced in Solar House I for this particular period. Collector area was reduced by one-half in March. Solar cooling load represented in Figure 6.5-16 is atypical because September is not a warm month in Fort Collins. As explained previously, experimental difficulties with phase-change storage prevented normal system operation during the summer months.

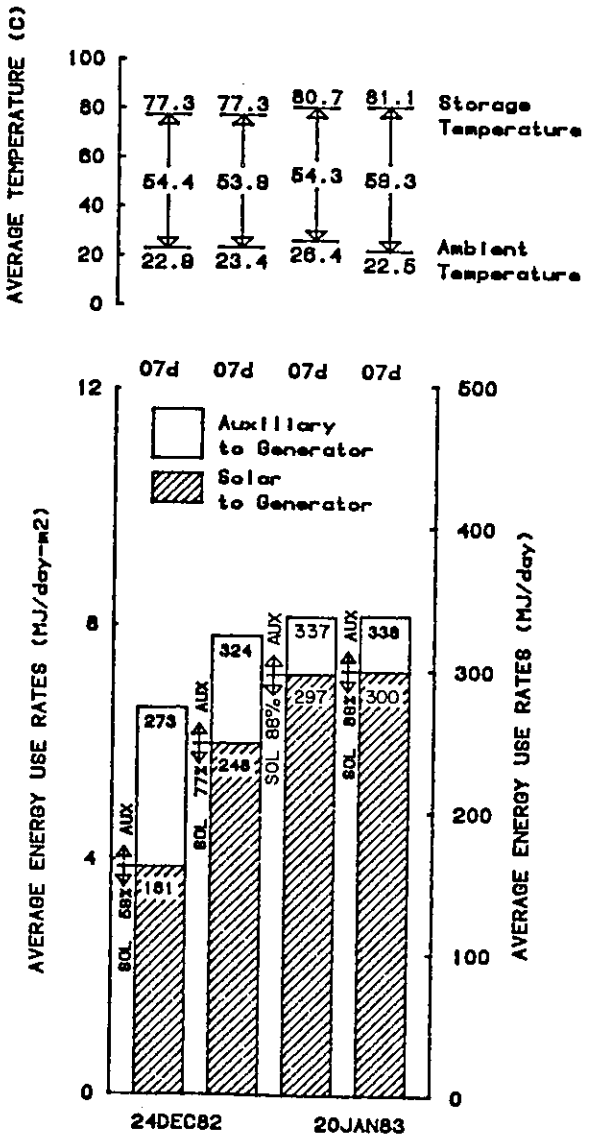

Figure 6.5-1. Average Energy Use Rate for Sydney University Evacuated Tubular Collector at Sydney, Australia, 24 December to 20 January 1983.

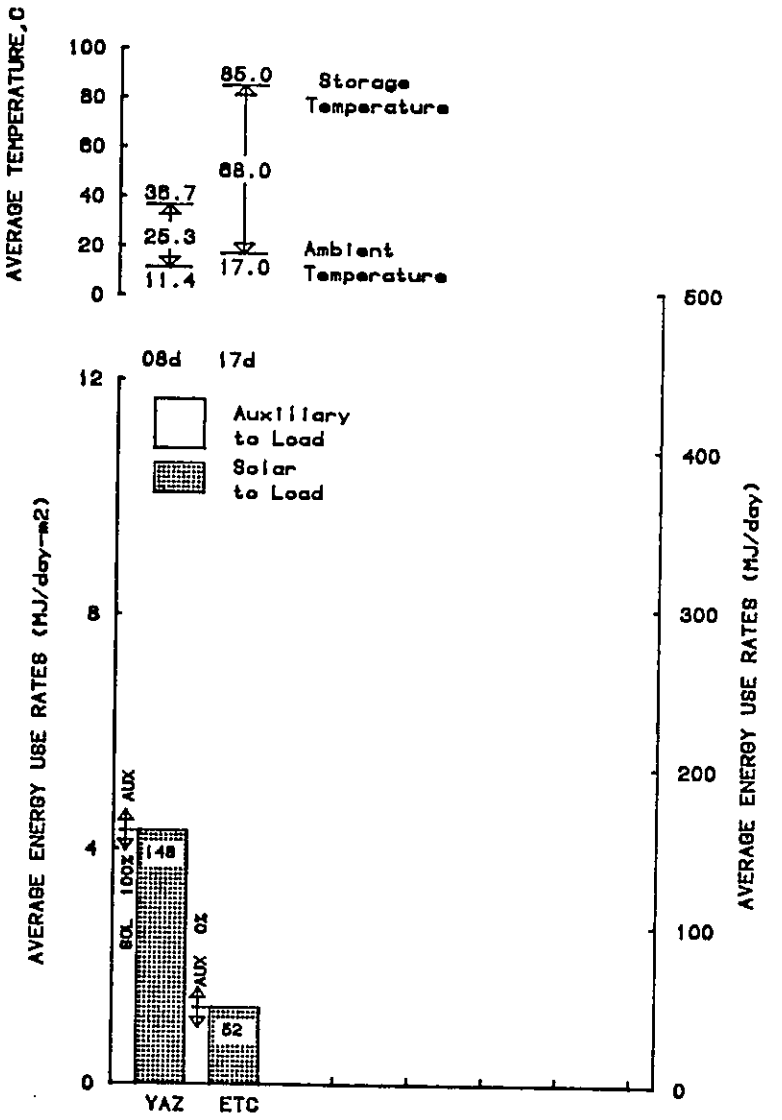

Figure 6.5-2. Average Energy Use Rate for Sydney University Flat-Plate Collector at Sydney, Australia, 8 July 1983 to 28 September 1983.

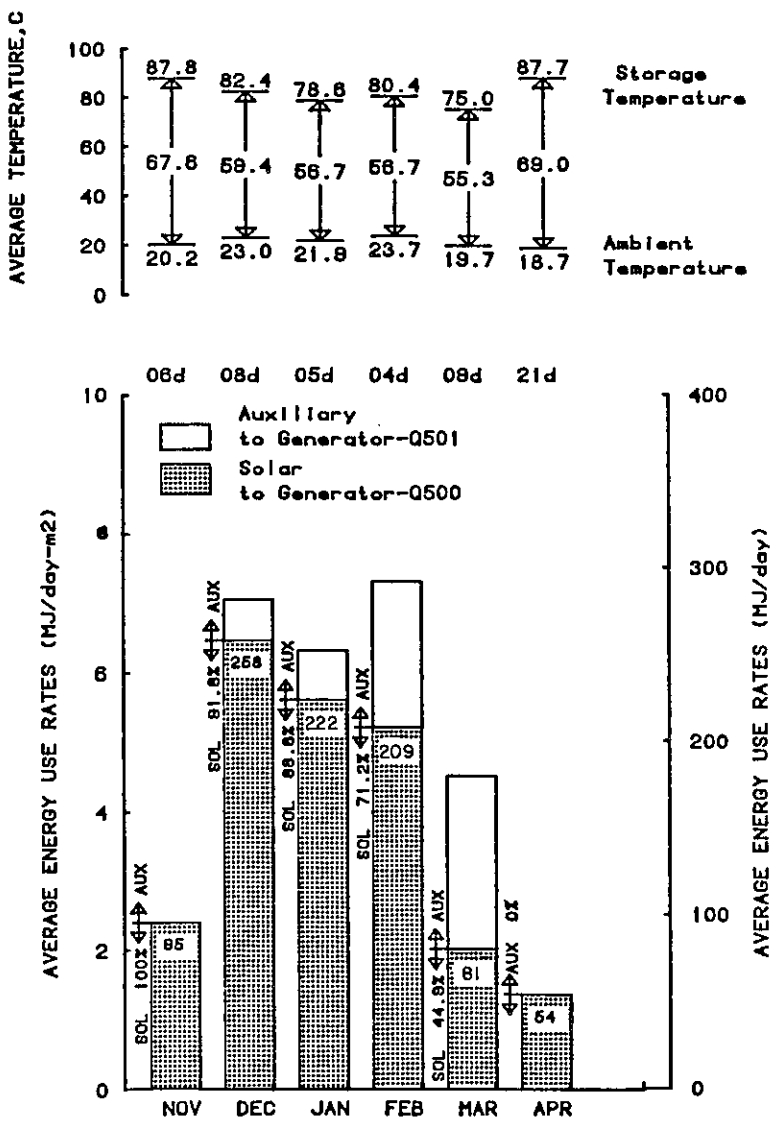

Figure 6.5-3. Average Energy Use Rate for Sydney University Evacuated Collector at Sydney, Australia, 1 November 1983 to 30 April 1984.

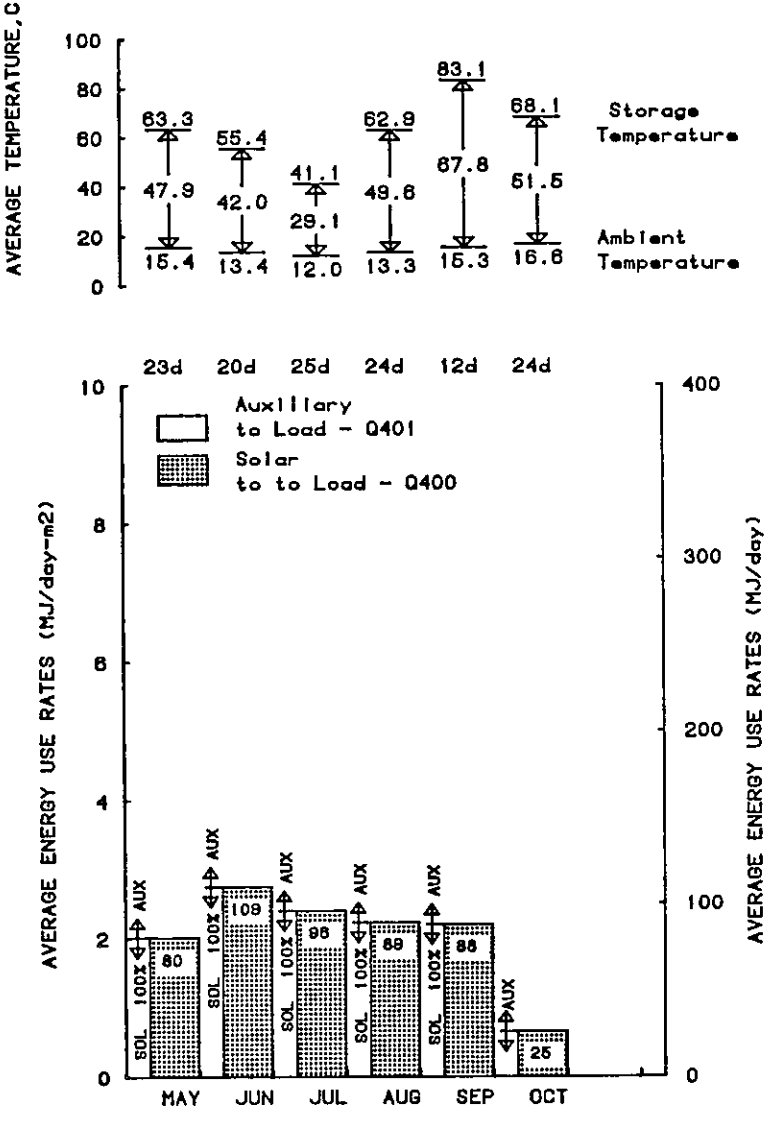

Figure 6.5-4. Average Energy Use Rate for Sydney University Flat-Plate Collector at Sydney, Australia, 1 May 1984 to 31 October 1984.

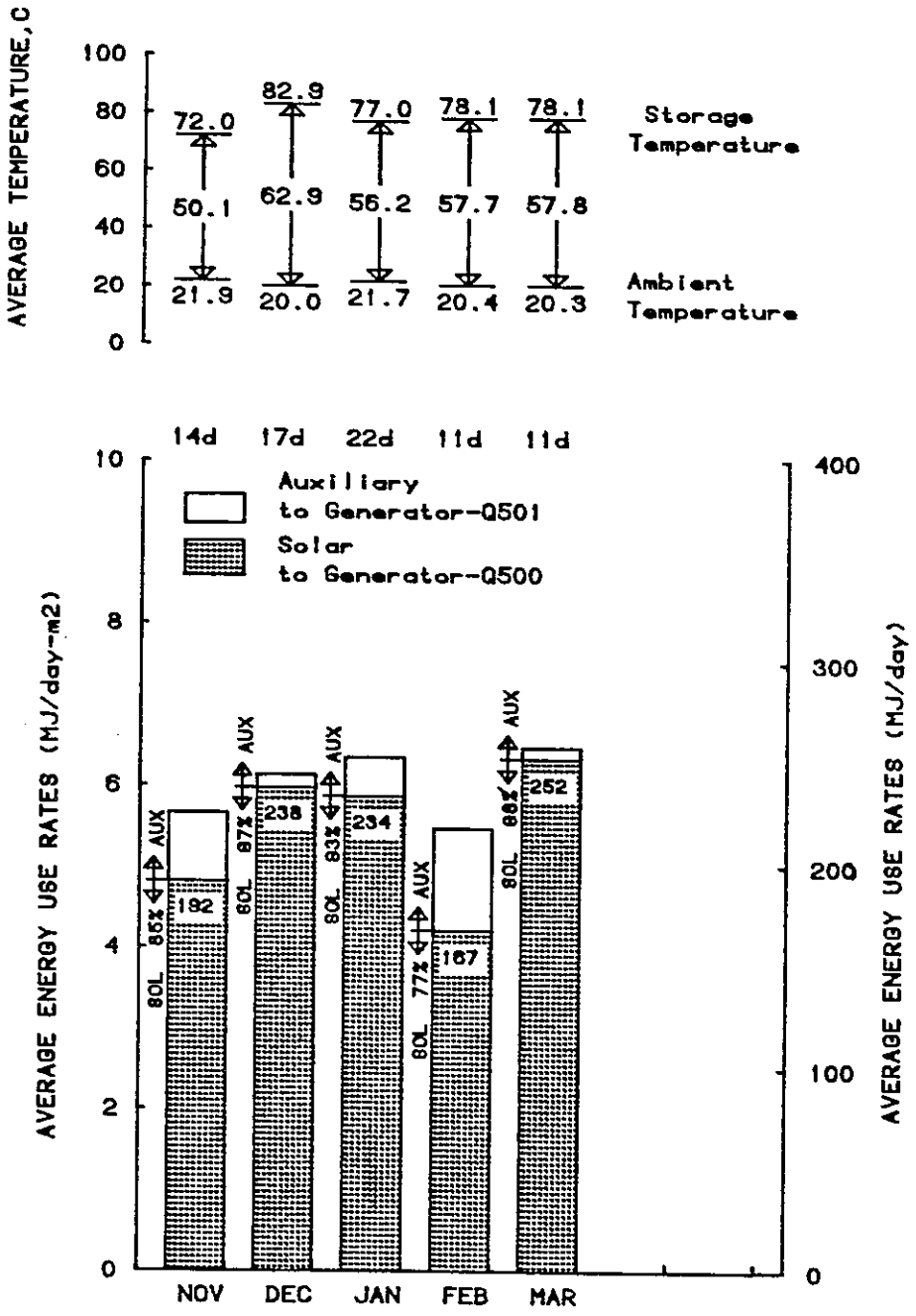

Figure 6.5-5. Average Energy Use Rate for Sydney University Flat-Plate Collector at Sydney, Australia, 1 November 1984 to 31 March 1985.

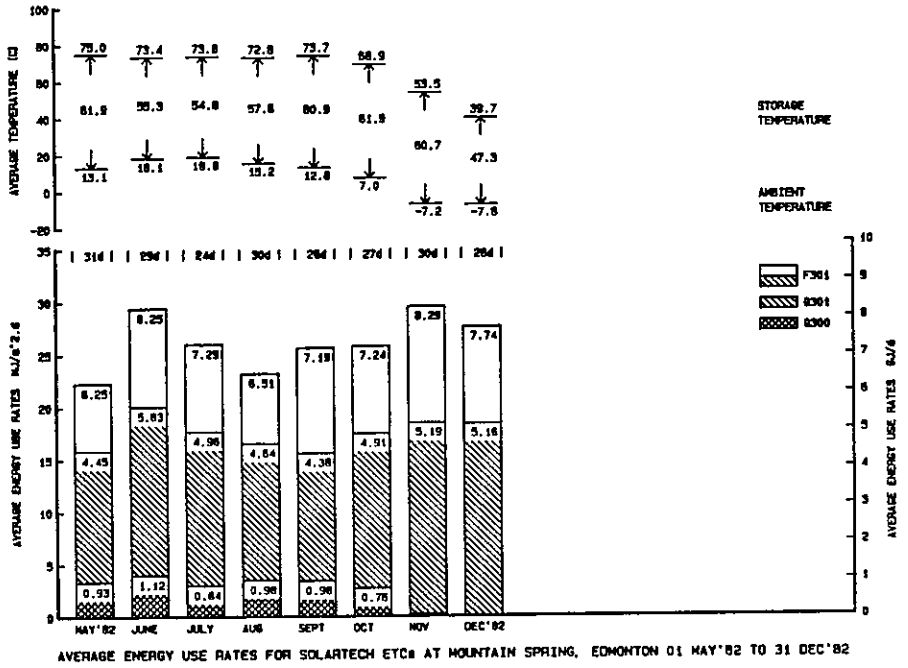

Figure 6.5-6. Average Energy Use Rate for Solartech Evacuated Tube Collectors at Mountain Spring, Edmonton, Canada, 1 May 1982 to 31 December 1982.

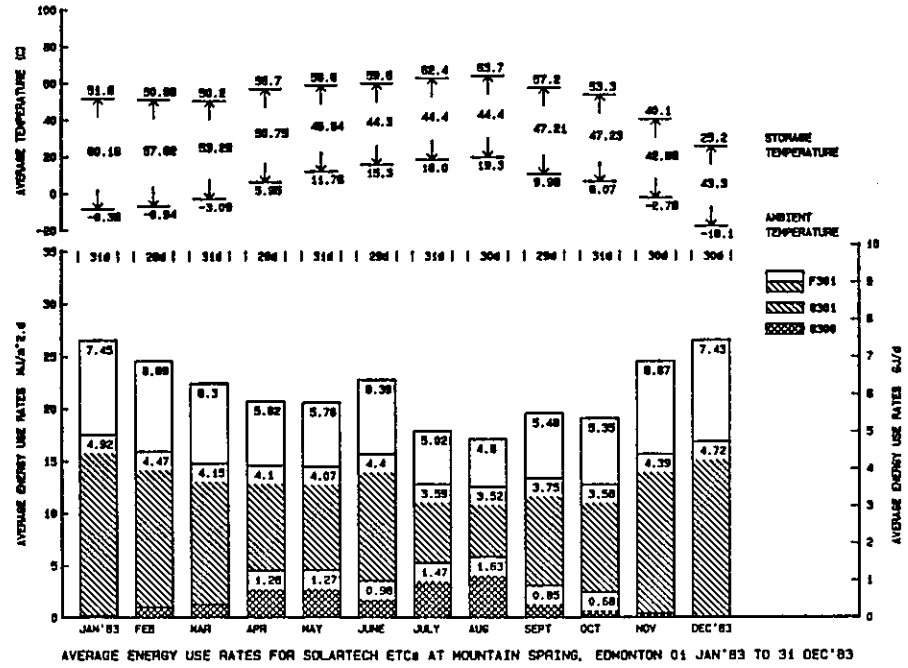

Figure 6.5-7. Average Energy Use Rate for Solartech Evacuated Tube Collectors at Mountain Spring, Edmonton, Canada, 1 January 1983 to 31 December 1983.

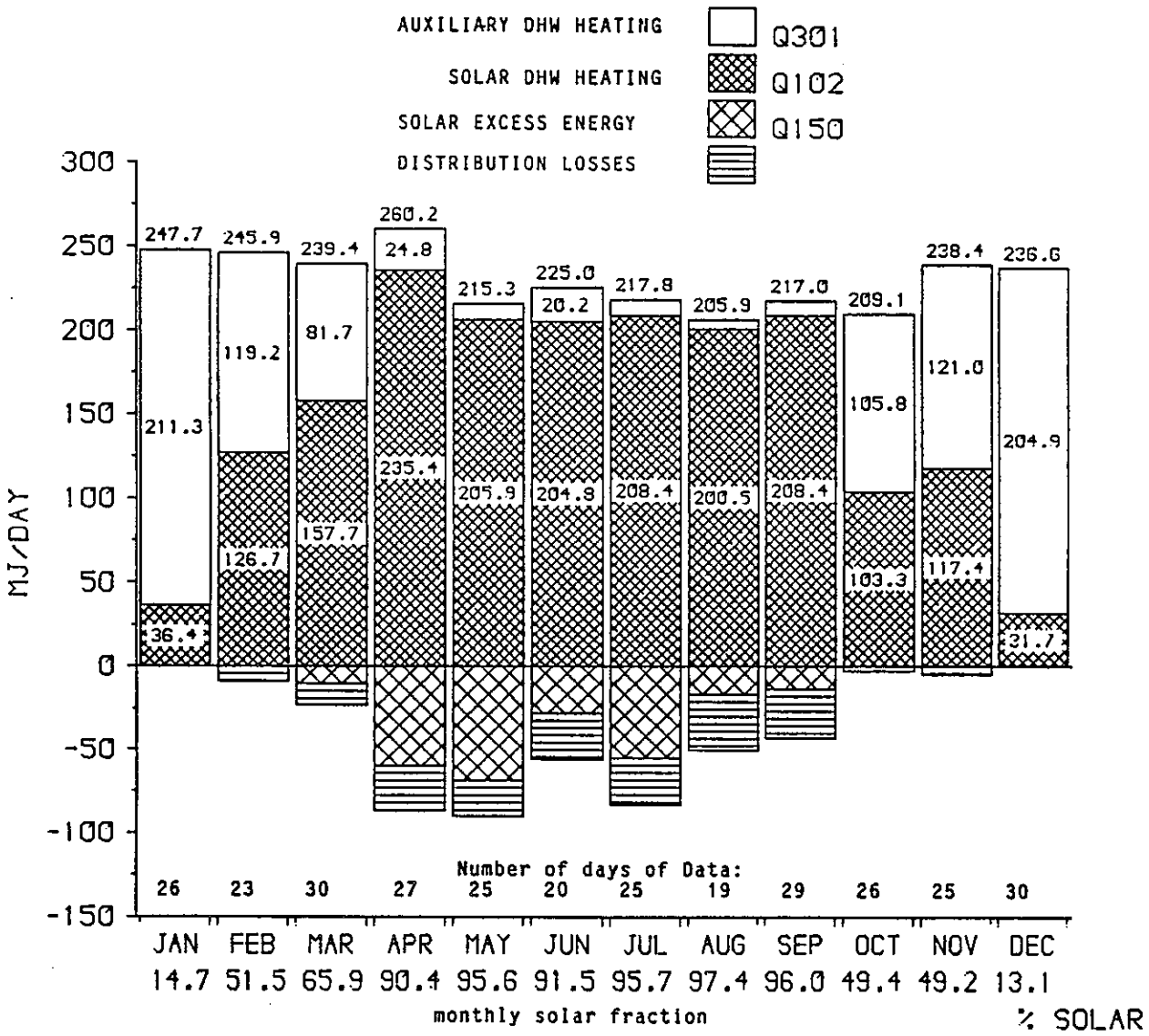

Figure 6.5-8. Average Solar Energy Use Rate of the Domestic Hot Water System at Solarhaus Freiburg (with sequential operation of the Corning Glass and Philips/Stiebel-Eltron Collectors), Federal Republic of Germany, 1982.

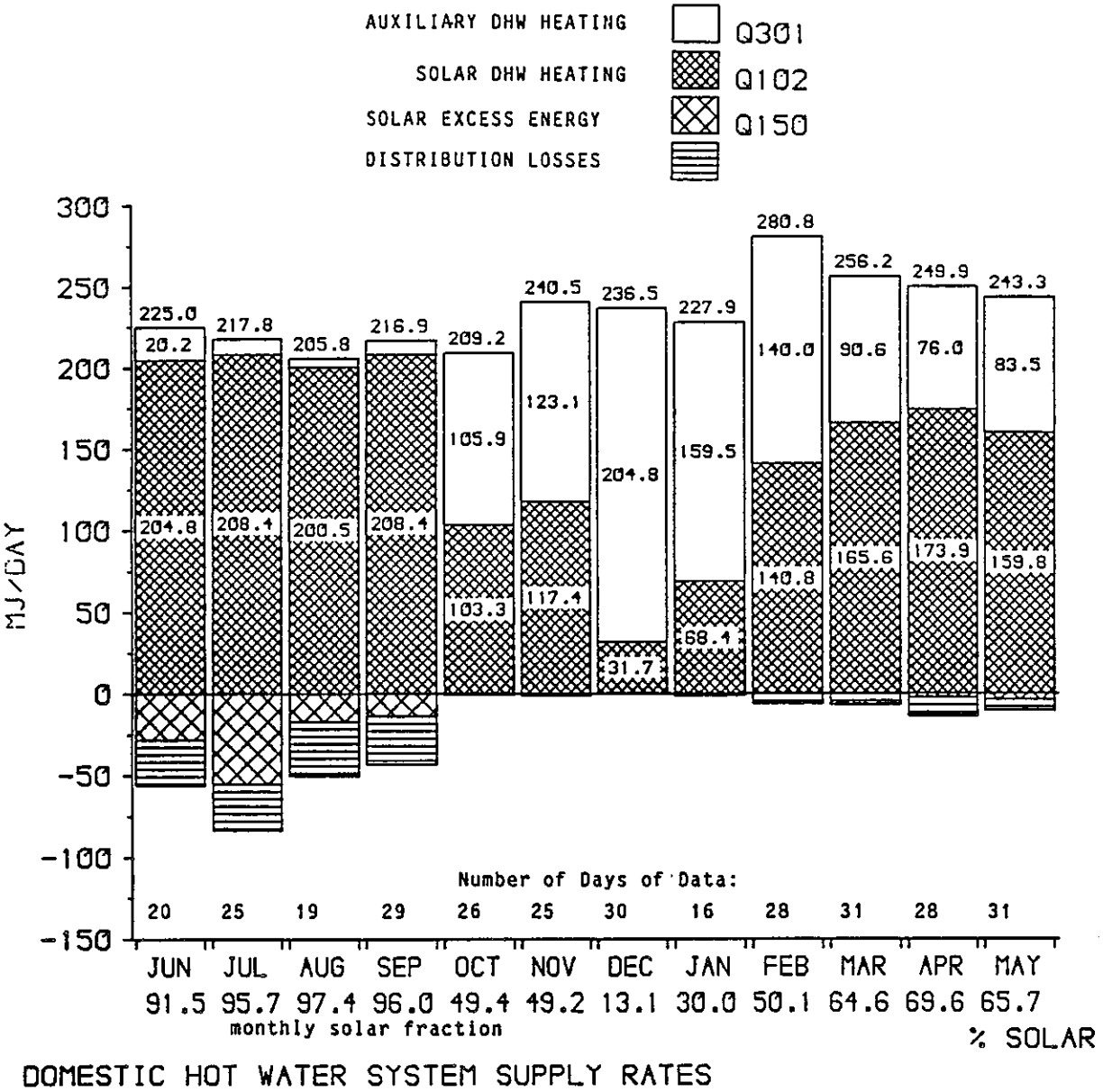

Figure 6.5-9. Average Solar Energy Use Rate of the Domestic Hot Water System at Solarhaus Freiburg with operation of the Philips/Stiebel-Eltron Collectors), Federal Republic of Germany, June 1982 to May 1983.

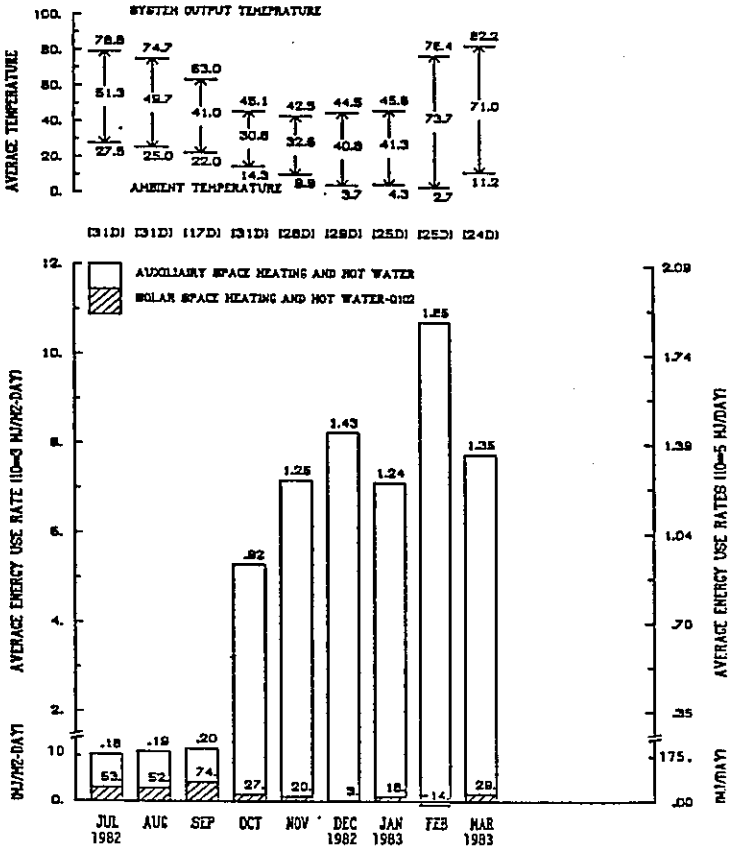

Figure 6.5-10. Average Energy Use Rate for Corning A+B Measurements Geneva, Switzerland, July 1982 to September 1983.

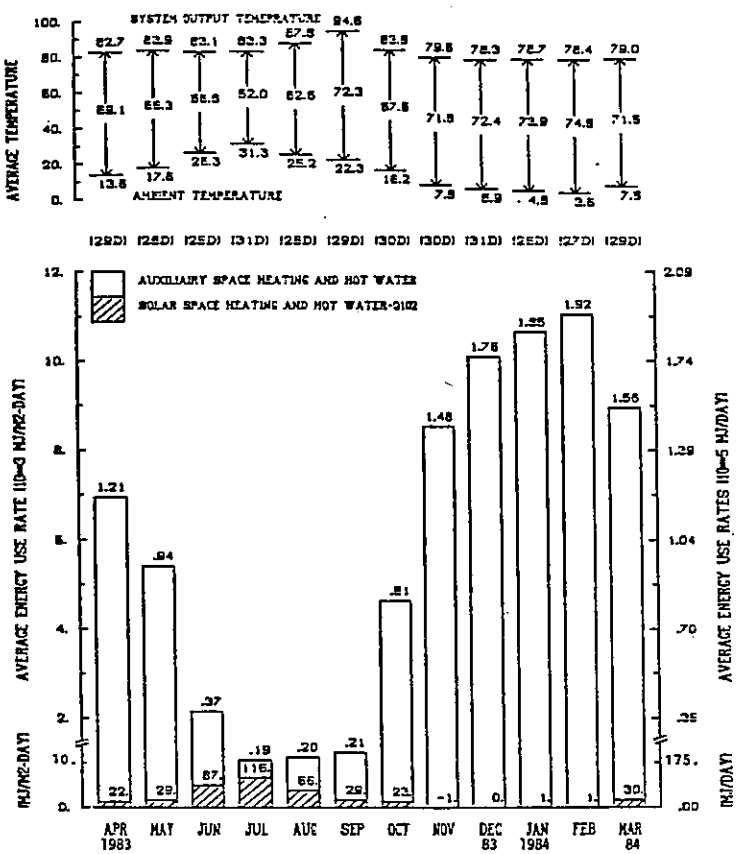

Figure 6.5-11. Average Energy Use Rate for Corning A+B Measurements Geneva, Switzerland, April 1983 to March 1984.

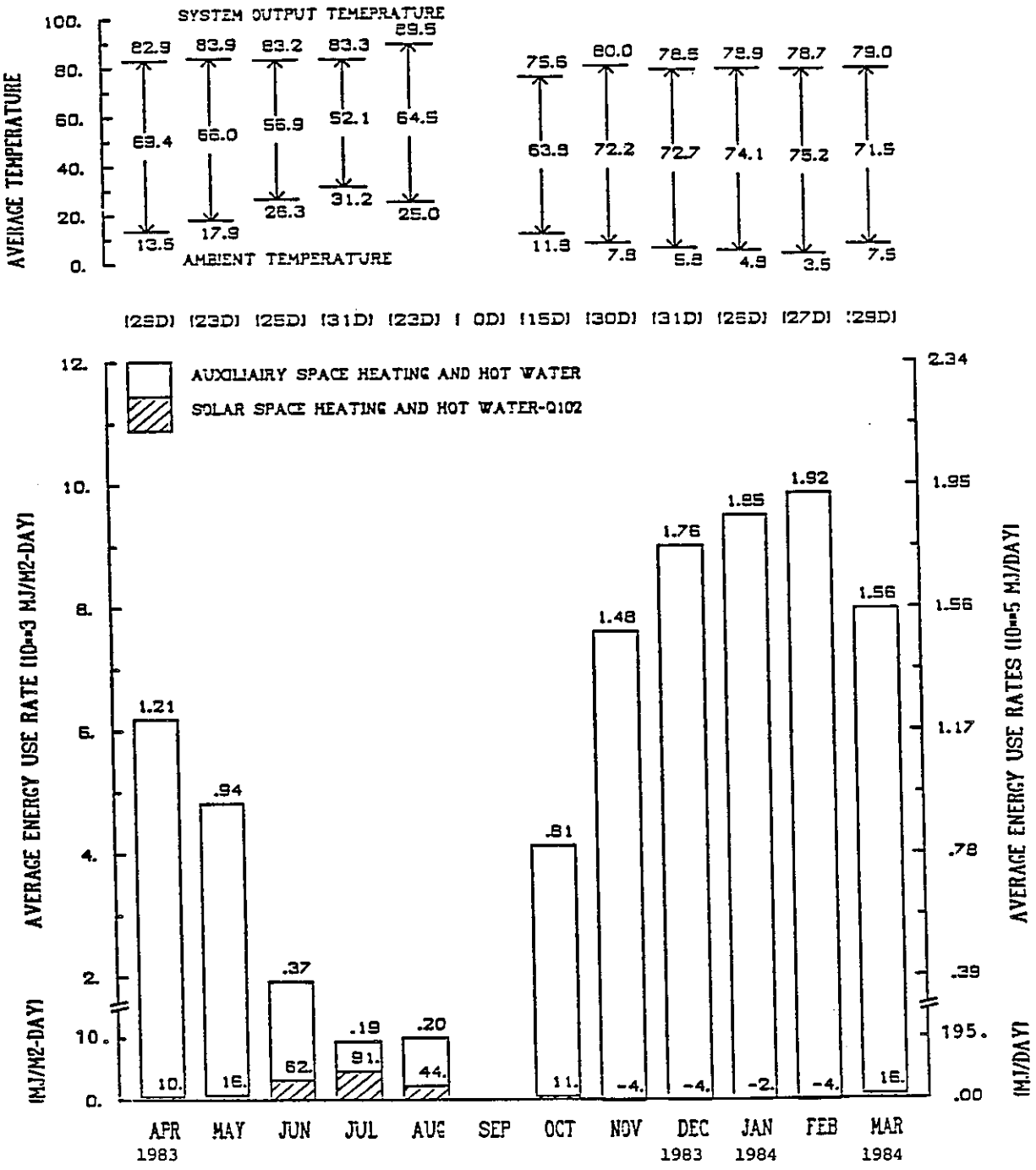

Figure 6.5-12. Average Energy Use Rate for Sanyo Measurements Geneva, Switzerland, April 1983 to March 1984.

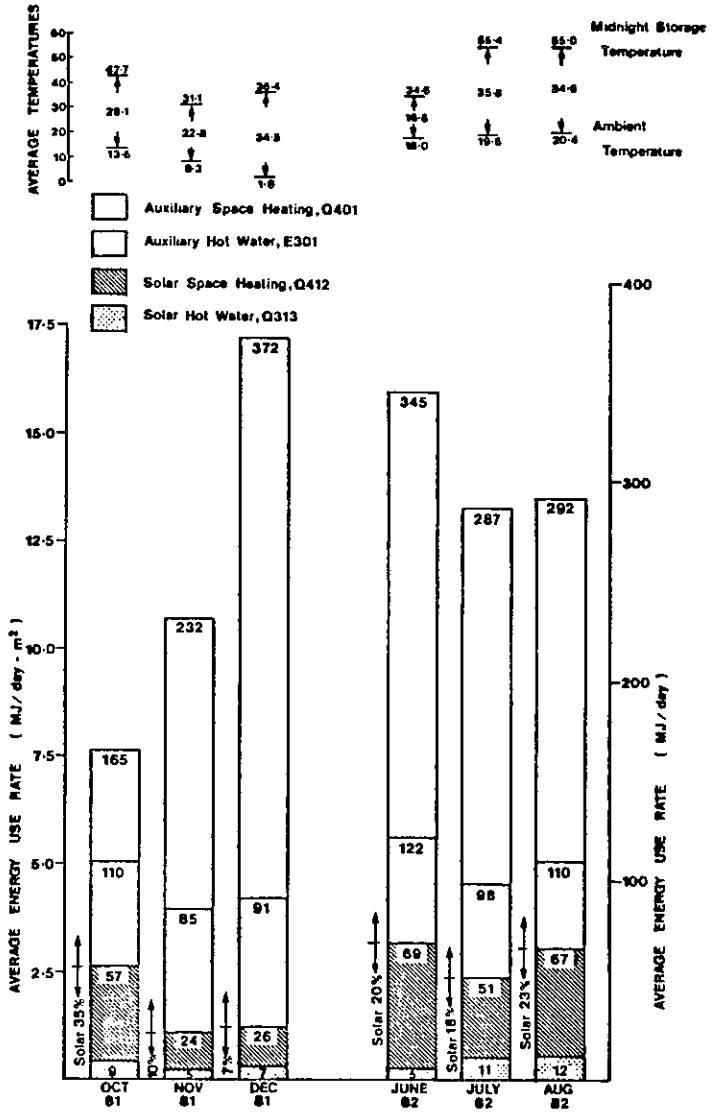

Figure 6.5-13. Average Energy Use Rate for Philips VTR151 Collectors at BSRIA Solar Test Facility with Simulated Loads. United Kingdom, UK-HTG-2, October 1981 to August 1982.

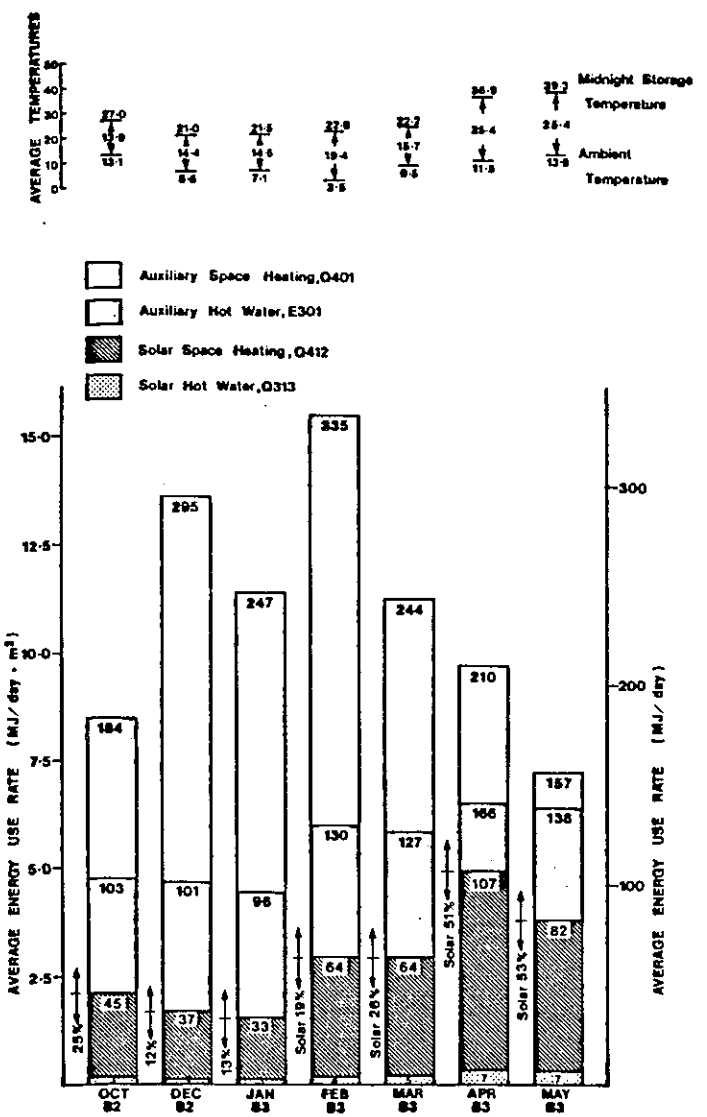

Figure 6.5-14. Average Energy Use Rate for Philips VTR151 Collectors at Bracknell Solar Test Facility with Simulated Loads, United Kingdom, October 1982 to May 1983.

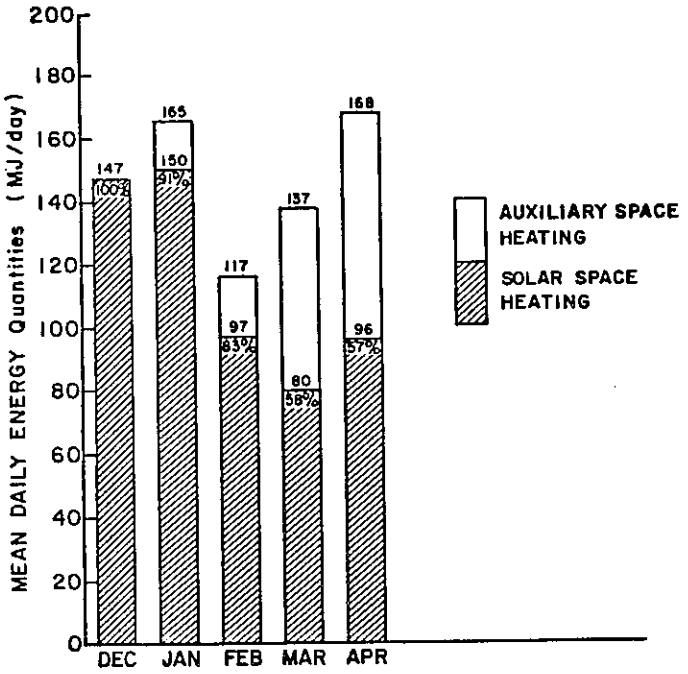

Figure 6.5-15. Energy Use for Space Heating, CSU Solar House I, Winter 1983.

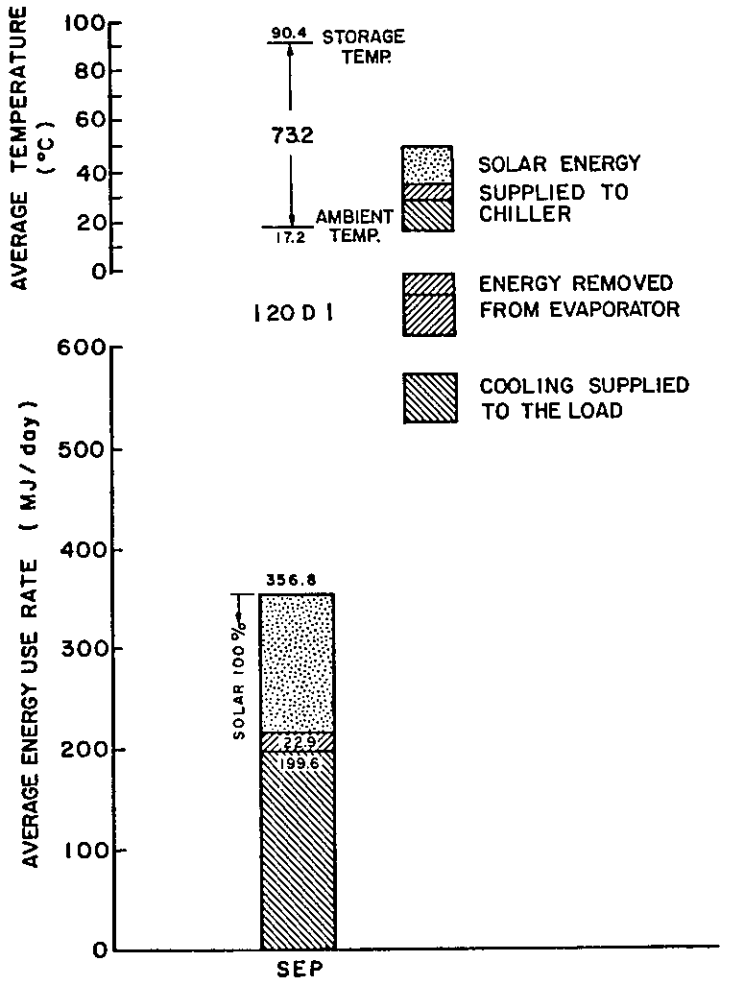

Figure 6.5-16. Energy Use for Cooling, CSU Solar House I, September 1983.

6.6 SYSTEMS EFFICIENCIES AND SOLAR FRACTIONS

Monthly systems efficiencies and solar fractions are provided in this section. Systems efficiency is the solar energy provided to the load divided by the solar energy falling on the collector aperture. Solar fraction is solar energy provided to the load divided by total load.

6.6.1 Sydney University Solar Heating and Cooling System, Sydney, Australia

Histograms of average monthly system efficiency and solar fraction are given in Figures 6.6-1 through 6.6-5.

Average monthly system efficiency during the intermediate months does not represent true system performance since loads are very small.

The first plot for cooling, Figure 6.6-1, covers four weeks in December 1982 through January 1893. The diagram for heating, Figure 6.6-2, is divided into two sections: 1. the operational period using Yazaki flat-plate collectors and 2. the period where Sydney University evacuated tubular collectors were used in the collection subsystem. The system efficiency drops sharply during evacuated tubular collector operation in August/ September 1983 due to the low loads. Similar graphs covering the period November 1983 to March 1985 are given in Figures 6.6-3 through 6.6-5.

6.6.2 Mountain Spring Bottle Washing Facility, Edmonton, Canada

Average monthly system efficiencies and solar fractions for the period 1 May 1982 to 31 December 1982, 1 January 1983 to 31 December 1983 and 1 January 8, 1984 to 30 November, 1984 are shown in Figures 6.6-6 through 6.6-8.

Once again the operation of the solar energy system from November through March is readily seen to be not practical. The improved system performance during 1983 is apparent by the improved values of Q300.

The seasonal nature of the load is shown with peaks in June and December. The June peak reflects the increase in inventory to meet the additional consumption of soft drinks over the summer holidays. The December peak results from the Christmas season. Additionally, from November through March there is an increase in the load reflecting the necessity in heating the bottles from the cold outdoor ambient temperature to 65^{o}C. The decrease in soft drink market is apparent from the reduction in the average height of the bars over the three years of data presented.

6.6.3 Ispra Solar Heated and Cooled Laboratory, Commission of European Communities

Since the only energy demand in the system of the Ispra Solar Laboratory is space cooling and solar fraction is always equal 1 (no auxiliary energy is provided for) these figures have been omitted.

6.6.4 Solarhaus Freiburg, Federal Republic of Germany

Figures 6.6-9 and 6.6-10 show the annual variation of the system efficiency for the solar DHW system together with the monthly solar fraction of the DHW load. The system operates with the highest system efficiency (47 to 50 percent) in the spring and fall season, when sufficient radiation is available and all collected energy can be used in the system. In mid-summer, system efficiency tends to decrease to values of about 37 to 39 percent due to the production of excess energy, although the collection efficiency remains at a rather high level of 52 to 54 percent.

6.6.5 Eindhoven Technological University Solar House, The Netherlands

No figures are presented.

6.6.6 Knivsta District Heating System, Knivsta, Sweden

Figures 6.6-11 through 6.6-16 show the average monthly system efficiency data for the Knivsta District Heating System. The solar fraction is less than 7 percent in this test system and is therefore not shown in the graphs.

6.6.7 The Södertörn District Heating Project, Södertörn, Sweden

Figures 6.6-17 through 6.6-21 show the average monthly system efficiency. The solar fraction is so low in this test system that the curve has been excluded. There is no drastic drop in efficiency when changing from 60°C to 80°C operation.

6.6.8 SOLARCAD Project, Geneva, Switzerland

Two experiments are presented separately in Figures 6.6-22, 6.6-23 and 6.6-24 even though they supply energy to the same load. Solar fraction can be added up for overlapping periods. Negative energy to the load occurs in some winter months due to pipe and capacitance losses. Refer to the remarks on the efficiency plot and arrow diagram in sections 6.1.8, 6.3.8, and 6.4.8.

6.6.9 SOLARIN Project, Hallau, Switzerland

Due to flowmeter failures, results are available only for the solar loop and not for the entire system. Refer to section 5.9.2.

6.6.10 Bracknell Solar Test Facility with Simulated Loads, United Kingdom

Average monthly system efficiency for the 1982/83 heating season is given and integrated over the heating season yields 36.8 percent and for the same period a solar fraction of 28.5 percent was yielded. Figure 6.6-25 is largely self-explanatory, since the space heating load reduces in the spring coincidental with increased radiation, the solar fraction and storage temperatures increase and the system efficiency decreases due mainly to storage losses, whereas for flat-plate collectors the system efficiency would drop-off rather more in the late spring.

6.6.11 Colorado State University Solar House I, United States

Monthly system efficiencies and system fractions for the winter season are shown in Figure 6.6-26. The low average monthly system efficiency of 18 percent for the winter season, was due in large part to the over-sized collector array, where a substantial portion of the collected heat was rejected to the atmosphere. High solar fractions for the coldest months of the year are indicated. After reducing the array area by 50 percent, system efficiency improved, but during each month of March and April, heat was still being rejected because the load also decreased.

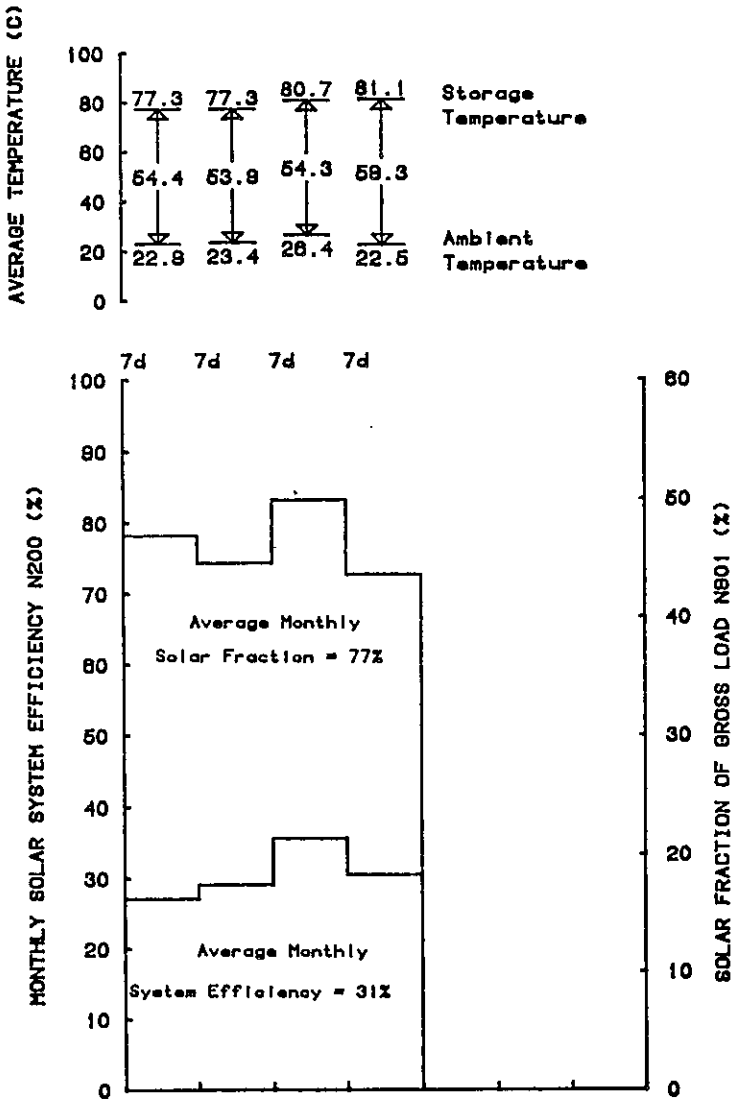

Figure 6.6-1. Average Monthly System Efficiency and Solar Fraction for Sydney University Evacuated Collectors at Sydney, Sydney, Australia, December 1982 to January 1983.

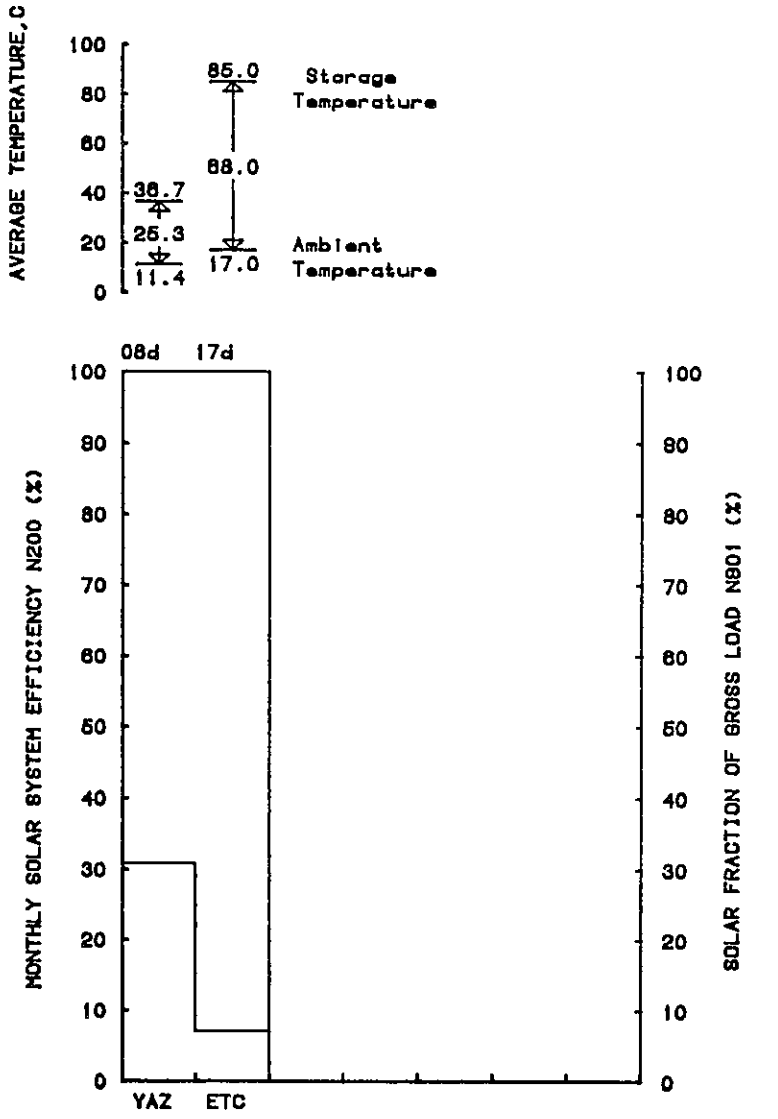

Figure 6.6-2. Average Monthly System Efficiency and Solar Fraction for Sydney University Flat-Plate Collectors at Sydney, Australia, 8 July 1983 to 28 September 1983.

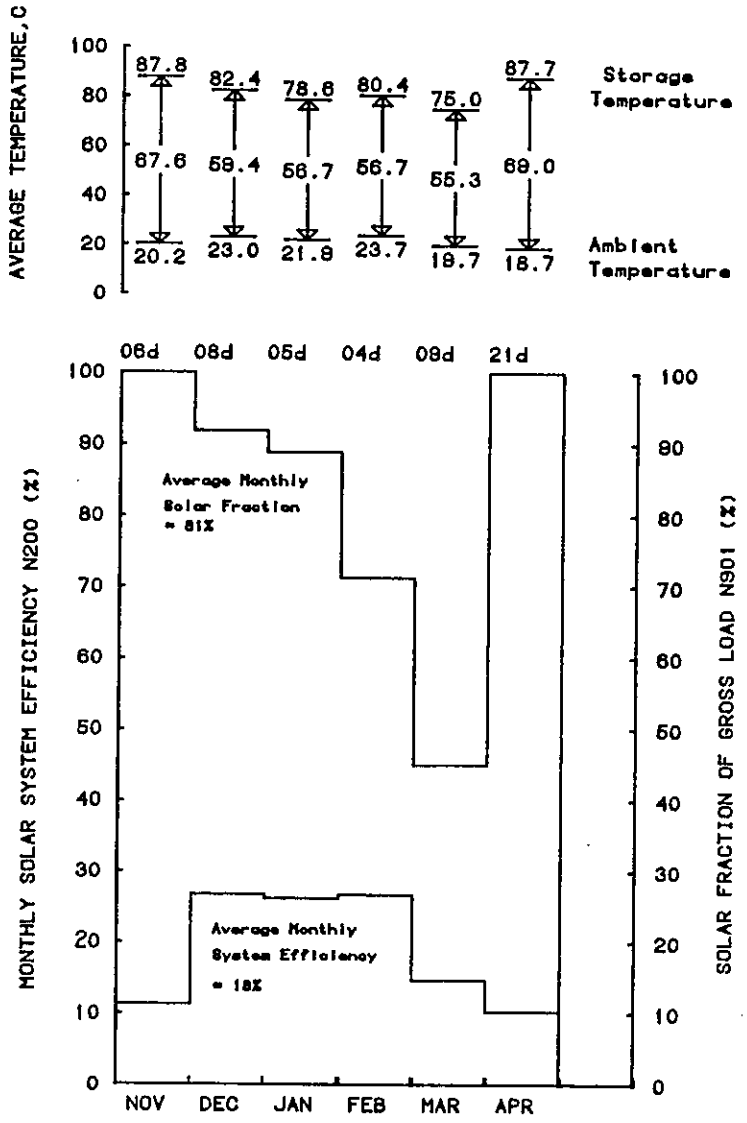

Figure 6.6-3. Average Monthly System Efficiency and Solar Fraction for Sydney University Evacuated Collectors at Sydney, Australia, 1 November 1983 to 30 April 1984.

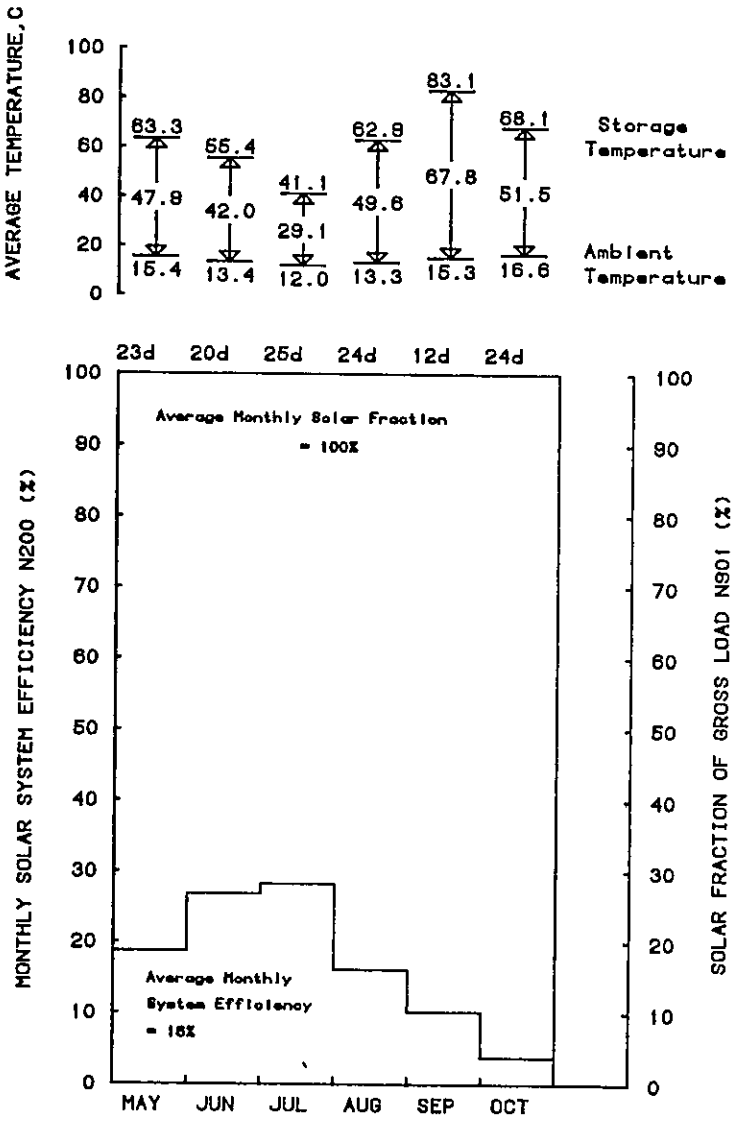

Figure 6.6-4. Average Monthly System Efficiency and Solar Fraction for Sydney University Evacuated Collectors at Sydney, Australia, 1 May 1983 to 31 October 1984.

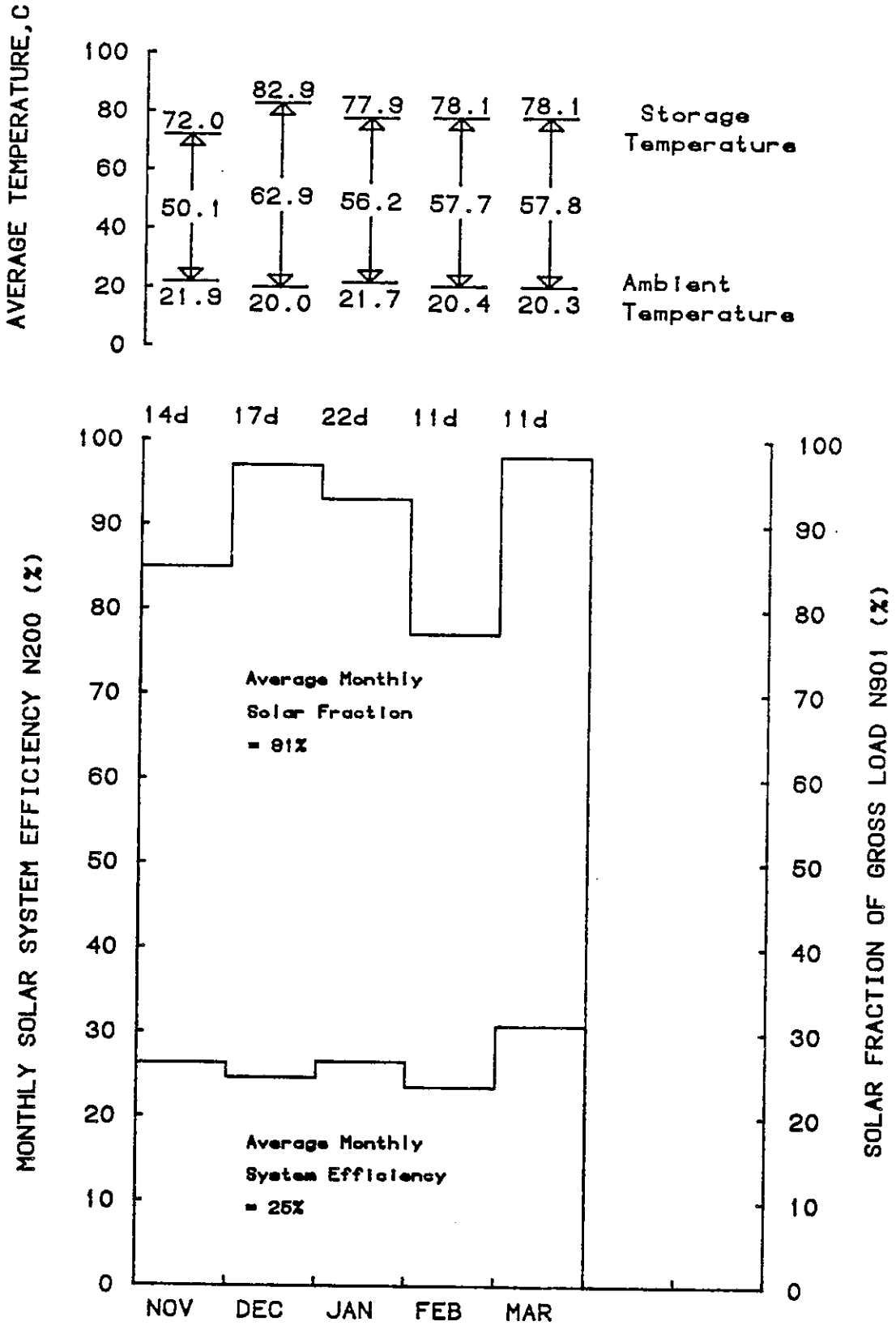

Figure 6.6-5. Average Monthly System Efficiency and Solar Fraction for Sydney University Evacuated Collectors at Sydney, Australia, 1 November 1984 to 31 March 1985.

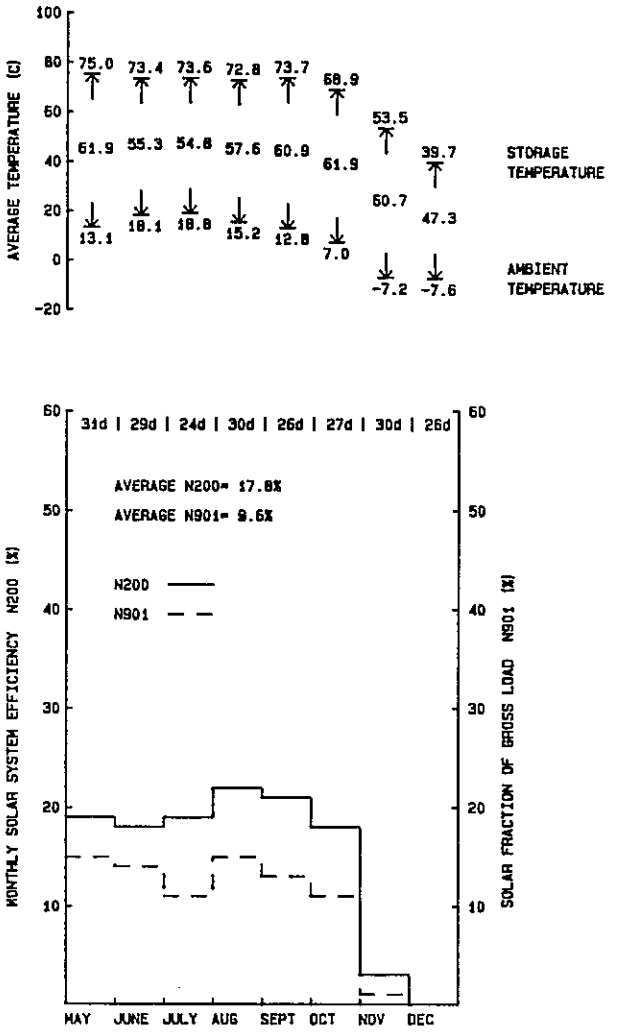

Figure 6.6-6. Average Monthly System Efficiency and Solar Fraction for Solartech ETCs at the Mountain Spring Bottle Washing Facility, Edmonton, Canada, 1 May 1982 to 31 December 1982.

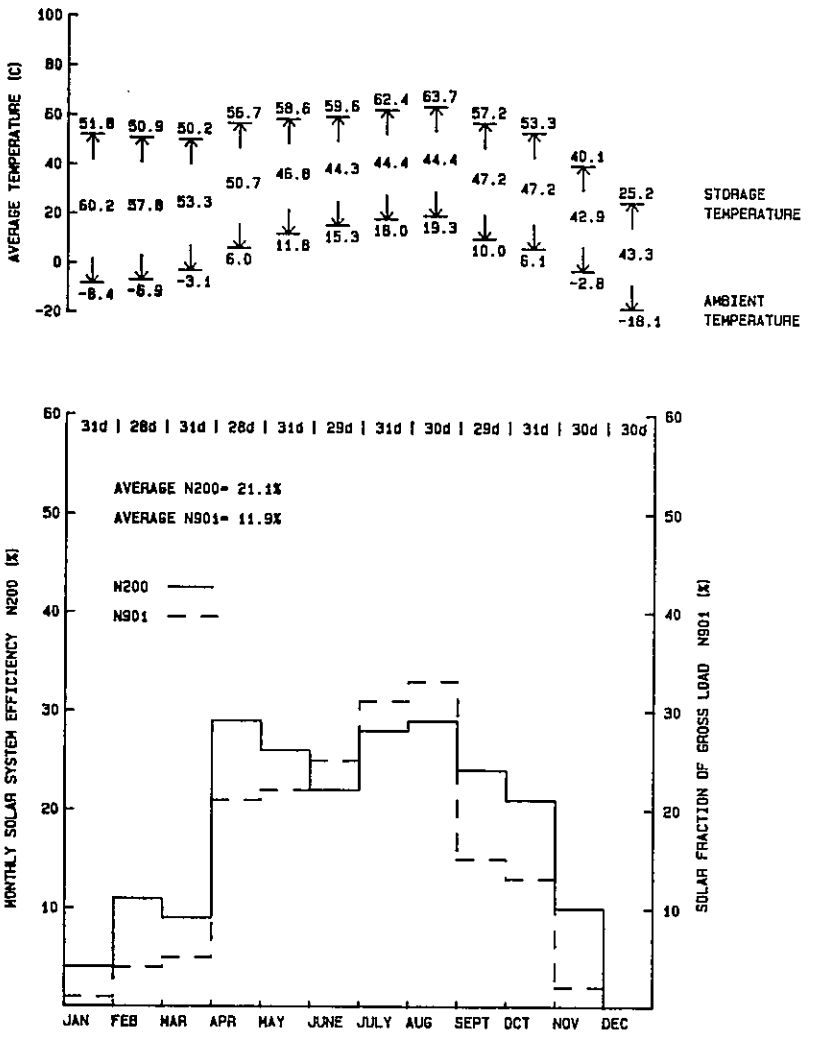

Figure 6.6-7. Average Monthly System Efficiency and Solar Fraction for Solartech ETCs at the Mountain Spring Bottle Washing Facility, Edmonton, Canada, 1 January 1983 to 31 December 1983.

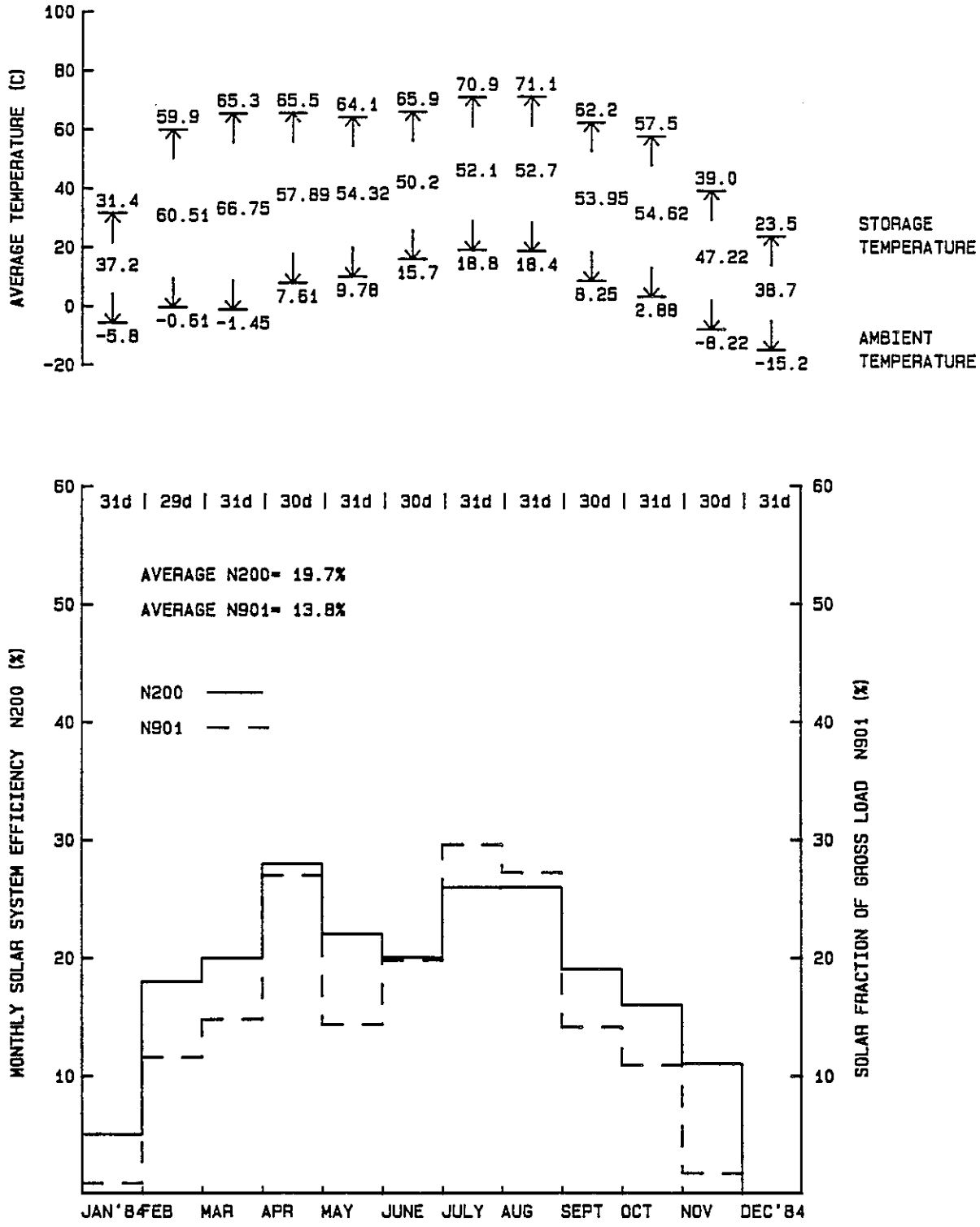

Figure 6.6-8. Average Monthly System Efficiency and Solar Fraction for Solartech ETC's at the Mountain Spring Bottle Washing Facility, Edmonton, Canada, 1 January 1984 to 31 December 1984.

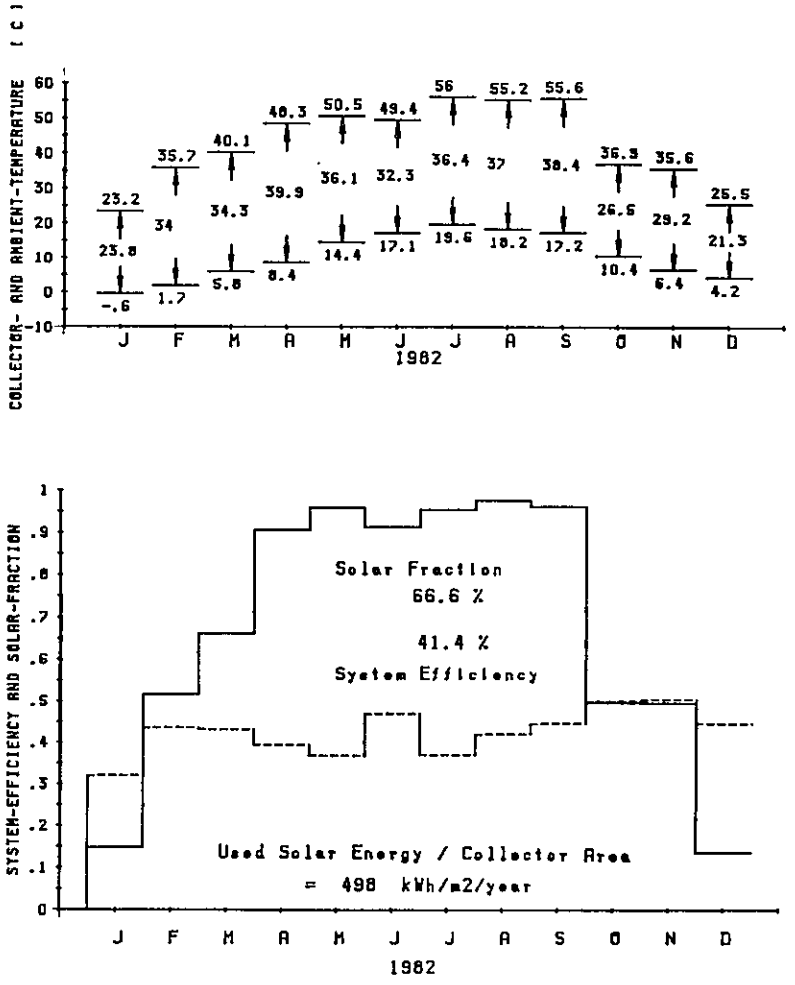

Figure 6.6-9. Average Monthly System Efficiency and Solar Fraction of the Domestic Hot Water System at Solarhaus Freiburg (with sequential operation of the Corning Glass and Philips/Stiebel-Eltron Collectors), Federal Republic of Germany, 1982.

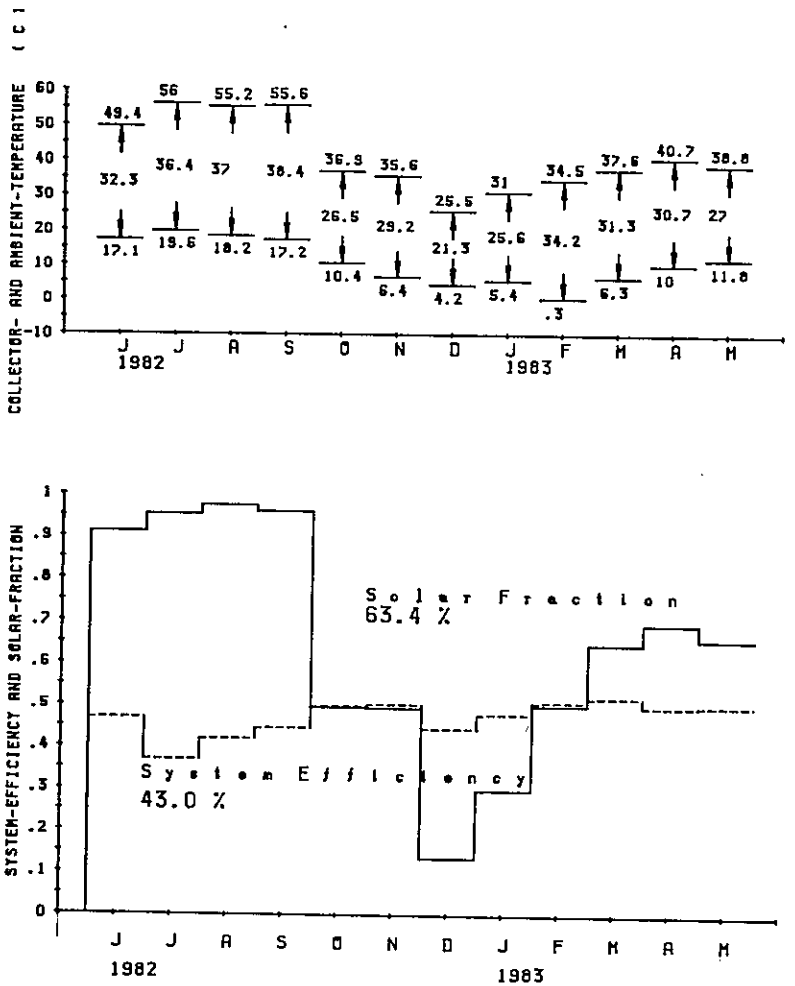

Figure 6.6-10. Average Monthly System Efficiency and Solar Fraction of the Domestic Hot Water System at Solarhaus Freiburg with operation of the Philips/Stiebel-Eltron Collector, Federal Republic of Germany, June 1982 to May 1983.

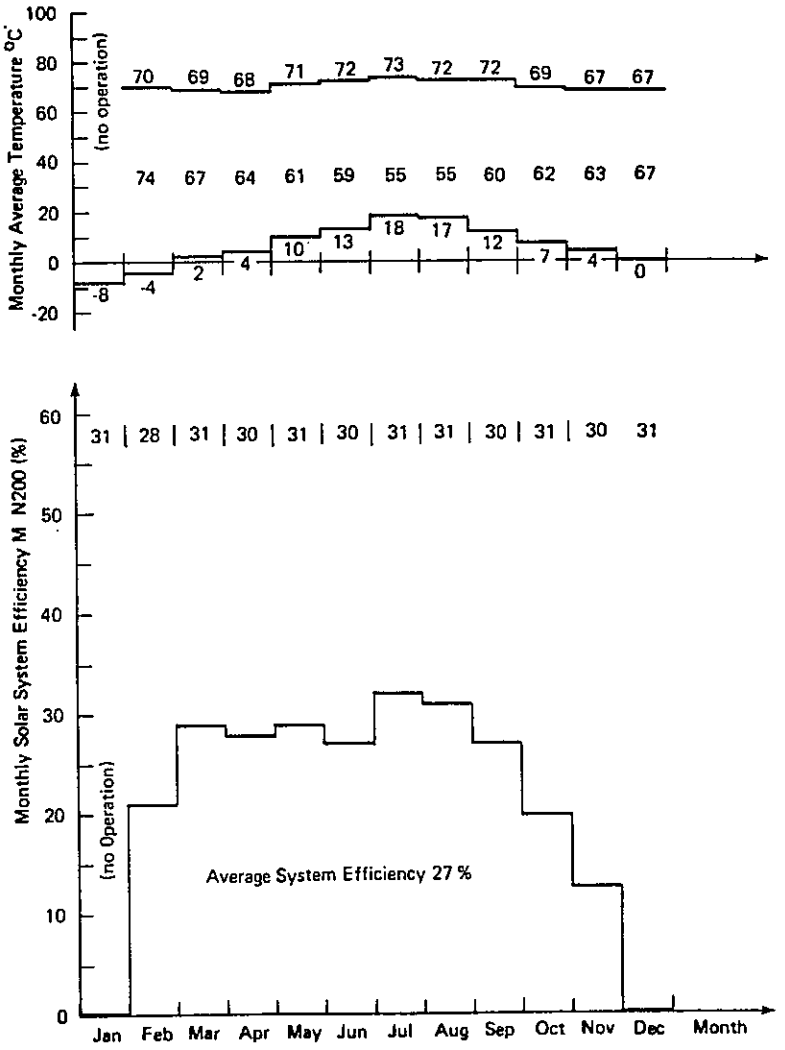

Figure 6.6-11. Average Monthly System Efficiency for General Electric TC 100, Knivsta, Sweden, 1 January 1982 to 31 December 1982.

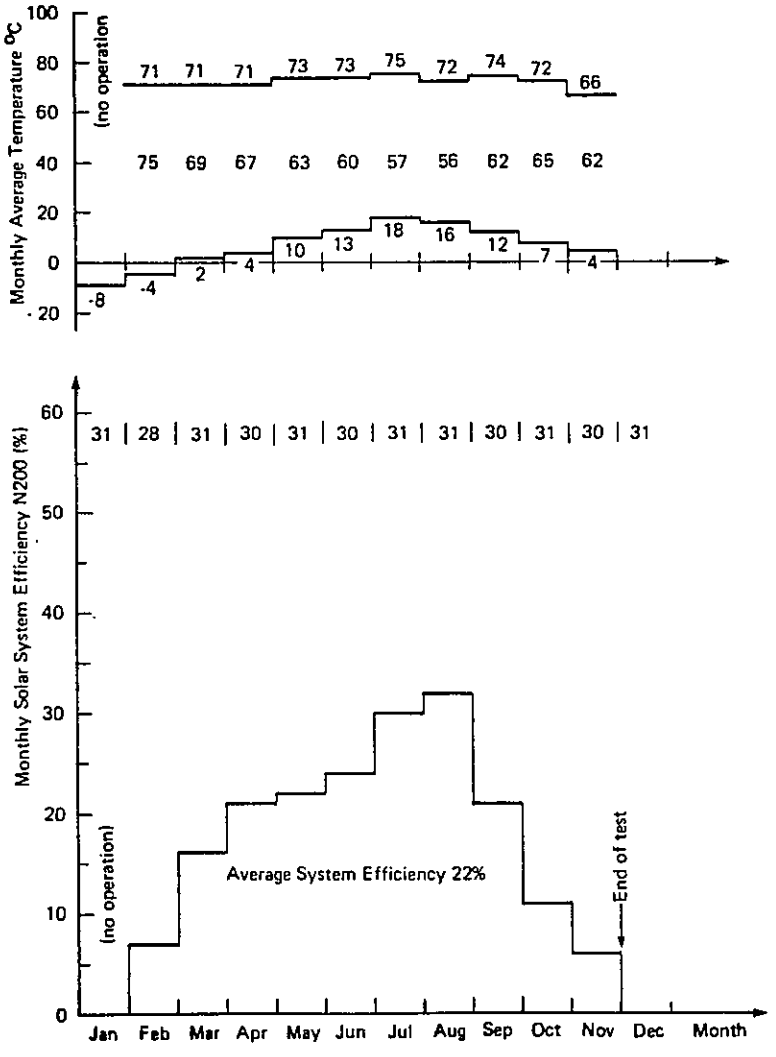

Figure 6.6-12. Average Monthly System Efficiency for Owens-Illinois Sunpak, Knivsta, Sweden, 1 January 1982 to 31 December 1982.

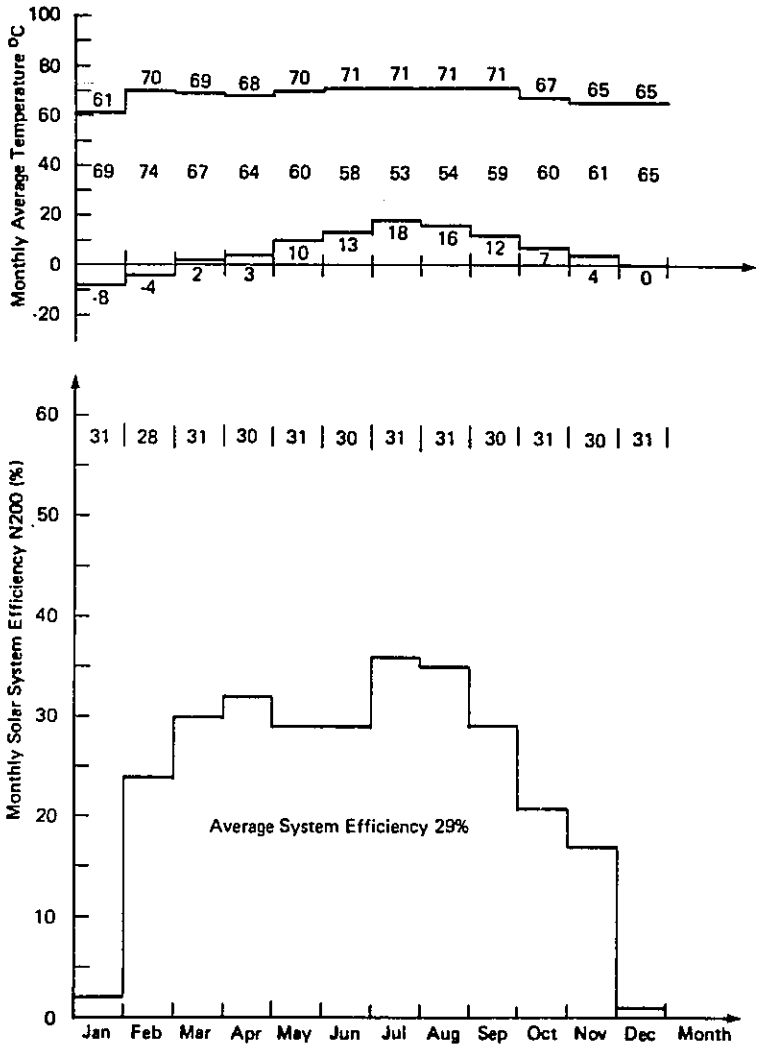

Figure 6.6-13. Average Monthly System Efficiency for Philips VTR 141, Knivsta, Sweden, 1 January 1982 to 31 December 1982.

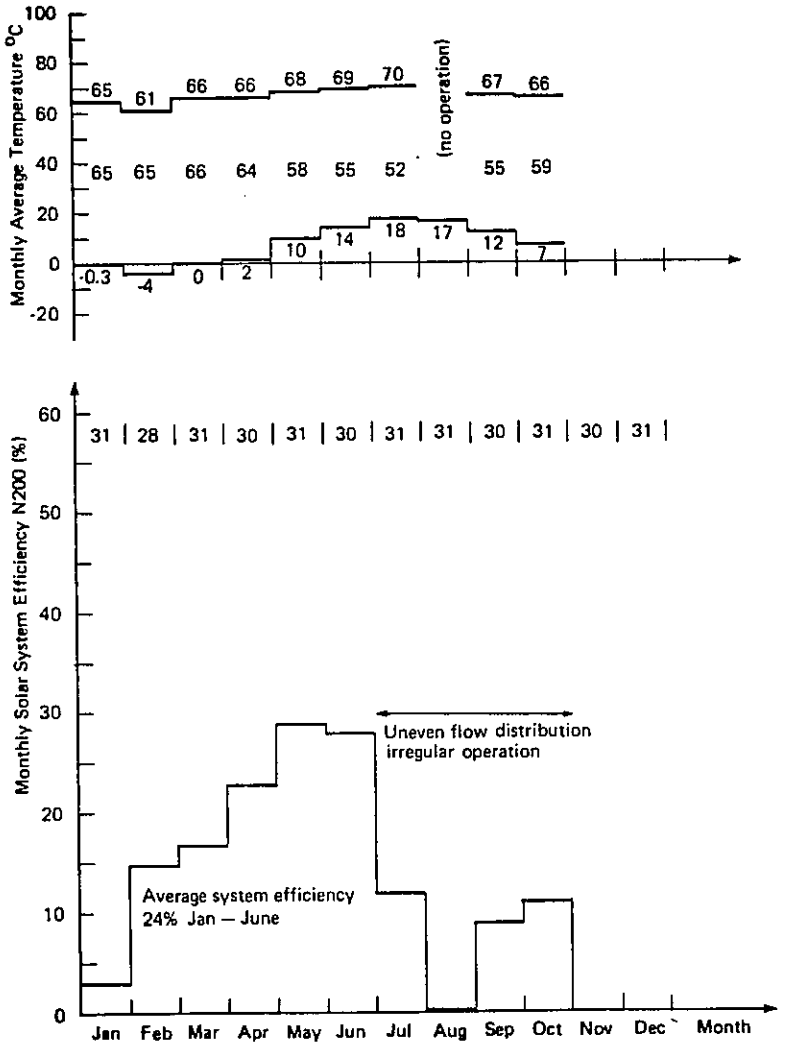

Figure 6.6-14. Average Monthly System Efficiency for General Electric TC 100, Knivsta, Sweden, 1 January 1983 to 31 December 1983.

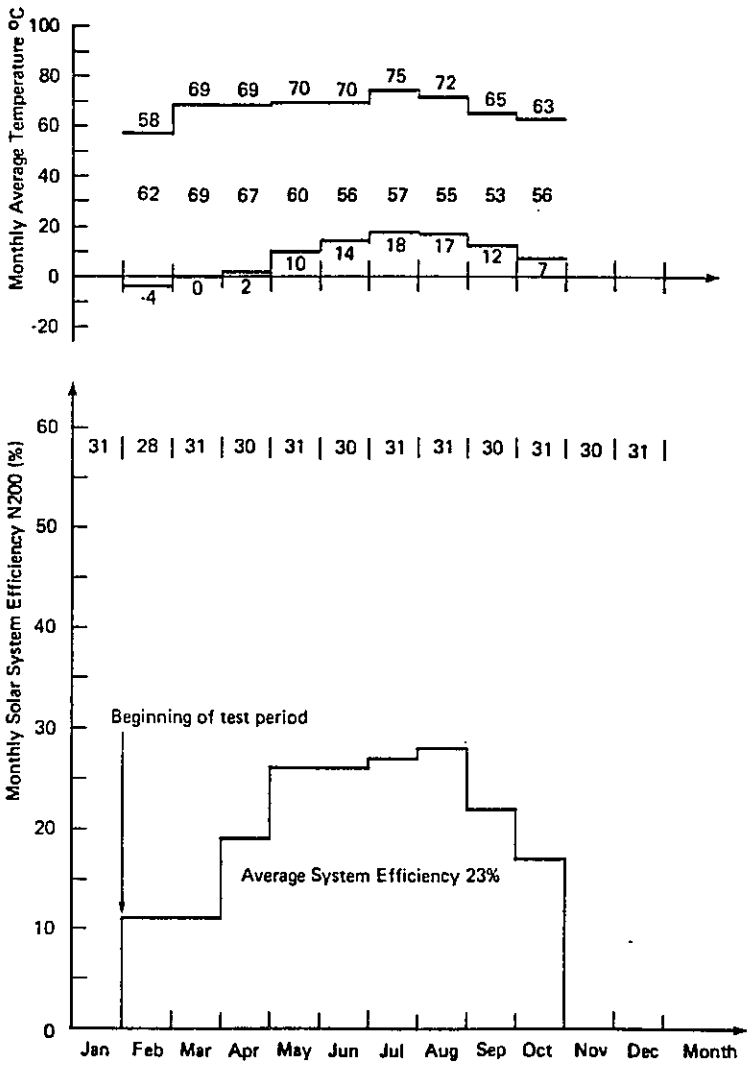

Figure 6.6-15. Average Monthly System Efficiency for Scandinavian Solar HT, Knivsta, Sweden, 1 January 1983 to 31 December 1983.

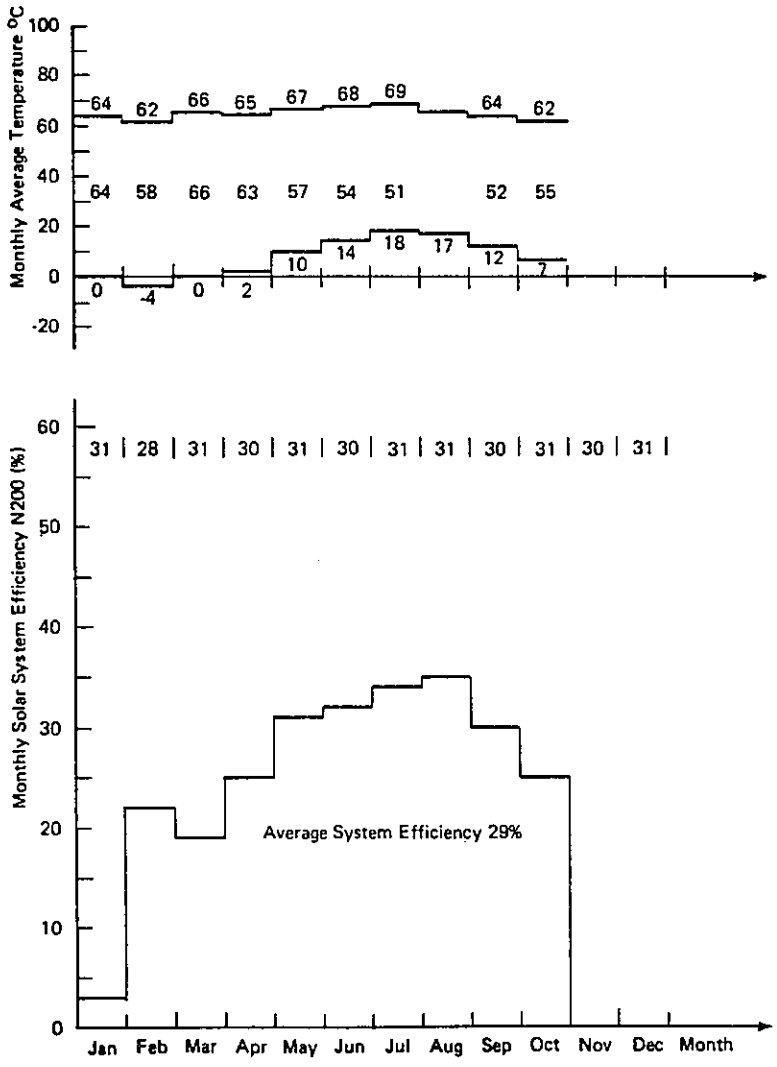

Figure 6.6-16. Average Monthly System Efficiency for Philips VTR 141, Knivsta, Sweden, 1 January 1983 to 31 December 1983.

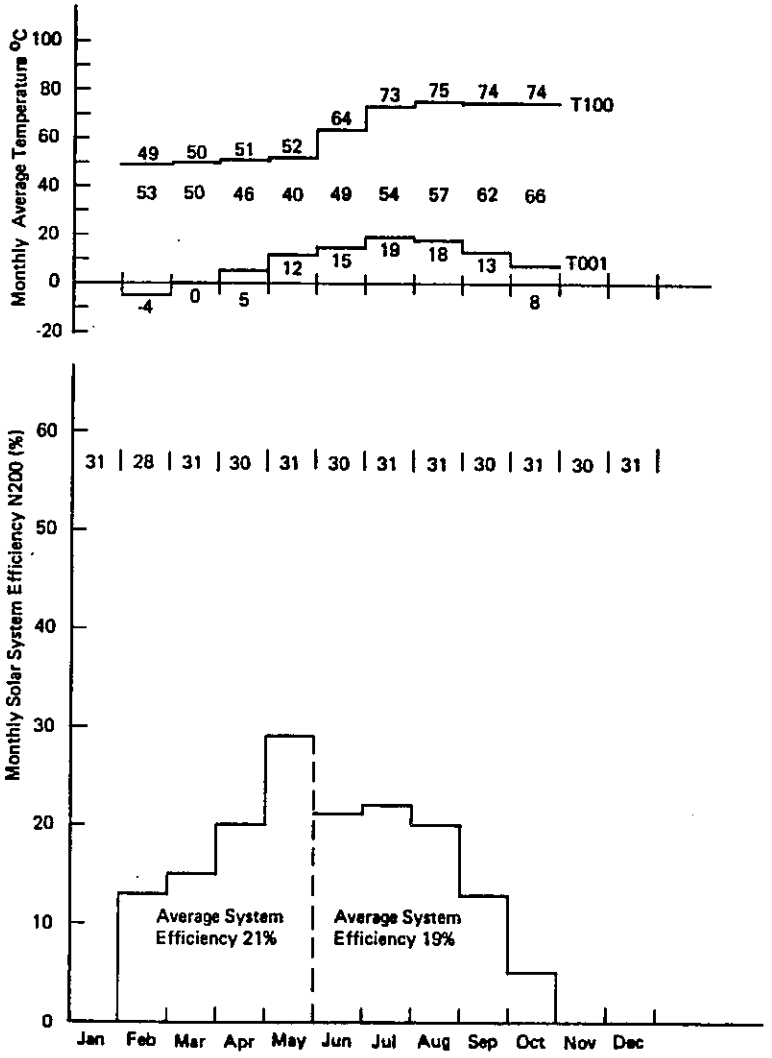

Figure 6.6-17. Average Monthly System Efficiency for Teknoterm, Södertörn, Sweden, 1 January 1983 to 31 December 1983.

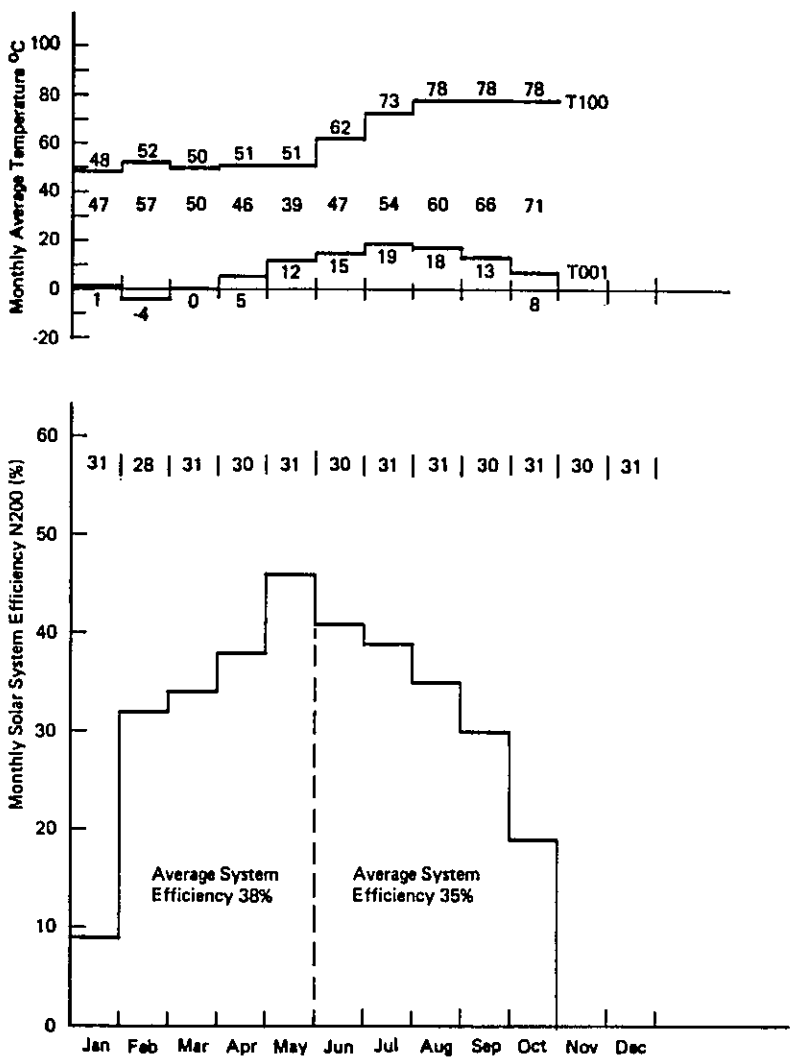

Figure 6.6-18. Average Monthly System Efficiency for Philips VTR 141, Södertörn, Sweden, 1 January 1983 to 31 December 1983.

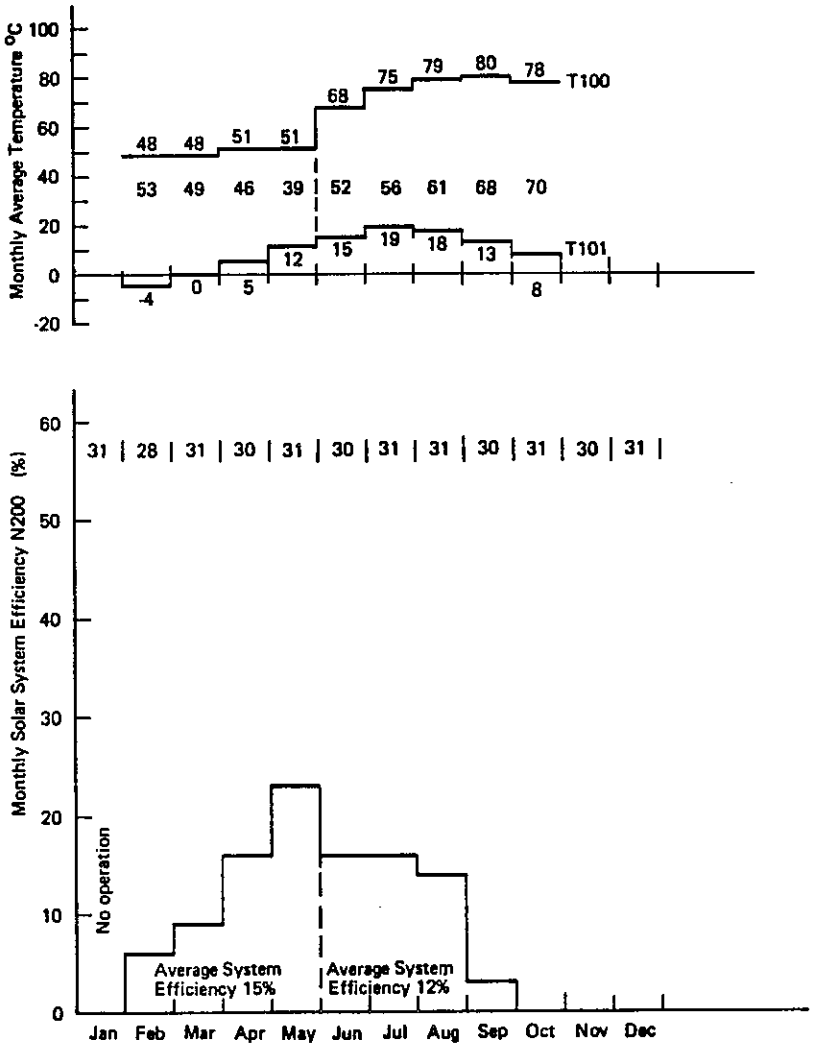

Figure 6.6-19. Average Monthly System Efficiency for Granges Aluminum, Södertörn, Sweden, 1 January 1983 to 31 December 1983.

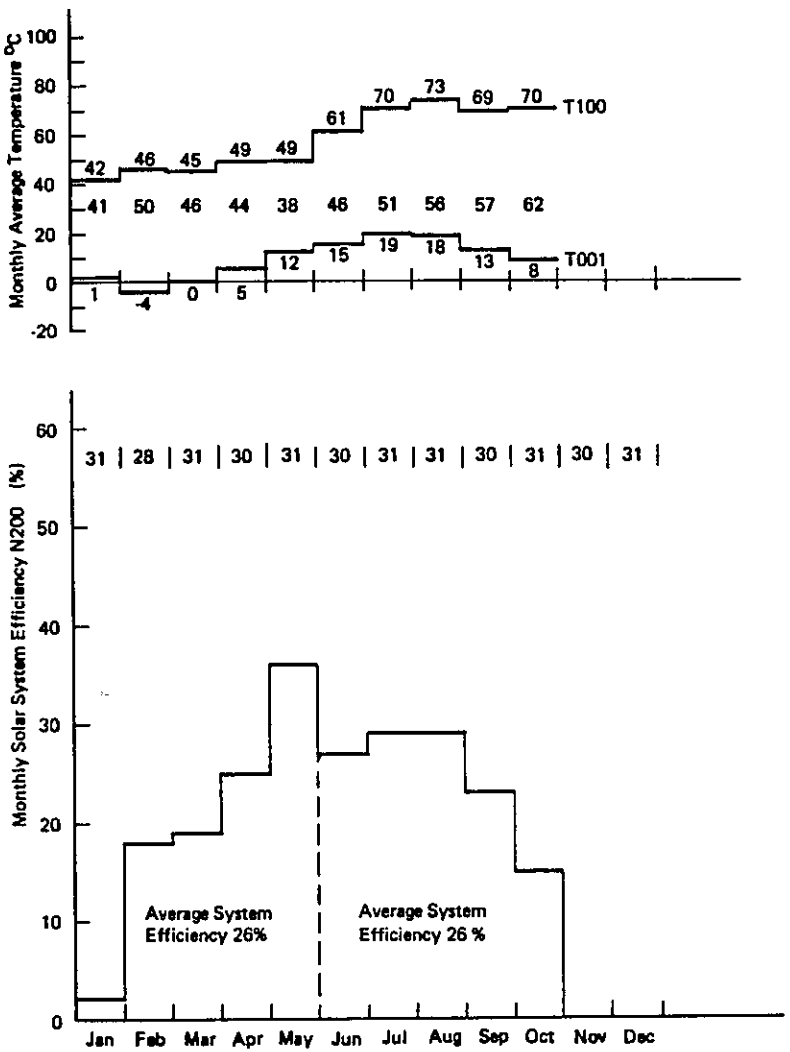

Figure 6.6-20. Average Monthly System Efficiency for General Electric TC 100, Södertörn, Sweden, 1 January 1983 to 31 December 1983.

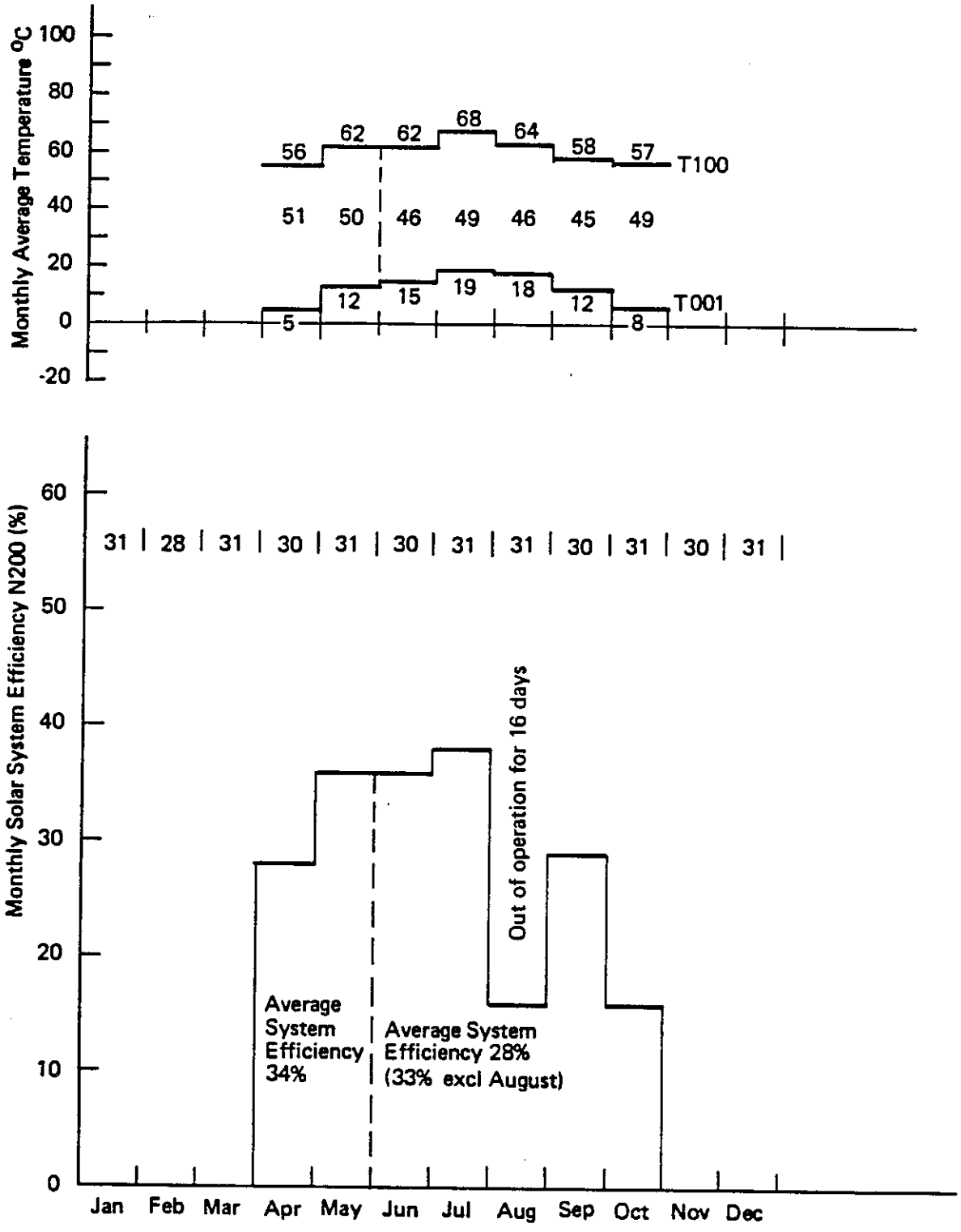

Figure 6.6-21. Average Monthly System Efficiency for Scandinavian Solar HT, Södertörn, Sweden, 1 January 1983 to 31 December 1983.

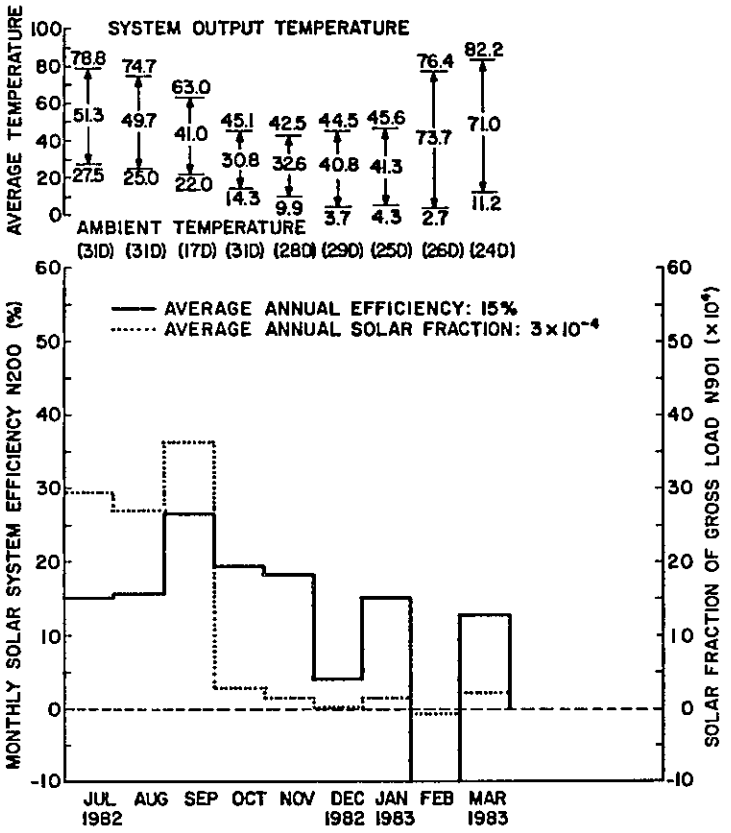

Figure 6.6-22. Average Monthly System Efficiency and Solar Fraction for Corning A+B Measurements, Geneva, Switzerland Switzerland, July 1982 to March 1983.

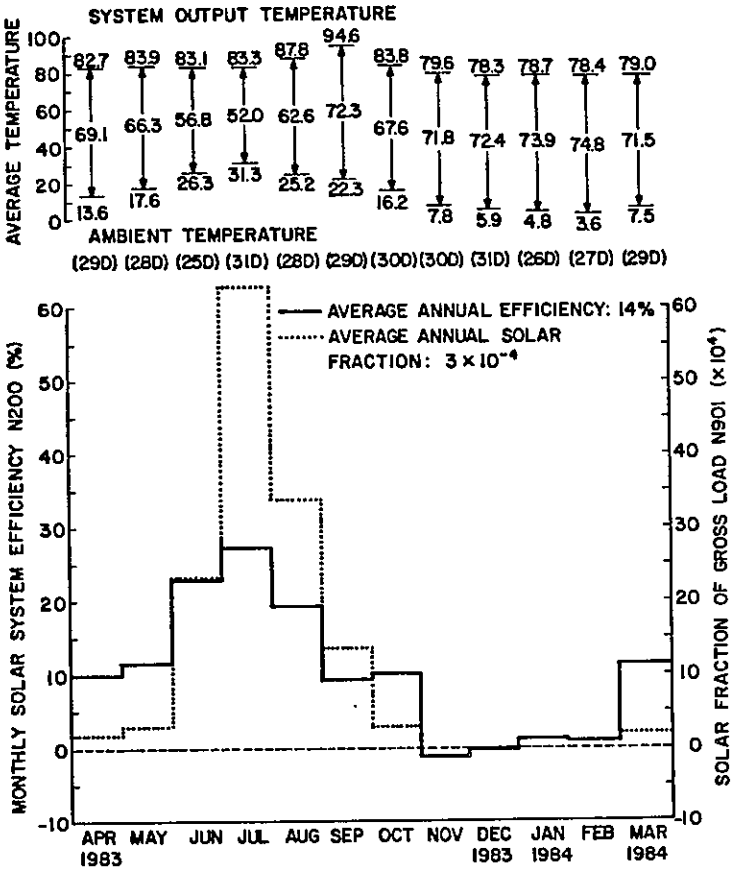

Figure 6.6-23. Average Monthly System Efficiency and Solar Fraction for Corning A+B Measurements, Geneva, Switzerland Switzerland, April 1983 to March 1984.

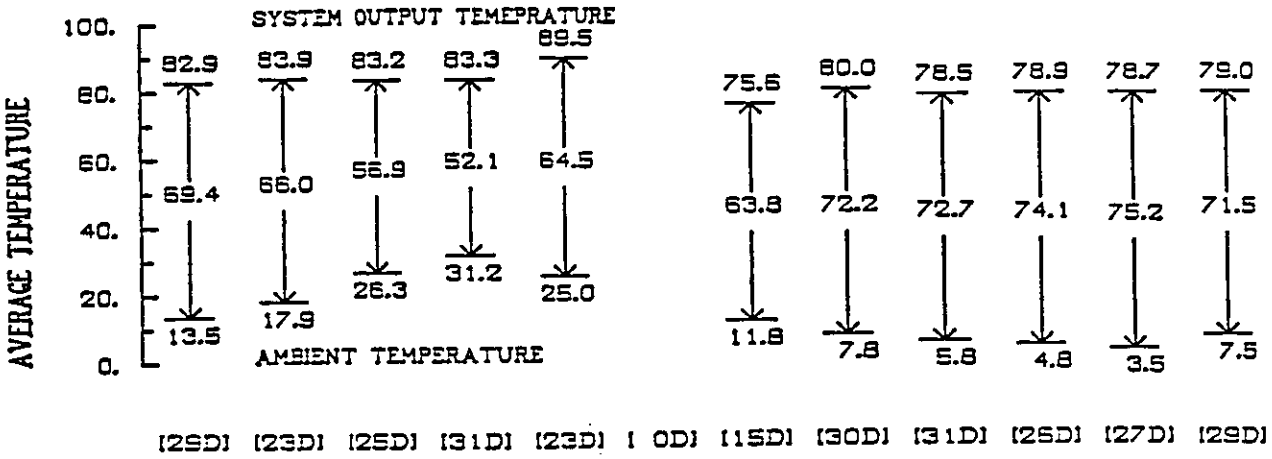

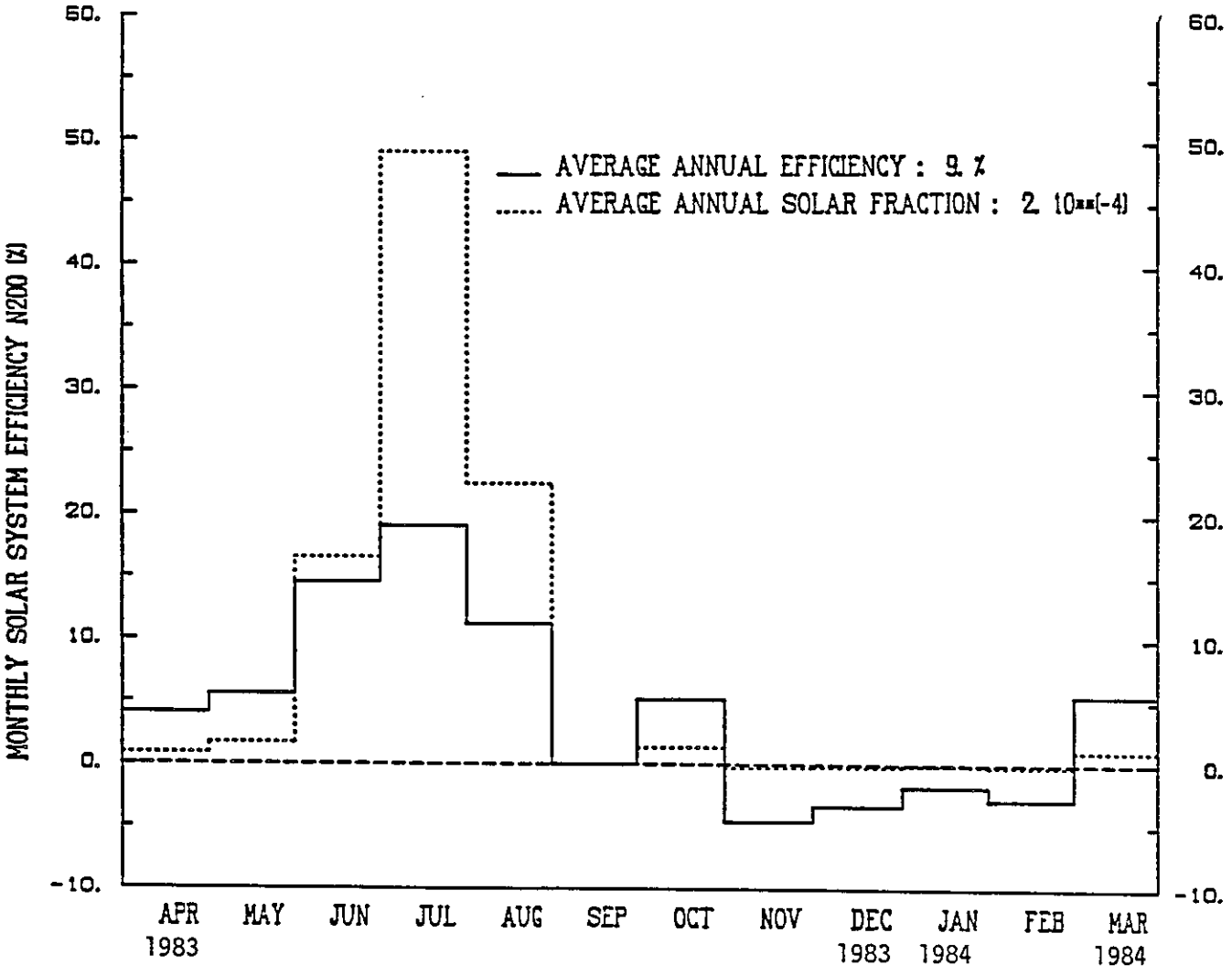

Figure 6.6-24. Average Monthly System Efficiency and Solar Fraction for Sanyo Measurements, Geneva Switzerland, April 1983 to March 1984.

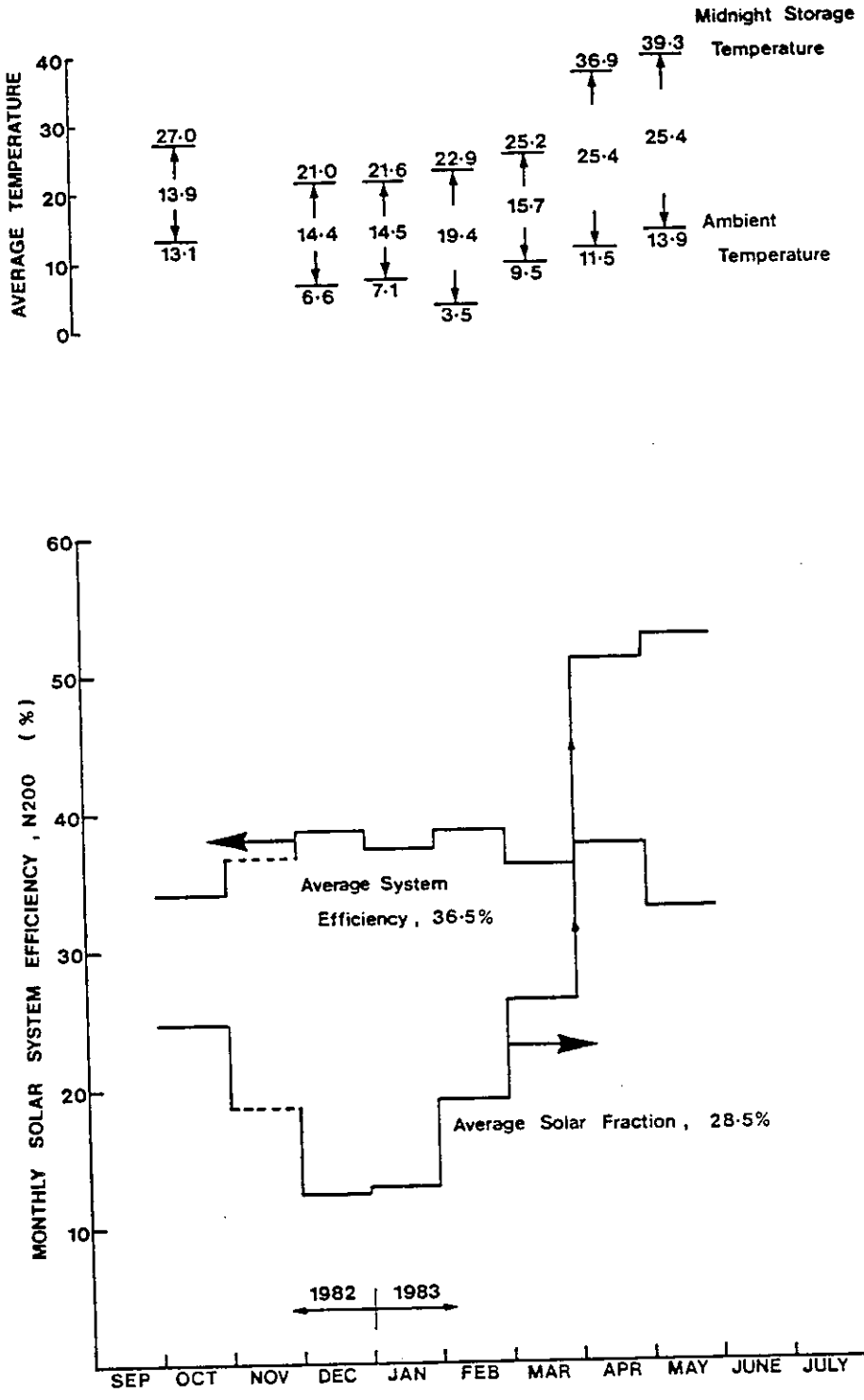

Figure 6.6-25. Average Monthly System Efficiency for Philips VTR141 Collectors at BSRIA Solar Test Facility with Simulated Loads, Bracknell, United Kingdom, 1 September 1982 to 31 August 1983.

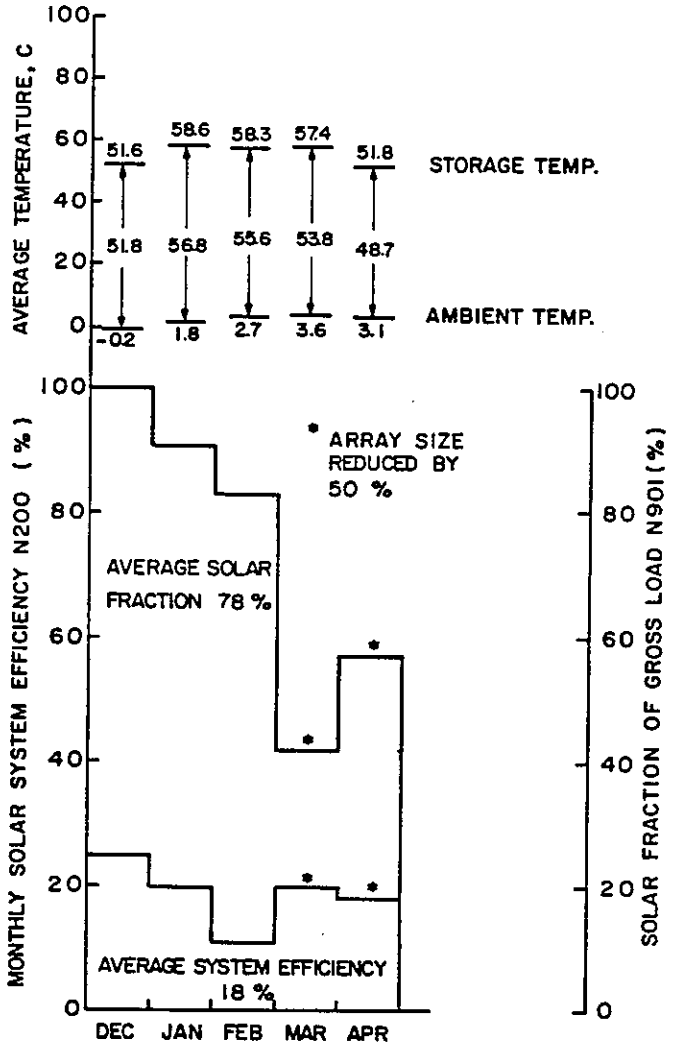

Figure 6.6-26. Average Monthly System Efficiency for the Winter Season at CSU Solar House I, United States, December 1983 to April 1984.

6.7 SHIPPING, RELIABILITY, MAINTAINABILITY AND OPERATION

Table 6.7-1 gives information on installation operating time, and on tube breakage and vacuum loss during shipping, installation and operation. Table 6.7-2 provides a description of maintenance problems encountered at each of the installations.

Table 6.7-1. Evacuated Collector Shipping, Installation, and Operating Problems

Country	Installation	Collector	Length of Operating Time (Months)	Total Number of Tubes	Breakage/Vacuum Loss During		Vacuum Loss During Operation	Breakage Loss During Operation
					Shipping	Installation		
Australia	Sydney University	Sydney University	26	480	40	0	2	0
Canada	Mountain Spring	Solartech	41	1728	16	150(1)	32	4
CEC	Ispra	Sanyo	36	120	--	--	--	1 (2)
		Philips VTR-261	24	95	--	--	4	42 (2)
		Philips VTR-361	18	42	--	--	--	--
FRG	Solarhaus Freiburg	US Corning	106	144	--	--	1	--
		Philips	30	180	--	--	1	--
Netherlands	Eindhoven University	Philips VTR-261	24	368	--	--	5	2
Sweden	Knivsta District							
Sweden	Södertörn District							
Switzerland	SOLARCAD District	Corning A & B	24	72	--	--	13	--
		Sanyo	24	80	--	--	--	--
Switzerland	SOLARIN Industry	Corning D	12	1680	2	--	--	-1
UK	Bracknell Facility	Philips VTR-141	24	300	4	2	2	0
USA	CSU Solar House 1	Philips VTR-261	13	336	--	--	10	--

(1) Hot start (thermal shock)
(2) Hail
(3) Pressure rise up to 0.5 Pascal

Table 6.7-2. Significant Maintenance and Reliability Problems

Country	Installation	Maintenance Problems
Australia	Sydney University	Module connection leak. Rubber hoses are used to connect the collector modules. Hose clamps need retightening and all the evacuated tubes needed to be checked for accumulation of water.
Canada	Mountain Spring	Continuing slow leakage at rubber hose connections between array piping and collector banks; two tube breakages causing large fluid loss.
CEC	Ispra	Tube breakage occurred due to hail.
FRG	Solarhaus Freiburg	None
Netherlands	Eindhoven University	None
Sweden	Knivsta District	Flow distribution problems due to facility deaeration and leakage (except for Philips VTR 141).
Sweden	Södertörn District	None for Philips VTR 141. Some tube breakages for GE TC-100.
Switzerland	SOLARCAD District	There was one pump failure, two control failures, one fluid leak and problems with rubber connections to the collectors.
Switzerland	SOLARIN Industry	There were serious failures of the microprocessor.
UK	BSRIA	Two tubes lost vacuum. Some connectors between modules failed causing loss of pressurization.
USA	CSU Solar House 1	None

6.8 SNOW COVER

Figure 6.8-1 gives a categorization of various degrees of snow cover for the Solartech collector. Tables 6.8-1 and 2 provide a record over two winter seasons of the number of days each month that the collectors spent in each degree of snowcover.

DIAGRAM	RATING	DESCRIPTION
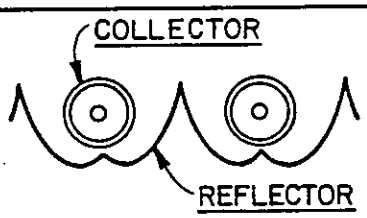	1	COLLECTORS FREE OF SNOW
	2	SCATTERED SNOW IN COLLECTORS, ALMOST TOUCHING BOTTOM OF TUBES
	3	UP TO 50% OF REFLECTORS FILLED WITH SNOW
	4	REFLECTORS FILLED MORE THAN 50%, BUT NO BUILD-UP OF SNOW ON TUBES
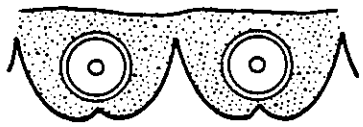	5	BUILD-UP OF 1-10 MILLIMETERS OF SNOW ON TUBES
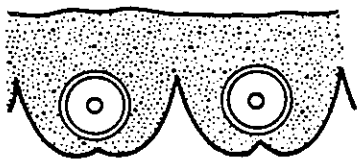	6	BUILD-UP OF MORE THAN 10 MILLIMETERS OF SNOW ON TUBES

Figure 6.8-1 Characterization of Snow Cover on Solar Collectors, Mountain Spring Bottle Washing Facility, Canada.

Table 6.8-1 Record of Snow Cover on Collectors[1,2], Mountain Spring Bottle Washing Facility, Edmonton, Canada, Winter 1981/1982.

	NATURAL CONDITIONS[3]						MANAGED CONDITIONS[4]					
Month/Rating	1	2	3	4	5	6	1	2	3	4	5	6
December	-	-	-	-	9	-	-	-	-	-	9	-
January	2	-	5	3	18	3	2	-	5	3	18	3
February	5	-	-	-	5	18	5	2	3	7	9	2
March	21	3	-	1	2	4	21	5	1	-	4	-
April	-	1	-	1	3	-	1	3	-	1	-	-
Total (days)	28	4	5	5	37	25	29	10	9	11	40	5

1 Entries indicate number of days with given snow condition
2 No observations before 81:12:23
3 Snow cover undisturbed
4 Regular removal of snow

Table 6.8-2 Record of Snow Cover on Collectors[1,2], Mountain Spring Bottle Washing Facility, Edmonton, Canada, Winter 1982/1983.

	NATURAL CONDITIONS[3]						MANAGED CONDITIONS[4]					
Month/Rating	1	2	3	4	5	6	1	2	3	4	5	6
October	27	1	0	1	0	2	27	1	0	1	0	2
November	13	2	1	3	9	2	13	6	4	2	3	2
December	26	2	1	2	0	0	26	2	1	2	0	0
January	22	1	3	4	0	0	22	1	5	2	0	0
February	12	7	4	1	4	0	13	6	5	1	3	0
March	17	1	2	2	5	4	18	0	9	2	1	1
April	28	0	2	0	0	0	28	0	2	0	0	0
Total (days)	145	14	13	13	18	8	147	16	26	10	7	5
Total (%)	69	7	6	6	9	4	70	8	12	5	3	2

1 Entries indicate number of days with given snow condition
2 No observations before 82:10:01 - 83:04:30
3 Snow cover undisturbed
4 Regular removal of snow

7. DISCUSSION OF RESULTS AND COMPARISONS

This chapter presents comparisons of thermal performance, shipping, reliability, maintenance, and operating experiences amoung different collector types. Also discussed is why operating periods of a day or longer are usually necessary when comparing performance of system components under real operating conditions.

7.1 INSTANTANEOUS PERFORMANCE

During collector testing, especially indoor testing, with all conditions held fixed and the incident radiation primarily beam and normal to the collector plane, instantaneous collection efficiencies fall nearly on a single curve[1] when plotted against $\Delta T/G$. Also, this curve can sometimes be approximated over most of its range by a straight line.

By contrast, it is very rare that instantaneous measurements of collection efficiencies in real systems during real operating conditions fall on the curve or curves produced by collector tests. There are a number of reasons for this.

7.1.1 Incidence Angle Effects

All glazed collectors show a variation in the amount of radiation reaching the absorber due to the angle at which it strikes the glass covers or to the shape or orientation of the absorber. Evacuated collectors are not optically symmetric. They have cylindrical glazings, sometimes have tilted or round absorbers, and may have CPC or ripple reflectors. These factors sometimes result in quite substantial incidence angle effects at different times of the day and during different seasons.

To see the extent of these various effects at different times of day and during different seasons, the instantaneous efficiencies of three evacuated collectors and a flat plate collector were calculated for clear and diffuse equinox, winter solstice, and summer solstice days. The round and flat absorber evacuated collectors were oriented south facing with slopes of 45° and positioned with their tubes running both north-south and east-west. The evacuated collector with the tilted absorber was oriented with its tubes running east-west and at a slope of 15° so that its absorber slope would be at 45° to the horizontal. The optically symmetric flat plate collector was positioned south facing with slope equal to 45°.

---

[1] Guisan et al. [3,20] point out that generally a single curve is not adequate.

The clear days are from actual Fort Collins, Colorado, USA latitude 40.6° data and the diffuse days are cosine curves for latitude 40.6° with a peak value of 500 w/m^2 and the proper day length. The collectors used are the Corning and Sydney University evacuated collectors and a good single glazed flat plate collector. The relevant thermal and optical parameters and dimensions of these collectors are given in Table 7-1 and the axial and transverse incident angle modifiers in Table 7-2.

Table 7-1 Collector Geometry, $F'(\tau\alpha)$, AND $F'U_L$

Collector	Pitch# (mm)	Tube Diameter (mm)	Tube Gap (mm)	$F'(\tau\alpha)$	$F'U_L$ W/Km^2 Aperture
ETC: Round Absorber	60.0	38	22.0	0.575	1.74
ETC: Flat Absorber	111.3	100	1.11	0.72	1.68
ETC: Tilted Absorber	111.3	100	1.11	0.72	1.68
Flat Plate	N/A	N/A	N/A	0.85	4.75

Centerline to Centerline Distance between Tubes
* Absorber Diameter

Figures 7-1 through 7-3 present the various calculated collector instantaneous efficiencies throughout the day for the clear winter solstice, equinox, and summer solstice days respectively. Figures 7-4 through 7-6 show the calculated efficiencies for the corresponding three diffuse days. Since the instantaneous efficiencies are symmetric about noon, only the hours after noon are provided in the figures.

As can be seen by comparing Figures 7-1 through 7-3, for a ΔT of 60°C the cylindrical absorber evacuated collector in the north-south orientation is quite effective at the mid-morning and mid-afternoon incidence angles due to presenting a maximum cross-section absorber at all angles. Shading by adjacent tubes causes a fall off in optical efficiency at higher incidence angles as in Figure 7.2. But, because all the radiation falling on the collector aperture falls on the tubes, the incidence angle modifier value remains high up to an incidence angle of nearly 90°.

Wide tube spacing does result in good utilization of the diffuse reflective background. However, it also produces an overall lower

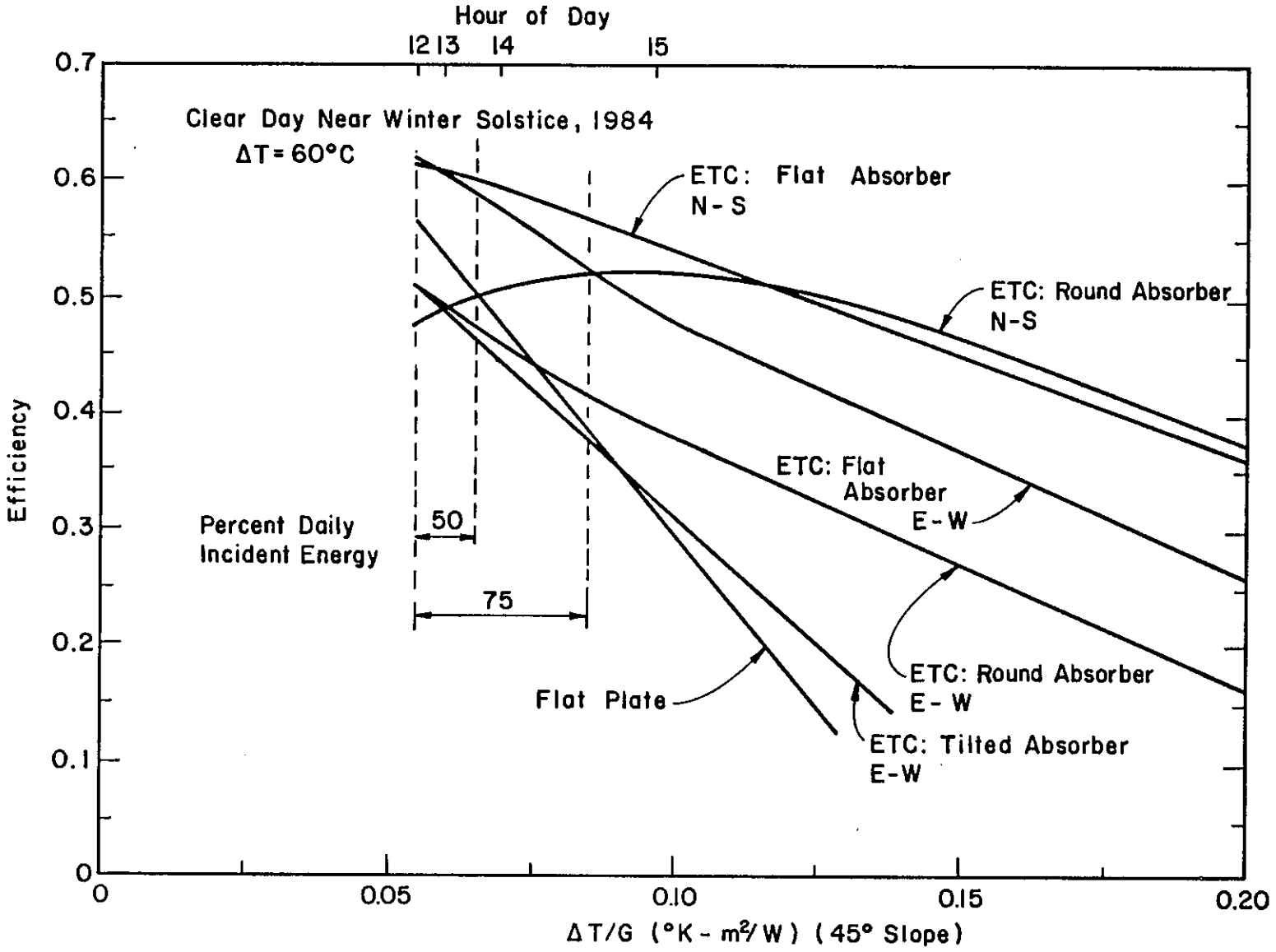

Figure 7-1 Calculated Effect of Incidence Angle on Collector Efficiency for a Clear Winter Solstice Day.

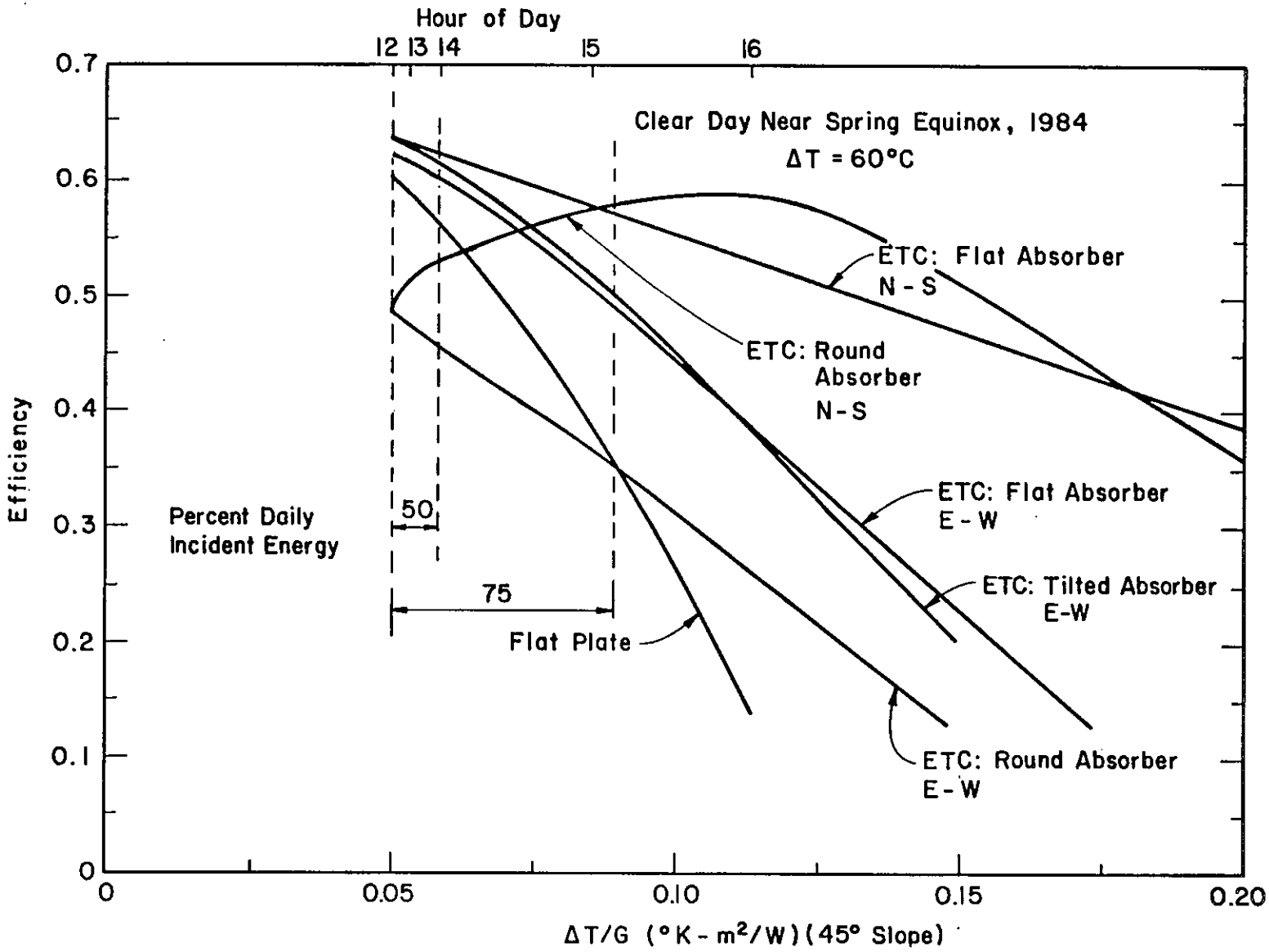

Figure 7-2 Calculated Effect of Incidence Angle on Collector Efficiency for a Clear Equinox Day.

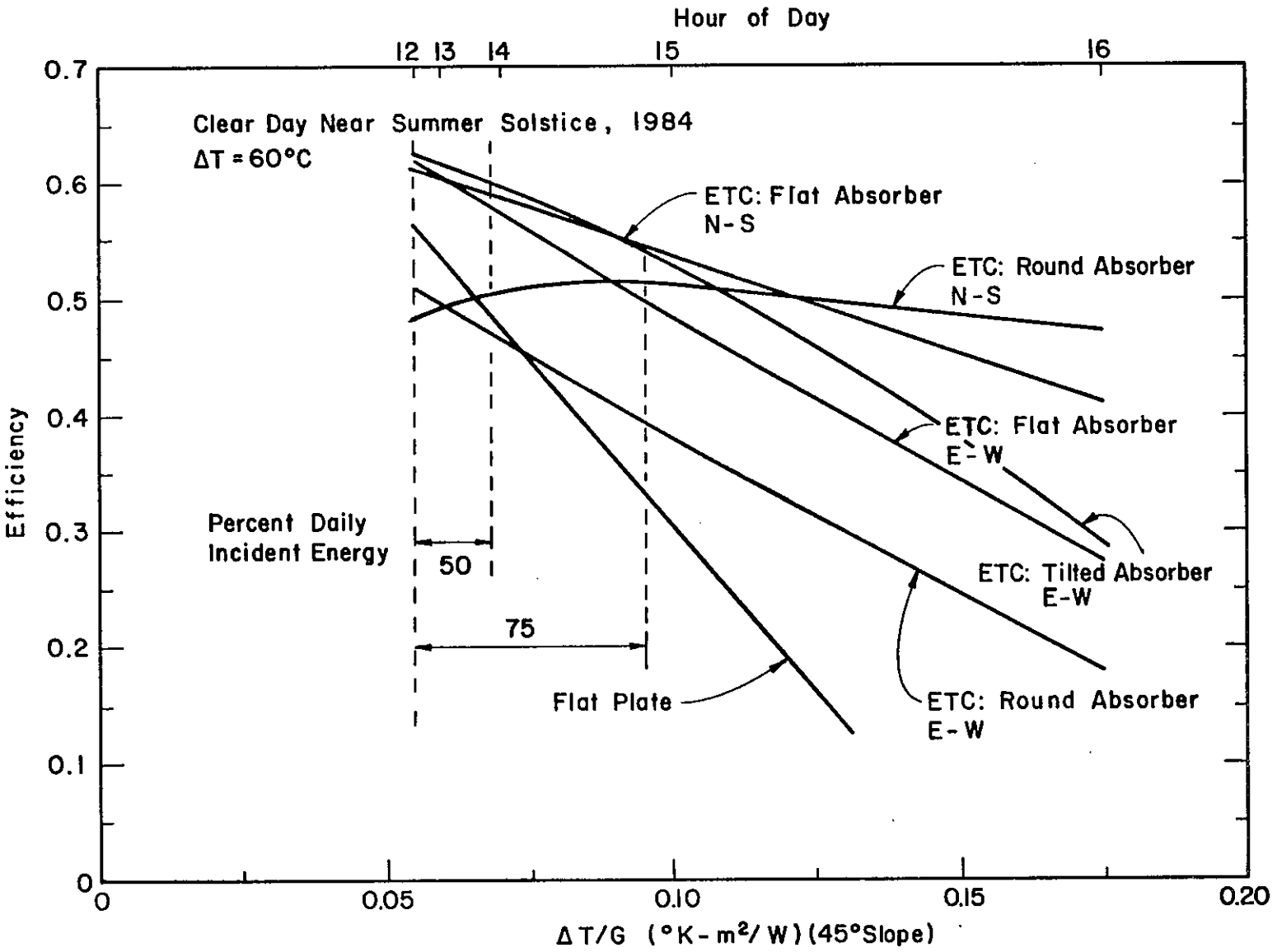

Figure 7-3 Calculated Effect of Incidence Angle on Collector Efficiency for a Clear Summer Solstice Day.

optical efficiency around noon. Overall losses per tube are also higher than with a flat absorber due to the $\pi/2$ to 1 ratio of their absorber areas.

Table 7-2 Incident Angle Modifiers

Collector	Day Length	IAM (γ) and IAM (β) for Beam Radiation Hour of Day 12	11 & 13	10 & 14	9 & 15	8 & 16	7 & 17
ETC: Round	9	1.00,0.98	1.03,0.98	1.08,0.98	1.20,0.98	1.38,0.98	1.14,0.98
Absorber	12	1.00,1.00	1.03,1.00	1.08,1.00	1.20,1.00	1.38,1.00	1.14,1.00
N-S	15	1.00,0.98	1.03,0.98	1.08,0.98	1.20,0.98	1.38,0.98	1.14,0.98
ETC: Flat	9	1.00,0.98	1.00,0.98	1.00,0.98	1.00,0.98	1.00,0.98	1.00,0.98
Absorber	12	1.00,1.00	1.00,1.00	1.00,1.00	1.00,1.00	1.00,1.00	1.00,1.00
N-S	15	1.00,0.98	1.00,0.98	1.00,0.98	1.00,0.98	1.00,0.98	1.00,0.98
Flat Plate	9	1.00,0.98	0.99,0.98	0.98,0.98	0.94,0.98	0.80,0.98	0.40,0.98
	12	1.00,1.00	0.99,1.00	0.98,1.00	0.94,1.00	0.80,1.00	0.40,1.00
	15	1.00,0.98	0.99,0.98	0.98,0.98	0.94,0.98	0.80,0.98	0.40,0.98
Tilted	9	1.25,1.00	1.25,0.99	1.25,0.97	1.25,0.91	1.25,0.79	1.25,0.40
Absorber	12	1.15,1.00	1.15,0.99	1.15,0.97	1.15,0.91	1.15,0.79	1.15,0.40
(E-W Only)	15	0.92,1.00	0.92,0.99	0.92,0.97	0.92,0.91	0.92,0.79	0.92,0.40
ETC: Round	9	1.06,1.00	1.06,0.99	1.06,0.97	1.06,0.91	1.06,0.79	1.06,0.40
Absorber	12	1.00,1.00	1.00,0.99	1.00,0.97	1.00,0.91	1.00,0.79	1.00,0.40
E-W	15	1.06,1.00	1.06,0.99	1.06,0.97	1.06,0.91	1.06,0.79	1.06,0.40
ETC: Flat	9	1.00,1.00	1.00,0.99	1.00,0.97	1.00,0.91	1.00,0.79	1.00,0.40
Absorber	12	1.00,1.00	1.00,0.99	1.00,0.97	1.00,0.91	1.00,0.79	1.00,0.40
E-W	15	1.00,1.00	1.00,0.99	1.00,0.97	1.00,0.91	1.00,0.79	1.00,0.40

For the cylindrical absorber collector, the north-south orientation is seen to be a better daily energy producer than the east-west orientation. It may also be seen in Figures 7-1 through 7-3 that the cylindrical absorber collector does not produce as much daily energy as the flat absorber collectors. However, if energy produced per meter of tube width is calculated rather than energy per unit area of collector aperture, as in the figures, this collector and orientation would provide more energy at a ΔT of $60^{o}C$ than any of the other collectors and orientations.

It may be seen for the east-west tube orientation that tilting the flat absorber at 30^{o} and orienting the collector at a 15^{o} slope provides nearly as much energy as orienting the same collector with no absorber tilt at a 45^{o} slope. It may also be seen from Figures 7-1 through 7-6

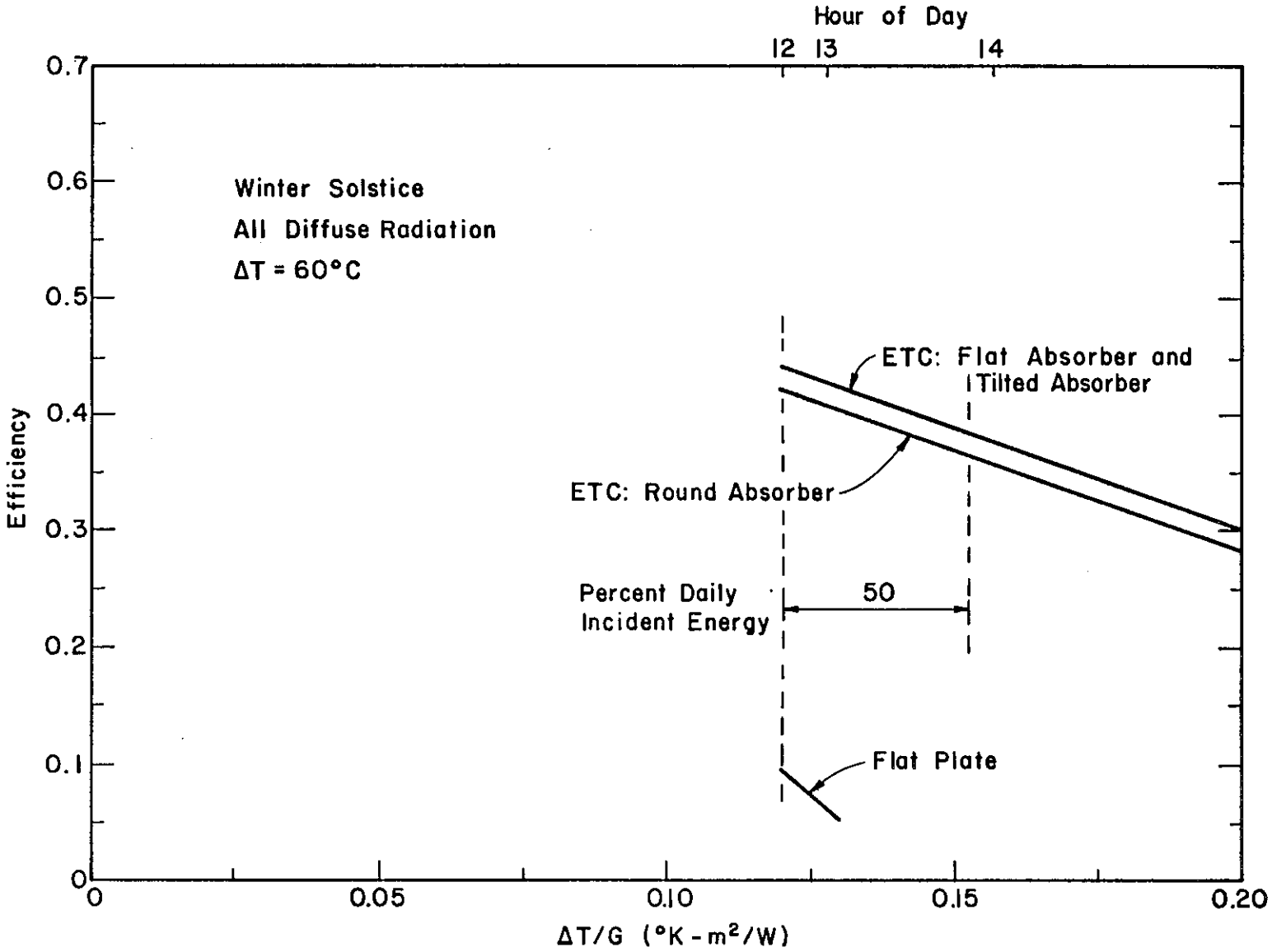

Figure 7-4 Calculated Effect of Incidence Angle on Collector Efficiency for a Diffuse Winter Solstice Day.

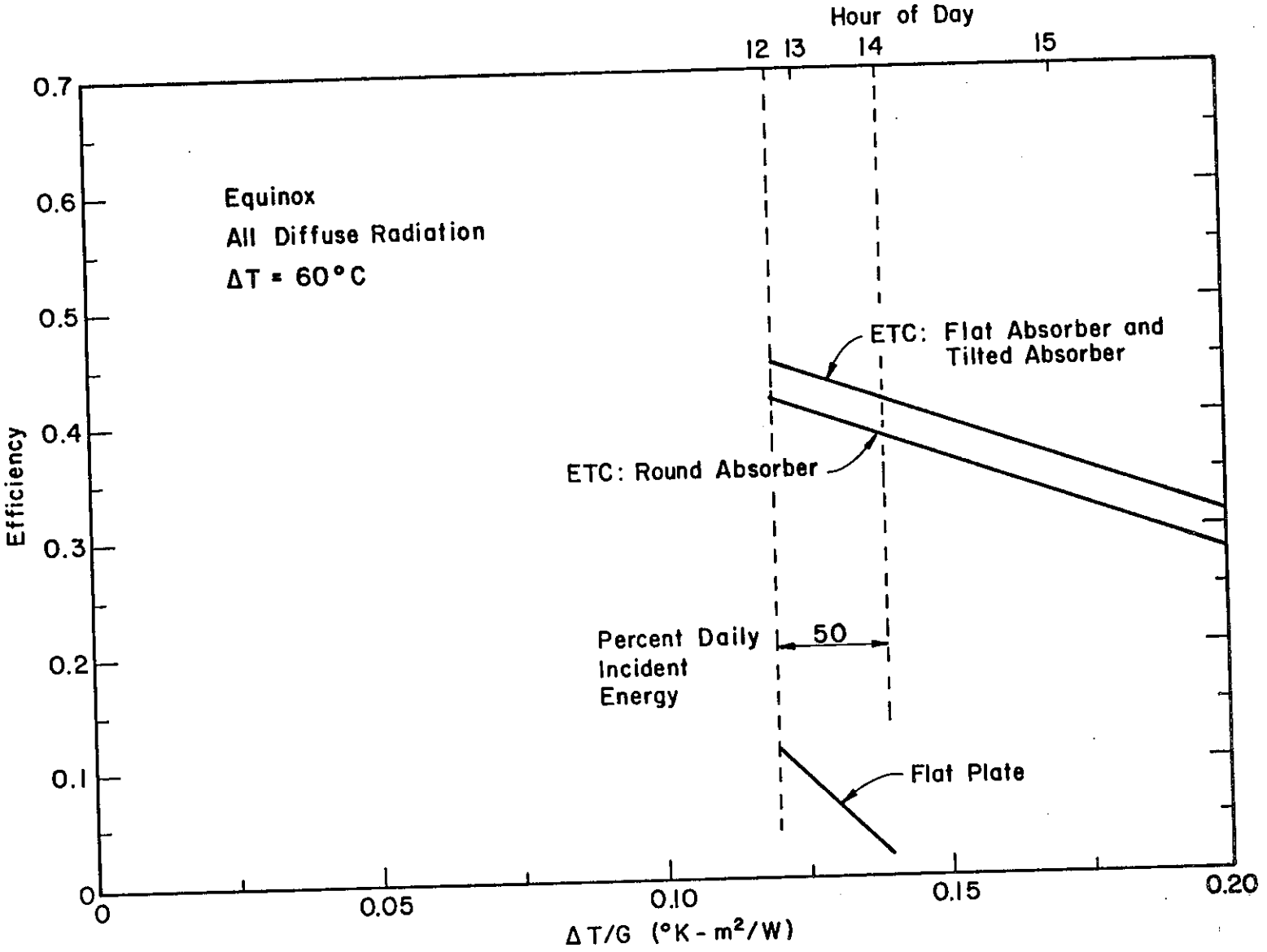

Figure 7-5 Calculated Effect of Incidence Angle on Collector Efficiency for a Diffuse Equinox Day.

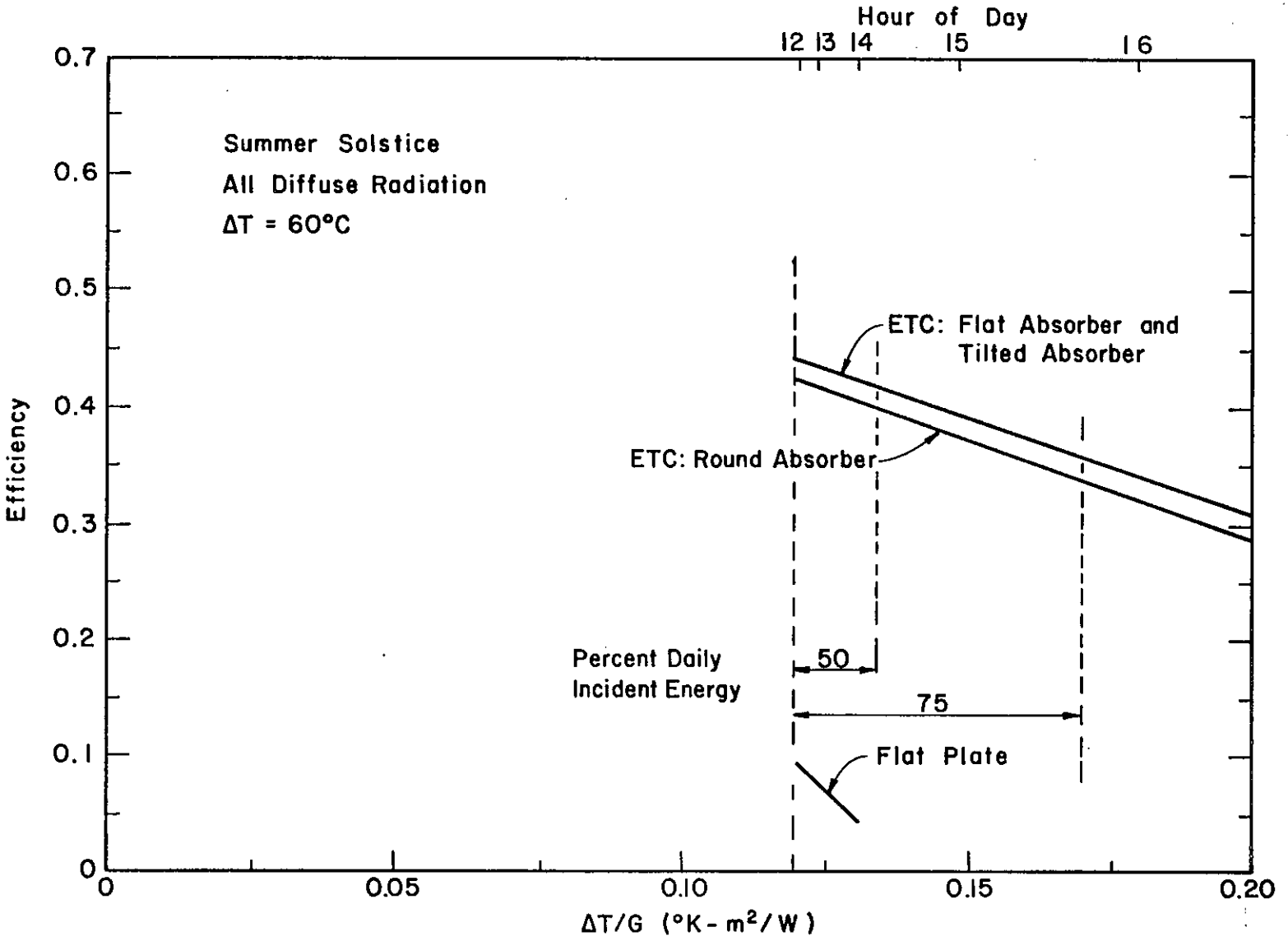

Figure 7-6 Calculated Effect of Incidence Angle on Collector Efficiency for a Diffuse Summer Solstice Day.

that the north-south tube orientation for the flat absorber evacuated collector provides more energy over a day than the east-west orientations. However, since a north-south tube orientation does not provide the possibility of a collector slope versus absorber slope tradeoff, the somewhat greater daily energy production may be offset in large arrays by interarray shading, greater structural cost for tilting the collectors, and greater interarray piping costs and losses.

Configuring the collector for one season or another may be more important since some applications, like space heating or space cooling, are seasonal. The ordering of the performance of the different evacuated collectors in Figures 7-1 through 7-6 does not change significantly from season to season, except for the cylindrical absorber north-south oriented collector. However, the magnitudes of the differences do. Whether the days are clear or diffuse, the performance of the flat absorber north-south oriented tube collector is the least affected by season changes.

The flat plate collector does not perform as well as some of the evacuated collector types and orientations for any part of the day during any of the seasons. Its performance looks comparatively best on a clear equinox day and worst on a solstice diffuse day.

7.1.2 Capacitance Effects

In the operation of real systems, measurements of energy collection may differ from calculated energy collection when capacitance effects are not included or cannot be included in the calculations. How capacitance will affect the measured performance of a collection system is shown in Figure 7-7 for the given set of collector parameters. This figure illustrates how measured efficiencies will change for different constant rates of increase or decrease in storage temperature at different levels of direct normal radiation. All other conditions are held constant.

In fact, measured instantaneous performance can be much more greatly affected by the capacitance of the collector and its fluid inventory than depicted in Figure 7-7. If the sun is suddenly covered by a cloud during an otherwise cloudless period of operation, measured insolation can drop fifty percent or more while measured energy collection is essentially undiminished due to energy stored in the collector. Measured collection efficiencies greater than one are not unusual in these cases. Such effects may also be caused by controls and other characteristics of system operation.

7.1.3 Collector Loss Temperature Dependence

Guisan et al[3] observes that, for typical evacuated collector operating temperatures, the temperature dependence of the collector loss factor can be modeled by a linear model of the temperature difference between the absorber and the ambient. Figure 7-8 uses this model to

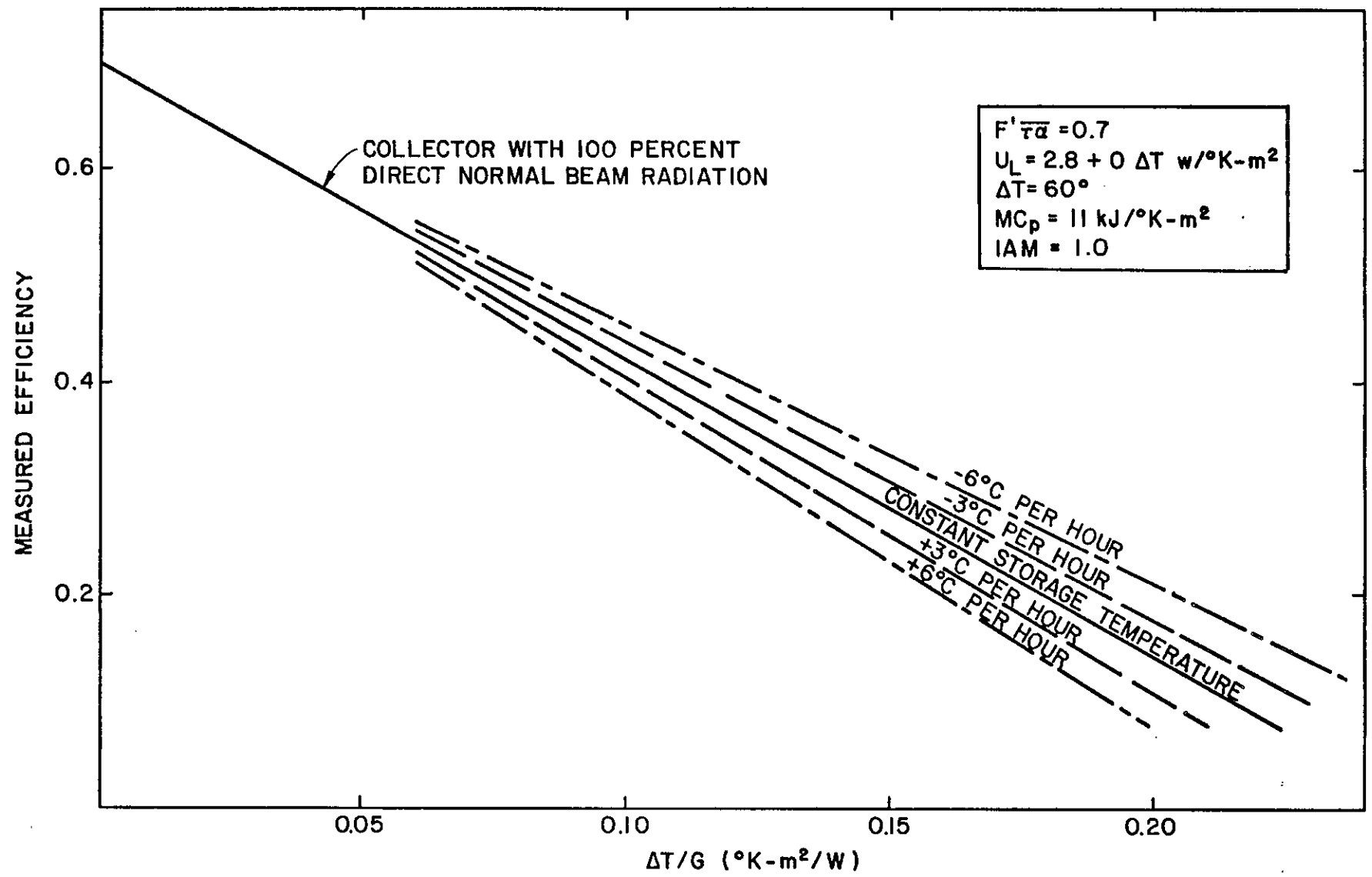

Figure 7-7 Calculated Instantaneous Collection Performance for Various Rates of Storage Temperature Change.

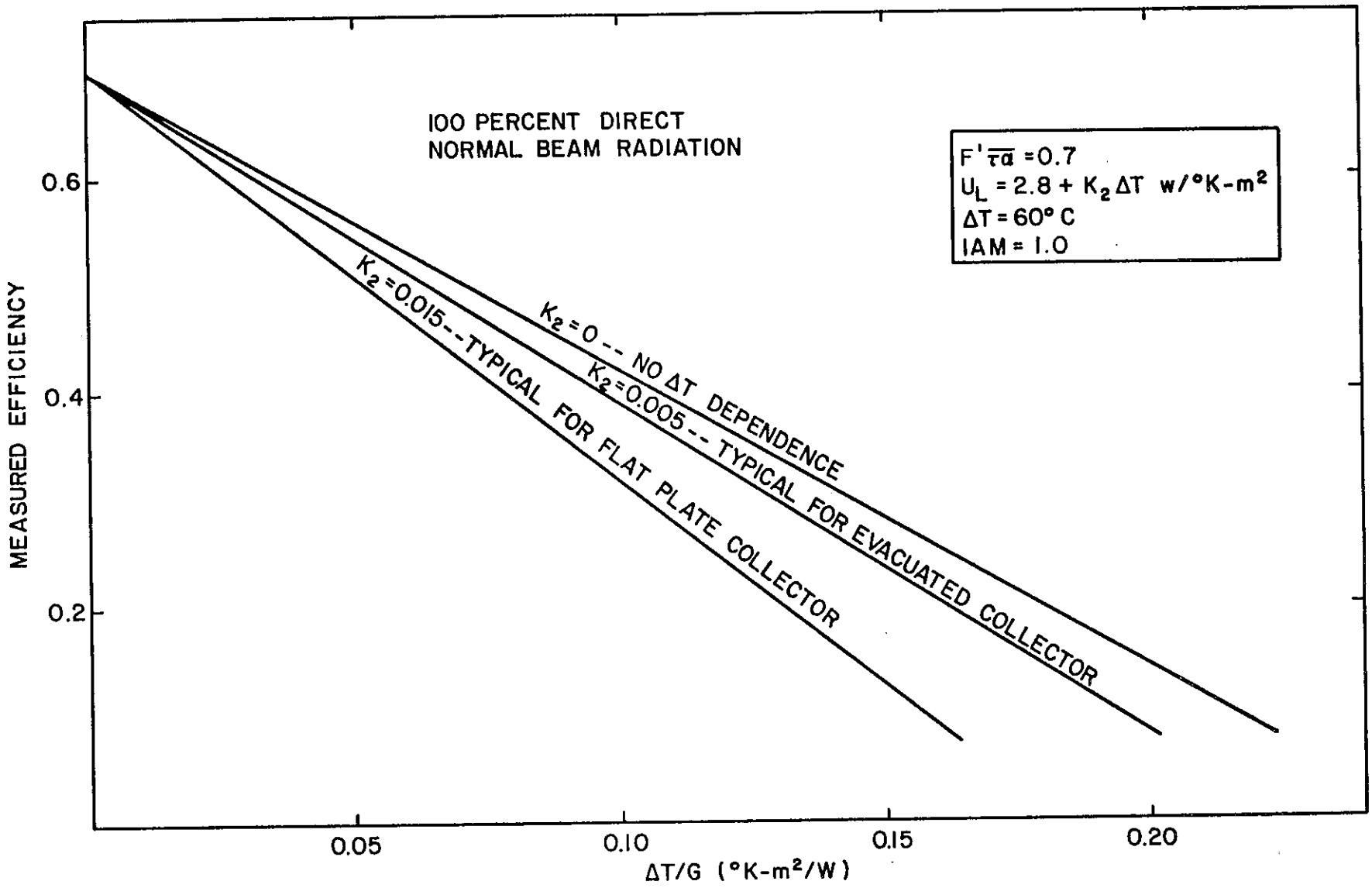

Figure 7-8 Calculated Instantaneous Collection Performance for Various U_L - ΔT Dependencies.

illustrate how instantaneous performance is effected by this dependency when all factors except insolation are held constant.

7.1.4 Other Factors

A number of effects other than capacitance, incidence angle, and collector loss temperature dependence can cause variations in collection efficiencies during operation of a system. Among these are shadowing effects of buildings and other collectors, reflection from the ground and surrounding structures, and unequal flow distribution in the collector field.

7.1.5 Installation Results

By now it should be clear that measured instantaneous performance of real systems under real operating conditions may fall far from the efficiency versus $\Delta T/G$ curves obtained from collector testing. Nevertheless, the effects discussed in the previous sections can often be identified in experimental measurement. For example, as can be seen in Figures 7-1 through 7-3, the Sydney University collector with the cylindrical absorber would be expected to show a rather small variation in efficiency across a range of $\Delta T/G$ values. This flat response can be clearly seen in Figures 6.1-5 and 6.1-6. The measured values in Figure 6.1-5 are restricted to 11 a.m. through 2 p.m. which is often close to direct normal insolation. When all day values are used in Figure 6.1-6, the greater incidence angle modifiers at higher incidence angles cause an almost completely flat efficiency curve.

In Figures 6.1-8, 6.1-10, 6.1-12, 6.1-14, 6.1-16, 6.1.18, and 6.1-28, effects of measured collection efficiencies much greater or much less than the average, due to energy storage in the collector, may be clearly seen. In Figures 6.1-51 and 6.1-53 a sequential pattern of the effect of energy storage in the collector on measured instantaneous performance may be clearly seen.

Figure 6-40 is an example of where we do not know which of the multiple efficiency curves to use because we have not segregated the points into ranges of G100. Thus, the linear curve that best fits the data is a weighted composite of operating conditions and is not likely to match the same curve generated during collector testing.

7.1.6 Predicting Longer Term Performance

Even if we could count on efficiency points of a real system under real operating conditions falling nearly on a line or curve, we still should not directly use efficiency curves to predict system performance since they provide no information about the $\Delta T/G$ values which are actually achieved during system operation. For example, we see by comparing Figures 6.1-24 and 6.1-25 that two collectors with similar efficiency curves supplying energy for different end uses during the same

period operate for different amounts of time at different values of $\Delta T/G$. Also, a collector that has a steeper efficiency curve slope, as in Figure 6.1-3, will operate in a narrow range of low values of $\Delta T/G$ whereas a collector with a shallower slope, as in Figure 6.1-5, will operate over a much wider range.

These differences in duration of operation at different values of $\Delta T/G$ could be determined by a detailed analysis, such as a simulation, but they are not at all obvious from the curves themselves. Thus, plots of instantaneous performance at direct normal incident radiation are not just a poor tool for estimating system performance, but potentially quite misleading. On the other hand, collection efficiencies during system operation and efficiency curves from steady state collector testing may be used to illustrate the effects which operating conditions have on performance as was done above, and, along with the proper incident angle modifiers, as collector models in detailed simulations.

7.2 DAILY PERFORMANCE

Daily energy input/output values, the ratio of daily energy output from the collector array to the solar energy input to it, provide a thermal performance measure that incorporates the effects that cause scatter in the collection efficiencies. The daily period is sufficiently long that the time constants involved in the various effects are short by comparison and any system biases, such as ground reflection or incidence angle effects, have run through a full cycle.

For a particular application, in a particular climate, and for a narrow operating temperature difference range, the daily energy input/output values form a straight line on a plot with a very high correlation, as may be seen in all the figures of section 6.2. Thus, two reliably determined sufficiently widely spaced points can determine a daily energy input/output curve. This has been done in Figures 7-9 through 7-11 by integrating the curves in Figures 7-1 through 7-6 over their incident energy distribution.

The following characteristics of input/output curves can be seen from close examination of these figures and from the work of Den Braven and Duff[53], Guisan et al[3], Boardman[34], and Hultin and Duff[29].

1. The slopes of the lines will be the same for collectors having similar optical characteristics, that is, similar absorber or absorber cross section to aperture ratios, similar absorber selective coating properties, similar absorber shapes, and similar reflector properties will produce lines with the same slopes.

2. The intercepts of the lines will depend on the daily losses of the collector array during the daily period of solar radiation. Losses during operation are affected by the magnitude the collector loss coefficient, the operating to ambient temperature difference, the length of the period of operation, and load patterns. The length of the non-

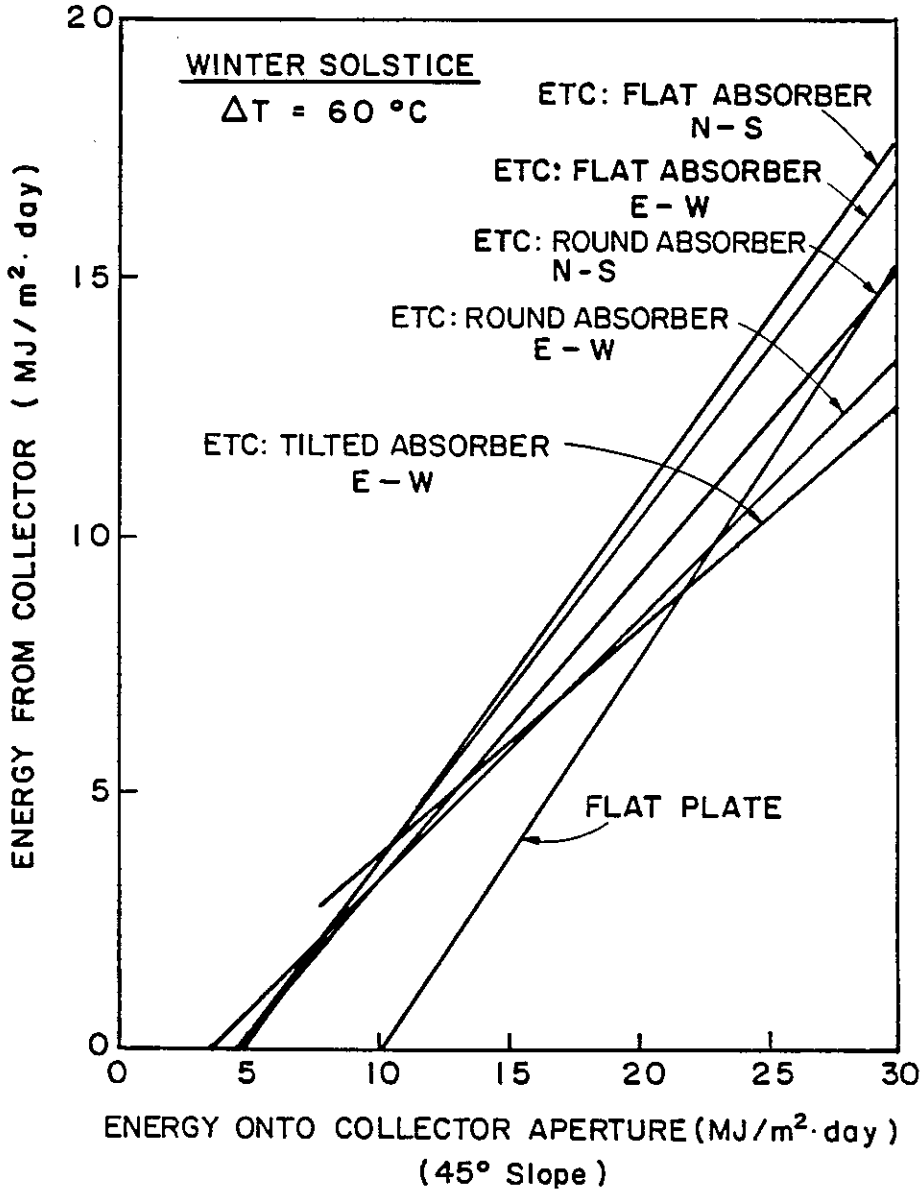

Figure 7-9 Daily Winter Solstice Energy Input/Output Curves Calculated from Figures 7-1 and 7-4.

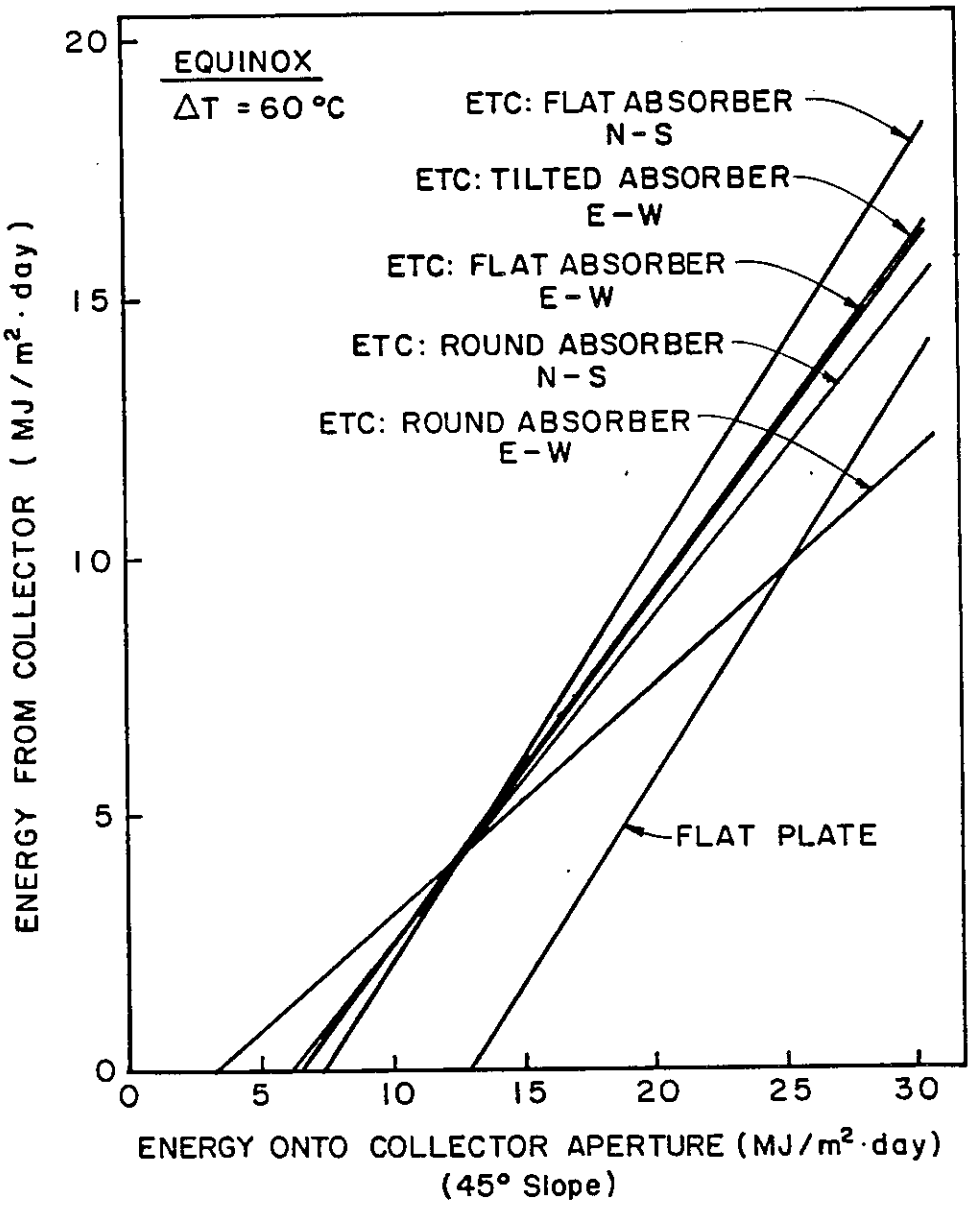

Figure 7-10 Daily Equinox Energy Input/Output Curves Calculated from Figures 7-3 and 7-6.

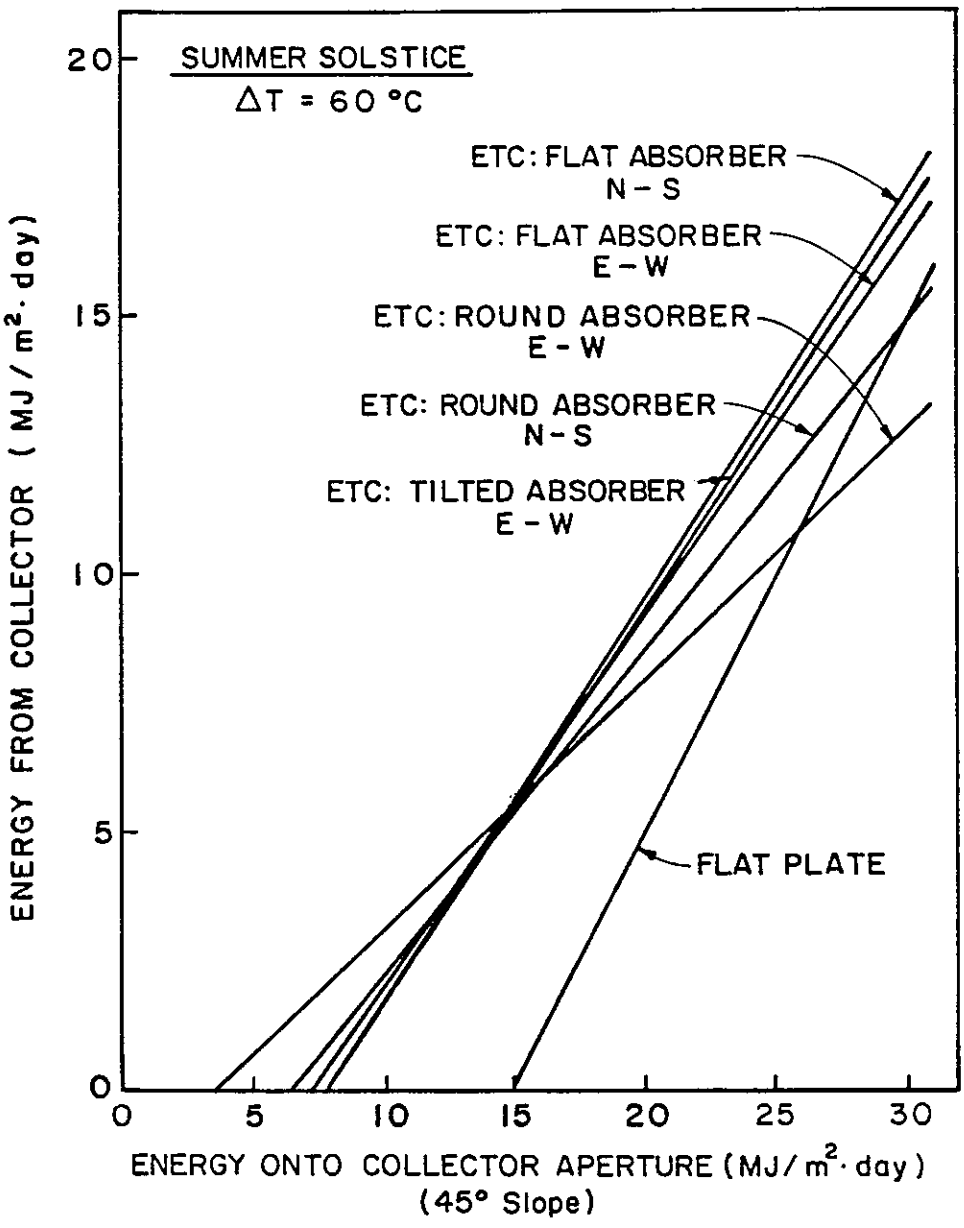

Figure 7-11 Daily Summer Solstice Energy Input/Output Curves Calculated from Figures 7-2 and 7-5.

operational period during periods of solar radiation can be substantial in large fields with high collector and interarray piping capacitance.

3. As ΔT, the temperature difference between the collector and ambient temperature, varies the intercepts, or equivalently the distances between the input/output lines, vary in a non-linear manner due to the dependence of the collector loss coefficient on temperature. That is, for the same collector an input/output line for a ΔT of $100^{o}C$ will be farther to the right of a $80^{o}C$ line than the $80^{o}C$ line is to the right on a $60^{o}C$ line.

4. For the same collector the most influential factor determining the output is of course the incident solar energy. After that the average ΔT is most important. Operating duration can also be important, particularly when contrasting the extremes of June and December. Load patterns and capacitance are usually lower order effects, though capacitance can be significant in large collector fields having substantial interarray piping.

5. Since the input/output curves of this report are regression fits they will differ in some cases in slope and intercept from the "true" curves due to the limitations of regression mathematics or the inadequacies of the data sets. If there is a cluster of the majority of points in one region and just a few points that are far removed, the far removed points will unduly influence the slope and intercept of the input/output curve. This effect is evident in some of the figures in section 6.2 and shows up in the lines not being parallel.

6. If there are points close to the lower part of the curve and excluded non-operational points, the curve may be pulled to the left at the bottom end due to the fact that some points have been "left off." It is also interesting that good evacuated collectors in low piping loss systems almost never encounter a non-operational day. This behavior is particularly evident in Figures 6.2-33 through 43, 6.2-48 through 51, and 6.2-93 through 95.

7. Thus, the same or similar collectors operating in similar systems with close to the same solar radiation duration and capacitance should produce nearly the same input/output curves. See Figures 7-12 through 14. These points provide a basis for using input/output curves to make thermal performance comparisons of different systems, collectors, climates, and seasons.

7.2.1 Tube Length and Width

Some manufacturer's early versions of their collectors, notably Philips and Sunmaster/Solartech, had tubes about two-thirds the length of those in current collectors. These shorter tube collectors had substantially poorer performance as can be seen in Figures 7-15 and 16. Sunmaster has also made substantial improvement in its selective surface when it went to longer tubes. Performance of these collectors are

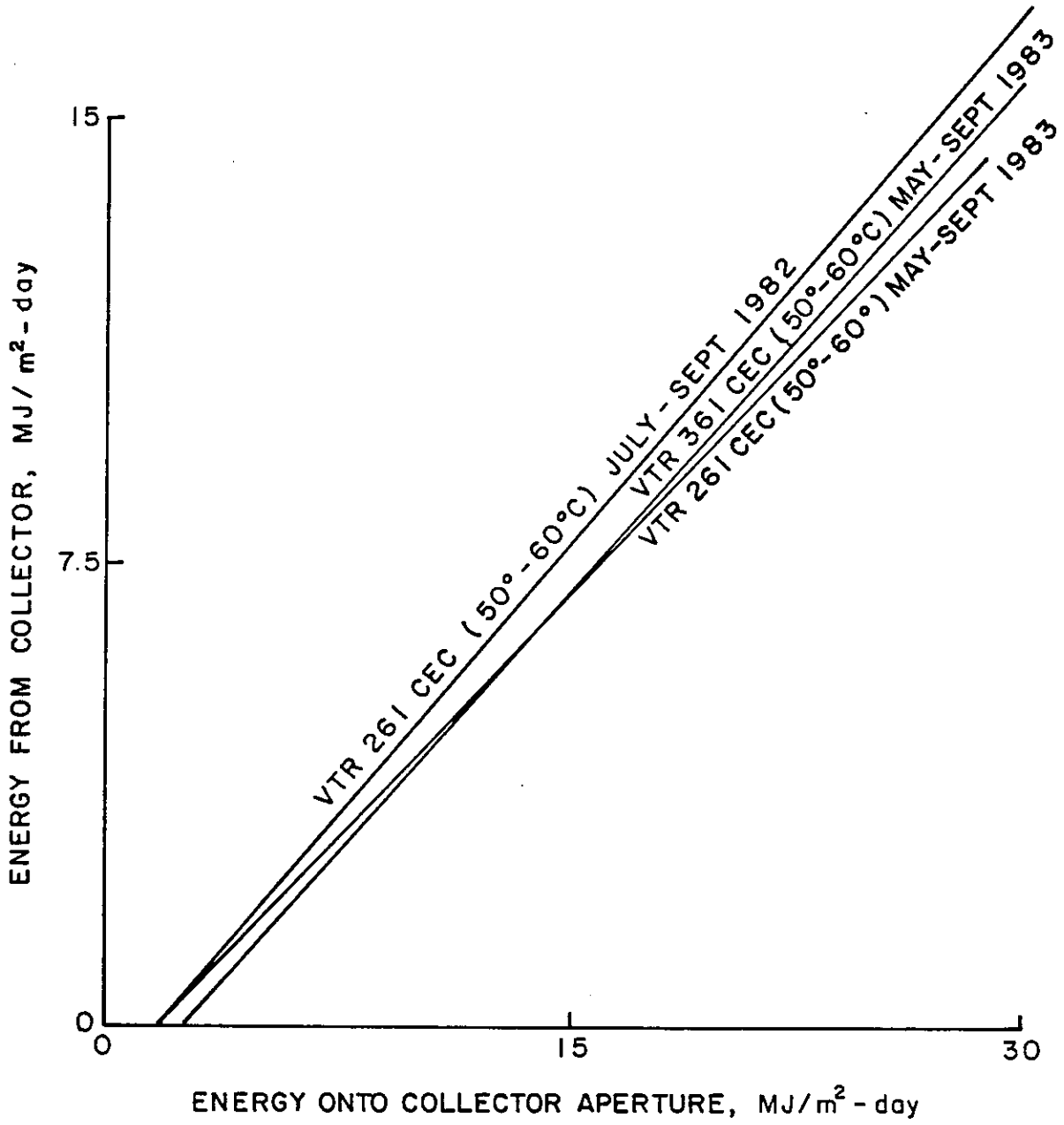

Figure 7-12 Daily Energy Input/Output Curves for Similar Collectors and Temperature Difference Ranges at the CEC Installation.

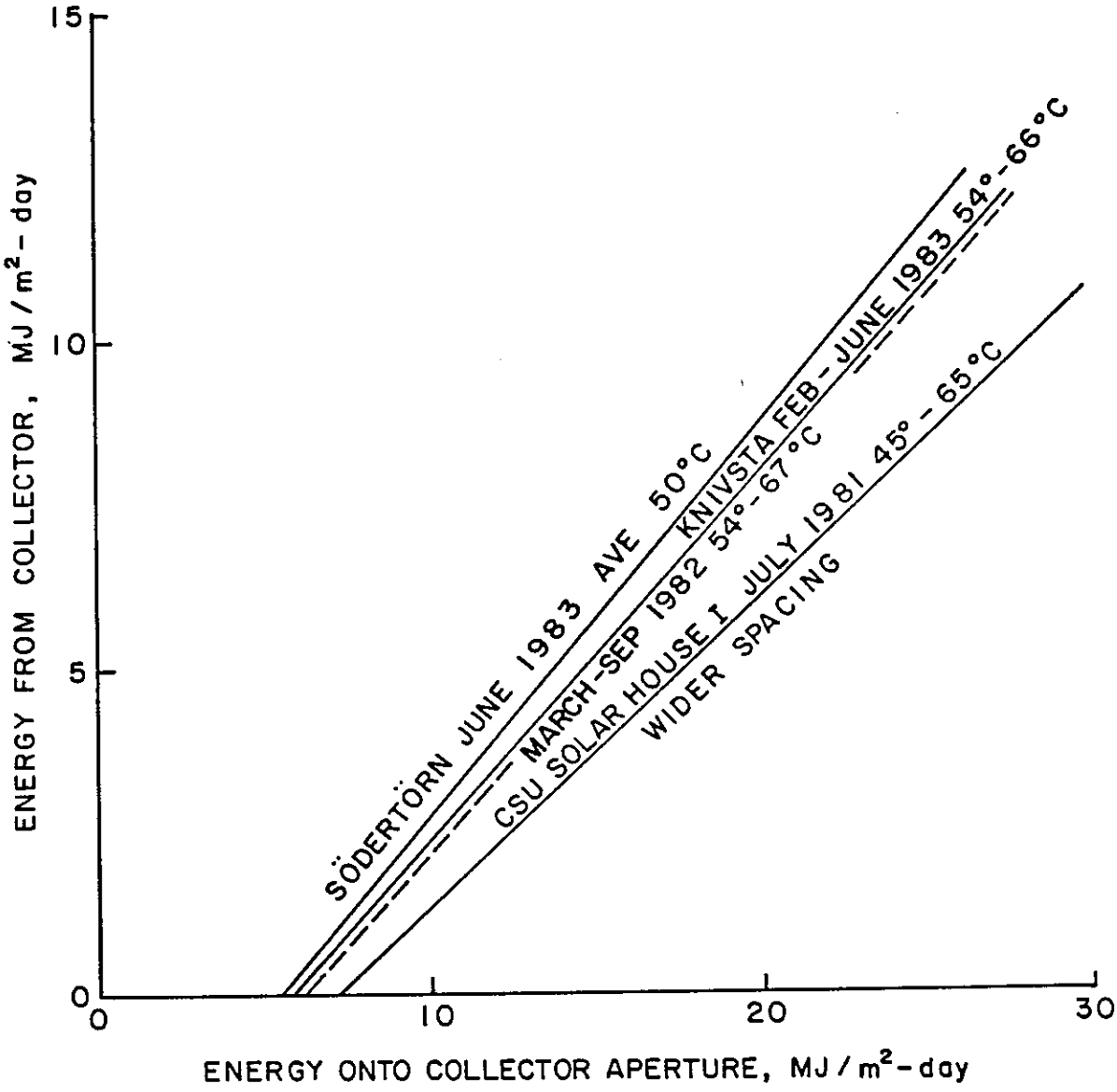

Figure 7-13 Daily Energy Input/Output Curves for the Philips VTR 141 in Various Locations.

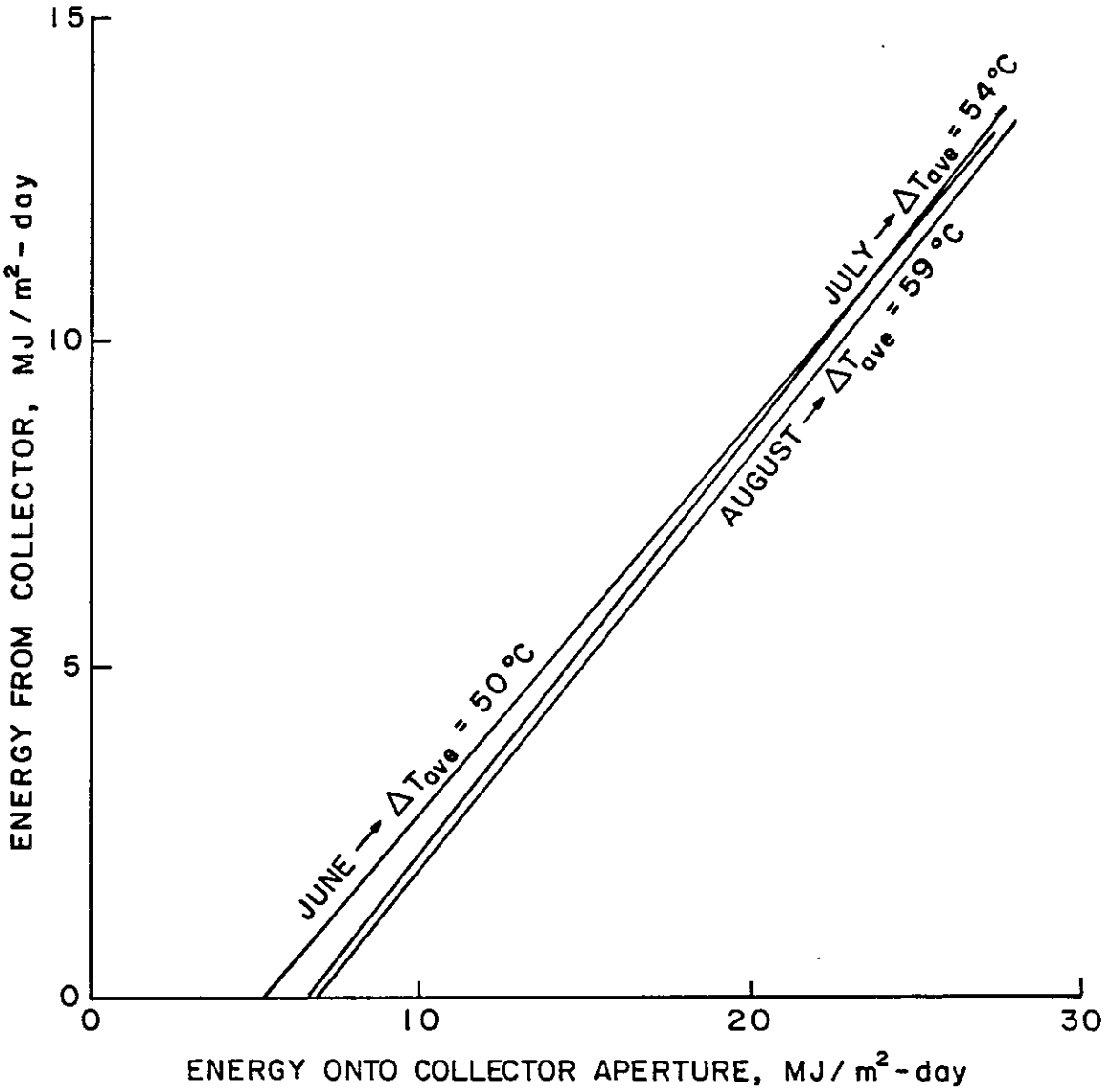

Figure 7-14 Daily Energy Input/Output Diagram for the Södertörn Philips VTR 141 Collector in 1983.

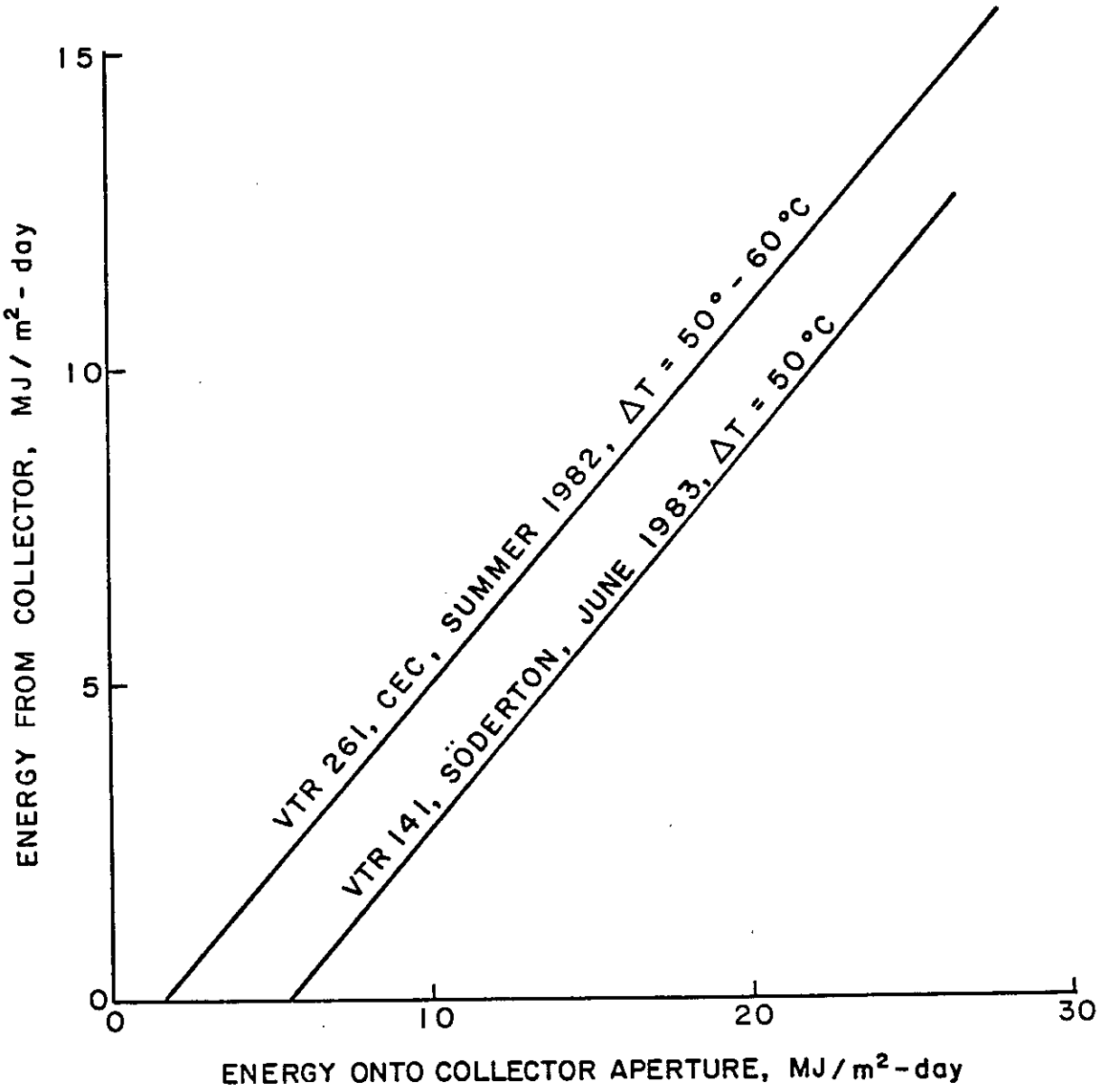

Figure 7-15 Comparison between Philips Long and Short Heat Pipe Evacuated Tube Collectors.

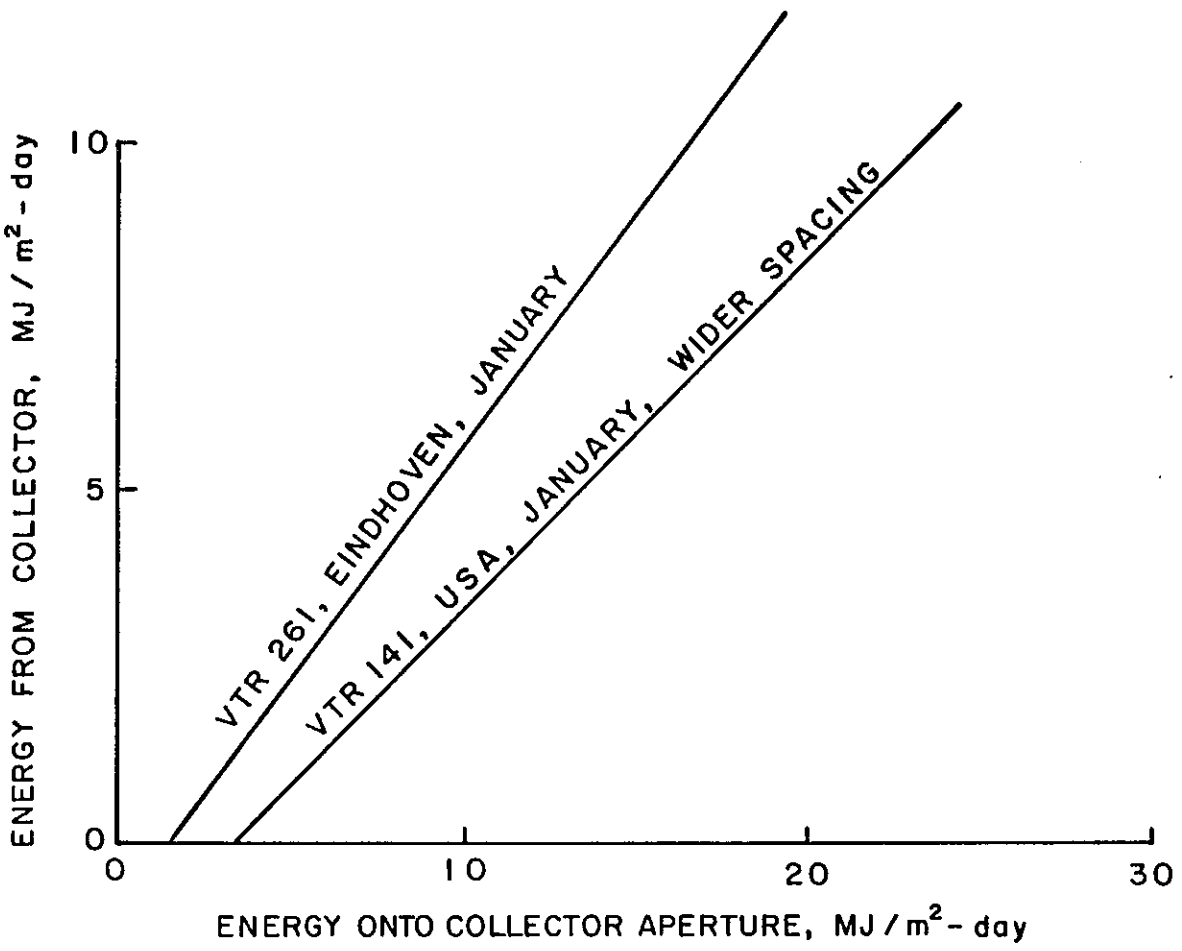

Figure 7-16 Comparison between Philips Long and Short Heat Pipe Evacuated Tube Collectors, Winter.

included in the supplementary installation performance results of Appendix E.

Lengthening a tube increases collector performance to a point of diminishing returns, due to the reduction in conduction losses per tube and the amount of manifolding required per unit of absorber area. Thus, collector module and array performance is improved. The same should be true when tube width is increased, although comparisons could not be made from Task VI installation results.

7.2.2 Different Evacuated Collector Types

Figure 7-17 shows the ranges of daily collection performance on an aperture area basis of the Task VI installations for a ΔT of 50^{o} to $60^{o}C$. The highest performance shown is for a Philips array of close packed VTR 261 tubes with a flat reflector. The lowest performance is for a General Electric array of widely spaced tubes with a CPC reflector. Also shown is a Solartech collector, with widely spaced tubes and a CPC reflector. Obviously, different evacuated collectors perform quite differently.

Figure 7-18 fills in Figure 7-17 with other Task VI collectors. As can be seen, the highest performers on an aperture area basis are the Corning and Philips VTR x61 series collectors. A few of the collectors shown are operated at higher ΔT's and thus their curves are shifted to the right. Also shown are some flat plate collectors which were included in some Task VI installation experiments.

7.2.3 Tube Spacing and Reflectors

Close packed tubes, like the Corning and some Philips VTR 261 collectors, and moderately close packed tube collectors with reflectors, like the Philips VTR 361 and some Philips VTR 261 collectors, perform about equally in the temperature ranges occurring in Task VI installations. This can be seen in Figure 7-18 and the appropriate figures in Chapter 6. When spacing is wide, as in the Solartech or General Electric collectors, daily performance based on aperture area is lower as can be seen in Figure 7-17.

7.2.4 Evacuated Versus Flat Plate Collectors

By far the most common solar collector sold, other than for low ΔT applications such as swimming pool heating, is the single glazed selective flat plate collector with one glass cover. Three of these collector types were included in Task VI installations. Also included was selective absorber flat plate collector with one glass top cover and two inner teflon glazings manufactured by Scandinavian Solar.

Figure 7-18 shows the daily performance of these collectors at ΔT's of 45^{o} - $60^{o}C$ compared to several evacuated collectors. At these

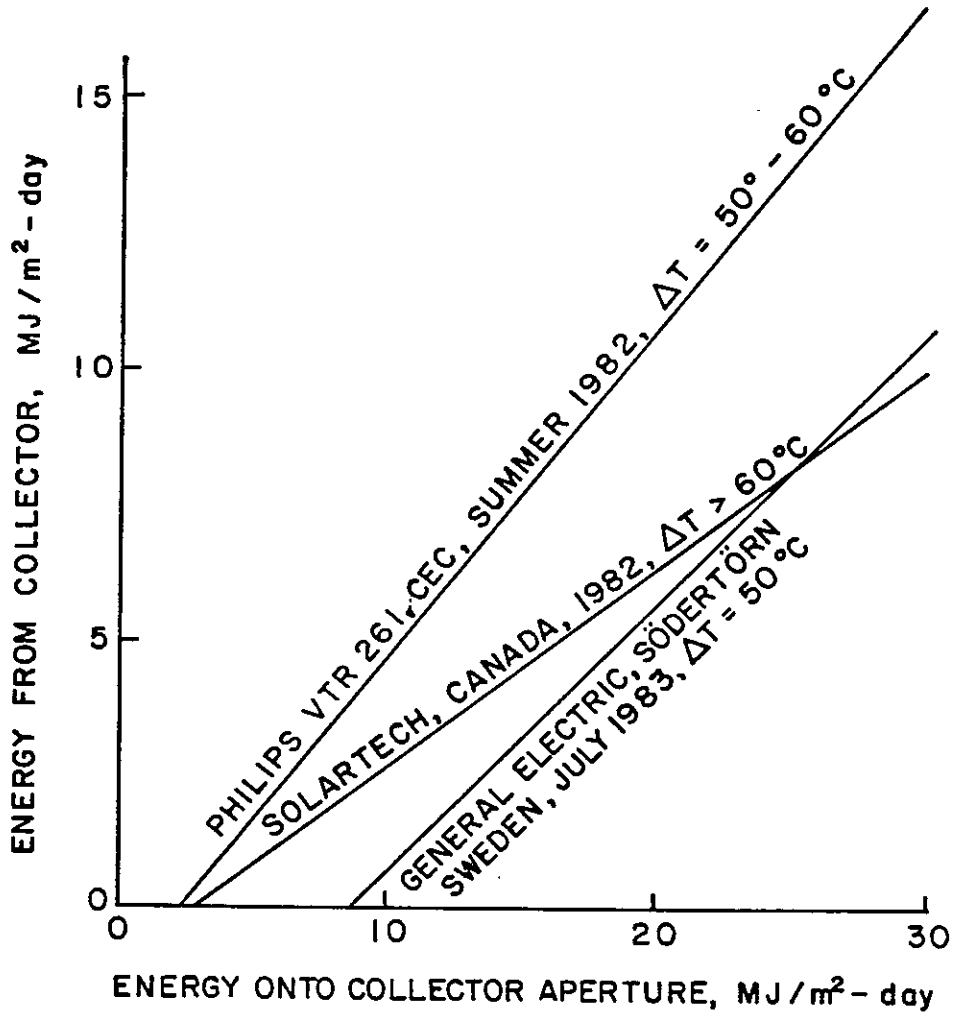

Figure 7-17 Ranges of Daily Performance.

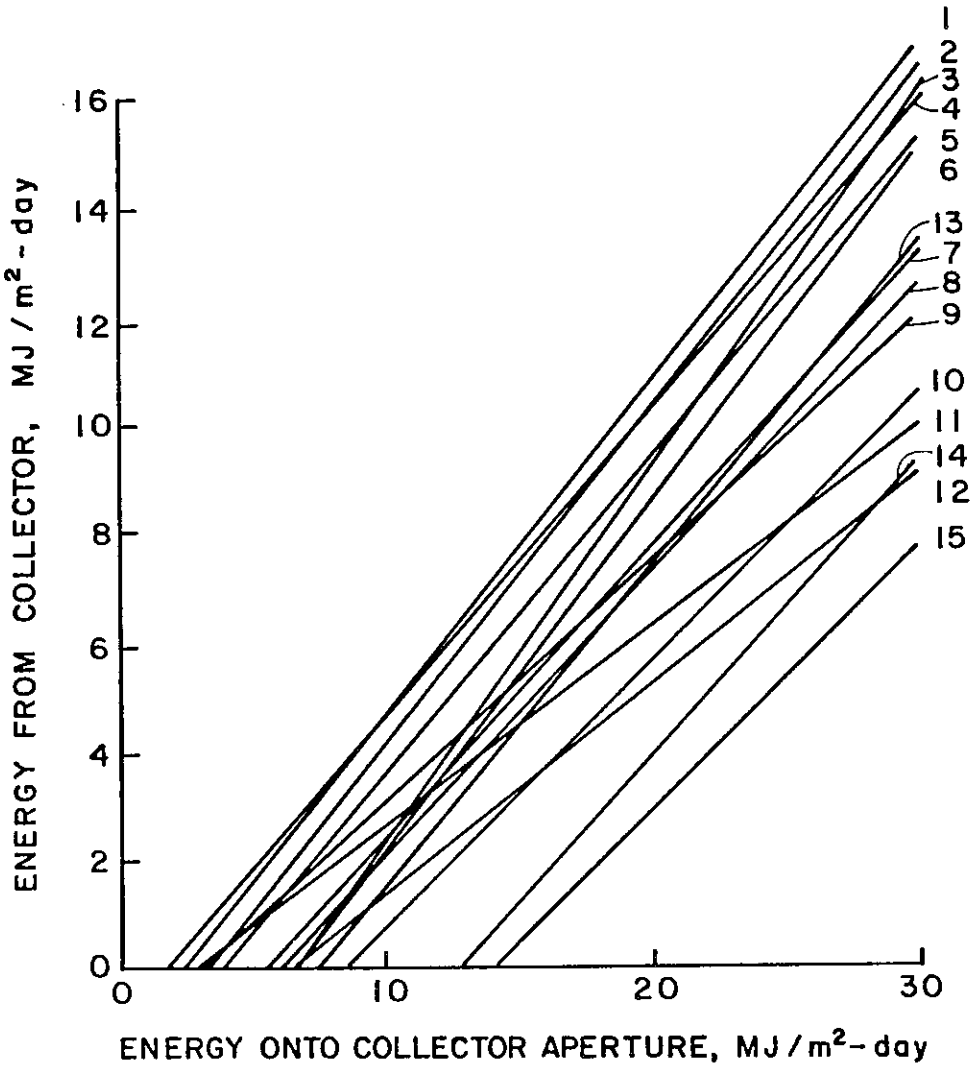

Evacuated Collectors

1. Philips VTR 261, CEC, Summer 1982, $\Delta T=50^{o}-60^{o}C$
2. Corning, USA, FRG, 1982, $\Delta T=45^{o}-60^{o}C$
3. Philips VTR 361, USA, September 1983, $\Delta T=65^{o}-75^{o}C$
4. Philips VTR 261, FRG, June-December 1982, $\Delta T=45^{o}-60^{o}C$
5. Corning Type A, Geneva, July-September 1983, $\Delta T=65^{o}-75^{o}C$
6. Philips VTR 141, Södertörn, Sweden, July 1983, $\Delta T=54^{o}C$
7. Sydney University, Summer 1983, $\Delta T=45^{o}-80^{o}C$
8. Sanyo, CEC, May-September 1983, $\Delta T=50^{o}-60^{o}C$
9. Philips VTR 141, UK, 1981-1983, $\Delta T=20^{o}-50^{o}C$
10. General Electric, Södertörn, Sweden, July 1983, $\Delta T=51^{o}C$
11. Solartech, Canada, 1982, $\Delta T=60^{o}C$
12. Sanyo, Geneva, April-August 1983, $\Delta T=60^{o}-75^{o}C$

Note: The above collectors are designated by tube type. The collectors may have different tube spacing and reflectors. Refer to Table 4-2.

Triple Glazed Selective Flat Plate Collector

13. Scandinavian Solar, Södertörn, Sweden, July 1983, $\Delta T=49^{o}C$

Single Glazed Selective Flat Plate Collectors

14. Technoterm, Södertörn, Sweden, July 1983, $\Delta T=55^{o}C$
15. Gränges Aluminum, Södertörn, Sweden, July 1983, $\Delta T=55^{o}C$

Figure 7-18 Daily Performance of Task VI Collectors.

temperatures the evacuated collectors substantially outperform the single glazed selective flat plate collectors and the best evacuated collectors substantially outperform the Scandinavian Solar flat plate collector.

Though data are not available to make the same comparisons in the ΔT range of 60^{o} - $75^{o}C$ or higher ranges, it is clear from the collector loss factors given in Table 4.2 what will happen. The loss factors for the flat plate collectors are much greater than those of the best evacuated collectors and thus in Figure 7-19 the flat plate collector curves will shift far more rapidly to the right as ΔT increases than the evacuated collector curves. The Solartech collector, with the smallest loss factor amoung the flat plate collectors, will have its curve shift a lesser amount.

7.2.5 Seasonal Differences

Because of longer day lengths in the summer, collectors tend to have longer operating time and hence greater daily losses at a given ΔT as compared to winter. Because of this, for a given amount of solar energy onto the collector, less energy is typically collected in the summer than in the winter. Thus the daily energy input/output curves are shifted to the right in summer. This behavior can be seen in Figures 7-20 and 7-21.

7.2.6 Preheating and Capacitance

Heating of collector arrays by nighttime circulation of heated fluid is one means of freeze protection. This approach is a net energy loser. However, if care is not taken in interpreting the daily energy input/output curves, one may erroneously assume that there is greater collection for the preheat mode. As collectors and their fluid inventory normally cool down to close to ambient temperature by morning, a collector array with large capacitance is given a substantial head start on energy collection for the day when it is preheated by nighttime circulation. This, of course, shows up in the daily energy input/output diagram as increased energy collection. What does not show up, is the even greater losses during nighttime circulation.

Figure 7-22 shows the magnitude of this effect in a high capacitance collector and Figure 7-23 the magnitude in a low capacitance collector. Comparison of the two figures gives a feeling for the magnitude of the difference in losses suffered when one chooses a high or a low capacitance collector.

7.2.7 Snowcover

The effect of snow cover on daily performance may be clearly seen in Figure 6.2-91 and 6.2-92 where points have been retained for days where snow covered the collector for some part of the day, although the points were not included in the regression analysis. Appreciable collection has

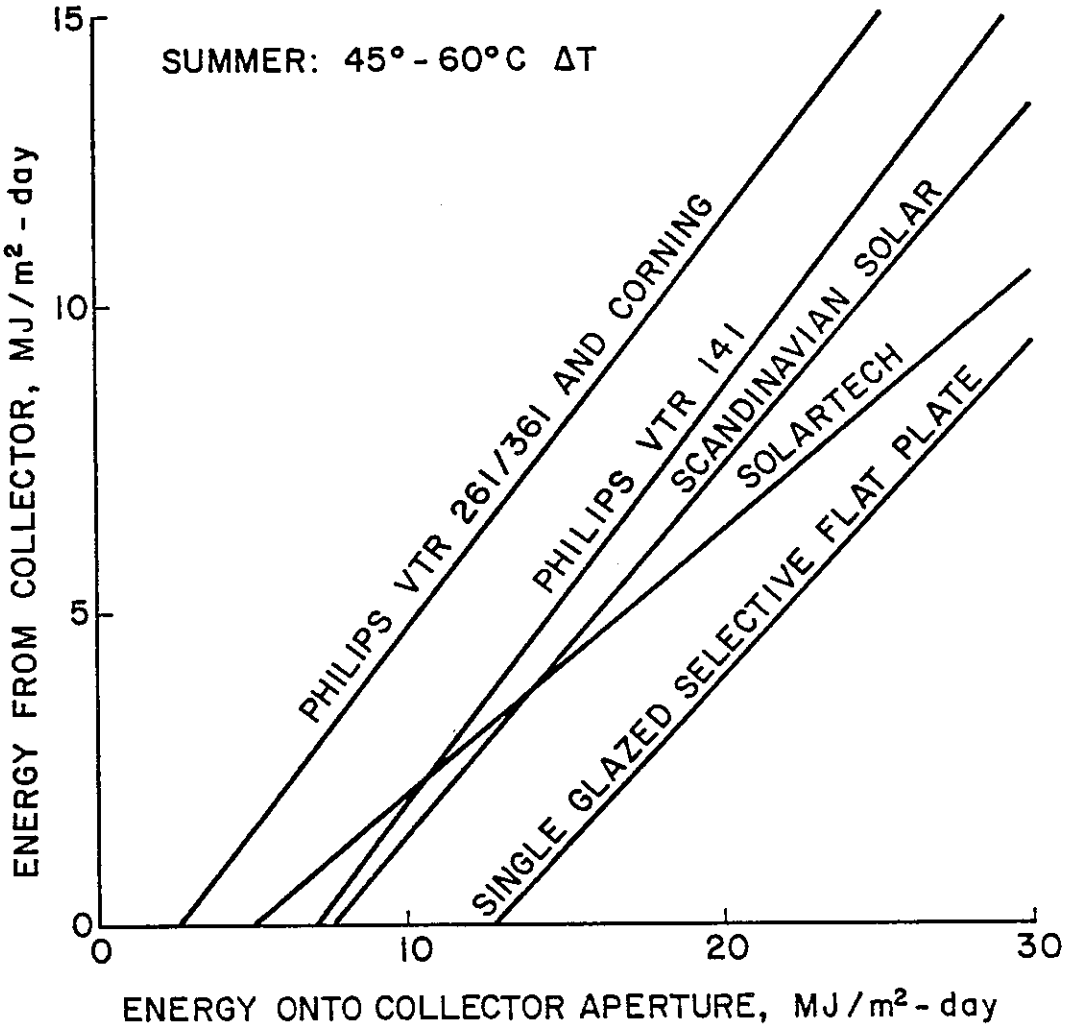

Figure 7-19 Comparison Between Evacuated and Flat Plate Collectors Daily Performance.

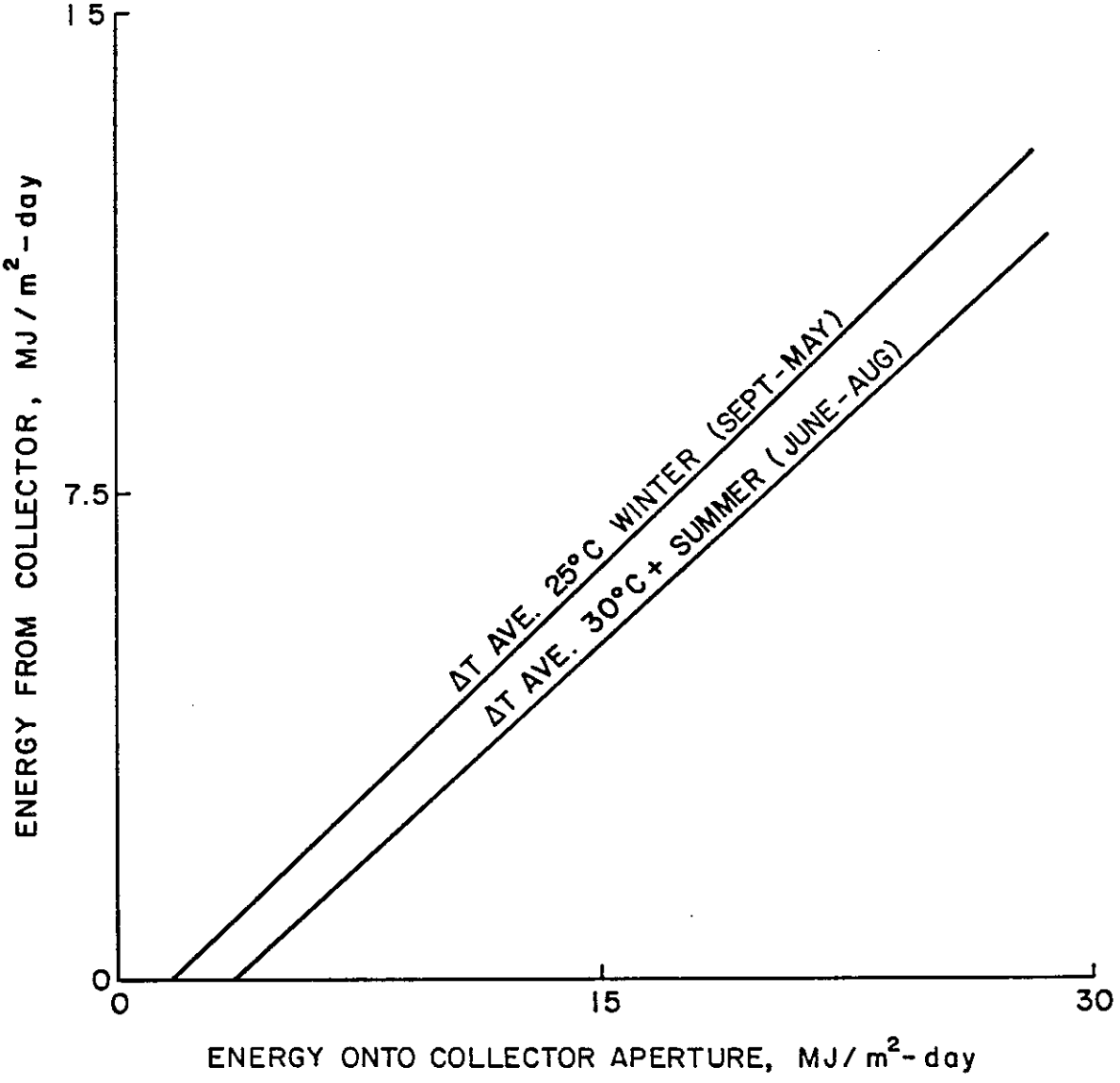

Figure 7-20 Seasonal Influence on Daily Performance for the UK Experiments.

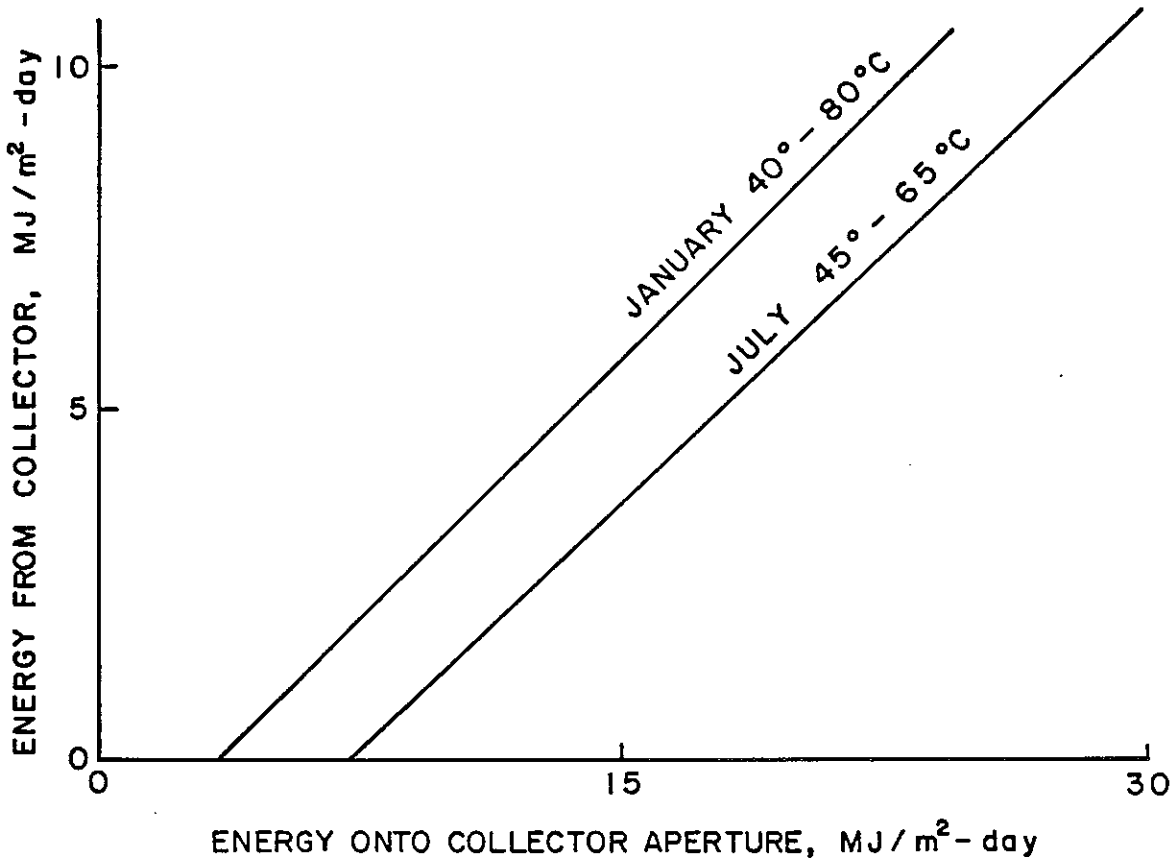

Figure 7-21 Seasonal Influence on Daily Performance for the USA Experiments.

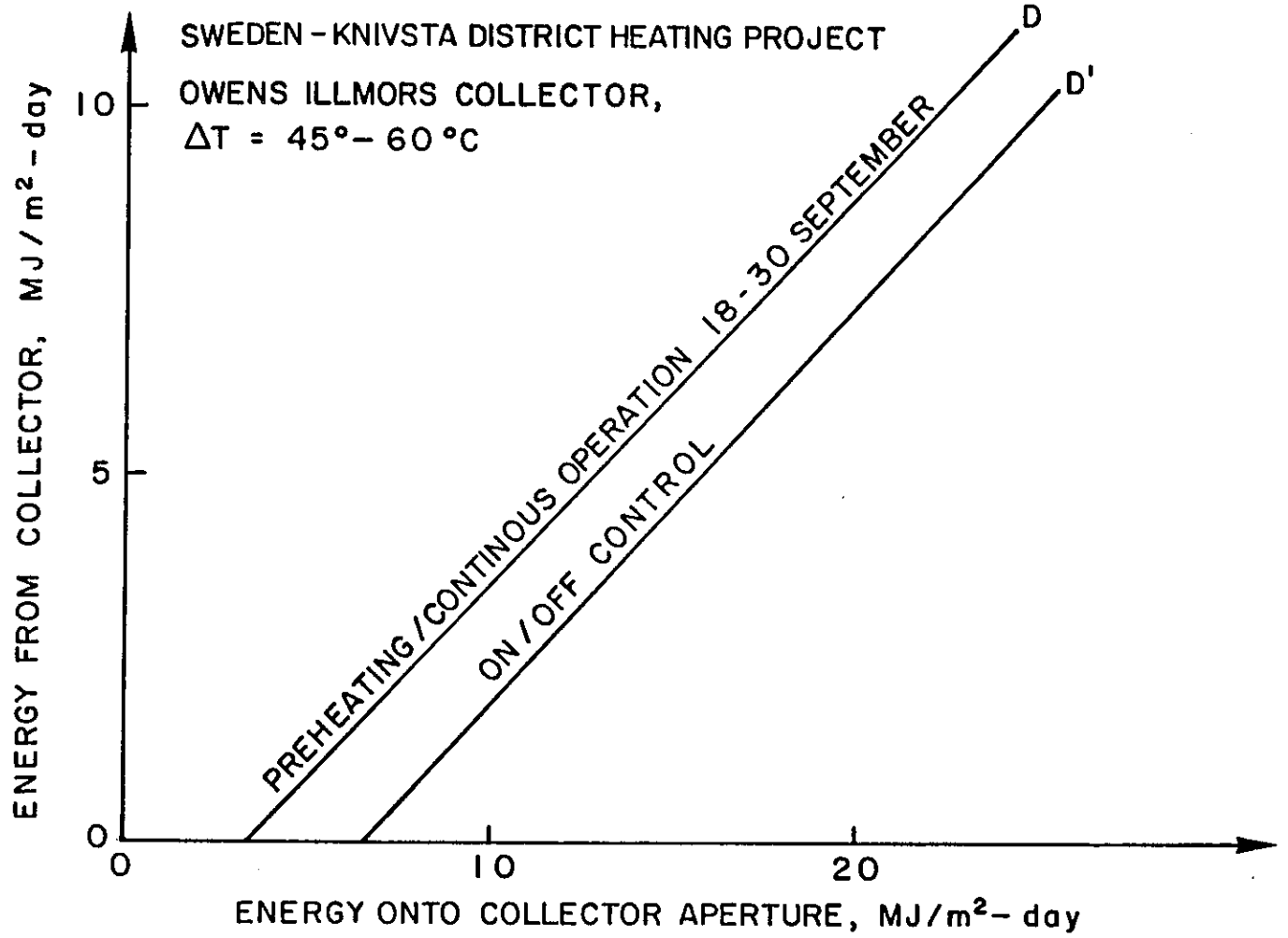

Figure 7-22 Effects of Preheating on Daily Performance of High Capacitance Collectors.

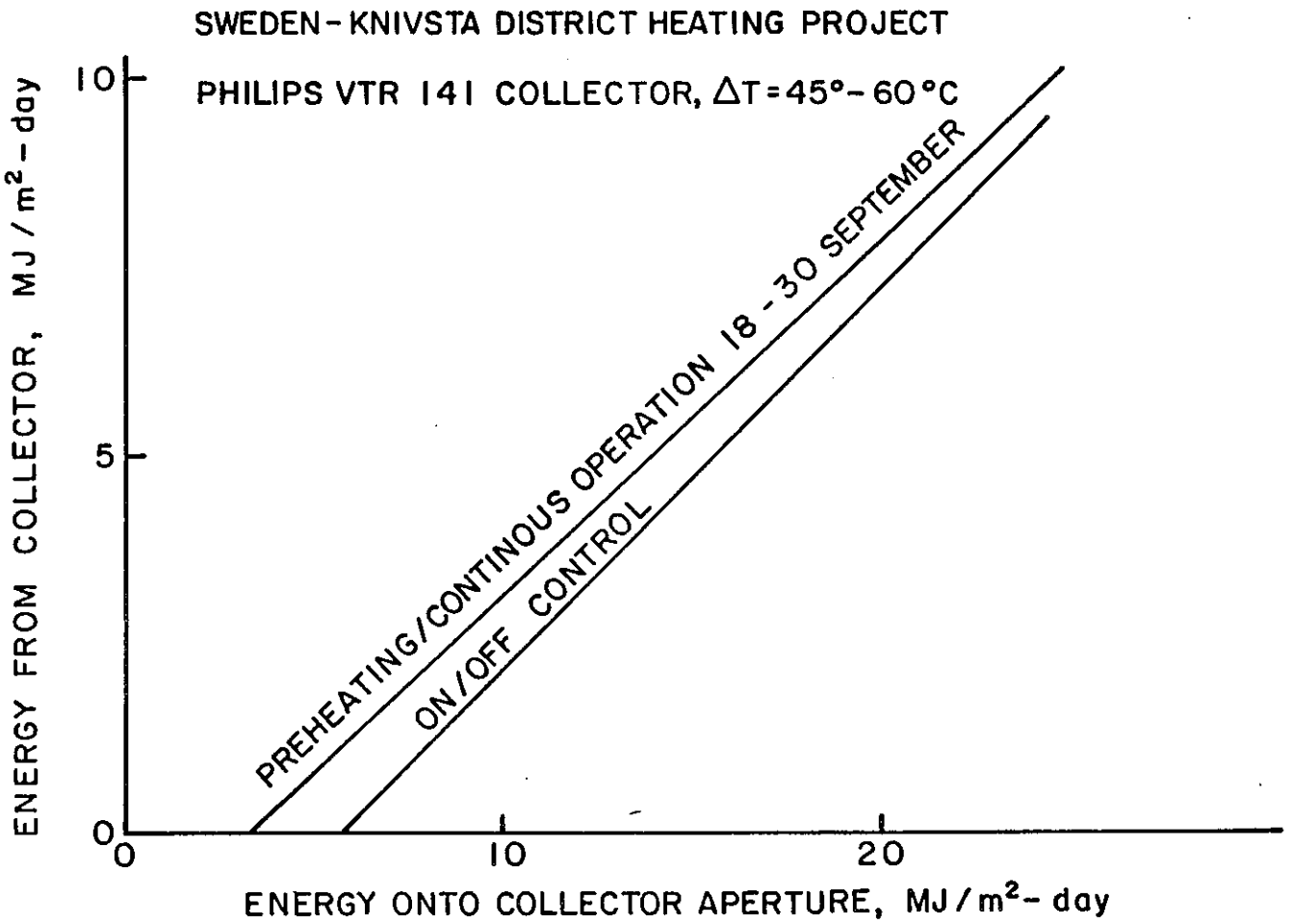

Figure 7-23 Effects of Preheating on Daily Performance of Low Capacitance Collectors.

been observed to take place when collectors are completely covered with snow, especially when the cover is thin and collection does not depend heavily on reflectors. Reflectors can be a factor in collecting and retaining snow as may be seen from the discussion in section 6.8. The best avoidance of deterioration of performance due to snow cover in locations where it may be a problem is by tubes not too closely packed with a substantial clearance from any background surface. The worst avoidance would be with widely spaced tubes with a specular reflector.

7.3 MONTHLY PERFORMANCE

From section 6.4 it may be seen that evacuated collector monthly midwinter, December or January, performance varies from a collection fraction low of 8 percent for Canada to a high of 50 percent for the USA and midsummer, June or July, performance varies from a low of 15 percent for Switzerland to a high of 54 percent for the FRG. Monthly collection fractions of 45 to 55 percent were common for the Corning and Philips VTR x61 series collectors and 40 to 50 percent for the Sydney University and Philips VTR x41 series for most months of the year.

7.4 ANNUAL PERFORMANCE

As can be seen in section 6.3, high annual collection fractions were achieved for some installations, notably 57 percent for the Philips VTR 261 collector in the 1982/83 FRG DHW system, 40 percent for the Philips VTR 141 collector in the 1982/83 Swedish Södertörn district heating system, and 51 percent for the Corning/Philips VTR 261 collectors in the 1982 FRG DHW system.

7.5 SYSTEM EFFICIENCY AND SOLAR FRACTION

In any of the Task VI installations it would be possible to achieve a high solar fraction with almost any type collector by installing an excessively large collector area. In many of the Task VI installations it would be possible to achieve a high systems efficiency with almost any collector by keeping the temperatures low and using a small collector area. High system efficiencies combined with high solar fractions in Task VI applications are only achieved with evacuated collectors. A particularly high value of both measures may be seen in section 6.6 for the FRG installation.

7.6 SHIPPING AND INSTALLATION

7.6.1 Shipping

Some problems were experienced in shipping collectors. Task VI results, consistent with other studies on tube breakage, are summarized

in Table 7-3. These difficulties were particularly evident when small quantities of tubes were shipped. In Table 7-3 more than two-thirds of the breakage resulted during small shipments. Only minimal breakage occurred in large, palletized shipments. It is clear that careful package design is important, especially for small shipments.

Table 7-3 Tubes Lost During Shipping

Total Tubes	Total Broken or Lost Vacuum
4188	62

7.6.2 Installation

Some collectors arrived on site as fully assembled units, while others were assembled in place. Both approaches have advantages and disadvantages. Fully assembled collectors are heavier, must be handled more carefully, and may require special equipment to lift them up to a roof. On the other hand, on site assembly can be costly, time consuming, and sometimes physically difficult.

No significant differences were observed for tube breakage during installation for the two different generic types.

Some collector designs impose strict requirements on the positioning of piping. For example, the drainable liquid-in-glass design of Sunmaster and Solartech requires that the header pipes be inclined. In other designs, such as the Corning and Sanyo collectors, high pressure drops in the collector require careful manifolding design to avoid large pumping power requirements. Finally, in collector designs with multiple parallel flow paths, care must be exercised in piping design and installation if reasonably uniform fluid flow through the collectors is to be achieved.

A problem in many installations was leakage, often caused by breakage of the flexible rubber couplings between collectors. Such couplings are usually required because of the substantial thermal expansion, about 2 mm per meter, possible in the headers of collectors. Leakage often occurred after a system stagnation.

It was found that the rubber hose connections aged and became hard and brittle. Present-day designs using such connections use silicone rubber hose, which is believed not to show these effects.

In addition, Philips collectors, which use Victaulic couplings, showed far fewer leaks and collectors which could be joined with soldered

fittings showed no leaks. Some collectors, such as the Sunmaster and Solartech designs, with one O-ring seal for each tube and four hose connections per module, have a higher potential for leakage.

Some collectors, such as Philips, Sydney University, Sunmaster and Solartech, required relatively simple plumbing. In the case of Sun master and Solartech, this is due to the incorporation within the collector module of the flow distribution system. For the Philips collector, the use of a single header pipe greatly simplifies the fluid distribution system.

Consideration of weight and wind loading is required for all collectors. Collector weight and site accessibility also may necessitate a crane during installation. The design of the collector support structure is also affected by the collector design and plumbing requirements. Some collector tubes, such as Corning, can be mounted horizontally with inclined absorbers, thus minimizing support hardware, giving close packing of tubes, and reducing external piping. The use of reflectors tends to restrict the flexibility of mountings.

Since the various collector types are so different in their mounting and plumbing requirements, it is usually necessary to determine the collector type to be used before the support hardware can be designed.

7.7 OPERATION

7.7.1 Thermal Shock

Some collectors, particularly the liquid-in-glass types are particularly sensitive to malfunctions of the operating system. Serious breakages have occurred with these collectors during start-up when hot collectors were filled with cold fluid. See Table 7-4. Correct operation of the system should prevent such an occurrence.

Table 7-4 Tubes Lost During Installation

COLLECTOR TYPE	TOTAL SHIPPED	TOTAL BROKEN OR LOST VACUUM
Metal Fin-in-Glass	1980	2
Dewar	2208	150*

* 150 lost due to a hot start

7.7.2 Stagnation

Collectors which are operating without heat extraction are said to be under stagnation. Evacuated collectors typically stagnate at 250-300°C under full insolation, although slightly higher temperatures can be achieved with concentrators or very low emittance selective surfaces. The collectors used in the Task installations showed no degradation effects which could be attributed to stagnation.

7.7.3 Loss of Vacuum and Breakage

In most installations, a very small number of tubes were observed to lose vacuum. In addition, a few breakages occurred during operation and these were often due to unidentified reasons. The number of such failures, on the order of one percent, is given in Table 7-5.

Table 7-5 Tubes Lost During Operation

COLLECTOR TYPE	TOTAL	LOST VACUUM	NUMBER BROKEN
Metal Fin-In-Glass	3295	36	50*
Dewar	2208	34	4

*43 lost due to large hail.

The low rate of such failures suggest that failures are not typical of evacuated tubes. A possible explanation for the failures that do occur during operation is that they are due to the relatively low production levels in most evacuated tube manufacturing facilities. Larger volume manufacture with more well developed quality assurance procedures should further reduce the occurrence of these infrequent failures.

7.7.4 Thermal Cycling

There is no evidence of acceleration of any degradation process due to thermal cycling.

7.7.5 Outgassing and Gas Permeation

No significant degradation of tubes was observed due to gas permeation from the outside into the vacuum space. Such gas can come from two sources. In borosilicate collectors, such as Corning, Solartech, Sunmaster and Sydney University, atmospheric helium will

permeate the hot inner glass tube during stagnation. A partial pressure of helium within the vacuum space approximately equal to that in the outside air will result. This amount of helium is known to degrade the performance of these tubes by only about one percent.

For metal-in-vacuum collectors, a possible degradation mechanism is penetration of gas such as hydrogen through the fluid circulation pipe into the vacuum space. However, no degradation due to such an effect has been observed. In summary, loss of vacuum and selective surface degradation is not a long term problem for evacuated collectors. Some Corning collectors have been operating continuously for almost twelve years without noticeable degradation.

7.7.6 Boiling

Collector arrays can experience local boiling at high temperatures and high levels of insolation. Although boiling could result in vapor locks, such effects have not been observed when boiling has occurred. Indeed, none of the Task VI systems has experienced any adverse effects due to boiling.

7.7.7 Heat Pipes

The effectiveness of a gravity feed heat pipe as a heat transfer device can be seriously affected under certain conditions. In particular, at temperatures close to the critical point, a large increase in vapor flow rate occurs at constant heat flow rates. This is due to the decrease in the latent heat of vaporization and condensation near the critical point. This increased vapor flow can choke the heat pipe by not allowing the liquid to flow down the tube rendering much of the evaporation section inoperative. Under these circumstances, the efficiency of a heat pipe collector can drop significantly and remain low until temperatures and radiation drop far below the initiating conditions.

Such effects have been observed at higher temperatures and insolation when organic fluids were used, as with earlier Philips collectors. Later Philips collectors using water in the heat pipe did not experience this condition. This potential characteristic of a heat pipe must be recognized and allowance made in collector and system design. In certain instances it could be used to advantage, for example, to provide protection from high temperatures.

7.7.8 Tube Replacement

When tube failure does occur it may be desirable, or essential for some collector types, to replace the faulty tube. In some collectors, such as Sydney University and Philips, this is a very simple procedure, not even requiring draining of the system. In the Sunmaster and

Solartech collector, tube replacement is also straight forward, and may be done without draining the system. In other collectors, such as Corning and Sanyo, replacement of a tube requires that the plumbing of the system be cut. Where operating temperatures are low enough the system may be operated with the faulty tube with little or no noticeable loss of performance. In some cases, such as the Sunmaster or Solartech collectors, a broken tube is a fluid leak and the tube must be replaced.

7.7.9 Freezing

Freeze protection of an array is achieved by the use of antifreeze solution and with drainback. Antifreeze solutions, such as glycol, are expensive for installations with a large volume of circulating fluid. Both the Philips and Sunmaster/Solartech collectors could be drained easily.

Another possible freeze protection method is circulation of water through the collector at night. This method may be particularly suitable for heat pipe collectors, such as Philips, where the thermal diode property of the heat pipe effectively isolates the tubes from the circulating heated fluid under zero insolation. It should be noted that heat pipes containing certain fluids cannot freeze under any likely external conditions, thereby protecting the most expensive part of the system, the tubes, from damage.

Some collectors such as Sydney University, Corning, and Sanyo cannot be drained easily. Such collectors can only be protected from freezing by use of an antifreeze solution.

7.7.10 Reflectors

In some studies, dirt accumulation has been shown to reduce the specular reflectance of reflectors by up to 25 percent. In Task VI systems with collectors incorporating reflectors, however, no measurable effects have been observed due to dirt on reflectors. Such a conclusion is drawn from the operating characteristics of collectors from year to year. It should be noted that none of the Task VI systems using reflectors is located near the ocean where irreversible degradation of reflectors is known to be a problem.

7.7.11 Hail

Hail can be a problem in locations where large hailstones, 5 cm or greater, are likely. Close packing of tubes and thin tube walls aggravate the problem. In one instance, see Table 7-5, the manufacturer is looking into the possibility of thicker tube wall.

7.7.12 System Design

The particular advantage of evacuated collectors, such as low thermal losses and insensitivity to ambient conditions, have been clearly demonstrated by Task VI results. In some systems these advantages have been largely negated by poor system design resulting in poor system performance. Causes of this are often large pipe and storage tank losses. Good system design practices which accommodate the advantages of evacuated collectors is clearly indicated.

8. CONCLUSIONS

Conclusions drawn from Chapters 6 and 7 and the previous Task VI experimental results report[1] are presented here. Additional conclusions specific to individual installations are presented in Table 8-1. Task wide conclusions on thermal performance are given in section 8.1, on non-thermal performance in section 8.2, and on measurement and reporting in section 8.3.

Future plans for the installations are presented in Table 8-2.

8.1 THERMAL PERFORMANCE

1. Instantaneous collection efficiencies around sixty percent were attained for temperature differences of about 80°C during most daylight hours.

2. Monthly collection efficiencies consistently above fifty percent were attained for a DHW and space heating application in a climate with a high level of diffuse radiation.

3. Monthly collection efficiencies consistently close to fifty percent were attained for a space cooling application.

4. Monthly collection efficiencies of up to forty-four percent were attained while operating at average monthly temperature differences between 88 and 96°C.

5. As compared with efficiencies determined when radiation was normal to the collector plane, evacuated collector efficiencies were greater at nearly every time of day all year long. For some types the difference was substantial, sometimes more than twenty percent greater during the times of the day that most energy is collected.

6. Cylindrical absorbers collected energy more effectively over a wider range of optical circumstances than flat absorbers.

7. Close packed tubes resulted in high module collection efficiencies at moderate collection temperatures and high radiation levels.

8. Wider tube spacing with use of reflectors resulted in higher module collection efficiencies at some combinations of high collection temperatures and low radiation levels.

9. Two evacuated collectors outperformed all other evacuated collectors and significantly outperformed the flat plate collectors at all but the lowest application temperatures.

10. The lowest performing ETC's performed as well or better than single glazed flat plate collectors at all but lower application temperatures.

11. The single glazed flat plate collector with convection suppression performed better than the lowest performing ETC at the temperatures studied, but not better than most ETC's.

12. Long tube evacuated collectors were decidedly better performers than short tube evacuated collectors.

13. Poor system design or construction was the most common cause of poor system performance, not the evacuated collectors.

14. Field capacitance can adversely affect energy output by a significant amount as a result of large amounts of interarray piping resulting in reductions of up to 50 percent in installation performance.

15. Preheating can increase system operation time and thus appear to yield better performance, but it extracts a greater penalty through non-operating losses.

8.2 SHIPPING, INSTALLATION, RELIABILITY, MAINTENANCE AND OPERATING CONSIDERATIONS

1. Evacuated collector reliability has been excellent given the newness of the technology.

2. In most cases no loss of performance has occurred, including those cases of evacuated collectors with reflectors.

3. In one case, there was no measurable loss of performance after nine years.

4. There was no evidence of performance loss due to selective surface degradation in any of the installations, even after months of stagnation.

5. The incidence of vacuum losses have been insignificant.

6. Most evacuated collectors have had insignificant breakage during operation.

7. Most types of evacuated collectors have proven to be highly resistant to environmental hazards, including hail.

8. The evacuated collectors required no maintenance in virtually all cases.

9. The performance of a few individual tubes degraded under operating conditions.

10. Some of the collectors, the Dewar types, were damaged by thermal shock when the collectors were filled when hot. Precaution must then be taken to see that this does not occur.

11. A heat pipe fin arrangement in an evacuated tube served as protection against freezing damage regardless of the design of the rest of the system.

12. Local boiling occurred, but was not a problem even in evacuated collector systems with inherent flow distribution imbalance.

13. Boiling has occurred routinely in the storages and collectors of a number of Task VI systems. There was no resultant damage as degradation to the storage or rest of the system.

14. Installation procedures varied widely in form and complexity depending on the collector type.

15. Extra precautions were necessary to avoid burns when installing evacuated collectors, which can reach temperatures of 250°C.

16. Horizontal mounting, which is possible with some evacuated collector designs, reduced interarray piping, mounting structure, installation labor, and thermal losses.

17. The short straight-through large diameter fluid passages in the manifold of the heat pipe collector modules minimized array pumping power and intermodule piping.

18. In some collectors individual tubes were replaced very easily. This can be a very useful feature, when a large number of tubes have been broken, say by vandalism, here and there in the array.

19. Under higher temperatures and insolation levels performance of some types of heat pipe tubes suffered sharp energy output drops. This effect may or may not be desirable depending on temperature required.

20. The higher temperatures possible with evacuated collectors reduced the number of viable options for interconnecting modules. The leaking problems of several installations, which often first occurred after stagnation, were corrected by proper connection choices.

8.3 MEASUREMENT AND REPORTING

1. Efficiency points and curves alone were not sufficient for comparisons of collection system performance for different collectors.

2. The effects of some factors, such as capacitance and incident angle, showed up in the sequential plots of efficiency points. However, their impact on daily performance was not readily ascertainable.

3. Daily energy input/output curves provided a very useful means of comparing collection system performance.

4. Differences in systems and climate showed up in the input/output curves.

TABLE 8-1 CONCLUSIONS

Sydney University Solar Heating and Cooling System, Department of Mechanical Engineering, University of Sydney, SYDNEY AUSTRALIA	Despite the relatively short involvement in IEA Task VI we have been able to compile performance information for system operation during cooling (December 1982, January 1983) and heating (June 1983 to September 1983). The Sydney University evacuated tubular collector has shown distinct performance advantages over a good quality flat plate collector in a heating/cooling application. Evacuated tubular collectors perform substantially better at elevated collector temperature necessary to power an absorption cooling cycle whereas in the Sydney climate at lower operating temperatures of 30 to 50°C (heating) the two collector types show similar performance. No problems were encountered with the operation of evacuated tubular collectors. Electrical problems as well as failure of other system hardware (e.g., tank leak) were major sources of down-times. For unknown reasons, chiller performance is very poor after an initial cooling season where the unit complied with the manufacturer's stated specifications. A considerable effort was spent in setting up the data acquisition/data reduction software. Program development has now reached a stage where data handling is achieved with a high degree of flexibility, little human interaction and according to Task VI reporting requirements.
Mountain Spring Bottle Washing Facility CANADA	Experience at the Edmonton facility has shown that long-term operation of a high-temperature ETC installation is technically feasible in a harsh climate such as Northern Canada. Major effects which reduce solar energy collection are snow cover, capacitance effects and pipe heat losses.
Ispra Solar Heated and Cooled Laboratory CEC	The experiments showed that ETC collectors can perform very well under sunny climatic conditions. High operating temperatures do not penalize the collector efficiency very much, due to the low heat loss coefficient and small heat capacity of the collector. This makes the ETC collector very attractive for many applications such as solar cooling, industrial process heat (up to about 120 C), district heating, etc. The problems encountered in these experiments, related mainly to the durability of the collectors. However, none of these problems look insurmountable. The optical losses are the principle inefficiency of the ETC's today. It should be possible to make improvements in this area. An important but often neglected aspect of solar collectors is the pressure drop over the collector. The concept of the Philips heat pipe collector is a great improvement in this sense. As far as the system is concerned it can be said that it operated as designed without major problems. The concept of the chilled water storage proved to be valid from a thermal point of view. The main system defect is the heat loss from the hot storage tank. The insulation of this storage will be improved.
Solarhaus Freiburg FEDERAL REPUBLIC OF GERMANY	The activities aimed principally at two objectives, i.e., • to demonstrate the performance of ETC in Central European weather conditions for DHW and space heating applications, to investigate the systems behavior and to develop and to validate design tools • to generalize and to extrapolate the results to other designs, consumers and/or climates by means of modeling. During a five years' operational period three different collector constructions have been tested. Reliability was excellent, servicing and maintenance minimal. The specific energy output was unparalled in comparable European

TABLE 8-1 (cont). CONCLUSIONS

installations [58]. The influences of various system schemes have been determined. The close cooperation with an ETC manufacturer provided valuable hints for a new collector construction.

A considerable effort was spent in the development, improvement and validation of simulation models. By these, the performance and the limitations of ETC systems in the temperature range of $\Delta T = 40$ to 150 C have been extensively investigated.

Eindhoven Technological University Solar House THE NETHERLANDS

The Philips VTR 261 collectors have shown high performance under unfavorable, cloudy weather conditions. No significant operational problems were encountered. The principles of the integrated storage-auxiliary heater-expansion tank were found to be sound, but some constructional modifications were required to achieve satisfactory practice. From the measurements it appears that the heat pipe ETC can not be characterized by an equation of the Hottel-Whillier-Bliss type. A new equation has been derived from data but its physical clarification is still lacking.

Knivsta District Heating Project KNIVSTA, SWEDEN

The experiences from three years of operation lead to some practical requirements for solar collector arrays, namely:

- it must be possible to easily replace a solar collector without emptying the system
- simple bleeding and deairation routines are needed
- solar collectors must be able to withstand stagnation temperatures
- obvious leakage risks must be eliminated.

There is no doubt that not all types of evacuated solar collectors fulfill these requirements and that further development is essential before large-scale installations with rational operation can be considered.

The results lead to the following conclusions:

- The Philips VTR 141 show the highest longtime efficiency compared to the Owens-Illinois, General Electric TC100 and Scandinavian Solar HT.
- The energy output from the Philips VTR 141 could be increased by changing the slope from 60 to 45 degrees.
- The large size of the piping system between the collector arrays and the district heating network has a significant influence on the system performance. Ten to 20 percent of the longterm array output is lost to the piping system for preheating in the morning at the Knivsta test installation. All this energy can not be transferred to useful energy even with a perfect system design due to the temperature requirements in this application. Q112 does not include this preheating array output as it is mainly very low temperature energy due to the 24 hour pump operatifon in the collector loop.
- The incidence angle modifier at large angles is important for the preheating period length. The Philips collectors utilizes the morning insolation even at angles above 90 degrees to preheat the collector which increases the net energy output.
- No significant degradation can be seen after three years of operation for GE and Ph.
- So far the flat-plate collector Scandinavian Solar shows good performance, somewhere inbetween General Electric TC100 and Philips VTR 141.

TABLE 8-1 (cont). CONCLUSIONS

Sodertorn District Heating Project SODERTORN, SWEDEN	• The Philips VTR 141 evacuated tube collectors shows the highest energy output and it can be further increased by changing the slope of the collectors to 40 degrees. • The highest system efficiency for a full year was 40 percent for the Philips collectors at 60 C operation. • The second generation of flat-plate collectors represented by Scandinavian Solar HT gives system efficiencies not so far from the evacuated tube collectors even at 80 C operation. Improvements are still possible for both kinds of collectors. The total system economy will decide whether evacuated tube collectors or flat-plate collectors are most suitable for district heating application. • A collector construction which minimizes the length of interconnecting pipes outside the collectors, as in case of Philips VTR 141 and Scandinavian Solar HT, show better performance both due to lower piping losses and longer operating time. • The change from 60 C operation to 80 C operation in June 1983 has reduced the systm efficiency from 40 percent to 35 percent for Philips VTR 141 and for example from 25 percent to 19 percent for the Teknoterm HT collectors array. The effective increase in operating ΔT has been 14 C for Philips and 13 C for Teknoterm. • The incident angle modifier at large angles has a significant influence on the all-day efficiency, as in case of Philips VTR 141 which accepts irradiation also from the back side, and starts to deliver energy early in the morning. • At these collector array sizes 121-216 m2 reasonable COP values of 30-40 have been measured, for both ETC and flat-plate collectors and improvements are possible by more careful sizing of the piping and pumps.
SOLARCAD District Heating Project, GENEVA, SWITZERLAND	A solar system connected to a district heating network must operate above a temperature threshold that may be quite high. All losses including collector efficiencies, thermal losses and capacity effects (or "off" losses") depend very strongly on temperature and very severely effect the overall system performance. After two years of measurements, studies, data analysis we now have a good understanding of our systems. It should be noted in this framework that the IEA collaboration is very helpful. The systems are not all optimized. However, methods of improving performance are available from shared experience. This "knowhow" so acquired is very helpful for future solar system designs at a national level. Also worthwhile has been our collaboration with Corning's French manufacturer: new collectors are significantly improved.
SOLARIN Industry Project HALLAU, SWITZERLAND	Operation of the plant following the reporting period has shown good average efficiency. Of the evacuated collectors, about 30 percent, although serious problems have been encountered with the microprocessor controls. Additional tests with focusing collectors have produced rather disappointing results. Apart from the solar loop, measurements on the rest of the system have been affected by control problems as well as flowmeter failures.

TABLE 8-1 (cont). CONCLUSIONS

BSRIA Solar Test Facility with Simulated Loads Bracknell, UNITED KINGDOM	
Colorado State University Solar House I Fort Collins, Colorado USA	On the basis of results presented here, the Philips VTR-361 evacuated tube heat pipe collector is a low capacitance, highly efficient collector. Tradiational flat-plate, two-parameter representation of collector efficiency is inadequate for this collector. Average daily collection efficiency is very high, even when average collector temperature is high. The phase-change HDPE storage unit tested during the summer of 1983 was not successful from a practical viewpoint. There is not sufficient data to support a technical conclusion about the PCM tested, but it appears that additional development and testing are necessary before it can be successfully included in a solar cooling system. A collector area of 54.5 square meters is too large for the heating needs of Solar House I. Even during the winter months it was occasionally necessary to reject heat from the collector to prevent overheating and overpressure.

TABLE 8-2 FUTURE PLANS

Sydney University Solar Heating and Cooling System, Department of Mechanical Engineering, University of Sydney, SYDNEY, AUSTRALIA	The existing water/lithium bromide absorption chiller will be replaced by a prototype ammonia/water cycle which incorporates novel printed circuit heat exchangers. Emphasis in the future will be on the evaluation of effects of changes in system operation (e.g., with/without chilled water storage, flat-plate collector versus evacuated tubular collector, simultaneous collector operation etc.). More specific investigations will be performed on particular system components (e.g., storage tank, piping, system control ...). We plan to be heavily involved in the modelling/simulation procedure which will enable us to obtain detailed understanding of the system investigated.
Mountain Spring Bottle Washing Facility CANADA	Monitoring of the system continued through mid-1985 in order to assess effects of improved control strategy and gain further experience in long-term reliability. In addition, part of the collector field has been replaced by more efficient Sunmaster TRS-81 collectors and the expected improved performance will be documented. Detailed performance evaluation and modeling studies will continue to October 1985.
Ispra Solar Heated and Cooled Laboratory CEC	The system will be operated during the summer of 1984 the same as it was in 1983. Some small improvements concerning the insulation of the hot storage tank will be made. Emphasis will be put on the detection of changes in collector performance from year to year. The replacement of the Sanyo collectors is foreseen for 1985.
Solarhaus Freiburg FEDERAL REPUBLIC OF GERMANY	The future activities shall cover both a generalization of the present knowledge (DHW applications) as well as an extrapolation to new areas (IPH applications). The performance of various DHW thermosiphoning systems both with flat plate and evacuated tubular collectors is currently investigated; after the validation of a relevant simulation model principles for an optimized design will be derived. Considerable efforts aiming at IPH applications are under way. The optical, thermal, and operational characteristics of various collector tubes are investigated (reflectors, absorber losses, degradation, outgassing, energy out coupling), whereas the systems' behavior shall be studied by means of a novel test facility, which shall cobine a high flexibilty as to component, operational and applicational aspects.
Eindhoven Technological University Solar House THE NETHERLANDS	Monitoring will be continued until summer 1985. The collectors fully meeting expectations attention will be directed towards system behavior and losses, and control.
Knivsta District Heating Project KNIVSTA, SWEDEN	The experimental period is ended and no further measurements will be done on this sytem.
Sodertorn District Heating Projerct SODERTORN, SWEDEN	Continued long-term operation and evaluation until June 1985.
SOLARCAD District Heating Project, GENEVA, SWITZERLAND	Two collector systems have been studied, (Corning and Sanyo) and their performances are very similar. Plans are to perform simulations and validations of these systems to help understand them and to optimize design tools. In 1984, a 1000 m2 solar system will be built in connection with the district heating network. Suitable high performance collectors will be chosen. Precise measurements will be taken and total performance evaluated. All these experiments should result in being able to predict the performance of evacuated collectors in Swiss climates.

TABLE 8-2 FUTURE PLANS

SOLARIN Industry Project HALLAU, SWITZERLAND	Control problems will be solved, flowmeters will be replaced and good measurements for the entire system should start soon in order to provide a full year of recorded data. In parallel, data analysis, characterization of all system components and simulation will be achieved. Comparisons with the SOLARCAD project should result in a broader overview of ETC systems in Swiss conditions. Also, further investigation of the installed focusing collectors is anticipated.
BSRIA Solar Test Facility with SImulated Loads Bracknell, UNITED KINGDOM	
Colorado State University Solar House I Fort Collins, Colorado USA	A new system is planned for Solar House I which will include new Philips collector tubes and a separate array of Sun Master evacuated tube collectors. Both arrays will be mounted on the roof of Solar House I but only one system will be operating at any one time.

9. REFERENCES AND BIBLIOGRAPHY

Task VI Reports

1. Duff, W.S., et al., "Eight Evacuated Collector Installations, Interim Report for the IEA Task on the Performance of Solar Heating, Cooling and Hot Water Systems Using Evacuated Collectors, Solar Energy Applications Laboratory, Colorado State University, Fort Collins, Colorado, November 1982.

2. M. Chandrashekar, K.H. Vanoli, "Data Collection and Performance Reporting Specifications for Solar Energy Projects," Report for the IEA Task on the Performance of Solar Heating, Cooling and Hot Water Systems Using Evacuated Collectors, June 1986.

3. Guisan, Olivier, et al., "Characterization of Evacuated Collectors, Arrays, and Collection Subsystems," Report for the IEA Task on the Performance of Solar Heating, Cooling and Hot Water Systems Using Evacuated Collectors, Group of Applied Physics, Geneva University, Switzerland, June 1986.

4. D. Buchen, et al., "Design Guidelines for Evacuat ed Collector Solar Energy Systems," Report for the IEA Task on the Performance of Solar Heating, Cooling and Hot Water Systems Using Evacuated Collectors, Buchen, Lawton, Parent Ltd., Canada, December 1986.

5. W.L. Gemmell, M. Chandrashekar, K.H. Vanoli, "Detailed Modeling of Evacuated Collector Systems," Report for the IEA Task on the Performance of Solar Heating, Cooling and Hot Water Systems Using Evacuated Collectors, University of Waterloo, Ontario, Canada, December 1986.

6. K. Schreitmüller, "Daily Energy Input/Output Oriented Modeling Approaches," Report for the IEA Task on the Performance of Solar Heating, Cooling and Hot Water Systems Using Evacuated Collectors, Institut für Solarenergieforschung GMBH, Hannover, Projected Publication July 1988.

Task VI Working Papers

7. Vanoli, K., "Data Acquisition and Measurement Systems in Solarhaus Freiburg". Technical Report 1978-79, IST Energietechnik GmbH, January 1980.

8. G.J. Baker, "The Development and Performance Evaluation of Liquid Solar Heating Systems Using Evacuated Collectors," IEA Task VI Working Document, April 1980.

9. N.V. Philips, "Preliminary Performance Data of the Evacuated Tubular Heat-Pipe Collectors for Applications Below 100°C," IEA Task VI Working Paper, May 1980.

10. K. Vanoli, K. Schreitmüller, "Evaluation of Collector Array Efficiency Under Non-Steady State Conditions by Multiple Regression," IEA Task VI Working Paper, August 1980.

11. W.S. Duff, Summary of the Task VI Working Group Meeting on Format, "Task VI Reporting Requirements". Pingree Park, Colorado, October 1980.

12. de Greijs, "Evacuated Tubular Collector heating and Hot Water System In the Solar House of the Eindhoven University of Technology," IEA Task VI Working Paper, November 1980.

13. Blondin, G., O. Guisan "SOLARCAD Project". Report under contract of Services Industriels de Geneve and Centre Universitaire d'Etude des Problems de Engergie, December 1980.

14. K. Vanoli, "Solarhaus Freiburg Data Summary 1980," IEA Task VI Working Paper, August 1981.

15. K. Schreitmüller, K. Vanoli, "Solarhaus Freiburg: On-Line Comparisons of Experimental Data with Computer Simularion Results," IEA Task VI Working Paper, August 1981.

16. P. Ineichen, et al., "Study of the Corrective Factor Involved When Measuring the Diffuse Solar Radiation by Use of the Ring Method," IEA Task VI Working Paper, February 1982.

17. K. Schreitmüller, "The Performance of Solar Energy Systems Using Evacuated Collectors," IEA Task VI Working Paper, May 1982.

18. Potter, I.N., J. Dewsburg, "Development and Performance Evaluation of Liquid Solar Heating Systems Using Evacuated Tubular Collectors". Contract 3002, Report No.3, United Kingdom, May 1982.

19. W.B. Veltkamp, C.W.J. van Koppen, "Optimization of the Energy Management of Low-Energy Houses with a Solar Heating and Hot Water System," IEA Task VI Working Paper, September 1982.

20. O. Guisan, "A Few Reflections About Efficiency Plots, I/O Diagrams and How to Average Temperature," IEA Task VI Working Paper, September 1982.

21. W.B. Veltkamp, C.W.J. van Koppen, "Optimization of the Flows in a Solar Heating System," IEA Task VI Working Paper, September 1982.

22. K.R. DenBraven, W.S. Duff, "An Analytic Model of Stratification for Solar Air and Liquid Heating Systems, IEA Task VI Working Paper, January 1983.

23. H. Zinko, et al., "Comparison of the Effective System Performance of Flat Plate and Evacuated Tube Collectors used for District Heating Purposes," IEA Task VI Working Paper, January 1983.

24. B. Perers, H. Zinko, "On Line Simulation for the Knivsta Installation," IEA Task VI Working Paper, January 1983.

25. K.R. DenBraven, W.S. Duff, and G.J. Favard, "An Event Time Simulation of Residential Solar Heating," IEA Task VI Working Paper, March 1983.

26. O. Guisan, "Stagnation Temperature for Evacuated Collectors," IEA Task VI Working Paper, July 1983.

27. O. Guisan, "Corning Collector Efficiency," IEA Task VI Working Paper, July 1983.

28. B. Perers, H. Zinko, "Presentation of I/O Model Preliminary Version for IEA Task VI Comparison," IEA Task VI Working Paper, August 1983.

29. S. R. Hultin, W.S. Duff, "Proposed Approach for Comparing Evacuated Tube Collector Results," IEA Task VI Working Paper, August 1983.

30. O. Guisan, "Simple Comparison/Extrapolation for Evacuated Tubular Collectors," IEA Task VI Working Paper, August 1983.

31. P.M. Nast, "Selected Materials from the Pyranometer Symposium in Norrköping, Sweden," IEA Task VI Working Paper, January 1984.

32. S. Harrison, "Characterization of Evacuated Solar Collectors," IEA Task VI Working Paper, September 1984.

33. K.R. DenBraven, "A Method of Collector Performance Prediction and Extrapolation," IEA Task VI Working Paper, March 1984.

34. E. Boardman, "Characterizing Collector Output," IEA Task VI Working Paper, March 1984.

35. B. Perers, H. Zinko, P. Holst, "Analytical Model for the Input/Output Energy Relationship," IEA Task VI Working Paper, March 1984.

36. W.S. Duff, K.R. DenBraven, "Simplified Methods Data," IEA Task VI Working Paper, March 1984.

37. E. Mannik, R. Schmid, "Evacuated Tubular Collector Performance - A Proposed Method of Extrapolating Results," IEA Task VI Working Paper, March 1984.

38. O. Rudaz, O. Guisan, "Corning Collector Efficiencies - IEA Task VI Meeting Stuttgart," IEA Task VI Working Paper, March 1984.

39. J.Y. Goumaz, W.S. Duff, "Comparison of Drain-Back and Dual Liquid Solar Heating and Domestic Hot Water Systems," IEA Task VI Working Paper, March 1984.

40. B. Perers, H. Zinko, P. Holst, "Analytical Model for the Daily Energy Input/Output Relationship for Solar Collector Systems," IEA Task VI Working Paper, May 1984.

41. E. Mannik, R. Schmid, "A Model of the Sydney IEA Task VI Evacuated Collector Array and its Use for performance Prediction and Extrapolation," IEA Task VI Working Paper, September 1984.

42. S.J. Harison, "The Effects of Operational and Meteorological Factors on Solar Collector Thermal Performance Test Results," IEA Task VI Working Paper, September 1984.

43. J.van Haaren, "The Experiences from the Quantity Production and Quantity Mounting of Solar Collector Systems Provided with Evacuated Tubes," IEA Task VI Working Document, September 1984.

44. O. Rudaz, O. Guisan, "Pump Characteristics for Solar Loop, Cornint Evacuated Tubular Collector Test Array," IEA Task VI Working Paper, September 1984.

45. B. Lachal, et al., "Measurement of Thermal Parameters," IEA Task VI Working Paper, September 1984.

46. O. Rudaz, O. Guisan, A. Mermoud, "Evacuated Tubular Collector Characteristics," IEA Task VI Working Paper, September 1984.

47. B. Lachal, "Solar Geometry and Shadowing for Corning Evacua ted Tubular Collectors with Tilted Absorbers," IEA Task VI Working Paper, September 1984.

48. B. Lachal, A. Mermoud, O. Guisan, "How to Take Into Account Absorber Tilt Angle for Evacuated Tubular Collector Comparisons," IEA Task VI Working Paper, September 1984.

49. O. Guisan, "Heat Pipe Evacuated Tubular Collector Characteristics," IEA Task VI Working Paper, September 1984.

50. K. Vanoli, K. Schreitmüller, E. Hahne, "The Impact of Collector Performance on the Level of Complexity of Design and Control of Solar Domestic Hot Water Systems," IEA Task VI Working Paper, February 1985.

51. B. Perers, "District Heating Systems Sweden Principle," IEA Task VI Working Paper, February 1985.

52. O. Guisan, "Heatpipe Evacuated Collectors - Search for a Capacitance Effect Due to Latent Heat of Vaporization," IEA Task VI Working Paper, February 1985.

53. W.S. Duff, K. DenBraven, "I/O Curve Working Group Report," IEA Task VI Working Paper, February 1985.

54. O. Guisan, et al., "SOLARCAD II: Results in the Task VI Format," IEA Task VI Working Paper, March 1985.

55. E. Mannik, R. Schmid, "I/O Curve Working Group Report," IEA Task VI Working Paper, March 1985.

56. O. Rudaz, A. Mermoud, O. Guisan, "Evacuated Collector System Characterization," IEA Task VI Working Paper, March 1985.

57. K. Schreitmüller, "Evaluation of Field Performance," IEA Task VI Working Paper, March 1985.

58. O. Rudaz, et al., "I/O Modelization," IEA Task VI Working Paper, March 1985.

59. K. Schreitmüller, "Input/Output Diagrams of the Solar Farm Systems," IEA Task VI Working Paper, March 1985.

60. W.S. Duff, K.DenBraven, "I/O Curve Working Group Report - VTR 361 Collector," IEA Task VI Working Paper, March 1985.

61. O. Rudaz, A. Mermoud, O. Guisan, "Power Curves," IEA Task VI Working Paper, March 1985.

62. K. Vanoli, "Seasonal Variations in I/O Diagrams," IEA Task VI Working Paper, April 1985.

63. W.S. Duff, K.R. DenBraven, G.J. Favard, "Development and Validation of a Day-by-Day Simulation of Solar Energy Systems (DAYSIM), IEA Task VI Working Paper, May 1985.

64. K. DenBraven, M. Riley, W.S. Duff, "Simplified Models Test Results," IEA Task VI Working Paper, July 1985.

65. E. Mannik, "Simplified Methods Comparison Exercise," IEA Task VI Working Paper, July 1985.

66. O. Guisan, "Tilted Absorber Effects - First Results Concerning SOLARIN Project," IEA Task VI Working Document, July 1985.

67. O. Guisan, et al., "New SOLARCAD 1000 m^2 in Geneva - Preliminary Results," IEA Task VI Working Paper, July 1985.

68. E. Mannik, "A Simple Method of Computing Evacuated Collector Performance," IEA Task VI Working Paper, July 1985.

69. W.L. Gemmell, M. Chandrashekar, W.E. Carscallen, "Performance Comparison of Simulated Solar Energy System Against Monitored Data," IEA Task VI Working Paper, July 1985.

70. E. Mannik, R. Schmid, "Performance Prediction of Evacuated Tubular Collectors - An analysis of Detailed Array Data," IEA Task VI Working Paper, July 1985.

71. K. Schreitmüller, "Task VI Simplified Models Approach," IEA Task VI Working Paper, July 1985.

72. K. Schreitmüller, "Proposal for a Concensus Test of Simplified Models," IEA Task VI Working Paper, March 1985.

73. Perers, Bengt et al., "Analytical Model for the Daily Energy Input Output Relationship for Solar Collector Systems. Swedish Council for Building Research, November 1985.

74. E. Mannik, "A Simplified Method for Computing the Long-Term Performance of Arrays and Systems Incorporating Evacuated Tubular Collectors," IEA Task VI Working Paper, January 1986.

75. B. Veltkamp, "Collector Characterization Comment to the Efficiency Hypothesis," IEA Task VI Working Paper, January 1986.

76. E.C. Boardman, W.S. Duff, "Simplified Modeling of Solar Process Heating Systems Using Stochastic Weather Input," IEA Task VI Working Paper, January 1986.

77. O. Guisan, et al., "A Simple Model for the Evaluation of the Thermal Output of a Solar Collector System on a Daily Basis," IEA Task VI Working Paper, June 1986.

78. W.B. Veltkamp, "Evacuated Tube Collector Characterization in the Low Flow Regime," IEA Task VI Working Paper, June 1986.

79. O. Guisan, et al., "Use and Validation of the Simplified G^3 Model," IEA Task VI Working Paper, May 1987.

Task VI Performance Reports

80. Löf, G.O.G., and W.S. Duff, "Comparative Performance of Two Types of Evacuated Tubular Solar Collectors in a Residential Heating and Cooling System". DOE Report COO-2577-19 for the period 1 October 1977 to September 1979.

81. Vanoli, K., K. Schreitmüller, "Solarhaus Freiburg Performance of Evacuated Tubular Solar Collectors in Domestic Hot Water and Heating Systems". IST Energietechnik GmbH, November 1980.

82. O. Guisan, Development and Performance Evaluation of a Large Solar Energy Facility Using Evacuated Collectors in Connection With a District Heating System - SOLARCAD Project," Interim Report, IEA Task VI, December 1980.

83. Löf, G.O.G., and W.S. Duff, "The Performance of Heat Pipe Evacuated Tubular Solar Collectors and Single Glazed Flat-Plate Collectors in a Residential Heating and Cooling System". DOE Report COO-2577-21 for the period 1 October 1979 to 30 September 1980, December 1980.

84. W.E. Carscallen, "Mountain Spring Project - Bottle Washing Facility," Interim Report, IEA Task VI, December 1980.

85. C.W.J. van Koppen, J.P. Simon Thomas, "Preliminary Performance of the Heating System in the Solar House of the Eindhoven University of Technology," December 1980.

86. Astrand, L., et al., "The Knivsta Project," Interim Report, IEA Task VI, December 1980.

87. W.E. Carscallen, "Mountain Spring Project - Bottle Washing Facility," Interim Report, IEA Task VI, December 1980.

88. K. Hinotani, et al., "Performance of the Evacuated Tubular Solar Collector in Sanyo Osaka Solar House," December 1980.

89. K. Vanoli, K. Schreitmüller, "Performance of Evacuated Tubular Solar Collectors in Domestic Hot Water and Heating Systems-Solarhaus Freiburg," December 1980.

90. Duff, W.S., and G.O.G. Löf, "The Performance of Evacuated Tubular Solar Collectors in a Residential Heating and Cooling System". DOE Report COO-2577-20 for the period 1 October 1978 to 30 September 1979, March 1981.

91. O. Guisan, A. Mermoud, "Development and Performance Evaluation of a Large Solar Energy Facility Using Evacuated Collectors in Connection with a District Heating System," Interim Report, IEA Task VI, July 1981.

92. K. Hinotani, et al., The Performance of Evacuated Tubular Solar Collectors in Space Cooling, Space Heating, and Domestic Hot Water Supplying Systems - Osaka Sanyo Solar House," Interim Report, IEA Task VI, August 1981.

93. I.N. Potter, J. Dewsbury, "Development and Performance Evaluation of Liquid Solar Heating Systems Using Evacuated Collectors - United Kingdom Project," Interim Report, August 1981.

94. MacLaren Plansearch Report for NRC/DERD/SEP, "Monitoring System Report - Mountain Spring ". October 1981.

95. K. Vanoli, K. Schreitmüller, "System Design and Experimental Performance of Two Types of Evacuated Tubular Solar Collectors in a Residential Domestic Hot Water and Heating System," Interim Report, IEA Task VI, January 1982.

96. E. Kjellsson, H. Zinko, B. Perers, "The Knivsta District Heating Project, Sweden," Interim Report, IEA Task VI, February 1982.

97. H. Zinko, P. Holst, "The Södertörn District Heating Project," Interim Report, IEA Task VI, October 1982.

98. Vanoli, K., K. Schreitmüller, "Solarhaus Freiburg". West German report revision, May 1982.

99. W.E. Carscallen, "Mountain Spring Project - Bottle Washing Facility," Interim Report, IEA Task VI, May 1982.

100. MacLaren Plansearch, Hubert Taube, "Data Acquisition System Report, Mountain Springs". Report for NRC/DERD/SEP, May 1982.

101. I.N. Potter, J. Dewsbury, "Development and Performance Evaluation of Liquid Solar Heating Systems Using Evacuated Collectors - United Kingdom Project," Interim Report, May 1982.

102. O. Guisan, A. Mermoud, O. Rudaz, "Development and Performance Evaluation of a Large Solar Energy Facility Using Evacuated Collectors in Conection with a District Heating System," Interim Report, IEA Task VI, May 1982.

103. Hinotani, K., et al., "Osaka Sanyo Solar House". Technical report for the period December 1979 to September 1981, Japan Interim Report, June 1982.

104. Löf, G.O.G., W.S. Duff, C.E. Hancock, and D. Swartz, "Performance of Eight Solar Heating and Cooling Systems in CSU Solar House I, 1980-1981". DOE Final Report COO-30122-27 for the period February 1980 to September 1981, June 1982.

105. DeGrijs, J.C., C.S.J. van Koppen, "Eindhoven Project". First Interim Report, Project funded by the Netherlands Energy Research Foundation, June 1982.

106. Astrand, L., et al., "The Knivsta District Heating Project," Interim Report, IEA Task VI, June 1982.

107. MacLaren Plansearch, Hubert Taube, "Solar Commissioning Report - Mountain Springs". Report for NRC/DERD/SEP, July 1982.

108. E. Kjellsson, H. Zinko, B. Perers, "The Knivsta District Heating Project, Sweden," Interim Report, IEA Task VI, December 1982.

109. E. Thomas Henkel, "Performance of the Wagner College Solar Energy Demonstration Project," Interim Report, IEA Task V, December 1982.

110. R.W.G. Bisschops, C.W.J. van Koppen, "The Assembly and First Three Months of Operating of the Solar Heating Installation - Eindhoven Project," Interim Report, IEA Task VI, December 1982.

111. O. Guisan, A. Mermoud, O. Rudaz, "Development and Performance Evaluation of a Large Solar Energy Facility Using Evacuated Collectors in Conection with a District Heating System," Interim Report, IEA Task VI, January 1983.

112. R.E. Collins, R. Schmid, "Sydney University Solar Heating and Cooling System," Interim Report, IEA Task VI, January 1983.

113. I.N. Potter, J. Dewsbury, "Development and Performance Evaluation of Liquid Solar Heating Systems Using Evacuated Collectors - United Kingdom Project," Interim Report, January 1983.

114. K. Vinoli, "Performance Evaluation of Three Types of Evacuated Tubular Solar Collectors Operating in a Multi-Family Residence Hot Water and Heating System," Interim Report, IEA Task VI, January 1983.

115. H. Zinko, P. Holst, B. Perers, "The Södertörn District Heating Project Sweden," Interim Report, IEA Task VI, August 1983.

116. O. Guisan, B. Lachal, O. Kaelin, "Development and Performance Evaluation of a Large Solar Energy Facility Using Evacuated Collectors to Provide Heat to an Industrial Plant - Hallau, Switzerland," Interim Report, IEA Task VI, December 1983.

117. O. Guisan, A. Mermoud, O. Rudaz, "Development and Performance Evaluation of a Large Solar Energy Facility Using Evacuated Collectors to Provide Heat to an Industrial Plant - Geneva, Switzerland," Interim Report, IEA Task VI, December 1983.

118. L. Astrand, et. al., "The Knivsta District Heating Project," Interim Report, IEA Task VI, December 1983.

119. R.E. Collins, et al., "The Sydney University Solar Heating and Cooling System," Interim Report, IEA Task VI, December 1983.

120. L. Astrand, et al., "The Knivsta District Heating Project, Sweden," Interim Report, IEA Task VI, August 1983.

121. H. Zinko, P. Holst, B. Perers, "The Södertörn District Heating Project, Sweden," Interim Report, IEA Task VI, August 1983.

122. O. Guisan, A. Mermoud, O. Rudaz, "Development and Performance Evaluation of a Large Solar Energy Facility Using Evacuated Collectors in Connection with a District Heating System," Interim Report, IEA Task VI, August 1983.

123. O. Guisan, et al., "Development and Performance Evaluation of a Large Solar Energy Facility Using Evacuated Collectors in Connection with a District Heating System," Interim Report, IEA Task VI, September 1984.

124. R.W.. Bisschops, C.W.J. van Koppen, "Solar House of the Eindhoven University of Technolory," Interim Report, IEA Task VI, January 1984.

125. K. Vanoli, "Solarhouse Freiburg," Interim Report, IEA Task VI, February 1984.

126. R. Schmid, et al., "The Sydney University Solar Heating and Cooling System," Interim Report, IEA Task VI, September 1984.

127. R. Schmid, E. Mannik, R.E. Collins, "The Sydney University Solar Heating and Cooling System," Interim Report, IEA Task VI, April 1985.

128. L. Astrand, U. Kraftvarme, "The Knivsta Project - Initial Report," December 1985.

129. W.B. Veltkamp, C.W.J. van Koppen, "Solar House of the Eindhoven University of Technology, The Netherlands," Interim Report, IEA Task VI, December 1986.

130. D. van Hattem, "Performance of a Solar Cooling System Using Different Types of Evacuated Tube Collectors - CEC," Interim Report, IEA Task VI, January 1986.

131. E. Mannik, R. Schmid, "Detailed Modelling of the Sydney University Evacuated Tubular Collector System," Interim Report, IEA Task VI, January 1986.

132. O. Guisan, A. Mermoud, O. Rudaz, "Development and Performance Evaluation of a Large Solar Energy Facility Using Evacuated Collectors in Connection with a District Heating System-SOLARCAD," Interim Report, IEA Task VI, January 1986.

133. O. Guisan, A. Mermoud, O. Rudaz, "Development and Performance Evaluation of a Large Solar Energy Facility Using Evacuated Collectors in Connection with a District Heating System-SOLARCAD," Interim Report, IEA Task VI, March 1986.

134. O. Guisan, A. Mermoud, O. Rudaz, "Development and Performance Evaluation of a Large Solar Energy Facility Using Evacuated Collectors to Privide Heat to an Industrial Plant - SOLARIN," Final Report, IEA Task VI, October 1986.

Other References

135. The Society of Heating, Air-Conditioning and Sanitary Engineers of Japan, "Dynamic Load Calculation Program (HASP/ACLD/7107)." Tokyo, 1972. SHASEJ, "Standard Meteorological Data for Osaka", Tokyo.

136. Duff, W.S., "Evaluation of the Corning and Philips Evacuated Tubular Collectors in a Residential Solar Heating and Cooling System." ERDA Final Report COO-4012-1 for the period May 1976 to 1 December 1976. Submitted to the Energy Research and Development Administration, March 1977.

137. Fischer, L.S., C.W.J. van Koppen, j.Th.T. van Wolde, Theorie und praxis der thermischgeschichteten Wasserspeicher. VDI berichte 288. VDI-verlag, Düsseldorf. pp. 33-37, 1977.

138. Duff, W.S., C.B. Winn, G.O.G. Löf, J. Leflar and D. Meredith, "Evaluation of a Residential Solar Heating and Cooling System with High Performance Evacuated Tube Collectors -- CSU Solar House I", Proceedings of the ISES Conference, Orlando, Florida, June 1977.

139. Winn, C.B., W.S. Duff, T.M. Conway, L. Lantz and M. Potishnak, "A Real Time Simulator for a Residential Solar Heating and Cooling System." Proceedings of the ISES Conference, Orlando, Florida, June 1977.

140. Duff, W.S., and N.S. Kenney, "Evaluation of Evacuated Tubular Collectors in a Residential Solar Heating and Cooling System", Proceedings of the International Conference on Energy Use Management, Tucson, Arizona, October 1977.

141. Leflar, J.A., and W.S. Duff, "Solar Evacuated Tube Collector-Absorption Chiller Systems Simulation." DOE Report COO-2577-13, December 1977.

142. Bruno, R., and W.S. Duff, "Solar Heating, Cooling and Hot Water Production: A Critical Look at CCMS Installations", Proceedings of the CCMS/ISES Conference on The Performance of Solar Heating and Cooling Systems. Dusseldorf, West Germany, April 1978.

143. van Koppen, C.W.J., J.P. Simon Thomas, "Preliminary Performance of the Heating System in the Solar House of the Eindhoven University of Technology." Report WPS3-78.11.R291. Eindhoven University of Technology, 1978.

144. Duff, W.S., T.M. Conway, G.O.G. Löf, D.B. Meredith and R.G. Pratt, "Performance of a Residential Solar Heating and Cooling System with Flat-Plate and Evacuated Tubular Collectors: CSU Solar House I." Proceedings of the CCMS/ISES International Conference on the Performance of Solar Heating and Cooling Systems, Dusseldorf, West Germany, April 19, 1978.

145. Loehrke, R.I., et al., "A Passive Technique for Enhancing Thermal Stratification in Liquid Storage Tanks". ASME preprint 78-HT-50, Palo Alto Conference, May 1978.

146. Sharp, M.K., and R.I. Loehrke, "Stratified Thermal Storage in Residential Solar Energy Applications." DOE Report COO-4523-1 UC-59(c), June 1978.

147. Duff, W.S., T.M. Conway, G.O.G. Löf, D.B. Meredith and R.G. Pratt, "Evacuated Tubular and Flat-Plate Collector Residential Solar Heating and Cooling Performance: CSU Solar House I," Proceedings of the 1978 American Section of the International Solar Energy Society, Denver, Colorado, August 28, 1978.

148. Conway, T.M., W.S. Duff, R.B. Pratt, G.O.G. Löf, and D.B. Meredith, "Evaluation of High Performance Evacuated Tubular Collectors in a Residential Heating and Cooling System: Colorado State University Solar House I." DOE Report COO-2577-14 for the period 1 October 1976 to 30 September 1977, July 1978.

149. Conway, T.M., W.S. Duff, G.O.G. Löf, and R.B. Pratt, "Comparative Performance of Two Types of Evacuated Tube Collectors in a Residential Heating System," Proceedings of the 1979 International Conference of the ISES, Atlanta, Georgia, May 1979.

150. Veltkamp, W.B., A Closed Drain-Down System in a Medium Size Solar Heating System. In K.W.Böer(Ed), SUN II. Pergamon, New York, Vol. 1, Chap 3, pp. 423-427. (1979).

151. Ward D.S., W.S. Duff, J.C. Ward and G.O.G. Löf, "Integration of Evacuated Tubular Solar Collectors with Lithium Bromide Absorption Cooling Systems". Accepted for publication in the International Journal for Solar Energy, 1979.

152. Duff, W.S., R. Kersten and K.R. Schreitmüller, "Evacuated Tubular Collector Concepts and Systems Applications", Proceedings of the 1979 International Conference of the ISES, Atlanta, Georgia, May 1979.

153. Loehrke, R.I., H.N. Gari, J.C. Holzer, "Thermal Stratification Enhancement for Solar Energy Applications." Technical Report HT-TS792, Department of Mechanical Engineering, Colorado State University, June 1979.

154. Fischer, L.S., C.W.J. van Koppen, J.J. Puts., Basic Aspects of the Seasonal Storage of Solar Heat in the Ground. In K.W. Böer (Ed), SUN II. Pergamon, New York, Vol. 1., Chap 3, pp. 609-613, 1979.

155. Gari, H.N., R.I. Loehrke, J.C. Holzer, "Performance of an Inlet Manifold for a Stratified Storage Tank." ASME preprint 79-HT-67, San Diego Conference, August 1979.

156. General Electric, "Solartron TC-100, Vacuum Tube Solar Collector", Document No. 78SD4215B, August 1979, USA.

157. IEA Solar Heating and Cooling Programme, "Data Requirements and Thermal Performance Evaluation Procedures for Solar Heating and Cooling Systems". Task I Report, December 1979.

158. Veltkamp, W.B., Evaluatie van het zonne - energieproject. De Ingenieur, nummer 12, jaargang 92, pp. 18-20, 1980.

159. Veltkamp, W.B., Thermal Stratification In Heat Storages. In C. den Ouden (Ed). Thermal Storage of Solar Energy. Martinus Nijhoff, The Hague, Chap. 2 pp. 47-59, 1980.

160. Isakson, P., W. Kennish and E. Ofverholm, "Reporting Format for the Thermal Performance of Solar Heating and Cooling Systems in Buildings". IEA Solar Heating and Cooling Programme Task I Report, February 1980.

161. Cuthbert, Daniel and Fred S. Wood, "Fitting Equations to Data", John Wiley and Sons, New York, 1980.

162. de Ron, A.J., Dynamic Modelling and Verification of a Flat Plate Solar Collector. Solar Energy 24. Pergamon Press, New York, No.2, pp. 117-128, 1980.

163. Duff, W.S., C.E. Hancock and G.O.G. Löf, "Operational Improvements in the CSU Solar House I System Supplied with Heating from Evacuated Collectors", Proceedings of the ASME Winter Annual Meeting, November 1980.

164. United Kingdom ISES: Text of seven papers given at the UK ISES Conference in London, January 1981.

165. Turrent, D., "Performance Monitoring of Solar Heating Systems in Dwellings". Proceedings of the ISES Solar World Forum, Brighton, England, 1981. p.82 ff.

166. Veltkamp, W.B., "On the Control of the Massflows in a Solar Heating and Hot Water System." Report WPS3-81-10-R321. Eindhoven University of Technology, 1981.

167. Veltkamp, W.B., Optimisation of the Mass Flow in the Heat Distribution Circuit of a Solar Heating System with a Stratified Storage. In D.O.Hall (Ed)., Solar World Forum. Pergamon, Oxford, Vol. 1, Chap. 2, pp.286-290, 1981.

168. van Koppen, C.W.J., Active Heating in Buildings. In D.O.Hall(Ed). Solar World Forum. Pergamon, Oxford, Vol. 1, pp.8-19, 1981.

169. Chandrashekar, M., and W.E. Carscallen, "Simulation of an Industrial Hot Water System with Evacuated Tubular Collectors Operating in Batch Mode," Presented at ISES, Brighton, England, 1981.

170. Sanyo Electric Company, Ltd., "R and D for Solar Cooling, Heating and DHW Supplying System". Annual Report of 1980 FY (in Japanese), March 1981.

171. Löf, G.O.G., W.S. Duff, and C.E. Hancock, "Development and Improvement of Liquid Systems for Solar Space Heating and Cooling - CSU Solar House I". Third Annual Systems Simulation and Economic Analysis/Solar Heating and Cooling Operational Results Conference, Reno, Nevada, April 1981.

172. Duff, W.S., G.J. Favard and K.R. Den Braven, "Development of a Day-by-Day Simulation of Solar Energy Systems", Third Annual Systems Simulation and Economic Analysis/Solar Heating and Cooling Operational Results Conference, Reno, Nevada, April 1981.

173. Goumaz, J.Y., and W.S. Duff, "Comparison of Drain-Back and Dual Liquid Solar Heating and Domestic Hot Water Systems", Proceedings of the ISES Meeting, Brighton, England, August 1981. Also accepted for publication in the International Journal for Solar Energy.

174. Window, B., I.M. Bassett, "Optical Collection Efficiencies of Tubular Solar Collectors with Specular Reflectors." Solar Energy, 1981, Vol. 26.

175. Duff, W.S., and C.B. Winn, "Modelling of Solar Thermal Systems," Chapter in Solar Energy Handbook McGraw-Hill, 1981.

176. Fietz, Evan, DMR and Associates, "Solar Energy Program, Data Acquisition System". Final report for NRC/DERD/SEP.

177. Duff, W.S., S. Karaki and G.O.G. Löf, "Performance of Three Well-Instrumented Residential Solar Energy Systems,"ASHRAE Transactions, Vol. 87, part 2, 1981.

178. Duff, W.S., "International Energy Agency Evacuated Collector Systems Project", Proceedings of the International Solar Energy Society Meeting, Brighton, England, August, 1981.

179. Sanyo Electric Company, Ltd., "R and D for Solar Cooling, Heating and DHW Supplying System". Annual Report of 1981 FY (in Japanese), October 1981.

180. Guisan, O., A.Mermoud, O. Rudaz, "SOLARCAD Project". Centre Universitaire d"Etude des Problemes de l'Energie and Groupe de Physique Applique, Universite' de Geneve, May 1982.

181. Veltkamp, W.B., SISOEN on the HP-41C. Report WPS3-82.12.R339. NOZ Report. indhoven University of Technology, 1982.

182. Veltkamp, W.B., "SISOEN a Fast Physical Model of a House and a Solar Heating Installation with a Stratified Storage and Optimum Control of the Flows." Report WPS3-82.09.R336, NOZ Report. Eindhoven University of Technology, 1982.

183. Veltkamp, W.B., "On the Performance of the Solar Heating and Hot Water System of the 'Keuringsdienst van Waren' at Enschede the Netherlands." Report BEOP-Z-82012. Eindhoven University of Technology, 1982.

184. Veltkamp, W.B., "Solar Energy in a Medium Size Commercial Building." Report WPS3-82.08.R332,BEOP-Z-82060. Eindhoven University of Technology, 1982.

185. Bisschops, R.W.G., C.W.J. van Koppen, W.B. Veltkamp, "Experimental Performance of the Second Generation Solar Heating System in the Solar House of the Eindhoven University of Technology. Solar World Congress, S.V.Szokoly Ed., Pergamon, Oxford, Vol.1, pp.84-88, 1983.

186. Veltkamp, W.B., C.W.J. van Koppen, A Two Level Simulation Model for Combined Active and Passive Solar Space Heating. In S.V. Szokolay (Ed)., Solar World Congress. Pergamon, Oxford, Vol. 1, pp. 939-943. 1983.

187. Horster, H., "Solare Heizung and Kuhlung von Gebauden Colorado - Freiburg, Teil A: Kollektorentwicklung". ET5041 Teil A. Philips GmbH, Forschungslaboratorium, Aachen.

188. Veltkamp, W.B., C.W.J. van Koppen, Balancing of Solar Heating Options. In C.den Ouden (Ed)., First E.C. Conference on Solar Heating. Reidel, Dordrecht, pp. 691-694, 1984.

189. Veltkamp, W.B., "Implementation of Stratified Storage Models in the EEC Model EMGP2." Report WOP-WET-84.030,NOZ Report, Eindhoven University of Technology, 1985.

APPENDIX A

TASK VI WORKPLAN (AS OF 1/1/85)

A.1 Objectives and Approach

The objective of Task VI of the IEA Solar Heating and Cooling Programme is to further the understanding of the performance of evacuated collectors in solar heating, cooling and hot water systems and to study, document and compare the performance characteristics of such collectors in various systems and climates. The execution of the Task emphasizes common reporting requirements, a variety of installations covering important evacuated collector applications, a comprehensive use of available evacuated collectors, use of the same collectors in several installations and some duplication in end uses. Cooperation in the Task provides a means of reducing duplication in each participant's national program and a reference point for future evacuated collector systems research, development and commercialization activities.

Exchange of performance results within the Task has been greatly enhanced by adoption of a mandatory common reporting structure utilizing the IEA performance reporting format that has been modified and made more specific and prescriptive. Performance comparisons can be made that would be difficult or impractical for non-coordinated projects. Thus, participants have as good or better access to, and gain as much or more information from each of the Task VI installations than if the installations were part of their national program.

A.2 WORK PLAN

A.2.1 Responsibilities of Participants

Each participant in this Task is responsible for the operation and analysis of at least one evacuated collector solar heating and/or cooling system. At the first meeting, the participants defined the general characteristics of acceptable systems and installations and developed a detailed program of work.

The general characteristics of acceptable installations and detailed program of work is as follows:

I. General Requirements for Participating Installations

1. Projects will provide the equivalent of one full-time data engineer responsible for instrumentation, data acquisition, and analysis. This individual, or equivalent, and the project support staff will identify and correct faults in the data collection and operating systems in a timely manner. This capability will be located on-site until system reliability and warning capability have been clearly established.

2. Continuity in project staff will be maintained, starting with installation design and continuing through data collection and reporting.

3. Projects will be sufficiently well instrumented to provide the required information at the specified accuracies.

4. A project minimum annual manning level of two years will be provided.

5. It is essential that the project be oriented toward the testing of the system, as opposed to collector testing.

II. Desired Features for Participating Installations

1. The relationship between the evacuated collector performance characteristics and system performance is important. Therefore this relationship should be well understood in the project design phase and should be further carefully explored throughout the experiment. These efforts should be coordinated with Task III.

2. The use of systems models, particularly simulation, as an integral part of the system design process and later to generalize the results to other locations and system variants is highly desirable. The study and use of models should be coordinated with Task I.

3. Excessive duplication of one type of project is undesirable. It is desirable to have a variety of different evacuated collector design, working fluids, system applications, working temperature ranges, and climates.

4. Applications where temperature differences to ambient are reasonably high, above $40^{o}C$, in sunny climates and moderate, above $20^{o}C$, in cloudy climates, should be sought. Also, applications where temperature differences are highly variable are desirable.

5. Real loads are preferred as simulated loads do not cover all operating problems, such as accidents, that must be experienced and dealt with before reliable evacuated collector systems are developed. However, one or two projects with simulated loads are desirable for more carefully controlled system experiments, identification of specific load factor influences, and the greater ease of conducting sensitivity analyses. The differences in capability between the real load projects and simulated load projects can be beneficial to the total Task efforts.

6. It is desirable that projects accepted in this Task be those for which the component suppliers and the project investigators not be the same organization.

III. Requirements for Instrumentation, Data Collection, and Performance Reporting

1. Well instrumented systems are required. Instrumentation will be sufficient to calculate the primary reporting quantities, and sensors will be precise enough to provide the accuracies given in the December 1979 report of "Data Requirements and Thermal Performance Evaluation Procedures for Solar Heating and Cooling Systems".

2. The instrumentation and data recording plan will ensure high data collection reliability.

3. Meetings will be held semi-annually.

   a. Annual reports will follow the IEA format for reporting the performance of solar heating and cooling systems, as given in the February 1980 report, with modifications, made at the September 1980 Pingree Park meeting and approved at the December 1980 Task VI meeting.

   b. Between annual reports, reporting for Task VI meetings should be patterned after the IEA format, if practical.

   c. To provide for adequate review time, each participant will send his report to each of the other participants at least one month before Task meetings.

   d. The Operating Agent will summarize the annual reports in a report to be submitted to the IEA Executive Committee and participants at the conclusion of the Task. The Operating Agent will also provide the required Task status reports to the IEA Executive Committee.

   e. Task meetings of the participating installations will be held semi-annually for the purpose of discussing Task and installation progress and results, exchanging information among participants, and reviewing proposals for new Task VI installations.

   f. The meeting date and location of the next meeting will be set at each meeting.

g. The Operating Agent will set the meeting agenda to make any necessary adjustments in meeting dates to accommodate timing of individual projects.

A.2.2 Procedures for Reviewing Proposed Installations

I. Design and data collection plans of proposed installations will be presented at Task VI meetings and will be sufficiently detailed so that the participants can evaluate if the proposals meet Task VI requirements. The participants will make recommendations on proposed installation designs and data collection plans. Approval of the plan for a proposed installation will be by consensus of the participants.

II. Revisions to projects that become necessary subsequently need not require approval of Task participants. However, recommendations on such matters should be sought, whenever practical.

A.2.3 Task Duration

The Task began officially in October of 1979 and will end December 1985.

A.2.4 Publications Policies and the Role of Evacuated Tubular Collector Manufacturers in Task Activities

Collector manufacturers are encouraged to take part in Task activities with supply of hardware, advice, evaluation and review. In such arrangements, the responsible participant in the Task shall give full consideration to the manufacturer's advice and opinions and provide the manufacturer with the opportunity to review and advise on reports and papers. The findings and reports shall be the sole responsibility of the participant.

A.2.5 Task Participants

The Task participants and applications are:

AUSTRALIA - Heating and Cooling of University Offices

CANADA - Industrial Process Heat

COMMISSION OF THE EUROPEAN COMMUNITIES (CEC) - Cooling of a Solar Laboratory

FEDERAL REPUBLIC OF GERMANY - Multi-family Residential Heating and Hot Water Production

JAPAN (a previous participant) - Single Family Residential Heating, Cooling and Hot Water Production

THE NETHERLANDS - Single Family Residential Heating and Hot Water Production

SWEDEN - District Heating

SWITZERLAND - District Heating and Industrial Process Heat

THE UNITED KINGDOM - Domestic Space Heating and Hot Water Production with Simulated Loads

USA - Single Family Residential Heating, Cooling and Hot Water Production

The CEC and Australia joined the Task in 1982. A second installation in Switzerland jointed the Task in 1983. Addresses and phone numbers of Task national contact persons and responsible researchers can be found in Appendix B.

A.3 BACKGROUND

Six of the nine current Task VI participants have been in the Task since it began in October 1979. These are Canada, the Federal Republic of Germany, Sweden, Switzerland, the United Kingdom, and the United States. The Netherlands joined the Task in October 1980, the CEC in May 1982 and Australia in October 1982. When the Task began, only Japan, a previous participant, the Federal Republic of Germany and the United States had operational evacuated collector systems with thoroughly tested data acquisition systems. As of September 1983 all installations, except the recently built Swiss industrial process heat application, were operating and collecting data.

APPENDIX B

ADDRESSES OF KEY TASK VI PERSONNEL

AUSTRALIA

R.E. COLLINS
School of Physics
University of Sydney
Sydney, NSW 2006
Australia
Telephone: (02) 692-3577
Telex: AA20056

ROLAND SCHMID
Department of Mechanical Engrg
University of Sydney
Sydney, NSW 2006
Australia
Telephone: (02) 692-3723
Telex: AA20056

ENN MANIK
Dept. of Mechanical Engrg.
University of Sydney
Sydney, NSW 2006
Australia
Telephone: (02) 692-3723

CANADA

W.E. CARSCALLEN
National Research Council Canada
Division of Energy
Montreal Road, Bldg. R92, Rm. 100
Ottawa, Ontario K1A 0R6
Canada
Telephone (613) 993-9224
Telex: 0533145

M. CHANDRASHEKAR
Dept. of Systems Design
University of Waterloo
Waterloo, Ontario N2L 3G1
Canada
Tel: (519) 885-1211 ext. ext 2897

HUBERT TAUBE
Maclaren Plansearch
#608 10240 - 124th Street
Edmonton, Alberta T5N 3W6
Canada
Telephone: (403) 482-7341

COMMISSION OF THE EUROPEAN COMMUNITIES

D. VAN HATTEN
Commission of European Communities
Joint Research Center Euratrom
I-21010 Ispra (VA)
Italy
Telephone: (0332) 78-9449
Telex: 380042

FEDERAL REPUBLIC OF GERMANY

K.R. SCHREITMULLER
DFVLR, Institut fur Technische Physik
Pfaffenwaldring 38-40
D-7000 Stuttgart-80
Federal Republic of Germany
Telephone: (0049) 0711-6862485 (2)
Telex: 072255689

K.H. VANOLI
IST Energietechnick GmbH
Ritterweg 1
D7842 Kandern-Wollbach
Federal Republic of Germany
Telephone: (07626) 7097 or 7098

JAPAN

KATSUHIRO HINOTANI
Research Center
Technical Operations
Sanyo Electric Company, Ltd.
1-18-13 Hashiridani, Hirakata
Osaka 573
Japan

THE NETHERLANDS

A. BOUWKNEGT
Philips Lighting Division
Development Department, Solar Collectors
Building EB5, Eindhoven
The Netherlands
Telephone: (040) 755741
Telex: 35000 PHTC NL

C.W.J. VAN KOPPEN
Eindhoven Univ. of Technology
Box 513, Eindhoven
The Netherlands

BART VELTKAMP
Eindhoven University of Technology
Box 513, 5600 MB Eindhoven
The Netherlands
Telephone: (40) 473152

SWEDEN

BENGT PERERS
Studsvik Energiteknik AB
61182 Nykoping
Sweden
Telephone: (46155) 27452
Telex: 64013 Studs 5

SWITZERLAND

O. GUISAN
University of Geneva
Section de Physique
32 Bd d'Yvoy
1211 - Geneva 4
Switzerland
Telephone: (22) 219355
Telex 421159 siao ch

B. LACHAL
University of Geneva
Section de Physique
32 Bd d'Yvoy
1211 - Geneva 4
Switzerland
Telephone: (22) 219355
Telex: 421159 siao ch

O. RUDAZ
University of Geneva
Section de Physique
32 Bd d'Yvoy
1211 - Geneva 4
Switzerland
Telephone: (22) 219355
Telex 421159 siao ch

A. Mermoud
University of Geneva
Section de Physique
32 Bd d'Yvoy
1211 - Geneva 4
Switzerland
Telephone: (22) 219355
Telex 421159 siao ch

UNITED KINGDOM

G. BAKER
BSRIA
Old Bracknell Lane
Bracknell, Berkshire
United Kingdom

I.N. POTTER
BSRIA
Old Bracknell Lane
Bracknell, Berkshire
United Kingdom

UNITED STATES

WILLIAM S. DUFF
Solar Energy Applications Laboratory
Colorado State University
Fort Collins, Colorado 80523
USA
Telephone: (303) 491-8487
Telex: 910-930-9000

S. KARAKI
Solar Energy Applications Lab
Colorado State University
Fort Collins, Colorado 80523
USA
Telephone: (303) 491-8617
Telex: 910-930-9000

OPERATING AGENT

WILLIAM S. DUFF
Solar Energy Applications Laboratory
Colorado State University
Fort Collins, Colorado 80523
USA
Telephone: (303) 491-8487
Telex: 910-930-9000

APPENDIX C

IEA TASK VI NOMENCLATURE

The nomenclature and reporting structure used in this report was developed by the Task to allow easily understood unambiguous communication of performance results among Task participants. A detailed presentation of the nomenclature and reporting structure is given in Chandrashekar and Vanoli [2]. Excerpts from this report are given in Tables C-1 through C-5 and Figure C-1.

TABLE C-1. SUBSYSTEM DESIGNATIONS

001-009	Climatological data group
100-199	Collection
200-299	Storage
300-399	Domestic Hot Water
400-499	Space Heating
500-599	Space Cooling
600-699	Energy Demand (eg., building, IPH)
700-899	Reserved for Future Use
900-999	Summary Data Group

TABLE C-2. QUANTITY OR ENERGY FORM LETTER DESIGNATORS

E*	Electrical energy (MJ)
F*	Fossil or chemical energy equivalent (MJ)
Q*	Thermal energy (MJ)
H	Solar irradiant energy or energy density (MJ or MJ/m^2)
G	Solar flux density (W/m^2)
T	Temperature (^oC)
R	Relative Humidity (%)
D	Spacial temperature difference (K)
W	Mass flow rate (kg/sec)
S	Status information
V	Velocity (m/sec)
N	Performance (units as derived)
A	Area (m^2)
C	Capacitance (MJ/K)
U	Heat transfer factor (W/K)

*time base for quantities will be given when values are stated. All designators are reserved. Additional designators will be allocated by the Operating Agent.

TABLE C-3. RESERVED DESIGNATIONS APPLICABLE TO ALL SUBSYSTEMS

Number	Designation
-00	Controlled energy from other subsystems
-01	Subsystems auxiliary energy
-02	Controlled energy to other subsystems
-03	Total subsystem operating energy
-04	Total subsystem heat loss. This quantity is frequently derived in more than one way. In such cases different derivations should be given different designations in the sub-system energy flow block diagram tables.
-05	Change in stored energy
-06	Total energy from otther subsystems
-07	Total energy to other subsystems
-08	Useable heat loss from solar
-09	Unuseable heat loss from solar stored energy
-10	Stored energy
-11	Thermal energy contribution to the subsystem by the operating energy
-12	Controlled energy to other subsystems excluding distribution systems effect
-13	Total useable heat loss
-14	Total nonuseable heat loss
-15	Cooling supplied by solar
-16	Transport heat loss
-17	Operating devices energy loss
-18	Total energy loss from auxiliary energy system
-30	Energy balance error

TABLE C-4. RADIATION AND TEMPERATURE DESIGNATORS

H001	total solar energy on collector plane	
H002	total horizontal	
H003	horizontal diffuse	In Units
H004	total solar energy on collector plane while the collector is on	of MJ/m^2-period
H005	diffuse solar energy on collector plane	
H006	beam solar energy on collector plane	
H007	total solar energy on collector plane corrected for shading	
H100	total solar incident on collector aperture	In Units
H101	solar incident on collector aperture while collector is on	of MJ/period

TABLE C-5. A LIST OF PERFORMANCE AND OTHER INDICIES

adjusted collector efficiency	N100=(Q112 + Q105)/H100
unadjusted collector efficiency	N100=Q112/H100
adjusted collector on efficiency	N101=(Q112 + Q105)/H101
unadjusted collector on efficiency	N111=Q112/H101
system collection efficiency	N102=Q102/H100
system collection on efficiency	N103=Q102/H101
system collection COP	N105=Q102/103
solar collection system and storage conversion efficiency	N104=Q212/H100
solar collection and storage COP	N106=Q212/E103
solar collection and storage system COP	N107=Q202/(E103 + E203)
normalized temperature difference	N108=(T100-T001)/G001
estimated shading factor	N109d (diffuse) N109b (beam)
solar energy collected per unit area	N112-Q112/A100
solar energy system efficiency	N200=(Q102 - Q209 - Q216)/H100
solar fraction energy consumer for domestic hot water	N301=Q300/(Q300 + Q301 + Q303)
solar fraction of energy delivered	N302=solar energy into hot for hot water water tank: (Q312 + Q301)
solar fraction of energy consumed for space heating	Q400 + Q908 N401 = Q400 +Q913 +Q401
solar fraction of energy consumed for space cooling	N501=Q500/(Q500 +Q501)
solar fraction of space cooling supplied	N502=Q515/Q502

TABLE C-5. (CONTINUED)

solar cooling thermal COP	N503=Q515/Q500
auxiliary cooling thermal	COP N504=(Q502 - Q515)/(Q501)
system solar fraction	N901= Q208 + Q202 Q202+Q901 + Q303 +Q913
system COP	N902 = Q202 Q903

APPENDIX D

ACKNOWLEDGMENTS

Those participating in the writing of participant contributions were:

Australia	Dick Collins, Roland Schmid, Enn Mannik
Canada	William Carscallen, Hubert Taube and M. Chandrashekar
CEC	Dolf van Hattem
Federal Republic of Germany	Klaus Vanoli and Konrad Schreitmüller
The Netherlands	Richard Bisschops, Rob Jetten, Chris van Koppen and Bart Veltkamp
Sweden	Elisabeth Kjellsson, Heimo Zinko and Bengt Perers
Switzerland	Olivier Guisan, Olivier Rudaz, Bernard Lachal
United Kingdom	Nigel Potter
United States	William Duff, Karen DenBraven, Michael Riley, Susumu Karaki, George Löf, Tom Brisbane

APPENDIX E

SUPPLEMENTARY PREFORMANCE REPORTS

NOTE

This appendix is a supplement to "Experimental Results from Eleven Evacuated Collector Installations." It presents work completed after the normal span of that report. Consequently, only new information and results are presented. To help the reader cross-reference this new material with material in the main body of the report, the numbering of sections of text, figures, and tables in the SOLARIN and SOLARCAD appendix sections have been made identical to those in the report main body.

SOLARIN Project at Hallau, Switzerland
November 1984 to October 1985

O. Guisan
B. Lachal
A. Mermoud
O. Rudaz

Table 2-1. Installation descriptions

Solarin Industry Project, Hallau/Switzerland

Evacuated collectors ($\sim$ 406 m^2) are installed on the roof of an alimentary factory (wine and fruit juice). They contribute to space heating and manufactory heat processing. Heat storage is achieved by use of 2 water tanks ($10m^3$ + $23m^3$). Conventional and existing burners provide auxiliary heating. A good solar fraction is expected in summer (50 - 90%), while lower values will characterize the winter months.

Table 2-2. Description of loads

Solarin Industry Project, Hallau/Switzerland

Hot water is needed for industrial processing and space heating.

In the former case (i.e. pasteurization, bottle and case washing) the load is 2900 GJ/year ranging between 35 and 430 GJ/month with a peak demand in autumn. The required temperature is between 90 and 110°C.

In the latter case and for the heating season, the load amounts to 640 GJ with a peak demand around 130 GJ/month. The temperature never exceeds 70°C. These figures correspond to long term averages.

The total monthly load varies between 120 and 560 GJ/month, with a yearly average value of 290 GJ/month.

The heat produced by solar is devoted to industrial processing in summer time and to space heating in winter time. The load is divided in different and complicated loops for processing and heating. Then it will be considered as a whole. Nevertheless it is possible to direct solar gains to low temperature uses if any.

Table 2-3. Current activities

Solarin Industry Project, Hallau/Switzerland

The whole solar system is installed and in operation since July 1983, with a rough and preliminary regulation. It was replaced by a microprocessor controled regulation by the end of 1983.

All measurement equipments have been built, calibrated and installed. The 50 sensors are connected to a microprocessor data acquisation system, which can be controled and read through a phone line at the University of Geneva (300 km away), where the analysis is achieved.

Measurements and regulation are fully separated.

Good data for solar loop have been taken, starting in January 1984. For the entire system, flowmeter failures in storage and load loop have been solved in autumn 1984, allowing complete measurements from November 84 to October 85.

Table 3-1. Climate at the Task VI locations

Hallau/Switzerland

latitude	47.6°N	
longitude	8.47°E	
elevation (meters)	420	
heating Degree-Days 18.3°C	3270	
heating season	Oct.-May	
average wet bulb temperature for cooling season	NA	NA = not applicable
colling season	NA	
relative humidity (%) (yearly average)	77	
typical daily insolation		
January (MJ/m^2 on horizontal)	3.1	
July (MJ/m^2 on horizontal)	20.8	
percent diffuse		
January (%)	64	
July (%)	39	
average daily temperature		
January (°C)	- 1.7	
July (°C)	17.4	
average maximum daily temperature		
January (°C)	8	deduced from meteorological data compilations
July (°C)	24	
average minimum daily temperature		
January (°C)	- 6	
July (°C)	11	
seasonal climate description	mesothermal forest; moist; rainfall all year	

Table 4-1. Evacuated Tube Collector Reference

Solarin Industry Project, Hallau/Switzerland

Corning Cortec 'D' (made in France)

Corning Cortec 'D' collectors are the same as Corning Cortec 'A' collectors but absorbers are tilted by 30^{o} as compared to the collector plane.

Note for interim report

Corning Cortec collectors used in Germany and in Switzerland are not the same. They should appear separately in Tables 4-1 and 4-2.

Collectors used in Geneva and Hallau could be refered to as:
Corning Cortec 'A' (made in France)
Corning Cortec 'B' (made in France)
Corning Cortec 'D' (made in France)

Collectors used in Freiburg could be refered to as :
Corning Cortec (made in USA)

All these collectors look similar (sizes, connections, etc....) but performances are different.

Table 4-2. Specifications for Evacuated Tube Collectors used in Task VI installations

Solarin Industry Project, Hallau/Switzerland

Collector	Corning Cortec 'D' 1)
Physical properties:	
No. tubes per module	6
Pitch (mm)	111
Absorber area (m^2) per module	1.12 x 2
Aperture area (m^2) par module	1.45
Absorber tilt angle / collector plane (^{o})	30^o
Absorber surface material	black chrome both sides
Collector/heat pipe fluid	any
Fluid volume per m^2 of aperture area (l/m^2)	$\sim$ 0.8
Collector capacitance per m^2 of aperture area ($KJ/m^2{}^oC$)	5.5
Typical temperature difference between absorber and fluid (^oC)	$\sim 1.6^oC$ for 500 W absorbed per m^2 absorber
Glass material	Pyrex
Tube material	Copper
Reflector provided by manufacturer	None
Performances:	
$F'\tau\alpha$	0.75
$F'U_L$ ($w/m^2{}^oC$)	1.1 - 5.0 (ΔT = 0-200 ^oC)
Manufacturer efficiency curve or other test data	test data for Cortec 'A'
Incidence angle modifier	NIA
Characterization of selective surfaces	NIA ($\alpha \sim 0.9$ $\varepsilon \sim 0.1$)

1) Same as Corning Cortec 'A' but absorbers tilted by 30^o/collector plane

Table 4-3. Characteristics of evacuated collector arrays in Task VI installations

Solarin Industry Project, Hallau/Switzerland

Collector	Corning Cortec 'D' [1]
No modules	280
Absorber area (m^2)	313.6
Aperture area (m^2)	406
Array capacitance per m^2 of aperture area ($kJ/m^2{}^oC$)	9.6
Fluid volume per m^2 of aperture area (l/m^2)	~1.33
Working fluid	32 % glycolen in water
Fluid flow rate (l/h) - array input (output) - through one module	~ 10.000 71
Tube material (piping)	iron
Module connections (serie/parallel)	7 branches in parallel; per branch: 20 series of 2 in parallel
Collector tilt angle (^{o})	2°/Hor.
Azimuth faced by array	3° W
Reflector / background	clear roof
Tube orientation	E/O

1) Same as Corning Cortec 'A' but absorbers tilted by 30°/collector plane

Reliability, maintainability aspects

Solarin Industry Project, Hallau/Switzerland

2 tubes broken during transport
1 tube broken by accident after mounting

No evidence for additional broken tubes in November 85 (visual check)

Table 4-5. Storage description

Solarin Industry Project, Hallau/Switzerland

Two horizontal steel cylinders filled with water and insulated by 150 mm of mineral wool are used for heat storage. Their volumes are 10 and 23 m^3; they correspond typically to one day and one weekend heat storage. Heat losses are theoretically 14 and 28 $W/^oC$, but experimental values are twice larger. For processing needs (summer time) the temperature ranges from 90°C to 120°C. For space heating (winter time) temperature down to 15°C can still be useful (preheating of air taken from outside).

Two tanks instead of one gives more flexibility for regulation and heat strategy. Although natural stratification is present and used, it will not play an important role because of frequent mixing and low temperature difference induced. Nevertheless 10 temperature sensors per tank will allow a detailed analysis and the unterstanding of the involved phenomena.

Table 4-6. Summary description of components and subsystems

Solarin Industry Project, Hallau/Switzerland

Collection

Corning Cortec 'D' collectors are used. They are mounted at 0.5 m above the flat roof of the factory. The roof is covered by gravel (white painted) and constitutes a clear background. The collector plane is tilted by 2^{o} from horizontal. Absorbers are tilted by 30^{o} with respect to the collector plane. Shadowing effects from one absorber to the other one can be important in winter time.

Allowance is given for testing other collectors (focusing type).

Heating

Solar gains are devoted to processing needs in summer time and space heating in winter time. Auxiliary heating is provided by existing and conventional burners. Low temperature heat use is sometimes possible: preheating, through an exchanger, of air taken from outside (space heating).

Controls

The solar radiation level controls the collector pump. Temperature conditions allow to act on other pumps and valves to orientate properly all heat flows. A rather complicated regulation is achieved by use of a microprocessor in order to allow different operations : direct use of solar, solar to storage, storage to load, choice of storage, choice of load, partial and/or combined operations.

Alltogether 12 sensors act on 3 pumps and 8 valves.
Also manual operations are possible.

Table 5-1. Experiment Descriptors, Modes, Components and operating dates

Solarin Industry Project, Hallau/Switzerland

Experiment	CH2 - HTG - 2
Mode	Industrial water heating
Dates	November 84 - October 85
Collector	Corning Cortec 'D'
Chiller	NA 1)
Auxiliary	oil burner
Main tank	$10m^3$ + $23m^3$ horizontal cylindrical steel tanks
Controls	microprocessor

1) NA = not applicable

CHAPTER 5

Solarin Industry Project, Hallau/Switzerland

The main objective of the project is to evaluate performances of evacuated collectors for industrial purposes in swiss climate conditions.

From previous experiments (see Solarcad project, Experiment CH-HTG-1 and 2), the Corning Cortec collector has been choosen. Allowance is also given for other collectors (focusing type).

The system diagram is shown separately (Fig. 5.1). The solar loop is connected through a heat exchanger to the main loop related to both storages and to the different uses. Precise and numerous sensors allow to evaluate all energy flows (especially - solar radiations, collector output, heat exchanger input/output, storage inputs and outputs, storage internal energies, heat to load) as well as intermediate losses.

Experiment CH2 - HTG - 2 (November 84 - October 85)

Evaluate performances for Corning Cortec 'D' collectors and for the whole system. Identify all collector ans system losses (thermal losses, capacity effects, ...). Understand physical and thermal behaviour of the system. Validate simulation or design procedures.

We present in this report data obtained from November 1984 to October 1985 (i.e. a full year). Solarin system is characterized by low temperature space-heating use during winter time (November → April; $\Delta T \sim$ 20 - 60 °C) and high temperature process use during summer time (May → October; $\Delta T \sim$ 60 - 90 °C).

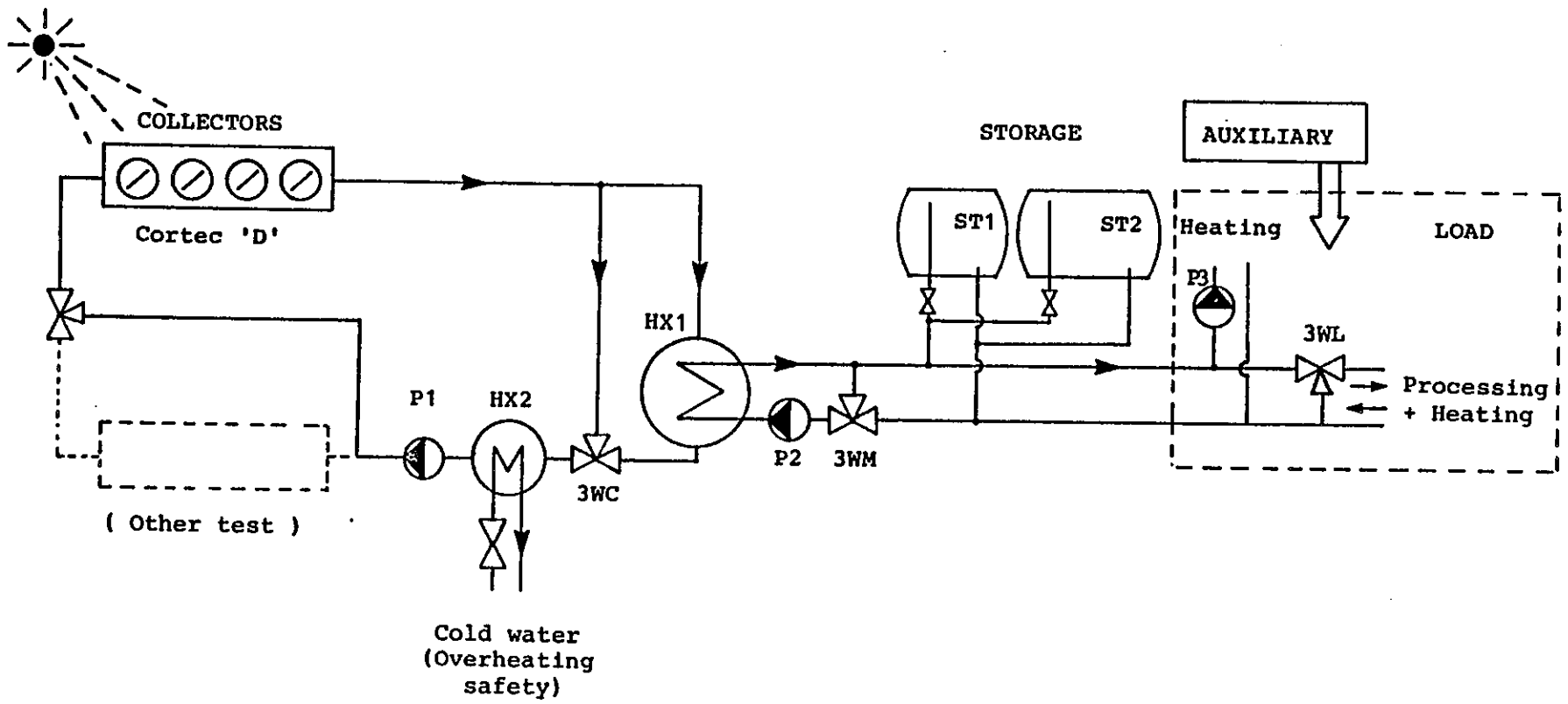

Figure 5.1 CH2 - HTG - 1. Hallau / Switzerland
Solar system schematic.

6.1.9 SOLARIN Project
Hallau, Switzerland

Figures 6.1.9-1 and 6.1.9-2 show hourly efficiencies for the one year period considered: November 1984 to October 1985.

Some points were rejected with respect to following criteria:

- pump should be "on" at least 6 min. before the considered hour
- no switching of valves is allowed during the considered hour (it may induce large temperature variations and then significant dynamic effects)
- capacitance correction (Q105) has to be smaller than one third of the delivered heat (Q112)
- snow cover, as measured at the closest meteorological station, must not exceed 1 cm
- measurement of the diffuse radiation has to be available and valid.

We recall that, for the used Corning Cortec ETC's, the absorber is tilted by 30° with respect to the collector plane (also tilted by 2° from horizontal). The poor collector orientation is compensated by tilting the absorber; it results in a better collector efficiency as compared to normal conditions, because the solar radiation is measured for the collector plane and tilting the absorber contributes to improve the "incidence angle modifier" factor. With respect to normal conditions we have less solar energy but almost the same heat gains. (See "Evacuated Collector Systems Characterization" report).

In 6.1.9-1, the reference solar energy is the measured collector plane solar radiation G001 (nearly horizontal), in 6.1.9-2 the reference radiation is the effective radiation reaching the absorbers G017:

G017 = DIF 2° S + DIR 2° S * TA (γ)

where

- DIF 2° S is the diffuse radiation onto collector plane, assumed to be close to the effective diffuse radiation reaching the absorbers.

- DIR 2° S is the beam radiation in collector plane

- TA(γ) is the gain when tilting the absorber, considered as an incidence angle modifier factor. This factor depends of the sun position via the transverse profil angle γ.

Heat losses are considered either constant or depending linearly on temperature:

$$F'U_L = K$$
$$\text{or } F'U_L = K + Kp \cdot \Delta T$$

The main conclusions from fits are:

1) When using the effective solar radiation as a reference, errors are significantly recuded (by a factor 2) as compared to the case where the solar radiation on the collector plane is considered as a reference.

2) The mean value for the gain when tilting the absorber

$$\overline{TA}(\gamma) = \frac{\eta o \text{ (Fit G001)}}{\eta o \text{ (Fit G017)}} = 1.12,$$ in good agreement with theorical expectations, where $TA(\gamma)$ varies from 1.05 in summer to 1.25 in winter.

3) Heat losses are the same for the two cases under consideration ($F'U_L$ = 2.31 and 2.25 $W°Cm^2$), as should be expected for the same average $\Delta T \cong 60\,°C$.

4) The best fit corresponds to consider both the effective solar radiation as the reference and heat losses as depending on temperature.

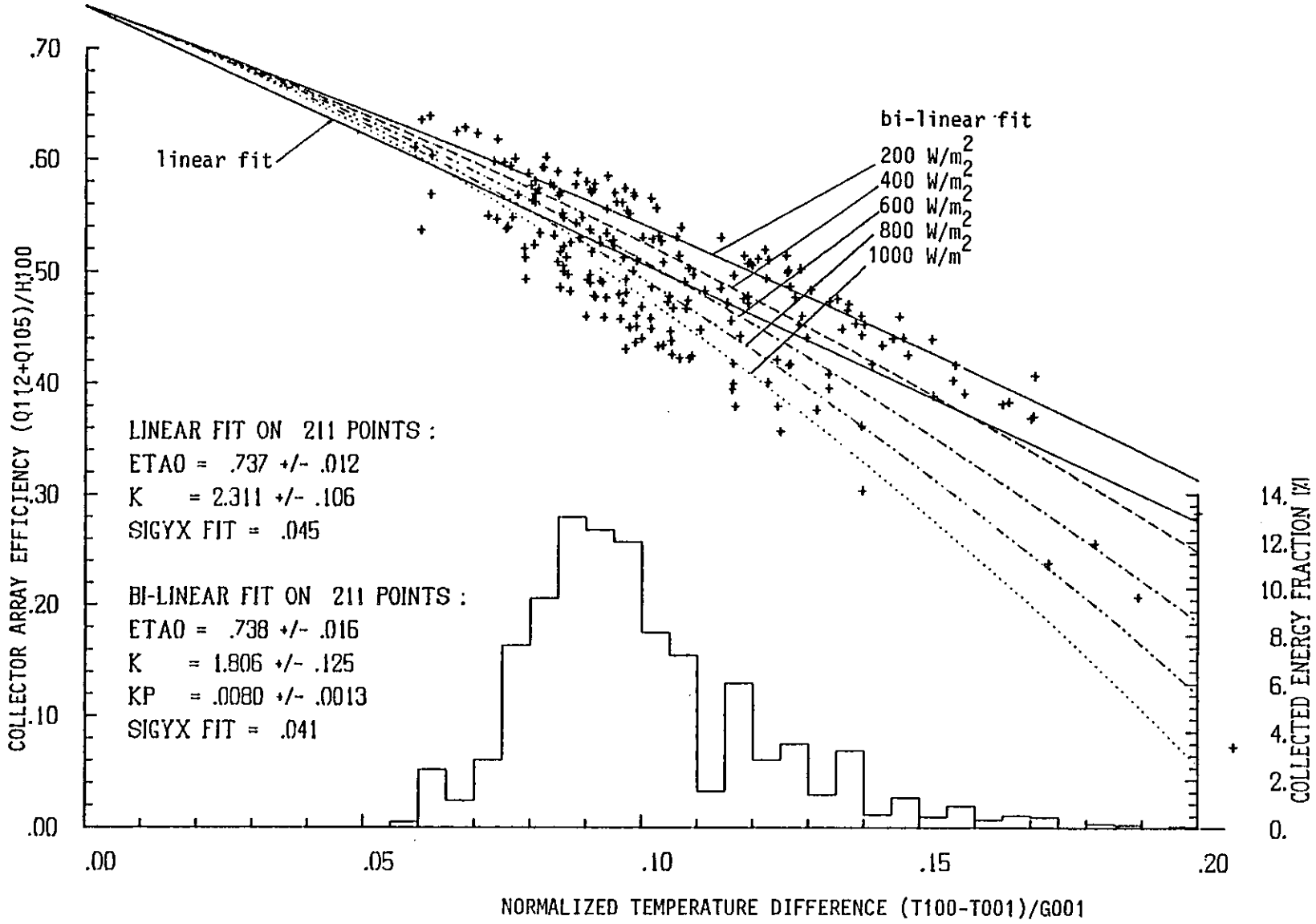

Figure 6.1.9-1 "CORTEC" ETC EFFICIENCY

SOLARIN SYSTEM AT HALLAU. 1/11/84 TO 31/10/85

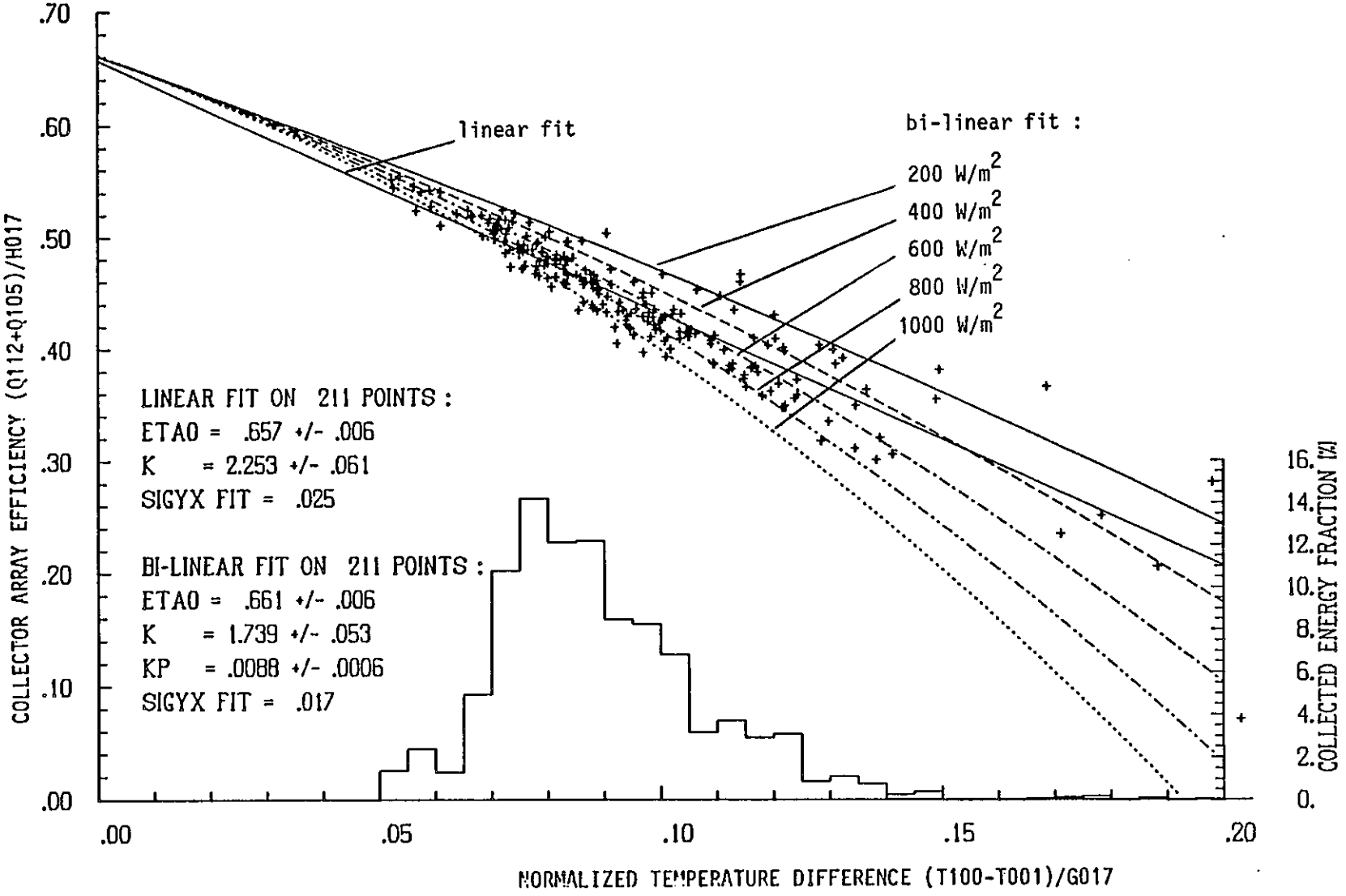

Figure 6.1.9-2 "CORTEC" ETC EFFICIENCY WITH ABSORBER SHADING CORRECTION
SOLARIN SYSTEM AT HALLAU. 1/11/84 TO 31/10/85

6.2.9 SOLARIN Project
Hallau, Switzerland

Figure 6.2.9-1 is a daily Input/Collector Output plot for the one year period under consideration.

Figure 6.2.9-2 gives the same plot, but when considering the effective solar energy H017 instead of H001.

Some daily data were rejected because of snow or regulation problems or bad diffuse radiation measurements.

Figure 6.2.9-3 and 6.2.9-4 are the corresponding plots with solar system energy Q102 as output. Additional capacity and heat losses in plumbing give lower but useful energy output.

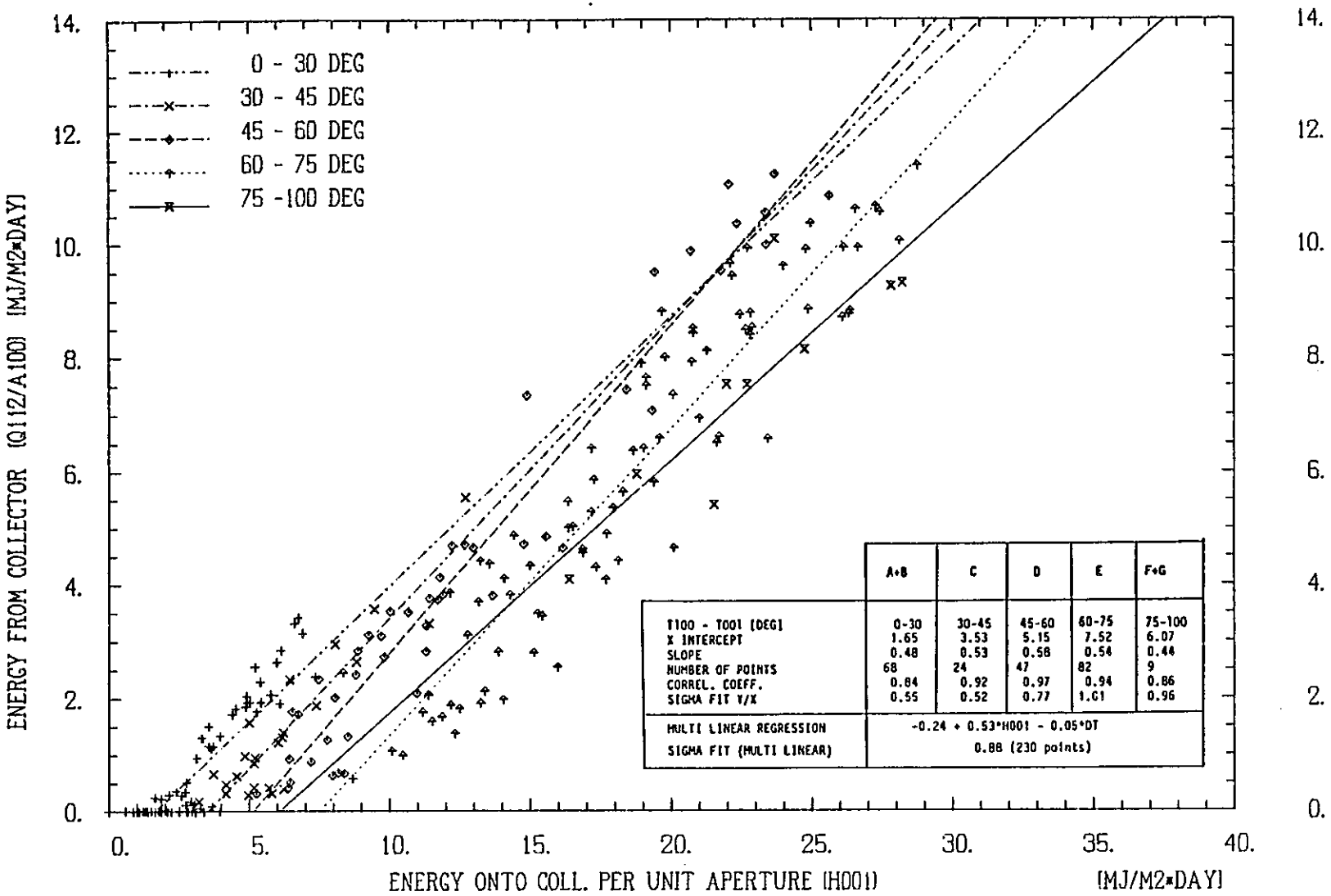

Figure 6.2.9-1 Q112 INPUT/OUTPUT DIAGRAM FOR "CORTEC" ETC AT HALLAU
VALUES FROM 1/11/84 TO 31/10/85

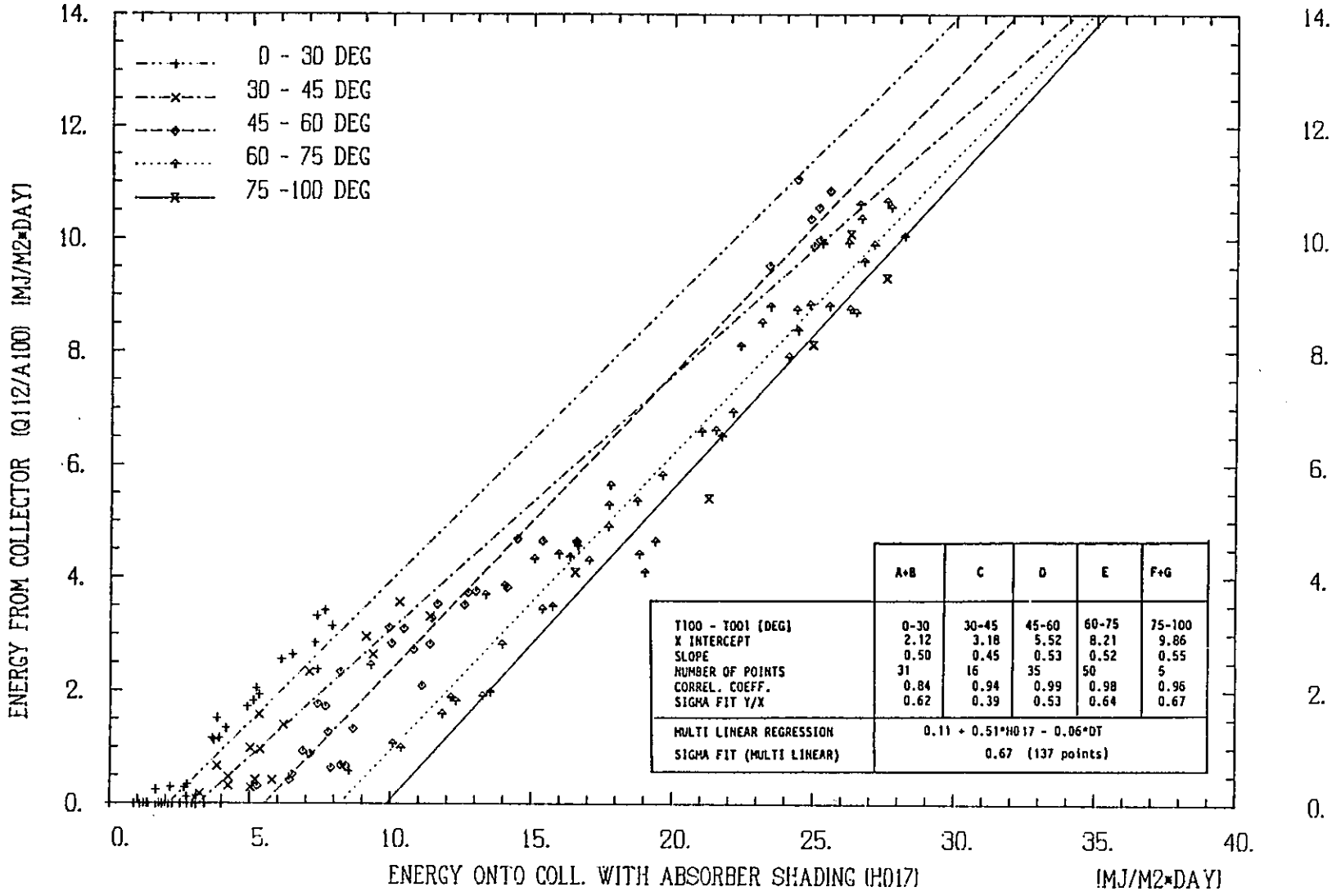

Figure 6.2.9-2 Q112 INPUT/OUTPUT DIAGAM FOR "CORTEC" ETC AT HALLAU WITH ABSORBER SHADING CORRECTION VALUES FROM 1/11/84 TO 31/10/85

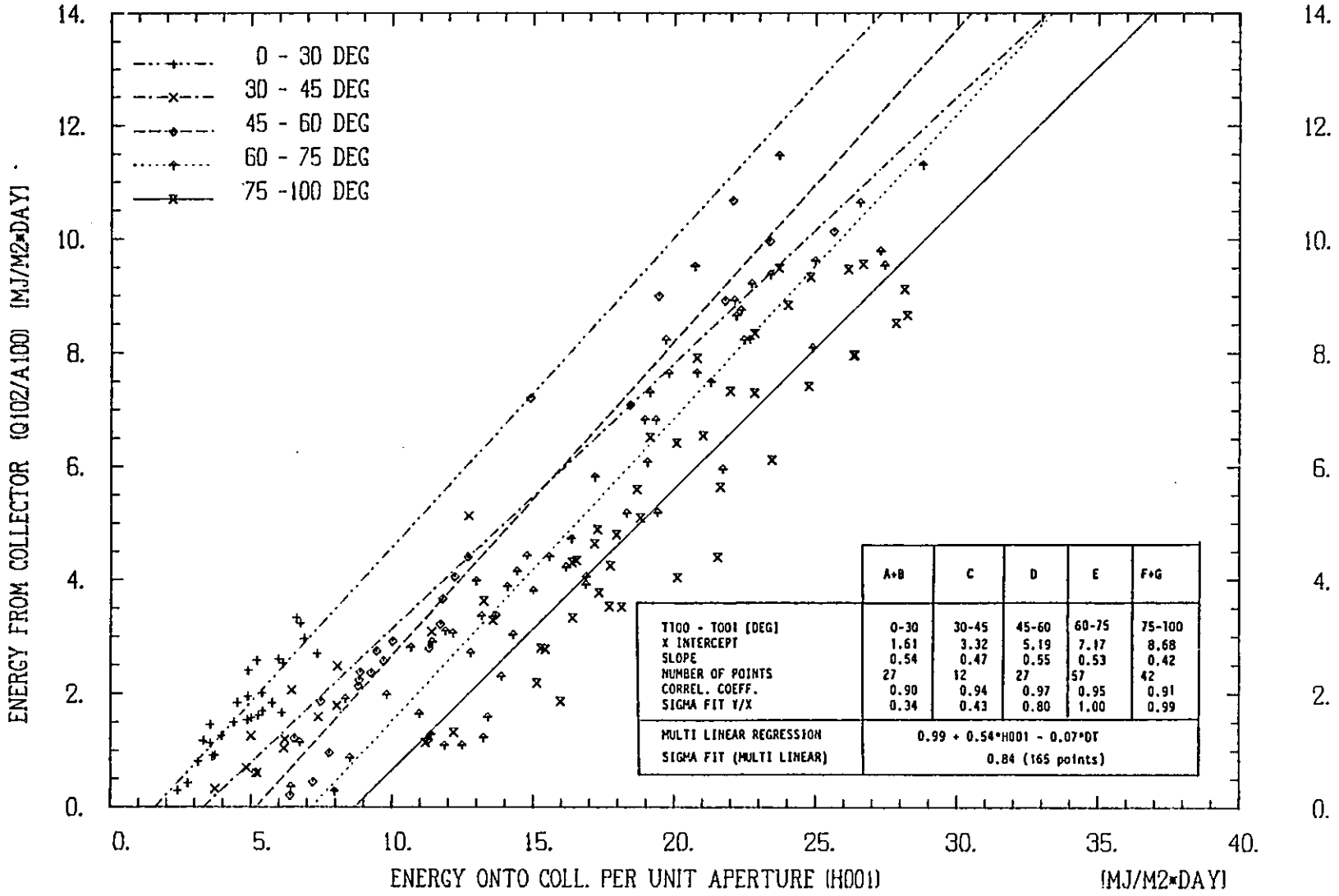

Figure 6.2.9-3 Q102 INPUT/OUTPUT DIAGRAM FOR "CORTEC" ETC AT HALLAU
VALUES FROM 1/11/84 TO 31/10/85

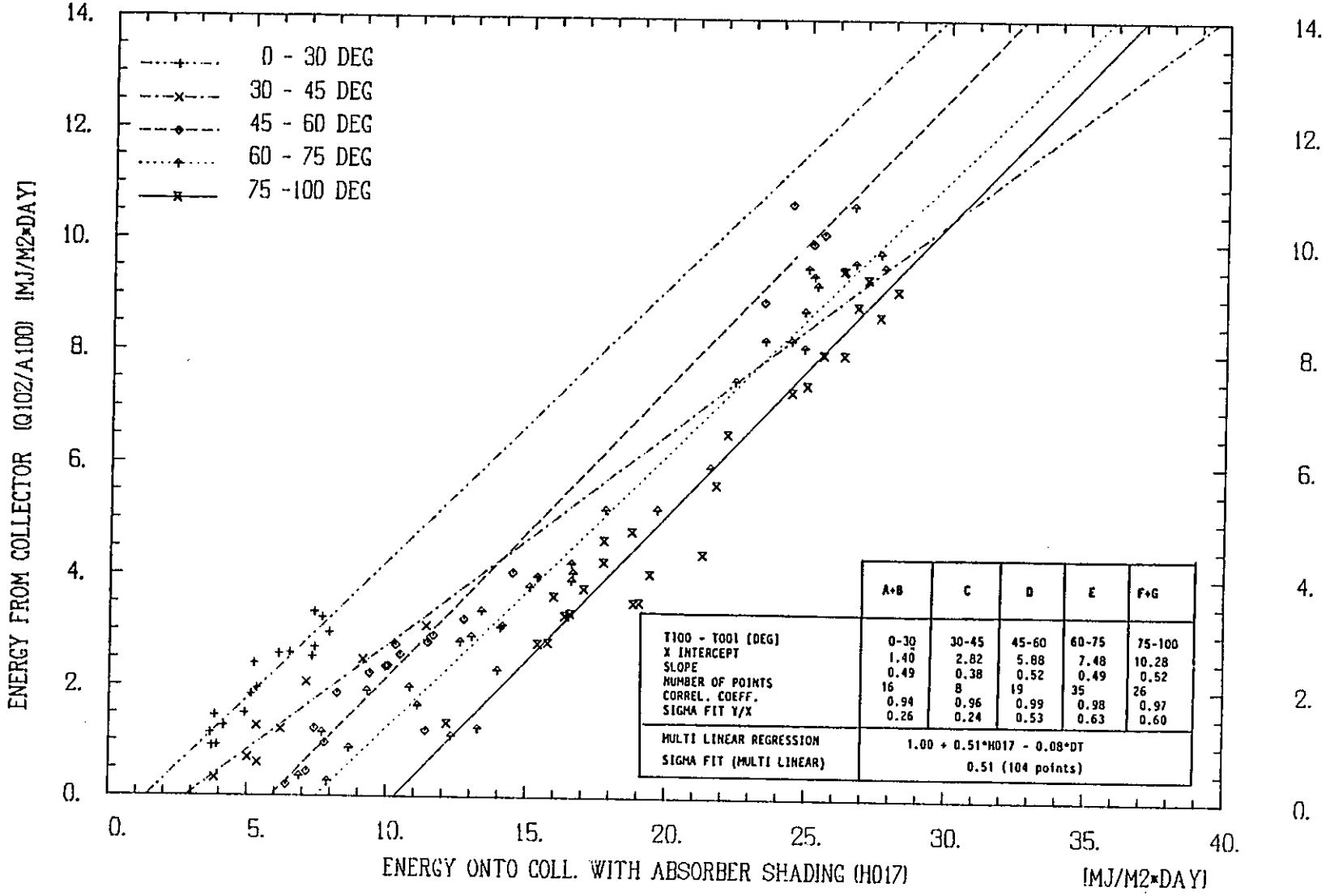

Figure 6.2.9-4 Q102 INPUT/OUTPUT DIAGRAM FOR "CORTEC" ETC AT HALLAU WITH ABSORBER SHADING CORRECTION

6.3.9 SOLARIN Project
Hallau, Switzerland

The total arrow diagramm is shown in fig. 6.3.9-1. Values are reported for 365 days. They are corrected on a monthly basis for failing daily datas (7%).

It can be seen that heat losses between the array and the rest of the system are reasonably low. But excess heat rejected amounts to roughly 10% of the delivered heat, it is partly due to a poor regulation.

For the rest of the system (including 2 storages) other losses amount to roughly 56000MJ what leads to a final system efficiency around 21%.

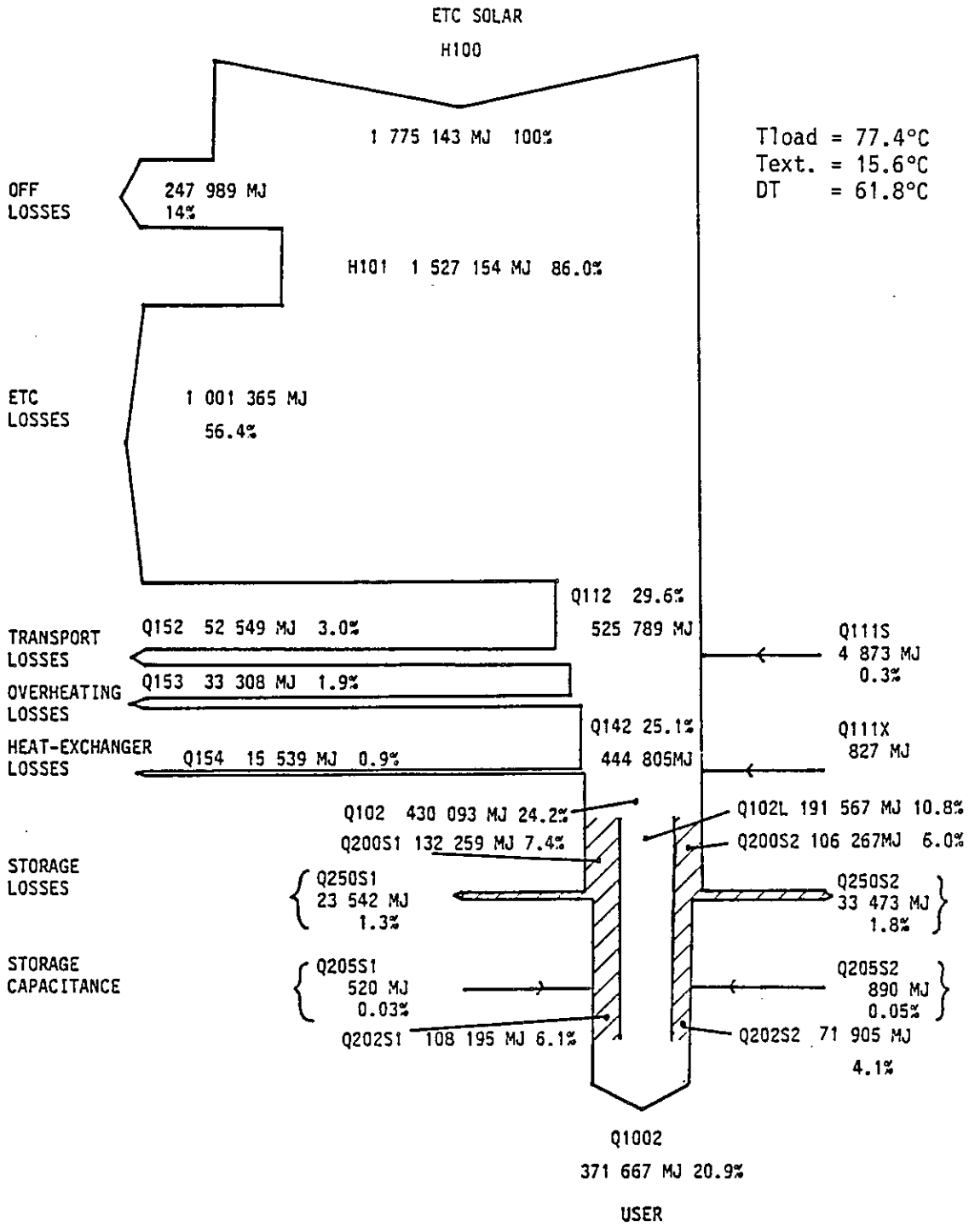

Figure 6.3.9-1 ENERGY FLOW ARROW DIAGRAM FOR CORTEC ETC AT HALLAU. FROM NOVEMBER 84 TO OCTOBER 85

6.4.9 SOLARIN Project
Hallau, Switzerland

Figure 6.4.9-1 gives bar chart for experiment CH2 - HTG-2.

Snow in January and part of February leads to very small figures. Heat losses between the collector array and the heat exchanger are mainly due to the rejection excess heat, what can be partly due to defects in the regulation. Winter regulation is correct, but summer regulation (May up to October) was not optimized : it appears clearly on Figure 6.4.9-1.

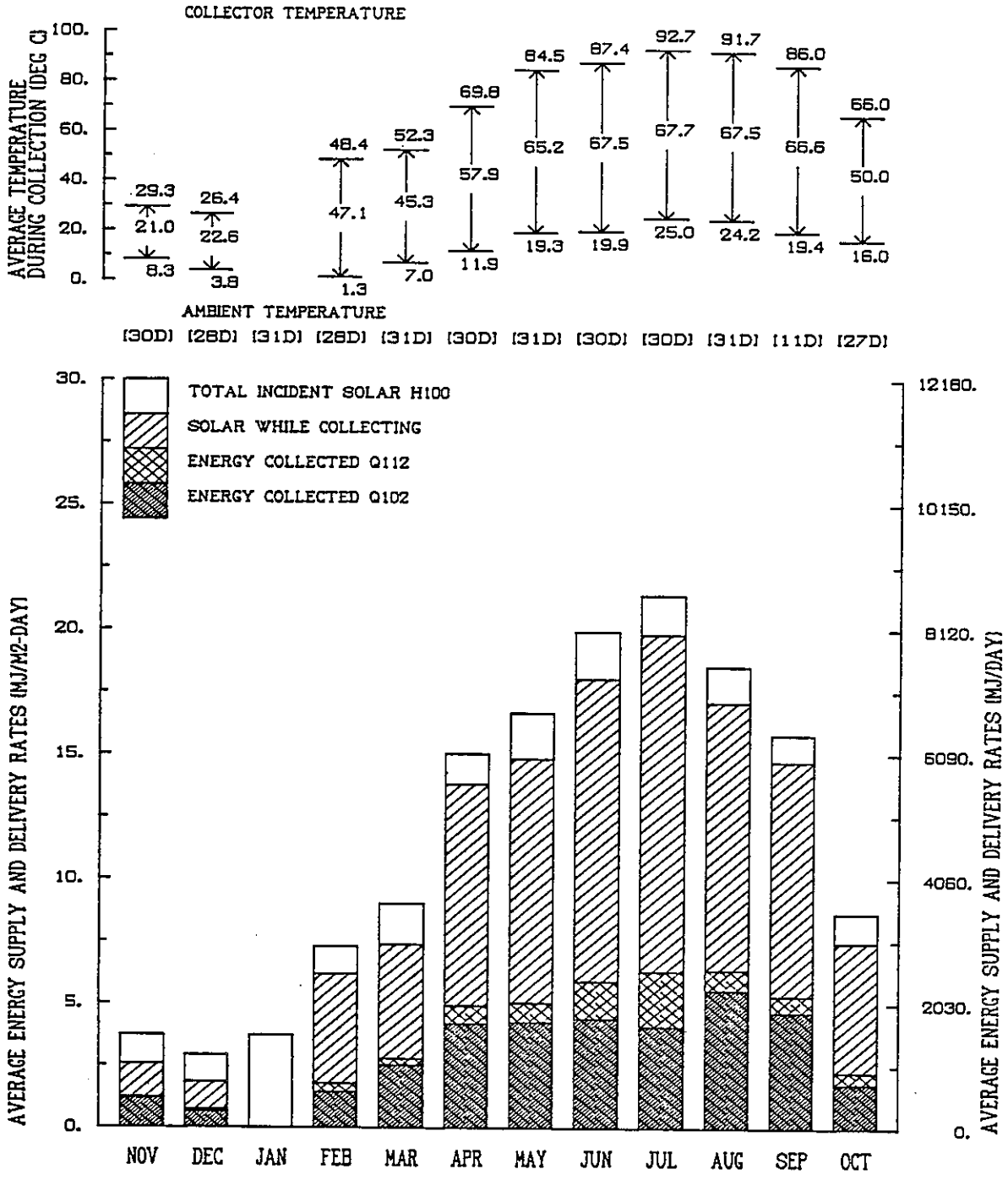

Figure 6.4.9-1 AVERAGE ENERGY SUPPLY RATES FOR CORTEC ETC AT HALLAU. FROM NOVEMBER 84 TO OCTOBER 85

6.5.9 SOLARIN Project
Hallau, Switzerland

The energy use bar chart is presented in figure 6.5.9-1. During winter month, when heating is needed, the total energy use is considered (heating + process). In this diagram, Q1002 is considered, i.e. it does not include storage heat losses and stored energy.

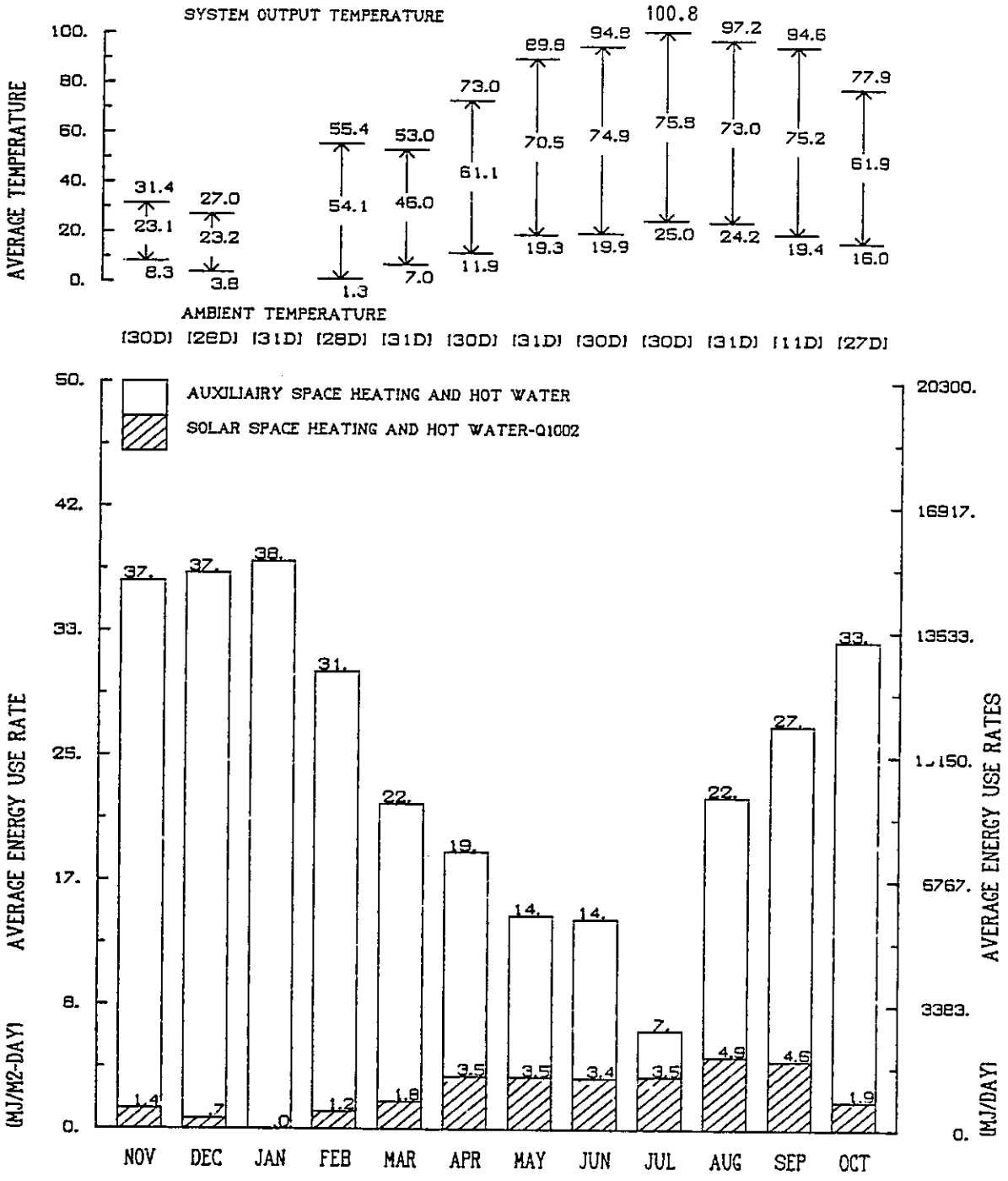

Figure 6.5.9-1 AVERAGE ENERGY USE RATES FOR CORTEC ETC AT HALLAU. FROM NOVEMBER 84 TO OCTOBER 85

6.6.9 SOLARIN Project
Hallau, Switzerland

System efficiency and solar fraction diagrams are shown in figure 6.6.9-1

Loading and unloading the storage correspond to a nearly constant system efficiency, except in January and February (snow) and in June and July (excess heat).

Spring efficiency is apparently reduced due to storage loading. Winter efficiency (November, December) is apparently increased due to storage unloading.

Solar fraction varies from 2% in December to 52% in July.

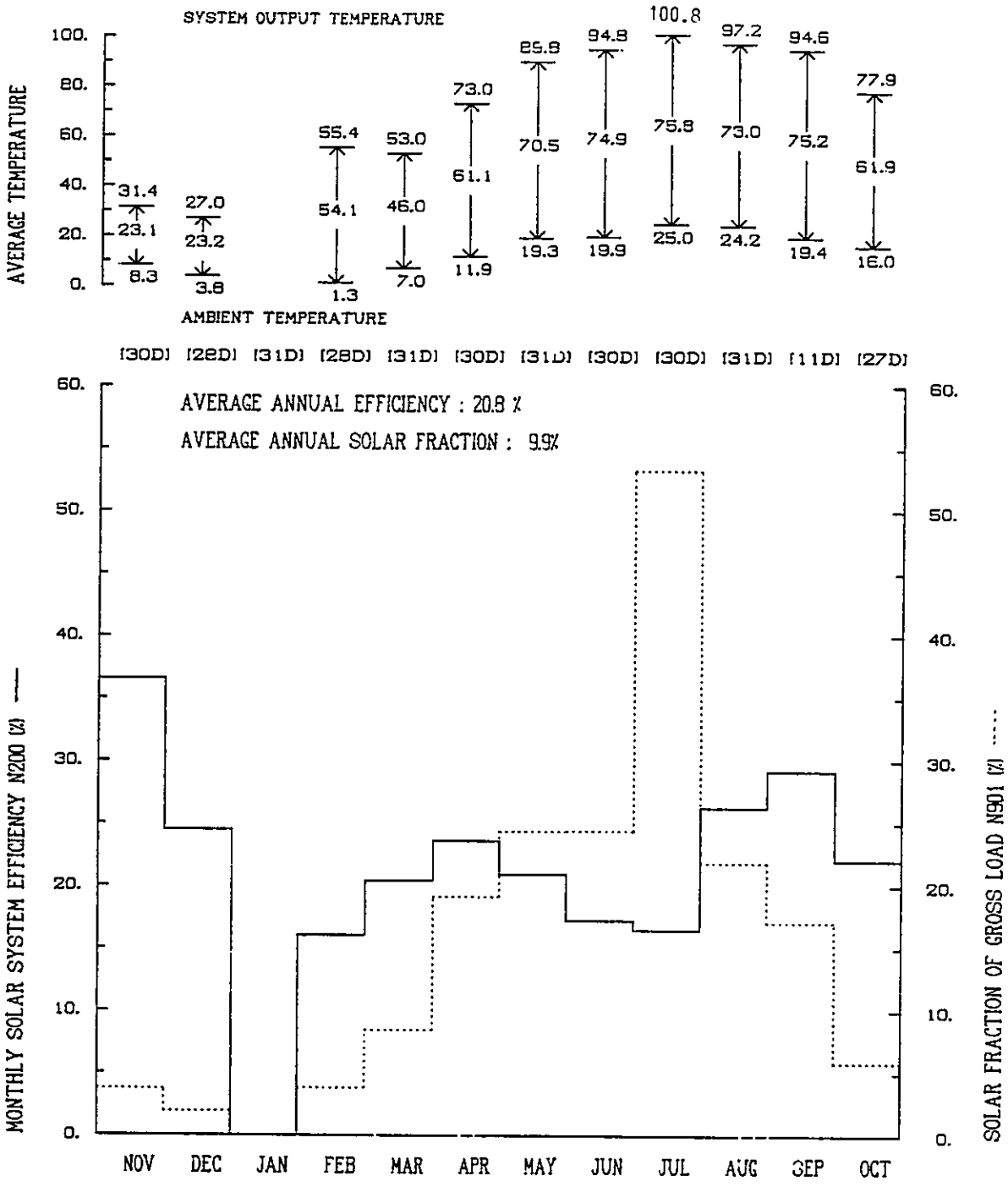

Figure 6.6.9-1 AVERAGE SYTEM EFFICIENCY AND SOLAR FRACTION AT HALLAU. FROM NOVEMBER 84 TO OCTOBER 85

7.1.9 SOLARIN Project
Hallau, Switzerland

Operation of the plan following the reporting format has shown good average efficiency of the evacuated collector (30%). Important losses are due to the excess heat during summer, when no heat is needed (4% of the total delivered heat), to the regulation problem (6% of the total delivered heat) and to the storage (15% of this heat). So total system efficiency is relatively low (21%).

Direct use and simple regulation are necessary to have high efficiency in a solar system.

Table 8-1. System Results Summary

SOLARIN Project
Hallau, Switzerland

	CH2 - HTG - 2
Net energy delivered $\frac{Q1002-Q111}{A100}$ (MJ/m² day)	2.51
System efficiency (%) (=Q1002/H100 in our case)	20.9
Collection subsystem COP (Q1002/E103)	76.3
System solar fraction (%) (Q1002/load in our case)	9.9
Average daily load per Aperture area (MJ/m²·day)	25.4
Average collector minus Average ambient temperature (°C)	61.8
Average daily insolation (MJ/m² · day)	13.3

SOLARCAD Project at Geneva, Switzerland
November 1984 to October 1985

O. Guisan
B. Lachal
A. Mermoud
O. Rudaz

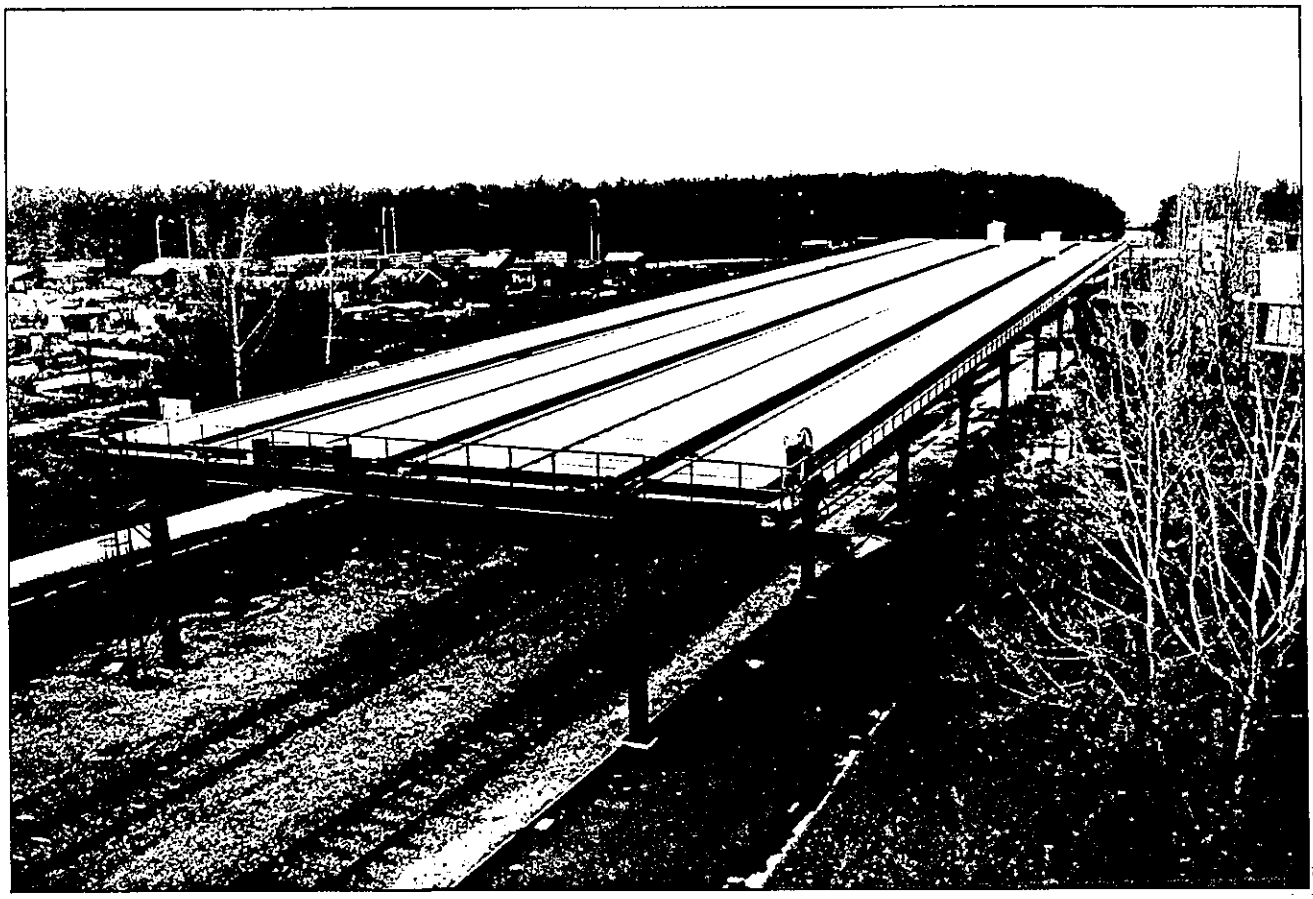

SOLARCAD 1000 District Heating Project, Geneva Switzerland.

Table 2.1. Installation description.

Solarcad 1000 District Heating Project
Geneva, Switzerland.

A solar ETC array of more than 1000 m² aperture area is connected directly to a district heating network without intermediate storage, since at any time the heat demand is much higher than the heat provided by solar. The district heating network supplies space heating and domestic hot water to surrounding buildings.

Table 2.2. Description of loads

Solarcad 1000 District Heating Project
Geneva, Switzerland.

Three different networks are connected to one central gaz furnace of 125 MW (450 GJh/h) capacity, and deliver heat to surrounding buildings for space heating and hot water purposes in combination, so that separate uses cannot be identified. Our solar plant is connected to the "return" branch of one particular network called "Avanchet", which is considered as the load and which is characterized by the following figures:

- power capacity of the "Avanchet" network: 190 GJ/h
- delivered power ranging from 3.5 to 90 GJ/h
- average daily load for the heating season (October-May): ≈ 650 GJ/day
- average daily load in summer (June-September)(DHW only): ≈ 230 GJ/day

Solar system has usually to operate above the "return" temperature of 80-90°C.

Table 2.3. Current activities

Solarcad 1000 District Heating Project
Geneva, Switzerland

A preliminary test installation of about 2x20 m² of different available ETC's (Sanyo STC - CU250L and Corning CORTEC with and without a selective coating on the back side of the absorbers, called "A and "B" types) was installed since 1981, and well measured in 1982-1984.

Taking advantage of previous experience, construction of the large facility (1026 m² aperture area), using improved Corning CORTEC "E" ETC's with tilted absorbers, was performed in 1984. Operation and measurements started in April 1985. After an operating breakdown of 6 months in winter 1985-1986, due to a maintenance problem, measurements will be prolonged up to the middle of 1987.

Summer data of 1985 are carefully analysed. Thermal and physical properties of the system (heat losses, heat capacities, pressure drop energies) are now well understood (estimations and measurements are in very good agreement). Detailed studies have still to be carried out about the Corning collectors, especially concerning tilted absorbers effects, longitudinal IAM effects and absorbers emissivity. Stagnation temperatures have been measured for a large sample of tubes.

A precise understanding of these physical parameters should lead to establish and validate very accurate models, either in a detailed or in a simplified day-by-day formulation.

Table 3.1. Climate at the Task VI locations

Geneva, Switzerland

		Comments
latitude	46°12'N	
longitude	6° 9'E	
elevation (meters)	400	
heating degree-days (18.3°C)	2740	
heating season	Oct.-May	
average wet bulb temperature for cooling season	NA	NA = not applicable
cooling season	NA	
relative humidity (%) (yearly average)	76	(ranges from 68 (summer) to 84 (winter)
typical daily insolation		
January (MJ/m^2) on horizontal	3.5	
July (MJ/m^2) on horizontal	19.5	
percent diffuse		
January (%)	68	
July (%)	40	
average daily temperature		
January (°C)	1.0	
July (°C)	19.0	
average maximum daily temperature		
January (°C)	10	) maximum or minimum in
July (°C)	24	) the month of the daily
		) average temperature
average minimum daily temperature		) taken from a reference) year
January (°C)	-2	
July (°C)	13	
seasonal climate description	Mesothermal forest; moist; rainfall all year	

Table 4.1. Evacuated Tube Collector Reference

Solarcad 1000 District Heating Project
Geneva, Switzerland

- Corning Cortec 'E' (made in France)

Note for interim report

Corning Cortec collectors used in Germany and in Switzerland are not the same. They should appear separately in Tables 4-1 and 4-2.

Collectors used in Geneva and Hallau could be referred to as:

Solarcad Test System	:	Corning Cortec 'A' (made in France)
Solarcad Test System	:	Corning Cortec 'B' (made in France)
Solarin	:	Corning Cortec 'D' (made in France)
Solarcad 1000	:	Corning Cortec 'E' (made in France)

Collectors used in Freiburg could be referred to as:
Corning Cortec (made in USA)

All these collectors look similar (sizes, connections, etc...) but performances are different.

Table 4.2. Specifications for Evacuated Tube Collectors used in Task VI Installations.

Solarcad 1000 District Heating Project, Geneva, Switzerland

Manufacturer and type:	Corning CORTEC "E" (made in France)

Physical Properties:

Number of tubes per module	6
Pitch	111 mm
Absorber area per module	1.12 m²
Aperture area per module (1)	1.45 m²
Gross area per module	1.86 m²
Absorber tilt angle on collector plane	27.5 °
Absorber surface material	black chrome, one side
Collector / Heat pipe fluid	any
Fluid volume per m² of aperture area	0.67 liter/m²
Fluid capacitance per m² of aperture area (if water)	2.8 kJ/K ·m²
Collector empty thermal capacitance per m² of ap. area	1.5 kJ/K ·m²
External glass equiv. capacitance per m² of ap. area	1.1 kJ/K ·m²
Total collector capacitance per m² of aperture area	5.4 kJ/K ·m²
Maximum operating pressure	6 bars
Typical temperature difference between absorber and fluid	≈ 1.6 °C for 500 W absorbed per m² absorber
Glass material	Pyrex
Absorber tube material	Copper
Glass outside diameter / thickness	100 / 2.7 mm
Reflector provided by manufacturer	none

Performances

$F'\tau\alpha$	0.64
$F'U_L$	1.3 to 2.4 W/m²K (T = 0 to 200 °C)
Source of information	EPFL test data for one CORTEC "E" module(2)
Incidence angle modifier	slight "transversal incidence angle" effect(3)
Characterization of selective surface	ε = .103 ± .013 (4,3) (at 250 °C)

(1) According to the revised IEA Task VI definition, i.e with no cos θ term for the tilted absorber.
(2) No background, no tilted absorber.
(3) See IEA-VI report: Evacuated Collector System Characterization
(4) According to stagnation temperature measurements on a large sample of tubes.

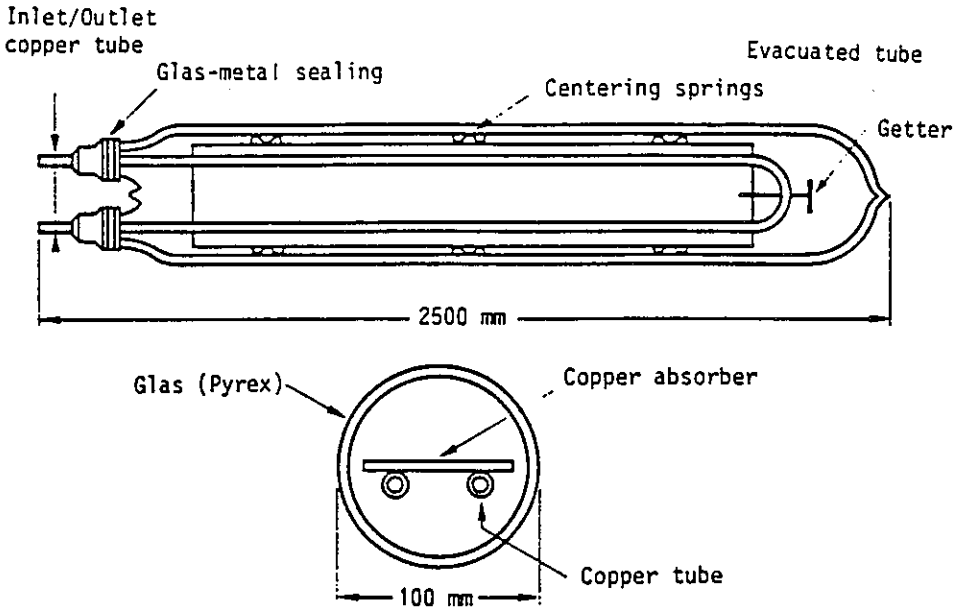

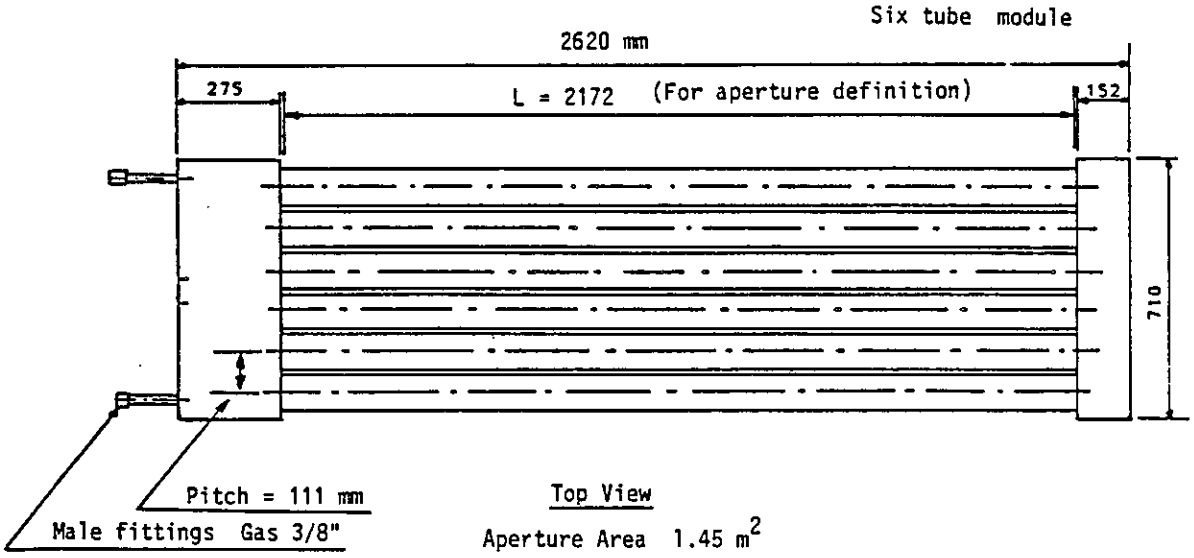

Mechanical features of the Corning "CORTEC" collector

Table 4.3. Characteristics of the Evacuated Collector Arrays in Task VI

Installations

Solarcad 1000 District Heating Project, Geneva, Switzerland

Evacuated Collector Type	Corning CORTEC "E"
Number of modules	708
Absorber Area	793 m^2
Aperture Area (1)	1027 m^2
Array heat capacitance per m^2 aperture area (calculated from components)	10.6 kJ/K·m^2 ap
Fluid volume per m^2 of aperture area	1.8 liter/m^2 ap
Working fluid	32 % V/V Ethylenglycol in water + corrosion inhibitors
Fluid flow rate per m^2 of aperture area	
One pump running (below 500 W/m^2 radiation)	21.4 l/h.m^2 ap
Two pumps running (above 500 W/m^2 radiation)	29.2 l/h.m^2 ap
Tube material (piping)	iron
Modules connexion	3 branches in parallel per branch: 118 pairs in parallel each pair being 2 modules in series
Collector plane tilt angle	2.5 ° on horizontal plane
Absorber plane tilt angle	27.5 ° on collector plane
Azimuth faced by array	4 ° West
Tube orientation	E - W
Background (behind collectors)	None (Ground 10 m below)
Shadow effects from surrounding environment	Negligible

(1) According to the revised IEA Task VI definition, i.e. with no cos Θ term for the tilted absorber.

Reliability, maintainability aspects

Solarcad 1000 District Heating Project
Geneva, Switzerland

Starting problems:

- 10 tubes broken during transport

- a large number of tubes (1% to 2%) suffered of vacuum loss and were replaced (free by manufacturer) just before starting up. Mainly due to too short order delays, resulting in a test period at the factory shorter than usual.

Running problems:

- System works very well from April to August 1986.

- End August, system is stopped during one week due to planned maintenance operation on the load (DHS utility). Antifreeze mixture is removed from the collectors, whose absorbers go up to the stagnation temperature level (≈ 270° C by 1000 W/m² radiation).

- When starting again, about 28% of the ETC's are partially or totally choked by corrosion residues. This has dramatic consequences since without heat removal, the ETC antifreeze contents first vaporizes, and then rises over 200° C, the limit operating temperature of the antifreeze. Repeated occurences of these extreme conditions cause a quick destruction of the antifreeze, which becomes trouble and corrosive in a few days.

- At beginning of Oktober, the collector field is emptied for precaution, and carefully rinced with water until problems are well understood, and a perfect cleaning is achieved. It is expected to start again in April 1986.

Table 4.5. Storage description

Solarcad 1000 District Heating Project
Geneva, Switzerland

No storage is used. Heat is transferred through exchangers directly to the district heating system.

Table 4.6. Summary description of components and subsystems

Solarcad 1000 District Heating Project
Geneva, Switzerland.

Collection

The collectors are mounted on a metallic frame, built 8 to 10 meters above a railway track. No background is used behind the tubes. The collector plane is tilted by 2.5° on horizontal, and absorbers are tilted by ≈ 27.5° with respect to the collector plane. Shadowing effects of one absorber to the next one may be important in winter time (up to 40%).

Heating

The load (district heating system) cannot be separated in heating and DHW components.

Controls

The solar radiation level controls the collector circulation pumps. Heat is transferred to the load (secundary pump) when solar loop temperature exceeds DHS temperature. A 3-way valve in the solar loop prevents freezing the exchanger water-filled secundary circuit in the cold morning starting-up. An overheating safety exchanger connected to the cold water network will be soon installed. Preset times and hysteresis avoid fast system oscillations. Altogether 6 sensors act on 6 pumps and 2 valves through a microprocessed control system.

Table 5.1. Experiment Descriptors, Modes, Components and Operating Dates

Solarcad 1000 District Heating Project
Geneva, Switzerland.

Experiment	CH - HTG - 3
Mode	District Space and DHW heating
Dates	10 May 1985 - 25 Aug. 1985 (1)
Collector	Corning CORTEC "E"
Chiller	NA
Auxiliary	Gas-fired burner
Main tank	NA
Controls	Microprocessorized with radiation sensor

(1) For clean data. In April 85 calibrations were performed, and in Septembre 85 the ETC array was partially obstructed.

Table 5.2. Climate Data for the Experimental Period

Solarcad 1000 District Heating Project
Geneva, Switzerland.

Experiment	CH - HTG - 3
Dates	10 May 1985 - 25 Aug. 1985
Degree-Days (°C-days) for "measured" days	—
Normalized monthly to all days	—
Average daily Insolation (MJ/m^2-day)	21.1
Average daily Ambiant Temperature (°C)	19.7
Average Daily Temperature (°C)	
max	27.7
min	7.3

Table 5.3. Actual average daily loads for the test period

Solarcad 1000 District Heating Project
Geneva, Switzerland(1)

Actual Average Daily Heating load (MJ/day)	
July	$225 \cdot 10^3$
January	$930 \cdot 10^3$
Actual Average Daily Cooling load	NA
Actual Average Daily Domestic Hot Water Load	NA(2)
Total Actual Average Daily loads (MJ/day)	1/5/85 - 31/8//85 $517 \cdot 10^3$

(1) The figures given here correspond only to the involved district heating network ("Avanchets") which consumes roughly 45% of the total district heating system.

(2) Use in an unseparable mixed way with heating load.

CHAPTER 5

Solarcad 1000 District Heating Project
Geneva, Switzerland

Objectives

The main objective of the project is to evaluate performance of a large solar plant for high temperature purposes in the swiss climate. Particular features of this project, as compared to other ones in Task VI, are:

- heat production for a large district heating system (DHS)
- no problems of storage: the DHS is always able to absorb produced energy
- high and stable temperature range: 80 to 100° C during the whole year
- use of tilted absorbers with respect to the collector plane. Such a geometry, which has a large effect on performances, is studied in only one other Task VI experiment (i.e. SOLARIN, second swiss project).

The system diagram is shown separately (fig.). The collector loop is connected through an heat exchanger to the "return" branch of the DHS network. Special care has been taken to minimize heat capacity of the solar loop and transport plumbing, as well as thermal losses.

Experiment CH-HTG-3

Evaluate performances of the whole solar system. Identify all collector and system losses (thermal losses, capacity effects, mechanical energy contribution of the pumps). Understand physical behaviour of the system to establish and validate simulations and design procedures.

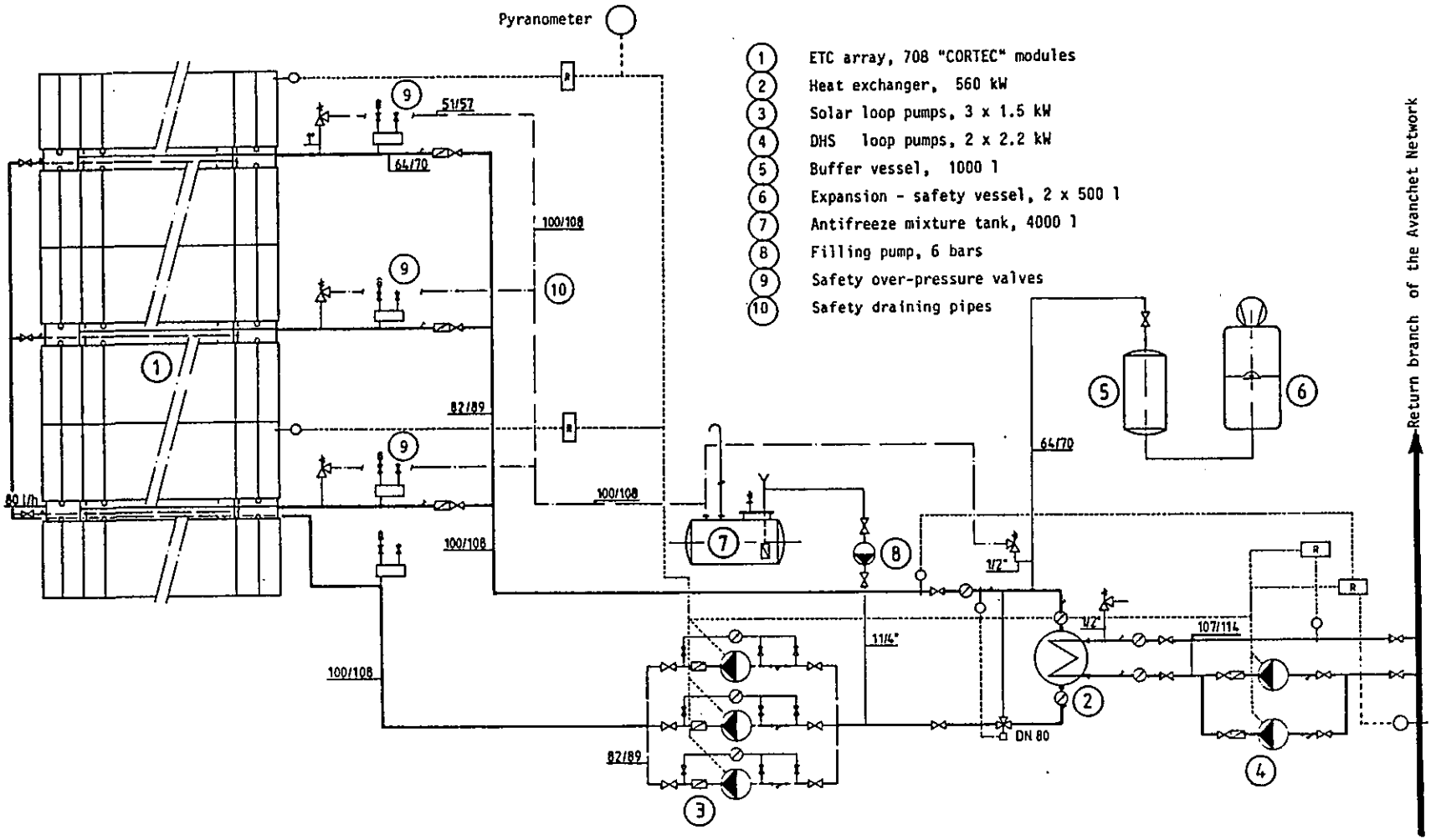

Solar System Schematics. SOLARCAD 1000 District Heating Project - Geneva, Switzerland.

CHAPTER 6 - Results

6.1 Efficiency Plots

Solarcad 1000 District Heating Project
Geneva, Switzerland

The usual way of reporting hourly data is derived from the following energy balance, where in our case (tilted absorber by respect to the collector plane) the input energy term involves the N127 tilt angle function (we neglect IAM(β) effects, which are not significant in the middle of the day):

$$\frac{Q112 + Q105F}{A100} = \underbrace{\tau\alpha \left(\frac{A_{abs}}{A_{ap}}\right)}_{\eta_o} \cdot N127 \cdot H001 - U_L \cdot (T100-T001)\ \Delta t$$

where: G001/H001 = global solar radiation/energy in collector plane
G016/H016 = direct solar radiation/energy in absorber plane
G013/H013 = diffuse solar radiation/energy on absorbers, including measured shading effects.
N109b = mutual absorber shading for CORTEC ETC estimated for beam component.
G017 = N109d · G016 + G013 = effective solar radiation on absorbers including shading effects.
N127 = G017/G001 = tilt angle factor.

Dividing the former expression by H001 leads to:

$$\frac{Q112 + Q105F}{H100} = N100 = \eta_o \cdot N127 - U_L \cdot \left(\frac{T100-T001}{G001}\right)$$

Therefore, a linear fit through these data will give an optical term modified by the N127 factor, which is depending on sun angles. Such a fit is obviously without great interest for the collector array characterization. The right way to get both η_o and U_L values from this equation would be to perform a bilinear fit in the N127 and $\Delta T/G001$ variables.

But a simpler way of analyzing data is to divide the last equation by the N127 factor:

$$\frac{Q112 + Q105F}{H117} = \eta_o - U_L \cdot \left(\frac{T100-T001}{G017}\right)$$

In this case the fitted parameters η_o and U_L should be identical to those of an equivalent ETC with no tilted absorber, regardless of its orientation or sun position (and neglecting incidence angle modifier effects).

It should be noticed that, due to our limited range in $\Delta T/G017$, only the set of parameters η_o and U_L is relevant, not individual values.

Efficiency plots are corrected for capacitance effects Q105F (the array thermal capacitance results from a computation, in very good agreement with special measurements achieved by night).

The dotted curves correspond to efficiency measurements achieved on one CORTEC "E" module (no tilted absorber) with a specialized testing facility (M. Van Kuijk, Ecole Polytechnique, Lausanne, Switzerland). They clearly show the dependence on both the temperature difference and the insolation, given by a heat loss factor of the form

$$U_L = k_1 + k_2 \cdot \Delta T$$

in the above expressions.

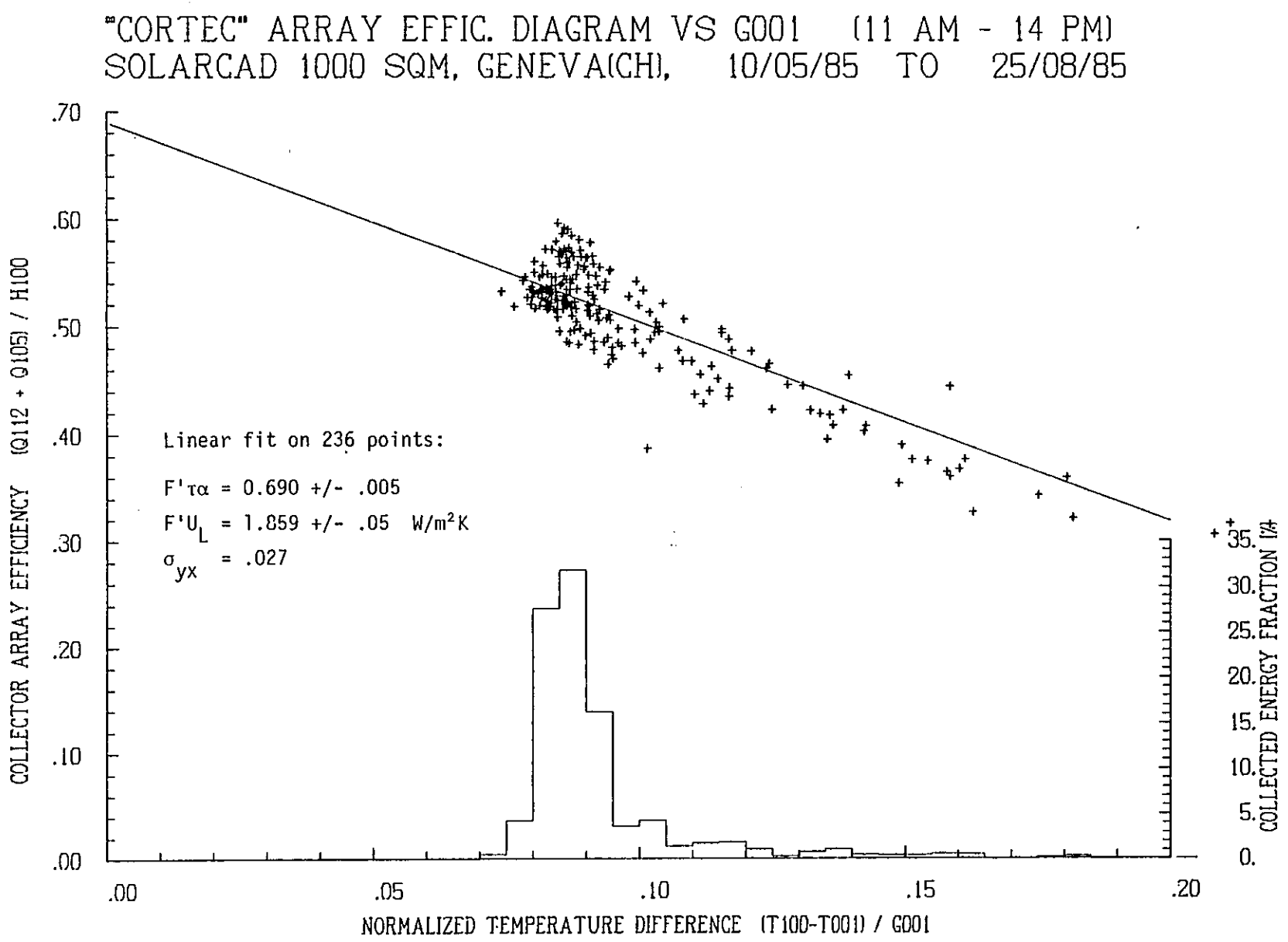
"CORTEC" ARRAY EFFIC. DIAGRAM VS G001 (11 AM - 14 PM)
SOLARCAD 1000 SQM, GENEVA(CH), 10/05/85 TO 25/08/85
COLLECTOR ARRAY EFFICIENCY (Q112 + Q105) / H100
.70
.60
.50
.40
.30
.20
.10
.00
Linear fit on 236 points:
F'τα = 0.690 +/- .005
F'U_L = 1.859 +/- .05 W/m²K
σ_yx = .027
COLLECTED ENERGY FRACTION (%)
35.
30.
25.
20.
15.
10.
5.
0.
.00
.05
.10
.15
.20
NORMALIZED TEMPERATURE DIFFERENCE (T100-T001) / G001

"CORTEC" ARRAY EFFIC. DIAGRAM VS G017 (11 AM - 14 PM)
SOLARCAD 1000 SQM, GENEVA(CH), 10/05/85 TO 25/08/85

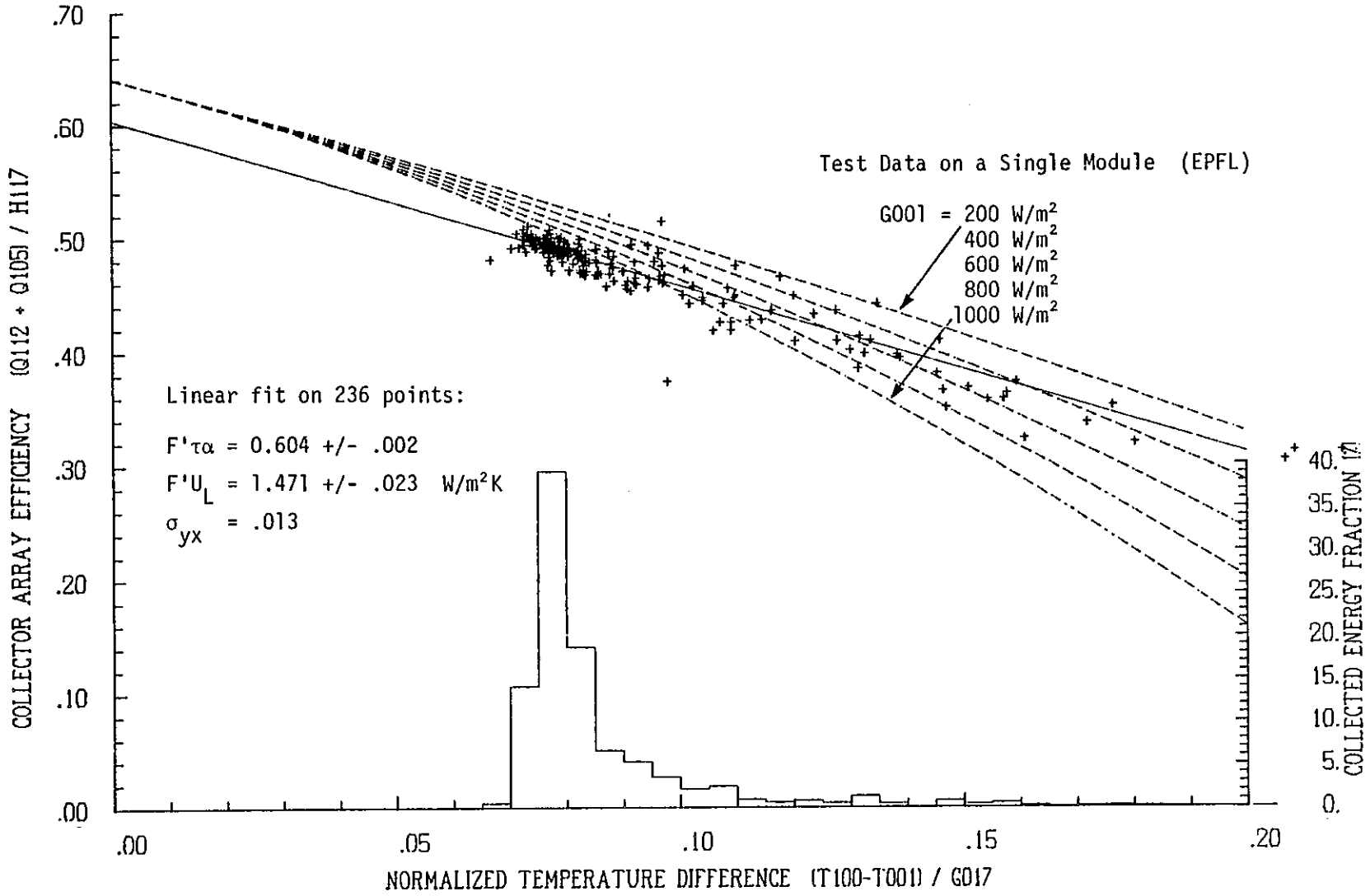

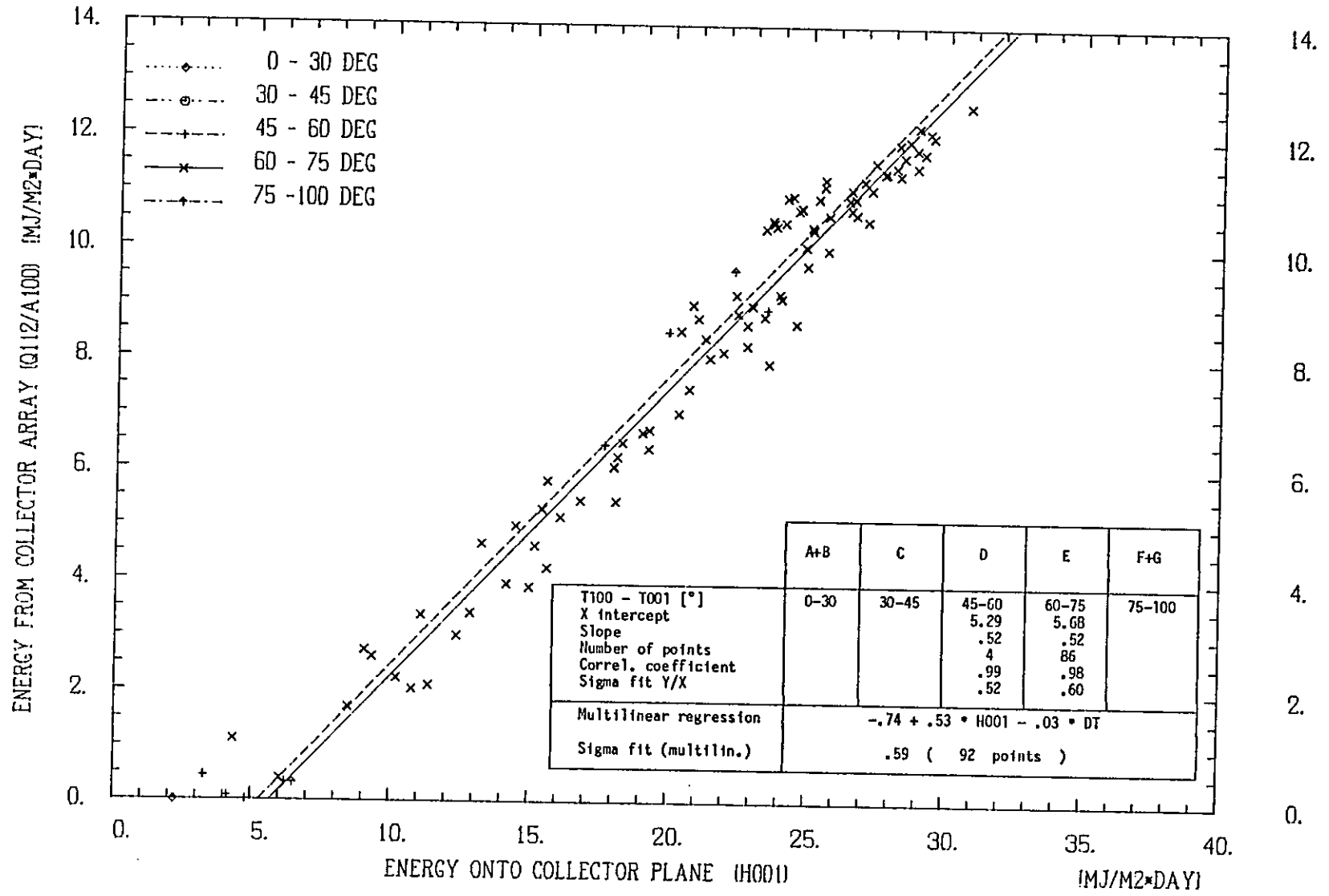

	A+B	C	D	E	F+G
T100 - T001 [°]	0-30	30-45	45-60	60-75	75-100
X intercept			5.29	5.68	
Slope			.52	.52	
Number of points			4	86	
Correl. coefficient			.99	.98	
Sigma fit Y/X			.52	.60	
Multilinear regression	-.74 + .53 * H001 - .03 * DT				
Sigma fit (multilin.)	.59 (92 points)				

Q112 Daily Input/Output diagram for "CORTEC" array vs H001.
Values from 10/05/85 to 25/08/85. SOLARCAD 1000, Geneva, Switzerland.

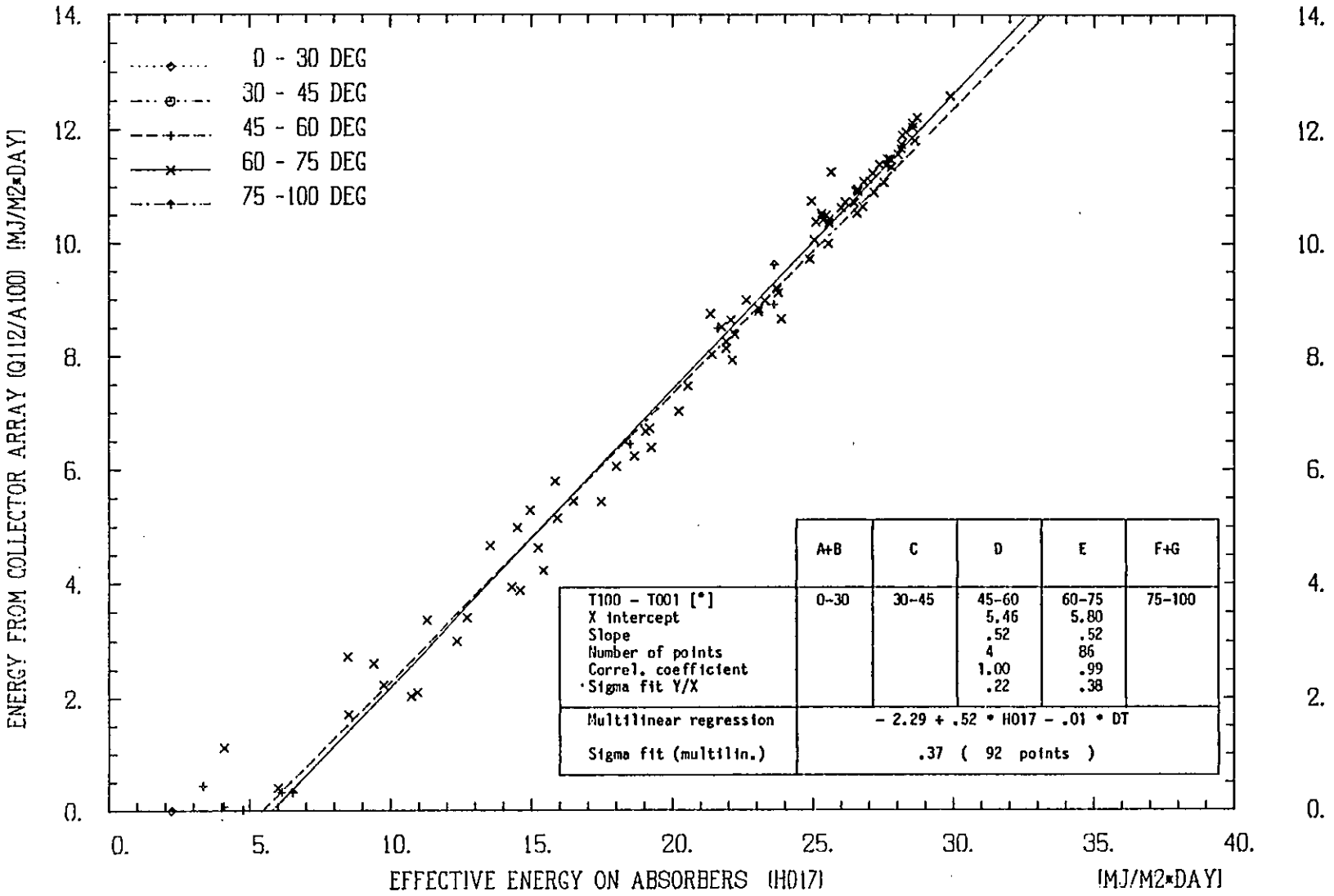

	A+B	C	D	E	F+G
T100 - T001 [°]	0-30	30-45	45-60	60-75	75-100
X intercept			5.46	5.80	
Slope			.52	.52	
Number of points			4	86	
Correl. coefficient			1.00	.99	
Sigma fit Y/X			.22	.38	
Multilinear regression	- 2.29 + .52 * H017 - .01 * DT				
Sigma fit (multilin.)	.37 (92 points)				

Q112 Daily Input/Output diagram for "CORTEC" array vs "Global Effective" H017.
Values from 10/05/85 to 25/08/85. SOLARCAD 1000, Geneva, Switzerland.

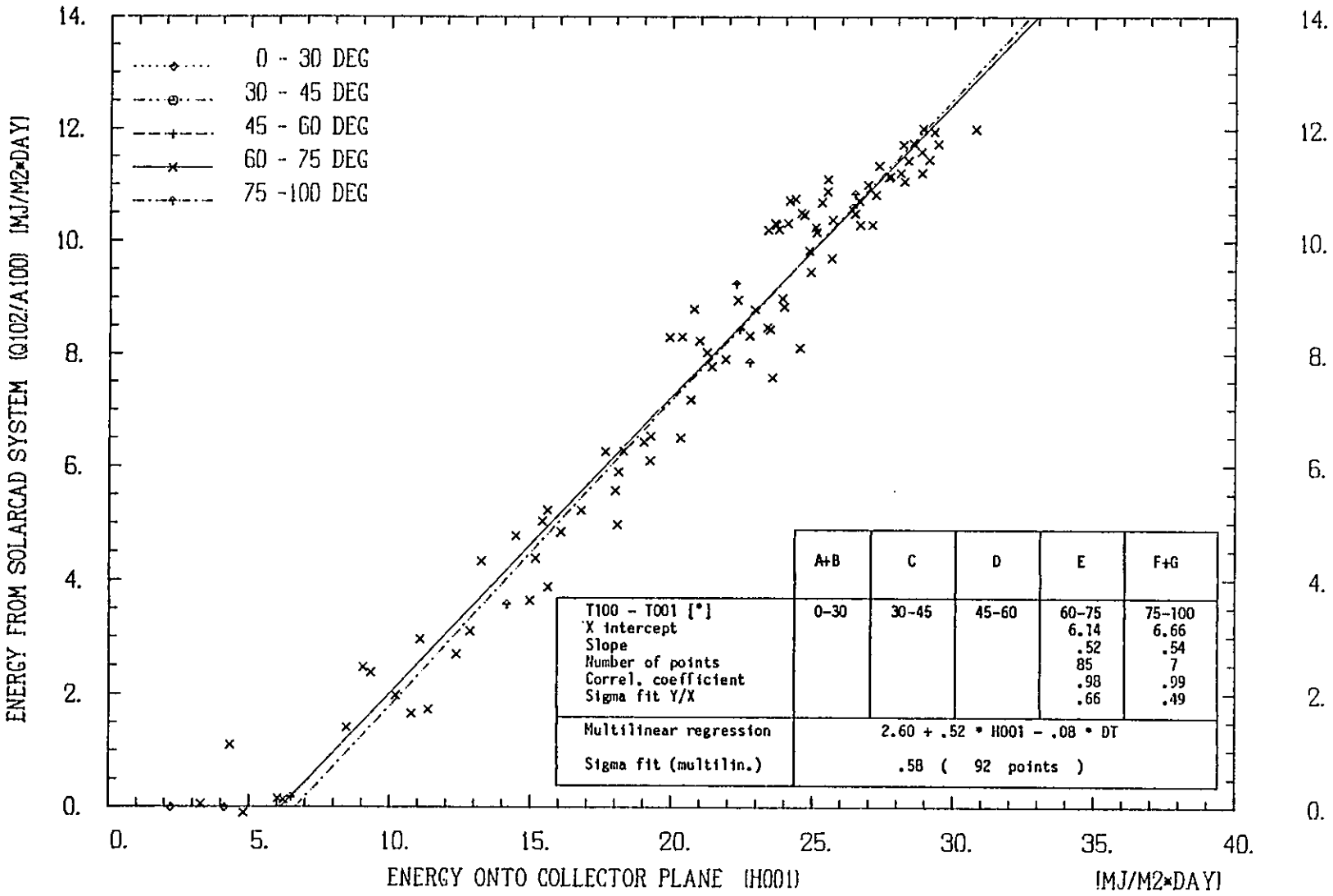

T100 - T001 [°]	A+B	C	D	E	F+G
	0-30	30-45	45-60	60-75	75-100
X intercept				6.14	6.66
Slope				.52	.54
Number of points				85	7
Correl. coefficient				.98	.99
Sigma fit Y/X				.66	.49
Multilinear regression	2.60 + .52 * H001 - .08 * DT				
Sigma fit (multilin.)	.58 (92 points)				

Q102 Daily Input/Output diagram for "CORTEC" system vs H001.
Values from 10/05/85 to 25/08/85. SOLARCAD 1000, Geneva, Switzerland.

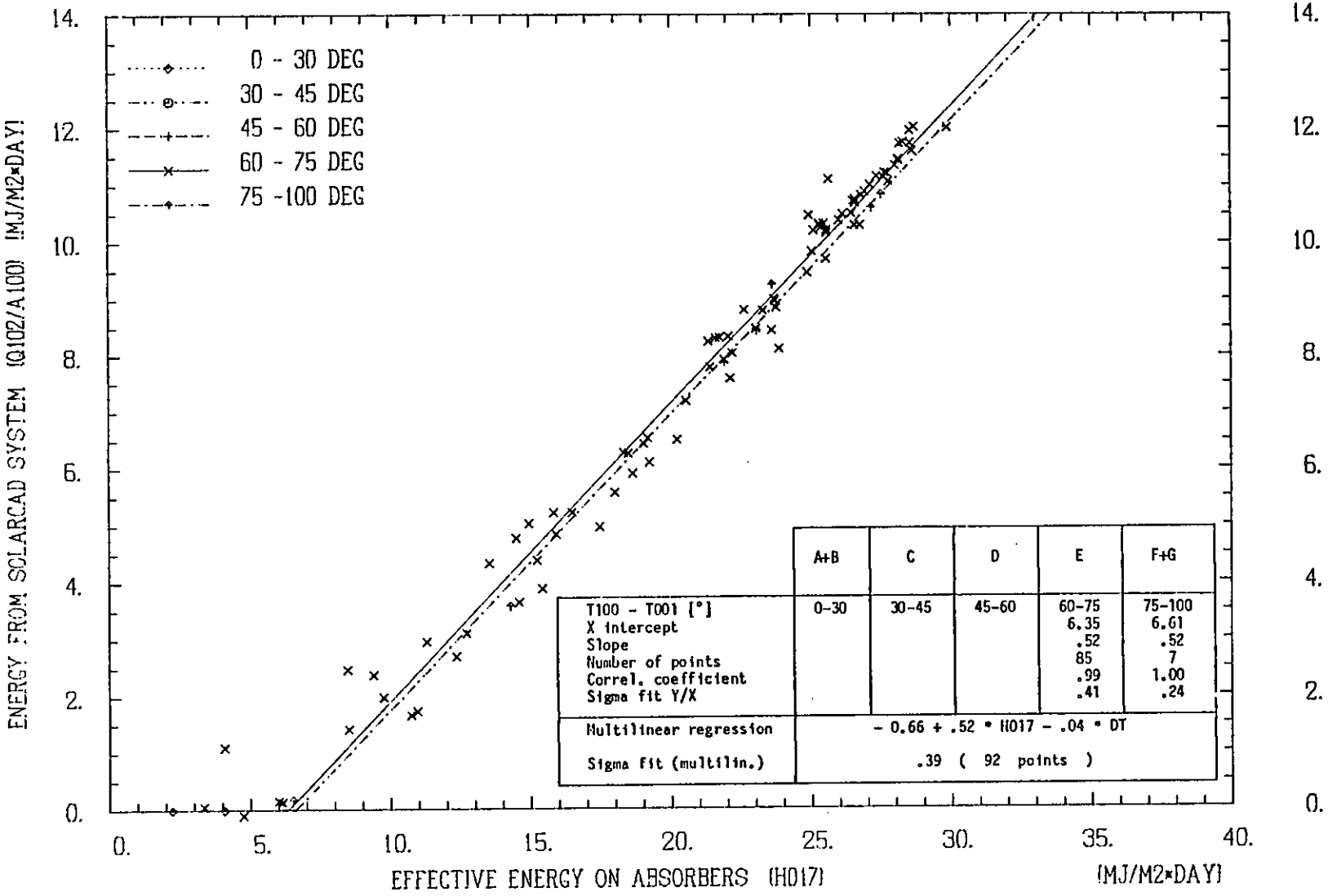

	A+B	C	D	E	F+G
T100 - T001 [°]	0-30	30-45	45-60	60-75	75-100
X intercept				6.35	6.61
Slope				.52	.52
Number of points				85	7
Correl. coefficient				.99	1.00
Sigma fit Y/X				.41	.24
Multilinear regression	- 0.66 + .52 * H017 - .04 * DT				
Sigma fit (multilin.)	.39 (92 points)				

Q102 Daily Input/Output diagram for "CORTEC" system vs "Global Effective" H017.
Values from 10/05/85 to 25/08/85. SOLARCAD 1000, Geneva, Switzerland.

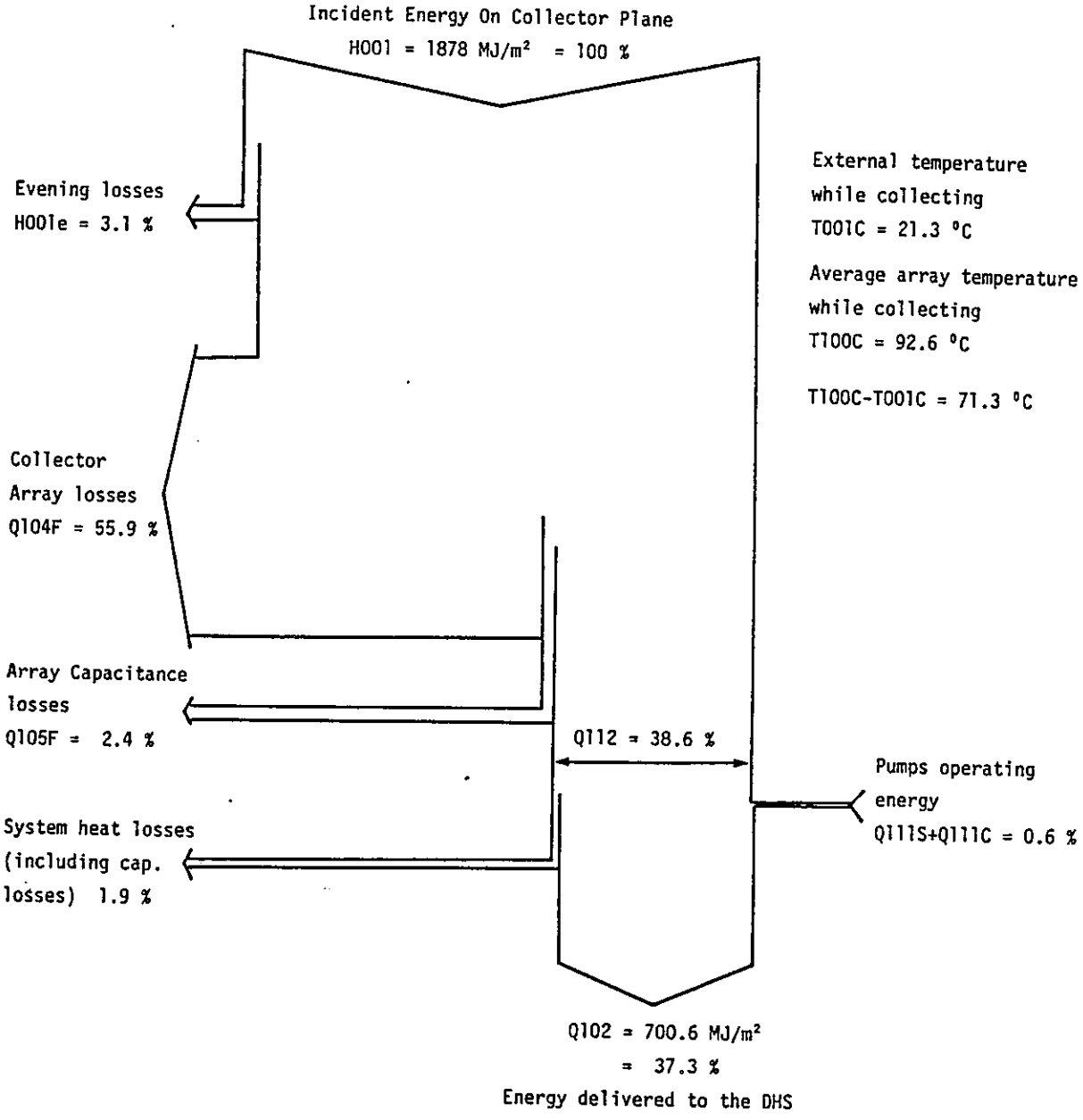

Simplified Energy Flow Arrow Diagram for the "CORTEC" system
at SOLARCAD 1000, Geneva, Switzerland.
Data of 89 days recorded between 10 May 1985 and 25 August 1985.

6.4. Energy Supply and Delivery Bar Chart

Solarcad 1000 District Heating Project
Geneva, Switzerland

Bar chart is given for the "summer" recorded period. Efficiencies are normalized to incident energy in collector plane (H100) but global effective energy on absorbers H117 is also shown (dotted lines). In April 85, some calibrations were performed on solarimeters, so that H117 is not determined for this period.

September 85 data are also shown, although the efficiency was significantly dropped due to the partial obturation of 28 % of the ETC modules.

6.5. Energy Use Bar Charts

Solarcad 1000 District Heating Project
Geneva, Switzerland

Because the heat produced by solar is much smaller than the load, different scales are used, which differ by a factor of 20. When dealing with a district heating system, space heating and domestic hot water contributions cannot be distinguished. The load temperature (input of the secundary loop of the exchanger), which is displayed here, is seen to lie about 5° C below the average collectors temperature (see bar chart figure).

See also remarks about bar charts.

6.6. System Efficiency and Solar Fraction

Solarcad 1000 District Heating Project
Geneva, Switzerland

System efficiency is related to the incident energy in the collector plane.

See also remarks about other plots.

DELIVERED SOLAR ENERGY
FOR CORTEC "E" ETC AT SOLARCAD 1000, GENEVA, SWITZERLAND

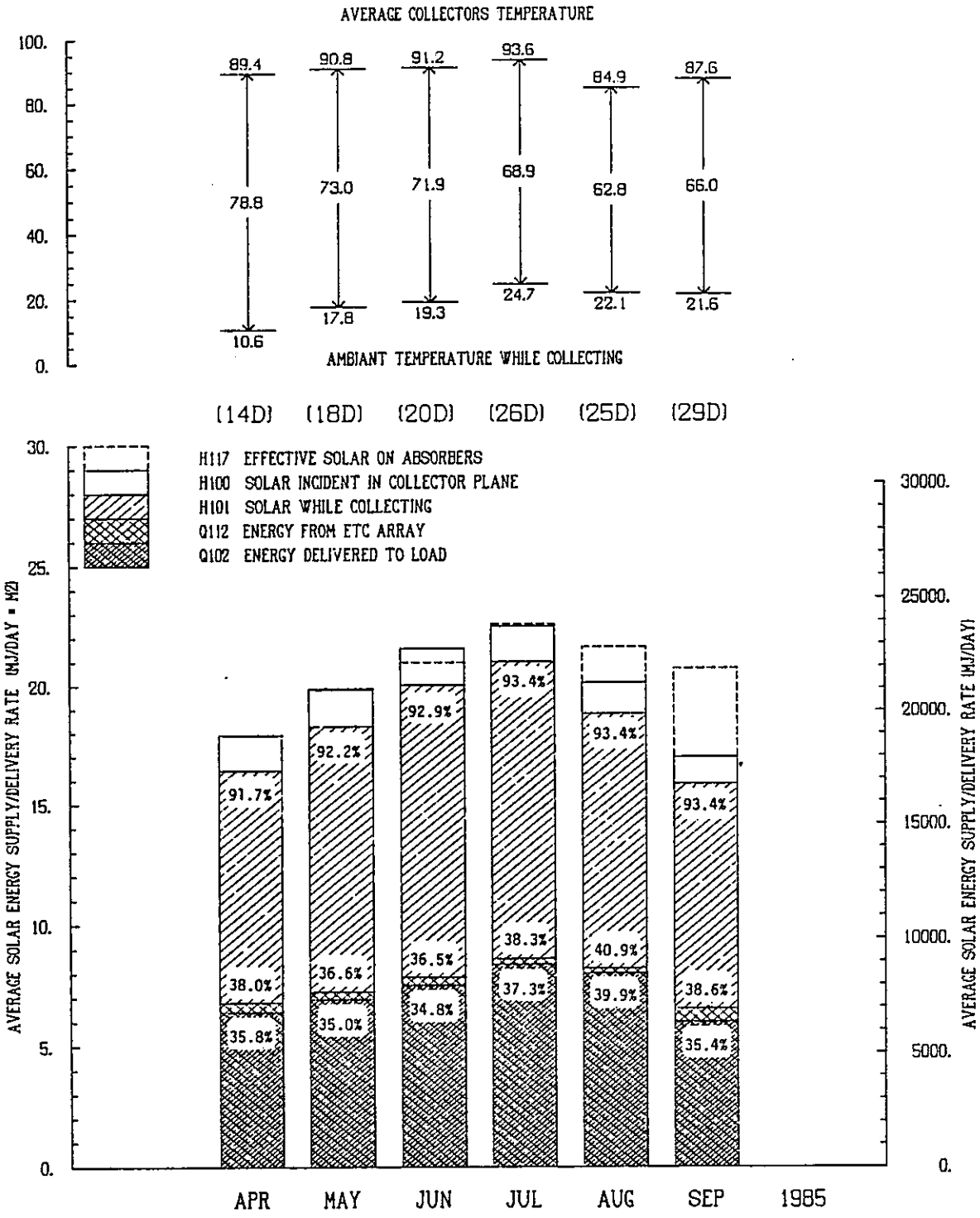

AVERAGE ENERGY USE RATE
FOR CORTEC "E" ETC AT SOLARCAD 1000, GENEVA, SWITZERLAND

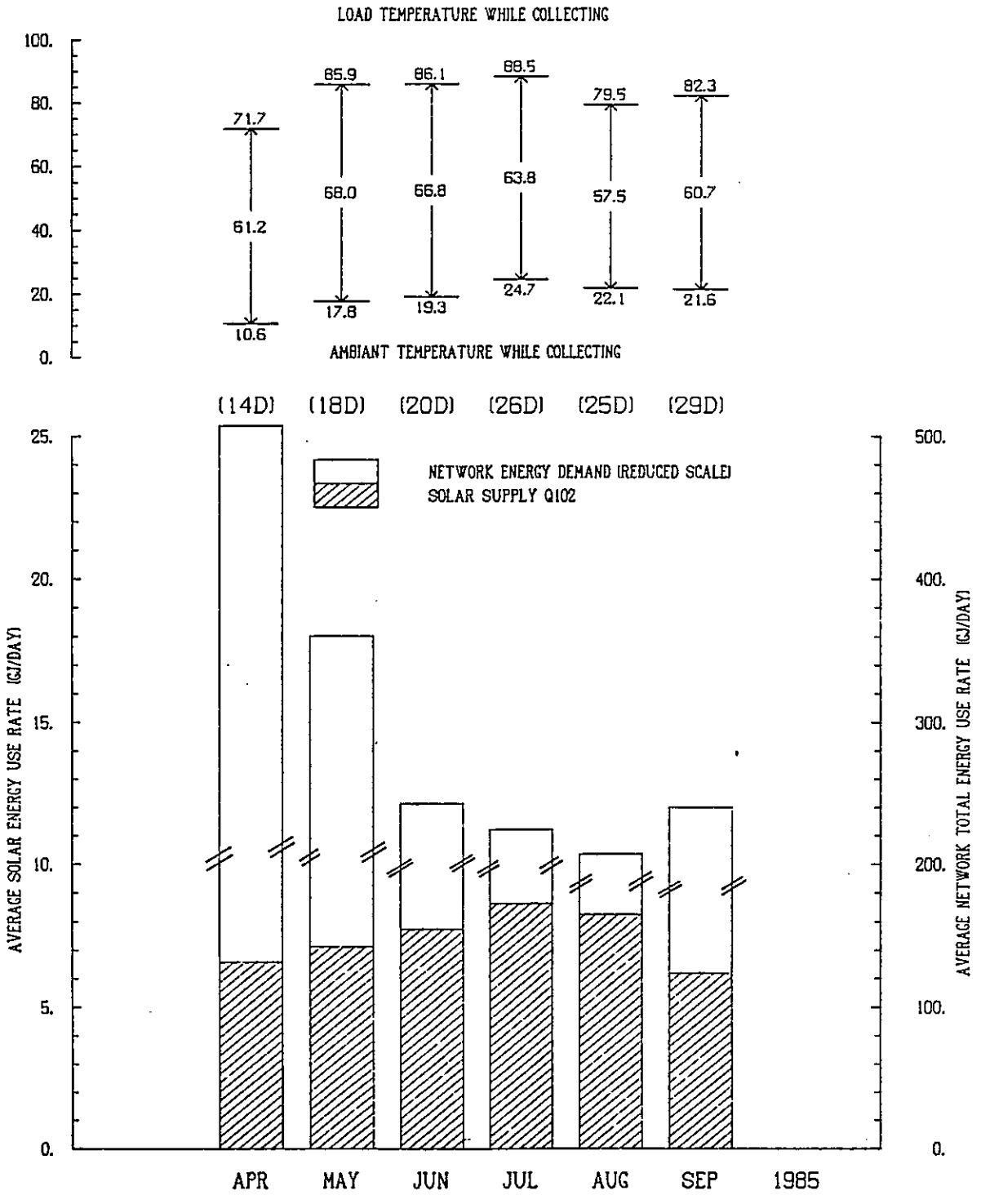

Table 6.1. System Results Summary

Solarcad 1000 District Heating Project
Geneva, Switzerland

	Experiment Results Summary
Net delivered energy (1) $\frac{Q102-Q111}{A100}$	7.75 $MJ/m^2 \cdot day$
System efficiency (= Q102/H100)	37.3 %
Collection subsystem COP (Q102/E103)	52.2
System solar fraction (Q102/load in our case)	1.54 %
Average Daily load per Aperture Area	503. $MJ/m^2 \cdot day$
Average Collector minus average ambiant temperature	71.3 °C
Average daily insolation H001	21.1 $MJ/m^2 \cdot day$

(1) Summer period, 10 May to 25 August 1985

AVERAGE MONTHLY SYSTEM EFFICIENCY AND SOLAR FRACTION FOR CORTEC "E" ETC AT SOLARCAD 1000, GENEVA, SWITZERLAND

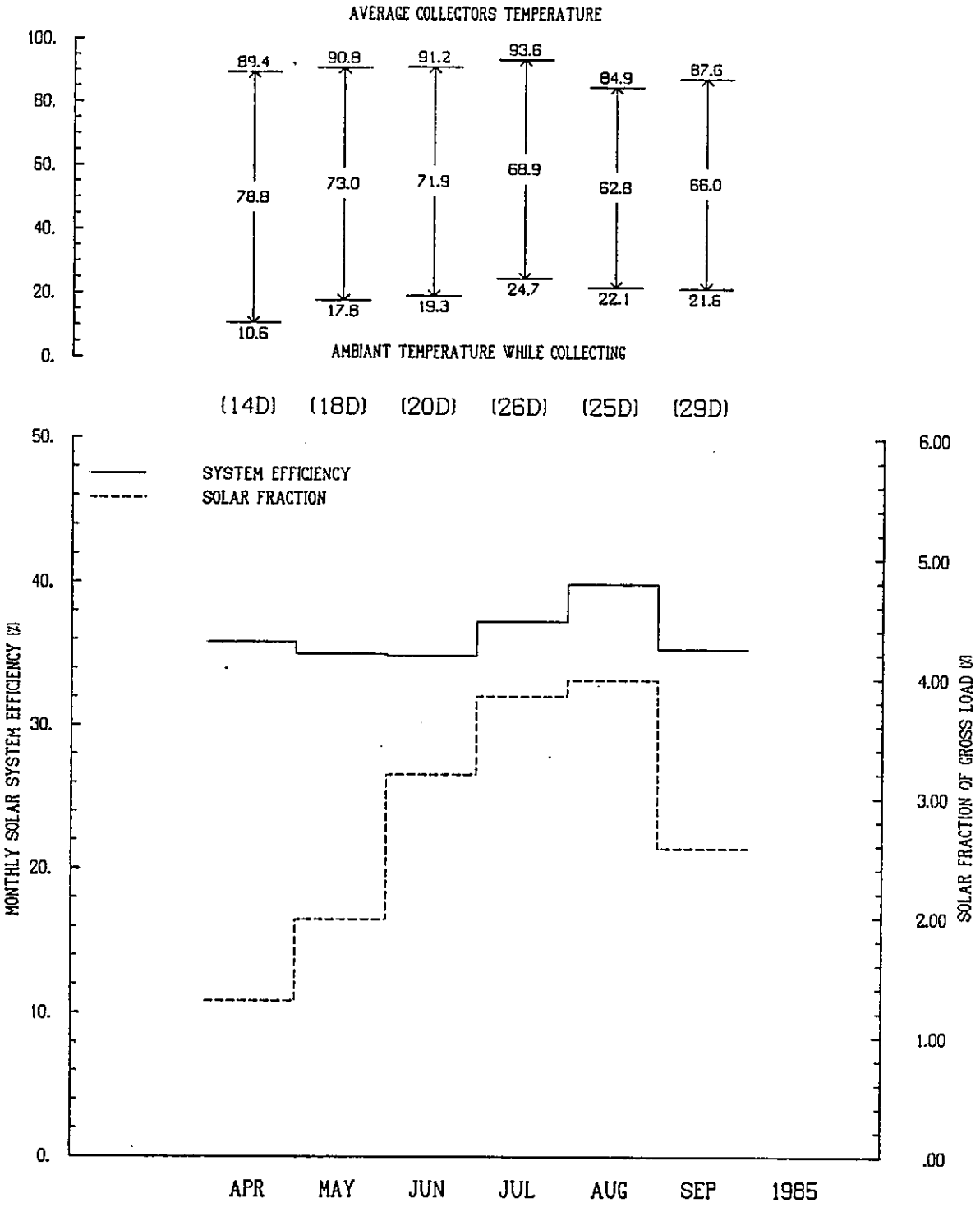

Table 8-1. Conclusions

Solarcad 1000 District Heating Project
Geneva, Switzerland

A solar system connected to a district heating network must operate above a high temperature theshold. All losses, including collector efficiencies, thermal losses and capacity effects (or "off" losses) depend very strongly on temperature and affect severely the system overall performance. But proper design can reduce these losses to acceptable levels.

With a quasi-horizontal collector plane, use of tilted absorbers results in a significant gain in energy intercepted. The collected energy is comparable to this of a tilted collector plane (corresponding to the absorber's plane) as long as no shadow of one absorber to the other occurs (i.e. from March to September in our case). Shading effect becomes important in winter, therefore the geometry choice is a delicate compromise depending on latitude, winter insulation and load seasonal profile.

Table 8.2 Future Plans

Solarcad 1000 District Heating Project
Geneva, Switzerland

We have studied test systems of 20 m^2, an industrial plant of 360 m^2 (SOLARIN project) and a DHS plant of 1000 m^2 (SOLARCAD 1000). All these experiments result in a good "know how" of evacuated collectors, their associated systems, their global performances and potentiality in swiss climate. We have also gained much experience in the collaboration with the other IEA Task VI participants.

We have still to establish models and design guide lines, which would summarize the whole experience gained for future solar designers at the national level.

Colorado State University Solar House I
Fort Collins, Colorado, United States

W.S. Duff
S. Karaki
G.O.G. Löf
T.E. Brisbane
D. Weirsma
G.Cler

Discussion

The material in this section was extracted from two reports: "Performance of a Solar Heating and Cooling System with Phase Change Storage" February 1985 and "Performance of Solar Heating and Cooling Systems Employing Evacuated-Tube Collectors - CSU Solar House I," both Colorado State University Solar Energy Applications Laboratory publications.

The Philips VTR 361 collector continued in operation through September 1984. A new collector, the Sunmaster TRS-1, was employed during the Winter of 1984-85. It is shown in Figures E-3-1 through E-3-3. Its characteristics are

Evacuated Tube Diameter	50.8	mm
Evacuated Tube Length	1.83	m
Pitch (Centerline Spacing between Tubes)	152	mm
Tubes per Module	8	
Gross Area per Module	2.43	m^2
Aperture Area per Module	2.14	m^2
Modules (Two Parallel Rows)	12	

Collector array efficiencies for the Philips VTR 361 on a clear day and at high operating temperature differences are shown in Table E-3-1.

Daily energy input/output diagrams for the Sunmaster TRS-1 collectors for operating collector to ambient temperature differences from 30 to 90°C are given in Figures E-3-4 through E-3-6. A comparison of the diagrams for the Philips VTR 361 and Sunmaster TRS-1 collectors is given in Figure E-3-7.

Energy flow diagrams for the Philips VTR 361 collector are shown in Figures E-3-8 and E-3-9 and for the Sunmaster TRS-1 collector, in Figure E-3-10.

Energy supply rates for the two collectors are given in Figures E-3-11 and E-3-12.

Table E-3-1 Collector Array Effficiencies for the Philips VTR 361 Collector at Colorado State University Solar House I, January 2, 1984

DAY	DATE	TIME	TOTAL SOLAR RAD H001	TOTAL SOLAR RAD H100	COLL INLET TEMP T100	COLL OUTLT TEMP T112	AVG FLUID TEMP T105	AMB AIR TEMP T001	CORR COLL ENRGY Q112'	CORR COLL EFF N100	Tav-Ta / GT
		hr	W/m2	MJ/m2	C	C	C	C	MJ/m2		Cm2/W
2	JAN 2	8:45	468	140.4	37.7	44.9	41.3	-8.5	76.5	.545	.1064
		50	495	148.5	38.1	45.9	42.0	-8.4	81.2	.547	.1018
		55	520	156.0	38.5	46.9	42.7	-7.9	86.4	.554	.0973
		9: 0	546	163.8	39.0	47.8	43.4	-8.0	91.9	.561	.0941
		5	572	171.6	39.4	48.7	44.1	-8.1	97.1	.566	.0912
		10	596	178.8	40.1	49.6	44.9	-7.6	102.5	.573	.0880
		15	621	186.3	40.6	50.7	45.7	-7.2	107.3	.576	.0851
		20	644	193.2	41.0	51.5	46.3	-7.2	111.7	.578	.0830
		25	668	200.4	39.8	51.0	45.4	-7.2	111.2	.555	.0787
		30	691	207.3	41.1	52.4	46.8	-6.8	126.7	.611	.0775
		35	712	213.6	41.5	53.2	47.4	-6.7	125.4	.587	.0759
		40	731	219.3	41.8	53.9	47.9	-6.8	129.4	.590	.0748
		45	751	225.3	42.0	54.6	48.3	-6.8	133.4	.592	.0734
		50	771	231.3	42.4	55.2	48.8	-6.8	136.5	.590	.0721
		55	790	237.0	43.0	55.8	49.4	-6.4	140.3	.592	.0706
		10: 0	809	242.7	43.4	56.5	50.0	-6.3	143.0	.589	.0695
		5	827	248.1	43.9	57.3	50.6	-5.9	146.4	.590	.0683
		10	843	252.9	44.5	58.1	51.3	-5.9	149.2	.590	.0679
		15	857	257.1	45.2	59.0	52.1	-5.8	152.2	.592	.0676
		20	872	261.6	45.9	59.9	52.9	-5.7	154.9	.592	.0672
		25	889	266.7	46.4	60.7	53.6	-5.4	156.8	.588	.0663
		30	904	271.2	46.9	61.4	54.2	-5.1	159.5	.588	.0655
		35	917	275.1	47.4	62.0	54.7	-5.0	161.5	.587	.0651
		40	929	278.7	47.8	62.9	55.4	-4.7	164.7	.591	.0646
		45	942	282.6	48.3	63.7	56.0	-4.7	167.3	.592	.0644
		50	954	286.2	48.9	64.5	56.7	-4.5	170.3	.595	.0642
		55	966	289.8	49.4	65.1	57.3	-4.2	172.1	.594	.0636
		11: 0	976	292.8	50.0	65.9	58.0	-4.1	175.1	.598	.0636
		5	986	295.8	50.6	66.7	58.7	-4.1	177.5	.600	.0636
		10	998	299.4	51.3	67.5	59.4	-4.0	180.2	.602	.0635
		15	1004	301.2	51.9	68.5	60.2	-3.6	182.8	.607	.0635
		20	1007	302.1	52.6	69.3	61.0	-3.4	181.6	.601	.0639
		25	1012	303.6	53.0	70.1	61.6	-3.5	185.5	.611	.0643
		30	1017	305.1	53.6	70.8	62.2	-3.4	186.7	.612	.0645
		35	1020	306.0	54.2	71.5	62.9	-3.1	188.5	.616	.0647
		40	1025	307.5	54.7	72.1	63.4	-3.0	188.8	.614	.0648
		45	1029	308.7	55.3	72.9	64.1	-3.0	190.8	.618	.0652
		50	1029	308.7	55.8	73.4	64.6	-2.5	190.8	.618	.0652
		55	1028	308.4	56.4	74.2	65.3	-2.5	192.4	.624	.0660
		12: 0	1027	308.1	57.1	74.7	65.9	-2.4	191.9	.623	.0665
		5	1028	308.4	57.7	75.4	66.6	-2.4	191.8	.622	.0671
		10	1028	308.4	58.3	76.0	67.2	-2.2	191.2	.620	.0675
		15	1028	308.4	59.0	76.6	67.8	-2.0	191.2	.620	.0679
		20	1023	306.9	59.6	77.0	68.3	-1.8	190.0	.619	.0685
		25	1027	308.1	60.1	77.6	68.9	-1.7	189.5	.615	.0687

Table E-3-1 (continued)

DAY	DATE	TIME	TOTAL SOLAR RAD H001	TOTAL SOLAR RAD H100	COLL INLET TEMP T100	COLL OUTLT TEMP T112	AVG FLUID TEMP T105	AMB AIR TEMP T001	CORR COLL ENRGY Q112'	CORR COLL EFF N100	Tav-Ta / GT
		hr	W/m2	MJ/m2	C	C	C	C	MJ/m2		Cm2/W
2	JAN 2	12:30	1028	308.4	60.7	78.2	69.5	-1.6	189.0	.613	.0691
		35	1028	308.4	61.3	78.7	70.0	-1.6	188.1	.610	.0696
		40	1027	308.1	61.8	79.1	70.5	-1.1	186.4	.605	.0697
		45	1024	307.2	62.5	79.5	71.0	-1.3	185.2	.603	.0706
		50	1015	304.5	63.1	79.8	71.5	-1.0	181.8	.597	.0714
		55	1006	301.8	63.6	80.1	71.9	-1.0	178.7	.592	.0724
		13: 0	1005	301.5	64.1	80.4	72.3	-1.0	175.8	.583	.0729
		5	1002	300.6	64.7	80.8	72.8	-0.6	173.7	.578	.0732
		10	994	298.2	65.3	81.1	73.2	-0.6	170.9	.573	.0742
		15	986	295.8	65.9	81.5	73.7	-0.8	168.6	.570	.0756
		20	974	292.2	66.5	81.8	74.2	-1.0	166.3	.569	.0772
		25	959	287.7	67.0	82.1	74.6	-1.1	163.4	.568	.0789
		30	944	283.2	67.5	82.5	75.0	-0.6	160.9	.568	.0801
		35	938	281.4	68.1	82.8	75.5	-0.7	158.7	.564	.0812
		40	926	277.8	68.8	83.2	76.0	-1.0	157.2	.566	.0832
		45	913	273.9	69.2	83.6	76.4	-0.5	154.5	.564	.0842
		50	900	270.0	69.7	83.9	76.8	-0.5	152.6	.565	.0859
		55	888	266.4	70.3	84.1	77.2	-0.2	150.5	.565	.0872
		14: 0	873	261.9	70.8	84.4	77.6	-0.5	148.0	.565	.0895
		5	856	256.8	71.2	84.6	77.9	-0.3	144.6	.563	.0914
		10	839	251.7	71.8	84.9	78.4	-0.2	142.5	.566	.0936
		15	819	245.7	72.3	85.1	78.7	0.2	138.8	.565	.0958
		20	798	239.4	72.7	85.3	79.0	0.0	135.7	.567	.0990
		25	778	233.4	73.2	85.5	79.4	0.3	133.0	.570	.1016
		30	755	226.5	73.7	85.8	79.8	0.4	130.2	.575	.1051
		35	731	219.3	74.3	85.9	80.1	-0.1	126.3	.576	.1097
		40	709	212.7	74.7	86.0	80.4	-0.3	122.1	.574	.1138
		45	684	205.2	75.2	86.0	80.6	0.0	117.8	.574	.1178
		50	657	197.1	75.5	86.0	80.8	-0.2	112.5	.571	.1232
		55	630	189.0	75.9	85.9	80.9	-0.3	107.5	.569	.1289
		15: 0	606	181.8	76.2	85.9	81.1	-0.4	102.5	.564	.1344
		5	583	174.9	76.6	85.8	81.2	-0.4	97.6	.558	.1400
		10	562	168.6	76.9	85.7	81.3	-0.4	92.9	.551	.1454
		15	537	161.1	77.3	85.5	81.4	-0.4	88.0	.546	.1523
		20	514	154.2	77.5	85.5	81.5	-0.2	83.0	.538	.1589
		25	492	147.6	77.9	85.2	81.6	-0.3	77.0	.522	.1664
		30	464	139.2	78.2	85.0	81.6	-0.5	71.3	.512	.1769
		35	434	130.2	78.4	84.7	81.6	-0.4	64.7	.497	.1888
		40	405	121.5	78.6	84.4	81.5	-1.0	58.4	.481	.2037
		45	376	112.8	78.8	84.0	81.4	-1.1	51.9	.460	.2194
		50	344	103.2	78.9	83.6	81.3	-1.1	44.8	.434	.2394
		55	315	94.5	79.1	83.2	81.2	-1.3	38.5	.407	.2617
26	JAN 26	8:45	503	150.9	70.7	78.2	74.5	3.7	77.6	.514	.1407
		50	528	158.4	71.1	79.0	75.1	4.1	80.6	.509	.1344
		55	553	165.9	71.4	79.9	75.7	4.3	85.6	.516	.1290

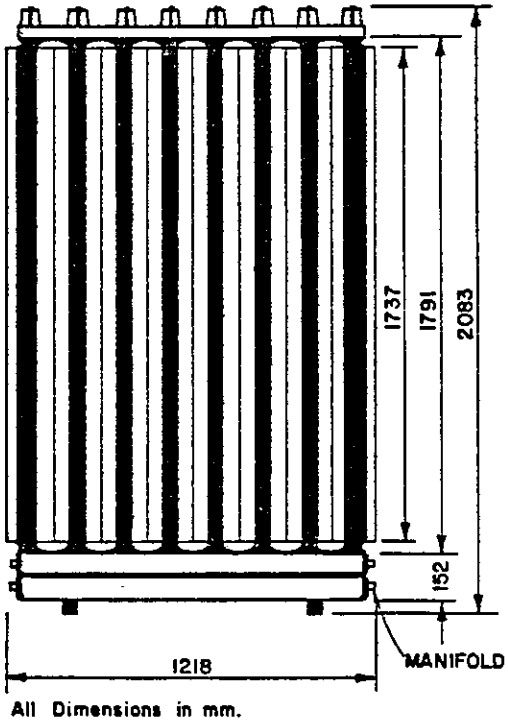

Figure E-3-1 Sunmaster TRS-1 Collector Module.

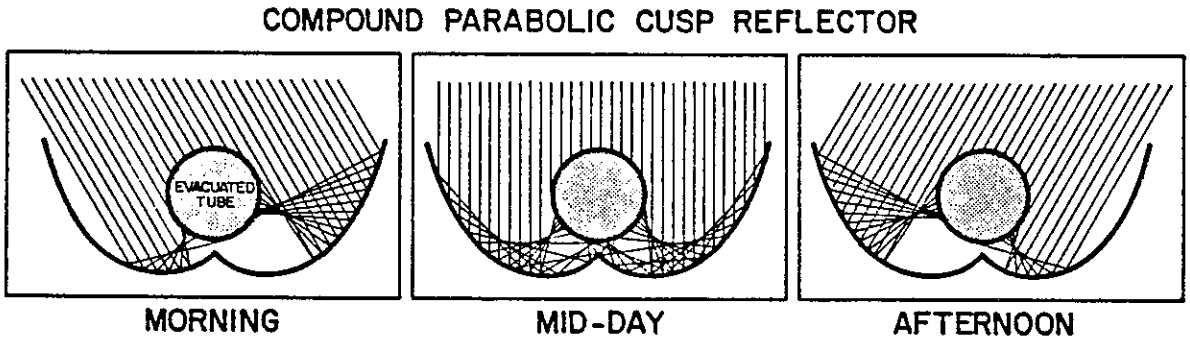

Figure E-3-2 Ray Traces from the CPC for Three Representative Periods of a Day.

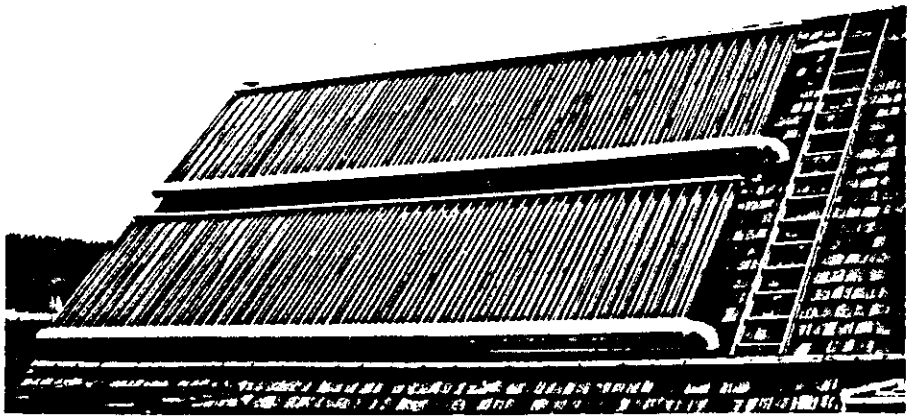

Figure E-3-3 Sunmaster Collector Array.

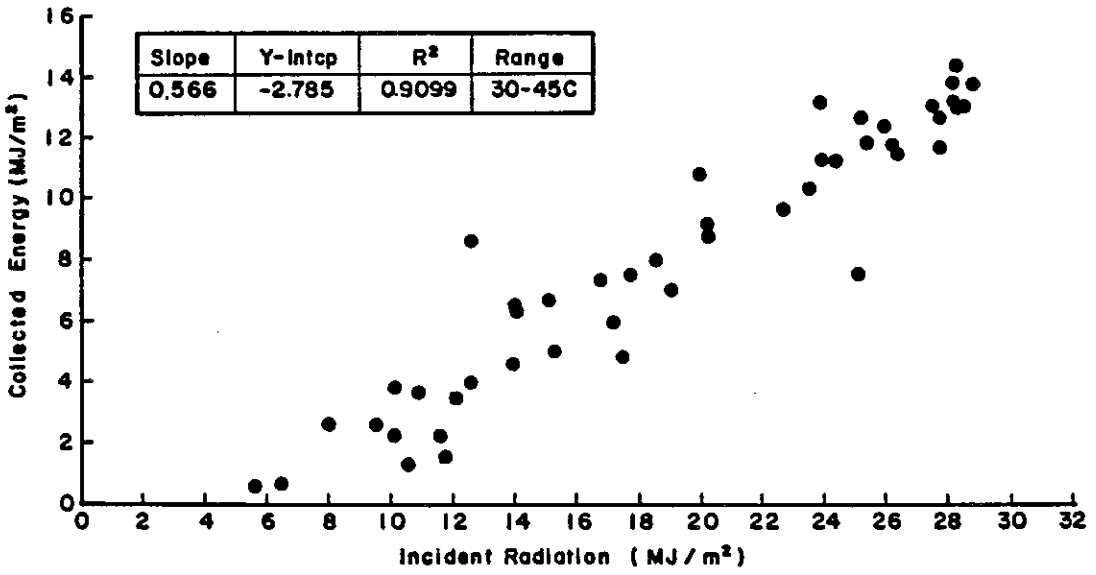

Figure E-3-4 Daily Energy Delivery from Sunmaster TRS-81 Collectors in ΔT Range 30-45°C.

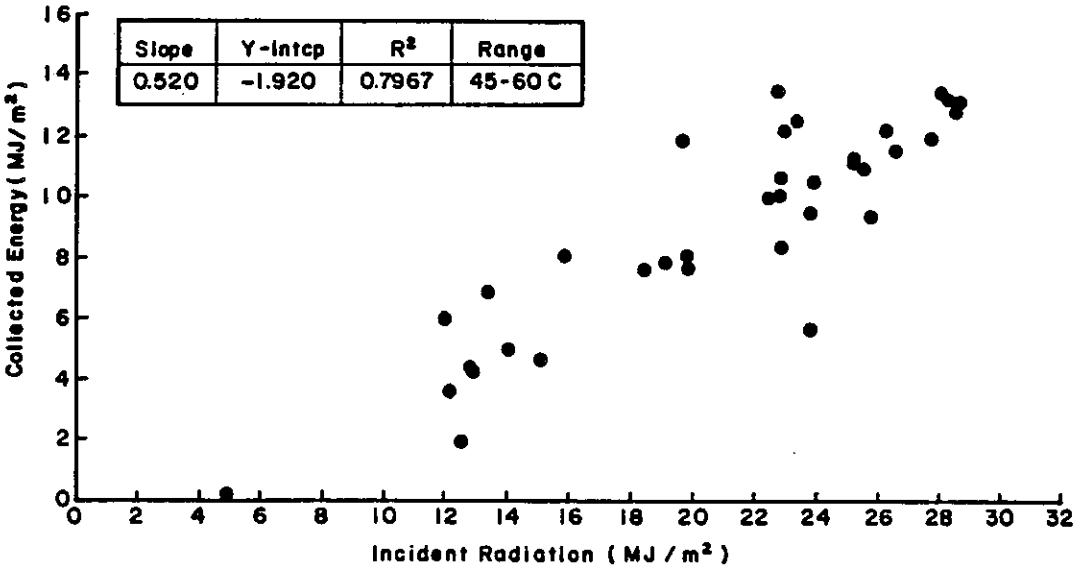

Figure E-3-5 Daily Energy Delivery from Sunmaster TRS-81 Collectors in ΔT Range 45-60^{o}C.

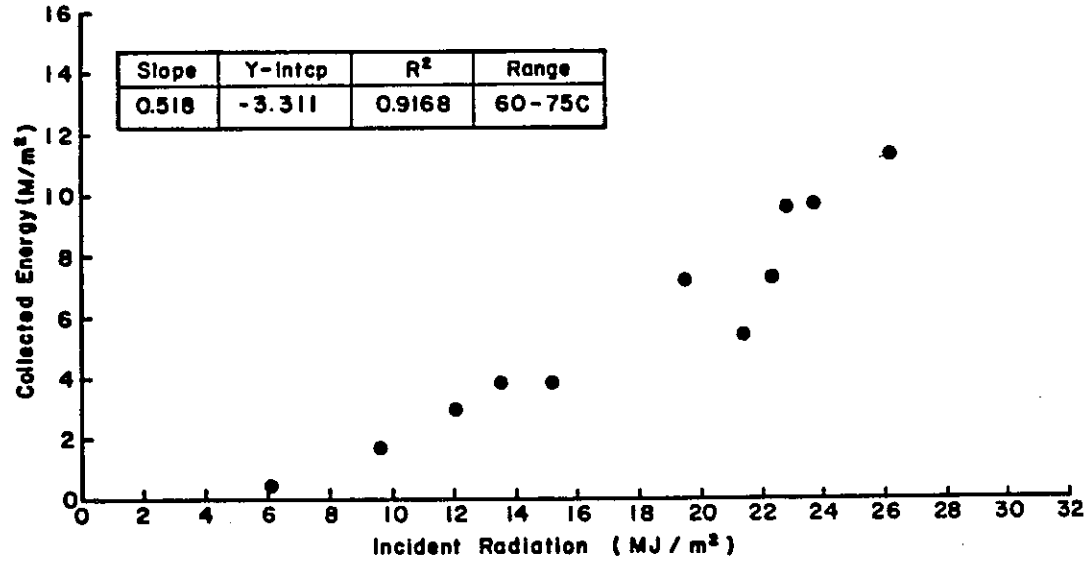

Figure E-3-6 Daily Energy Delivery from Sunmaster TRS-81 Collectors in ΔT Range 60-75^{o}C.

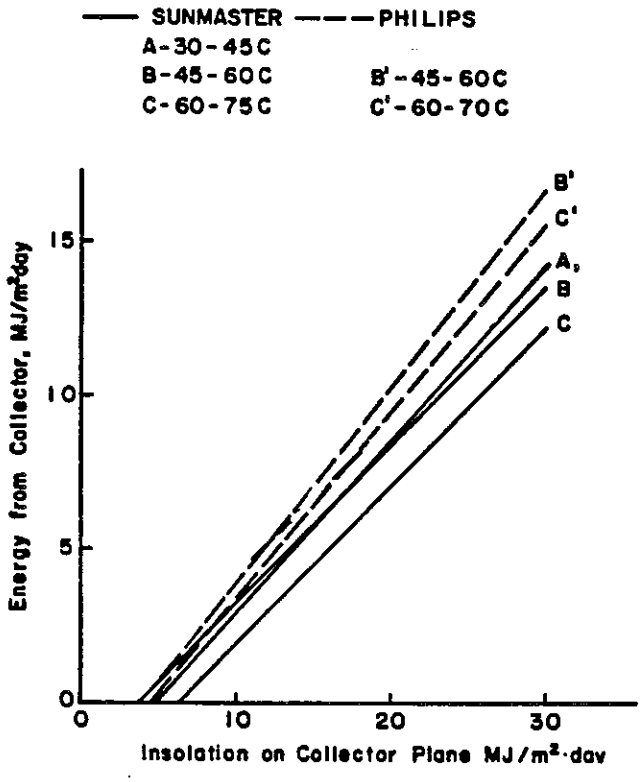

Figure E-3-7 Composite Representations of Energy Delivery from Sunmaster and Philips Collectors.

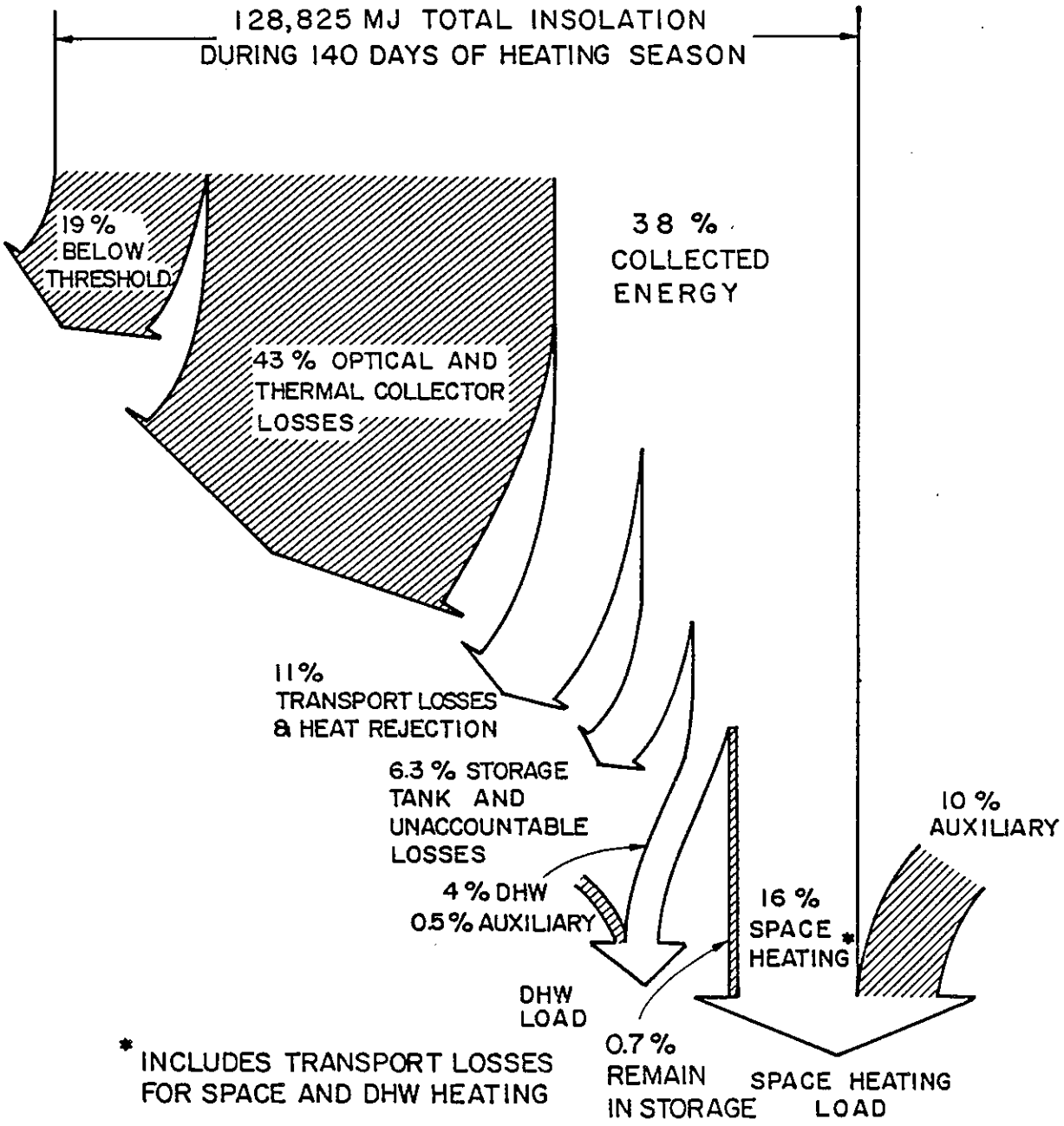

Figure E-3-8 Energy Flow Diagram for the Philips VTR 361 Collectors at Colorado State University Solar House I, Winter 1983-84.

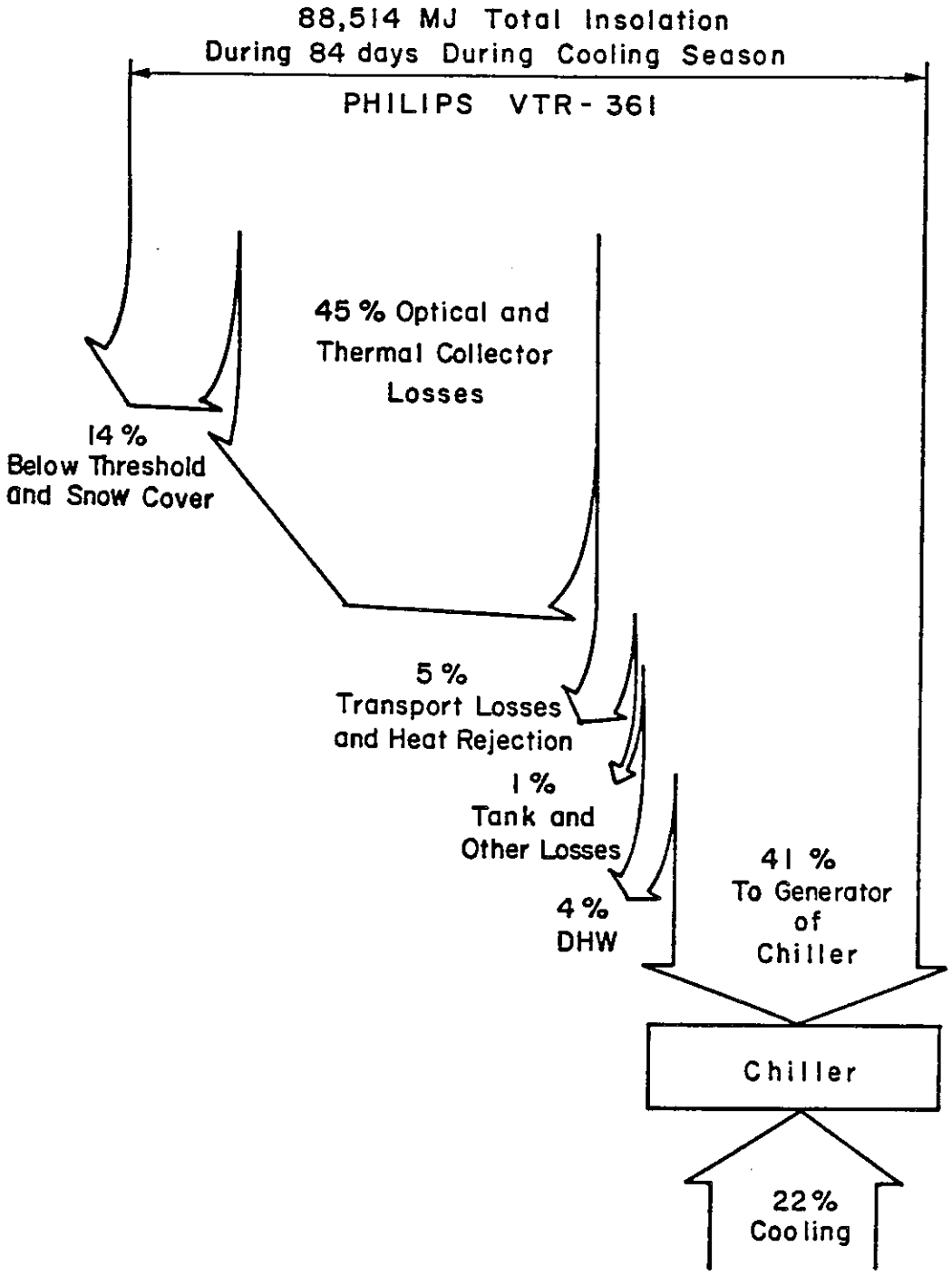

Figure E-3-9 Energy Flow Diagram for the Philips VTR 361 Collectors at Colorado State University Solar House I, July through September 1984.

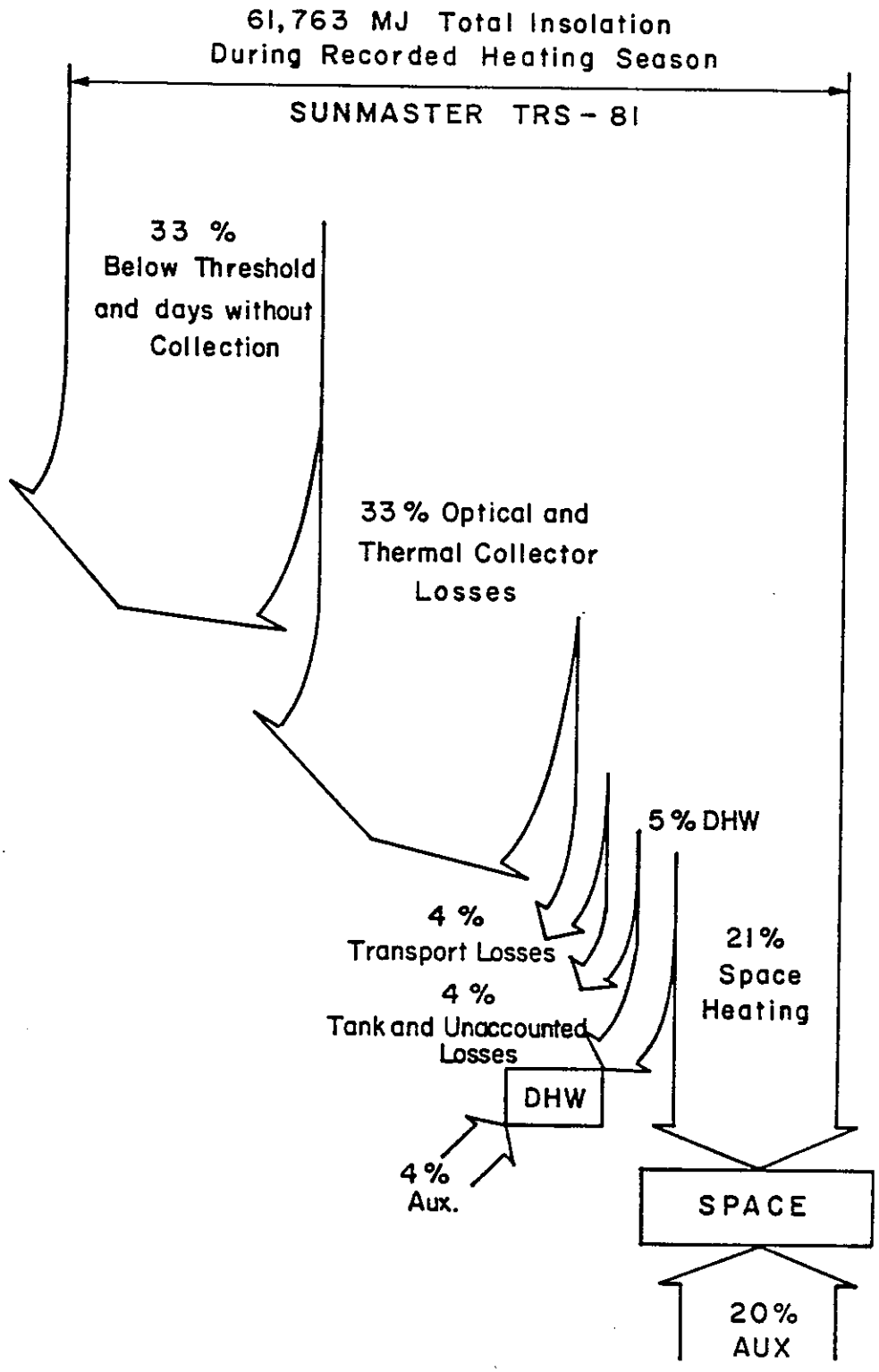

Figure E-3-10 Energy Flow Diagram for the Sunmaster TRS-81 Collectors at Colorado State University Solar House I, January through May 1985.

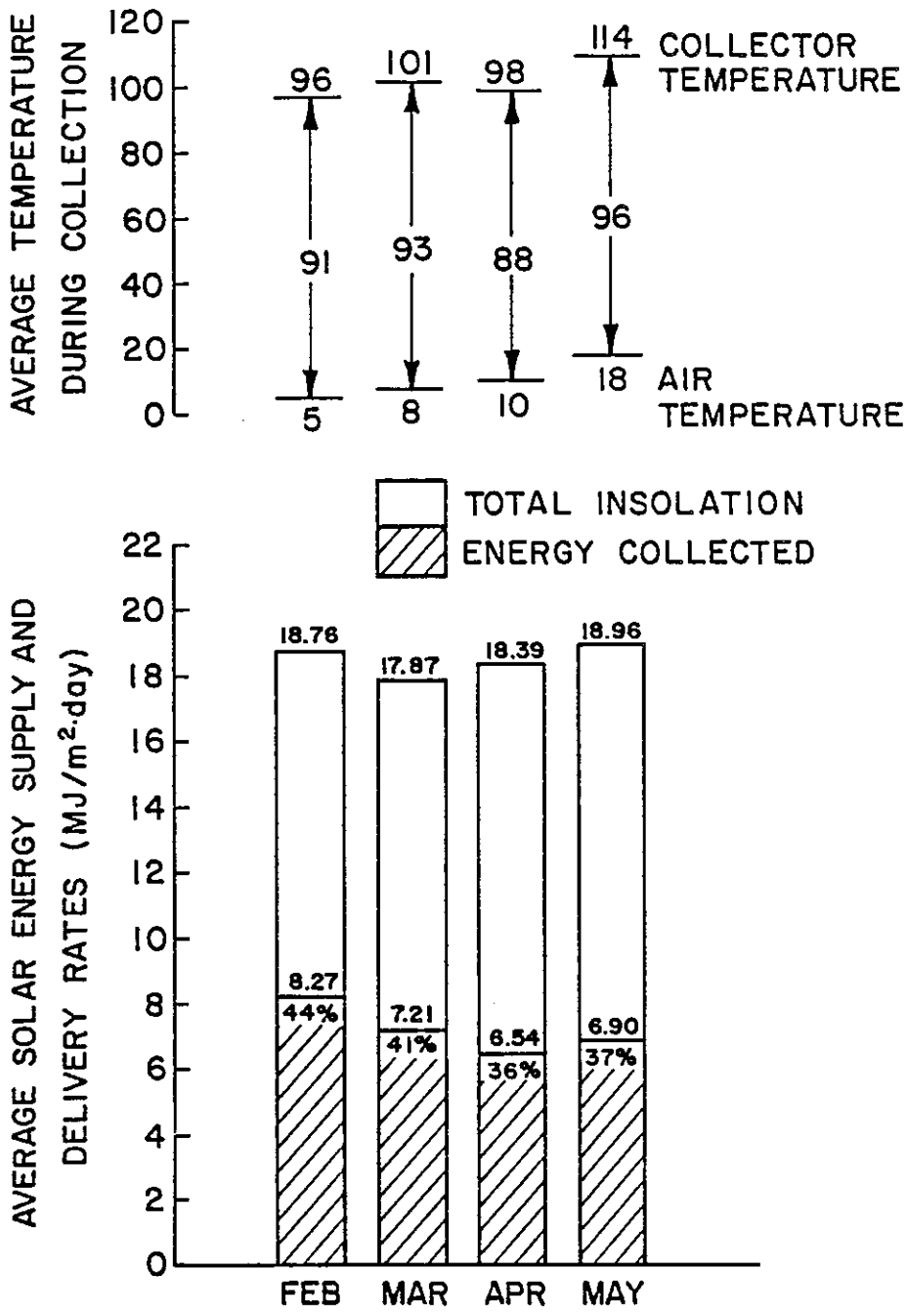

Figure E-3-11 Average Energy Supply Rates for the Philips VTR 361 Collectors at Colorado State University Solar House I, February to May 1984.

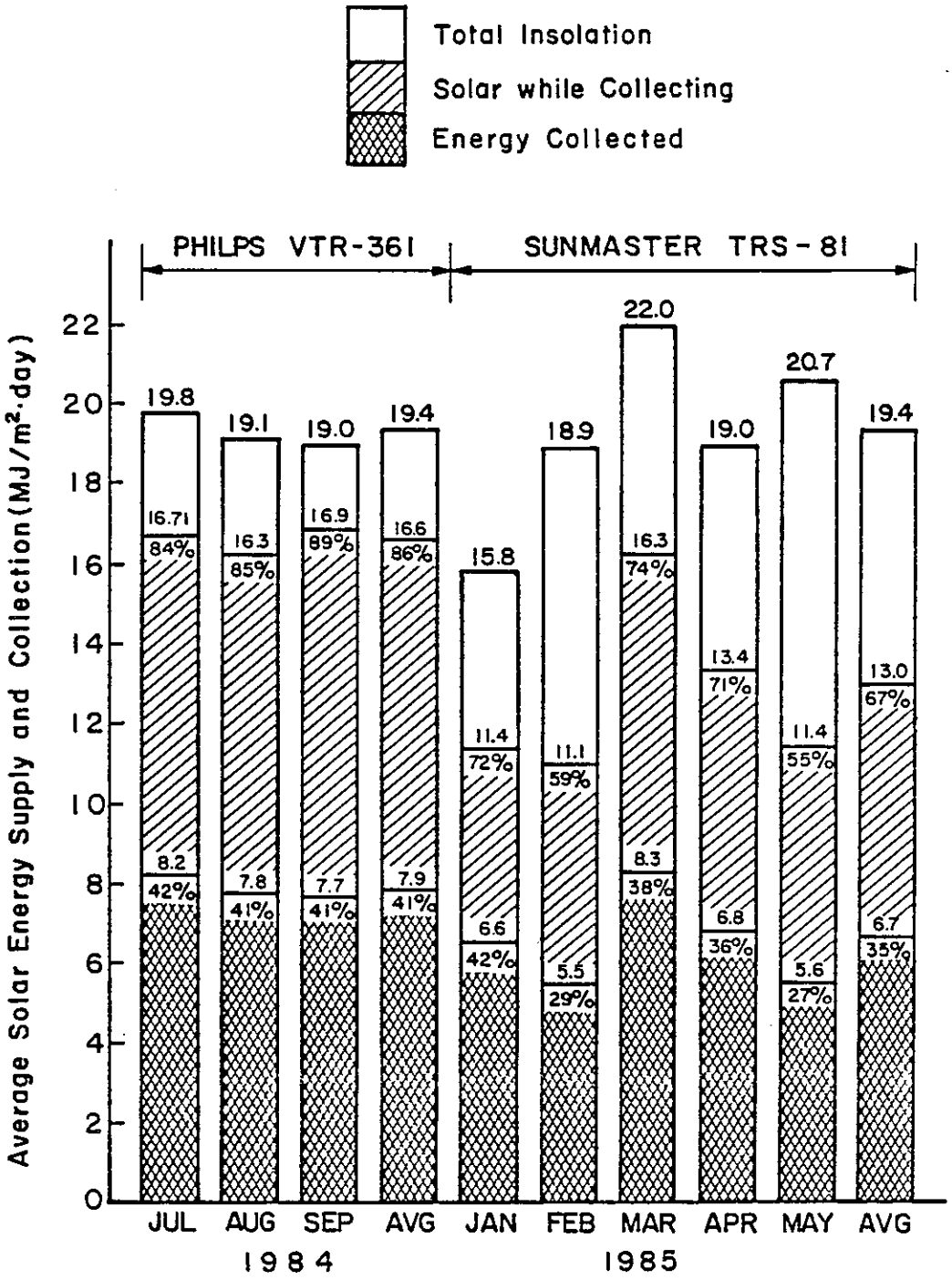

Figure E-3-12 Average Energy Supply Rates for the Philips VTR 361 and Sunmaster TRS-81 Collectors at Colorado State University Solar House I, July 1984 to May 1985.